University of Reading

Assessment of the hydrological status of Iraq using a combination of remote sensing and drought indices

A Thesis Submitted in Fulfilment of the Requirements for the Degree of Doctor of Philosophy

School of Human and Environmental Sciences

Geography and Environmental Science Department

Ahmed AlArazah

August 2017

Declaration of original authorship

Declaration

I confirm that this is my own work and the use of all materials from other sources has been properly and fully acknowledged.

Ahmed Alarazah

Acknowledgements

There are a number of people without whom this thesis might not have been written, and to whom I am greatly indebted.

I am grateful to Iraq, for providing me with the scholarship and their support to study for a PhD Degree. Deep thanks go to the School of Geography & Environmental Science, University of Reading for allowing me to conduct my research and providing any assistance requested.

I am extremely grateful to my supervisor Prof. Anne Verhoef for her guidance, support, constructive comments throughout this work, in addition, their valued time spending for reading the draft of this project, and for nurturing me through the months of writing.

I would also like to thank Dr Kevin White for his assistance, enthusiasm and advice and Dr. Shovonlal Roy for providing valuable advices.

Very special thanks go to staff, for their support. I would like to extend my loving thanks to my friends at Reading, and who directly or indirectly, have lent their hand in this venture.

A special feeling of gratitude to my loving family, for their care, support, affection in particular and encouragement.

Ahmed AlArazah

Reading, August, 2017

Abstract

This research deals with the assessment of drought over Iraq, a country which has been affected by recurrent droughts of medium to long duration, with serious socio-economic consequences. The overarching aim of this work is to identify reliable large-scale drought monitoring and assessment methods, using a range of freely available meteorological and remote sensing data, as well as model simulations of the water balance. The thesis starts with an overview of Iraq's climate, soil, land use and socioeconomic issues, as well as an inventory of commonly used methods to assess and express drought.

Historical droughts in Iraq have been studied between 2001 and 2013, using a combination of meteorological drought indices, remote sensing products, and water balance estimates by the SWAP model and ERA-Interim reanalysis. Drought is assessed for a number of key land surface types (desert, rangeland, agricultural land, and marshland), with the first three representative of the different climatic zones in Iraq. Their evolutions of drought have been compared and contrasted.

The research uses Standardised Precipitation Index (SPI) and Standardised Precipitation Evaporation Index (SPEI) drought indices, derived from ERA-Interim/in-situ data of rainfall and temperature, that are applied to evaluate meteorological droughts in Iraq. The effect of the meteorological droughts has also been analysed using land surface temperature (LST), Normalised Difference Vegetation Index (NDVI) and near-surface soil moisture content (SMC), derived from remote sensing data, in isolation and together with SPI/SPEI, for the years 2001 to 2015. NDVI has been used widely to detect changes in vegetation extent; LST was employed as a proxy of land surface evapotranspiration. NDVI was obtained from MOD13A2 products (16-Day L3 Global 1km SIN Grid VI datasets), which were designed for vegetation. LST was obtained through MOD11A2 products available at a spatial resolution of 1km and a temporal resolution of 8 days. SMC was derived from the Soil Moisture and Ocean Salinity (SMOS) product at a resolution of 40 × 40 km.

The evolution NDVI and SMC overall followed that of the drought indices, but the interannual variations of seasonal LST courses were not deemed useful for drought assessment. Furthermore, regression analyses were conducted between SPI3/SPEI3 and NDVI as well as LST to investigate the potential of drought inference from the sign and strength of the

correlation coefficient of the slope. This approach appeared promising for the marshlands, but less so for desert, rangeland, and agricultural regions.

Finally, the soil water balance Assessment (SWAP) model was used, driven by in-situ and ERA-Interim data. Water balance components for each land surface type were studied over time, to determine the effect of meteorological droughts on the variation of predicted ecosystem and agricultural system's hydrological behaviour. Comparisons were also made between the various land surface types, and between SWAP and ERA-Interim actual evapotranspiration estimates. The outcomes showed that the lowest mean actual evapotranspiration and water storage was found between 2008-2010, and 2012, as a result of lack in rainfall, whereas the monthly averages of actual evapotranspiration and water storage were the highest in 2013 and 2014. The data of the surface latent heat flux (ERA-Interim), actual evapotranspiration (SWAP), and soil moisture corresponded well for the desert and rangelands but not for the agricultural region. This is the result of the fact that ERA-Interim does not cater for (irrigated) crops whereas SWAP does.

The thesis concludes with recommendations with regards to the usefulness of the various (meteorological and remote sensing-based) drought indices, and combinations thereof, for assessment of drought in Iraq and similar climatological conditions.

Table of contents

Table of figures

List of tables

List of appendices

List of abbreviations

Ks	Water stress coefficient
°C	Degree Celsius
E	Soil evaporation
ET	Actual evapotranspiration
ET0	Reference evapotranspiration
GCM	General Circulation Models
GIS	Geographic information system
Ha	Hectare
IPCC	Intergovernmental Panel on Climate Change
Kc	Crop transpiration coefficient
KcTr, x	Maximum crop transpiration coefficient
Ksat	Saturated hydraulic conductivity
LAI	Leaf area index
NDVI	Normalized differential vegetation index
SWC	Soil water content
SMOS	Soil Moisture and Ocean Salinity
LST	Land surface temperature
SPI	Standardised precipitation index
SPEI	Standardised precipitation evapotranspiration index
T_{pot}	Potential transpiration
E_{pot}	Potential evaporation
ET_{pot}	Potential evapotranspiration
T_{act}	Actual transpiration
E_{act}	Actual evaporation
ET_{act}	Actual evapotranspiration
SLHF	Surface latent heat flux
STR	Net longwave radiation
SSR	Net shortwave radiation
SSHF	Surface sensible heat flux
Rn	Net radiation
SWAP	Soil, water, atmosphere and plant
ERDAS	Earth resource development assessment system

1. Chapter one: Introduction

Drought is a reoccurring worldwide environmental disaster. Increased water demands, climate variability (in particular variability in rainfall intensity and duration) and climate change, salinization and contamination of water supplies all together play a significant role in the occurrence of drought and its impacts. A natural hazard is recognized as a threat of a naturally occurring event that has a negative impact on both people and the environment. Drought as a natural hazard is a topic of great interest to physical and social scientists, as they are attempting to understand the causes of drought to help improve advice for practitioners to manage drought, and policy makers to mitigate drought impacts.

Drought presents a large number of negative impacts, which influence the environmental, social and economic standard of living. In environmental terms, drought not only reduces crop and forest productivity, surface and groundwater stores, and increases fire hazard, but also can cause an increase in desertification (Wilhite, Svoboda et al. 2007, EDEN 2012).

When studying drought, one needs to understand the difference between aridity and drought. Permanent drought (aridity) can be defined in meteorology and climatology, as "the degree to which a climate lacks effective, life-promoting moisture" (*Glossary of Meteorology*, American Meteorological Society). Aridity can be estimated by comparing long-term averages of precipitation to long-term averages of evapotranspiration. The climate is arid when evapotranspiration is higher than precipitation, *on average*. While a temporary drought is "a period of abnormally dry weather sufficiently long enough to cause a serious hydrological imbalance". A temporary drought refers to a moisture imbalance that occurs on a month-to-month or more frequent basis. Therefore, when the precipitation is less than evapotranspiration *for a given month*, and the month is abnormally dry; a drought occurs accompanied by at times serious hydrological impact if the drought is persistent in time and space (https://www.ncdc.noaa.gov/monitoring-references/dyk/drought-aridity).

Because of the fact that drought depends on many variables, predicting the start and end of temporary drought is quite difficult. Furthermore, typical characteristics of drought, such as frequency and intensity, vary from one climate regime to another (Solomon 2007).

The spatiotemporal occurrence of drought is a complex problem, because dry spells are tightly coupled to atmospheric and hydrological processes; in dry areas of a large extent, the moisture in the upper soil layers will be depleted, thus decreasing evapotranspiration rates, which in turn leads to a decrease in atmospheric relative humidity, which will have implications for rain-forming processes (Shrestha 2012), (Bierkens, Dolman et al. 2008).

Mesopotamia was recently affected by an intense and long-term drought episode during the four hydrological years from 2007 to 2010. Due to very low precipitation amounts, a steep decline in agricultural productivity occurred in the rain-fed Tigris and Euphrates drainage basins (Kaniewski, Van Campo et al. 2012). The worst drought affected regions in the Middle East were Iraq, Syria, and Iran. Consequently, this recent drought caused major socioeconomic issues, which clearly challenged the common belief that agricultural societies, by technological innovation and societal adjustment, can adaptively protect themselves from variability in natural precipitation'' (Wright Jr, McAndrews et al. 1967). The large arid and semi-arid zones of the Middle East generally rely on fragile systems of rain-fed or irrigated cultivation and are especially vulnerable to periodic fluctuations in climate and, most of all, to changes in the hydrological cycle. Anticipated repetitive drought episodes may exacerbate the vulnerability of communities unprepared to mitigate their adverse effects (Sowers, Vengosh et al. 2011). During the last 40 years, many Middle eastern dryland countries (Iran, inland Israel, Jordan, Turkey) have experienced warming and precipitation declines (Kafle and Bruins 2009), (Tayanç, İm et al. 2009), (Al-Qinna, Hammouri et al. 2011), (Soltani, Saboohi et al. 2012). Droughts occurred in an irregular and non- uniform manner, with highest severity, magnitude, and duration over the last decade (Bronk Ramsey 2009). Throughout the recent crisis and its aftermath (Weiss, Courty et al. 1993), eastern Syria reveals the same environmental vulnerability as in antiquity that may severely impact farming communities (Chen, Zhao et al. 2006)

Drought in Iraq has been increasing in occurrence and severity over the past decade. The principle cause of this is appears to be climate variability (Jouhari Nadiah 2012). Consequently, drought impacts, drought monitoring, and management in Iraq should be investigated.

1.1. Types of drought

Drought in Iraq has been earmarked as an important issue and as a potentially serious disaster facing Iraq, according to the High-Level Committee for Disaster Risk Reduction (HLCDRR) report. The occurrence and severity of droughts have been increasing since 1969, causing a reduction in surface and ground water stores, and an increase in soil salinization, water salinity and desertification of large areas of land (Jouhari Nadiah 2012).

The principal factors causing drought in Iraq are climate variability and associated global warming, growing water demand, reduction in water release from dams in riparian areas, and dust storms.

Drought events, including those in Iraq, can be classified into 3 different categories:

- **Meteorological drought**: is defined on the basis of the degree of dryness or precipitation deficiency over a pre determined time and period, in comparison to a normal or average amount, and the duration of the dry period (Mishra and Singh 2010).

- **Agricultural drought:** crops do not receive adequate levels of soil moisture, as caused by meteorological or groundwater drought. In other words, it is caused by the lack of availability of soil moisture that is needed to support forage and crop growth.

- **Hydrological drought:** water reserves in rivers, streams, lakes, aquifers and reservoirs fall below statistical averages; caused by meteorological droughts, but also by increased human water demand and consumption, changes in land use, land degradation(Jouhari Nadiah 2012).

1.2. Impacts of drought

Impacts of drought in Iraq are widespread, including serious erosion of both farm and non-farm incomes, increased poverty, increased workloads (both on and off-farm), the need to seek alternative livelihoods, health and welfare issues, problematic access to basic services, overload on service providers, and increased risks of conflict (Jouhari Nadiah 2012).

1.2.1. Social impacts

Severe droughts in Iraq forced people to migrate, often to cities, in search of alternative livelihoods, in turn also adversely affecting labour market conditions in urban areas. For example, the excess supply of unskilled and semi-skilled labour as a result of rural-to-urban migration can negatively affect wage and other employment conditions for both migrants and host communities. Drought in Iraq has contributed to population displacement; from 2004 to 2009 approximately 100,000 people have been displaced as a result of drought according to United Nations Educational, Scientific and Cultural Organization (UNESCO) observations. Furthermore, the International Organization for Migration (IOM) estimated that more than 500 families were displaced from Kirkuk, Salah al-Din and Ninewa provinces alone during 2009 – 2010 due to continued drought conditions and water scarcity as the principle factor which encouraged the increasing rural to urban migration. (Jouhari Nadiah 2012).

In Iraq, drought has not only led to decreasing Iraqi strategic reservoir levels, but also caused increasing levels of water (surface/groundwater) and soil salinity. Furthermore, a number of shallow surface wells have now fully dried up due to drought conditions. Consequently, these environmental impacts affect humans in terms of good-quality water available for consumption (Jouhari Nadiah 2012).

1.2.2. Economic impacts

Droughts affect a range of economic sectors such agriculture, tourism, construction, and energy. FAO reported that the contribution of agriculture to the Gross Domestic Product (GDP) has dropped from about 9% in 2002 to 4% in 2009, due to drought and desertification occurring throughout the country. In addition, drought caused a decrease of almost 40% in cropland coverage throughout Iraq. Consequently, forcing the country to significantly increase their food imports, at a great cost to the Iraqi Economy.

Furthermore, the livestock population greatly dropped in 2007-2008 due to drought impacts, which caused increasing poverty, unemployment and reduction of family income, as was documented by IOM. This also meant a continuing rise in food prices. Ultimately, economic drought caused a strain on the income of the average Iraqi household; approximately 3.1 % of the Iraqi population currently has no guaranteed access to a sufficient and secure amount of food, while 9.4% is close to slipping into this state according to a FAO report (Jouhari Nadiah 2012).

1.2.3. Environmental impacts

Recent droughts, in particular due to decreases in annual rainfall, have also resulted in a decrease in vegetation cover. The removal of the land vegetation cover has contributed to wind erosion and related degradation of agricultural lands in Iraq. Consequently, large areas of agricultural land have changed to drylands and are no longer suitable for agriculture. Fig. 1.1 illustrates the effect of drought on agriculture area; 46-56% of cropland area has been affected by drought in the northern part, and less so in the western and southern parts.

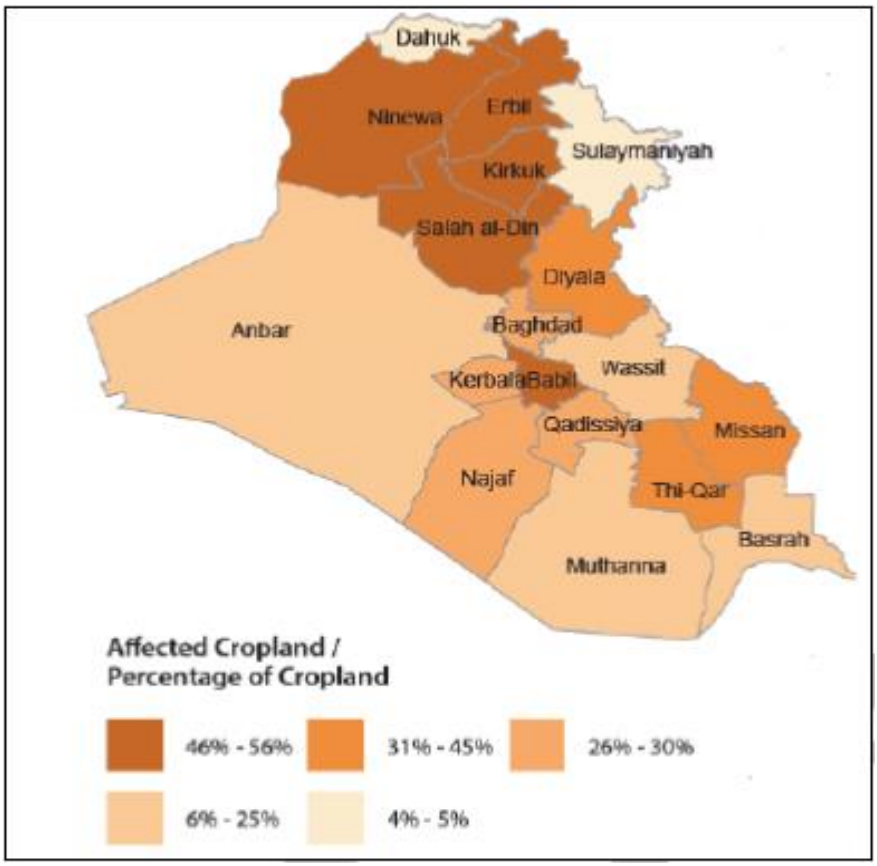

Figure 1.1 Impacts of drought on agricultural land area in Iraq during 2007-2009 ((FAO 2009))

Crop yields in Iraq today are low by any international comparison (FAO 2012). This is due, in part, to the effects of droughts, a serious water shortage problem (Al-Ansari 2013). However, consecutive years of severe drought and inadequate availability of agricultural inputs during 1999 to 2001 have negatively affected the Iraqi agriculture sector, as reflected by a substantial reduction in planting and yields. In 1999, total cereal production was estimated at 1.6 million tons, which was nearly 40 percent below the previous five-year average. Winter crops in this year were represented by approximately 1.2 million hectares under cereals; equivalent to 46 % of the total cultivated area was affected by severe droughts. In 2000, crop yields were substantially below the poor harvest of 1999. Central and southern regions were affected most severely with regards to reduction in land cover of natural vegetation and cropped area. Roughly 75% of barley and wheat crop areas were damaged by the drought and were mostly grazed by livestock instead. In 2000, yields had decreased to all time low levels.

Drought conditions dramatically affected water resources in rivers, lakes, dams, and canals, and resulted in the drying up of some of these water resources, thus creating unfavourable conditions for the upcoming irrigated summer crops.

It was not only drought that affected cereal production but also the lack of other agricultural inputs, such the serious shortages of fertilizers, and spare parts for agricultural machinery. Production of cereals (mainly barley and wheat) in 2001 was estimated at 1.8 million tons, which was 12% below average.

Basically, most farming in Iraq entails planting and harvesting a single crop per year. In the rainfed areas the winter crops, primarily small grains, are planted in the fall and harvested in late spring or early summer. In the irrigated areas of central and southern Iraq, summer crops predominate.

Even with some double or triple cropping, the intensity of cultivation is usually on the order of 50 percent because of the practice of leaving about half the arable land fallow each year. In the rainfed regions, land is left fallow so that it can accumulate moisture. The fertility of fallow land is also increased by ploughing in weeds and other plant materials that grow during the fallow period. On irrigated land, fallow periods also contribute some humus to the soil (Jaradat 2003).

Drought in the rainfed areas is a recurrent annual event, and a number of farming methods have evolved to deal with it in various ways such as: storing grain to feed animals during the dry periods, selling failed crops for grazing, using all of the crop residues for animal feed; using fallow, having more than one source of income, and being flexible enough to move to find employment or grazing.

At the same time, the drought problem has increased with increasing water demands for agricultural, domestic and industrial uses. Droughts do not only affect agricultural crops or rangelands (used for grazing). Due to recurrent drought events in 2008-2009, Iraq's recently restored marshlands' extent (see Section 2.9) started shrinking again, and only very slightly recovered during the winter months of 2009/2010 (Initiative 2010). In 2008, the marshlands were covering approximately 4950 km^2 which was reduced to 3420 km^2 in April 2009, and to

2313km^2 in July 2009 (Dempster 2010). The recovery rate from January 2010 to January 2011was similar.

1.3. Agricultural drought background and its effect on vegetation over Iraq

Agricultural drought is a disaster that affects vegetation in general and cropland specifically in Iraq. In recent years, arable lands in Iraq experienced increasing land degradation that led to desertification (Almamalachy 2017). Although drought has no universal definition, it can be simply described as "deficiency in precipitation over an extended period, usually a season or more, resulting in a water shortage which adversely affects agriculture on vegetation" (NOAA 2008). Van Loon 2015 described the impacts of the different stages of drought development, where a drought event starts with a prolonged shortage in precipitation rate, called a meteorological drought, and usually leads to a reduced water availability in root-zone soil moisture, ultimately resulting in decreased vegetation cover; this is known as an agricultural drought.

Trigo, Gouveia et al. 2010 state that hydrological drought emerges after the development of meteorological and agricultural droughts, and that it can be defined as the long-term below-normal amount of water available in the terrestrial part of the hydrological system including surface water, and ground water. The historical region of Northern Mesopotamia recently experienced an intense and prolonged drought episode during the four hydrological years between 2007 and 2010, that generated a steep decline in agricultural productivity in the rain-fed Euphrates and Tigris drainage basins.

Iraq was also subjected to a number of drought events in the period of 2003-2012, where different factors contributed to the occurrence of these events including shortage of rainfall rates and above-average temperatures. These meteorological factors resulted in a range of different environmental impacts over this region such as a lower discharge of the Tigris and Euphrates, inducing a hydrological drought, and agricultural degradation (UNESCO 2014). Crop production levels in rain-fed and irrigated areas over Iraq were low due to the combination of both climatological and hydrological drought. Al Qatrani 2012 was that cultivated areas reduced by 60% during the agricultural season of 2008/2009, causing a reduction in agricultural production. It was also reported that a major decline in vegetation cover occurred between 2009 and 2012 where the land cover vegetation loss was estimated at 65%, 47%, and 41%,

respectively (UNESCO 2014). Eklund and Seaquist 2015 studied drought in the northern part of Iraq using Enhanced Vegetation Index (EVI) to assess agricultural drought between 2000 and 2011. They concluded that the study area experienced agricultural drought between 2007 and 2009. Likewise, Atyah, Abbas et al. 2012 used NDVI to monitor areal variation in vegetation cover over Babylon governorate in 1976, 1986, 1992, 2003, and 2010. The results of that study showed that a decrease in vegetation cover referred to that vegetation cover decreasing over time.

1.4. Study area

1.4.1. Location

As discussed in Chapter 1, this study focusses on drought in Iraq. Fig. 1.2 shows that Iraq shares borders with six countries. It is located in the Middle East, in southwest Asia, between latitudes 29° and 37° N. It has a total area of 437065 km^2. Drought indices and related remote sensing indices, together with SVAT model runs, have been calculated and conducted for all climatic zones (with specific land use (see Section, 2.6, and 2.8)), as well as for the marshlands area (see Section 2.9 apart from the SWAP runs as the model is not equipped to deal with water bodies).

Figure 1.2 Map of Iraq (Malinowski 200)

1.4.2. The climate of Iraq

Generally, total rainfall and temperature are the most important climatic variables in Iraq, through their control on the main components of the water balance. Over the last three decades, total rainfall rates have decreased, and temperatures have been higher than average. This, combined with recurring dust storms, have caused many agricultural areas to turn into barren land.

However, a high contrast among the values of meteorological variables for Iraq is clearly observed; between the northern and southern regions and between summer and winter seasons. The northern region of Iraq has high values of rainfall compared with the southern and central regions, in January. The total rainfall rates tend to increase from the southern to the northern parts. For July, rainfall is rare over the entire region. In the western regions in Iraq, there are very small amounts of rainfall throughout whole year, which are considered not significant. For these reasons, the northern parts of Iraq are almost always characterised by permanently vegetated areas, while the southern and central parts are suffering from a lack in vegetation.

The central and the southern regions are warmer than the northern region of Iraq, with the temperatures in the south and south-east being the highest in Iraq.

The low precipitation amounts and high temperatures in the south gradually turn into wet, cool weather in the north. For total actual evaporation, values in winter are 22.19 and 109.2mm in the north and the south, respectively.

The distinct climatic zones in Iraq has led to the development of three different regions, as explained below, Figs. 1.3, 1.4, see also Fig 1.5.

Mediterranean climatic region: This climate is cool and wet in winter, and hot and dry in summer. It is found in the mountainous areas; therefore, snowfall often occurs. The amount of rainfall varies; around 400 mm yr^{-1} at lower altitudes, and nearly 1000 mm yr^{-1} at higher altitudes. In summer, the average temperature is less than 35 ℃ on the lower slopes, and much lower on higher slopes.

Semiarid climate region: This climate type is characterised as a transitional climate between the Mediterranean type in the north and the desert or arid climate type in the south. It has small

amounts of rainfall and high temperatures. Annual rainfall is between 200 mm to 400 mm yr^{-1}; it falls during the cool period of the year when the evaporation rate is the lowest.

Arid climatic region: Typically, the climate of the lowlands of Iraq is a desert climate. This is an area of high shortwave and longwave radiation and clear skies in summer; air temperature rises to a maximum of 45-50℃, with a large diurnal temperature amplitude (Tday-Tnight), whereas nights are relatively cool. In winter, the prevailing weather is warm and sunny, and temperature very rarely drops below freezing point, (Jaradat 2003).

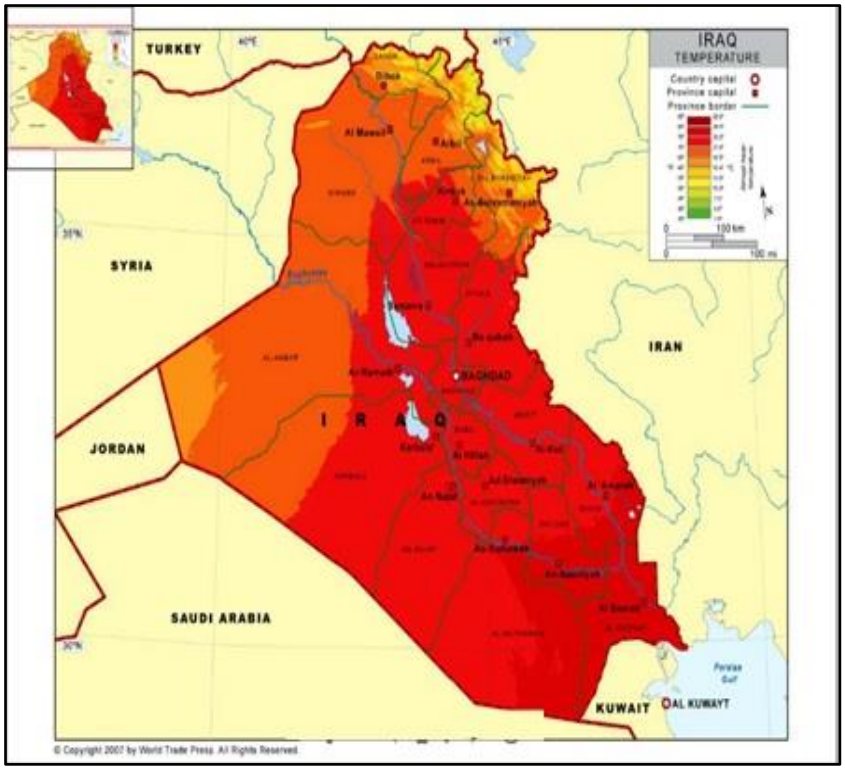

Figure 1.3 Annual mean temperature (℃) map of Iraq

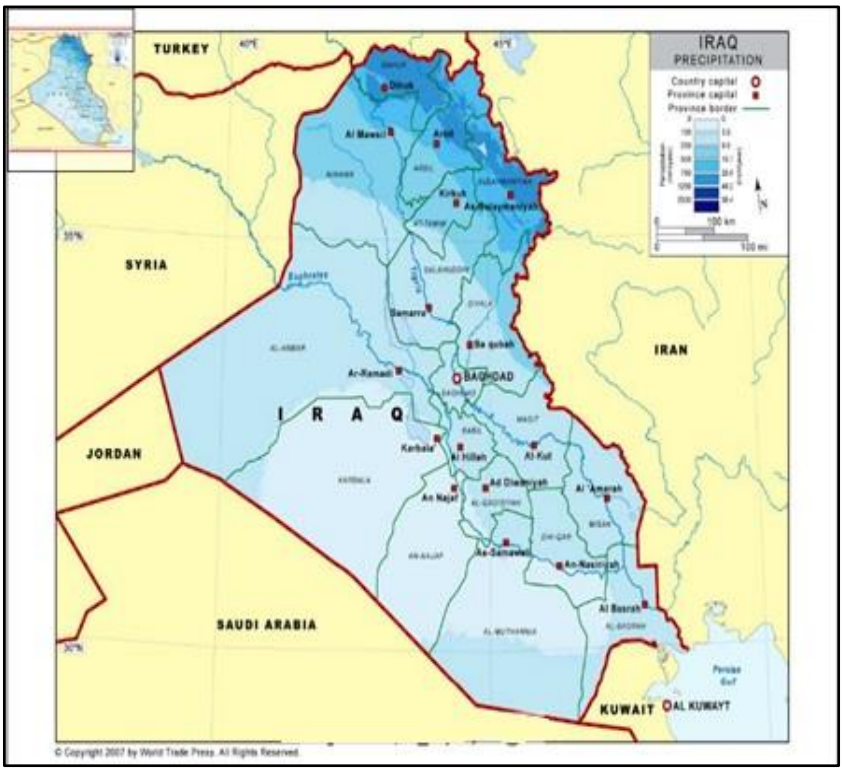

Figure 1.4 Annual mean precipitation ($mm\ yr^{-1}$) map of Iraq

Figure 1.5 Map of climatic zones of Iraq (FAO 2011).

1.4.3. Physiography

All regions are shown in Fig. 1.6 and discussed separately below.

1.4.3.1. Zagros region

An area composed of valleys and high mountains, reaching to 1000 to 4000 m. A limestone ridge is the main component for this region, varying from soft chalk to very hard dolomitic limestone. There are less steep slopes on the northeastern part of the ridge Soils.

1.4.3.2. Foothills region

The foothills region comprises hills at the foot of the Zagros Mountains, with altitudes ranging from 500 to 1000mm. It mainly consists of sandstone, beds of gravel and conglomerate. The conglomerate and gravel are alternated with thin layers of clay and reddish loam. These red loam and clay layers are severely eroded at the top in some places, forming gullied land, so called 'bad lands'. This region is mostly covered by grasses during spring and winter seasons. The vegetation cover gradually decreases in summer, because it is extremely hot and dry. Hills are generally rounded, and have thin soil. The level areas within the valleys commonly consist of three different terraces; the lowest terrace being the most extensive, and the most important from a cultivation point of view, because it has good soils (Buringh 1960), (Omer 2011).

1.4.3.3. Jazeerah region

The Jazeera Region is an uplands region (Library of Congress, 1988), a steppe and desert plateau, which comprises the remnants of an old inland sea where mainly gypsum was deposited. This relatively flat area has low mountain ridges and hills, which are an extension of the mountain ridges to the east. These mountain ridges follow an east-west direction. Gypsum is the main rock in the east part, while the limestone and sandstone dominate in the east and north of the region. Lime and gypsum crusts cover large areas, which are exposed at the surface. The wadi Tharthar is the main source of drainage in this region, running into the large Tharthar Depression. Jazeera is considered a grazing area, due to the presence of natural vegetation in this area, particularly in the southwest and steppe in the northeast. Recently, in the north of the region, some areas have been ploughed to grow barley and wheat (Jaradat 2003).

1.4.3.4. Desert region

In this region, we find a different kind of limestone, which was deposited on the old shelf. The northwestern part is the highest, gradually sloping down to east. The vegetation is of Irano-Turanian type in the northern part and of Sahara-Sindian type in the south. The desert in the northern part, and the northern part of the southern desert, are rock plains, which developed on limestone crust.

The western deserts are intersected by numerous wadis, they are mostly dry riverbeds that direct occasional rainfall east towards the Euphrates (Held 2000). Water erosion affects large parts of the desert; in some places, wadis or deep gullies have been shaped. There is some vegetation in the wadis, particularly in northern parts that have an average rainfall of around 150 mm, and sparse vegetation is present in parts with average rainfall up to 70 mm (see map 1.4) (Buringh 1960), (Jaradat 2003).

1.4.3.5. Mesopotamian plain region

The Mesopotamian Plain is a geological depression, a plain of the Tigris and Euphrates rivers that is generally low and flat. It is mostly filled by river sediments, occupying land that is located in central and southern parts of Iraq within semi-arid climate zone. Geographically, the northern part, which extends between Samarra and Deltwa, consists of three distinct river terraces, which are higher than the present river level. These old river terraces thus form high plains, which are never flooded by the river. The lowest terrace is the most important for agricultural irrigation. It is situated on both sides of the Adhaim River. The plains in central Iraq are nearly level; it is for this reason that large areas are flooded every year, almost always during spring.

In the southern parts, the plain can be divided into the delta plain, the marshes region and the estuary region. In the delta plain, that starts from the south of Kut and Hilla, the rivers split up into many branches. It is relatively flat land, with high ground water levels, and the natural drainage is quite poor. In the south of the Delta. The main natural vegetation in the marshes is composed of reeds. Close to the coast, there is the estuary region, where the sedimentation is in the form of extensive saline soils. There are narrow strips of well-drained land along the river (Jaradat 2003).

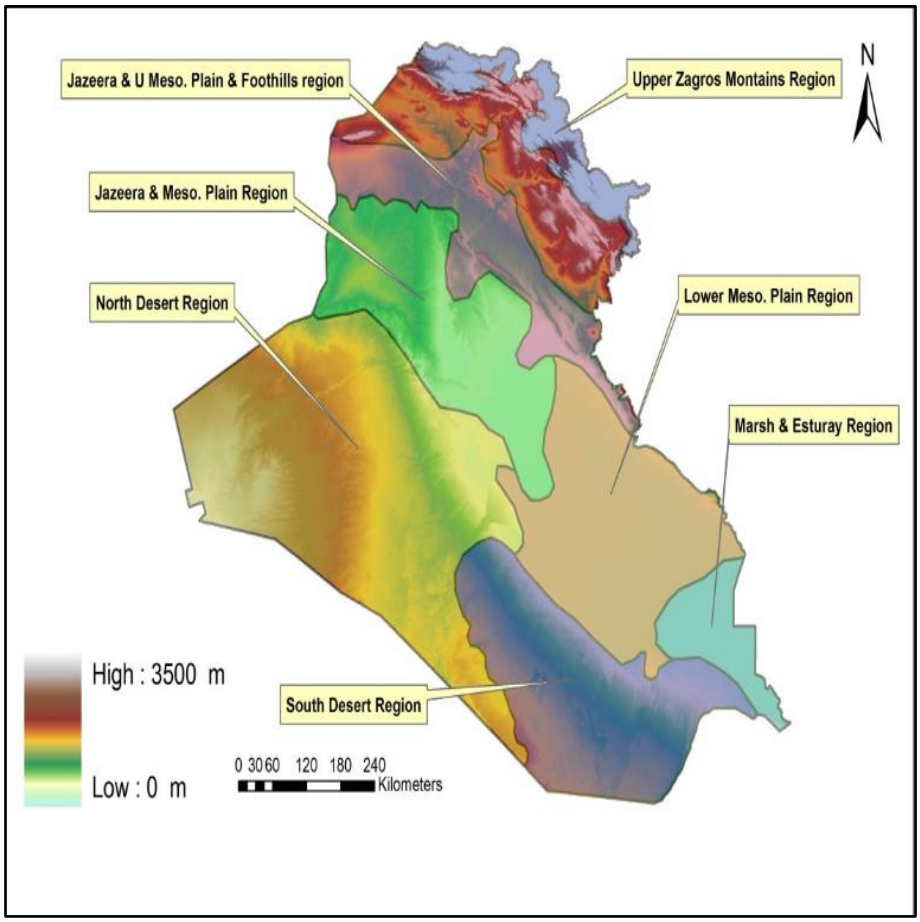

Figure 1.6 Physiographic regions of Iraq (Copyright © 2014 IJAIR)

1.4.3.6. Marshlands region

A number of marshes exist in the centre of Iraq, as shown in Fig. 1.7. As a result, the water source nourishing the marshes is almost entirely dependent on the surface run-off, generated in the humid Anatolian highlands and Zagros Mountains (> 1,000 mm in rainfall) in the north and east, respectively. The extent of the marshes is highly variable, expanding and contracting with seasonal flooding and annual changes in water flows. Prior to dam construction, discharges into the Tigris and Euphrates peaked in April and May, with flow volumes lowest in August and September. This oscillation, generated by snowmelt flood pulses during the spring and gradual water recession over the summer months, plays a critical role in the dynamics of marshland ecology (Al-Ansari and Knutsson 2011).

Drought-related investigations were performed as part of this thesis in the form of a case study on the marshlands in the south of Iraq, which is located in the Mesopotamian plain that has an arid to semi-arid climate. In these areas, vegetation is affected by high diurnal and seasonal variations of temperature, low amounts of precipitation and high potential evaporation (Dehghan 2011). The wetland area lies between 29°55'N and 32°45'N to 45°25'E and 48°30'E, covering an area of approximately 15000-20000 km^2 in the lower part of the Mesopotamian basin where the Tigris and Euphrates Rivers flow (Al-Ansari and Knutsson 2011). The marshland consists of three main areas: Hammar, Chibyish and Haweezah marshes are shown in Fig. 1.7. Further details are given below.

1.4.3.6.1. Hammar marshes

The Hammar Marshland is situated south of the Euphrates, extending from near Nasiriyah in the west to the outskirts of Basrah on the Persian Gulf Sea in the east. During the 1970s, Hammar marsh covered an area of approximately 2800 km^2 of permanent marsh and lake (approximately 120 km long and 25 km wide). The maximum water levels in this marshland were ranging from 1.8 to 3 meters in time and space. Large parts of the lake's shoreline dry out during summer, and banks and islands emerge. They receive an influx of water mainly from tributaries of the Euphrates River, from groundwater recharge, as well as a considerable amount of water originating from the Tigris River, overflowing from the Chibyish Marshlands (Al-Ansari and Knutsson 2011).

1.4.3.6.2. Chibyish marshes

The Chibyish marshes are bordered by the Tigris River to the east, and by the Euphrates River to the south. They cover an area of approximately 3000 km^2. This marsh area is fed primarily from Tigris distributaries branching southward from the Mayssan province. It is densely covered by tall reed beds, interspersed with several large water-filled depressions (Al-Ansari and Knutsson 2011).

1.4.3.6.3. Haweezah marshes

The Haweezah marshes lie to the east of the Tigris River, straddling the Iran-Iraq border. In the west, they are largely fed by three main distributaries departing from the Tigris River near Mayssan; the Musharah, Kahlah and Majriyah. An important water influx also comes from the Karkheh River in Iran. Historically, the Haweezah covered an approximate area of at least 3,000 km^2, expanding to over 5,000 km^2 before draining. The northern and central parts of the

marshes are permanent but the lower southern sections are mostly seasonal. Large permanent lakes up to six meters deep are still found in the northern part of the marshes. The Haweezah marshes represent the most intact part of the original Mesopotamian wetland complex and are of major importance as a biodiversity store (Al-Ansari and Knutsson 2011).

Figure 1.7 Major Iraqi Marshlands **(**Source: CIA World Factbook, 2001 in IRAQ geography)*
Note: Qurnah refers to Chibyish marshes, and Hawizah refer to Haweezah.

1.5. Research questions

The following research questions will be addressed in this thesis

- What has been the recent evolution of droughts over Iraq, for a range of land surface types, namely desert, rangeland and agricultural lands, as well as marshlands?
- Has the occurence of drought increased over time?
- Which parts of Iraq are most prone to drought?
- How can the severity of agricultural drought stress on vegetation, water balance, energy balance, land surface temperature and soil moisture best be estimated?
- Which drought indices are best suited for analysing the extent and severity of drought in Iraq and similar areas?
- Can the change in vegetation cover over time be explained by variation in drought indices?
- How can remote sensing help to assess drought in Iraq?
- To what extent can SPI and SPEI, and remote sensing detect drought?
- What is the most suitable meteorological drought index for Iraq?
- How can land surface modelling be used to further our understanding of droughts in Iraq?
- How will the findings inform water resources management in Iraq?

1.6. Research design

The methods employed for this study include three main steps:

- **Chapter 2, Literature review**: Literature study on the hydrological balance and related meteorological, land surface and plant processes that ultimately link to hydro-meteorological drought indices (e.g. SPI-3) and related vegetation indices derived from remote sensing. Further literature studies on drought and drought indices; how to use remote sensing techniques in drought assessment; and evapotranspiration and methods to estimate it.

- **Chapter 3, Methodology** Time series of normalised difference vegetation index (NDVI) MODIS (MOD13A2) products and land surface temperature MODIS

(MOD11A2) with 1 km resolution were used for 2001-2015; SMOS near-surface soil moisture data were also extracted for Iraq, spanning the period 2010-2015. Detailed long-term meteorological data for Iraq were obtained from the Iraqi Meteorological Office; these data were checked and gap-filled where necessary. ERA interim data were downloaded from ECMWF as an alternative driving data set for the SWAP model (see below). ERA interim output data (surface latent heat flux) were also obtained for SWAP model verification.

- **Drought assessment**: The first step involved processing and filtering of the satellite and meteorological data obtained during data collection. Next, various drought indices were compared and their interannual variability and trends were interpreted in the context of the meteorological input data. Subsequently, remote sensing (RS) indices that relate to vegetation density and greenness, and hence implicitly to drought, were calculated. Time series of NDVI and LST and its relation with SPI and SPEI were analysed. Finally, runs were conducted with a Soil-Vegetation-Atmosphere-Transfer model (SWAP) to help explain the differences in NDVI observed, e.g. through differences in soil type, vegetation type, management etc.

2. Chapter two: Theoretical background

The first chapter of the thesis provided an introduction to the concept of drought, and an overview of the research project in context of the research objectives. This chapter will present the literature on drought indices, vegetation monitoring using remote sensing technologies, and hydrological models.

2.1. The hydrological cycle

The global hydrological cycle describes the continuous movement of water, at its three phases: liquid, solid, and gas, between and within Earth's continents, oceans, and atmosphere (Bierkens, Dolman et al. 2008).

The total mass of water is fairly constant on Earth, but there are variations within the reservoirs of saline water, ice, and fresh water, mainly depending on climate variability. Water moves from continents to oceans and from oceans to the atmosphere; these movements are driven by the physical processes of runoff, precipitation, evaporation, infiltration, and condensation. Water flows to the oceans from land via rivers, in this case, the precipitation must be more than evaporation over land. The nature of the Earth surface (e.g. vegetation type, cover, and status, as well as soil type and soil moisture status) is a major factor, which strongly influences the hydrological cycle. Hydrological processes can operate at different time scales over land and ocean.

Ecologically, the water balance affects the functioning and survival of ecosystems on planet Earth, and can influence the climate via heat exchanges. For example, evaporation causing cooling of the environment. On the other hand, energy will be released, thereby warming the environment, through condensation processes. (Trenberth, Smith et al. 2007).

Fig. 2.1 summarises the annual average global hydrological cycle. Oceans evaporate around 413×10^3 km^3 yr^{-1} of water, i.e. nearly 1200 mm per year, although on average about 90% of this is returned as precipitation to ocean. Precipitation over land occurs due to the transfer of evaporated water from ocean to land, apart from landlocked areas where re-cycling of terrestrial evaporation also plays a role. Approximately 65% of terrestrial precipitation is re-evaporated. Nearly 35% of the terrestrial precipitation returns to the oceans as surface runoff (Bierkens, Dolman et al. 2008).

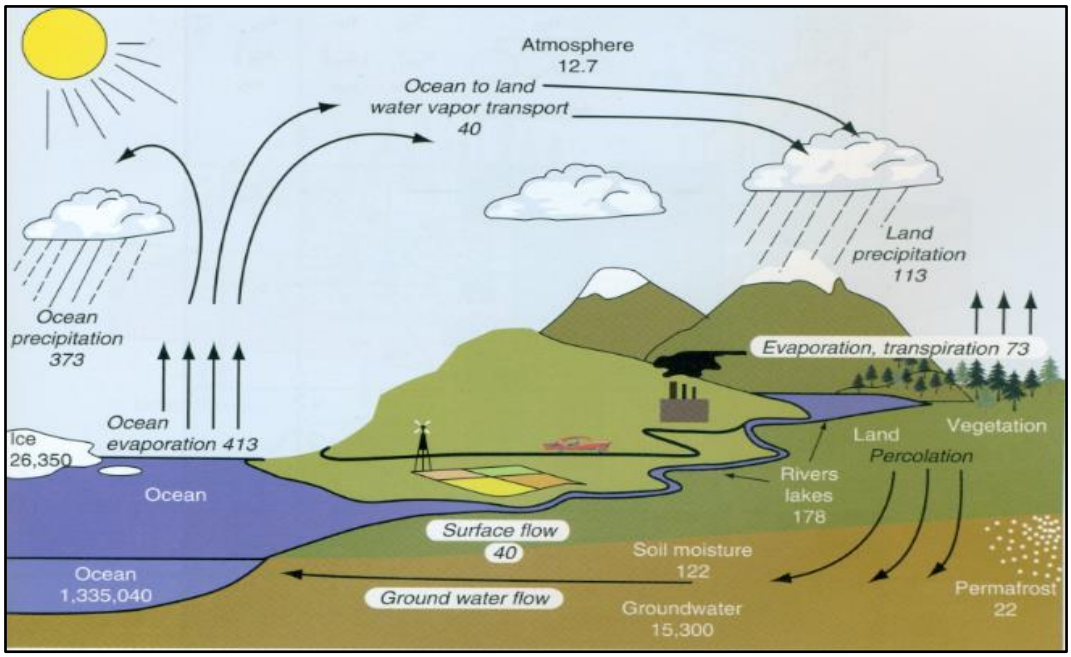

Figure 2.1 The global annual average hydrological cycle including estimates of the main water reservoirs (in plain font in unit of $10^3 km^3 yr^{-1}$), and the flow of moisture between stores (in Italic in units of $10^3 km^3 yr^{-1}$), Copy right 2007 American Meteorological Society (AMS).

Eq. 2.1 uses the principle of mass conservation in a closed system. The movement of water throughout an ecosystem system can be represented by water entering this system via precipitation, which is then transferred into either evaporation, surface runoff (eventually leaving in the form of river discharge), or stored in the ground. A water balance can be used to predict where there might be water shortages, and help to manage water supply (Fish 2011). It is crucial in the context of drought prediction and management.

The water balance is calculated as follows from field-or catchment scale inputs and outputs.

$$\Delta S = P + G_{in} - (Q + ET + G_{out}) \qquad 2.1$$

where P is the precipitation, G_{in} groundwater inflow, Q surface water runoff, ET evapotranspiration, G_{out} groundwater outflow, and ΔS change in water storage.

2.2. General overview of drought indices

Drought indices have been developed to detect, assess and monitor drought. Widely used drought indices include Crop Moisture Index (CMI), Palmer Drought Severity Index (PDSI), Surface Water Supply Index (SWSI), Standardized Precipitation Index (SPI), Standardized Precipitation Evapotranspiration Index (SPEI) and Standardised Vegetation Index (SVI). (Hayes, Svoboda et al. 1999). Some indices are more suitable for certain applications than others. For instance, the U.S. Department of Agriculture has widely used the PSDI to decide when to grant emergency drought assistance. However, the PSDI works better for large areas of uniform topography. Water resources planning authorities in Western states of the USA, with mountainous terrain and resulting complex regional microclimates, find it useful to supplement PSDI values with other indices such as the SWSI that is based on snow pack. Meanwhile, the National Drought Mitigation Centre is using SPI to assess soil moisture supply conditions. Features that distinguish this index are that it identifies emerging droughts months sooner than the PSDI and that it can be computed on various time scales. Most water supply planners find it useful to consult one or more indices before making a decision related to water management.

Using SPI may help scientists and planners to develop a climatology of the intensity and spatial extension of droughts, which will provide a wider understanding of its characteristics and an indication of the probability of recurrence of drought at different levels of severity. (Ji and Peters 2003) assessed vegetation response to drought in the northern Great Plains by using drought indices and estimates of land cover of vegetation. They studied the relationship between SPI and NDVI at different time and spatial scales. They concluded that the SPI-3 had the highest correlation to NDVI, and that SPI-3 was the best for determining drought severity and duration. In addition, it was found that seasonality has a very significant effect on the relationship between NDVI and SPI-3.

Drought indices can be split into several categories: meteorological, hydrological, agricultural and groundwater indices. In the sections below the various drought indices will be discussed briefly

2.2.1. Standardized Precipitation Index (SPI)

SPI is commonly based on the long-term precipitation record that includes the period of interest. It can be calculated for different time scales; this versatility offers the possibility to express the drought in terms that are relevant for long term water resources, such as stream flow, groundwater supplies, lake and reservoir levels; and short-term water supplies, such as soil moisture which is a useful indicator of agricultural production. Therefore, it is considered a powerful, flexible index that is simple to calculate due to the fact that precipitation is the only required input variable that can be computed for different time scales, thereby providing early warning of drought and helping to assess drought severity. The long term precipitation record is fitted to a gamma probability distribution, then transformed into a standardized normal distribution (z-distribution), so that the mean of the SPI is zero for the desired period (Lloyd-Hughes and Saunders 2002). The gamma probability density function performs well over Iraq, and has been tested for a wide range of locations and at different time scales (Al-Timimi and Al-Jiboori 2013).

SPI values should have similar and consistent results, even if they are computed from different lengths of records as long as they have a comparable gamma distribution over different periods of time. However, there will be a significant difference in SPI values when the distributions are different. Because precipitation is seasonal in nature there will be many zero precipitation values. Therefore, SPI will not be the index of choice in arid to semi-arid climatic zones because of the limitation of the fitted gamma distribution and the highly skewed underlying precipitation distribution. This may cause large errors when simulating precipitation distributions in dry climates from small data samples (Mishra and Singh 2010).

Table 2.1 shows a classification system used to define drought intensities based on the SPI (as well as SPEI, see Section 2.2.2) values, where positive SPI values refer to values greater than median precipitation while negative values indicate less than median precipitation. Because the SPI is normalized, wetter and drier climates can be monitored using the same index. A drought event occurrence might happen any time, once the SPI is continuously negative and also reaches a value of -1.0 or less. The end of the drought event is represented by SPI returning to positive values (McKee, Doesken et al. 1993).

Table 2.1 Drought category according to SPI and SPEI value (McKee, Doesken et al. 1993)

SPI and SPEI	Category
2.0 and more	Extremely wet
1.5 to 1.99	Very wet
1.0 to 1.49	Moderately wet
-0.99 to 0.99	Near normal
-1.0 to -1.49	Moderately dry
-1.5 to -1.99	Severely dry
-2 and less	Extremely dry

SPI was proposed by McKee et al. (1993) to provide early warning of drought and to help assess drought severity for multiple time scales (Naresh Kumar, Murthy et al. 2009). It is widely used by a range of national Meteorological and Hydrological Services throughout the world, as a part of drought assessments and early warning efforts (Svoboda, Hayes et al. 2012).

Using SPI approach allows the user to plot a time series of interannual SPI variation, which offers a good indication of the drought history for a given station or area. SPI was originally calculated for 3, 6, 12, 24 and 48-month timescales by McKee and others (1993). These timescales reflect the impact of drought on the availability of different water resources. Groundwater, stream flow and reservoir storage reflect long-term precipitation anomalies. Soil moisture conditions typically respond to precipitation anomalies on a relatively short-term timescale (e.g. 3 months or less).

The SPI is generally calculated using the following formula:

$$\text{SPI} = \frac{P_i - \bar{P}_i}{\sigma} \qquad 2.2$$

where, P_i is the seasonal precipitation, $\bar{P}_i$ is the long term seasonal mean, and σ is the standard deviation.

2.2.2. Standardised Precipitation Evapotranspiration Index (SPEI)

The use of drought indices that include temperature data in their formulation (such as the SPEI) is preferred to the use of SPI, especially for arid and semi-arid areas where drought is strongly affected both by high potential evapotranspiration and lack of rain. Therefore, an alternative drought index, the Standardized Precipitation Evapotranspiration Index (SPEI), has recently been formulated that is based on precipitation and potential evapotranspiration, PET. The SPEI combines the sensitivity of PDSI to changes in evaporation demand (which is mainly caused by temperature fluctuations and trends) with the simplicity of calculation and the multi-temporal nature of the SPI. The new index is particularly suited to monitoring, detecting, and exploring the impacts of global warming on drought conditions (Vicente-Serrano, Lopez-Moreno et al. 2011), (Vicente-Serrano, Beguería et al. 2010).

SPEI was developed by (Vicente-Serrano, Beguería et al. 2010) to assess drought in terms of duration, onset, severity, extent and end. Recently, most studies related to drought analysis and monitoring systems have been conducted using SPEI.

The approach is similar to that of the SPI drought index and the values are also expressed on the basis of different timescales. The SPEI is based on a monthly water balance (the difference between precipitation (P_i) and potential evapotranspiratio (PET_i) for the month), adjusted using a three-parameter log-logistic distribution to take into consideration common negative values.

$$D_i = P_i - PET_i \qquad 2.3$$

A key step in the quantification of SPEI is the determination of evapotranspiration, which can be calculated using a number of equations, covering a range of complexity and with varying input requirements. Considered the most reliable equation, the Penman-Monteith equation calculates evapotranspiration based on solar radiation, air temperature, wind speed and relative humidity(Allen, Pereira et al. 1998).

In general, SPEI is based on a simple climatic water balance, which is calculated at different time scales. PET in this thesis is calculated based on Thornthwaite's (1948) equation, which only requires monthly average temperature data to calculate SPEI. Among a number of methods for calculation of the water balance, the Thornthwaite (1984) model is considered as

one of the most appropriate methods for arid and semi-arid regions, and has been adopted widely over these areas, in particular over Iraq (Saud, Said et al. 2016), (Henderson 2012), (Ibrahim 2012), (Anderson, Jin et al. 2012), (Djaman, Balde et al. 2015), (Saud, Said et al. 2016).

A number of studies examined the most appropriate methods to estimate PET in semi-arid parts of Iraq; these methods included the Thornthwaite, Blaney-Criddle, Kharufa and Ivanov methods. These equations have been employed to estimate and identify the spatiotemporal variations of PET over certain parts of Iraq. Calculated PET was compared with the average actual pan-evaporation in the meteorological stations to establish the accuracy of the PET estimation. Thornthwaite equation provided a relatively low value in comparison with the other methods (Ali 2008), (Mohammad 2008), (Ibrahim 2012), (Al-Shamaa and Ali 2011), (Al-Maliki 2005).

Other studies compared the Blaney- Criddle, Thornthwaite, and Penman-Monteith methods in the central part of Iraq and found that these methods gave different results with regards to consumptive water use. It was concluded that these three methods exhibit the similar temporal evolution and tendency. The Penman Monteith was not found to be the most suitable method in this region compared with observed data (Obid, Khaleel et al. 2013).

The main objective of using SPI and SPEI in this thesis is to enable comparison of historical drought assessment based only on assessment of precipitation with that based on the combined effects of precipitation and potential evapotranspiration. Both drought indices are obtained using the same log-logistic probability distribution that shows a very close fit to the series of differences between precipitation and evapotranspiration (Vicente-Serrano, Beguería et al. 2010), and also to the monthly precipitation records.

Using the same probability distribution will allow for reliable comparisons among the series of these two drought indices, to ensure that any differences between the series are only related to the impact of temperature on drought conditions, and not from the calculation method. These two indices have therefore been selected for this study, together with NDVI as a measure of vegetation vigour.

Several studies have shown that the 3-month time scale is the most appropriate for determining drought severity. Therefore, this particular time scale was used throughout the thesis (Otgonjargal 2012).

2.3. Monitoring land surface hydrological status from space

Obtaining hydrological information from ground-based measurements can pose serious difficulties, in particular for less developed regions, or those situated in areas that are considered unsafe for political reasons. Furthermore, there is the issue of scale, as a large amount of information is required to obtain a reliable water budget and related drought assessments. Remote sensing (RS) can play a substantial role in observing weather, climate and land surface processes and properties. As already explained above it also has the potential to provide useful data for drought monitoring (see Section 3.1.3 in Chapter 3). Via sensors mounted on satellites, remote sensing allows us to quantify, directly and indirectly, the components of the hydrological cycle and watershed water balances (river and lake levels, precipitations, soil moisture, evaporation and total water storage). Furthermore, useful information can also be derived on the variations of vegetation condition, such as plant health and productivity, from a moving platform such as a satellite or an aircraft. Because of its generally widespread nature, monitoring of drought requires a large spatial scale approach, therefore satellite remote sensing is particularly useful for drought observation. In addition, it can provide information at a high temporal and spatial resolution to provide a comprehensive insight of the drought development. In recent years, RS data have quickly become the preferred choice when observing the large-scale energy and water cycles of the land and atmosphere. The challenge of using RS techniques for monitoring drought is that there is a disconnection between what is required for quantification of drought via pertinent vegetation or hydrological indices, and what satellites actually measure (Sheffield and Wood 2012).

In general, radiation is measured from satellite borne sensors over one band or more across the electromagnetic spectrum. These radiances need to be converted into quantities and surface parameters that are associated to the hydrological variables, to next provide a quantitative description of drought. In practical terms, the emitted, reflected or backscattered radiation from the earth's surface (soil, water bodies and vegetation) need to be related to the state of the land surface, in particular that of the vegetation. The retrievals of remote sensing variables are often restricted to certain so-called atmospheric windows, which are 'transparent' and allow sensors to observe the land surface. These windows are the result of the scattering of radiation and

strong absorption of oxygen, water vapor, aerosols and CO_2 over certain electromagnetic bands.

RS bands are divided into visible, infrared, short wave, thermal and microwave. There exists a multitude of data products from recent satellite missions that can help estimate the components of the water budget, at various time and space scales (Sheffield, Andreadis et al. 2009). For example, precipitation can be retrieved by multi sensor microwave data, and from infrared data, using a variety of techniques (Huffman, Bolvin et al. 2007). Vegetative health has been quantified from visible and near infrared data for several years now (Petach, Toomey et al. 2014). Evapotranspiration can be evaluated from analyses of the surface energy balance, given remote sensing inputs of net radiation and surface meteorology (Su, McCabe et al. 2005) and large scale products are progressively becoming available (Liou and Kar 2014). Changes in the total water surface and subsurface storage can be derived from gravity, e.g. the recent GRACE mission (Forootan, Safari et al. 2017). Stream flow and surface water storage can be estimated by using laser altimetry technologies (Alsdorf and Lettenmaier 2003).

2.3.1. Normalised difference vegetation index (NDVI)

Monitoring land cover vegetation changes over time is necessary to inform regulatory actions and policy decisions related to water management, and possible subsequent (changes in) land use activities. Traditionally, weather station observations have been used to help monitor the water balance, and drought, but the drawback is the lack in continuous spatial coverage needed to monitor and characterise the detailed spatial pattern of drought and its impacts (Huffman, Bolvin et al. 2007).

The normalized difference vegetation index (NDVI) is a simple indicator that can be obtained using the normalised reflectance difference between the near infrared (NIR) and visible red bands (Tucker 1979). NDVI records the changes in chlorophyll content via absorption of visible red radiation (VIS), and in spongy mesophyll via reflected NIR radiation within the vegetation canopy.

The NDVI for each pixel is calculated according to the normalised difference between the red and near infrared bands from an image. NDVI can be derived from data collected by the Moderate Resolution Image Spectrometer (http://earthexplorer.usgs.gov/).

Since the MODIS sensor is carried on both the Terra and Aqua satellites, it is generally possible to obtain images in the morning (Terra) and the afternoon (Aqua) for any particular location. The MODIS instrument on the Terra satellite was launched in December 1999 with 36 spectral bands ranging between 0.405-14-385 μm, which is more sensitive than AVHRR. MODIS presents NDVI imagery at three different resolutions: 250m, 500m, and 1000m. (Gallo, Ji et al. 2004). The NDVI is generally calculated as follows:

$$NDVI = \frac{NIR - RED}{NIR + RED} \qquad 2.4$$

where NIR and RED are the reflectance in the near infrared (NIR) and red bands, respectively.

The values commonly range from -1 to 1, positive values indicate that the vegetation is healthier than those with negative values (Boken, Cracknell et al. 2005). The long-term deviation of NDVI is useful to determine droughts and to characterise the health of vegetation, in most regions. Low NDVI can be caused by cool temperatures or by low radiation due to heavy cloud cover.

2.3.2. Land surface temperature (LST)

The land surface temperature (LST) derived from the thermal bands of satellite images provides implicit information on the spatiotemporal changes of the surface energy balance and is of basic importance in many applications (Kerr, Lagouarde et al. 2004).

LST is important for environmental studies and is widely used in formulating the land surface water budget, because the water and energy balances are related via the evapotranspiration (latent heat flux), see Section 4.6. It is a major factor in determining the partition of the available energy into sensible and latent heat fluxes (see section 2.4). In this context, LST is a useful variable to determine evapotranspiration, soil moisture, vegetation water stress, and thermal inertia (Jang, Viau et al. 2006), (Anderson, Norman et al. 2007). Vegetation abundance and condition is also known to influence LSTs and drought conditions through the process of evapotranspiration. Therefore, investigations into the relationship between NDVI and LST can be informative in the context of drought, especially where this phenomenon is more pronounced, and where mitigation measures are needed (Patel, Parida et al. 2012).

2.3.3. Soil moisture

Knowledge on soil moisture over large scales can provide powerful information for monitoring of drought. Soil moisture estimates from microwave remote sensing are usually obtained from model-data fusion, where microwave radiation emitted from soil through the vegetation canopy, atmosphere and then to the satellite sensor is simulated using a microwave emission model. The rationale of this type of model is based on the large contrast between the dielectric properties of liquid water and dry soil. Microwave radiation is the most appropriate wavelength to measure soil moisture, regardless of its restrictions. It also has the potential to quantitatively determine soil moisture under a variety of vegetation types, cover densities and conditions, and topography. However, the main challenge is that the microwave signal is restricted to the top centimetres of the soil. This is because the penetration depth depends on the signal frequency. The signal is attenuated in densely vegetated regions and so retrievals are limited to sparsely vegetated regions at biomass values of less than 5 kg/m^2 (Sheffield and Wood 2012). Passive microwave sensors use frequencies of 6 GHz or higher, although L band is deemed optimal and more suitable for soil moisture monitoring in terms of the relative strength of the vegetation and soil signals.

However, the relatively high spatial variability of soil moisture in the field makes interpretation of data obtained at 25 km (e.g. using SMOS) problematic (Sheffield and Wood 2012). Therefore, the most recent missions have merged active and passive products in order to overcome these limitations, and to improve the coverage and resolution. The European Space Agency Soil Moisture Ocean Salinity (SMOS) mission has been launched relatively recently, but it uses passive microwave only. However, the NASA Soil Moisture Active and Passive (SMAP) mission uses L band passive microwave instruments that should improve accuracy and penetration depth into the soil, as well as active microwave to improve the spatial resolution. Unfortunately, the active sensor failed approximately 6 months after launch.

2.4. The energy balance

2.4.1. Determination of surface latent heat flux from energy balance form part of land surface models

The Surface Energy Balance (SEB) is closely linked to the water balance, via the evapotranspiration (ET), see Fig. 2.2. Hence the SEB is often used to determine ET, once the other terms (often easier to determine directly) are known, either from in-situ measurements or via RS. The SEB is given by

$$R_n = \lambda E + G + H \qquad 2.5$$

where R_n is the net radiation, G the soil heat flux and H the sensible heat flux, all in W m^{-2}.

The net all-wave radiation flux density depends on incoming and outgoing radiation at the land surface. The net radiation equation may be written as:

$$R_{ns} = \left((1 - a)R_s\right) + (R_I \downarrow - R_I \uparrow) \qquad 2.6$$

where R_s is the total downward solar radiation flux density (W m^{-2}), a the surface albedo, and R_I the longwave radiation flux density (W m^{-2}). Upward and downward arrows represent upwelling and downwelling fluxes, respectively. All fluxes represent radiation through a horizontal plane.

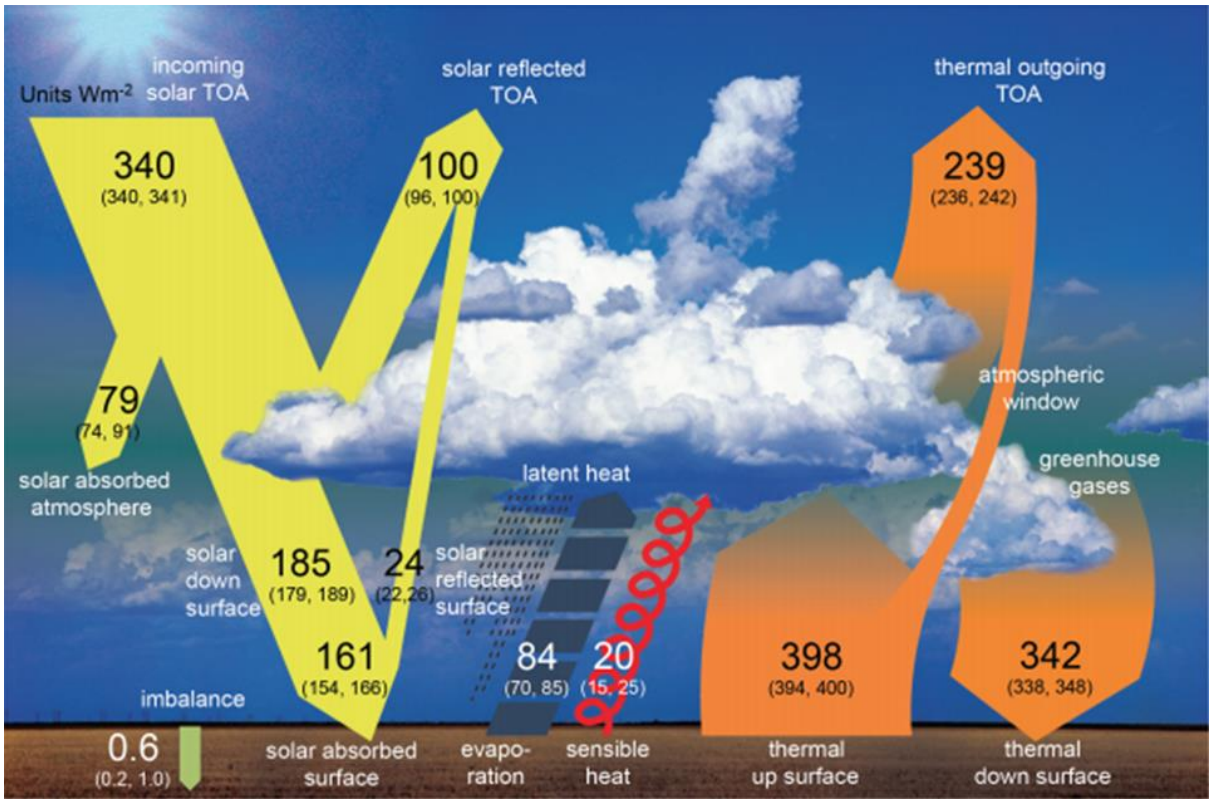

Figure 2.2 Schematic diagram of the global mean energy balance of the earth. Numbers indicate best estimates for the magnitudes of the globally averaged energy balance components (W m^{-2}) together with their uncertainty ranges, representing present day climate conditions at the beginning of the 2121 (Wild, Folini et al. 2015).

For the radiation balance, we need the flux density of atmospheric longwave radiation through a horizontal plane at the surface, $R_I \downarrow$. If we assume the atmosphere is a grey radiator at air temperature, the sky has an apparent emissivity, ε_a. The following formula, i.e. the modified Stefan Boltzmann's law, can be derived for longwave radiation reaching a horizontal surface.

$$R_I \downarrow = \varepsilon_a \, \sigma \, T_a^4 \qquad 2.7$$

where ε_a is the mean apparent atmospheric emissivity, σ is the Stefan-Boltzmann constant and T_a the temperature of the atmosphere (in K).

Sky emissivity, ε_a, is usually found from a combination of a formula describing clear sky emissivity, $\varepsilon_a(0)$, and a correction for the occurrence of clouds. Different parameterizations have been proposed to find a value of $\varepsilon_a(0)$, mainly depending on the atmospheric conditions

under which they were developed (Wang, Wan et al. 2005) Most of them are a function of air temperature, T_a, and/or vapour pressure, e_a. Both variables are usually taken at screen height for convenience. The formula of is widely used and will be applied in this thesis for calculations of $\varepsilon_a(0)$:

$$\varepsilon_a(0) = 1.24(e_a/T_a)^{1/7} \quad 2.8$$

Surface temperature sets the boundary condition for latent and sensible heat transport through vegetation, soil and atmosphere. Therefore, it is an important parameter in the SEB. Together with surface emissivity, it determines the outgoing longwave radiation. The modified ($\varepsilon_s < 1.0$) Stefan-Boltzmann law is a good estimator of $R_I \uparrow$. The Earth, being a grey radiator, emits longwave radiation according to the following equation:

$$R_I \uparrow = \varepsilon_s \sigma T_s^4 + (1 - \varepsilon_s) R_I \downarrow \quad 2.9$$

where ε_s is the surface emissivity, σ the Stefan-Boltzmann constant and T_s the surface temperature (in K). The second term on the right-hand side of Eq. 2.10 presents the re-emitted incoming longwave radiation.

2.4.2. Determination of surface latent heat flux from energy balance closure and LST data

The equations under Section 2.4.1 form part of land surface models such as H-Tessel (LSM used for ERA-Interim) and combined with so-called bulk transfer equations they are used to calculate the sensible and latent heat fluxes.

In this thesis, the SEB has also been used separately to calculate the SHLF for the marsh lands. The issue here is that ERA-Interim's spatial resolution is too coarse to resolve for the marshes explicitly: the large grid boxes would contain water bodies as well as vegetated/bare soil land surface types.

To solve this problem separate LST timeseries for the three marshes were used to calculate sensible heat flux using the equation employed in (Verhoef, Allen et al. 1999)

$$H = c(T_{s.1400} - T_{a.max}) \quad 2.10$$

Where: $T_{s.1400}$ is the surface temperature at 1400 GTM, and $T_{a.max}$ is the maximum daily air temperature.

Finally, SHLF was determined as the residual of the SEB, with knowledge of net radiation and assuming soil heat flux zero. These values of SHLF determined from LST, $T_{a.max}$ and R_n were plotted together with NDVI and shown in Section 4.3.8, Figs 4.15.

2.5. Modelling drought

Apart from in-situ hydrometeorologial data and drought estimates based on remote sensing, computer models of the water-and/or energy balance can provide data, which have the potential to allow for drought estimation for a range of climate systems and land-surface types. Models have a number of advantages, such as providing temporally and spatially consistent and continuous fields of key variables at a range of scales (from field to global). These models can also present reasonably realistic depictions of climate and hydrology at timescale of decades to centuries. On the other hand, models, and hence their simulations or predictions of drought, are imperfect and are subject to biases in their outputs, resulting from uncertainties in their driving data and model parameters. Drought analyses can be derived from hydrological models (field (e.g. SWAP) to catchment (e.g. SPHY model) or global scale (HadGem family of GCMs) or land surface models (LSMs, e.g. JULES) that can be used on their own at field scale, or be embedded in regional climate models (RCMs) or global climate models (GCMs).

Hydrological models and land surface models have originally been derived by different research communities, but there is now a considerable overlap between them. These models can simulate the physical processes of the land hydrological cycle (and energy- and carbon balance in the case of LSMs), when driven by surface climate observations (air temperature and relative humidity, radiation, wind speed and precipitation). In addition, most regional to global scale models now simulate stream flow as well as the other hydrological variables, which makes them highly suitable for drought assessment.

GCMs, in coupled mode, can simulate the atmospheric processes and their interactions with the land and ocean from seasonal to decadal time scales. Furthermore, they can simulate the observed global distribution of climate and its variation over different time scales, when given time series of external forcing (atmospheric and sea surface temperatures (SSTs)) and initial conditions such as atmospheric humidity profiles or soil moisture content. However, due to

their coarse spatial resolution and the fact that they use parameterizations for finer scale processes, errors and biases can occur. Some of these climate models have resolutions as high as 10 – 50 km, a change which has made the simulation of fine scale, more complex, processes, such as tropical storms, possible (Knutson, Sirutis et al. 2007). RCMs have generally higher spatial resolutions than GCMs, and are applied over regional scales and driven by atmospheric boundary conditions taken from GCMs. Until not that long ago, the land component of GCMs was represented by a simple form of the hydrological water budget model. Recently, land surface and hydrological models have increased in accuracy, but also in complexity, due to the increasingly recognised importance of the role of land surface processes (Orth, Dutra et al. 2016).

Now, the attention is moving towards Earth system models (ESMs) because of the recognised need to incorporate as many of the complex feedbacks between all Earth system components as possible, which include detailed ecosystem dynamics and ocean biogeochemistry (Evensen 2003).

Another relatively recent development is the merging of observations, generally consistent and continuous fields of hydrological or atmospheric variables (from in-situ observations or RS), with models in a process that is called data assimilation). This provides a number of advantages, most importantly guiding the simulation by the available observations. This development has resulted in a number of widely used 'model reanalyses' than can be defined as historic simulations of the global atmosphere – land system at multiple decades through using a climate model, which ingests the observations from ground, satellites, balloons, buoys etc. The most widely used examples of reanalyses are the European Centre for Medium-Range Weather Forecasts (ECMWF) ERA-Interim reanalysis (Dee et al., 2011), the US National Centre for Environmental Prediction/National Centre for Atmosphere Research ((Kalnay, Kanamitsu et al. 1996) reanalysis and the NCEP North American Regional Reanalysis (NARR) (Mesinger, DiMego et al. 2006). These models are used for diagnosing the physical mechanisms of the hydrology and climate variation, including those that lead to drought by analysing the connection between different parts of the coupled physical system that they represent (Sheffield and Wood 2012). For instance, Atmosphere Only (AO) GCMs can provide general insights for forecasting mechanisms of historical drought events, such as the influences of patterns of cool or warm SSTs (Hoerling and Kumar 2003). Because of the lack of observational data about the

variability and occurrence of drought, much of recent research focussing on large-scale drought has favoured model based approaches, thereby providing opportunities to gain further insight into the mechanisms that manage and control drought persistence and development. Apart from the coupled ocean atmosphere mechanisms mentioned there are land surface-atmosphere feedbacks, which contribute to the persistence of droughts (Sheffield and Wood 2012).

The land surface has gained acceptance in the climate system, therefore the use and development of land surface modelling schemes has increased in recent years (Entekhabi, Rodriguez-Iturbe et al. 1996). The state of the art schemes can simulate the energy and water cycles at the land surface and physical processes including those related to soil water dynamics, evapotranspiration and snow, and interaction with wetlands, lakes and rivers. Current investigations are looking to simulate the effects of vegetation dynamics (overgrazing, deforestation, growth, die off, species competition and disturbance such as fire), biochemistry, which includes the nitrogen and carbon cycle, and human activities (river diversion, reservoirs, land use change and irrigation) on drought. These schemes use a variety of advanced techniques, including multi-layer soil models with full energy and water accounting and sub grid variability of the hydrological processes (Sheffield and Wood 2012). Modelling the storage and transport of water in detail, all of these schemes are deemed highly suited to the analysis of the intensity and occurrence of drought. With the ever increasing advent of observational data (in-situ and remotely sensed) combined with advances relating to increased computational speed and telemetry, as well as the availability of state-of-the-art global datasets (e.g. reanalyses), it is now possible to hydrological historical and prognostic data products at large scales (Mitchell, Lohmann et al. 2004). Historical model simulations can provide reliable estimates of the variation of the terrestrial water cycle and its extremes, including drought over the last 50 – 100 years, when observational data were available (Sheffield and Wood 2012)

This thesis will make use of historical and current model simulations to describe and discuss drought in Iraq using a range of model (products) and in-situ and remote sensing data to drive or verify the models.

Finally, Soil-vegetation-transfer models (SVATs) are very similar to land surface models, but they are not part of RCMs or GCMs. They are sometimes described as a 1-dimensional hydrological model. They can be used to calculate the water balance for surfaces representing different combinations of vegetation, soil and management under a range of climate conditions.

An example of such as SVAT model is the SWAP Model (Van Dam et al 2008), that will be used in this thesis to assess the water balance over Iraq, through focussing on different climatic zones (Sections 3.2.5).

2.6. Agricultural systems in Iraq

Over 90% of Iraq's rainfall occurs during the November-April period. However, precipitation may vary greatly from one year to the next in intensity, timing, and frequency. Generally, precipitation levels increase from lower to higher elevations (Fig. 2.3). During the dry period from May to October, extremely high temperatures and a dry north-westerly wind lead to very high evaporation rates from water surfaces, irrigated land, and plants. This exacerbates summer water shortages and soil salinization in irrigated areas (Schnepf 2004). The hill country of northern Iraq has sufficient precipitation to support rain-fed agriculture. From the foothills of north-central Iraq, a broad, arid rolling plain (used primarily for desert grazing and marginal agriculture) sweeps downward to the fertile valleys of the Tigris and Euphrates rivers where irrigated agriculture predominates. South-western and western Iraq is mostly desert, extending into Syria, Jordan, and Saudi Arabia.

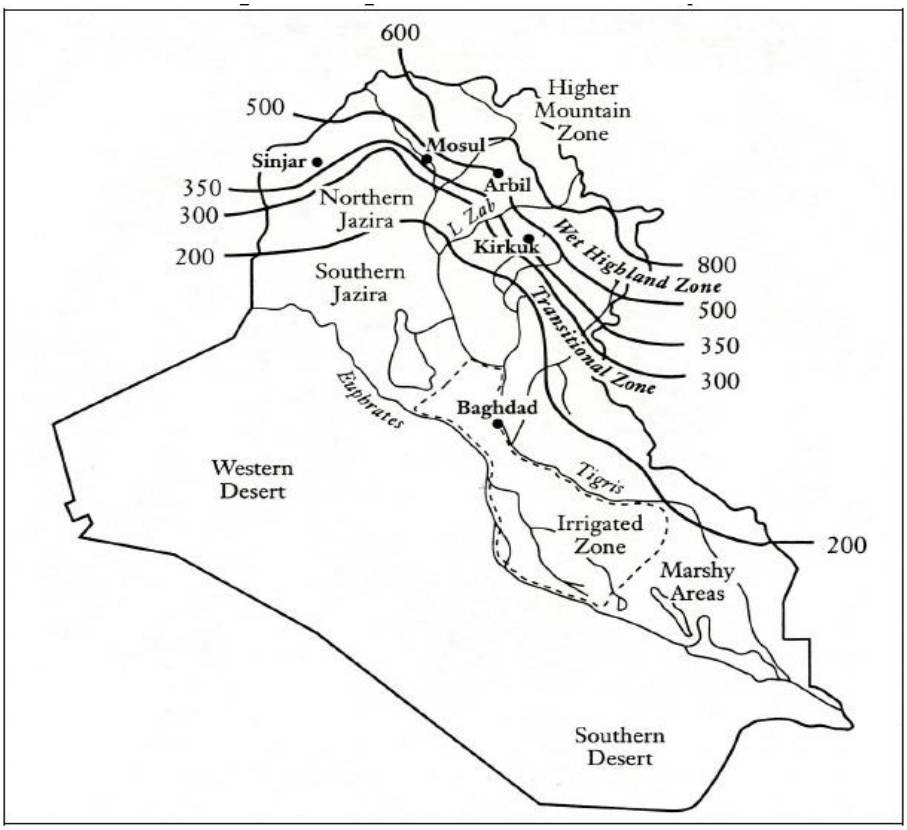

Figure 2.3 Agro-climatic Zones in Iraq, with rainfall isohyets indicated (Kamil 2002a).

The total area of Iraq is approximately 440 000 km^2. Land potentially suitable for agricultural production however is not more than 120 000 km^2, or 27% of the total area of the country. The rest includes deserts with extremely low rainfall and rocky/steep mountains which are the natural grazing grounds for the million sheep and goats in the country. The total area of agricultural production is about 8 million ha (80 000 km^2) which is almost 67% of the potentially cultivable area. However, due to certain limitations such as soil salinity, drought, shortage of irrigation water in summer, and fallowing, it is estimated that the average area actually cropped each year ranges from 3 to 4 million ha (Omer 2011).

Historically the most significant types of land use and food production in Iraq have been irrigated agriculture, which requires substantial investment and is an intensive form of land use, and pastoralism, which requires relatively little investment and is extensive. These have been combined with dry land farming in the semi-arid areas of northern Iraq. Although these basic types are technologically very different, they have been closely interrelated, socially and

economically, for thousands of years. Environmental problems generally derive not from basic technologies such as types of irrigation or grazing, but from the scale of the productive activity in relation to the resource. Before the first attempt to develop irrigation in modern-day Iraq, irrigation had already served as the basis of vast agricultural projects, and had environmental effects which reduced productivity seriously. Perennial irrigation in Iraq, which requires storage and gradual release of the water through the period of minimum flow, was largely introduced during the twentieth century. This kind of irrigation has allowed major increases in areas under cultivation and intensification of cropping but it also magnified the adverse effects of irrigation: soil salinity and water logging develop faster and some of the adverse effects are more difficult to reverse. Water resources in Iraq are controlled by the Twin Rivers, the Tigris and the Euphrates. Both are international rivers with their source in Turkey. The Tigris river basin in Iraq has a total area of 253 000 km², or 54% of the total river basin area. The history of irrigation started 7 500 years ago in the land between the Tigris and the Euphrates when the Sumerians built a canal to irrigate wheat and barley. Irrigation was estimated in 2006 at over 5.15 million ha, of which 60% is in the Tigris basin, 37% in the Euphrates basin, and 3% in the Shatt Al-Arab basin. Considering the soil resources, it is estimated that about 6 million ha are classified as excellent, good or moderately suitable for flood irrigation. With the development of water storage facilities, the regulated flow has increased and changed the irrigation potential significantly, since it was estimated at 4.05 million ha only in 2007. However, irrigation development depends to a large extent on the volume of water released by the upstream countries. The relative area of land used for the major crops in Iraq may be summarized as below in Figs. 2.4, and 2.5.

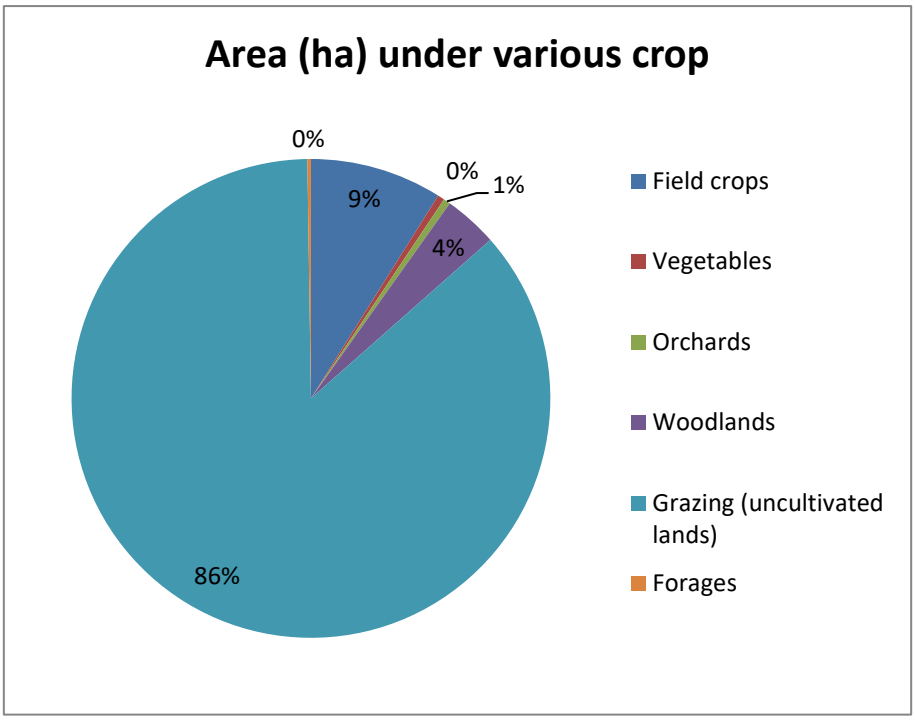

Figure 2.4 Area (ha) under various crops in Iraq (FAO Statistics 2011).

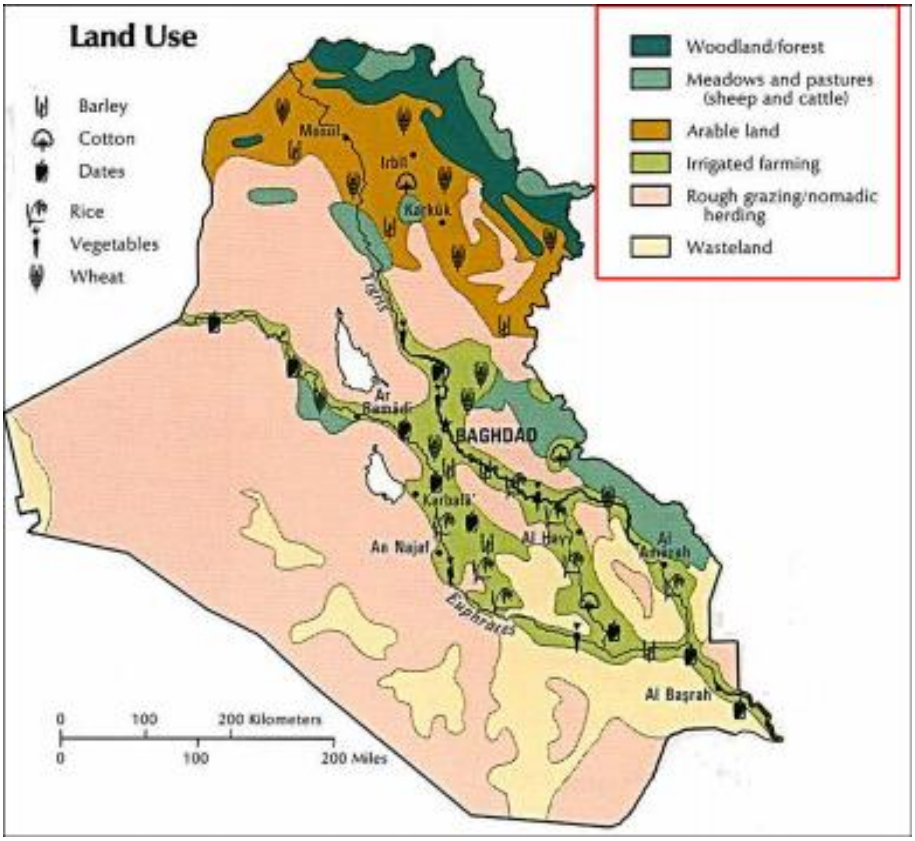

Figure 2.5 Land use in Iraq. Source: (CIA Atlas of the Middle East, 1993)

2.6.1. Agriculture sector

Iraq has great agricultural potential and it was once one of the breadbaskets of the Middle East, but today the yield gaps, defined as the differences between actual or observed yields and simulated potential yields in a given area (Nin-Pratt et al. 2011), are very significant (Schnepf 2004).

Iraq's agricultural sector plays a vital role in Iraq's economy sector. In 1976, agriculture contributed about 8% of Iraq's GDP. During the period 1971 to 1990, the population in Iraq had grown at an annual rate of 3.2% as compared with only 1.2% growth rate for Iraq's cereal production. Hence, food demand has risen faster than food production and created a growing reliance on agricultural imports to close the gap between food demand and availability. However, the agricultural sector has a long track record of government intervention, and mismanagement of agricultural policies. 'Investment in the sector has been discouraged by a history of shifting land and water property rights that has ebbed and flowed with the government's changing role' (Schnepf 2004).

In general, the most important crops in Iraq include barley, wheat, rice, dates, vegetables, and cotton. In the late 1980s, crop production accounted for about two-thirds of revenues in the agricultural sector. Winter crops, such as wheat, are normally planted in the second half of October. Planting is occasionally delayed due to inadequate rainfall early in the season. In addition, the production is also likely to be limited by the serious shortages of essential agricultural inputs. Crop production in Iraq is reported to be low especially in relation to the nation's food demand (FAO 2009), (FAO 2012), (Bishay 2003), (Schnepf 2004).

An assessment was carried out in 2003 by the World Bank and the United Nations Development Group; they concluded that Iraq's agricultural sector has been in decline since the 1980s. It was found that the agricultural production between 1988–2003 declined by approximately 1.1 percent annually, and the per capita agricultural production by about 3.9 percent annually (Bank 2003). The assessment also mentioned the production of key cereal crops such as barley and wheat; it was noted that cereal crops in particular suffered dramatically during this period.

The Food and Agriculture Organization of the United Nations (FAO 2009) stated that average wheat crop yields decreased by 11 percent between 2002 and 2007, and average barley crop

yields declined by 21 percent during the same period. More recent FAO statistics (FAOSTAT 2013) show that although these crops' yields have experienced significant and frequent degradation recently, overall, yields for both barley and wheat have followed something of an upward path since the beginning of the century. Wheat and barley are the most important crops in Iraq; Table 2.2 shows that wheat and barley represent almost half of the total cultivated cereal area in Iraq, which is 31.4 percent and 15.7 percent, respectively, of all cultivated cereal crops.

Most of the rain-fed harvested land areas in the central and northern are used for barley wheat production. Vegetables and fruits covers up 15.2 percent of the total land of cultivated area, and about one third of cultivated land to other crops.

Table 2.2 Yields of main crops in Iraq during 2000-2009, (FAO Statistics 2011).

Yields of main crop in Iraq		
Crop	**Area harvested (hectares)**	**Total area harvested (%)**
Cereals	2015790	52.7
Vegetables and fruit	581070	15.2
Other crops	1224766	32
Total area	3821626	100

Several studies provide a comparison of wheat and barley yields for Iraq with yields in nearby Syria and Turkey, from 1961 to 2012. It shows that wheat yields are higher overall in Turkey; there has been a steady and consistent increase in yields since 1961. Iraq, on the other hand witnessed an increase in yield rates only since 2001. Syria outperformed Iraq in the mid-1970s, and has experienced the most erratic history in wheat crop yields, with frequent declines and surges along the country's overall trend towards increased yields.

In terms of barley yields, there is a difference in performance between Iraq and the other two countries. Since the 1960s, Iraq has performed slightly better than Syria. However, barley yields in both countries show a trend over the past half century, where yields have been far less

erratic at compared with those recorded in Syria. Turkey, however, remains the dominant barley producer among the three countries; it is outperforming Iraq and Syria in both wheat and barley yields, and it has also achieved a steady growth in barley crop yields (Al-Haboby, Breisinger et al. 2014).

Given the comparable agro-ecological conditions found in Iraq, Syria, and Turkey, these differences in yield suggest large room for improvement in agricultural productivity in Iraq. While there is not much literature on estimated yield gaps in Iraq, it is known that significant gaps exist in the dry areas that stretch across the Middle East and North Africa (MENA). A 2011 assessment carried out by the International Center for Agricultural Research in the Dry Areas (ICARDA) on wheat yield gaps in Morocco, Syria, and Turkey indicates that there is significant potential to increase wheat yields in the West Asia and North Africa (WANA) region, which includes Iraq. ICARDA's research finds that wheat yields can be increased by 1.6–2.5 times in Morocco, 1.7–2.0 times in Syria, and 1.5–3.0 times in Turkey (Pala, Oweis et al. 2011).

2.6.2. Cropping patterns-farming systems in rainfed regions

Cereal-fallow and continuous cereals (mainly wheat and maize) are the main two farming systems in Iraq. The cereal-fallow system leaves the stubble of the previous year's crop and relies on volunteer plants based on seeds from the previous crop. The fallow fields are normally ploughed in March-April before the plants have produced seed and before the last spring rains. Farmers tend to use this system because it allows for conservation of soil moisture, control of weeds, and build-up and release of mineral nitrogen.

The production of livestock (for meat and milk) plays a vital role in the present farming system. In the northern part of Iraq, there are over 5.8 million goats and sheep and also 1 million cattle, horses, and buffaloes. These animals need supplementary feeding during some part of the year with grains and roughage of some kind. In addition, to feed the poultry, it was estimated that the requirement is about 12 000 Mtonnes of legume grains and 60 000 Mtonnes of cereal grains. The exceptions to the pattern of settled agriculture are the migratory goat and sheep herds. Because of the fact that herders have to supplement the grazed feed of their livestock with feed grains bought from local farmers, they move from the south of Iraq and the plains in the centre to the north for grazing and conversely, whenever there is a sufficient supply of feed. A

proportion of farmers in the north move down from the mountains during winter to avoid the feed deficiency.

Historically, the cereal–fallow system has been used for thousands of years, while the cropping system of continuous wheat is more recent. With this system (cereal-fallow) only the stubble can be used by livestock - for the remainder of the year, the livestock are fed by barley grains along with wheat/barley straw. Before sowing, the stubble is ploughed in, then tilled while soil is in dry state and the crop is sown at the preferred time or soon after the first autumn rains.

2.6.3. Zones of crop production in Iraq

With respect to crop production, the agricultural sector in Iraq can be divided into two regions, the predominantly rain-fed North and the predominantly irrigated Center-South. Generally agricultural production occurs on smallholdings, although the rainfed farms of the North are relatively large, approximately 10 to 30 hectares compared to the irrigated farms in the Center-South that average 1 to 2.5 hectares (Schnepf 2004).

2.6.4. Rain-fed agriculture

Winter wheat and barley account for about one-third of cereal production that predominantly is produced under rainfed conditions in the northern foothills region. This region can be classified into three rainfall regimes: high (700-1100 mm), medium (400-700 mm), and low (under 400 mm). Barley is the main crop in the low-rainfall zone, wheat occupies most of the medium-rainfall zone, Fruit orchards and vegetable productions dominate in the high-rainfall zone in the northern parts. Winter wheat and barley are planted in the fall (October-November) and harvested in the late spring (April-June) in accordance with the rainfall pattern.

In the rain-fed crops regions, yields are generally poor and vary significantly dependent on rainfall amounts. A biennial fallow system is predominantly used in these areas in order to regenerate the depleted soils and also to provide protection against diseases and pests. A winter crop of barley or wheat is grown once every two years under this system, and alternate halves of the field are left fallow for successive years. The crop rotations are selected carefully; very low inputs in terms of fertilizers, herbicides, and pesticides, and generally poor crop management practices prevail. Farmers have been rotating previously mono-cropped cereals with leguminous forage crops such as alfalfa since the early 1990s. This was done to partially

offset the sharp decline in imported feed grains and to break a slump in productivity due to declining soil fertility.

2.6.5. Irrigated agriculture

The irrigated production zone runs along and between the Euphrates and Tigris rivers, extending from the central region southeast heading to the marshlands of the Euphrates-Tigris Delta. Agriculture in this region is mostly based on irrigation because relatively little rain falls in the center-south zone. Approximately two-thirds of the irrigated region is occupied by cereal production. This includes both summer rice and corn crops and winter wheat and barley production. Vegetables and cotton are other main irrigated summer crops in the irrigated areas. Biennial fallow is the traditional system in the irrigated zone. Farmers tend to use this system to prevent salinization, because the fallow period allows the water table to drop sufficiently to allow the salt accumulation in the topsoil to be leached downwards.

However, the use of the biennial fallow system has recently declined; this is because during the 1990s, the government policies encouraged more intensive land cultivation, and a land tenure system, which encourages short term exploitation over long term investment in soil health. In recent decades, a single crop has been planted each year; a cycle of mono-culture has encouraged plant pests and disease in many cases. Occasionally, some double cropping, either wheat and maize and multiple cropping of vegetables has been practised when and where irrigation water is available. Irrigated summer crops are planted in April-May and harvested in September-October, although this may vary by crop. (Qureshi and Al-Falahi 2015).

2.7. Irrigation approaches in Iraq

2.7.1. Irrigation governance

There are regulatory policies and laws relating to various aspects of water resources in Iraq. In the case of irrigated agriculture areas, the law provides that all farmers benefiting from a scheme in which the state has invested must comply with the agricultural programme (that include laws and rules) set by government. The current bulk water distribution network includes 45 main regulators to regulate the main irrigation channels and divert water to branch canals. There are about 27,000 km of canals for water distribution. About two thirds of Iraq's irrigation system is gravity fed, through major canal systems controlled either by river intakes, diversion weirs, or off-takes directly from reservoirs. About a third of off-takes are pumped from rivers and major channels, with about 100 major pumping stations. The responsibilities of the Ministry of Water Resources (MoWR) include irrigation management through its offices at the districts and sub-districts. At the level of distributary canals, typically commanding 900-1250 ha, an official, called the "irrigation foreman", is responsible for water distribution. Water service charges were instituted by Law 112 of 1986, which was intended to create more farmer responsibility for operation and maintenance. The operation and maintenance expenditure of MoWR is financed by the central government budget. Although this allows services to continue, such subsidies have strong disadvantages: irrigation becomes dependent on fiscal and political factors unrelated to the needs of the irrigation sector, decisions on allocation of the budget are taken administratively by officials independent of any local voice, service levels are unrelated to farmer contribution, and agencies are not accountable to farmers for water service delivery. Moreover, it is also responsible for the water allocation, water planning, the construction, operation and maintenance of facilities for bulk water supply, flood prediction and mitigation. In addition, MoWR also operates dams, irrigation and drainage pumping stations (275 irrigation pumping stations serving almost the entire irrigated area), hydropower stations reservoirs, barrages and regulators (Water 2006).

On the other hand, the Ministry of Agriculture (MoA) is the other key institution related to water in Iraq including water conveyance to on-farm irrigated agricultural production. It is entrusted with providing farmers with small size booster pumps to lift the rationed surface irrigation water from nearby canals and rivers or open surface wells onto their flood irrigated fields. Furthermore, it is responsible for assigning cropping patterns to the farmers to produce "strategic crops", for distributing input rations at subsidized prices, and for marketing outputs

at controlled prices. The MoA exercised control through Agricultural Directorates in each province. In addition, there were 12 state boards and companies for various purposes that worked under MoA. The tasks of the MOA such as: managing land tenure, especially lease contracts, which govern tenure of lands redistributed under land reform; secure production contracts with farmers, which specify what is to be grown, the related entitlements to subsidized inputs and output prices to be received from the state marketing monopolies; market inputs and outputs, including the provision of agriculture inputs to all farmers and organizing the purchase of outputs by the state monopolies; and distribute subsidized equipment such as tractors and water saving equipment. At the local level, the various rules and regulations on irrigation and agriculture were determined and supervised by the local Agricultural Committee comprising of relevant government officers in the sub-district. This committee included representatives of both MoWR and MoA (Water 2006).

2.7.2. Irrigation extent in Iraq

In Iraq, the areas irrigated by surface water are estimated at 3.3 million ha, of which 105,000 ha (3 %) are in the Shatt Al-Arab river basin, 2.2 million ha (67%) in the Tigris river basin, and 1million ha (30%) in the Euphrates river basin' (Jaradat 2003). However, it should be noted that most of these areas are not completely irrigated, because a large part of these lands has been abandoned as a result of salinity and waterlogging. In 1993, the actual irrigated areas were estimated at about 1,936,000 ha. In 1990, nearly 220,000 ha were irrigated from groundwater, with some 18,000 wells. About 8,000 ha were under micro irrigation.

Based on available soil resources it was estimated that approximately 6 million hectares can be classified as excellent, good or moderately suitable for flood irrigation (Jaradat 2003).

Irrigation systems in Iraq have faced severe problems such as widespread discontinuation of maintenance of most of the agricultural amenities, especially the extensive network of irrigation and drainage infrastructure. In 2008, over 500 drainage and irrigation pumps were evaluated as in critically bad condition and not suitable for use. There was also substantial damage to the canal network due to lack of maintenance and repair. The cost of making the water available depends on the frequency of irrigation, the agricultural area (regardless of the consumed quantity of water), and the crop types.

However, the main irrigation method in Iraq is flood irrigation, a traditional method commonly used by most farmers, since it overcomes the unevenness of the land, and does not need costly grading or furrowing. Iraqi farmers still widely use this method of irrigation, despite its disadvantages. It causes waterlogging, increasing salinization, and has a very low efficiency on average; not more than 40 percent of the applied irrigation water is used by the plant.

The quality of land is poor due to soil degradation (including diminishing fertility) often as a result of overuse, and wind and water erosion. Wind erosion affects about 35% of the total area, while water erosion affects 17%. Approximately, 70% of the cultivable land suffers from salinity that leads to as much as 20 to 30% of the irrigated area not being farmed because of the high salinity. Salinity has always been a major issue; in 1970, it was estimated that about half of the irrigated areas in southern and central Iraq were degraded as a result of water logging and salinity.

Over the last decade, water stored in rivers has declined because of the long periods of droughts. Moreover, the contamination levels of river waters have steadily increased by discharges of untreated domestic wastewater directly into the rivers. Industrial wastewater has also caused increased sedimentation in reservoirs. Consequently, increased water pollution due to high temperatures and sub-standard water treatments caused eutrophication, which contributed to further water scarcity through reducing the water usability downstream (FAO 2012).

2.7.3. Irrigation system constraints in Iraq

According to FAO, the total irrigation area in Iraq was estimated at about 3.4 million hectares. Flood irrigation represented about 97%, about 3.1 million hectares are provided from rivers' diversions, and 300,000 hectares from direct river pumping. Well-based water systems irrigated 220,000 hectares in 1990. However, often less than 30% of annual irrigation water is used by crops. Furthermore, irrigation is often supplied in sub-optimal amounts or at the wrong time. Inefficient management of irrigation system has led to poor distribution of irrigation water, also due to inadequate levelling of the ground (causing lack of water in certain parts of the field and waterlogging in others) and other poor water management practices (e.g. poor maintenance of the irrigation canals)

In many cases, farmers invest the least amount possible in their crops to avoid the economic risks, which in turn reduces crop productivity.

2.7.4. Salinity caused by irrigation

Most of the irrigated agriculture in Iraq takes place in a very flat alluvial plain (Mesopotamian plain), that is poorly drained, and contains much salt in the soil and groundwater. The leakage of water from the associated irrigation network, the application of irrigation water, storage, distribution, and drainage channels have all caused a rise in ground water levels and even caused inundation in some areas. This process mobilises the stored salt and when the water table comes close to the soil surface, soil salinization and waterlogging result, which negatively affects the agricultural production.

Increased salinity in irrigation water and soil has reduced plant growth and crop yields due to the reducing ability of plants to take up moisture from saline soils. Large areas of agricultural land have been planted with more salt tolerant plants or the land has fallen out of irrigated production due to increasing salinisation over time. This adversely affects crop choices, crop yields, and under such circumstances, farmers may be only able to use the land for halophytic forages production.

2.7.5. Irrigated cropping

Crop intensity varies temporally and spatially in the winter season, approximately 80–90% of lands are used along the irrigation canals, and on the present levees of the Tigris and Euphrates rivers. Further away from the central canals, the soil salinity increases, and the cropping intensity decreases, falling to almost zero in saline basins. In summer, the intensity of cultivation is approximately 50%. The agricultural economy in Iraq is essentially based on the irrigation water that is supplied by the Euphrates and Tigris River. Traditionally, flood irrigation techniques are mostly used by farmers, planting on the slopes of furrows. This is attributed to the fact that most farmers are not very familiar with modern irrigation techniques or can't afford them. Drip and spray of irrigation systems are still in the first stages of adoption. The 9% of the land that is associated with irrigated agriculture represents about 2.5 million ha. In 1990.

Fig. 2.6 shows the irrigated area is spread out in central and southern Iraq, in the area adjacent to and between the Tigris and Euphrates rivers, known as the Mesopotamian plain.

The rivers deposit a large volume of sediments in large, irregular floods that spread across the plain. The plain itself has a very arid climate, with less than 200 mm annual rainfall. Hardly

any river water entering the floodplain leaves by surface flow. Major aquifers systems drain into the plain from the north, west, and east, and groundwater drains slowly from the plain to the Persian Gulf to the south. The aquifers of the floodplain are also connected to the surface water in the rivers and exchange depending on the relative hydraulic gradients. The low rainfall and the very shallow topographic gradient to the coast mean that there has been little opportunity for flushing of salts from this landscape. The high salinity manifests itself as widely distributed gypsiferous and saline soils.

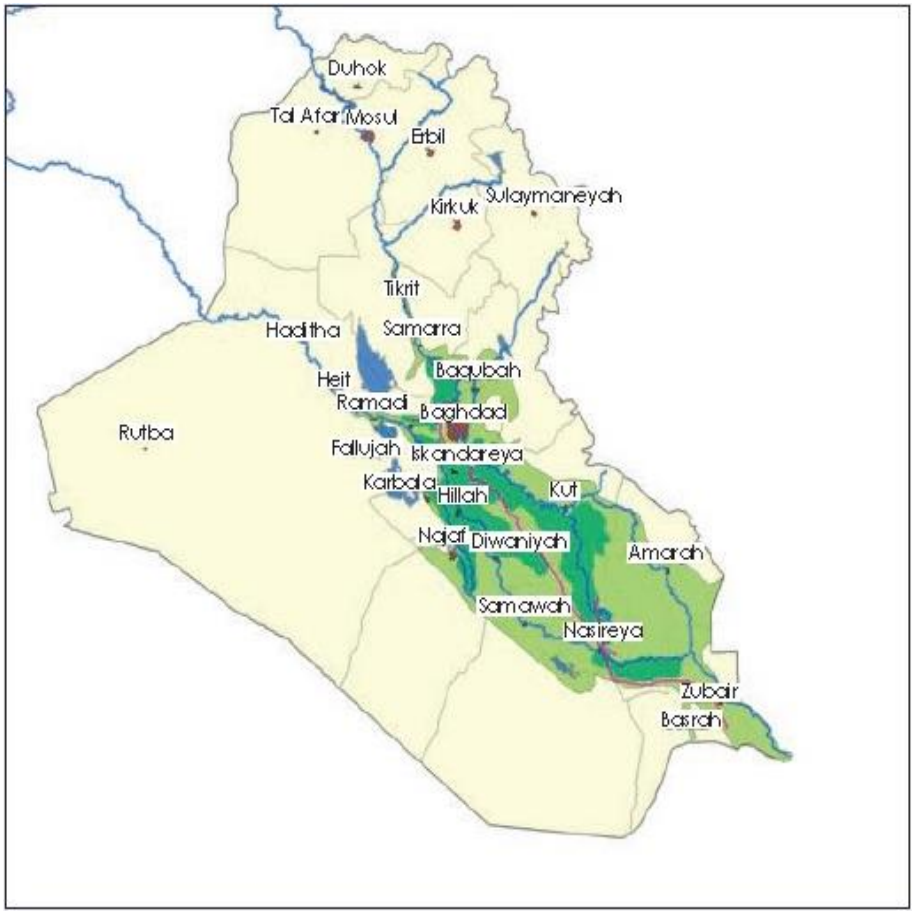

Figure 2.6 A map of Iraq showing the Mesopotamian plain, where irrigated agriculture is conducted (dark green are most irrigated areas in the plain), (ICARDA 2012).

2.8. Rangeland and grazing resources

Rangelands play a major role in determining the size and number of the national herds due to its contribution to livestock feed. In the past, these rangelands were deemed as one of the vital sources to meet livestock feed requirements. The main supplemental feeds for livestock in these rangeland areas are wheat and barley grains. Livestock used to contribute an appreciable proportion to the total earnings of the farming communities. In the low rainfall areas of Iraq, some ruminants, such as goats and sheep represented a principal economic output and contributed a large proportion of the income of herders and farmers.

Prior to 1990, the government encouraged livestock producers to increase their herd sizes because of the increasing demand for animal products coupled with favourable price ratios between livestock products and barley. Feed subsidies and other measures intended to mitigate the effects of feed shortages, especially in drought years, have provided further incentives to retain greater numbers of animals.

In the past, the rangeland vegetation provided sufficient feed to the large proportion of small ruminant population. Unfortunately, the majority of the rangelands have now been substantially degraded: both in the southern and northern rangelands more than 70% of pastoral lands are degraded. It has become no longer possible to meet the current feed demand, and also the absolute levels of feed sources have decreased. The contribution of natural grazing to the total feed needs has declined from 70% in the 1950s to about 10-25% at present.

Rangeland productivity declined massively, mainly due to changes in the climate, rapid exhaustion of cultivated lands, loss of water e.g. through evaporation, desert encroachment, semi desert area overgrazing, expansion of cultivation at the expense of rangelands, uprooting of shrubs for fuel wood, ploughing of some sites, desertification, overexploitation to supply the urban centres with animal products, lack of management of grazing resources, and due to the migration of large numbers of livestock from other different neighbouring countries to exploit the available forage in grazing seasons (Omer 2011). Overgrazing and barley cultivation in the semi-desert and steppe in years of above average rainfall contributed to degradation process of the rangeland in Iraq. Rangelands provided about 60-80% of the small ruminant's diet in the last four decades, nowadays, barley can only produce 5 to 10 percent of these requirements.

Consequently, the country faces a serious shortage of livestock feed and hence of animal products, particularly during dry periods.

2.9. Marshlands area

The Mesopotamian marshlands constitute the largest wetland ecosystem in the Middle East and Western Eurasia and support a rich biota (Al-Ansari and Knutsson 2011), (UNEP . Nairobi 2010). These wetlands cover 20,000 km^2 of open water, and include both permanent and seasonal marshes. Three major areas are the Chibyish, Hammar, and Haweezah Marshes, that together form the core of the marsh lands of southern Iraq. These wetlands in the southern part of Iraq play a vital role in the maintenance of biodiversity in the Middle East, due to their large size, their richness of aquatic vegetation and their isolation from other comparable systems (Bedair et al. 2006). The historical marshlands were part of the largest and most valuable habitats for different aquatic species and wildlife in the Middle East; and served as an important stopover site for migrating birds (Scott 1995). Reed (Pharagmites communis, Typha augustata) covers large areas of the marshes. The vegetation in the mud flats is usually Carex and Juncus spp., Scripus brachyceras. In the fresh water lakes aquatic herbaceous vegetation dominates like hornwort (Ceratophyllum demersum), eel grass (Vallisneria sp.) and pondweed (Potamogeton lucens spp.), as well as bottom vegetation such as stonewart (Chara spp.). In the smaller lakes and back swamps, floating vegetation such as waterlilies (Nymphaea and Nuphar spp) can be found (Fitzpatrick 2004), (Richardson et al. 2005), (Mahamed 2008), (Sama et al. 2012).

Over the past decades, this extensive Iraqi wetland system has been heavily affected by both climate and anthropogenic factors. Desiccation was one of the most dramatic environmental disasters that occurred to the marshlands area (Garstecki and Amr 2011). The marshes were drained during the early 1990s for political reasons; and the negative impact of and feedbacks resulting from this desiccation converted approximately 90% of the wetlands into deserts (UNEP 2001). This prolonged drainage was sustained from 1990 to 2003 and has caused severe damage to these aquatic systems (Sama et al. 2012), (Beaumont 1998). Large parts of the drained wetland area were re-flooded again in April 2003, which encouraged the remainder of the aquatic habitat to re-establish thus giving hope to the local communities that the ecological values of the Mesopotamian marshlands could be restored (Douabul, Al-Saad et al. 2012). In

2008-09, the marshlands were heavily impacted by a drought event, causing their extent to decline again; a brief recovery was observed in the winter of 2009/10 (Victoria 2010a).

2.9.1. Draining of the Mesopotamian marshes

The draining of the marshes since the 1990s has severely disrupted the hydrological regime of the Marshes. These marshlands have been affected by the construction of tributary canalisations and embankments. A Turkish Dam in the upper reaches of the Tigris and Euphrates impacted the water distribution throughout the basin, and continues to strongly affect downstream water availability (Beaumont 1998). Flood control structures changed the hydro-period of the downstream rivers, diverting peak floods into depressions and thereby creating reservoirs. The marshes have been also affected by Turkey's development project that includes 22l dams and 19 hydropower plants, as well as by Iran's large-scale water management projects on the Karun and Karkeh Rivers (the latter a key tributary feeding the Haweezah Marshes), that started in the mid-1990s. Due to upstream dams, the discharge and hydro-period of the Tigris and Euphrates were significantly reduced after 1990. Furthermore, a large-scale hydro-engineering programme was initiated by a previous hydrological regime to drain the Marshlands after the second Gulf War 1991 for politician reasons, thus a large part of the Euphrates was diverted into the Main Outfall Drain (Partow 2001), (Naff and Hanna 2003).

Originally, both the Chibyish and Hammar marshes were covering more than 4000 km². In 2000, ~98 km² of the Chibyish Marshes remained, around 3% percent of the surface area of the original marshes (Vinez and Leanard 2010). Moreover, the approximately 120 km long Lake of Hammar marsh practically disappeared between 1992 and 1994 (Munro and Touron 1997, Mitchell 2002), leaving Hammar marsh with only 6% of its original marsh land area. Al-Haweezah is the least affected marsh; in 2000, it had a third of its original marshland remaining. Overall, the re-channelization of the Tigris and Euphrates river flow had destroyed more than 9000 km² of marshland and eliminated entire habitats (UNEP 2001).

'The overall area of permanent marshland shrunk - according to one typical estimate - by 84% and the area of open water by 90%, while the area of seasonal marshes increased by 48% (Brasington 2002). Another estimate put the figures at 87% and 66% loss of permanent marshes and lakes, respectively, with another 87% loss in seasonal shallow lakes' (UNEP 2001).

The marshlands had shrunk to less than 7% of their 1973 extent and a new phase of active and widespread restoration started in March 2003, after the collapse of the former Iraqi regime. Local communities immediately tried to reclaim the marshland, but this was initially often conducted in an uncontrolled and haphazard fashion by breaching embankments and dikes, dismantle drainage structures, opening flood gates and sealing diversions (Lawler 2005). Because of the breaching of levees and dams, and coincidental plentiful rain in the following two years, the marshlands superficially recovered and regained about 50-60% of their former extent by 2005 (Initiative 2010). The year 2003 was also the end of a three-year drought period (2000-2003), and combined by good precipitation levels in the Euphrates and Tigris headwater catchment, the effect of re-flooding was further increased, causing a significant and rapid environmental change in the Iraqi marshlands during 2003-2005. By March 2004, more than 20 per cent of marshland area had been inundated; more than 50% of the former marshes had been re-flooded by May 2005. At the same time, wetland vegetation rapidly increased, at the significant rate of over 800-900 km^2 per annum. Since 2003, there has been an increase in wetland area and vegetation by about 50 to 60%. In November 2005, the flooded area gradually decreased to approximately 41% during this period due to the high evapotranspiration rates in the preceding hot summer months (Partow et al. 2005).

3. Chapter three: Materials and methods

This chapter describes the methodology used to achieve the research objectives. The first section of this chapter describes the study area, summarising the climatic zones of Iraq and the marshlands region, as well as the soils. The second section describes the methods used to obtain the meteorological and remote sensing data. The third section describes the methodology used for land use/land cover mapping. The fourth part describes how the meteorological drought indices were calculated over the study period. This is followed by a description of the methodology used to study changes in vegetation productivity and land surface temperature over the study period. The fifth part of this chapter describes the methodology used for the simulations with the SWAP model. Finally, the last section of the chapter discusses the methodology used for drought assessment based on meteorological and remote sensing data. It also describes the different remote sensing indices that are evaluated to see whether they can reliably indicate the occurrence, degree and duration of drought.

3.1. Data collection

3.1.1. In situ meteorological data

Historical records of daily and monthly rainfall (P), maximum ($Tmax$) and minimum temperature ($Tmin$), relative humidity (RH), wind speed (WS), and sunshine hour (SH) datasets were acquired for Iraq, for a period of 33 years, from 1980-2013, for 14 stations distributed throughout Iraq, see Fig. 3.1. The data were collected from the Iraqi Meteorological and Seismology Organisation and the stations are shown in Table 3.1. Meteorological data have been used to calculate drought indices, to drive the SWAP model (to give water balance components), and to help explain remote sensing time series/patterns of NDVI, LST, and energy balance. More detail on the meteorological data is presented in Table 3.2.

The Weather Observing Department is responsible for preparing basic data on weather variables needed by the Iraqi Meteorological Organisation (IMO) technical and related departments. Surface observing stations are distributed in different Iraqi provinces. At every station operators visually observe changes in weather variables (such as cloud cover and type, range of visibility, occurrence of thunderstorms, and other weather phenomena), in addition to using meteorological instruments, together with automatically recording devices, for determination of weather data such as temperature, air pressure, humidity, surface wind, solar incoming radiation, rain, and potential evaporation. These data are sent to the weather forecasting center in Baghdad, every 3 hours, which means eight times daily, by phone. All these stations operate around the clock. In addition, there are two main weather observing stations in each of Baghdad's international airports, and a meteorological station in Basrah international airport. IMO is responsible for collecting, checking and analysing the data originating from the weather observing stations. They issue the Iraqi climate atlas yearly, as well as publish monthly bulletins containing climate elements averages. In terms of data quality, the ISO 9001-2008 has been awarded to IMO and the related organisation of seismology (http://www.meteoseism.gov.iq).

Table 3.1 The meteorological stations over Iraq selected for this study (based on data quality and length of climatic records). The location of the stations/site (through their capital letter ID) is shown in Fig. 3.1

Station	ID in the map	WMO code
Ramadi	A	642
Karbala	B	656
Najaf	C	670
Samawa-Muthana	D	674
Basrah	E	689
Nasiriya	F	676
Dywania	G	672
Kut-AlHay	H	665
Babil	I	657
Baghdad	G	650
Biji-Tikrit	K	631
Kirkuk	L	621
Mosul	M	608
Rabiaa-Nainvah	N	602

3.1.2. ERA-Interim meteorological data

ERA-Interim is the latest global atmospheric reanalysis produced by the European Centre for Medium-Range Weather Forecasts (ECMWF). ERA-Interim reanalysis daily data were obtained from the ECMWF website (https://www.ecmwf.int) for the period 1 January 1980 to 31 December 2015. In this study, precipitation, minimum and maximum temperature at a height of 2 m, solar radiation, 10 metre wind speed, 2 metre dewpoint temperature to calculate relative humidity, net shortwave and longwave radiation, sensible heat flux, and latent heat flux were extracted at a resolution of 0.125 ° x 0.125°. The data were provided in netcdf format. For instantaneous variables such as temperature, wind speed, and dewpoint temperature data were extracted as a daily average. In order to obtain accumulated daily totals for precipitation and radiation variables, a start time was selected of 00:00 (midnight) and 12:00 (midday), so that daily totals were obtained by summing these values. After extraction, the model variables were compared with observed data for all study sites, mainly for quality assurance (Section. 4.5). The meteorological data (in-situ and ERA-Interim) were used for water balance simulations with the SWAP model. These data were also used to derive the hydrometeorological drought indices.

3.1.3. Satellite data

Several MODIS Terra multi temporal data products were acquired over the study area. MODIS data were downloaded from NASA's website for the period 2001 to 2015. MODIS acquires earth observation in 36 spectral bands crossing the equator at approximately 11:00 AM. The acquired data include Normalised Difference Vegetation Index (NDVI), and land surface temperature (LST). These data were obtained in HDF format.

3.1.3.1. NDVI data

The Moderate Resolution Imaging Spectroradiometer (MODIS) NDVI data of Iraq were used for this study. MODIS data were obtained from the USGS Earth Explorer (EE) (http://earthexplorer.usgs.gov/). NDVI was obtained from MOD13A2 products (16-Day L3 Global 1km SIN Grid VI datasets), which were designed for vegetation, in Geographic lat/long (WGS 84) projection. With all of the recent MODIS products available in different formats and resolutions, it is important to learn from previous research, i.e. which MODIS wavebands, vegetation indices, spatial resolutions, radiometric calibration methods, and temporally

processed products have been successful in detecting vegetation disturbances at the regional scale.

3.1.3.2. LST data

Land Surface Temperature (LST) data were obtained from MOD11A2 products available at a spatial resolution of 1km and a temporal resolution of 8 days. MODIS Land Surface Temperature and Emissivity (LST/E) products provide per-pixel temperature and emissivity values. These level-3 MODIS global Land Surface Temperature (LST) and Emissivity data are composed from the daily 1-kilometer LST product (MOD11A2) with a spatial resolution of 1km and temporal resolution of 8 days in sinusoidal projection represented as the average values of clear-sky LST during 8-day period. The MODIS products were calibrated by using the relevant scale factors for MODIS products; the scale factor of NDVI and LST is 0.0001 and 0.02 respectively.

3.1.3.3. Soil moisture data (SMOS)

Soil moisture (SMC) over the period 2010-2015 was obtained from the ESA soil moisture and ocean salinity (SMOS) mission. Soil moisture data were extracted from the SMOS archive onto a 40km×40km grid. Data were averaged to monthly values over the study sites for each of the years from 2010 to 2015.

Table 3.2 List of meteorological data from measured data and remote sensing

Data available		Description	Spatial resolution	Temporal resolution
In Situ data	Maximum temperature (℃)	The data (01 Jan 1980 to 31 Dec 2013) derive from climate observations made at 14 meteorological stations over Iraq	Point	Daily
	Minimum temperature (℃)		Point	Daily
	Rainfall (mm)		Point	Daily
	Relative humidity (%)		Point	Daily
	Wind speed (m/s)		Point	Daily
	Sun shine hours (hr)		Point	Daily
ERA Interim data	Maximum temperature (K)	This is a global atmospheric reanalysis. The data were obtained for 35 years (01 Jan 1980 to 31 Dec 2015).	0.125˚ × 0.125˚	Daily
	Minimum temperature (K)		0.125˚ × 0.125˚	Daily
	Rainfall (m)		0.125˚ × 0.125˚	Daily
	Dew point temperature (K)		0.125˚ × 0.125˚	Daily
	Wind speed (m/s)		0.125˚ × 0.125˚	Daily
	Surface shortwave radiation downward $(W\ m^{-2}\ s)$		0.125˚ × 0.125˚	Daily
			0.125˚ × 0.125˚	Daily
	Net longwave radiation $(W\ m^{-2}\ s)$		0.125˚ × 0.125˚	Daily
	Net shortwave radiation $(W\ m^{-2}\ s)$		0.125˚ × 0.125˚	Daily
	Latent heat flux $(W\ m^{-2}\ s)$		0.125˚ × 0.125˚	Daily
Remote sensing data	NDVI	The monthly NDVI (MOD13A2) product and LST (MOD11A2) product	1 km	16 days
	LST (K)		1 km	8 days
	SMC (m^3/m^3)	SMOS (2010-2015)	40 × 40 km	Daily

3.2. Methodology

3.2.1. Land cover classes

Land use/cover mapping using remote sensing data is commonly performed by digital image classification (Campbell 2002). The MODIS land cover classes (MCD12Q1) 2007 were downloaded from NASA LP DAAC website (https://lpdaac.usgs.gov/data access). The MODIS land cover type products have a 0.5 km spatial resolution that provided broad information on Iraq's land cover classes. A supervised classification (Schowengerdt 2006) was carried out to create the MODIS land cover types involving high quality land cover training sites. This approach was developed by utilizing a combination of ground reference data and fine spatial resolution imagery to increase the accuracy of the product (Muchoney, Strahler et al. 1999). The seven land cover types included water, shrub lands, grass lands, crop lands, urban, natural vegetated, and barren lands as shown in the map (Fig. 3.1) showing MODIS land cover types in 2007 over Iraq. The map indicates that land cover is dominated by barren land, but marshlands and shrublands also make up a significant part of the study area. Note that this map also shows the sites of the meteorological stations, and the nearby sites selected for the remote sensing studies, labelled by their numbers given in Table 3.1.

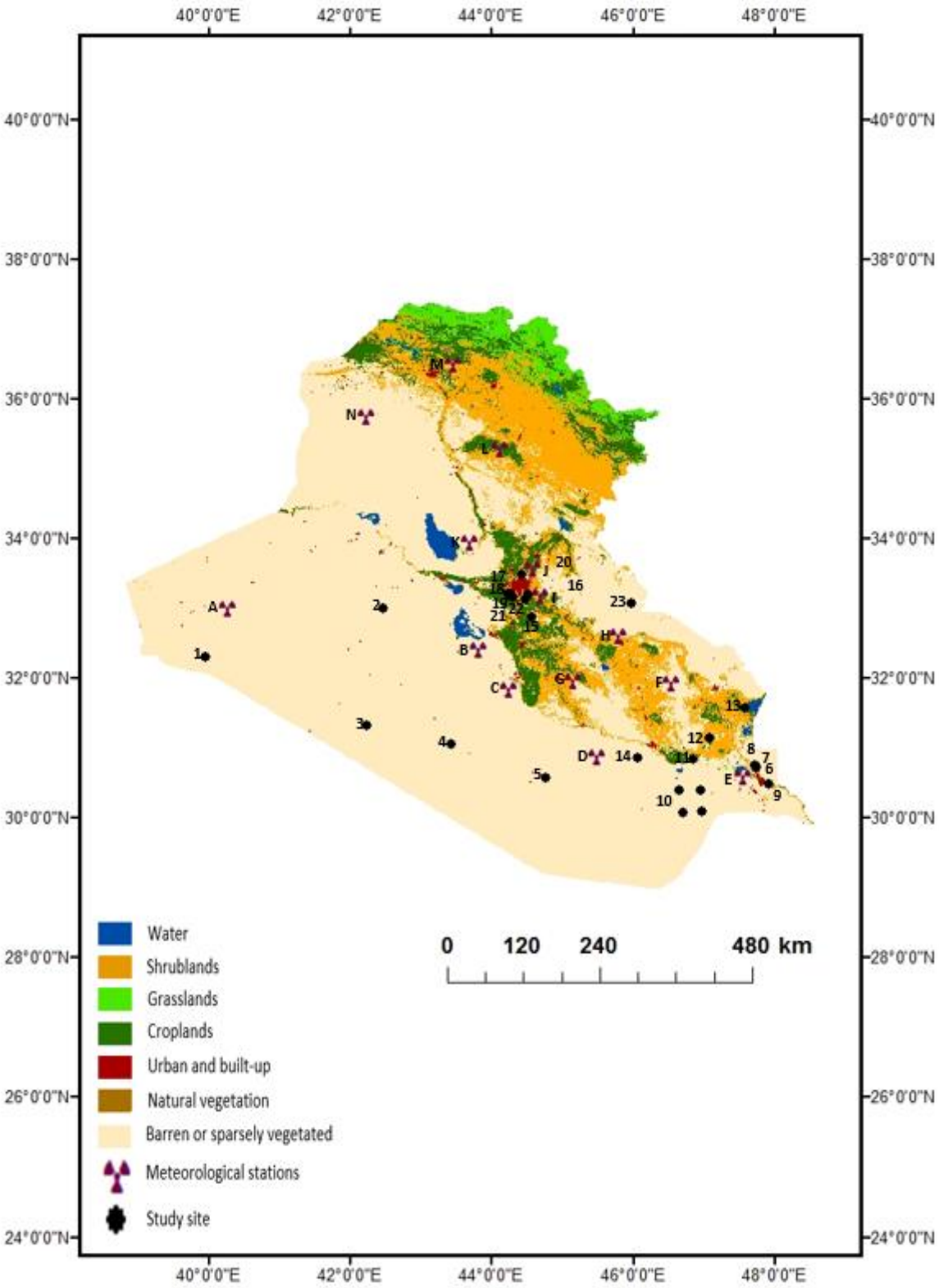

Figure 3.1 Maps of MODIS land cover classes with a spatial resolution of 250m for 2007 (https://lpdaac.usgs.gov/dataaccess).

3.2.2. Estimation of potential evapotranspiration (PET)

There are various empirical equations serving to convert the climatic data into PET.

The Penman-Monteith equation is the most commonly used method for estimating reference crop evapotranspiration (ETo). Using this method requires a considerable number of meteorological data, yet few stations with adequate meteorological data may exist in a region. Reference evapotranspiration, ETo (mm/day), is given by:

$$ET_0 = \frac{0.408\Delta\,(R_n - G) + \gamma \frac{900}{T+273}\,u_2\,(e_s - e_a)}{\Delta + \gamma(1 + 0.34\,u_2)} \qquad 3.1$$

where Δ is the slope of saturation vapor pressure vs. air temperature curve (kPa °C^{-1}), R_n = net radiation received at the crop surface (MJ m^{-2}d^{-1}), G = soil heat flux density at the soil surface (MJ m^{-2}d^{-1}), T = mean daily air temperature at 1.5 – 2.5 m height (°C), u_2= mean daily wind speed at 2 m height (m s^{-1}), es = the saturation vapor pressure (kPa), ea = actual vapor pressure (kPa), es − ea = saturation vapor pressure deficit (kPa). All parameters and variables necessary for computing ETo were computed according to the procedure described in FAO irrigation and drainage manual 56, by Allen et al.(1998).

The Hargreaves (Hargreaves and Samani 1985) equation is an empirical radiation-based method, which is extensively used when limited weather data are available.

It is expressed as:

$$ET_0 = 0.0023\,(T_{mean} + 17.8)\,(T_{max} - T_{min})^{0.5}\,R_a \qquad 3.2$$

where, Ra: extraterrestrial radiation (mm day^{-1}); Tmean: mean air temperature (°C);Tmax: daily maximum air temperature (°C); Tmin: daily minimum air temperature (°C).

Setting up a station that records the required data for Penman-Monteith equation is expensive and maintenance of the instruments is labour-intensive. Alternatively, the Thornthwaite (Thornthwaite 1948) equation is a simpler method for estimating ETo since it is a temperature-based method:

$$PET = C\left(\frac{10\,T_{mean}}{I}\right)^{a}\left(\frac{d}{12}\right)\left(\frac{N}{30}\right) \quad 3.3$$

in which PET is the adjusted monthly potential evapotranspiration (mm); C = 16 (a constant), $T_{mean}$is the monthly average temperature; d is the duration of average monthly daylight (hr); and N is the number of days in a given month, $a = 67.5 \times 10^{-8} I^3 - 77.1 \times 10^{-6} I^2 + 0.0179I + 0.492$; in which I is the annual heat index.

3.2.3. Meteorological drought indices

A time scale of 3-months was selected to calculate the various drought indices as it is the most appropriate for determining drought severity (Ji and Peters 2003). Therefore, this particular time scale was used throughout the thesis. It was computed on a monthly data so that drought characteristics can be more readily identified. The 3-month time scale is based on the precipitation total for 3 months, which includes the month against which the SPI value is plotted. For instance, the 3-month time scale SPI for March, 2001 is based on the precipitation total for January, February, and March 2001. Meteorological data between 1980 to 2015 were used to get a long-term assessment of drought in Iraq. This period is long enough to perform statistically reliable drought magnitude analyses (Otgonjargal 2012).

3.2.3.1. Drought assessment using standardised precipitation index (SPI)

The temporal occurrence of meteorological drought based on SPI was examined, where the monthly precipitation data were used as main parameter of interest. The program was downloaded from the http://drought.unl.edu website. Drought was identified according to the outputs, positive values indicates wetter than normal conditions, and negative values refer to drought conditions as categorised in Table (2.1).

3.2.3.2. Drought assessment using standardised precipitation evapotranspiration index (SPEI)

The standardized precipitation evaporation Index (SPEI) was calculated from spatially interpolated monthly values of precipitation and temperature data (to calculate PET, using the Thornthwaite equation, also at timescales of 3 months. To investigate the performance of this drought index, correlation analyses were conducted with simulated soil moisture and SMOS and NDVI. A comparison with SPI, a drought index that does not incorporate temperature (i.e. ignores the effect of changes in potential evapotranspiration), was also conducted.

3.2.4. MODIS images processing

MODIS satellites images have been processed in ERDAS (2013) and ArcMap (10.2). From the global dataset, the images for the study area were selected and NDVI data were derived and analysed. MODIS NDVI values range from -1999 to 10000, 2000 is the fill value. After multiplying with the scale factor (= 0.0001. Thus, time-series of NDVI over Iraq were derived for the years 2001 to 2015. The following steps were carried out in consecutive order: 1.

Importing MODIS satellite images into ERDAS IMAGINE 2013, data are already projected to latitude/longitude geographic co-ordinates and WGS84 datum; 2. Extraction of the Study Area using a polygon file of the outline of the study sites from the land cover map; 3. Extraction of NDVI and LST seasonal monthly average. The NDVI and LST values were converted from IMG to ASCII format. The result of this pre-processing is a spreadsheet containing NDVI and LST values of the study area, only covering the period 2001 to 2015 (because suitable remote sensing data were not available before then). LST values of the study area between the years 2001 and 2015 were calculated, and averaged monthly. Temperatures were extracted in Kelvin then converted to centigrade. The digital numbers (DN) of LST data were converted to degree Celsius using:

$$LST = (DN \times 0.02) - 273.15\ °C \qquad 3.4$$

3.2.5. Soil water balance model simulations

SWAP can simulate transport of solutes, water, and heat in the vadose zone in interaction with vegetation development (see Fig. 3.2). SWAP's scale in the horizontal direction is the field scale, whereas in the vertical direction the model domain reaches from a plane above the canopy to a lower boundary which is situated below the root zone. In well-drained soils (with 'free drainage' occurring at the bottom boundary) this level could represent unsaturated soil layers, whereas for poorly drained soil the lower boundary could be below the groundwater level. In this soil-plant-atmosphere system the transport processes are predominantly vertical; it is therefore SWAP is a one dimensional, vertically directed model.

The main input data consist of crop growth, meteorological, and drainage data. SWAP can be used to analyse water management options, through calculations of the water balance.

The model employs standard soil physical theory to simulate soil moisture and heat movement in variably saturated soils, including root water extraction. It can also account for macroporous flow and water repellency (Kroes, Van Dam et al. 2008). SWAP simulates soil heat flow taking into account heat capacities and thermal conductivities. The generic crop growth module WOFOST is incorporated to simulate leaf photosynthesis and crop growth. The soil moisture, heat and solute modules exchange status information for each time step to account for all kind of interactions. Crop growth is affected by the actual soil moisture and salinity status on a daily

basis. The model is considered as very flexible with regards to its intake of input data at the bottom and top of the soil column (Kroes, Van Dam et al. 2008).

The main input file includes information regarding the simulation input and output data (e.g. time step and numerical considerations), soil water flow, meteorology, irrigation, crop rotation scheme, heat flow and solute transport. For the meteorological data files, daily time steps are commonly used. The meteorological data required to run SWAP, are daily maximum temperature, minimum temperature, humidity, wind speed, rain, and solar radiation.

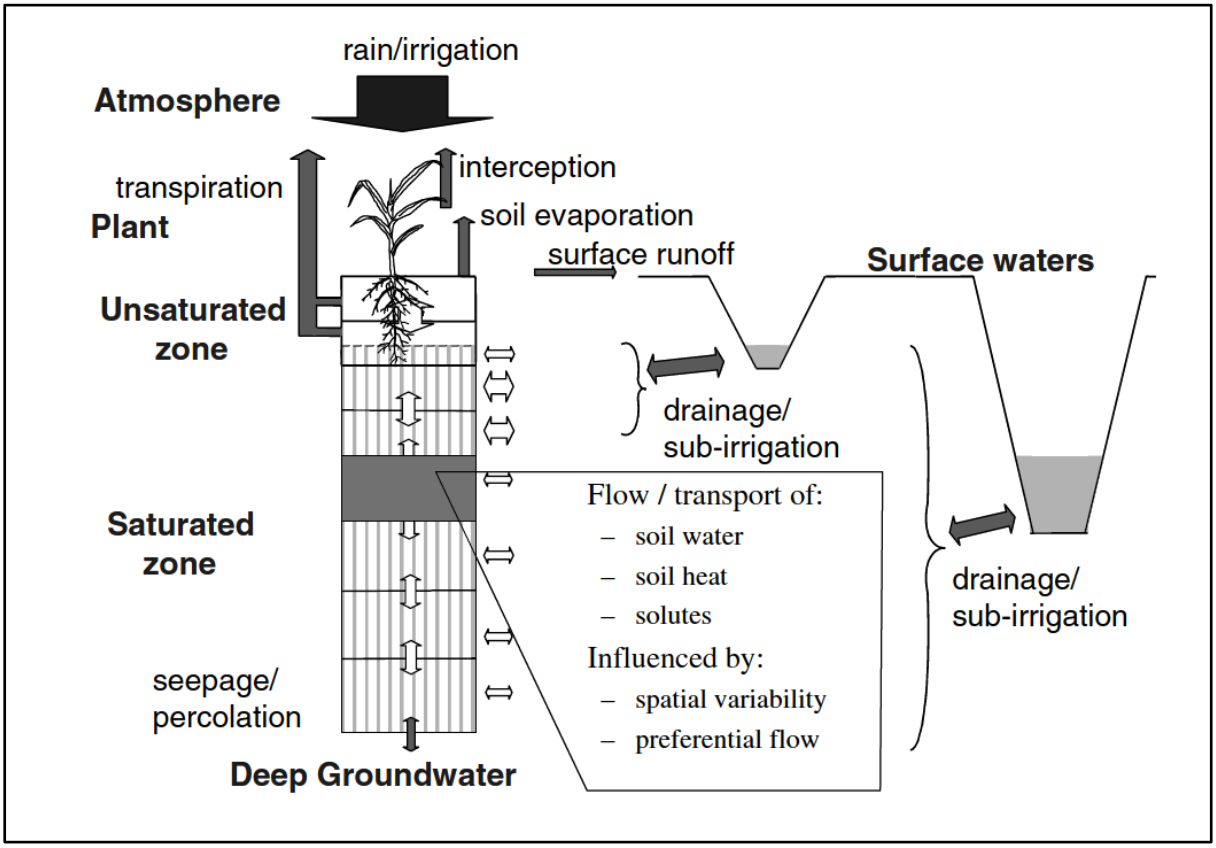

Figure 3.2 A schematization of the hydrological processes incorporated in SWAP (van Dam 2000).

SWAP model applies the Richards equation via a finite difference scheme adapted from those described by (Haverkamp, Vauclin et al. 1977) and (Belmans, Wesseling et al. 1983). The wide

range of lower and upper boundary conditions being offered in SWAP is one of the key advantages of SWAP. The soil profile is modelled as a sequence of layers, each layer has its own hydraulic characteristics. The layers are divided into smaller compartments adopted in the finite differences solution scheme. Soil retention curves θ (h) and unsaturated hydraulic conductivity K(θ) of these layers are also described by the analytic equations of (Mualem 1976), (Van Genuchten 1980)respectively. With regards to the crop development, SWAP includes a relatively simple module that needs the time series of soil cover fraction (CF) or leaf area index (LAI), root depth and distribution, crop height, or alternatively, a detailed crop growth model (Hijmans, Guiking-Lens et al. 1994) can be used. Interception is modelled by the analytical model that was proposed by (Braden 1985). The potential evapotranspiration $ET_{pot}(cm\ d^{-1})$ was calculated by the Penman-Monteith equation (Allen et al., 1998). ET_{pot} is divided into potential soil evaporation rate E_{pot} $(cm\ d^{-1})$ and potential transpiration rate $T_{pot}(cm\ d^{-1})$ based either on the leaf area index LAI m^2/m^2or the soil cover fraction SC (-), both as a function of crop development. Reduction of the potential soil evaporation rate into actual soil evaporation rate, $E_{act}(cm\ d^{-1})$depends on the maximum soil water flux in the top soil according to Darcy's law or is calculated by an empirical function following either (Boesten and Stroosnijder 1986).The actual evaporation $E_{act}(cm\ d^{-1})$ depends on the capacity of the soil to transport water to the soil surface, while the actual transpiration $T_{act}(cm\ d^{-1})$ is derived from the potential accounting for soil cover, moisture and salinity conditions in the root zone (weighted by the root density). Regarding irrigation, it may be prescribed at fixed times or scheduled according to a number of criteria. The scheduling options allow for the evaluation of alternative application strategies.

3.2.5.1. SWAP model theory

According to SWAP the water balance (cm) of a vertical soil column with vegetation during a certain period can be written as:

$$\Delta W = P + I - R - P_i - T_a - E_a - E_w + Q_{bot} \quad 3.5$$

where ΔW is the change in soil water storage, $P$is precipitation, I is irrigation, R is surface runoff, $P_i$is interception by vegetation, T_a is actual transpiration, E_a is actual soil evaporation,

E_w is evaporation of ponding water and $Q_{pot}$is water percolation at the soil column bottom (+ upwards).

3.2.5.2. Soil water flow

Soil water movement is governed by the gradient of the hydraulic head, H (cm) which be

written as:

$$H = h + z \quad 3.6$$

where h is the soil water pressure head (cm) and z is the vertical coordinate (+upward). In unsaturated soils water flow is predominantly vertical. Using Darcy's law, the water flux density q (cm d^{-1}) can be expressed as (+ upward):

$$q = -K(h)\frac{\partial(h+z)}{\partial z} + 1 \quad 3.7$$

where K is the unsaturated hydraulic conductivity (cm d^{-1}) as function of soil water pressure head. The law of mass conservation of a soil column with root water extraction S_a (d^{-1}) gives:

$$\frac{\partial\theta}{\partial t} = -\frac{\partial q}{\partial z} - S_a(z) \quad 3.8$$

where θ is the volumetric soil water content (cm^3 cm^{-3}) and t is time (d). Combination of Eqs. 3.7 and 3.8 yield the general soil water flow equation, which is known as Richards' equation:

$$C(h)\frac{\partial h}{\partial t} = \frac{\partial}{\partial z}\left[k(h)\left(\frac{\partial h}{\partial z} + 1\right)\right] - S_a(z) \quad 3.9$$

where $C(h) = \partial\theta/\partial h$ is differential water capacity (cm^{-1}). SWAP solves the Richards' equation numerically for specified boundary conditions and with known relations between the soil

variables θ, h and K. The relation between θ and h (retention function) might be described with the analytical equation proposed by Van Genuchten

(1980):

$$\theta(h) = \theta_{res} + \frac{\theta_{sat} - \theta_{res}}{[1+|\alpha h|^n]^{\frac{n-1}{n}}} \quad 3.10$$

where θ_{res} is residual water content ($cm^3\ cm^{-3}$), θ_{sat} is saturated water content ($cm^3\ cm^3$), and α (cm^{-1}) and n (-) are empirical shape factors. Equation 3.10 in combination with the theory of Mualem (1976) provides a versatile relation between θ and K:

$$K(\theta) = K_{sat} S_e^{\lambda} \left[1 - (1 - S_e^{n/n-1})^{\frac{n-1}{n}}\right]^2 \quad 3.11$$

where K_{sat} is the saturated hydraulic conductivity (cm d-1), ⅄ is an empirical coefficient (-), and S_e is the relative saturation ($\theta - \theta_{res}$) / (θ_{sat} - θ_{res}).

3.2.5.3. Top boundary condition

The top boundary condition is determined by the potential evapotranspiration, irrigation and precipitation fluxes. The potential evapotranspiration can be estimated by the Penman-Monteith equation (Allen, Pereira et al. 1998):

$$ET_p = \frac{\frac{\Delta_v}{\lambda_w}(R_n - G) + \frac{p_1 \rho_{air} C_{air} e_{sat} - e_a}{\lambda_w \quad r_{air}}}{\Delta_v + \gamma_{air}\left(1 + \frac{r_{crop}}{r_{air}}\right)} \quad 3.12$$

where ET_p is the potential transpiration rate of the canopy ($mm\ d^{-1}$), Δ_v is the slope of the vapour pressure curve (kPa $°C^{-1}$), λ_w is the latent heat of vaporization ($J\ kg^{-1}$) , R_n is the net radiation flux at the canopy surface ($J\ m^{-2}\ d^{-1}$) , G is the soil heat flux ($J\ m^{-2}\ d^{-1}$) , p_1 accounts for unit conversion (=86400 s d^{-1}), ρ_{air} is the air density ($kg\ m^{-3}$) , C_{air} is the heat capacity of moist air ($J\ kg^{-1}\ °C^{-1}$) , e_{sat} is the saturation vapour pressure (kPa), e_a is the actual vapour pressure (kPa), γ_{air} is the psychrometric constant (kPa $°C^{-1}$), r_{crop} is the crop resistance ($s\ m^{-1}$) and r_{air} is the aerodynamic resistance ($s\ m^{-1}$).

The potential evaporation is given by:

$$E_p = ET_p e^{-k_{gr} LAI} \quad 3.13$$

where k_{gr} (-) is the extinction coefficient for global solar radiation. In wet soil conditions, the actual soil evaporation rate E_a (cm d^{-1}) will be equal to E_p. In dry soils conditions, E_p is governed by maximum soil water flux, E_{max} (cm d^{-1}) in top soils, which can be determined by

Darcy's law as:

$$E_{max} = k_{1/2}\left(\frac{h_{atm} - h_1 - z_1}{z_1}\right) \quad 3.14$$

where k_{gr} (LT^{-1}) is mean hydraulic conductivity between the soil surface and first node, $hatm\ (cm)$ is soil water pressure head in equilibrium with the air humidity, h1 (cm) is the soil water pressure head of first node, and $z1\ (cm)$ is the soil depth of the first node. In our experience, the Darcy flux of Eq. (3.14) overestimates the actual soil evaporation flux. Therefore, in addition to Eq. (3.14) was used the empirical function of (Black, Gardner et al. 1969) to limit the soil evaporation flux to $Eemp$. In our analysis SWAP determined actual evaporation rate by taking the minimum value of Ep, $Emax$ and $Eemp$. The potential transpiration rate, Tp (LT^{-1}), follows from the balance:

$$T_p = \left(1 - \frac{P_i}{ET_{p0}}\right) ET_p - E_p \quad 3.15$$

where P_i (cm d^{-1}) is the water intercepted by vegetation and ET_{p0} is the potential evapotranspiration of a wet crop, which can be estimated by the Penman-Monteith equation assuming zero crop resistance. The ratio P_i / ET_{p0} denotes the day fraction during which interception water evaporates and transpiration is negligible. Bottom boundary condition

In case of deep groundwater levels (< 3 m below soil surface) we will assume free drainage conditions. In that case the percolation flux at the bottom of the soil column will be calculated from:

$$q = -K(h)\left(\frac{\delta h}{\delta z} + 1\right) = -k(h)(0 + 1) = -k(h) \quad 3.16$$

In case of shallow groundwater levels (within 3 m of soil surface) the measured groundwater levels were specified as bottom boundary condition.

3.2.5.4. Model driving variables

Weather variables required for SWAP model runs are solar radiation ($KJ\ m^{-2}\ day^{-1}$), minimum (℃) and maximum temperature (℃), rainfall amount (mm), wind speed and actual ($m\ s^{-1}$), vapour pressure (kpa). Table (3.2) shows the weather data during the simulation period. The solar radiation (derived from extyra-terrestrial radiation and the difference between the maximum and minimum temperature) and actual vapour pressure (derived from air relative humidity and average air temperature) were calculated based on standard equations (Allen, Pereira et al. 1998).

3.2.5.5. Crop parameters

Detailed data on vegetation parameters (crops and rangeland) were required for the SWAP simulations, as detailed mostly in the. crp files. The 'simple' crop files, supplied with each SWAP release, for wheat and maize, natural grass, and bare soil were chosen for agriculture, rangeland, and desert simulations, respectively. Data for wheat and maize crops, such as rooting depth, sowing date, harvest date, typical application rates of irrigation water and soil cover values as a function of crop development stage were derived from previous published work. Leaf area index (LAI) for rangeland areas NDVI were used to estimate LAI (Fan, Gao et al. 2009):

$$LAI = 0.128 \times \exp(\frac{NDVI}{0.311}) \quad 3.17$$

In terms of agricultural sites, SWAP was simulated twice according to the source of LAI. The standard LAI was retrieved from a previous literature review (Qureshi et al. (2013)), and also calculated as equation shown below (Gigante, Iacobellis et al. 2009):

$$LAI = -0.39 + 6 \times NDVI \quad 3.18$$

3.2.5.6. Soil layers and parameters

In SWAP, the maximum number of soil layers allowed is ten (with the present setting) but each layer can be divided into smaller compartments to ensure stability in the numerical computations. In this research study, five layers were considered. The layers were divided into compartments; their thicknesses were varied for each site due to the differences in the land surface types as shown in the map 3.1. This was done to ensure that the water table depth was within the limits of the soil profile.

Soil hydraulic properties were described by the Van Genuchten-Mualem (VGM) parameters (Mualem 1976), (van Genuchten 1987). These parameters are saturated soil moisture content (θ_{sat}), residual soil moisture content (θ_{res}), saturated hydraulic conductivity (K_{sat}), empirical shape parameters (r, a, n). These parameters were derived from pedo-transfer functions (Wösten, Lilly et al. 1998) as a function of texture.

3.2.5.7. Bottom boundary condition

The selected bottom boundary condition was that of a flux determined by the groundwater level. This is option based on calculation the bottom flux as a function of groundwater level using an exponential relation.

3.2.5.8. Model spin-up

A number of 30-year SWAP simulations were conducted with the first years serving as model spin up years, for soil moisture to reach steady state. The water balance simulations SWAP model was used to simulate the historical water balance components for the various study regions, as defined by climate zones and related land use, include potential soil evaporation and transpiration, actual soil evaporation transpiration., and soil water storage changes for desert, rangeland, and agricultural areas. The simulations were conducted from January 1990 to December 2013, driven by daily meteorological data. The simulated soil water contents at different climatic zones will be compared with the NDVI, hydro-meteorological drought indices, and measured soil moisture (SMOS).

3.2.5.9. Running SWAP model

SWAP was simulated for desert, rangelands, agricultural regions that is located in an arid, semi-arid, and mediterranean climatic zones based on measured and ERA interim data. For agricultural region, the simulation was also carried out with calculated LAI (see equation 3.17 and 3.18) and standard LAI. (see table 3.3).

Table 3.3 Overall simulation framework to estimate water balance for desert, rangeland, and agricultural regions, using measured and ERA interim data

Simulation set: Desert-In situ data					
Land cover type	**Site (See map 3.7)**	**Climate zone**	**Weather data**	**Soil properties**	**LAI**
Desert areas	Site (1)	Arid	Same data	Same data	Different data
	Site (2)	Arid			Different data
	Site (3)	Arid			Different data
	Site (4)	Arid	Different data	Different data	Different data
	Site (5)	Arid	Different data	Different data	Different data
	Site (10)	Arid	Different data	Different data	Different data

Simulation set: Desert-ERA interim data					
Land cover type	**Site**	**Climate zone**	**Weather data**	**Soil properties**	**LAI**
Desert areas	Site (1)	Arid	Different data	Same data	Same data
	Site (2)	Arid	Different data		
	Site (3)	Arid	Different data		
	Site (4)	Arid	Different data	Different data	Same data
	Site (5)	Arid	Different data	Different data	Same data
	Site (10)	Arid	Different data	Different data	Same data

Simulation set: Rangelands-In situ data-Calculated LAI					
Land cover type	**Site**	**Climate zone**	**Weather data**	**Soil properties**	**LAI**
Rangelands	Site (16)	Semi-arid	Same data	Same data	Different data
	Site (20)	Semi-arid			Different data
	Site (21)	Semi-arid			Different data
	Site (14)	Semi-arid	Different data	Different data	Different data
	Site (23)	Mediterranean	Different data	Different data	Different data

Simulation set: Rangelands-ERA interim data- Calculated LAI					
Land cover type	**Site**	**Climate zone**	**Weather data**	**Soil properties**	**LAI**
Rangelands	Site (16)	Semi-arid	Different data	Same data	Same data
	Site (20)	Semi-arid	Different data		
	Site (21)	Semi-arid	Different data		
	Site (14)	Semi-arid	Different data	Different data	Same data
	Site (23)	Mediterranean	Different data	Different data	Same data

Simulation set: Agricultural- In situ data-Calculated LAI					
Land cover type	**Site**	**Climate zone**	**Weather data**	**Soil properties**	**LAI**
Agricultural areas	Site (17)	Semi-arid	Same data	Same data	Different data
	Site (18)	Semi-arid			Different data
	Site (19)	Semi-arid			Different data
	Site (22)	Semi-arid			Different data
	Site (6)	Semi-arid	Same data	Same data	Different data
	Site (7)	Semi-arid			Different data
	Site (8)	Semi-arid			Different data
	Site (9)	Semi-arid		Different data	Different data
	Site (15)	Semi-arid	Different data	Different data	Different data

Simulation set: Agricultural- ERA Interim data-Calculated LAI					
Land cover type	**Site**	**Climate zone**	**Weather data**	**Soil properties**	**LAI**
Agricultural areas	Site (17)	Semi-arid	Same data	Same data	Different data
	Site (18)	Semi-arid			Different data
	Site (19)	Semi-arid			Different data
	Site (22)	Semi-arid			Different data
	Site (6)	Semi-arid	Same data	Same data	Different data
	Site (7)	Semi-arid			Different data
	Site (8)	Semi-arid			Different data
	Site (9)	Semi-arid	Different data	Different data	Different data
	Site (15)	Semi-arid	Different data	Different data	Different data

Simulation set: Agricultural- In situ data-Standard LAI					
Land cover type	**Site**	**Climate zone**	**Weather data**	**Soil properties**	**LAI**
Agricultural areas	Site (17)	Semi-arid	Same data	Same data	Same data
	Site (18)	Semi-arid			
	Site (19)	Semi-arid			
	Site (22)	Semi-arid			
	Site (6)	Semi-arid	Same data	Same data	Same data
	Site (7)	Semi-arid			
	Site (8)	Semi-arid			
	Site (9)	Semi-arid		Different data	
	Site (15)	Semi-arid	Different data	Different data	Different data

Simulation set: Agricultural- ERA interim data-Standard LAI					
Land cover type	**Site**	**Climate zone**	**Weather data**	**Soil properties**	**LAI**
Agricultural areas	Site (17)	Semi-arid	Same data	Same data	Same data
	Site (18)	Semi-arid			
	Site (19)	Semi-arid			
	Site (22)	Semi-arid			
	Site (6)	Semi-arid	Same data	Same data	Same data
	Site (7)	Semi-arid			
	Site (8)	Semi-arid			
	Site (9)	Semi-arid	Different data	Different data	Different data
	Site (15)	Semi-arid	Different data	Different data	Different data

Note: 'Same data' represents sites that have same observed weather, soil texture properties, and LAI data, and 'Different data' represents sites that have different observed weather, soil texture properties, and LAI data, as obtained from NDVI (see Eqs 3.17 and 3.18).

3.3. Drought assessment

Analysing and assessing drought is essential in planning and managing water resources. Drought can be assessed in different ways, based on hydrological, socio-economic, meteorological, and agriculture aspects (Nagarajan 2009). Assessment of drought depends on the impacts of drought and factors that caused the drought. An improved understanding of historical droughts, and related impacts, is required for reliable drought assessment (McKee 2000). Historic drought data are a valuable source in quantifying current drought conditions; this is because it allows for comparison and thereby an objective assessment of the relative severity of drought. Necessarily, a long series of data must be available for addressing current conditions in the framework of previous events. Moreover, improving of drought prediction relies upon a sound knowledge of factors that cause drought, their impacts on human and ecological systems, and propagation of hydrological drought to agricultural drought (Boken, Cracknell et al. 2005).

Severity and intensity of drought are the main parameters used for drought assessment, often combined into drought indices (Rossi, Benedini et al. 1992) There are various drought indices used throughout the world, such as Standarised Precipitation Index (SPI), Crop Moisture Index (CMI), Evaporation Deficit Index (ETDI), Palmer Drought Severity Index (PDSI), and (Mishra and Singh 2010).

In the past, assessment of drought was based on ground observations only. Recently, models and remote sensing techniques have started to play a substantial role in the observation of weather, climate and land surface variables and processes; they are increasingly being used to provide data for drought monitoring. Fig. 3.3 shows the methodology of drought assessment in current study

3.3.1. Water balance and drought assessment

In the current study, the water balance study and drought assessment was carried out in Iraq to analyse the water balance components and their seasonal and temporal variations during drought and non-drought years.

3.3.2. Comparison between SPI and SPEI

A key objective of computing SPI and SPEI was to enable a comparison of historical drought assessment based only on precipitation with that based on the combined effects of precipitation and potential evapotranspiration. Both drought indices were obtained using the same log-logistic probability distribution that shows a very close fit to the series of differences between precipitation and evapotranspiration, and also to the monthly precipitation records.

The same probability distribution was used for both indices to allow for reliable comparisons among the series of these two drought indices, to ensure that any differences between the series are only related to the impact of temperature on drought conditions, and not from the calculation method.

3.3.3. Comparison of water balance and drought indices from measured and ERA interim data

This study compares ERA interim data with the measured data to evaluate the quality. The quality of ERA-Interim data. These datasets were used to drive the water balance and drought assessment. The quality of ERA-Interim was assessed by comparing with satellite-based and ground-based observations. In particular, estimates of drought indices (SPI3 and SPEI3), water balance components, and latent heat fluxes (the response of latent heat flux to NDVI)

3.3.4. Monitoring drought based on drought indices and remote sensing

A continuous yearly time series analysis has been carried out in order to study the seasonal, and in terannual course and detect the presence of statistically significant trends in the time series of NDVI, LST and SPI/SPEI. In the present study, LST and NDVI were retrieved to estimate the spatiotemporal distribution of desert, rangeland, agricultural, and marshlands land surface temperature and vegetation status from 2001 and 2015. The remote sensing products together (LST versus NDVI) as drought indicators and also have compared the meteorological drought indices with the remote sensing-based indicators.

The relationship between commonly used meteorological drought indices and soil moisture (a more direct indicator of drought) was also examined, using soil moisture data derived from SMOS. Since the vegetation (NDVI) is significantly associated with drought, soil moisture (SMOS) was used to evaluate the effect of variations in soil moisture on vegetation density.

Monthly and yearly soil moisture (SMOS) was derived, then related to LST, NDVI, and SPI/SPEI to evaluate the link between meteorological drought indices and the soil moisture contents.

3.3.5. The relationship between LST and NDVI

The current study focusses on assessing the evolution of the hydrological state of desert, rangelands, agricultural, and during re-flooding (restoration) and natural drought periods, based on data on vegetation cover, drought indices derived from meteorological variables, and land surface temperature (LST). Different types of vegetation indices are available to estimate the vegetation cover, but the Normalized Difference Vegetation Index (NDVI) is the most efficient, and most commonly used one (Liu and Huete 1995). There exists a strong correlation between LST and NDVI. LST is a good indicator of the relative effects of evapotranspiration and warming of the lower atmosphere by the land surface which can provide important information about the surface biophysical properties and state, as also affected by the local climate. Therefore, this study assesses the temporal evolution of the Iraqi regions state, as affected by natural or human-induced changes to the local hydrology, using MODIS derived multi temporal data of NDVI and LST.

Assessing desert, rangelands, agricultural, and wetland ecological function is important in order to evaluate how the recovery processes and the restoration methods that have been used are achieving their goals; by understanding the past and current land cover vegetation, combined with information on marshland ecosystem functioning as is implicit in variables such as land surface temperature.

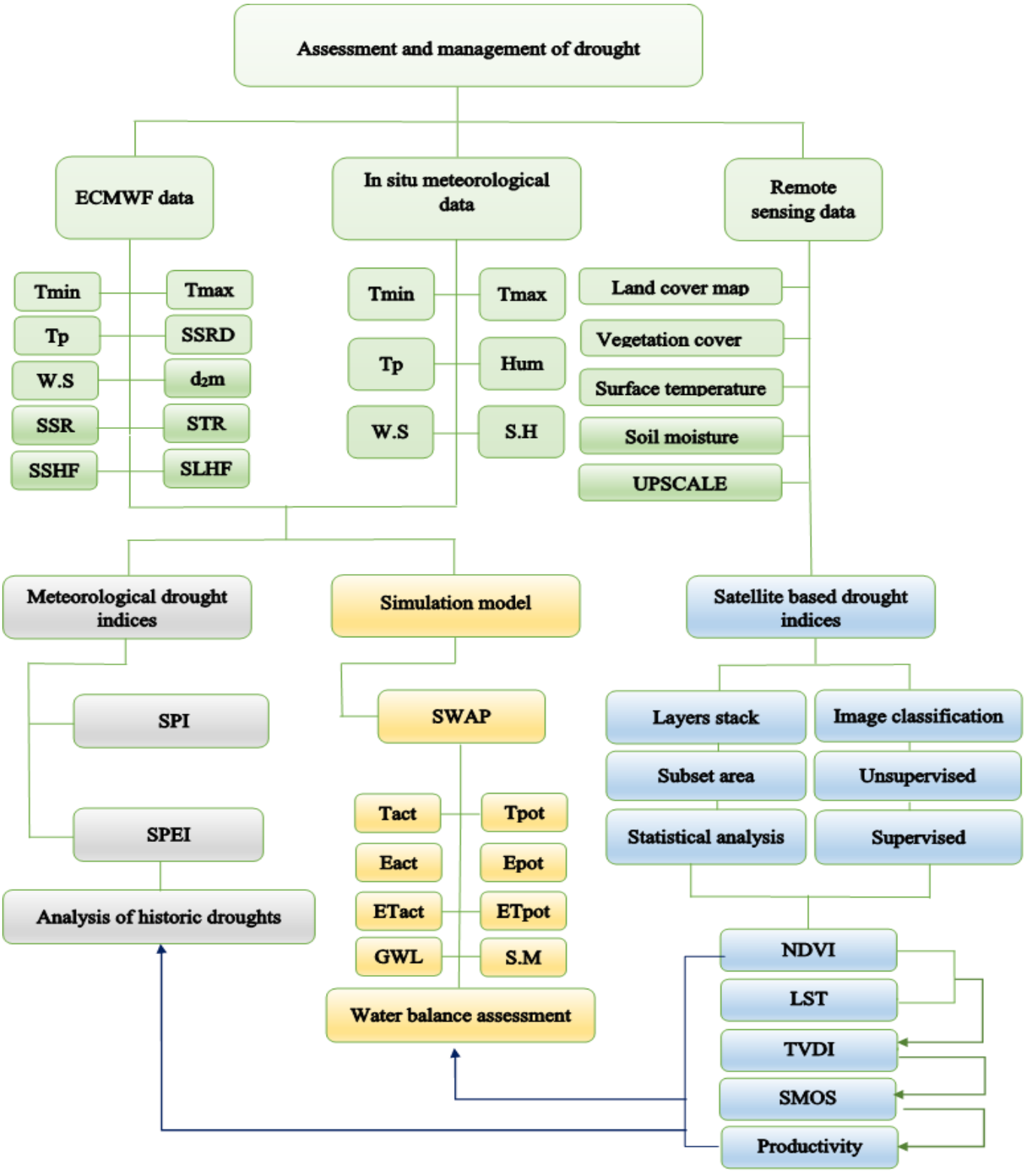

Figure 3.3 Framework of drought assessment

Where: T_{min}: Minimum temperature, T_{max}: Maximum temperature, T_p: Total precipitation, $W.S$: Wind speed, d_2m: Dewpoint temperature, HUM: Humidity, $S.H$: Sunshine hours, $SSRD$: Surface solar radiation downward, STR: Net longwave radiation, SSR: Net shortwave radiation, $SLHF$: Surface sensible heat flux, T_{pot}: Potential evapotranspiration, E_{pot}: Potential evaporation, ET_{pot}: Potential evapotranspiration, T_{act}: Actual transpiration, E_{act}: Actual evaporation, ET_{act}: Actual evapotranspiration, GWL: Ground water level, $SMOS$ Soil Moisture and Ocean Salinity, LST: Land surface temperature, $NDVI$: Normalised difference vegetation index, SPI: Standardised precipitation index, $SPEI$: Standardised precipitation evapotranspiration index, $SWAP$: Water balance model simulation, $R.S$: Remote sensing data.

4. Chapter four: Results chapter

4.1. Introduction

This chapter presents the results obtained from data collection (meteorological and remote sensing data), data generation (e.g. from models) and analysis. The results are arranged following the order of the specific objectives of the research (see Section 1.5). In relation to the first objective, an analysis of historical drought using meteorological drought indices over the study area is provided. These indices are then evaluated together with remote sensing and reanalyses data, i.e. NDVI, LST, SMOS, and latent heat flux from ERA-Interim, for the second objective. The latter part of the chapter presents the results of objective three; i.e. assessment of the water balance through SWAP model simulations and comparison of the water balance between surfaces.

Note that a number of sites were available for reach region, each with their own time series of in-situ and ERA-Interim derived meteorological data. However, in the sections below only one representative site is shown for each region, as typified by its main land cover/use (desert (site 4), rangeland (site 23), agricultural area (site 19)). This was done to reduce the number of plots, so that repetition was avoided and the story line remained clear. The other plots, and related discussion are presented in Appendices.

4.2. Estimation methods for potential evapotranspiration (PET)

Fig. 4.1 shows that the three methods used to calculate PET (see Section 3.2.2) exhibit the same temporal behaviour and tendency, as expected for site 23 (based on Penman-Monteith), that showed ET0 slightly decreased from 2005 to 2012. The average values of daily weather variables for the period 2001–2013 are employed in the FAO P–M equation for the calculation of monthly averages of ET0 for representative sites for each of the three main sites; Fig. 4.1 shows that ET0 values derived from the FAO P–M values are higher than those generated by the Hargreaves and Thornthwaite method. Thornthwaite's equation produces lower values when compared to the other equations, but many researchers use this equation to estimate the water balance of watersheds in semi-arid areas, such as Iraq. (Saud, Said et al. 2014).

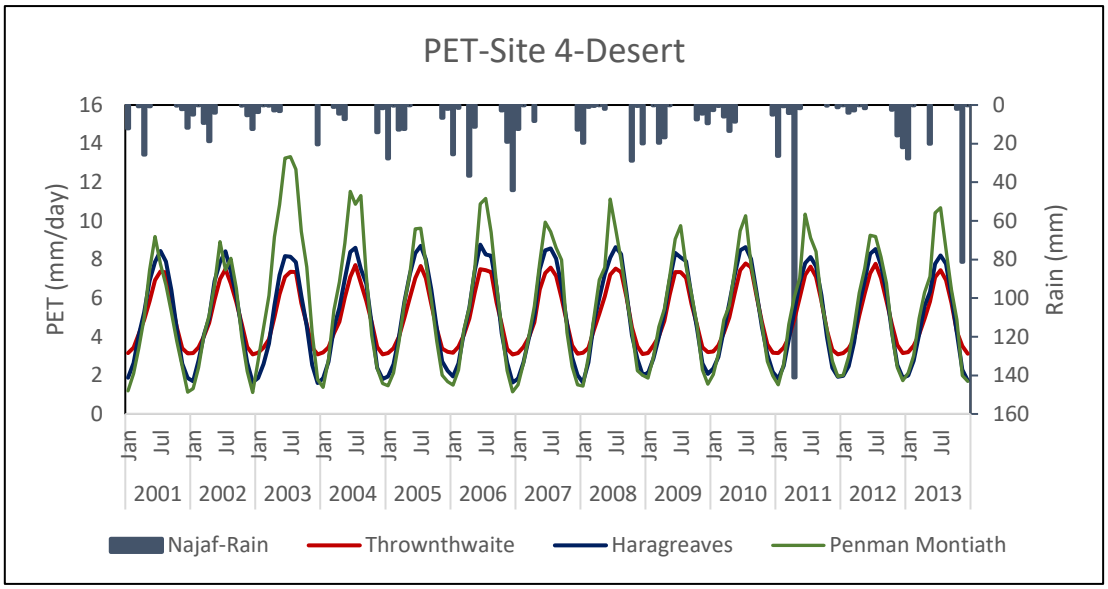
PET-Site 4-Desert
PET (mm/day)
Rain (mm)
Najaf-Rain
Thrownthwaite
Haragreaves
Penman Montiath

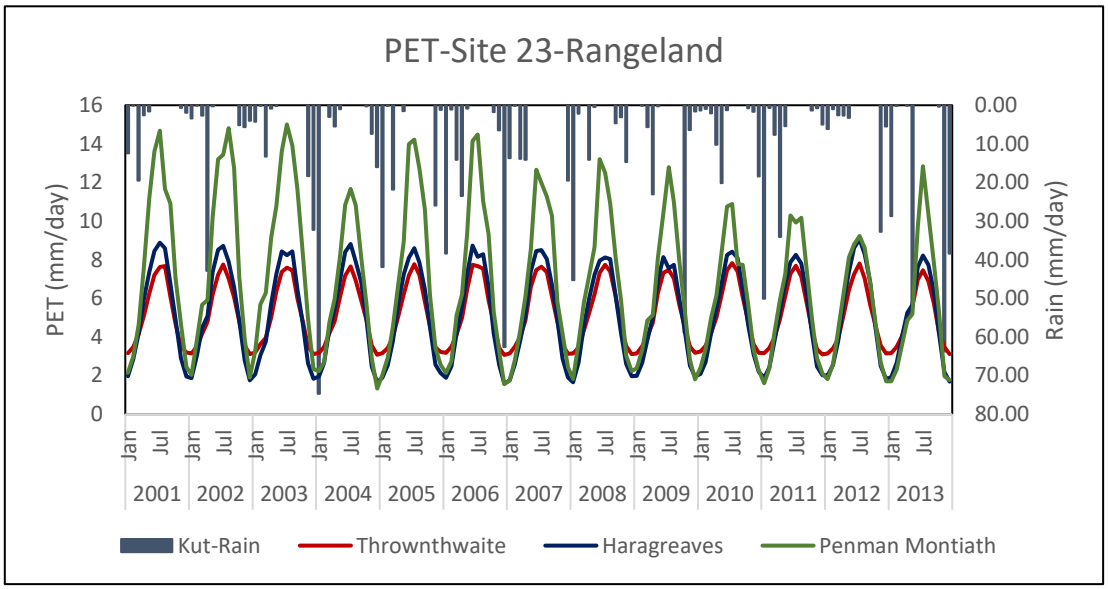
PET-Site 23-Rangeland
PET (mm/day)
Rain (mm/day)
Kut-Rain
Thrownthwaite
Haragreaves
Penman Montiath

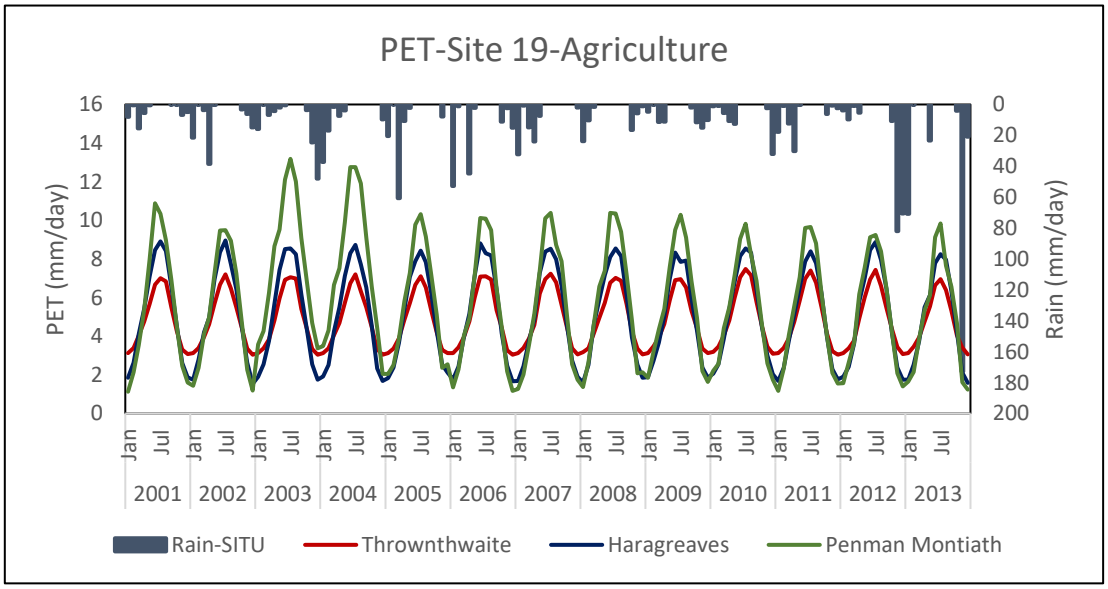
PET-Site 19-Agriculture
PET (mm/day)
Rain (mm/day)
Rain-SITU
Thrownthwaite
Haragreaves
Penman Montiath

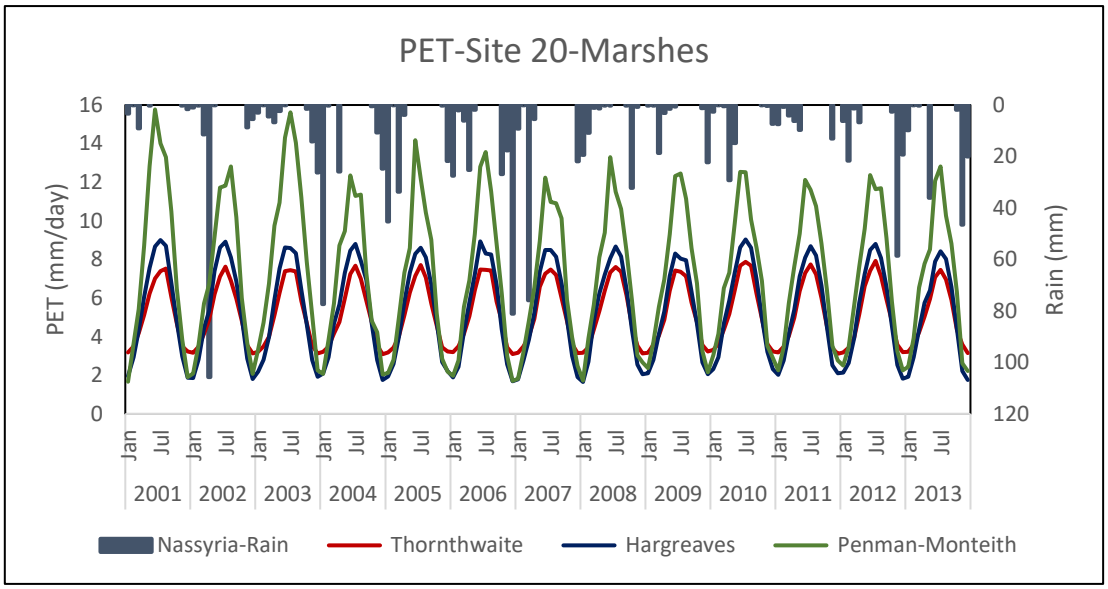

Figure 4.1 A Comparison of methods for the calculation of potential evapotranspiration (PET) for three typical surface types, and marshlands area in Iraq during 2001-2013.

4.3. Assessment of spatiotemporal drought in the Iraqi area during the period 2001-2015

4.3.1. The standardised precipitation drought index (SPI-3)

The yearly SPI-3 values (Fig 4.2), as derived from the *measured datasets*, showed that most years were representative of near normal to slightly wet conditions; 2013 was the wettest year during the study period for all study regions. SPI-3 values derived from the *ERA interim dataset* indicated that the drought conditions for the study period could be classified as near normal, with the highest SPI-3 values (hence the wettest conditions) observed from 2013 to 2015 for all regions.

4.3.2. The standardised precipitation evapotranspiration drought index (SPEI-3)

Based on *measured meteorological data*, Fig 4.2 shows that SPEI-3 values indicated normal to moderate drought conditions during the study period. It appeared that all sites in the desert, agricultural, and rangelands areas experienced near normal to moderate drought conditions from 2001 to 2009. However, in general, there were more drought occurrences between 2006 and 2010; between these years SPEI-3 values were much more negative compared with drought years during the period of 2001 to 2005 ($\geq$ -1). Also, 2010 can be classed as a severe drought year for nearly all sites (SPEI-3 nearly -2). Furthermore, 2014 was classified as the wettest year in the study period; SPEI-3 was positive for all sites. Compared to the other regions, Site (23) was least affected by drought, for example 2010 was classified as a moderate rather than severe drought year (SPEI-3 roughly ~ -1).

According to SPEI values calculated using the *ERA interim dataset*, near normal ($-1.00 \leq$ SPEI-3 $<$ -1.00) to moderate drought conditions were observed from 2001 to 2009 throughout the country. ERA-based SPEI-3 values also indicated an increased drought occurrence from 2006 to 2010 over the three climatic zones. Mostly, moderate drought conditions occurred between 2007 to 2009 in the desert region, while values were near normal for agricultural and rangelands areas.

This study also investigated the frequency and severity of drought for the marshlands region in Iraq; (Fig. 4.2) show values are typically near to normal at most of years based on SPI-3. It shows that SPEI-3 values calculated for the marshes indicated that the period from 2001 to 2007 could be considered wet (near normal). In contrast, during the period 2008 to 2012 the

marshlands experienced drought most frequently in the entire time series (almost always near normal to moderate drought, except for 2010 which was a severe drought year).

Fig 4.2 also shows that severe drought conditions occurred in 2010 for desert sites. ($-2.00 \leq SPEI < -1.50$), while drought was moderate for the other land use types. The years 2013 to 2015 were the wettest during the period 2001–2015.

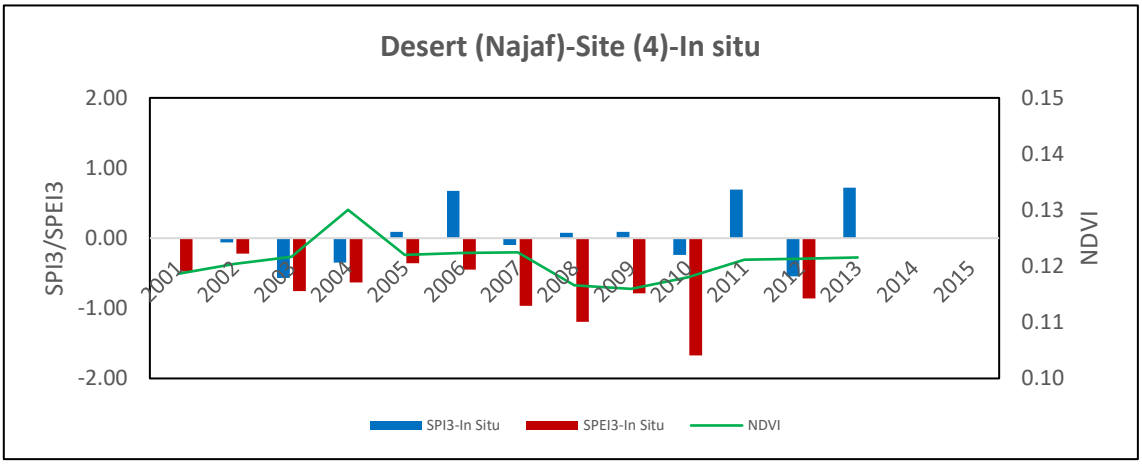
Desert (Najaf)-Site (4)-In situ
SPI3/SPEI3
NDVI
2.00
1.00
0.00
-1.00
-2.00
0.15
0.14
0.13
0.12
0.11
0.10
2001 2002 2003 2004 2005 2006 2007 2008 2009 2010 2011 2012 2013 2014 2015
SPI3-In Situ
SPEI3-In Situ
NDVI

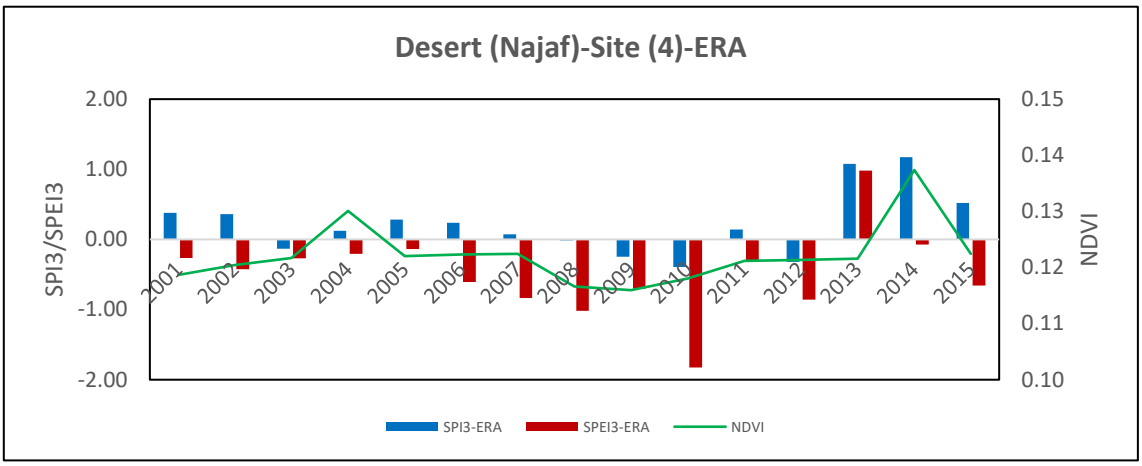
Desert (Najaf)-Site (4)-ERA
SPI3/SPEI3
NDVI
2.00
1.00
0.00
-1.00
-2.00
0.15
0.14
0.13
0.12
0.11
0.10
2001 2002 2003 2004 2005 2006 2007 2008 2009 2010 2011 2012 2013 2014 2015
SPI3-ERA
SPEI3-ERA
NDVI

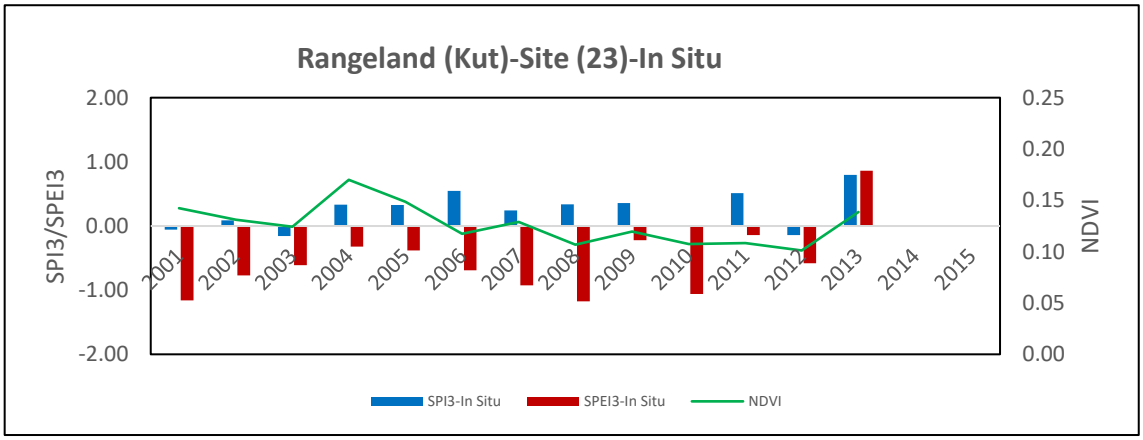
Rangeland (Kut)-Site (23)-In Situ
SPI3/SPEI3
NDVI
2.00
1.00
0.00
-1.00
-2.00
0.25
0.20
0.15
0.10
0.05
0.00
2001 2002 2003 2004 2005 2006 2007 2008 2009 2010 2011 2012 2013 2014 2015
SPI3-In Situ
SPEI3-In Situ
NDVI

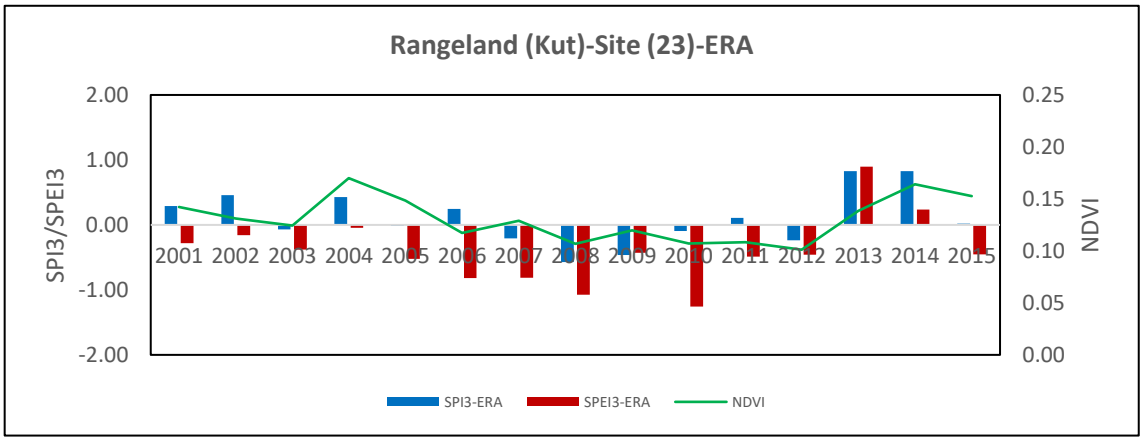
Rangeland (Kut)-Site (23)-ERA
SPI3/SPEI3
NDVI
2.00
1.00
0.00
-1.00
-2.00
0.25
0.20
0.15
0.10
0.05
0.00
2001 2002 2003 2004 2005 2006 2007 2008 2009 2010 2011 2012 2013 2014 2015
SPI3-ERA
SPEI3-ERA
NDVI

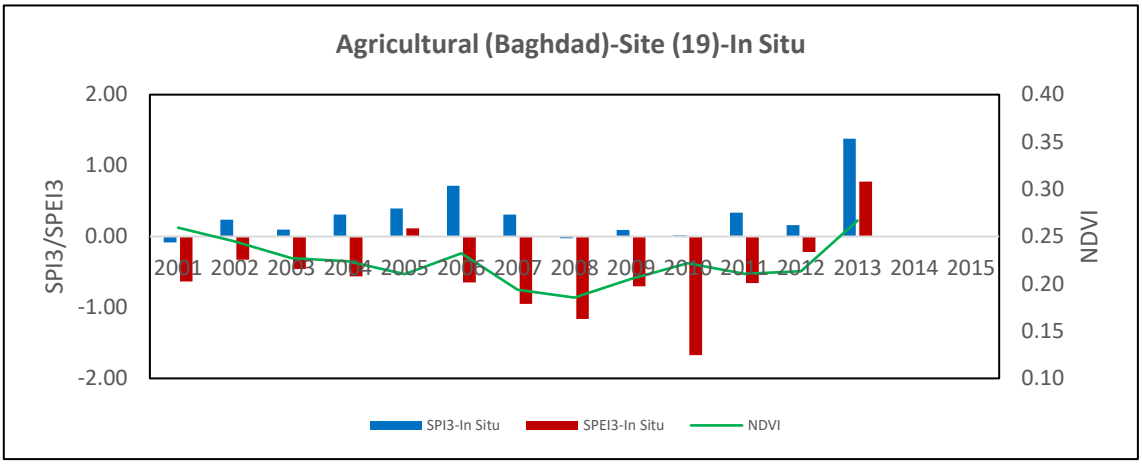
Agricultural (Baghdad)-Site (19)-In Situ
SPI3/SPEI3
NDVI
2.00
1.00
0.00
-1.00
-2.00
0.40
0.35
0.30
0.25
0.20
0.15
0.10
2001 2002 2003 2004 2005 2006 2007 2008 2009 2010 2011 2012 2013 2014 2015
SPI3-In Situ
SPEI3-In Situ
NDVI

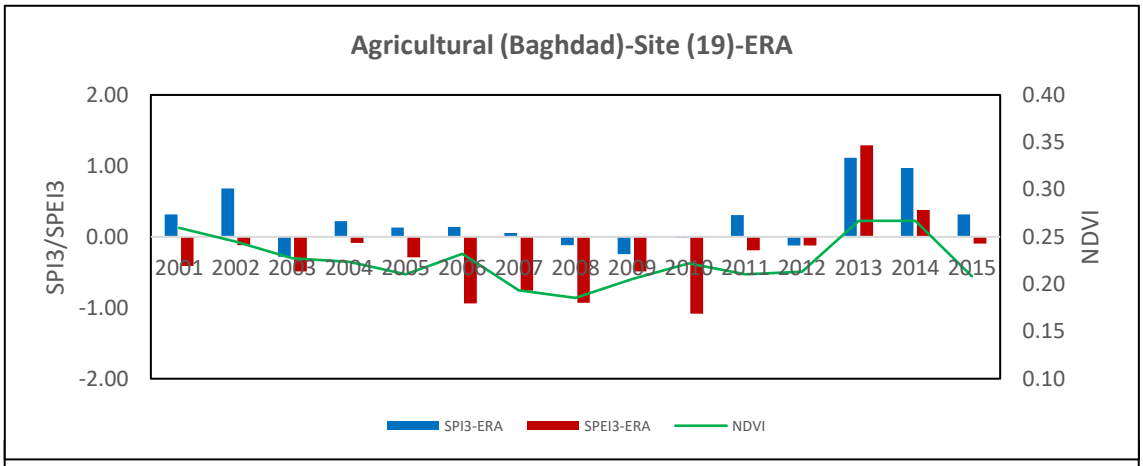
Agricultural (Baghdad)-Site (19)-ERA
SPI3/SPEI3
NDVI
2.00
1.00
0.00
-1.00
-2.00
0.40
0.35
0.30
0.25
0.20
0.15
0.10
2001 2002 2003 2004 2005 2006 2007 2008 2009 2010 2011 2012 2013 2014 2015
SPI3-ERA
SPEI3-ERA
NDVI

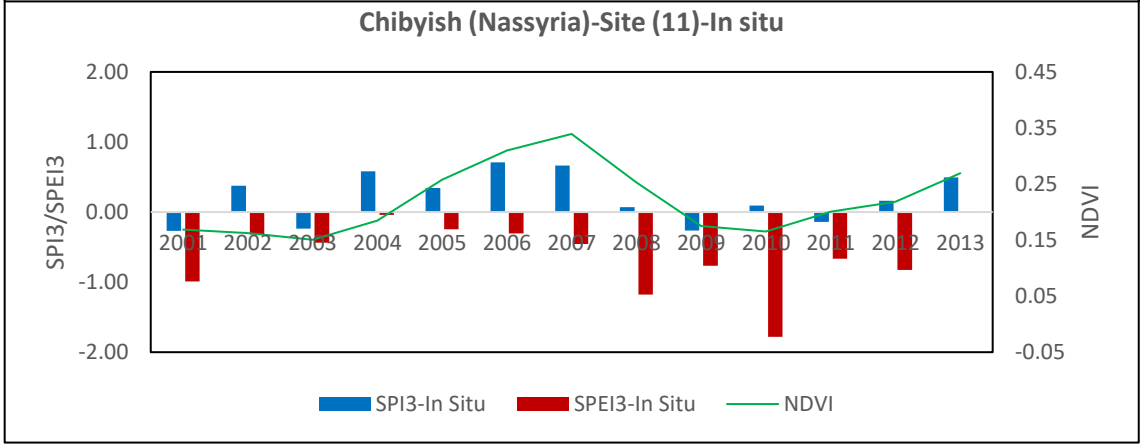
Chibyish (Nassyria)-Site (11)-In situ
SPI3/SPEI3
NDVI
2.00
1.00
0.00
-1.00
-2.00
0.45
0.35
0.25
0.15
0.05
-0.05
2001 2002 2003 2004 2005 2006 2007 2008 2009 2010 2011 2012 2013
SPI3-In Situ
SPEI3-In Situ
NDVI

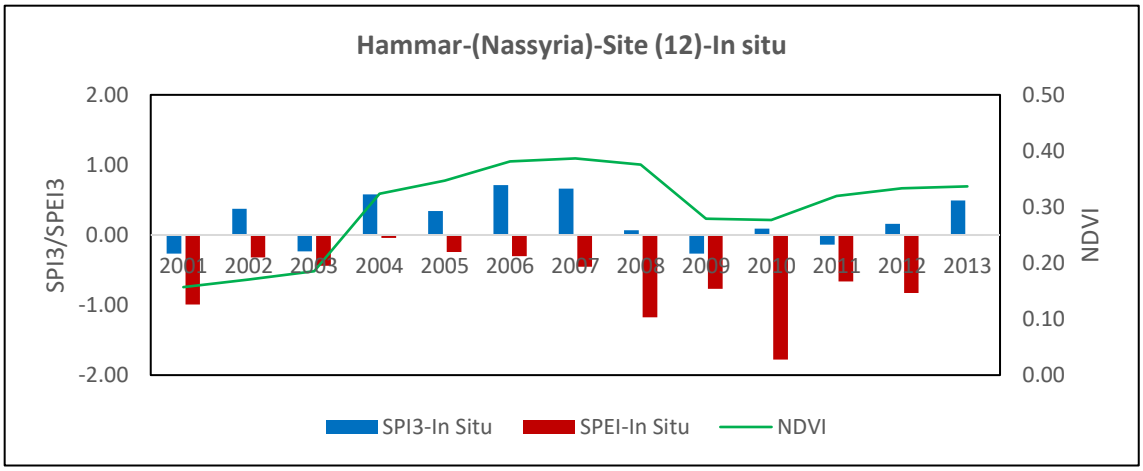
Hammar-(Nassyria)-Site (12)-In situ
SPI3/SPEI3
NDVI
2.00
1.00
0.00
-1.00
-2.00
0.50
0.40
0.30
0.20
0.10
0.00
2001 2002 2003 2004 2005 2006 2007 2008 2009 2010 2011 2012 2013
SPI3-In Situ
SPEI-In Situ
NDVI

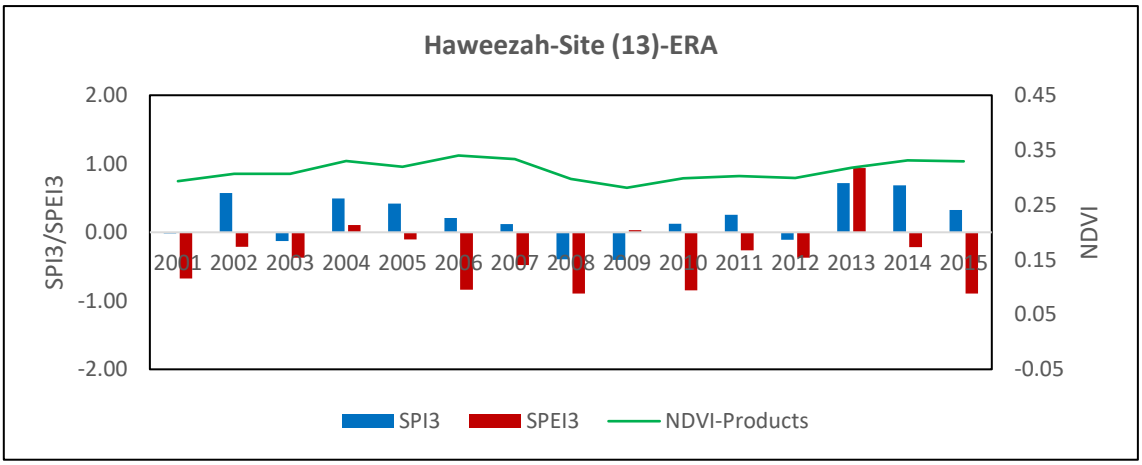

Figure 4.2 Yearly averaged SPI-3 and SPEI-3 values over the period 2001–2015, calculated using measured and ERA interim dataset for different land covers (desert, rangeland, agriculture and marshlands, see Appendix A for other sites). Also shown are NDVI values in green (to be discussed in Section 4.3.3).

4.3.3. Spatiotemporal variability of NDVI

To demonstrate the spatiotemporal variation of NDVI, an indicator of vegetation greenness, and hence an implicit indicator of drought, the monthly NDVI evolutions (green lines) for typical sites selected for the desert, agricultural, and rangelands regions are shown in Fig 4.3 and Appendix B, again between 2001-2015. Overall, NDVI ranged between 0.10-0.5. For the desert site, NDVI varied between 0.10 to 0.17, for the agricultural site values ranged from 0.10 to 0.50, while values between 0.10 to 0.25 were found for the rangelands site. This figure also highlights a clear peak in vegetation in 2004. Overall, the values decreased somewhat from 2006 to 2010. The vegetation condition returned to that before 2006 between 2013 and 2014.

The NDVI plot for the rangeland shows a similar evolution; there was also a tendency of a decreasing NDVI during the years 2006-2010, and 2015. The vegetation was at its greenest between 2013 and 2014. However, this recovery period was followed by heavily reduced values of NDVI in 2015. For the agricultural site (in the semi-arid region), NDVI was reduced from the beginning of the year 2007 to 2010. In general, the vegetation greenness between 2001 to 2012 was lower than that found for 2013 and 2014. For Site 9 in particular (NDVI decreased sharply and fell to the lowest point between 2007 to 2013, to return to more normal values in 2014. NDVI values showed more intra- and inter-annual variations for the rangeland

and agricultural sites (in particular site 19, see Fig. 4.3). This was most likely caused by larger (compared to desert region), and more variable, rainfall events (rangeland) and supplemental irrigation of cultivated crops (mainly wheat in winter season and maize in summer season) in the agricultural region.

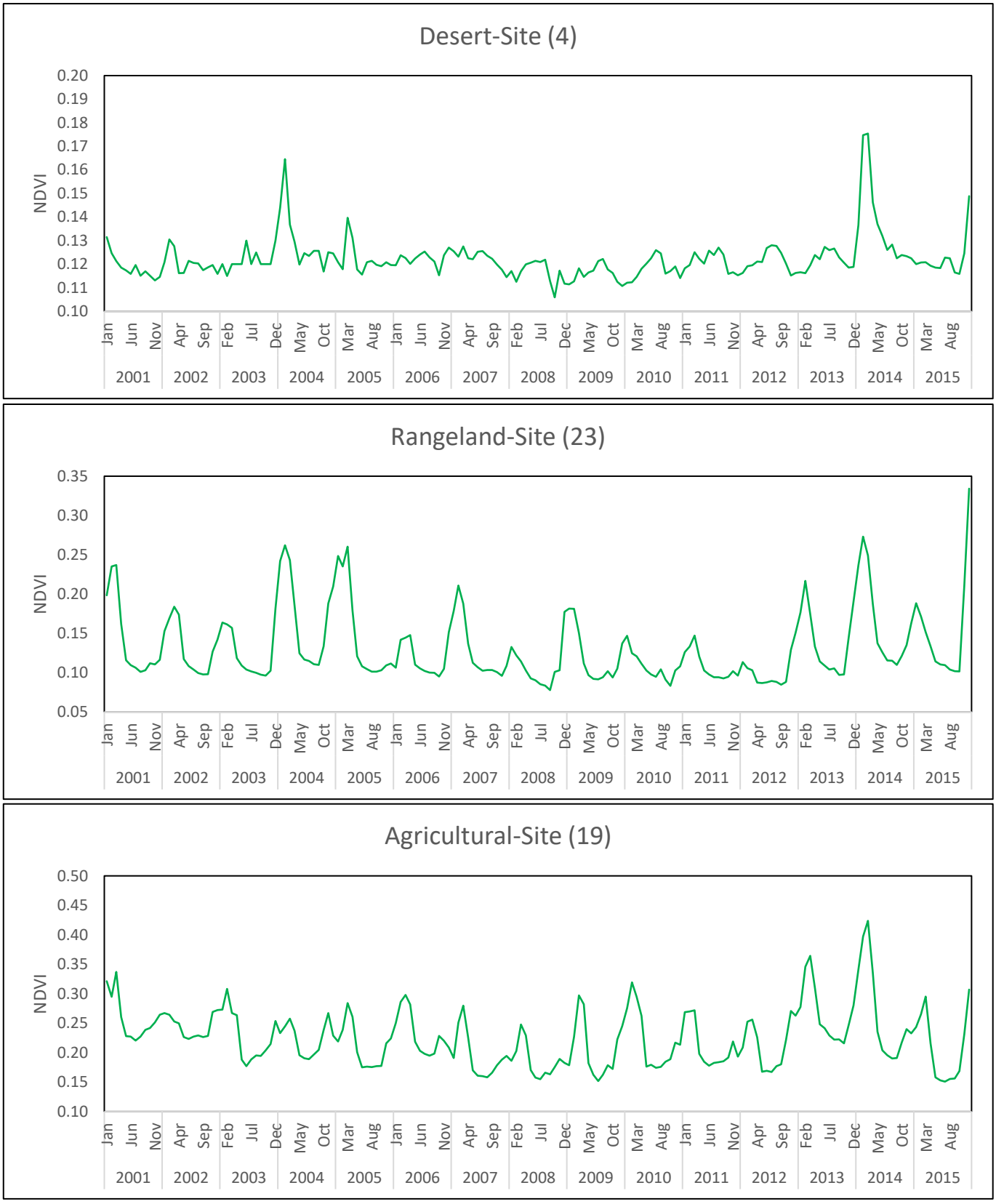

Figure 4.3 Spatiotemporal seasonal and interannual variation in the NDVI for three typical surface types in Iraq during 2001–2015**.**

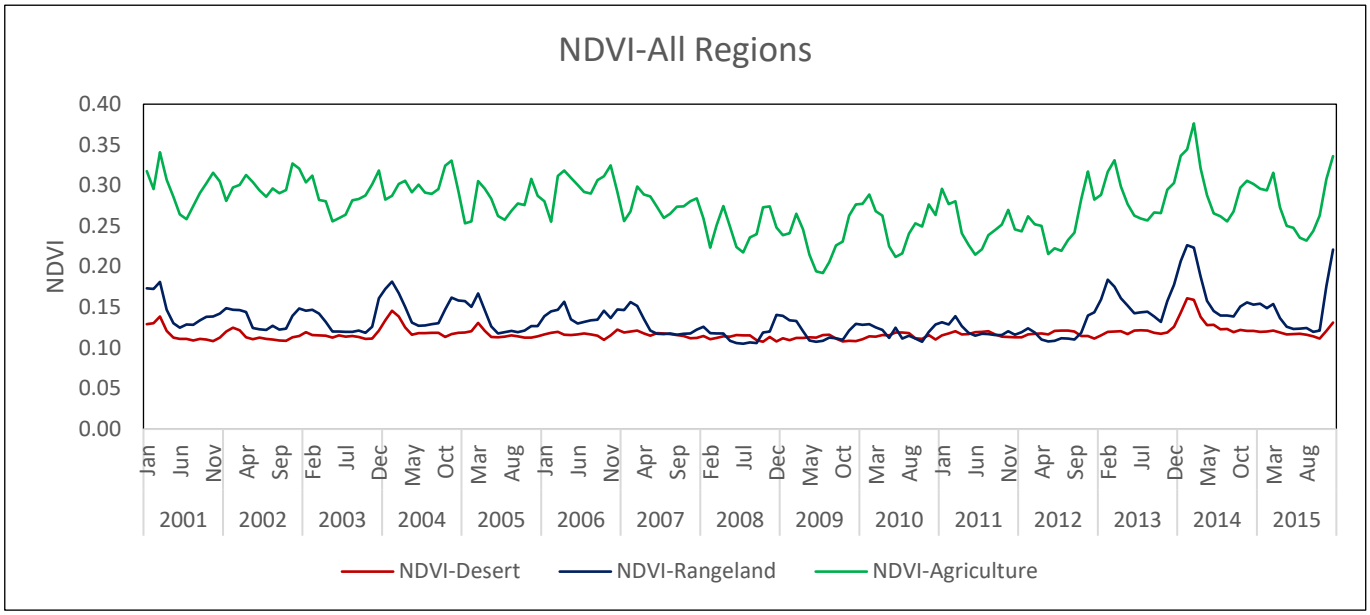

Figure 4.4, showing the average NDVI evolution for each surface types, indicates that there are clear differences between the three land cover types, even when all sites in each region are averaged, in desert (6 sites), rangelands (5 sites), and agricultural (9 sites) regions during 2001-2015.

particular with regards to their NDVI range; 0.10-0.15 for deserts, 0.10-0.25 for rangelands and 0.20-0.40 for agricultural areas. The years from mid-2012 to mid-2015 stands out as a period of more lush vegetation for the agricultural and rangeland sites. For the desert, a flush of vegetation was only implied in 2004 and in particular in 2014. For some years, desert and rangeland NDVI values are at their lowest and very similar to each other (Fig, 4.4); these are the dry years between 2007-2012, when agricultural NDVI went down and SPEI-3 values were largely negative (see Fig. 4.2).

For marshlands, Fig 4.5 shows that NDVI values vary from 0.10 to 0.50 for the overall marshland area. Chibyish marsh had the lowest NDVI values in particular during drainage years (2001-2003, see Section 2.9 for more background on the marshland and their anthropogenic influences), when NDVI values stayed between 0.15-0.22. NDVI started to increase significantly after 2003, and reached its maximum values in 2007 (around 0.40). Hereafter, it decreased sharply reaching values between 2008 and 2010 to values that were nearly as low as during the drainage years. The temporal evolution of NDVI for Hammar marsh

was very similar to that of Chibyish marsh; on average, NDVI reached maximum values between 2004 to 2008, with values as high as 0.45 (year 2007) during the peak of the rainy seasons. In years before 2003, NDVI was relatively low (< 0.20) and the difference between rainy and dry season peaks was much less pronounced. Similarly, low values were also found for the years 2009 and 2010. NDVI reached peak values in 2006 and 2008, then it began to decrease gradually until 2010, picking up again between 2010-2015, when NDVI ranged from 0.20 to 0.35.

Finally, NDVI values of Haweezah marsh showed a much less pronounced periodical variation compared to the other two marshlands. NDVI values vary between 0.25 and 0.40. Maximum values were calculated for years 2006, 2007, and 2012. In 2008 and 2009, NDVI values declined to about 0.25, after which they varied approximately between 0.30-0.35.

Figure 4.5 The monthly average (between 2001 to 2015) of normalized difference vegetation index (NDVI) for the 3 marshland areas.

4.3.4. The relationship between NDVI and drought indices

Time series analysis of NDVI suggests that vegetation in the study area was stressed during the period 2006 to 2010. A more obvious decrease was observed from 2008 to 2010, this indicates low vegetation cover and is most likely to be a result of the severe drought during this period. NDVI values recovered to more normal levels in all regions of the study area in 2011, 2013, and 2014. The ERA interim data showed a similar trend to the SPEI-3 that is based on measured data. It also showed that the wettest years were in 2013 and 2014, when the NDVI values were the highest.

For marshlands, Fig 4.2 shows the NDVI together with both drought indices between 2001 and 2013, for the three main marshes. As already indicated in Fig. 4.5, the NDVI varies considerably, and appears related to the drought indices. The vegetation condition returned to normal after the restoration period, roughly from late 2003 onwards. The NDVI evolution shows that growth was even better than normal during restoration period at all marshes. The vegetation greens up and increases its density from 2004 to 2007 due to increased availability of water, as indicated by SPI-3 values that were continuously larger than zero, and SPEI-3 that had values that are typically classified as near to normal. However, there was a series of drought years after 2008. SPEI-3 was lower than normal in 2009 and a very severe drought was observed in 2010 for Chibyish and Hammar, whereas SPEI values were near to normal at Haweezah. The year 2010 was the most serious drought year; it caused NDVI to decrease sharply so that it reached its lowest point in the timeseries. For that year the SPEI-3 was nearly –2, indicating that there was a severe deficit in the precipitation (SPI-3 was nearly zero), whereas potential evapotranspiration reached its maximum. SPEI-3 was considered as it represents the monthly water balance (the difference between precipitation and PET) which was deemed give a better result for identifying drought sensitivity. The NDVI values were compared to SPEI-3 during draining and drought periods (2001 to 2003), drought years (2008 to 2010), and relatively wet years (2005 to 2008); a peak of NDVI is observed during 2007. The results shown in Figure 4.2 indicates that there was clear difference between the SPEI-3 values of these years. The values remained less than -1 for the drought years (2008 to 2010) and values remained around zero indicating wet conditions for non-drought years (2005 to2007).

The link between drought and changes in vegetation cover is also illustrated by the relatively high correlation coefficients between NDVI and the meteorological drought indices, SPI-3 in particular (see Table 4.1). Values for R (NDVI versus SPI-3 regressions) range between 0.22 (in-situ) and 0.55 (ERA-Interim) for deserts, between 0.57 and 0.75 for rangeland, between 0.48 and 0.58 for agricultural sites and 0.69 and 0.57 for Chibyish and Hammar marshes respectively. Values for NDVI versus SPEI-3 correlation coefficients are generally smaller (0.23 to 0.58), because water supply is more important in determining greenness than atmospheric demand. The results demonstrated the advantage of using SPEI over SPI due to its capability in identifying and exploring the role of evapotranspiration variability, largely via temperature variability.

Table 4.1 Correlation coefficients between SPI-3 and SPEI-3, and NDVI based on measured and ERA interim meteorological data over Iraq. Maximum values per region are shown in bold, minimum values in red. Average values per region are also given.

Region	Site	SPI-NDVI (In Situ)	SPEI-NDVI (In Situ)	SPI-NDVI (ERA)	SPEI-NDVI (ERA)
Desert	1	0.02	0.18	0.65	0.37
	2	0.006	0.17	0.54	0.29
	3	0.25	0.19	0.13	0.22
	4	0.12	0.30	0.58	0.36
	5	0.50	0.26	0.65	0.35
	10	0.45	0.37	0.74	0.18
Average		0.22	0.25	0.55	0.30
Rangeland	16	0.65	0.52	0.78	0.60
	20	0.55	0.60	0.80	0.64
	21	0.79	0.69	0.84	0.74
	14	0.67	0.67	0.69	0.33
	23	0.17	0.26	0.62	0.57
Average		0.57	0.55	0.75	0.58
Agricultural	15	0.39	0.52	0.64	0.61
	17	0.33	0.34	0.64	0.37
	18	0.28	0.43	0.67	0.50
	19	0.45	0.51	0.75	0.61
	22	0.38	0.53	0.76	0.66
	6	0.74	0.55	0.67	0.01
	7	0.66	0.43	0.48	0.07
	8	0.64	0.43	0.50	0.006
	9	0.45	0.21	0.12	0.18
Average		0.48	0.44	0.58	0.34
Marshlands	Chibyish (11)	0.69	0.31	-----	----
	Hammar (12)	0.57	0.14	----	----
	Haweezah (13)	----	----	0.63	0.02
Average		0.63	0.23	0.63	0.02

4.3.5. Variation of land surface temperature

Fig. 4.6 and Appendix C shows the land surface temperatures derived from MODIS for three locations representing the three land surface types. It shows that the highest temperature is between 50℃ and 60℃ in the summer, whereas the minimum temperature in the winter dips below 20℃. Fig 4.6 shows that winter minima vary more in time than summer maxima, and that maxima are considerably lower for the agricultural sites (see also Appendix C. Drought years, nor the period 2008-2010, do not have LSTs that stand out. Rangelands seem to have two summer peaks, or rather a brief and small dip during the period when LST were highest, for the dry years in particular. This phenomenon could potentially be related to pasture phenology.

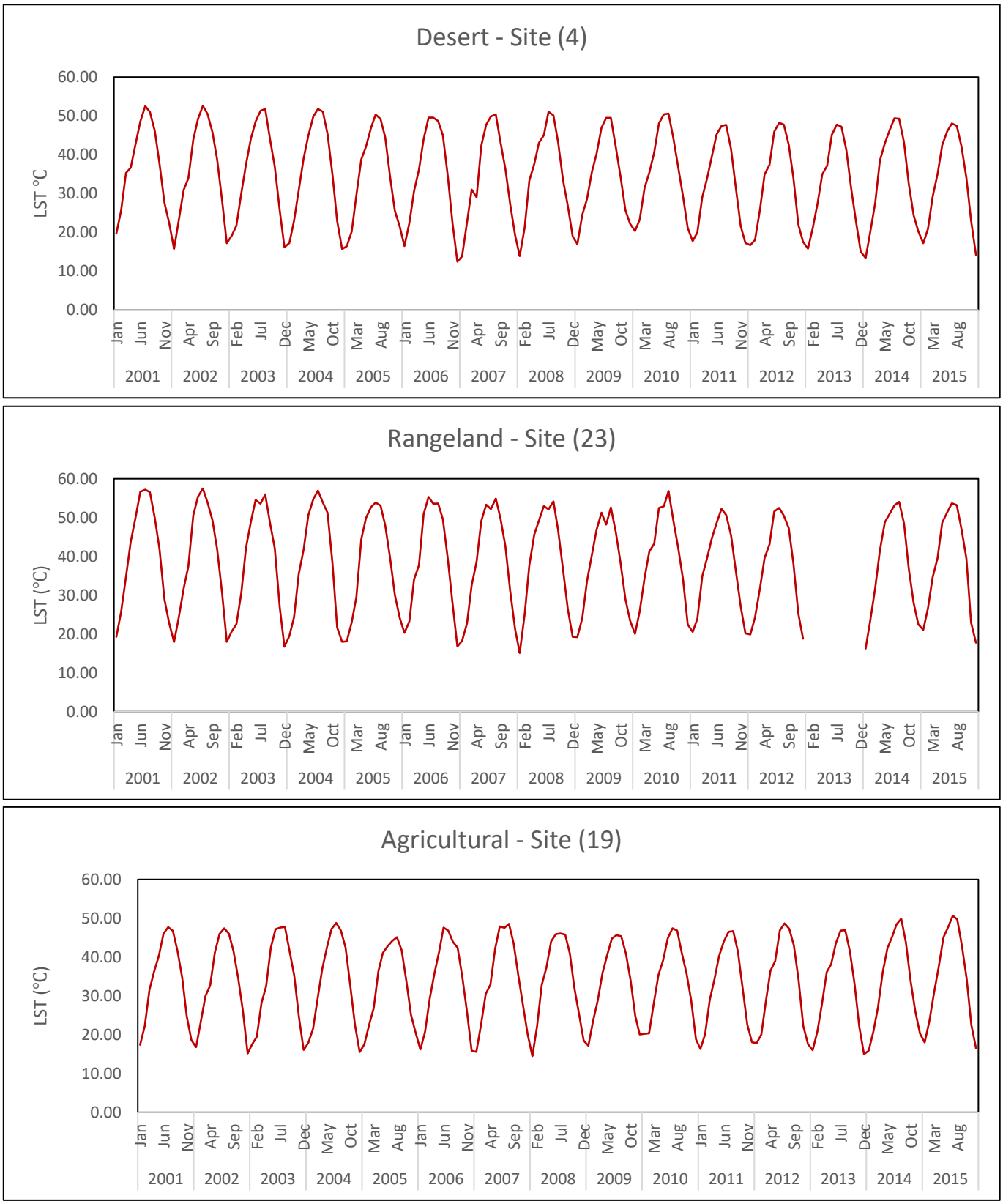

Figure 4.6 Spatiotemporal seasonal variation in the LST (℃) for typical desert, rangeland, and agriculture sites during 2001–2015.

The multi-site averages of land surface temperature for the desert, rangeland, and agricultural regions are shown in Fig 4.7. As per Fig. 4.6, desert and rangeland averages are virtually

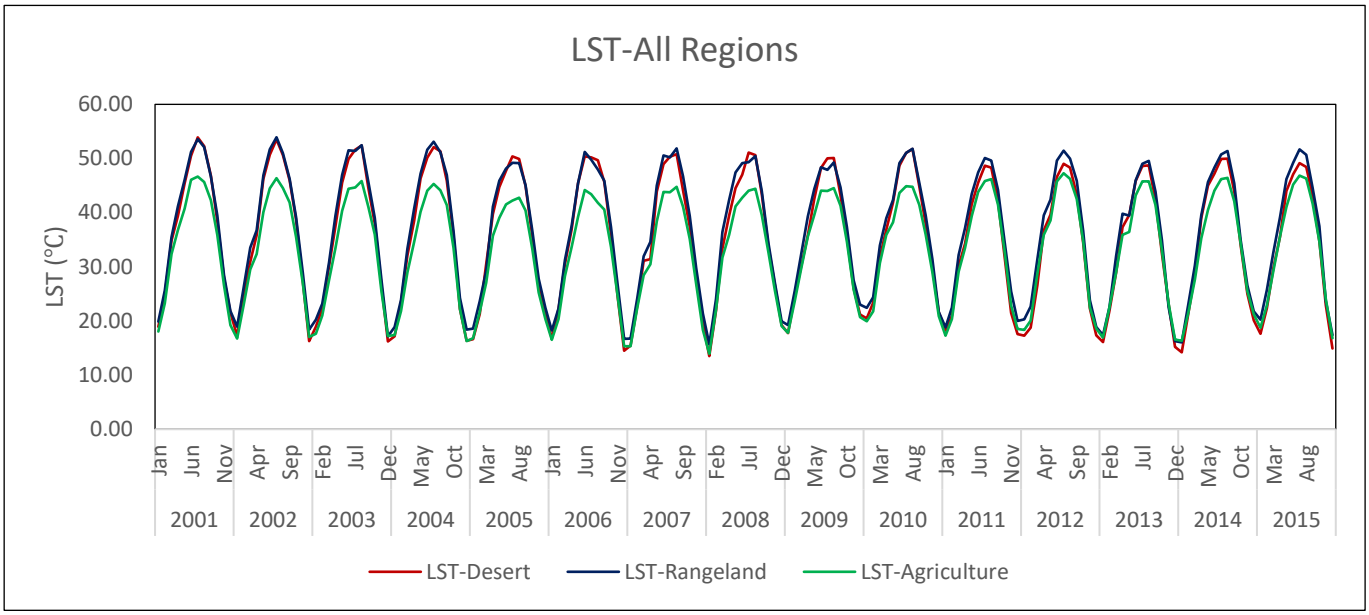

Figure 4.7 Spatially averaged evolution of LST throughout desert, rangelands, and agricultural regions during 2001-2015. Each line is based on 6, 5 and 9 sites for desert, rangeland and agricultural regions, respectively.

indistinguishable, whereas the average for the agricultural areas is up to 8 degrees or so lower in summer, although these differences are much less pronounced for the years 2011-2015 (wetter years). During winter differences are small, although rangeland is often slightly higher. In more recent years, winter LSTs for the desert zone have been found to be lower than that of the other zones.

Fig 4.8 shows that LST values vary from 10 to 60℃ for the overall marshland area. LST of Chibyish marsh had the highest values, in particular during drainage years (2001-2003). LST started to decrease after 2003, and reached its minimum values in 2005 to 2007. Hereafter, it increased sharply reaching values between 2008 and 2010 that were nearly as high as during the drainage years.

The temporal evolution of LST for Hammar marsh was very similar to that of Chybyish marsh; on average, LST reached its lowest values between 2004 to 2008, during the peak of the rainy seasons. In the years before 2003, LST was relatively high. Similarly, high values were also found for the years 2009 and 2010. LST was relatively low in 2006 and 2008, then it began to increase gradually until 2010, after which it settled at lower values between 2010-2015.

LST values of Haweezah marsh showed a much less pronounced periodical variation compared to the other two marshlands. Maximum and minimum values of LST were almost constant throughout 2001-2015, and lower than the values observed for Chibyish and Hammar marshes.

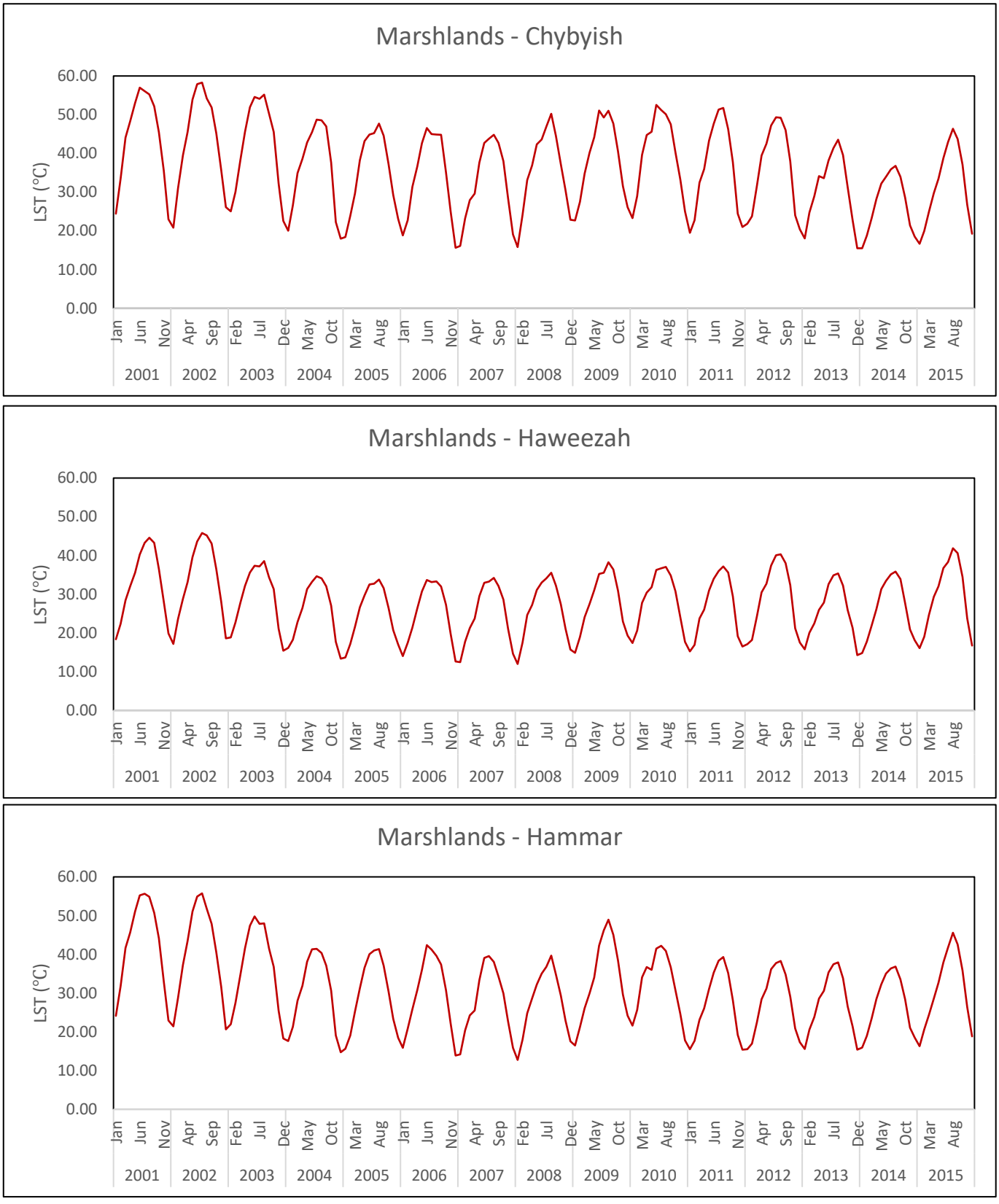

Figure 4.8 Spatiotemporal seasonal variation in the LST (℃) throughout marshes during 2001–2015.

Section 4.3.6 investigates the generality of the NDVI and LST relationship over a wide range of climatic regimes encountered over Iraq. Standard precipitation index (SPI) and standardised precipitation evapotranspiration index (SPEI), which are measures of drought and assessed from meteorological data, were used to verify the remote sensing results.

4.3.6. Relationship between Vegetation-indices and LST

By computing the values of NDVI and LST of the marshland sites for each month for the years between 2001 and 2015 and plotting them against each other, separately for each year, it was found that there is a strong relationship between NDVI and LST over Chibyish marshes area for most years (Fig 4.9). The spatiotemporal variations of surface temperature are affected by the considerable changes in vegetation cover between 2001 to 2015 in the marshes. For the years when the marshes were drained or affected by drought, NDVI has an inverse relation with LST; this strong inverse relationship is evident for Chibyish and Hammar (see Appendix D) marshes from 2001 to 2003. NDVI-LST correlation coefficient (R) was -0.94 and -0.93 for 2001, -0.78 and -0.95 for 2002, and -0.86 and -0.54 for 2003 and 2004, for Chibyish and Hammar marshes, respectively, and have statistically significant positive correlations (p-value < 0.05). In contrast, an increasing NDVI was accompanied by an *increase* in surface temperature during the marsh restoration periods (e.g. 2004); the correlation converted to positive in this period. The highest positive correlation was observed in 2007 for Chibyish ($R= 0.75$, P-value < 0.05), and in 2012 for Hammar marshes ($R=0.89$, P-value < 0.05). Haweezah had much lower, albeit still positive, correlations for this period. As a result of reduced vegetation density due to drought in 2009 to 2010, a strong inverse relationship between surface temperature and NDVI value was found again for Chibyish marshes; R-values of -0.60 and -0.85, respectively, were recorded for these years, (which showed a significant increase (p-value < 0.05) in surface temperature over Chibyish marshes). Haweezah had R- values of -0.34 and -0.46 for 2009, and 2010, respectively, while correlation was weaker for Hammar marshes (-0.21 in 2009, and in fact positive (0.33) for 2010). Draining of the marshes between 2001 to 2003, and droughts events in 2009-2010 caused a decrease in vegetation cover resulting in decreasing NDVI values of the marshes.

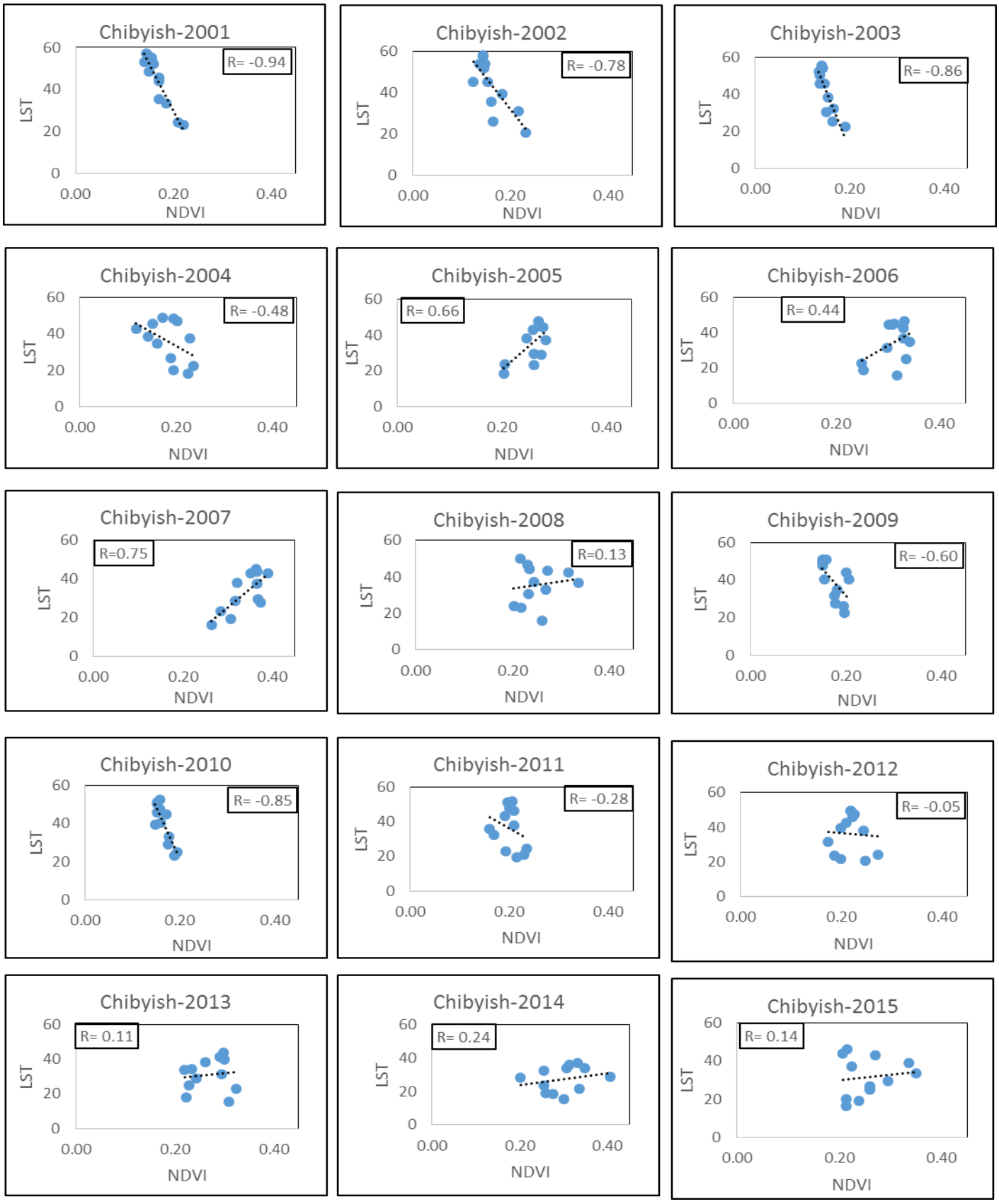

Figure 4.9 Mean values of LST and NDVI over Chibyish marshes

A joint plot of NDVI and LST over the three regions is shown in Fig 4.10. It was observed that NDVI and minimum LST both decreased between 2008 to 2010 for all regions. Conversely, a different scenario was apparent for the period from 2011 to 2015, where NDVI increased while the minimum LST decreased at the same time. From an evapotranspiration perspective, the second type of behaviour makes more sense as more vigorously growing vegetation cover implies higher transpiration values and therefore lower LSTs. Nevertheless, LST is also influenced by the other fluxes in the energy balance (see section 2.4.2) and by the air temperature, so it is often hard to point at the exact reason why LST is going up or down during a certain period.

For the desert region, the relationship between LST and NDVI was found to be positive after 2008 at many sites in this region, while high negative R values were seen at sites 1, 10) and 5 during 2002 and 2003. For rangelands and the sites in the agricultural region, the highest negative R values were found during 2001 to 2004, and 2008 to 2009 for sites 14, 21, and 23, (see appendix D). This links well with SPEI-3 values, see Figs. 4.2.

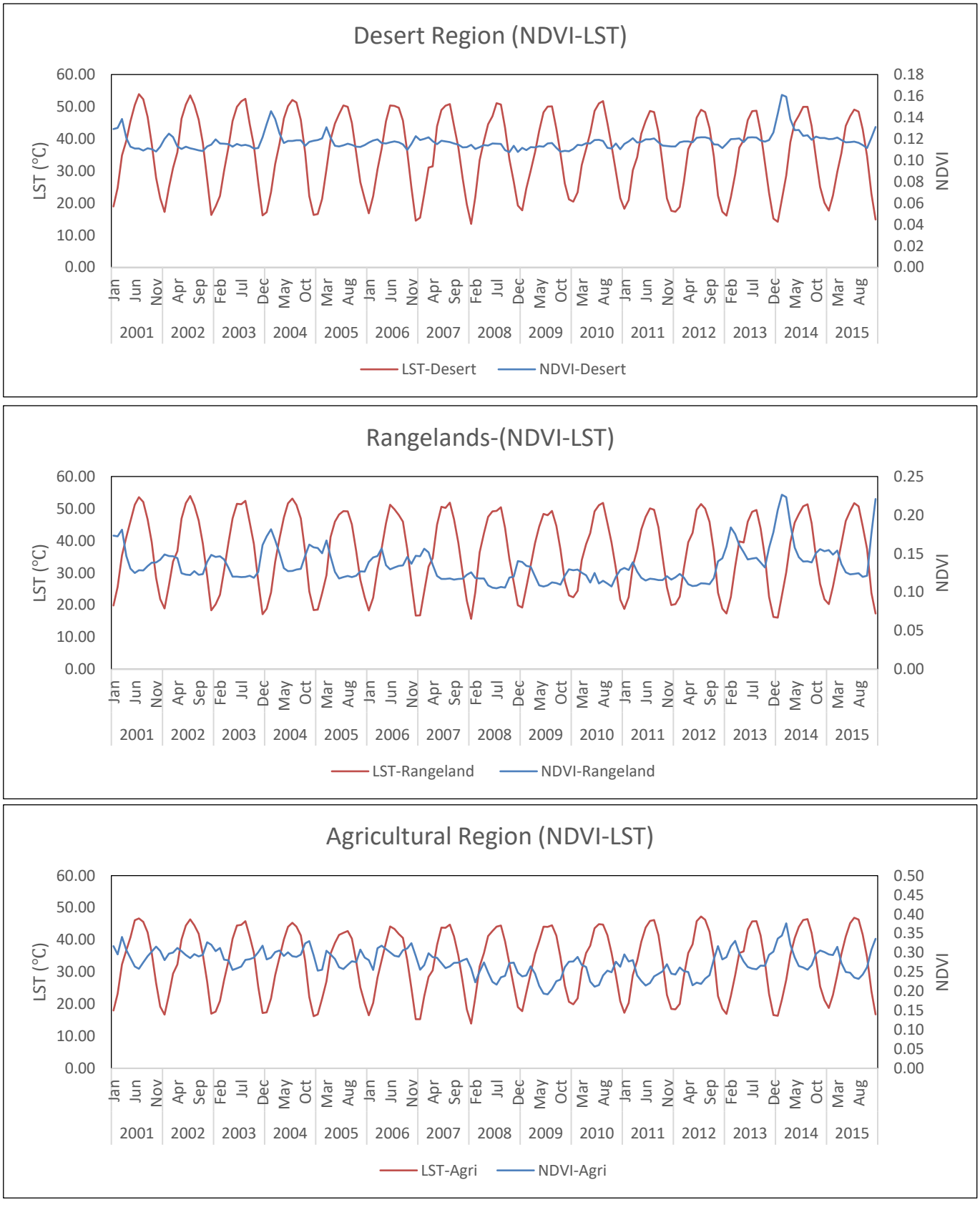

Figure 4.10 Spatiotemporal seasonal variation in the LST (℃) and NDVI throughout desert, rangeland, and agricultural during 2001–2015.

4.3.7. Soil moisture from SMOS data and comparison with NDVI

Fig. 4.11 shows the values of SMOS-retrieved surface soil moisture content (SMC) between 2010 to 2015 over all study-sites, averaged per zone, in Iraq. SMOS data were not available prior to this period. The results show a similar temporal evolution of SMC for all zones, but with Mediterranean (rangelands) and semi-arid (agricultural, most of these irrigated, although not during war years) zones having a more pronounced seasonal and interannual variation than that observed for the arid (desert) zone. Overall, all years exhibit a relatively dry period extending from May to September, and higher SMC values in January, February, November, and December; March, April and October have intermediate SMC values. The years 2010-2012 overall exhibited lower SMC values than years 2013-2015.

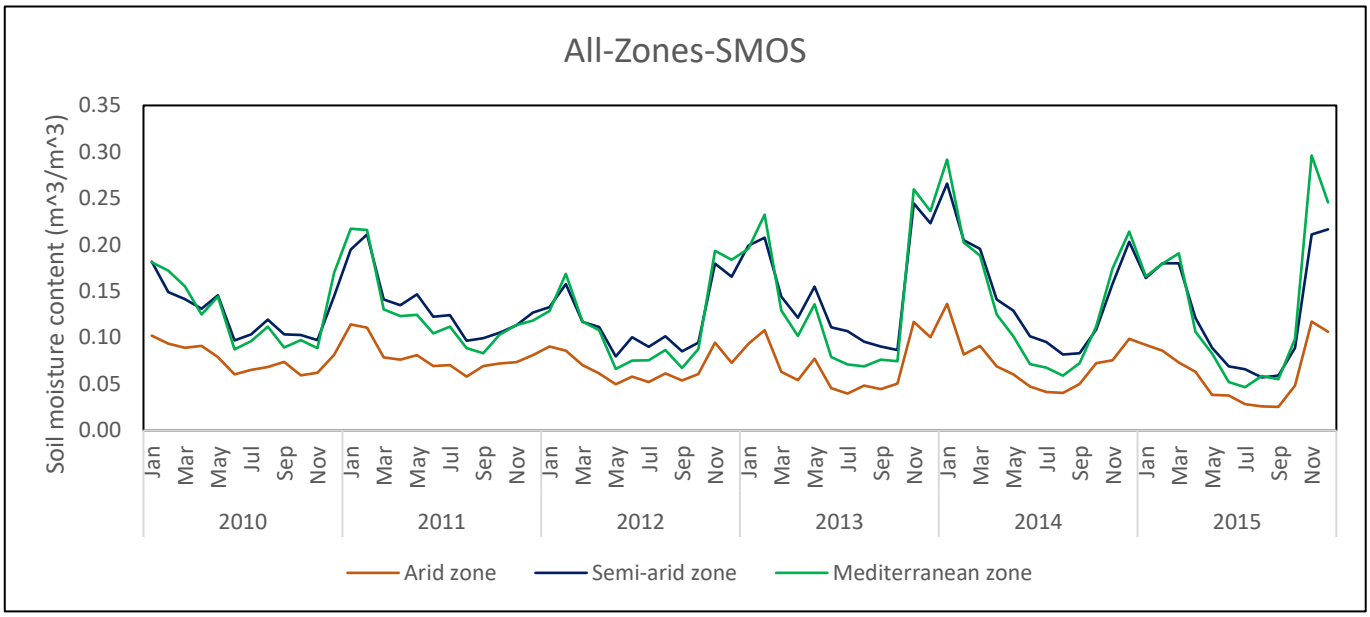

Figure 4.11 Monthly mean area-averaged soil moisture content (derived from SMOS data) over the period 2010–2015 for the three regions (desert (arid zone), rangeland (semi-arid and Mediterranean zone), and agricultural (semi-arid)) considered in this study.

Fig 4.12 shows the SMC separately for a typical desert, rangeland and agricultural site, together with their NDVI. The SMOS data indicate overall much drier soil conditions in 2010, when soil moisture content was the lowest during the study period as a result of reduced rainfall content (see Figs. 4.16 and 4.17). There are also notable differences for the wet months (November to February) of 2013 and 2014 when soil moisture status improved considerably for all study regions.

These results indicate a switch to higher than average SMCs for all regions in 2013 and 2014, following relatively dry values in 2010 and 2012 (2011 less so). Although there is considerable variability over the whole period, it is hypothesized that this split is caused in part by droughts years when rainfall is decreased (see Fig. 4.2) and increase evapotranspiration (see Fig. 4.2) and therefore cause the occurrence of soil moisture drought.

The NDVI also clearly illustrates a divide of ‘less vigorous (lower SMC)’ and ‘more vigorous (higher SMC)’ vegetation periods: NDVI improved in 2013 and 2014, when SMC was the highest. This is evident particularly for the rangeland and agricultural areas, as expected. The SMOS data for the desert site appear to fluctuate much more than the corresponding NDVI. This simply relates to the fact that although SMC varied and caused variations in soil evaporation, the lack of vegetation in the desert did not cause any changes in NDVI (apart from during the first half of 2014).

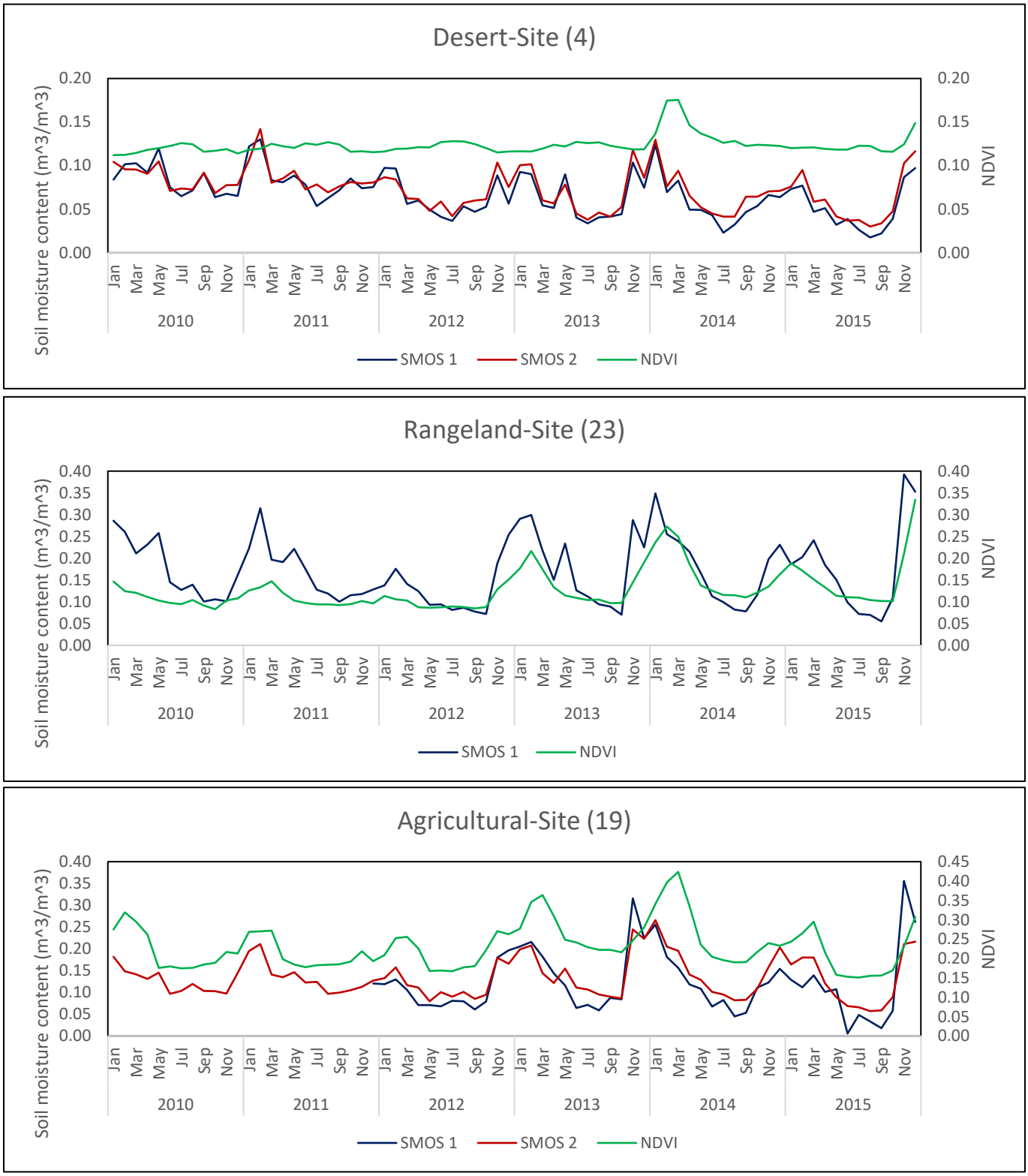

Figure 4.12 Spatiotemporal variability in soil moisture contents (SMOS) and NDVI in Iraq during 2010-2015, for a typical desert, rangeland and agricultural site. SMOS 1 represents the pixel located most closely to the sites, whereas SMOS 2 represents a large number of pixels covering an area inclusive of, and around, the site. For other sites see Appendix E.

4.3.8. The relationship between NDVI and surface latent heat flux (SLHF)

The sections above described the potential of meteorological drought indices (SPI/SPEI) and RS-indices (NDVI) or variables (LST, SMOS) to capture drought (strength and duration) for Iraq. In this section, we move to model products as tools to indicate drought. The seasonal surface latent heat fluxes (SLHF) or evapotranspiration rates for all three regions are shown in Fig 4.13, which give monthly spatial temporal means over each site per land cover type, derived from ERA-Interim output data for the period between 2001 to 2015. There are relatively large values of latent heat fluxes at the beginning and end of the year during winter (wet season), and much smaller values during the summer months (dry season). Particularly high values of SLHF were found for 2001 and 2007 over all three regions. Values rapidly decreased during the period between 2008 and 2010. Throughout 2012 the (SLHF) was very low for all regions. The highest values were observed from 2013 to 2015. There are differences between the three land cover types in particular with regards to their SLHF range; 0-3.5 MJ m^{-2} day^{-1} for deserts, 0-5 MJ m^{-2} day^{-1} for rangelands and 0-4 MJ m^{-2} day^{-1} for agricultural areas. NDVI has been plotted together with SLHF (Fig 4.14). It is shown that NDVI increases concurrently with SLHF, e.g. during the years 2013 and 2014 in particular for the following sites 4, 23, and 19.

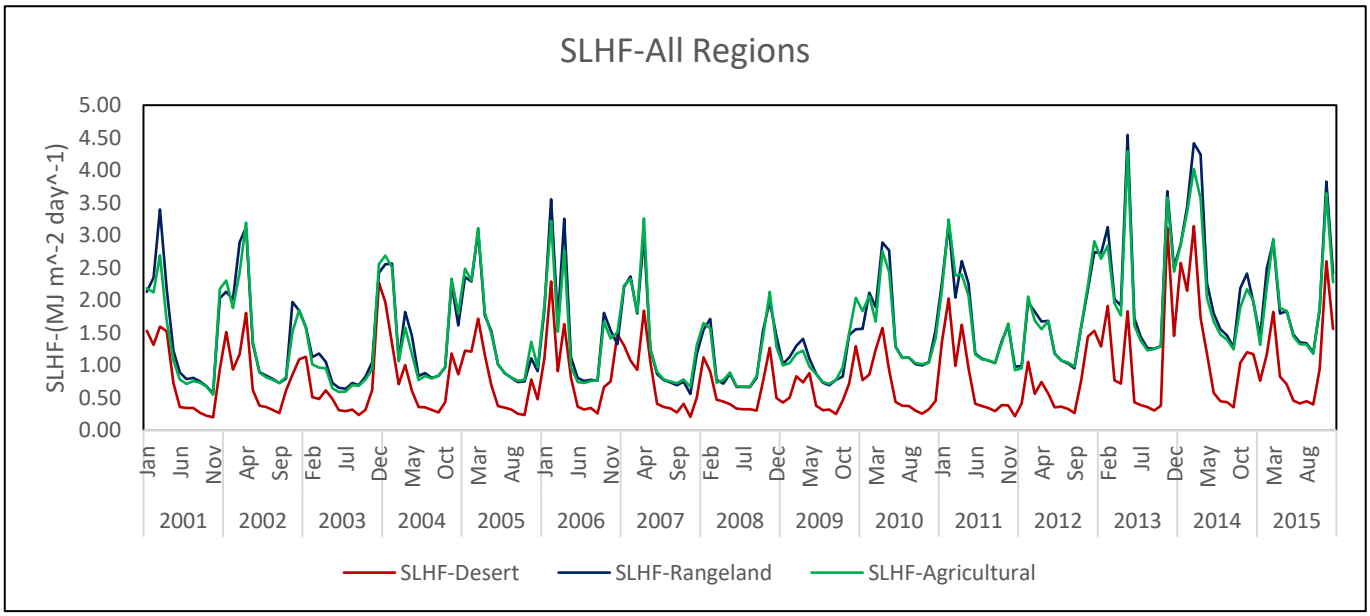

Figure 4.13 Interannual and seasonal variation in the SLHF as obtained from ERA-Interim throughout desert, rangeland, and agricultural sites (each line represents the average of 6 sites for desert, 5 sites for rangelands, and 9 sites for agriculture) during 2001-2015.

Fig 4.15 shows the evolution of the marshes' surface latent heat flux as calculated from in-situ net radiation and Eq. 2.10 that employs the remotely sensed LST and maximum monthly air temperatures. It has been plotted together with NDVI.

Although the absolute values of SLHF are at times nonsensical (i.e. negative values during drought conditions), their relative values follow NDVI fluctuations very closely, in particular for Chibiyish and Hammar. It shows again that while LST on its own may not be that useful for drought assessment, when incorporated into a more relevant product, using a combination of in-situ and RS data, it is able to provide some powerful information on land surface moisture status.

Surface latent heat flux values for Haweezah marsh follow those for the other two marshes closely, but the correspondence with NDVI is poor. In fact, annual peak value of NDVI correspond to low values of SLHF, which is counter-intuitive. It is not clear what the reason for this is. It could be related to the spatial resolution of the different RS (LST & NDVI) products or due to the fact that the method described in e.g. Verhoef et al. (1997), is not suitable for (near) permanently wet land.

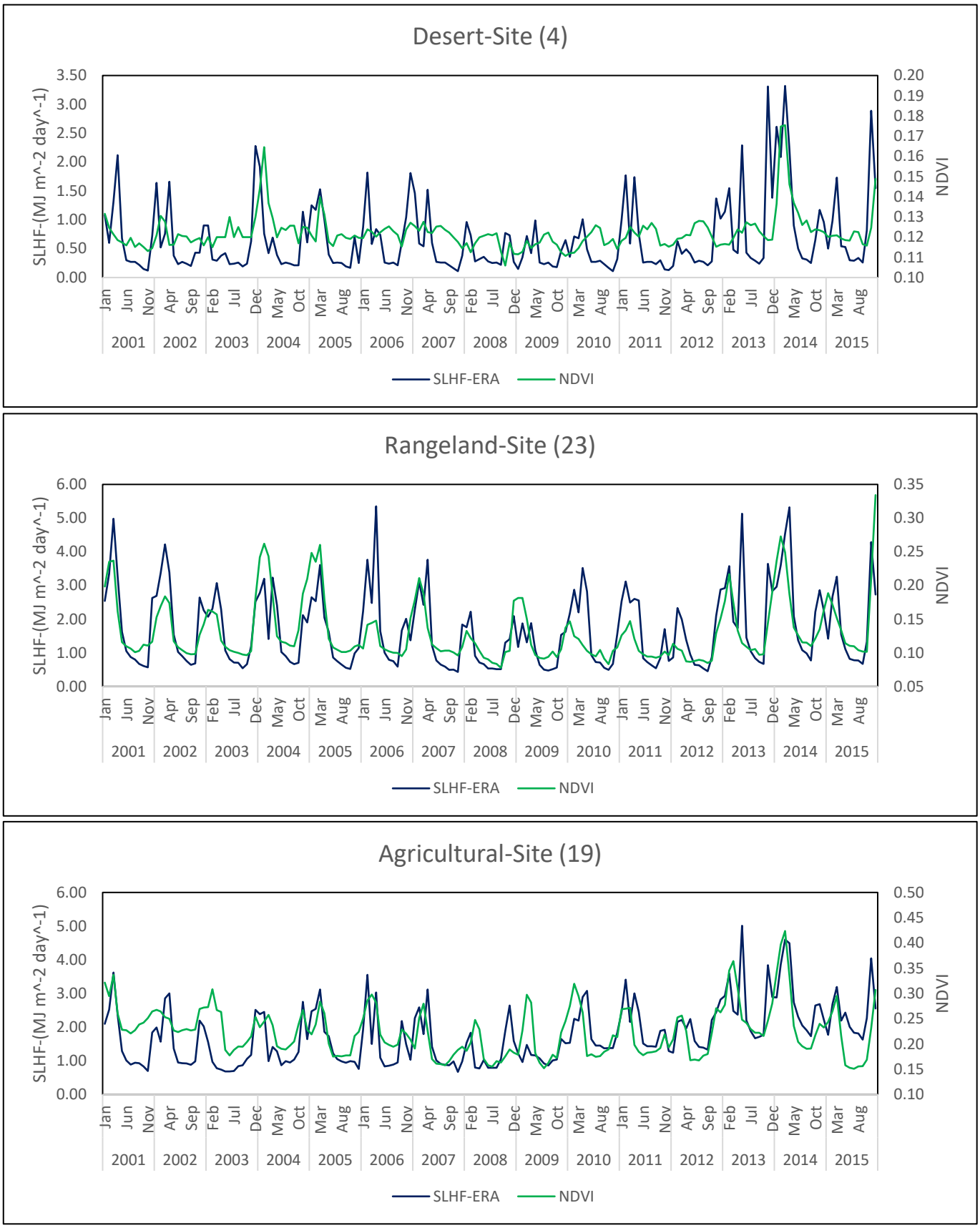

Figure 4.14 Seasonal and interannual and variation in the SLHF (blue lines), as derived from ERA-Interim outputs, for a typical desert, rangeland and agricultural site during 2001-2015.

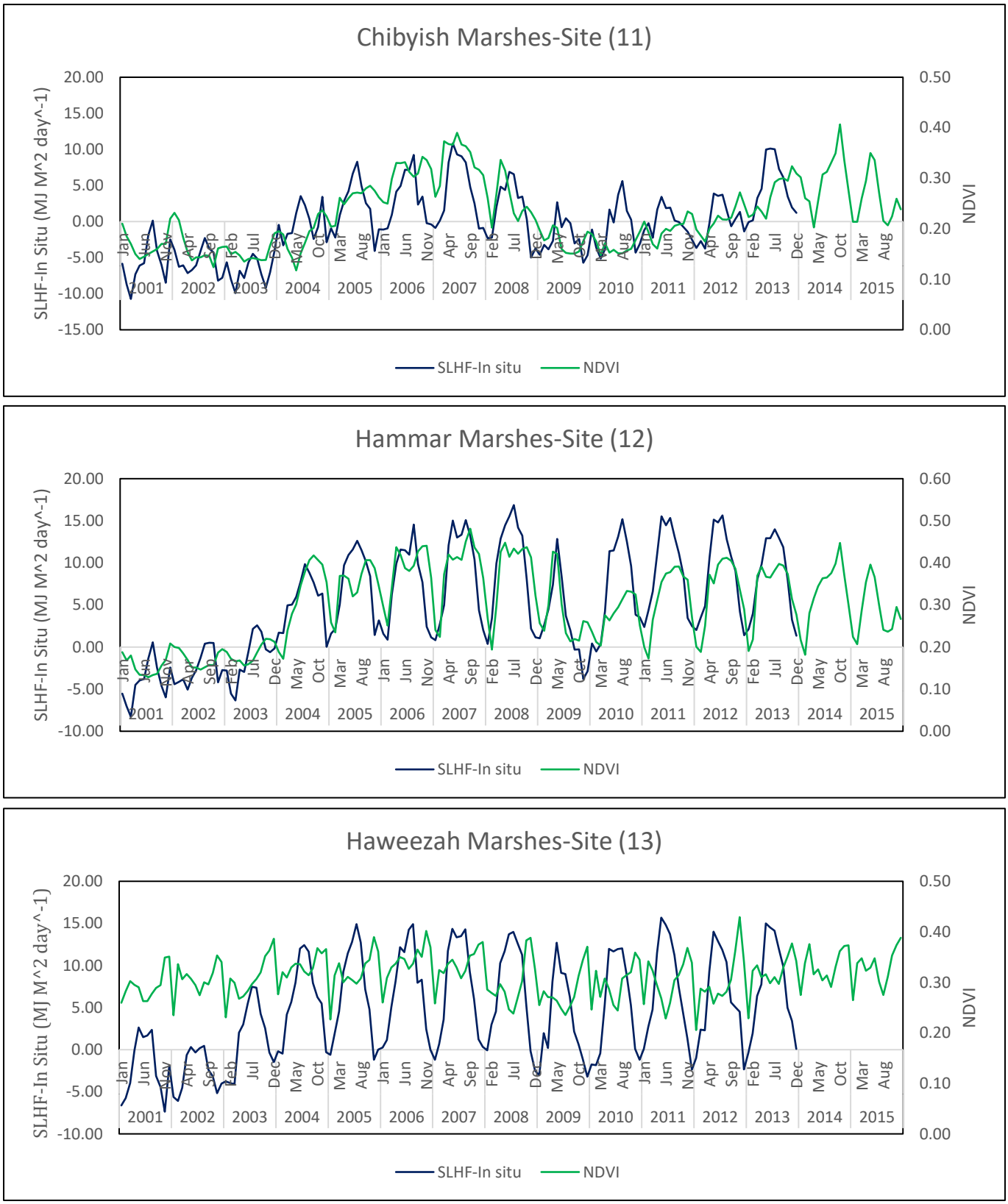

Figure 4.15 Seasonal and interannual and variation in the SLHF (blue lines), as derived from measured data outputs, for a Chibyish, Hammar, and Haweezah marshes during 2001-2015.

4.4. Assessment of water balance components from SWAP runs

Whereas Section 4.9 only described the evapotranspiration (as denoted by the surface latent heat flux, SHLF) as obtained from the standard low-resolution ERA-Interim product, Section 4.4 gives the results for the entire water balance, this time obtained using the field-scale SWAP model with bespoke soil hydraulic and vegetation data (development stage and LAI), as well as with standard LAI data. This section describes the water balance components as calculated by the SWAP model (see Section 3.2.5 in Chapter 3) per vegetation cover/climate zone; other sites can be found in Appendix G for desert, H for rangeland, and I for agricultural sites.

Before the water balance fluxes are discussed, first the driving data are presented for the different regions, as it is their absolute values and variation that will largely determine the relative size and fluctuation of the fluxes and soil water storage.

4.5. Driving variables

4.5.1. Meteorological driving data

Figs 4.16-4.17 below show the interannual variations of the seasonal courses (expressed as monthly sums for rainfall and radiation and averages for the other variables) of the in-situ and ERA-Interim meteorological driving variables, together with their spatial variability, per region.

4.5.1.1. In-situ data

When comparing the three regions, the largest differences are found in rainfall, in size and timing. ERA-Interim has the largest rainfall event occurring in late 2013 (72, 92 and 105 mm day^{-1} for desert, rangeland and agricultural region, respectively. The in-situ rainfall maxima occur at different times, e.g. in 2011 (110 mm day^{-1}), for the desert. For all regions air temperature have their lowest values in January 2008, between 7 (desert) to 9 (rangeland) deg. C. Maximum values range from 37 (desert) to 39 (rangeland); agricultural region reached 38.3 maximum.

The range in minimum and maximum incoming shortwave radiation is also very similar, with lowest winter values found for the rangeland and agricultural region (~ 9.6-9.8 MJ m^{-2} day^{-1}). Maximum values in summer are all around 28 MJ m^{-2} day^{-1} or so.

Actual vapour pressure is a little more variable, with lowest values of 0.6, 0.9 and 0.75 kPa for D, R and A, respectively. Maximum values are 1.6, 2, and 2 kPa, respectively. With air temperatures fairly similar (and saturated vapour pressure depending on Ta), vapour pressure deficits would have been largest for the desert.

Finally, monthly averaged windspeed is overall the lowest for the desert region (which seems a little strange seeing roughness length would have been low and displacement height zero), with a minimum of 1 m/s and a maximum of 5 m/s as compared to 2/6.5 and 2/5.3 m/s for the rangeland and agricultural regions, respectively.

4.5.1.2. ERA-Interim data

ERA-Interim data courses of driving data are mostly very similar, but the largest differences are observed for rainfall (size and timing), vapour pressure (ERA-Intermin about 0.5 kPa lower on average) and windspeed (higher minima). Radiation amounts and air temperatures are very similar so potential evaporation will be very similar.

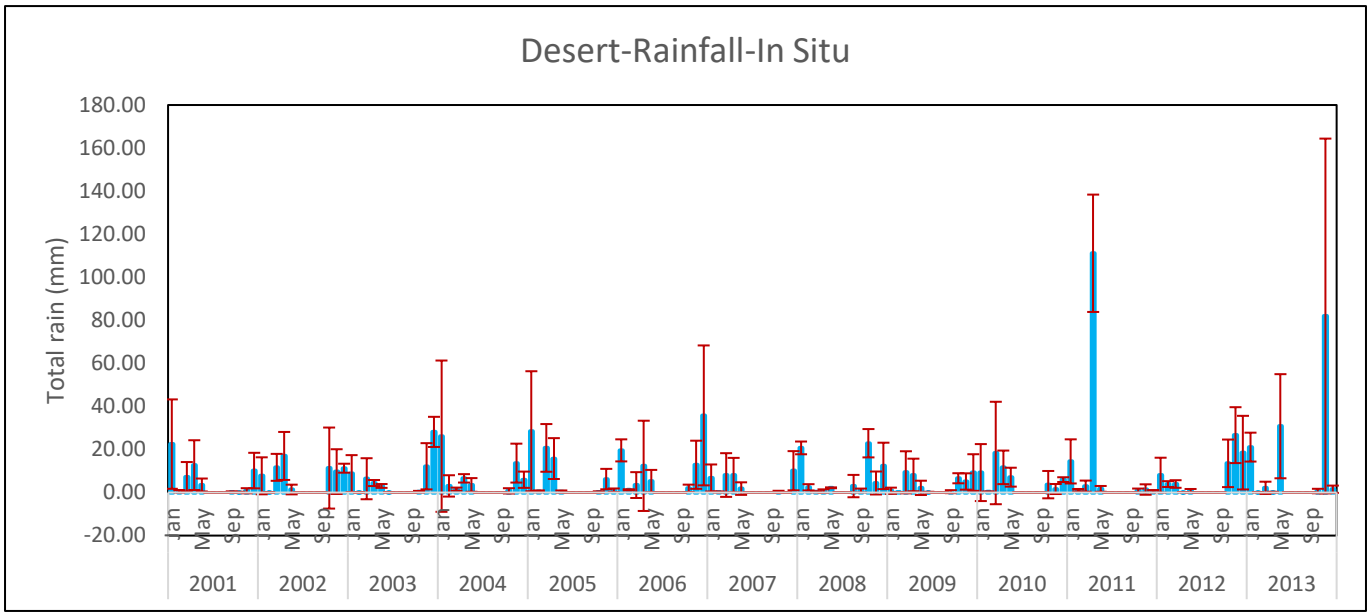
Desert-Rainfall-In Situ
Total rain (mm)
180.00
160.00
140.00
120.00
100.00
80.00
60.00
40.00
20.00
0.00
-20.00
Jan May Sep
2001 2002 2003 2004 2005 2006 2007 2008 2009 2010 2011 2012 2013

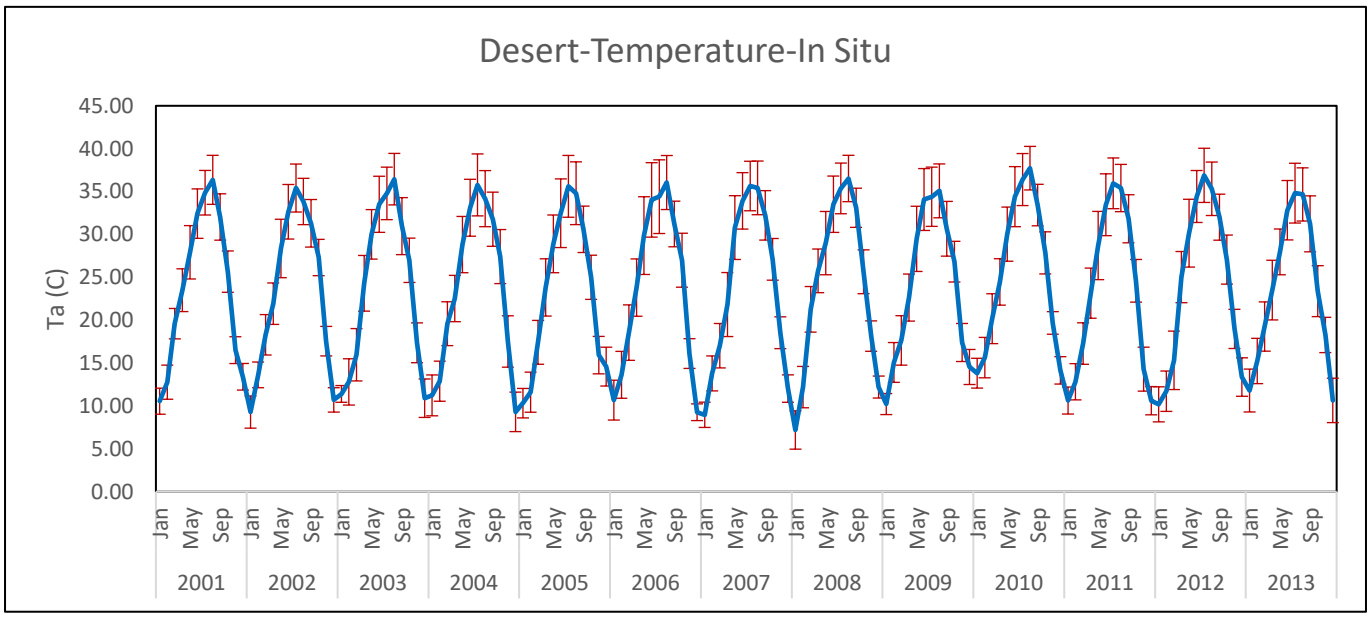
Desert-Temperature-In Situ
Ta (C)
45.00
40.00
35.00
30.00
25.00
20.00
15.00
10.00
5.00
0.00
Jan May Sep
2001 2002 2003 2004 2005 2006 2007 2008 2009 2010 2011 2012 2013

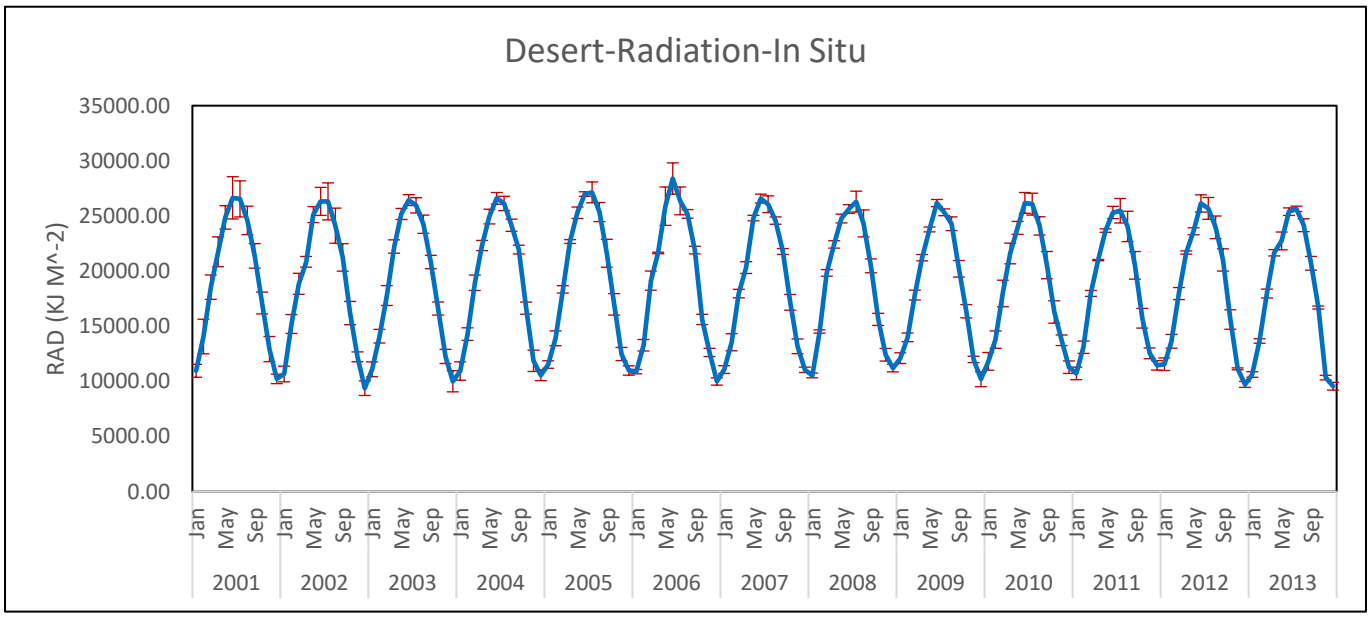
Desert-Radiation-In Situ
RAD (KJ M^-2)
35000.00
30000.00
25000.00
20000.00
15000.00
10000.00
5000.00
0.00
Jan May Sep
2001 2002 2003 2004 2005 2006 2007 2008 2009 2010 2011 2012 2013

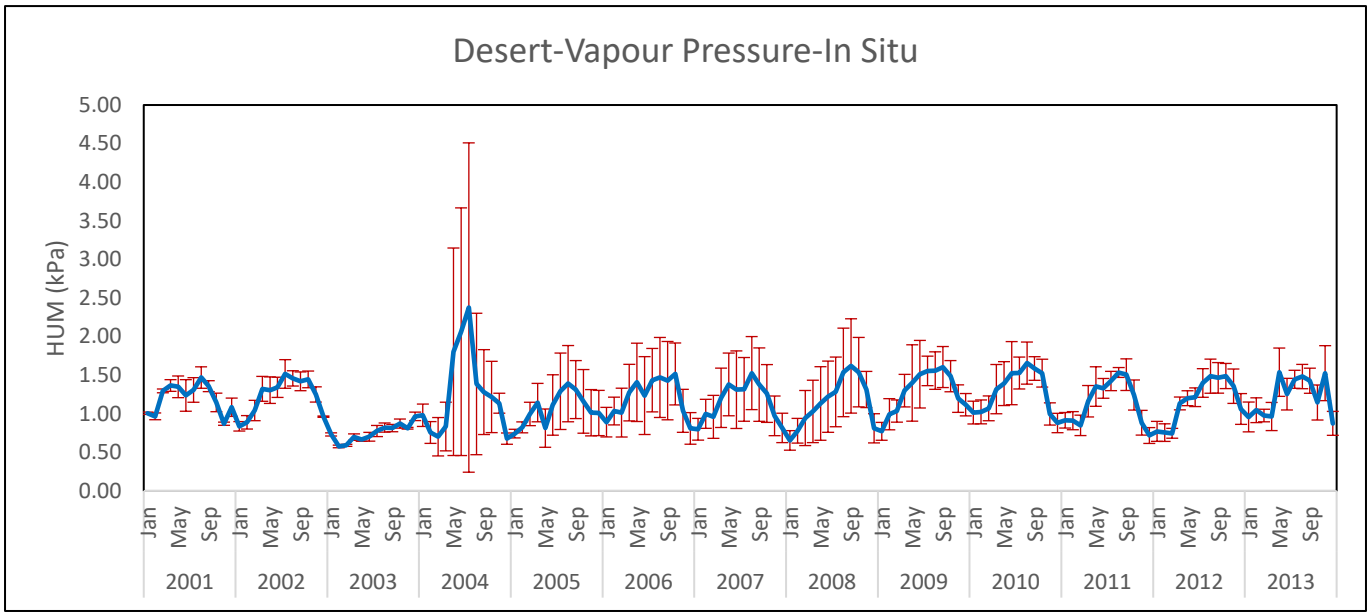
Desert-Vapour Pressure-In Situ
HUM (kPa)
5.00
4.50
4.00
3.50
3.00
2.50
2.00
1.50
1.00
0.50
0.00
Jan May Sep
2001 2002 2003 2004 2005 2006 2007 2008 2009 2010 2011 2012 2013

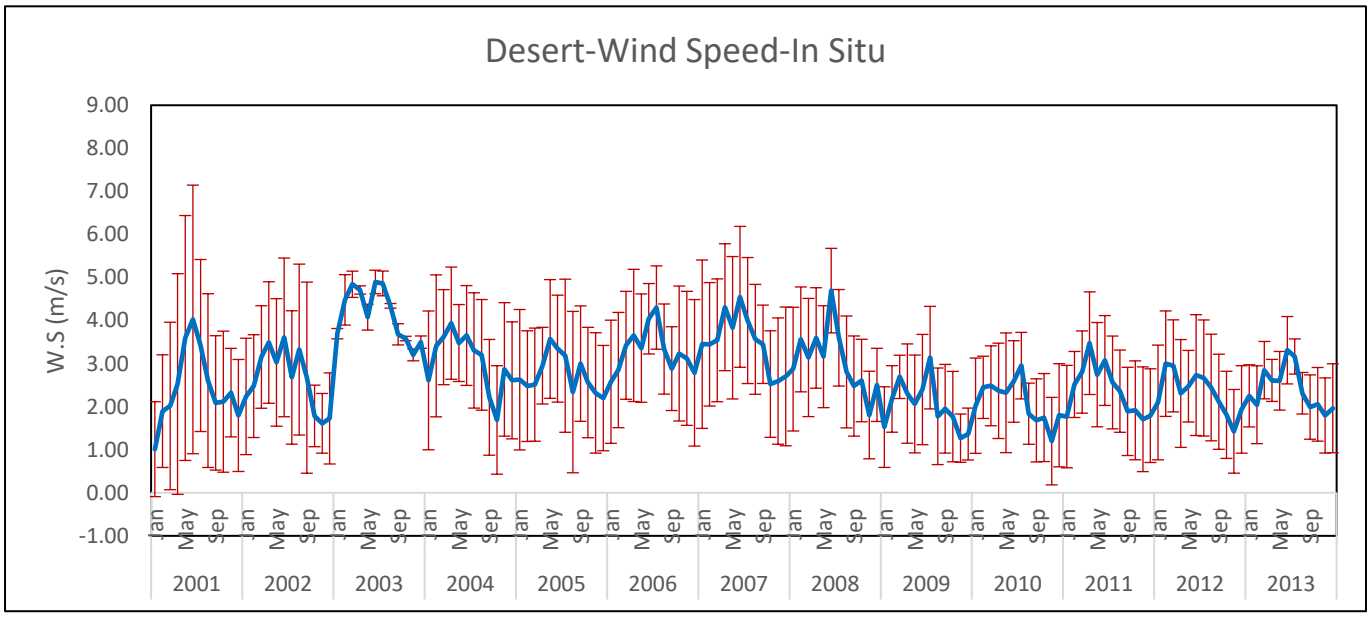
Desert-Wind Speed-In Situ
W.S (m/s)
9.00
8.00
7.00
6.00
5.00
4.00
3.00
2.00
1.00
0.00
-1.00
Jan May Sep
2001 2002 2003 2004 2005 2006 2007 2008 2009 2010 2011 2012 2013

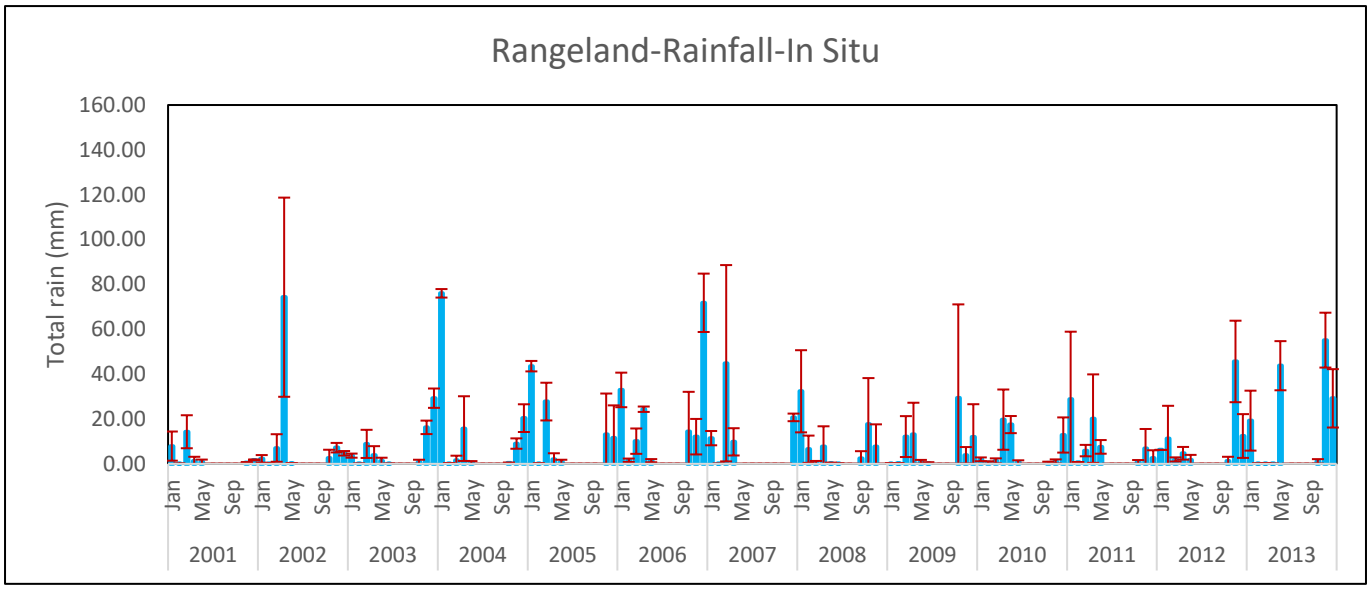
Rangeland-Rainfall-In Situ
Total rain (mm)
160.00
140.00
120.00
100.00
80.00
60.00
40.00
20.00
0.00
Jan May Sep
2001 2002 2003 2004 2005 2006 2007 2008 2009 2010 2011 2012 2013

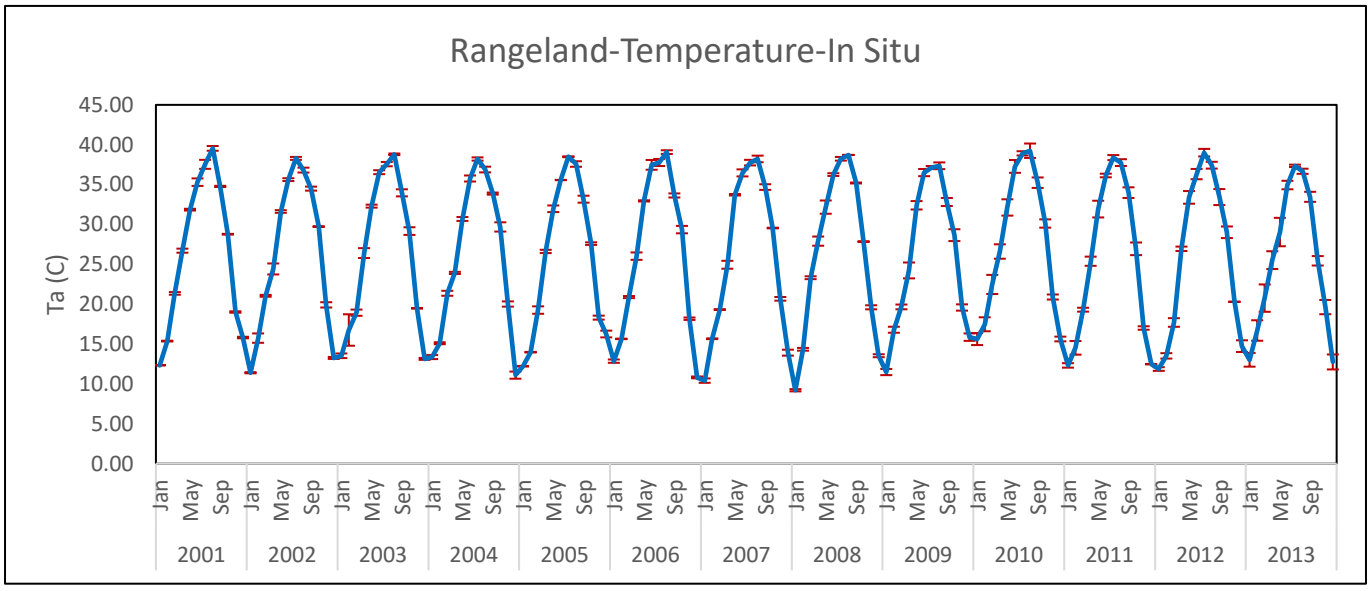
Rangeland-Temperature-In Situ
Ta (C)
45.00
40.00
35.00
30.00
25.00
20.00
15.00
10.00
5.00
0.00
Jan May Sep
2001 2002 2003 2004 2005 2006 2007 2008 2009 2010 2011 2012 2013

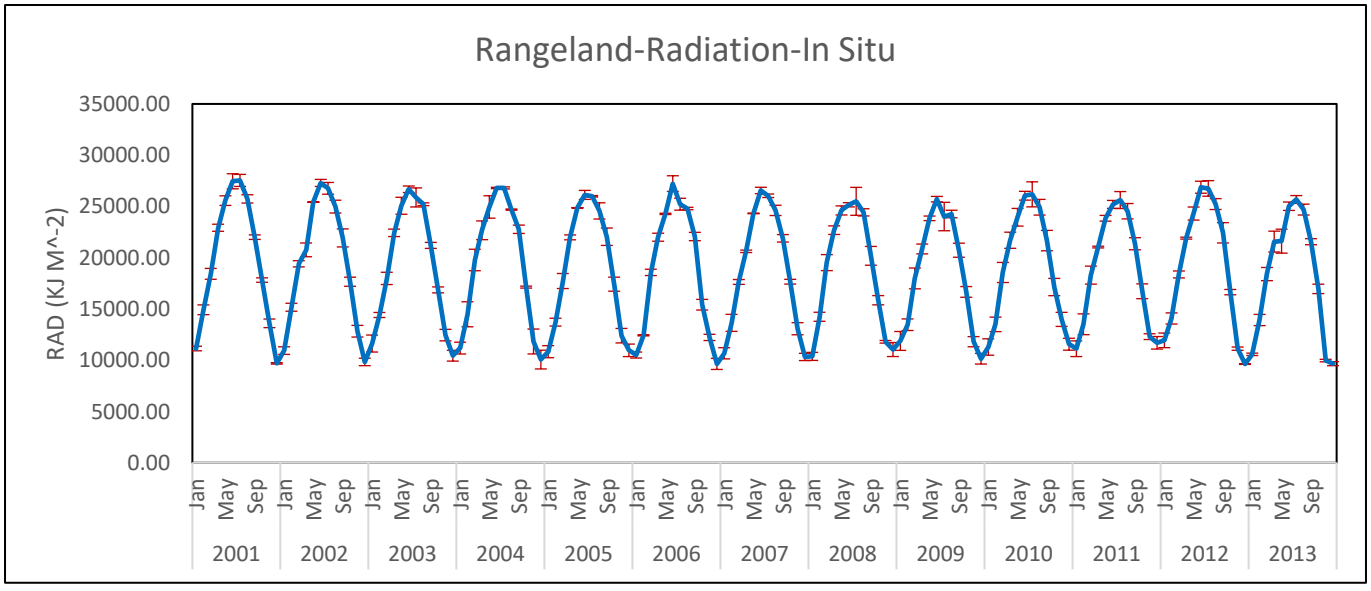
Rangeland-Radiation-In Situ
RAD (KJ M^-2)
35000.00
30000.00
25000.00
20000.00
15000.00
10000.00
5000.00
0.00
Jan May Sep
2001 2002 2003 2004 2005 2006 2007 2008 2009 2010 2011 2012 2013

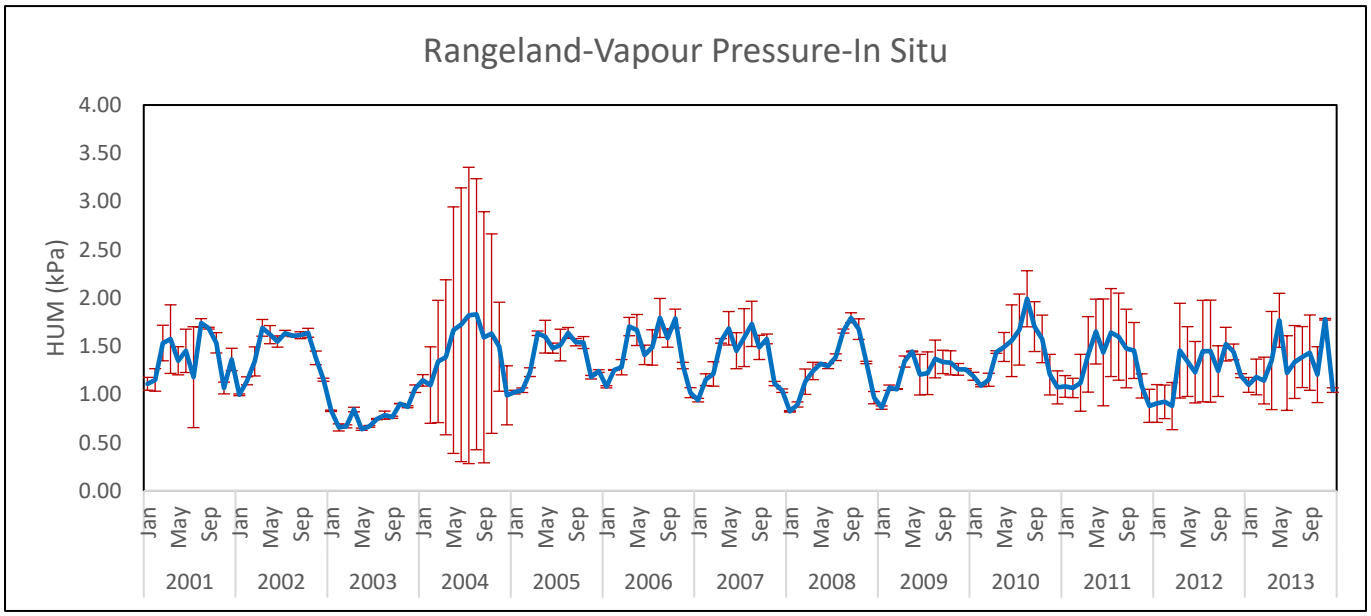
Rangeland-Vapour Pressure-In Situ
HUM (kPa)
4.00
3.50
3.00
2.50
2.00
1.50
1.00
0.50
0.00
Jan May Sep
2001 2002 2003 2004 2005 2006 2007 2008 2009 2010 2011 2012 2013

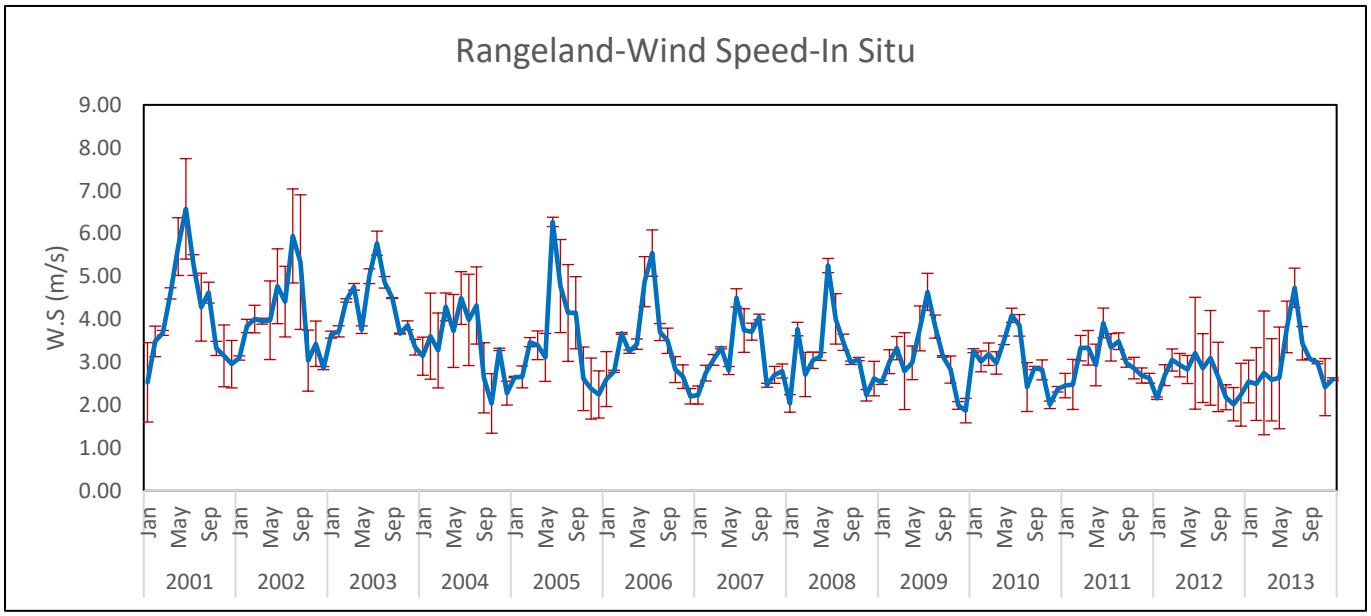
Rangeland-Wind Speed-In Situ
W.S (m/s)
9.00
8.00
7.00
6.00
5.00
4.00
3.00
2.00
1.00
0.00
Jan May Sep
2001 2002 2003 2004 2005 2006 2007 2008 2009 2010 2011 2012 2013

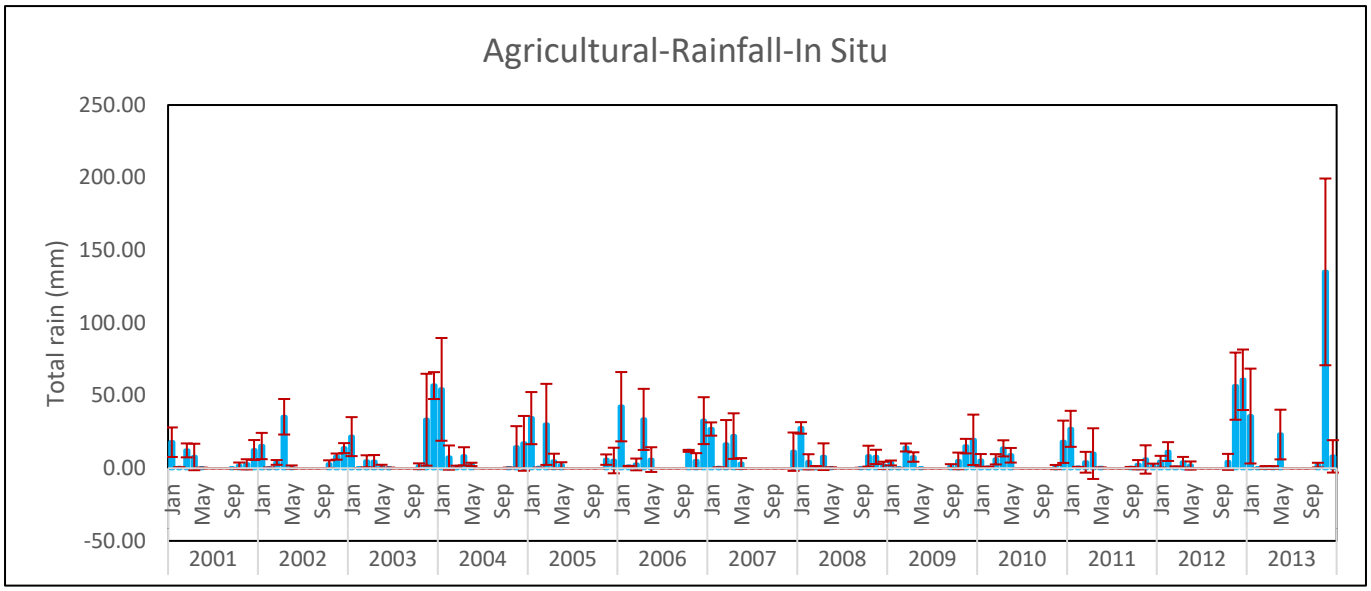
Agricultural-Rainfall-In Situ
Total rain (mm)
250.00
200.00
150.00
100.00
50.00
0.00
-50.00
Jan May Sep
2001 2002 2003 2004 2005 2006 2007 2008 2009 2010 2011 2012 2013

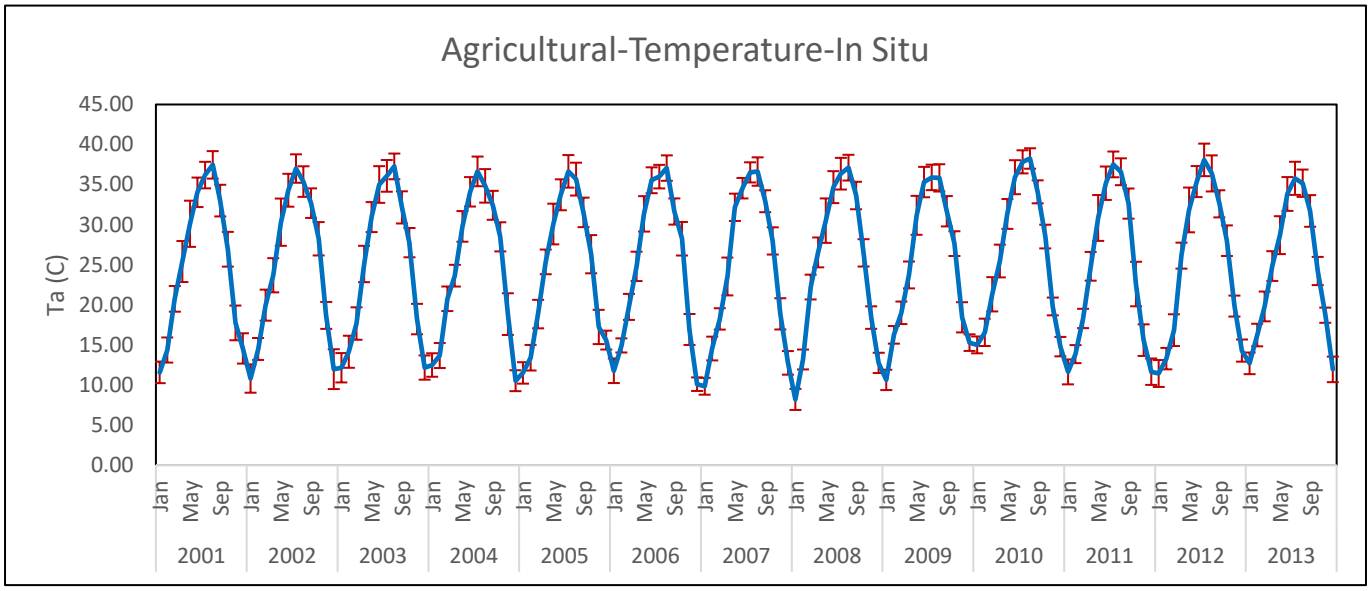
Agricultural-Temperature-In Situ
Ta (C)
45.00
40.00
35.00
30.00
25.00
20.00
15.00
10.00
5.00
0.00
Jan May Sep
2001 2002 2003 2004 2005 2006 2007 2008 2009 2010 2011 2012 2013

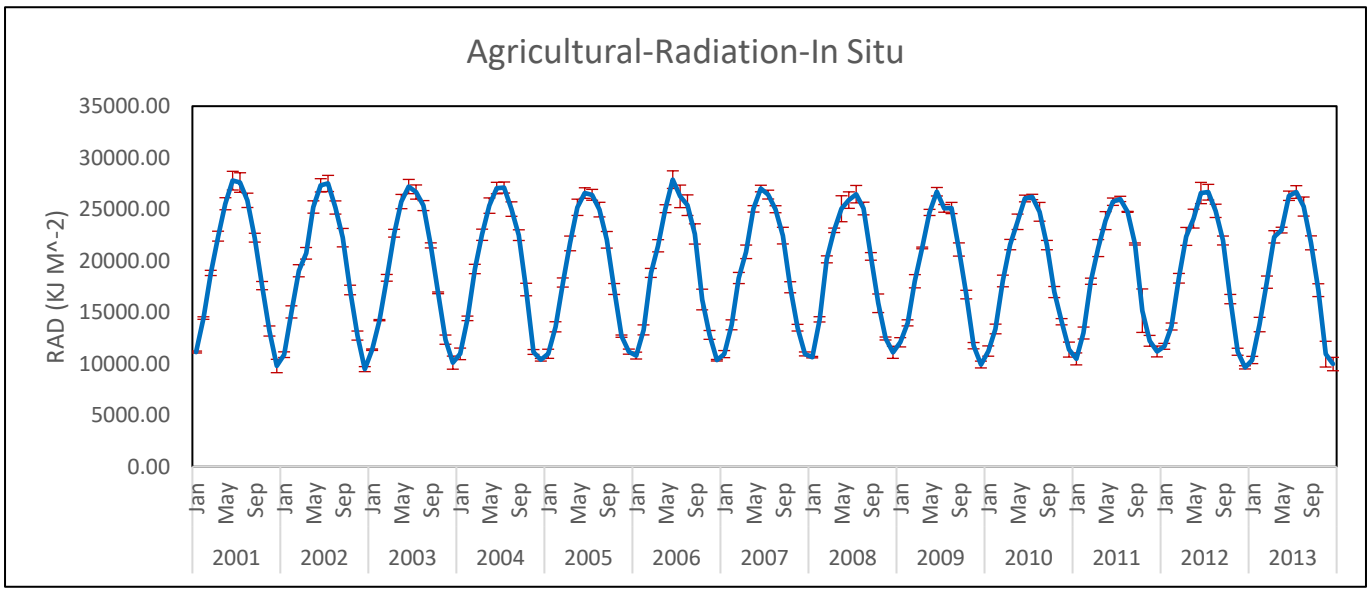
Agricultural-Radiation-In Situ
RAD (KJ M^-2)
35000.00
30000.00
25000.00
20000.00
15000.00
10000.00
5000.00
0.00
Jan May Sep
2001 2002 2003 2004 2005 2006 2007 2008 2009 2010 2011 2012 2013

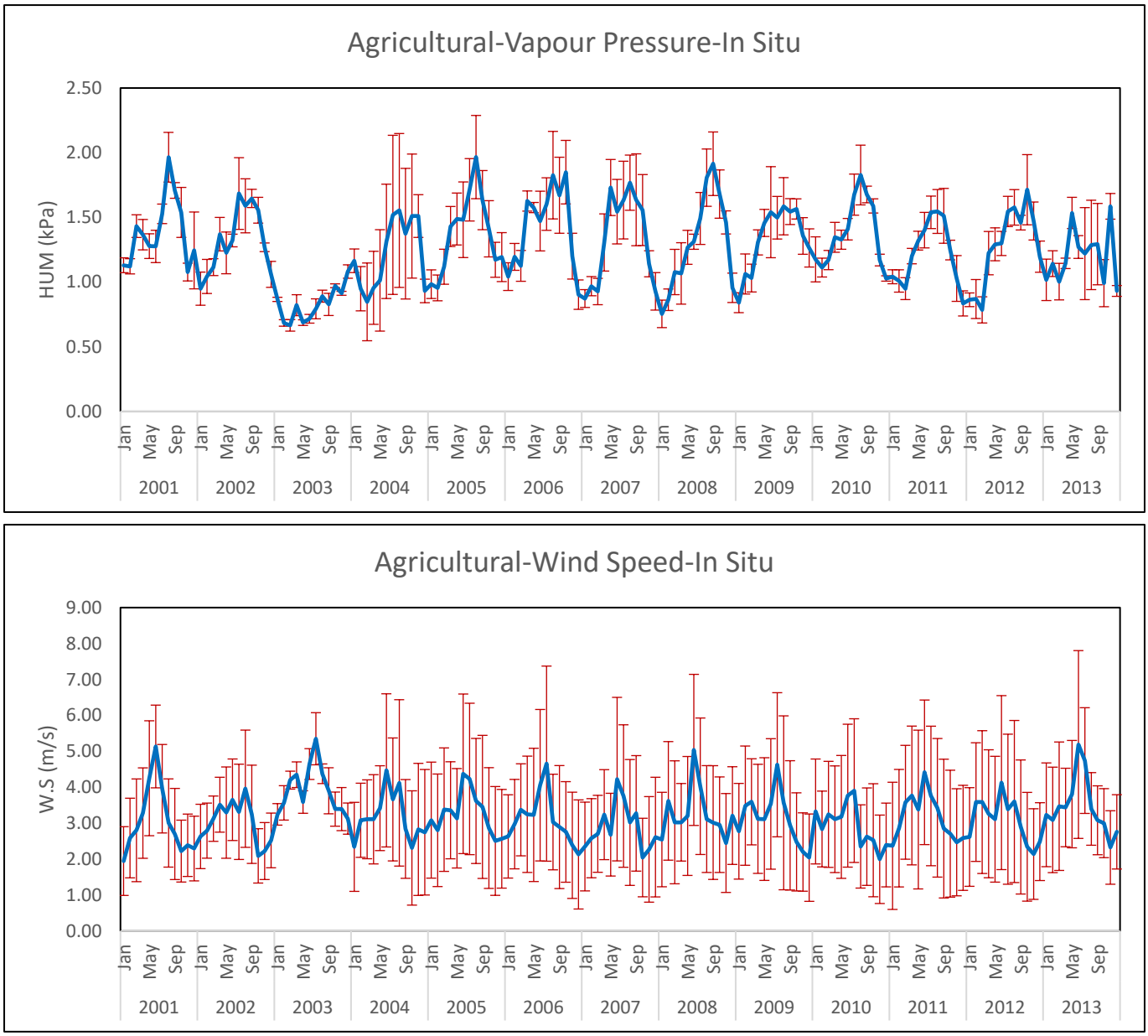

Figure 4.16 The interannual variations of the seasonal courses of the measured meteorological driving variables, expressed as monthly sums for rainfall and radiation and averages for the other variables during 2001-2013.

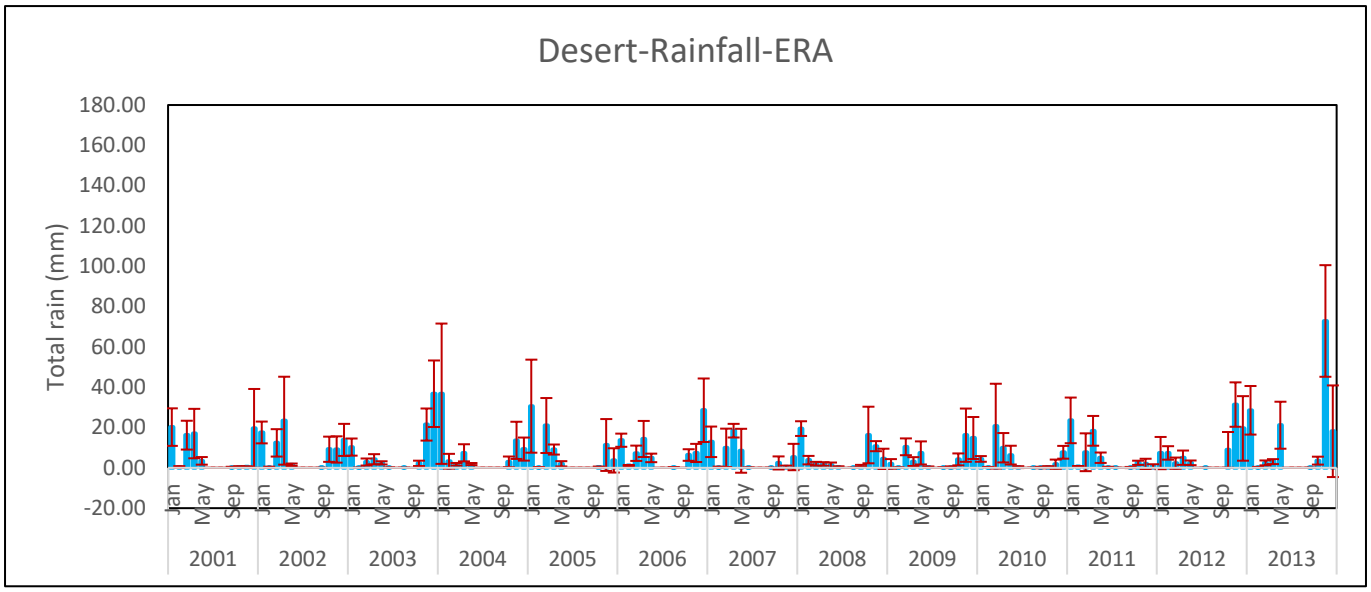
Desert-Rainfall-ERA
Total rain (mm)
180.00
160.00
140.00
120.00
100.00
80.00
60.00
40.00
20.00
0.00
-20.00
Jan May Sep
2001 2002 2003 2004 2005 2006 2007 2008 2009 2010 2011 2012 2013

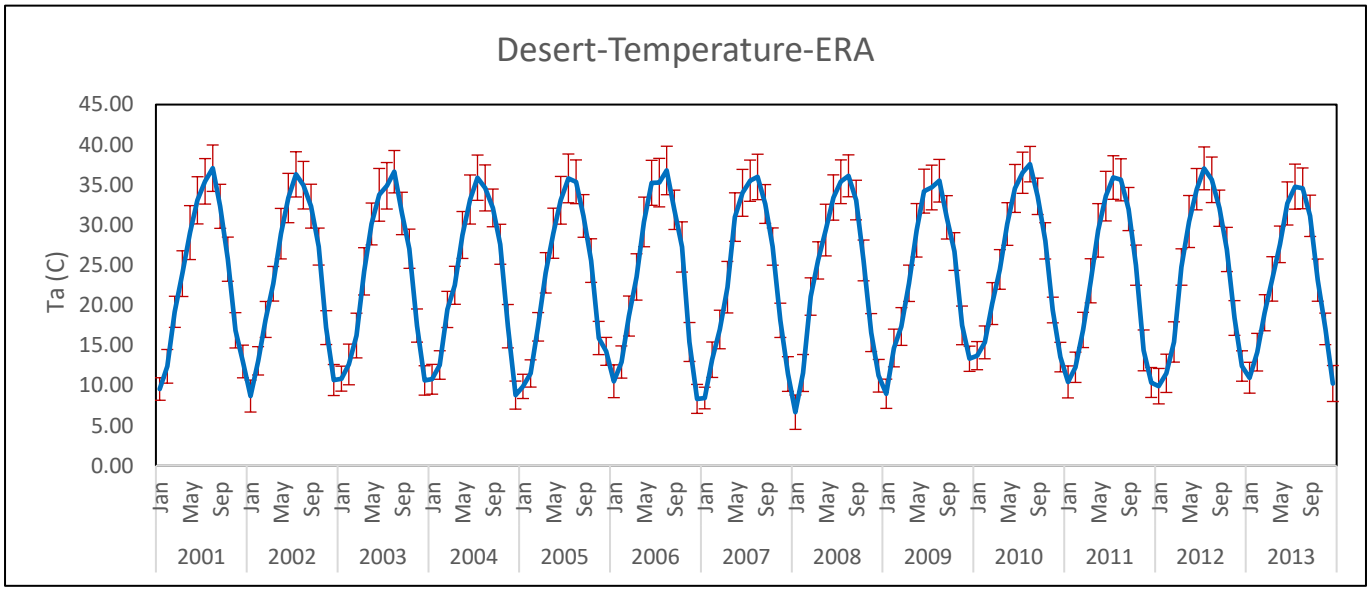
Desert-Temperature-ERA
Ta (C)
45.00
40.00
35.00
30.00
25.00
20.00
15.00
10.00
5.00
0.00
Jan May Sep
2001 2002 2003 2004 2005 2006 2007 2008 2009 2010 2011 2012 2013

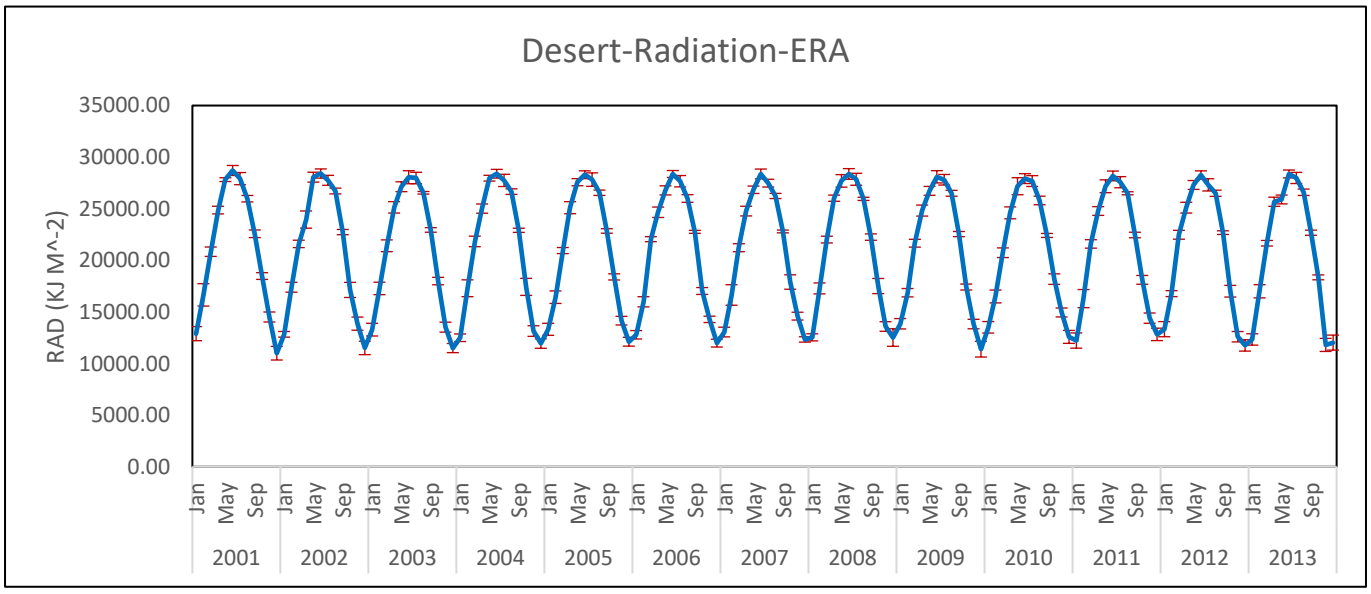
Desert-Radiation-ERA
RAD (KJ M^-2)
35000.00
30000.00
25000.00
20000.00
15000.00
10000.00
5000.00
0.00
Jan May Sep
2001 2002 2003 2004 2005 2006 2007 2008 2009 2010 2011 2012 2013

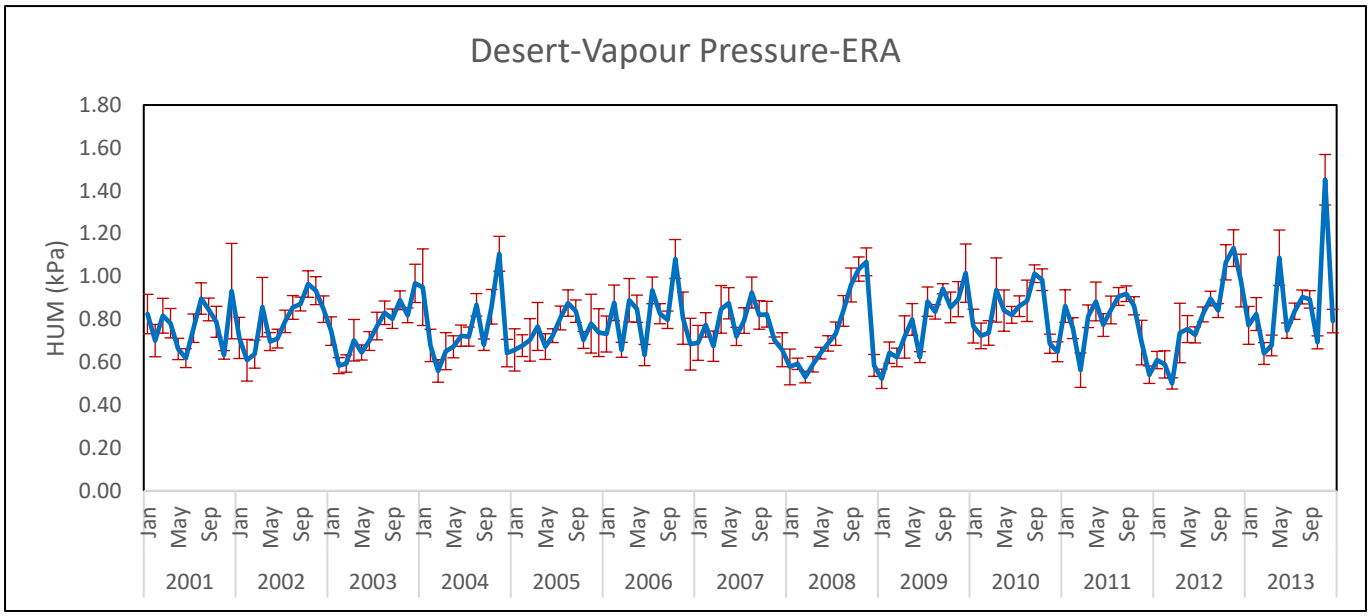
Desert-Vapour Pressure-ERA
HUM (kPa)
1.80
1.60
1.40
1.20
1.00
0.80
0.60
0.40
0.20
0.00
Jan May Sep
2001 2002 2003 2004 2005 2006 2007 2008 2009 2010 2011 2012 2013

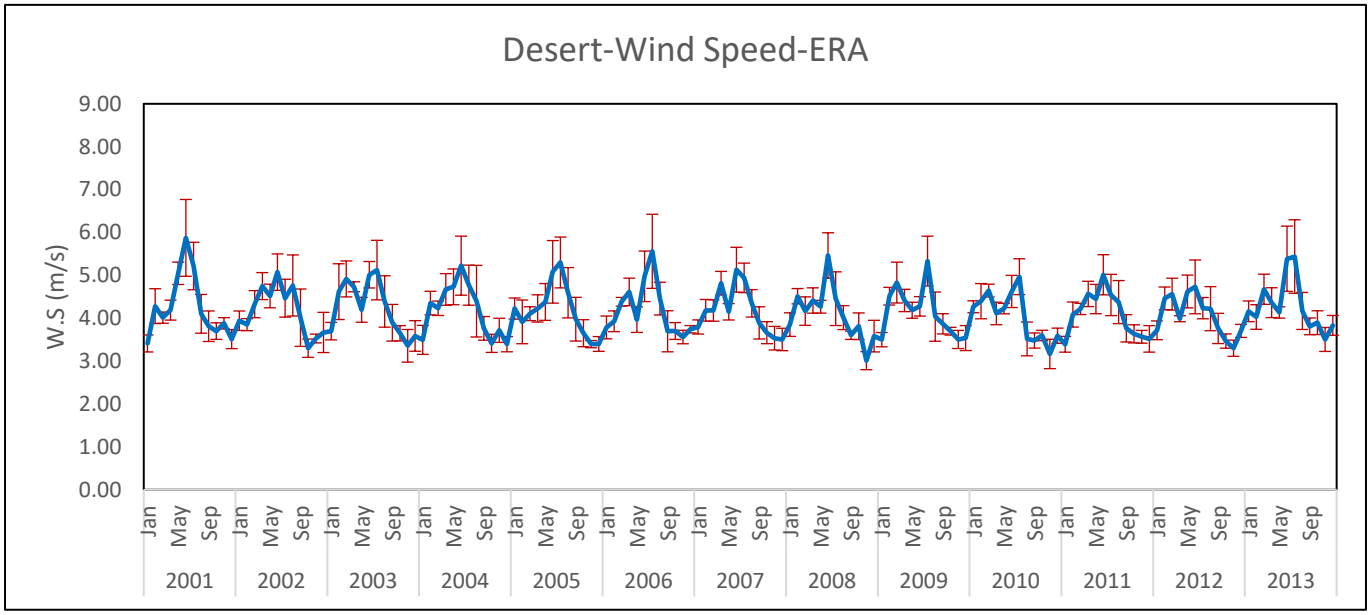
Desert-Wind Speed-ERA
W.S (m/s)
9.00
8.00
7.00
6.00
5.00
4.00
3.00
2.00
1.00
0.00
Jan May Sep
2001 2002 2003 2004 2005 2006 2007 2008 2009 2010 2011 2012 2013

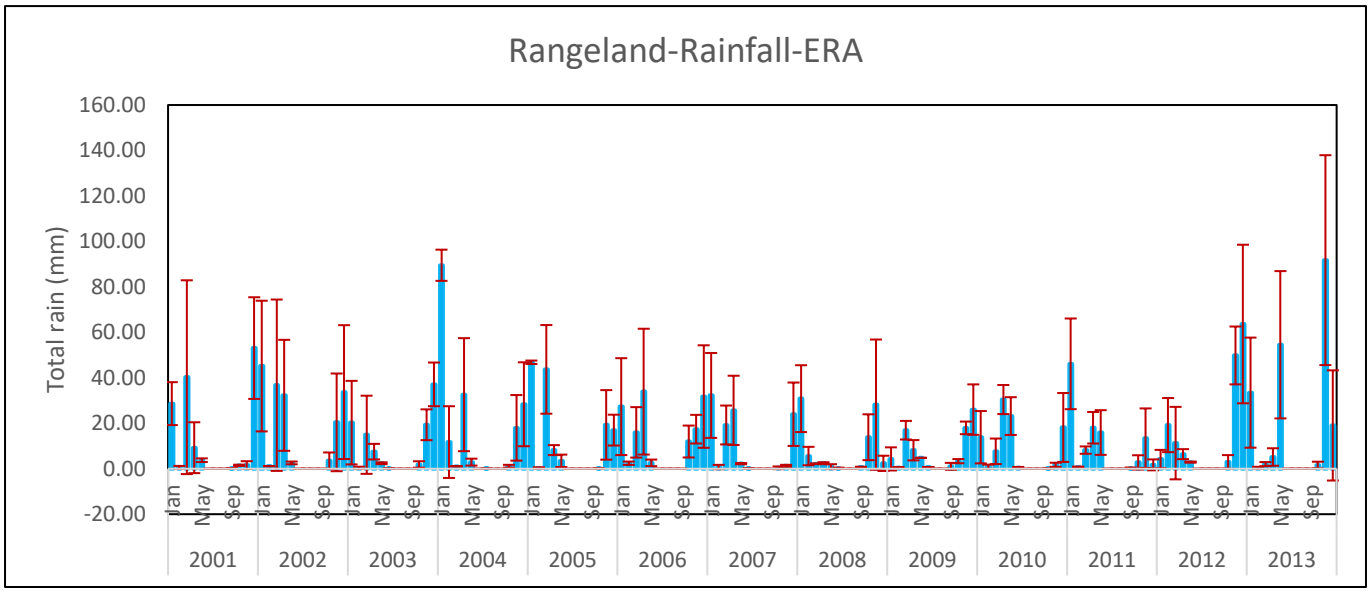
Rangeland-Rainfall-ERA
Total rain (mm)
160.00
140.00
120.00
100.00
80.00
60.00
40.00
20.00
0.00
-20.00
Jan May Sep
2001 2002 2003 2004 2005 2006 2007 2008 2009 2010 2011 2012 2013

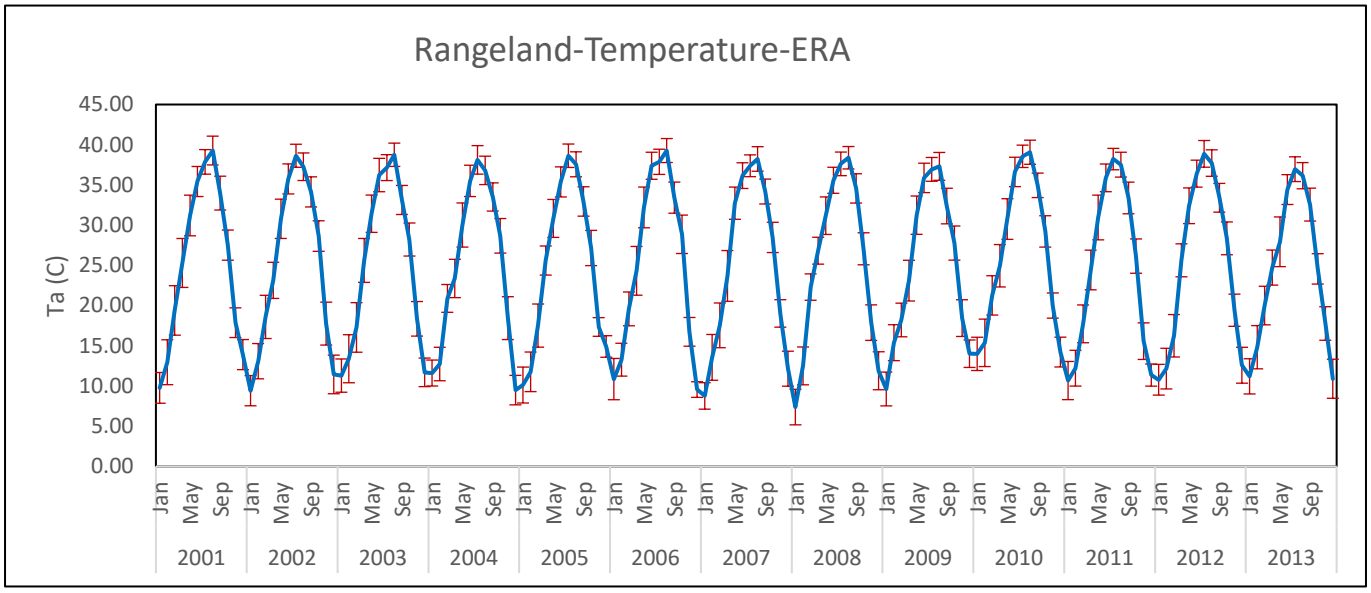
Rangeland-Temperature-ERA
Ta (C)
45.00
40.00
35.00
30.00
25.00
20.00
15.00
10.00
5.00
0.00
Jan May Sep
2001 2002 2003 2004 2005 2006 2007 2008 2009 2010 2011 2012 2013

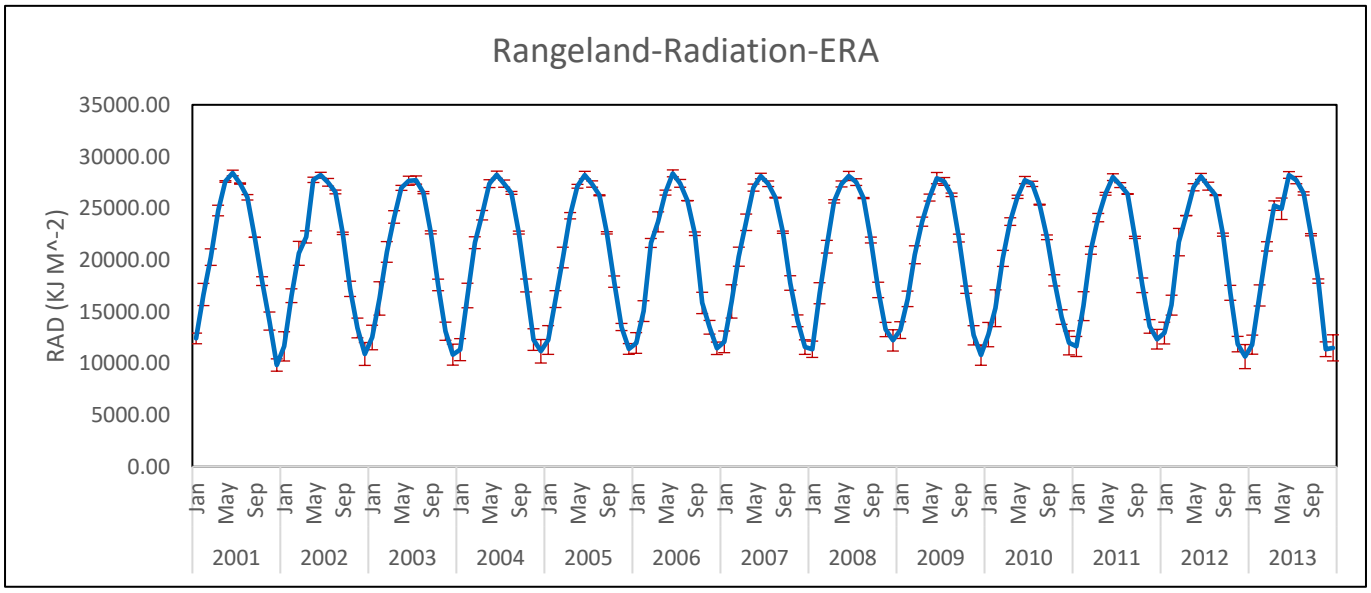
Rangeland-Radiation-ERA
RAD (KJ M^-2)
35000.00
30000.00
25000.00
20000.00
15000.00
10000.00
5000.00
0.00
Jan May Sep
2001 2002 2003 2004 2005 2006 2007 2008 2009 2010 2011 2012 2013

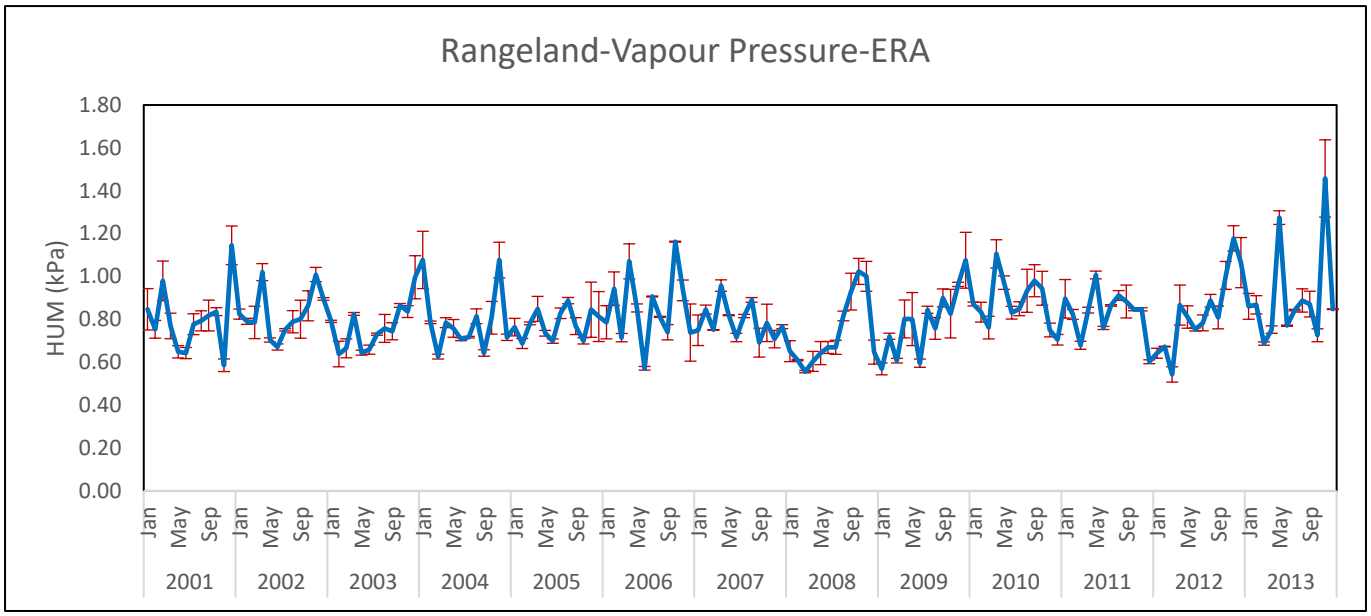
Rangeland-Vapour Pressure-ERA
HUM (kPa)
1.80
1.60
1.40
1.20
1.00
0.80
0.60
0.40
0.20
0.00
Jan May Sep
2001 2002 2003 2004 2005 2006 2007 2008 2009 2010 2011 2012 2013

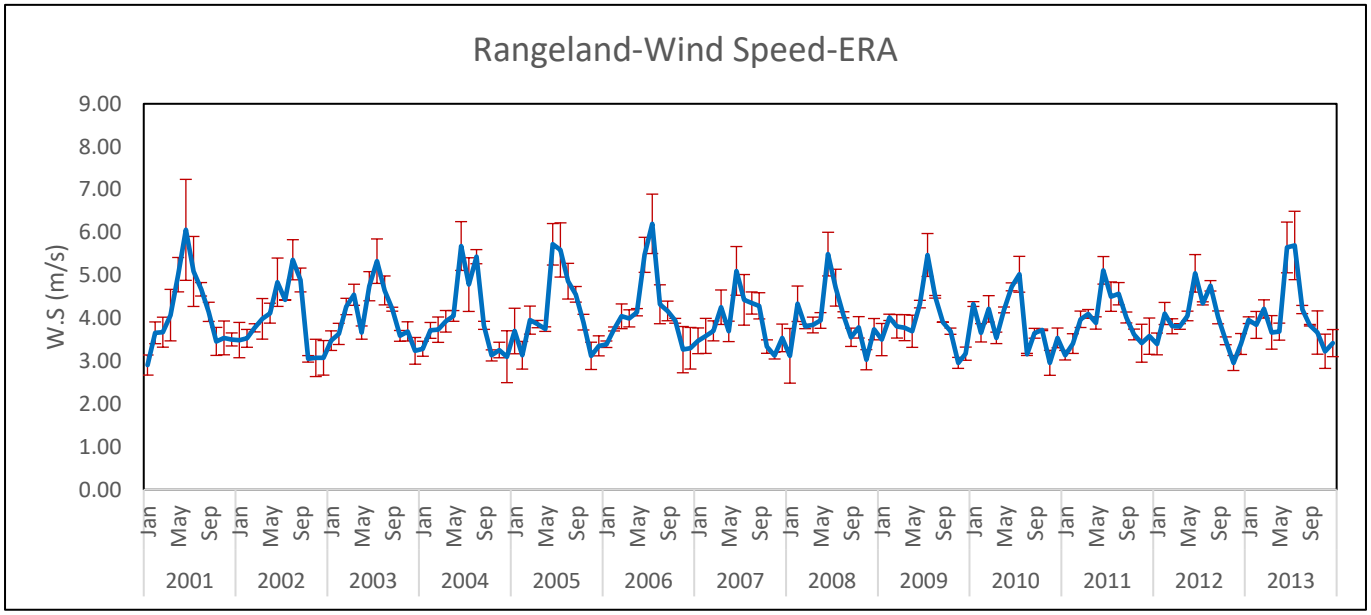
Rangeland-Wind Speed-ERA
W.S (m/s)
9.00
8.00
7.00
6.00
5.00
4.00
3.00
2.00
1.00
0.00
Jan May Sep
2001 2002 2003 2004 2005 2006 2007 2008 2009 2010 2011 2012 2013

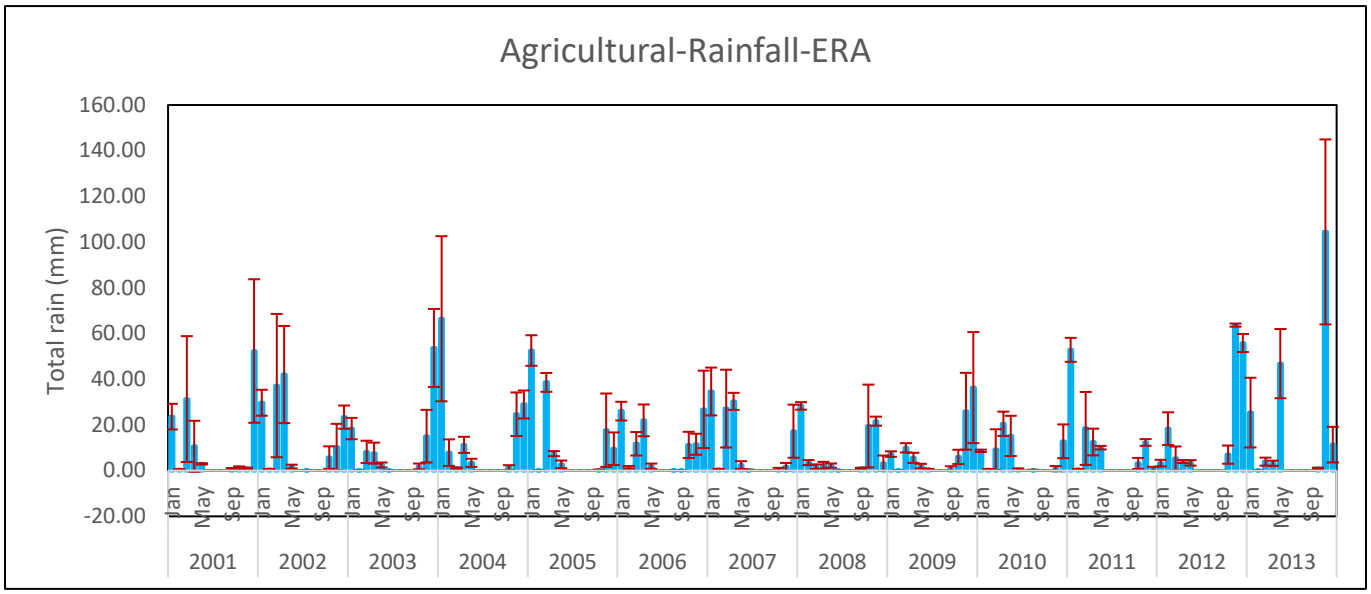
Agricultural-Rainfall-ERA
Total rain (mm)
160.00
140.00
120.00
100.00
80.00
60.00
40.00
20.00
0.00
-20.00
Jan May Sep
2001 2002 2003 2004 2005 2006 2007 2008 2009 2010 2011 2012 2013

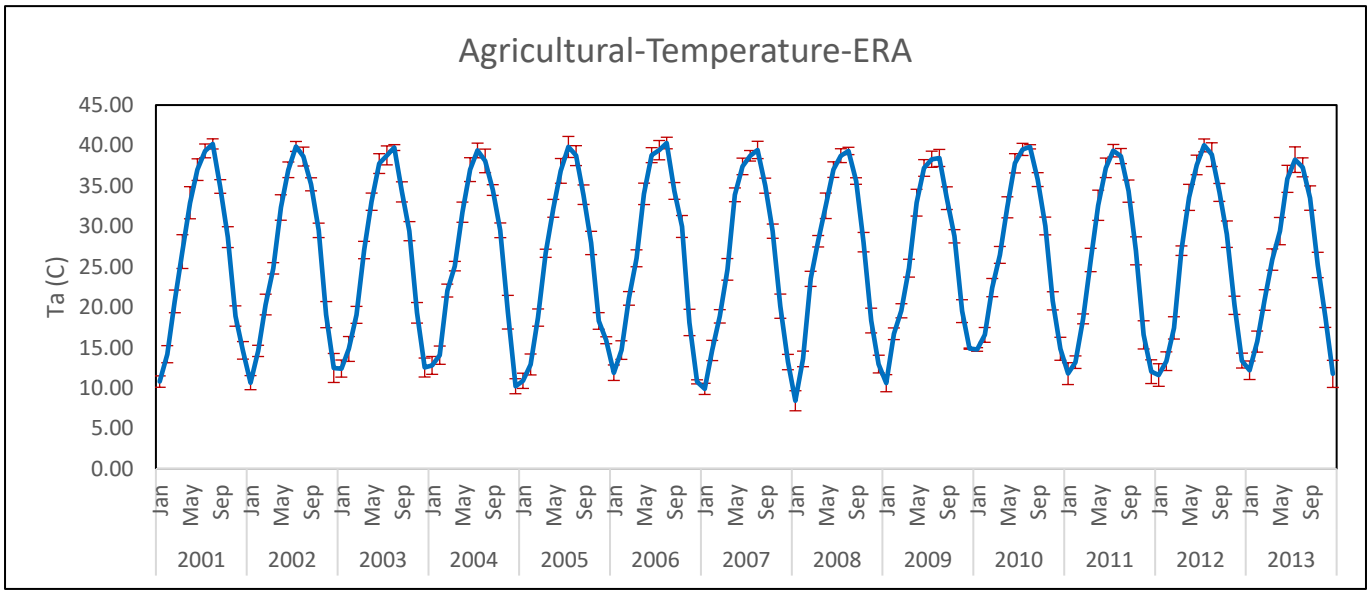
Agricultural-Temperature-ERA
Ta (C)
45.00
40.00
35.00
30.00
25.00
20.00
15.00
10.00
5.00
0.00
Jan May Sep
2001 2002 2003 2004 2005 2006 2007 2008 2009 2010 2011 2012 2013

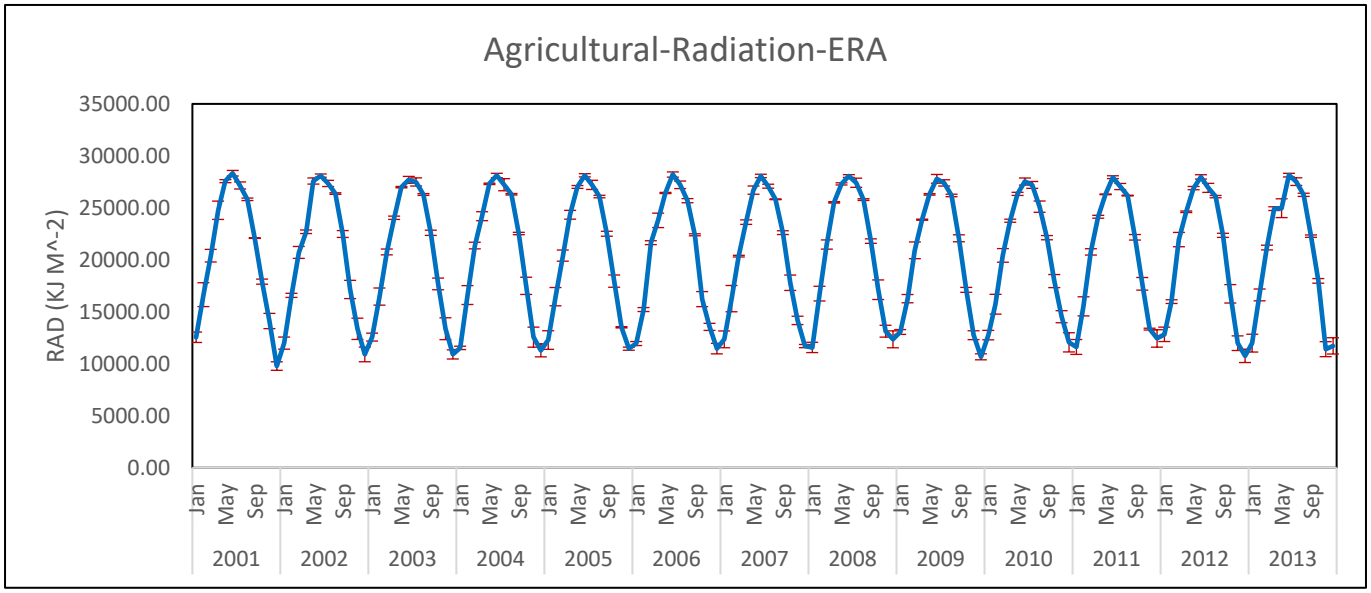
Agricultural-Radiation-ERA
RAD (KJ M^-2)
35000.00
30000.00
25000.00
20000.00
15000.00
10000.00
5000.00
0.00
Jan May Sep
2001 2002 2003 2004 2005 2006 2007 2008 2009 2010 2011 2012 2013

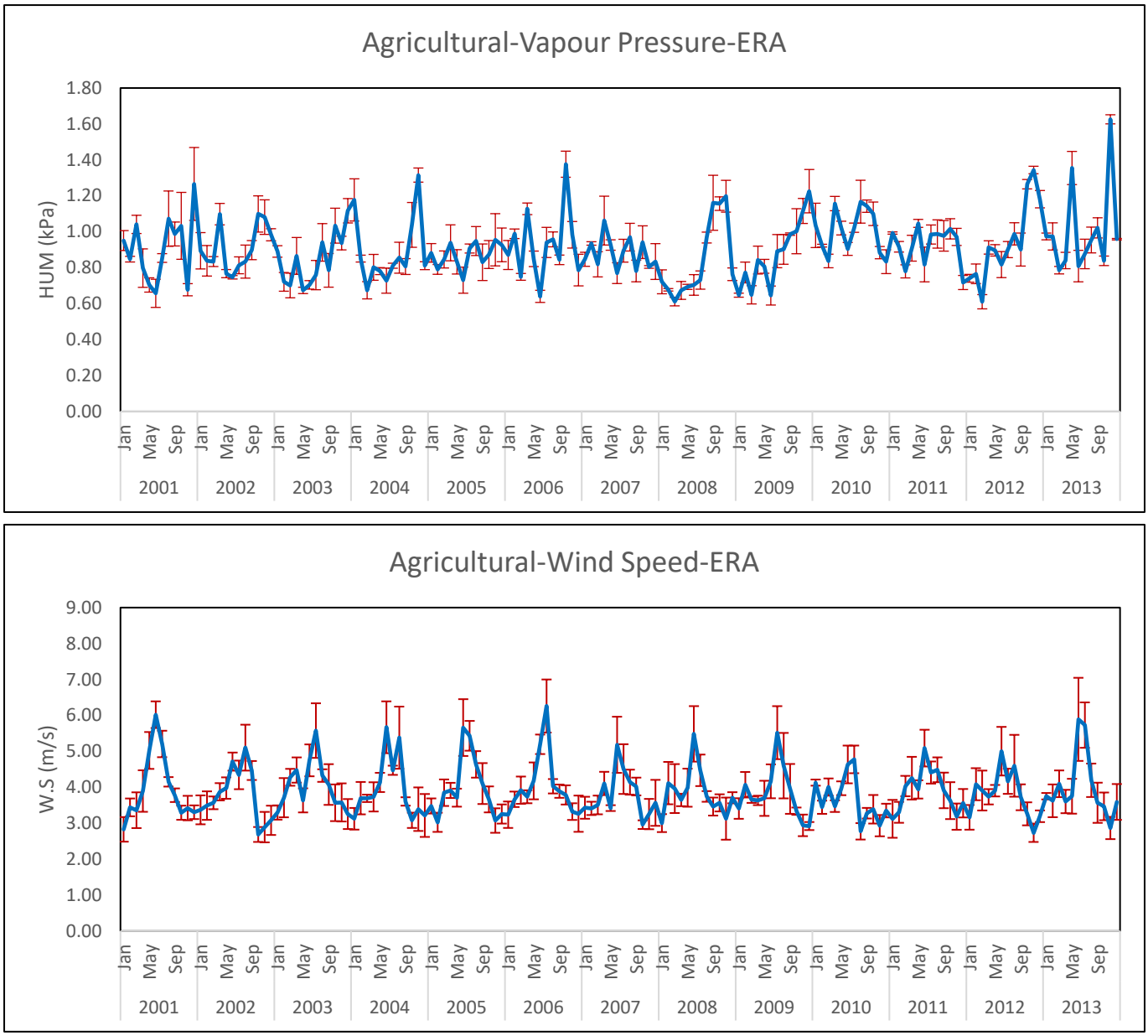

Figure 4.17 The interannual variations of the seasonal courses of the ERA interim meteorological driving variables, expressed as monthly sums for rainfall and radiation and averages for the other variables during 2001-2013.

4.5.2. Desert region

4.5.2.1. Potential transpiration (Tpot)

Values for the desert $Tpot$ are not presented as bare soil only was assumed in the model runs.

4.5.2.2. Potential evaporation (Epot)

Based on *measured in-situ driving data*, Fig. 4.18 shows that the dry season E_{pot} over the desert area initially had relatively low values at site 4 which varied from 6 to 8$mm\ d^{-1}$. E_{pot} for site 4 started to increase around 2004 and its peak values remained constant with a further slight increase between 2006 to 2008. E_{pot} *derived from ERA interim data* was almost identical for all desert sites (only site 4 is show here as an example, for brevity). $Epot$ (ERA) was larger than $Epot$ (in-situ) by up to 2.5 mm day^{-1} (i.e. year 2001) for most years, apart from 2003, when values were very similar.

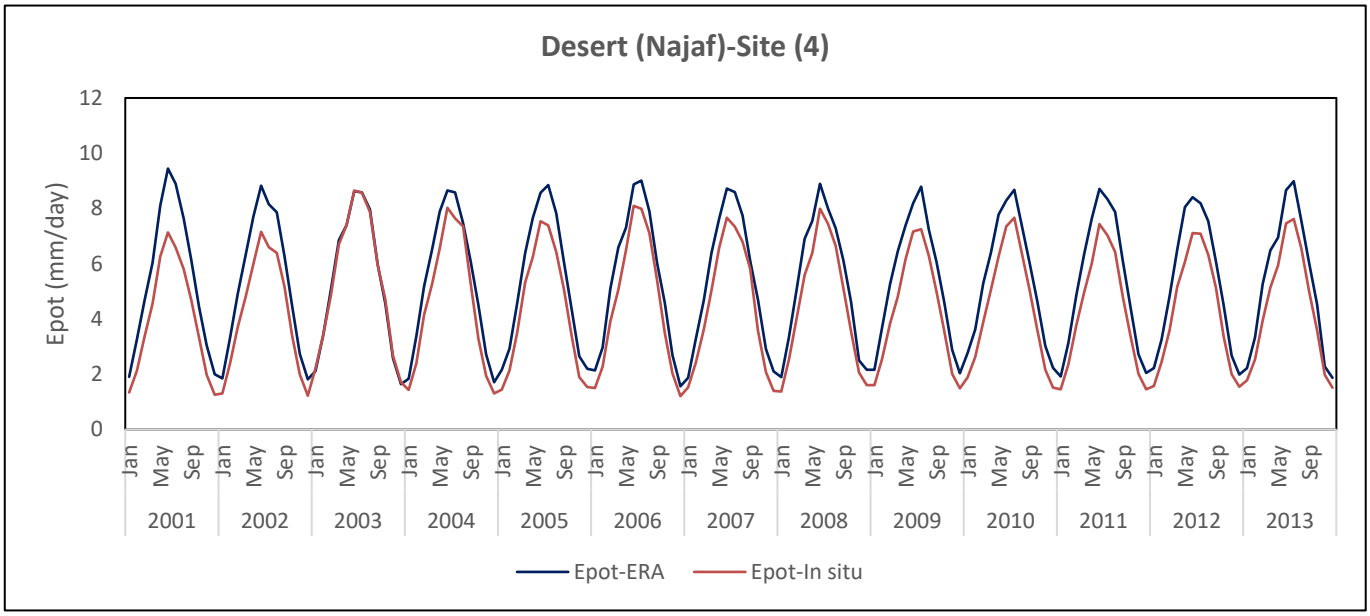

Figure 4.18 Temporal variations in E_{pot} for a representative desert site over Iraq during the period 2001-2013, using measured meteorological driving data and driving data from the ERA interim dataset.

4.5.2.3. Potential evapotranspiration (ETpot)

$ETpot$ is the sum of $Epot$ and $Tpot$. No results are shown for the desert, because $ETpot$ = $Epot$ (see Fig. 4.18).

4.5.2.4. Actual evaporation (Eact)

Actual evaporation ($Eact$) occurs for all land surface cover types and while its potential rate largely depends on the LAI (rangeland and crops only), its actual rate also depends on near-surface soil moisture content (see section 3.2.5 in Chapter 3 and the hydraulic properties of the soil type. Top-soil soil moisture content shows considerable seasonal, interannual and spatial differences (see section 4.3.7 and Appendix E) and hence $Eact$ is expected to vary in a similar fashion.

Fig. 4.19 presents the evolution of $Eact$ for the desert region (again using site 4 as an example) over the study period. Based on SWAP runs driven by measured data, generally, for each year, apart from 2012, two peaks were observed, relating to an increased rainfall during wet seasons. The results for site 4 illustrate that dry season $Eact$ varied from 0.4 to 0.6 $mm\ d^{-1}$ over the period 2001 to 2004, i.e. only a fraction of what is potentially possible ($Epot$, see Fig. 4.18), while $Eact$ was very low for sites 1, 2, and 3). Highest values occurred in 2006, 2009, and 2013. From 2005 to 2006, the maximum $Eact$ increased, ranging between 0.6 to 0.8 $mm\ d^{-1}$, whereas values were notably decreased in 2007 and 2008 (around 0.5 $mm\ d^{-1}$).

SWAP runs driven with *ERA interim data as weather input* show that $Eact$ had low dry season values compared with the period 2008 to 2010, site 1 excepted, where $Eact$ for year 2011 was quite high (see Appendix G). The results also showed that $Eact$ was high in 2013 in the desert region, especially compared to 2008 to 2010; in 2013, a peak close to 0.9 mm day^{-1} was observed. Fig. 4.19 shows that there is a considerable difference between both time-series of $Eact$, in particular for 2004, 2006, 2009.

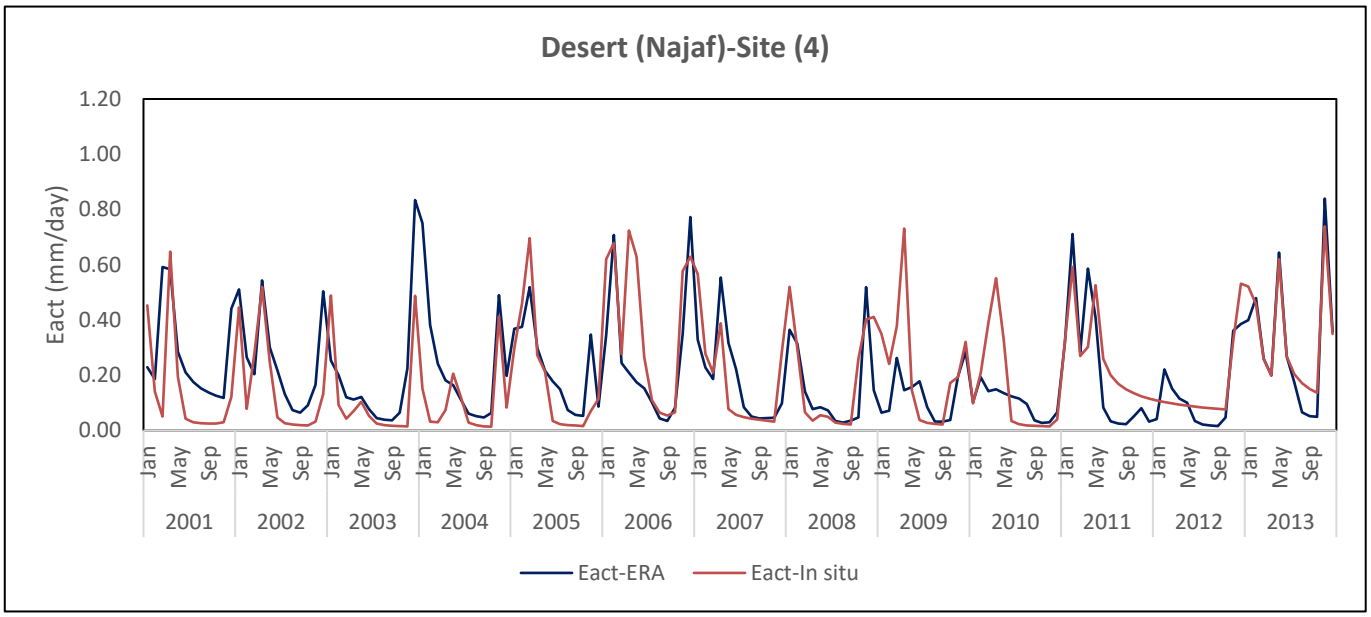

Figure 4.19 The temporal changes in seasonal E_{act} for site (4) over Iraq during 2001-2013 using measured and ERA interim dataset to drive the SWAP model.

4.5.2.5. Changes in soil water storage

For all surface types changes in soil water storage are the result of the balance between incoming terms (precipitation, irrigation where applicable) and outgoing terms ($ETact$, and surface- and subsurface runoff). Negative values mean a temporary loss of water from the soil profile, positive values denote the opposite. Changes in the total soil profile water storage as calculated by SWAP for the desert area site 4 are shown in Fig 4.20. When SWAP was driven by measured meteorological data, the year 2011 had a very wet season for this site (ΔS = 130 mm). The year 2013 also had a high soil moisture storage value (~ 60 mm).

SWAP results based on ERA interim driving data show that the evolutions of ΔS were overall similar to those found with in-situ driving data.

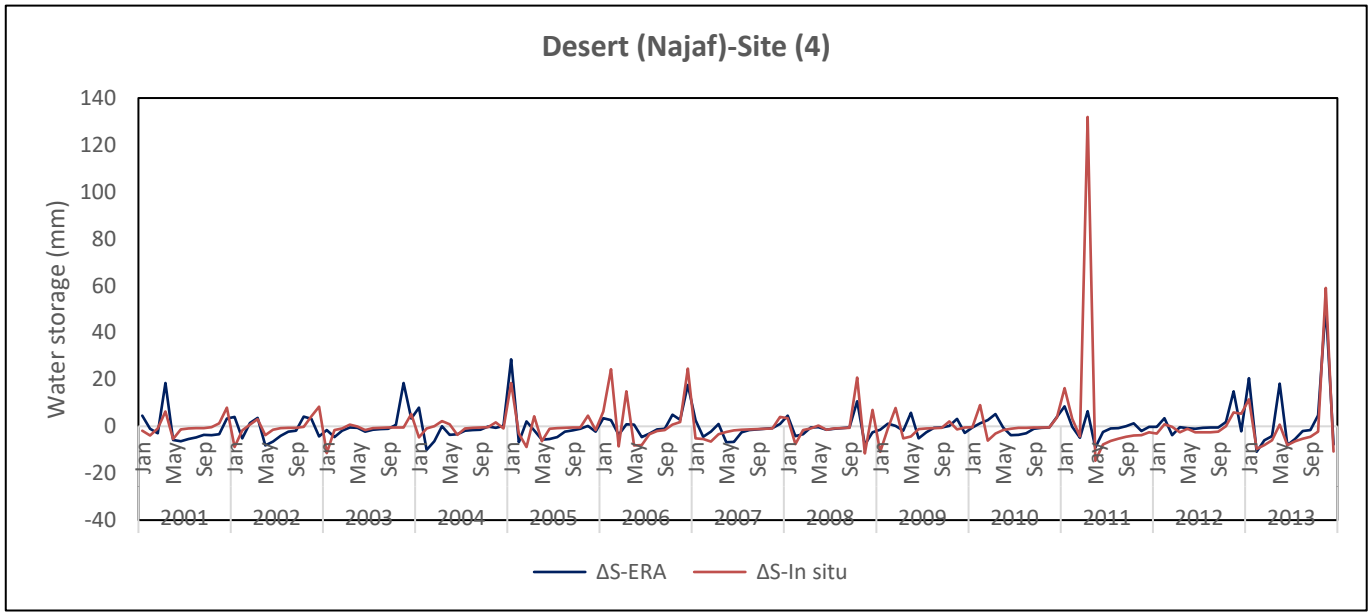

Figure 4.20 The temporal changes in seasonal ΔS for a typical desert region site (4: Najaf) over Iraq during 2001-2013 using measured and ERA interim dataset.

Generally, the profile soil water storage was highest for the years where most rain was received. This is illustrated by the rainfall as indicated by the bars in each of the figures below (Figs. 4.21 and 4.22). The large purple bars for May 2011 and November 2013 in Fig.4.21, and their effect on ΔS are apparent. The ERA rainfall driving data also indicate a peak for November 2017, but not for May 2011. Instead, they have comparatively large values for January 2005 and December 2006. These figures also summarise the other water balance components, as already discussed above.

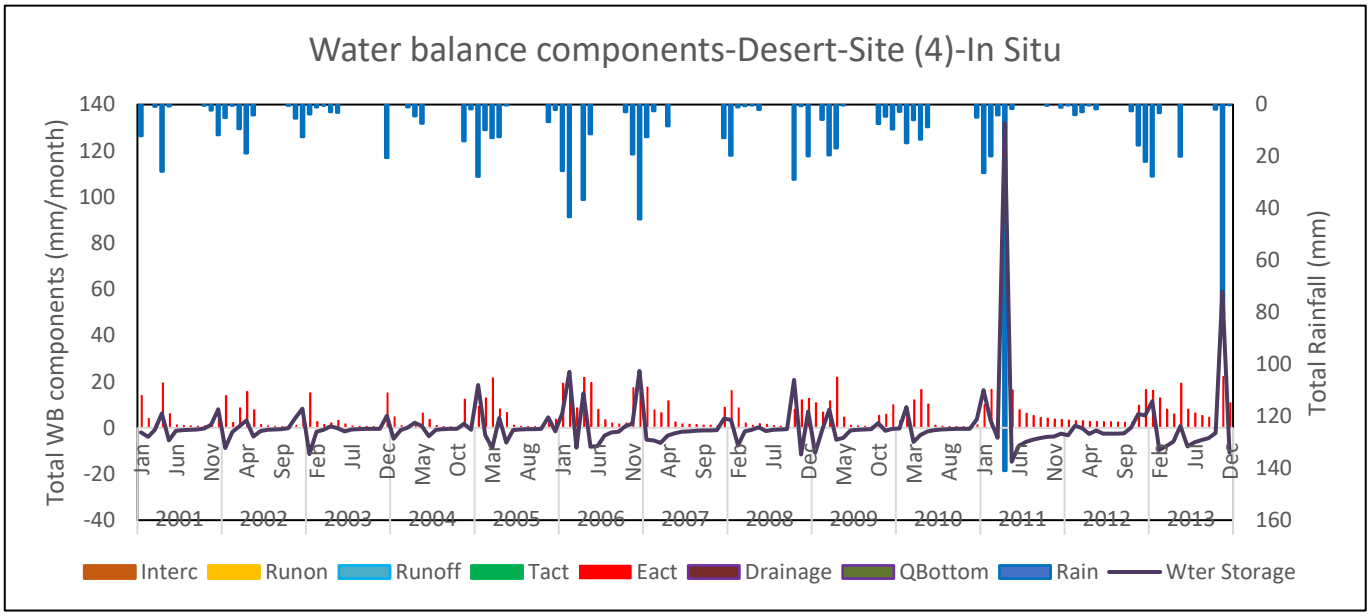

Figure 4.21 SWAP Water balance components over site 4 during 2001-2015, based on measured data, (QBottom, Drainage, Runoff, Runon, Tact, and Interc fluxes equal to zero).

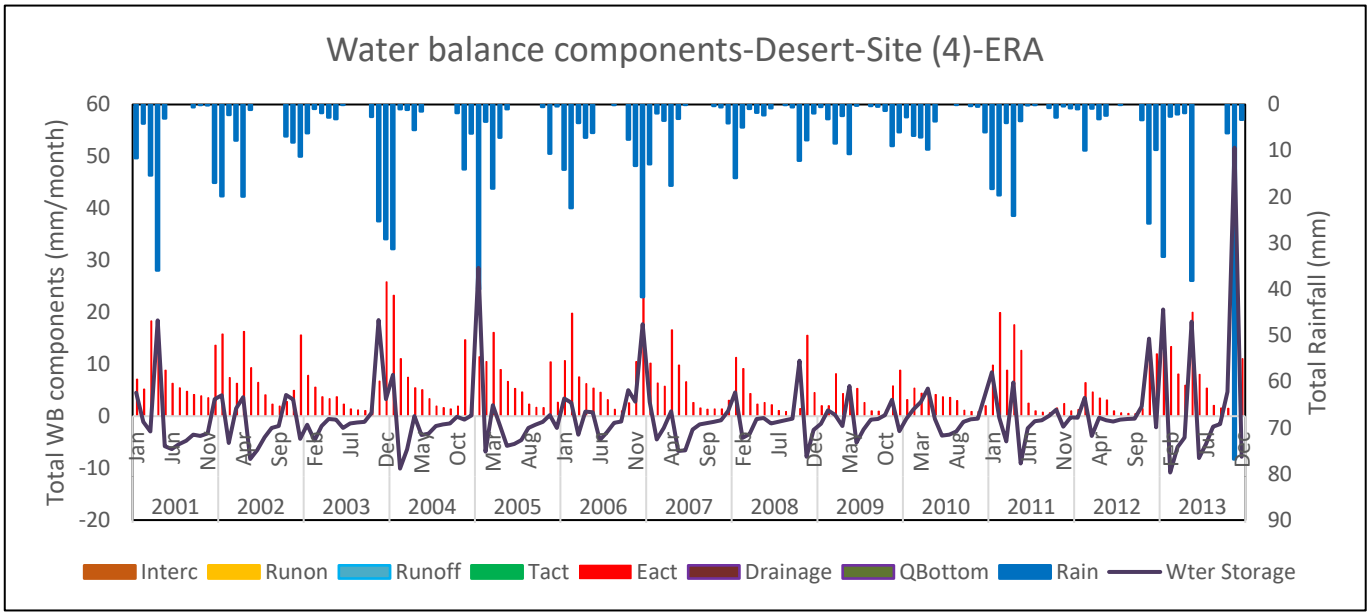

Figure 4.22 SWAP water balance components over site 4 during 2001-2015, based on ERA interim driving data, (QBottom, Drainage, Runoff, Runon, Tact, and Interc fluxes equal to zero).

4.5.3. Rangelands region

4.5.3.1. Potential transpiration (Tpot)

The monthly T_{pot} $(mm\ d^{-1})$ values for the rangelands region over 13 years (2001 to 2013) are presented in Fig. 4.23. Based on the SWAP results for the *observed meteorological data*, for site 23, the highest value was observed in 2001 (above $5mm\ d^{-1}$), and raised values were also found for 2002. Generally, there was a small increase of T_{pot} from 2007 to 2009, whereas during 2010 and 2012 SWAP predicted a significant decrease. T_{pot} slowly increased again in 2013.

T_{pot} was almost constant from 2001 to 2006 (ranging from 5 to 7 $mm\ d^{-1}$) when SWAP was *driven by ERA interim data*. Compared to the period 2001 to 2006, T_{pot} was somewhat lower (peak values of approximately $5mm\ d^{-1}$) during the dry seasons between 2007 to 2010, although there was a slight increase during winter seasons. T_{pot} values were the lowest in 2011 and 2012, and increased again in 2013 when ERA-Interim precipitation increased, similar to the in-situ values. T_{pot} values simulated with both driving datasets overall compared well, apart from for years 2004, 2010-2012 when ERA Interim $Tpot$ was considerably higher. The year 2003 was the only year when in-situ $Tpot$ > ERA $Tpot$.

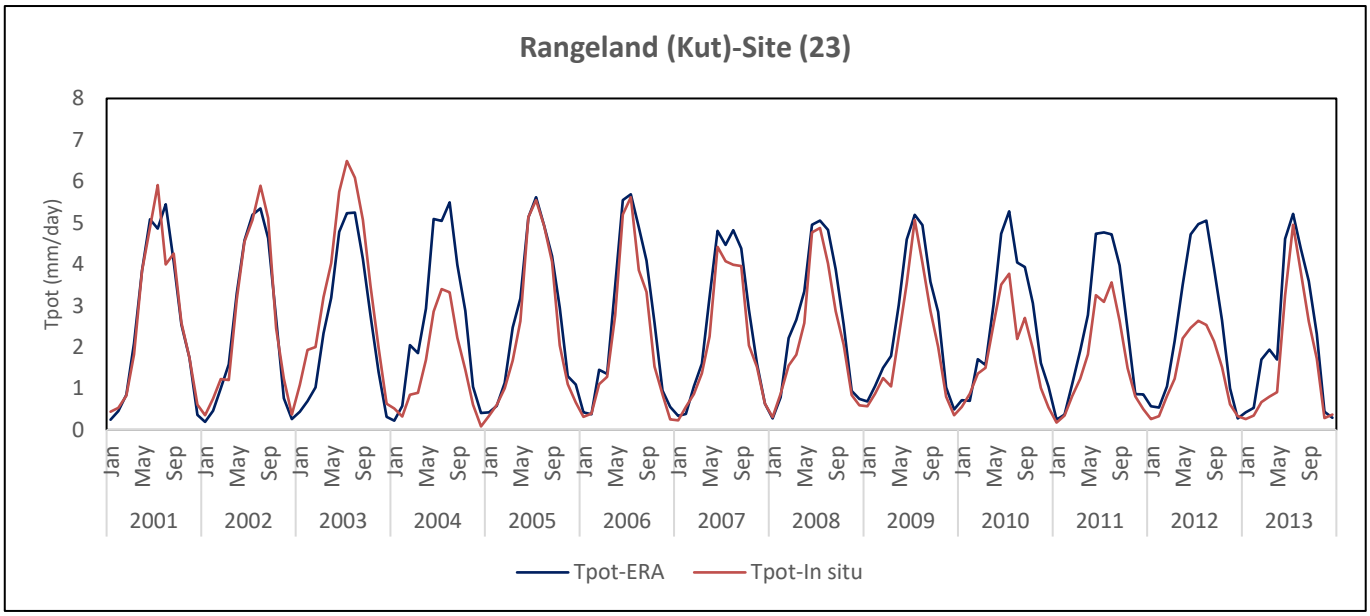

Figure 4.23 Seasonal and interannual and variations in T_{pot}as calculated by the SWAP model for the site 23 during 2001-2013 using measured and ERA interim driving datasets.

4.5.3.2. Potential evaporation (Epot)

The evolution in seasonal E_{pot} for the rangeland region based on *measured meteorological driving data* is shown in Fig. 4.24. Dry season E_{pot} over the whole rangeland region exhibited a modestly decreasing trend from 2009 to 2012 compared with the period from 2001 to 2008. However, dry season E_{pot} witnessed an increase in 2013 for all sites (see Appendix H).

Fig. 4.24 also shows E_{pot} based on SWAP simulations *driven by ERA interim data*. The data sequence shows some periods of relatively constant maximum and minimum values of E_{pot} throughout the period of 2001 to 2006, and a slight decrease between 2007 to 2013; during 2013 values increased somewhat again.

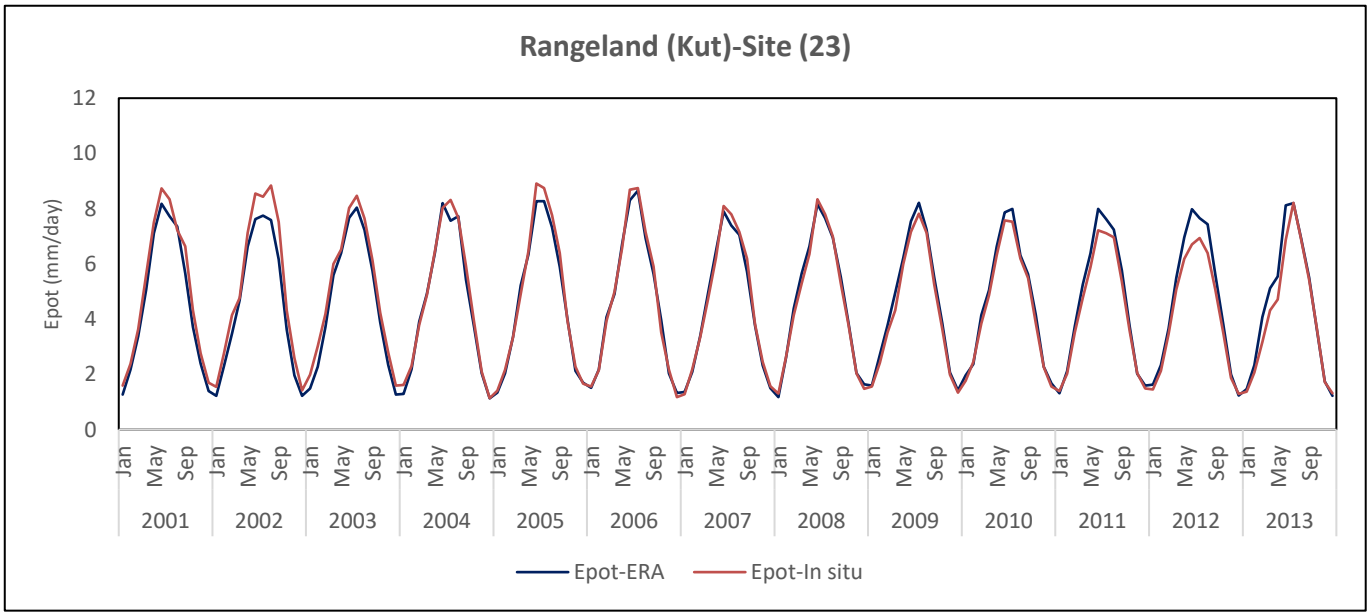

Figure 4.24 Interannual variations in seasonal E_{pot} predicted by SWAP for site 23during 2001-2013 using measured and ERA interim driving data.

Differences between the two $Epot$ timeseries are small, but note that in-situ data generated slightly higher values of $Epot$ between 2001-2005, whereas the reverse was true from 2010-2013.

4.5.3.3. Potential evapotranspiration (ETpot)

Driven by measured meteorological data, SWAP predicted gradually decreasing dry season ET_{pot} values from 2001 to 2013 (Fig. 4.25). ET_{pot}had the highest rate (between 12 to 14 $mm\ d^{-1}$) between 2001 to 2004 for all study sites in this region (see Appendix H), after which a decrease was observed between 2005 to 2009 (average values around 12 $mm\ d^{-1}$). ET_{pot} decreased further between 2010 to 2012, so that peak values were < 12 $mm\ d^{-1}$; a slight increase was observed in 2013.

The typical ET_{pot} evolution can be clearly observed at site 23. For this site, ET_{pot} ranged from 2 to 14 $mm\ d^{-1}$, stayed in this range from 2001 to 2006, and then decreased gradually to peak values of approximately 12 $mm\ d^{-1}$ from 2007 to 2009. It slowly decreased again down to peak values of 8 $mm\ d^{-1}$ in 2012. In 2013, a dramatic increase to peak values of 14 $mm\ d^{-1}$ was observed.

The results for $ETpot$ when SWAP was *driven by ERA interim driving data* showed ET_{pot} to have decreased during the study period for all sites in this region. For site 23 peak values were at between ~ 14 to 16 $mm\ d^{-1}$ between 2001 to 2006. It fluctuated much more strongly during the years 2010 to 2012 than between 2001 and 2009, and ET_{pot} increased in 2013. Biggest differences between the runs driven with the two datasets were observed for 2010-2012.

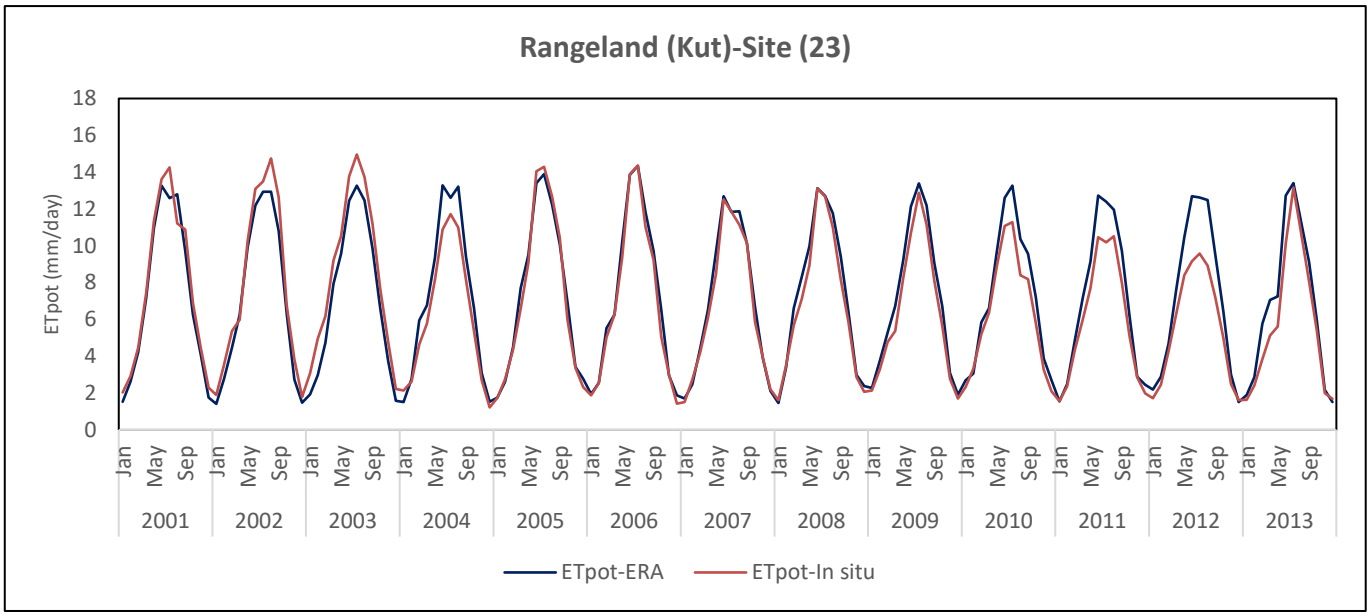

Figure 4.25 Interannual variation of seasonal ET_{pot} for rangelands region (Site 23 as a typical example) over Iraq during 2001-2013 using measured and ERA interim datasets to drive SWAP.

4.5.3.4. Actual transpiration (Tact)

The interannual variation of seasonal actual transpiration ($Tact$) obtained by using *measured meteorological data* to drive SWAP is presented in Fig. 4.26. $Tact$ for the dry season was very low in 2001, mainly because of low LAI and precipitation values, see Figs. 4.27 and 4.16 increased to ~ 0.3 $mm\ d^{-1}$ in 2002, then dropped down to less than 0.1 $mm\ d^{-1}$ in 2003, and increased again to values around 0.5 $mm\ d^{-1}$ in 2004. In general, a strongly decreasing trend in $Tact$ was present between 2005 to 2012, $Tact$ was approximately 0.6 $mm\ d^{-1}$ in 2005, and reached values of around 0.5 and 0.2 $mm\ d^{-1}$ in 2006 and 2007, respectively, after which $Tact$ was the lowest from late 2007 to 2010 and 2012, with near-zero values. Finally, the rates of $Tact$ during the dry season of 2013 were the highest during the study period, with values up to 1.0 $mm\ d^{-1}$. For site 23 $Tact$ values were comparable to those calculated for the other rangeland sites, albeit with slightly higher overall than the values found for other sites in this region.

SWAP output obtained with *ERA interim driving data* indicated that in 2001 and 2002 $Tact$ was comparatively high, and ranged from 0.8 to 1.2 $mm\ d^{-1}$. $Tact$ values underwent a sudden decrease during 2003 (values just above 0.2 $mm\ d^{-1}$). A slightly increasing trend was observed for $Tact$ during 2003 to 2005; from 0.6 to 0.8 $mm\ d^{-1}$. Generally, a small decreasing trend in $Tact$ was apparent from 2005 to 2012, with the lowest values occurring between 2008 to 2010, and 2012. $Tact$ experienced a large increase in 2013 (reaching values of approximately 0.9 $mm\ d^{-1}$). The overall evolution for site 23 was very similar to the one described above for in-situ data, but with higher values of $Tact$. Fig. 4.27 shows the rangeland LAI derived from NDVI (see Eq. 3.17) for site 23. Values are low, ranging between 0.18-0.30, but these values are typical for sparse rangelands in dry climates.

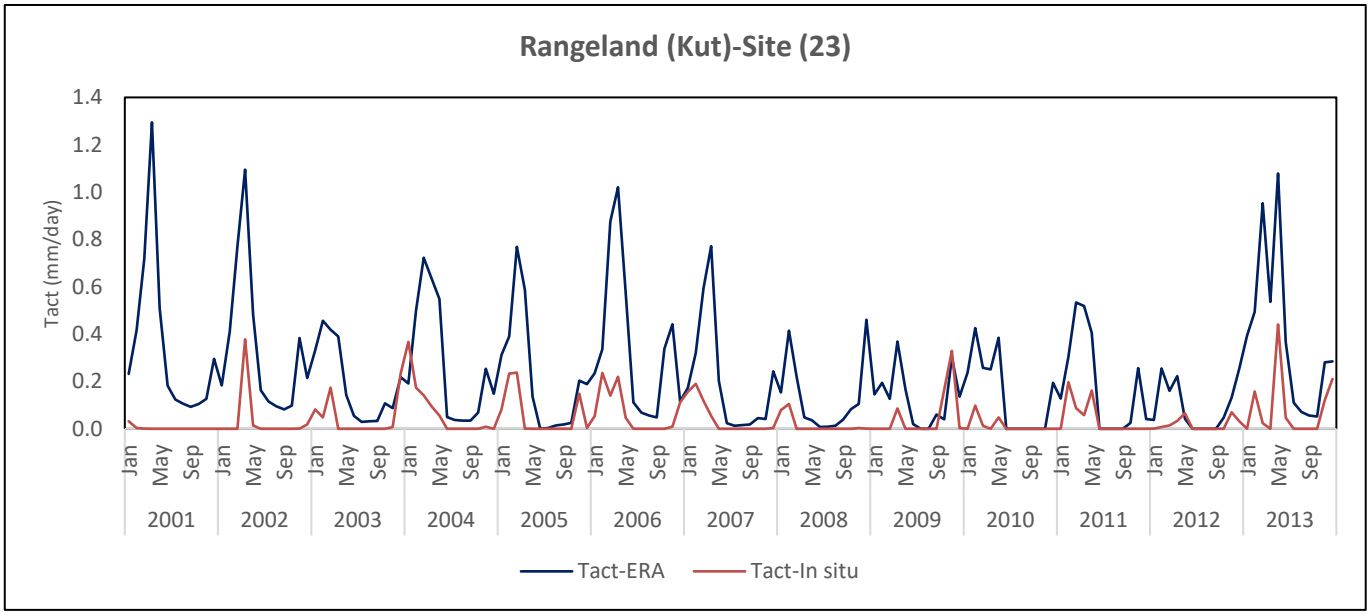

Figure 4.26 Variation in seasonal T_{act} for rangeland region over Iraq during 2001-2013 using measured and ERA interim dataset to drive SWAP.

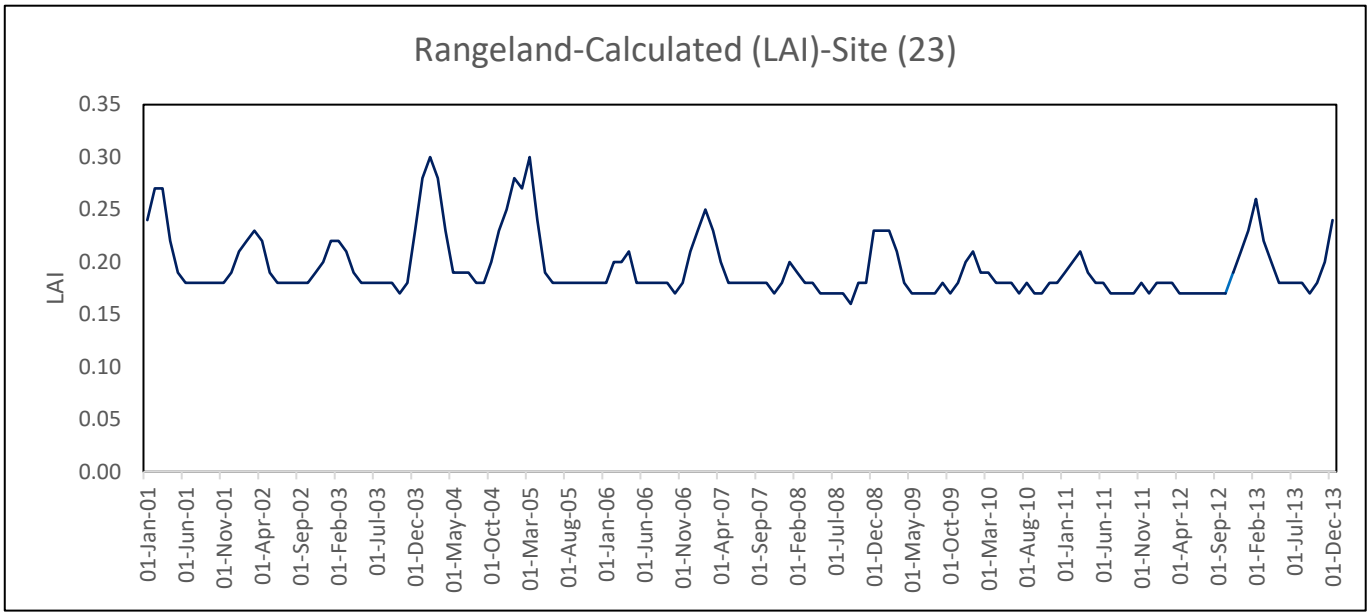

Figure 4.27 Estimation LAI of site 23 based on NDVI during 2001-2015.

4.5.3.5. Actual evaporation (Eact)

Fig. 4.28 shows $Eact$ for the rangeland region, obtained with SWAP. When using in-situ data, dry season $Eact$ increased gradually from 2010 to 2013 for all sites in this region. However, late in 2002 and at the beginning of 2003 at site 14, $Eact$ was very low, and 2011 and 2012 had a similar scenario (see Appendix H). *SWAP driven by ERA-Interim data* results in relatively similar spatiotemporal $Eact$ variations, with large differences in 2002, 2003, and 2012.

Overall, values for rangeland are slightly larger than those for desert. Note that these land surface types occur in different climatic zones (see Fig. 2.3), with atmospheric variables affecting $Epot$ and hence $Eact$. Furthermore, $Eact$ and Tact are affected by near-surface and root-zone available SMC, respectively, so that $Eact$ and Tact are considerably lower than their potential counterparts.

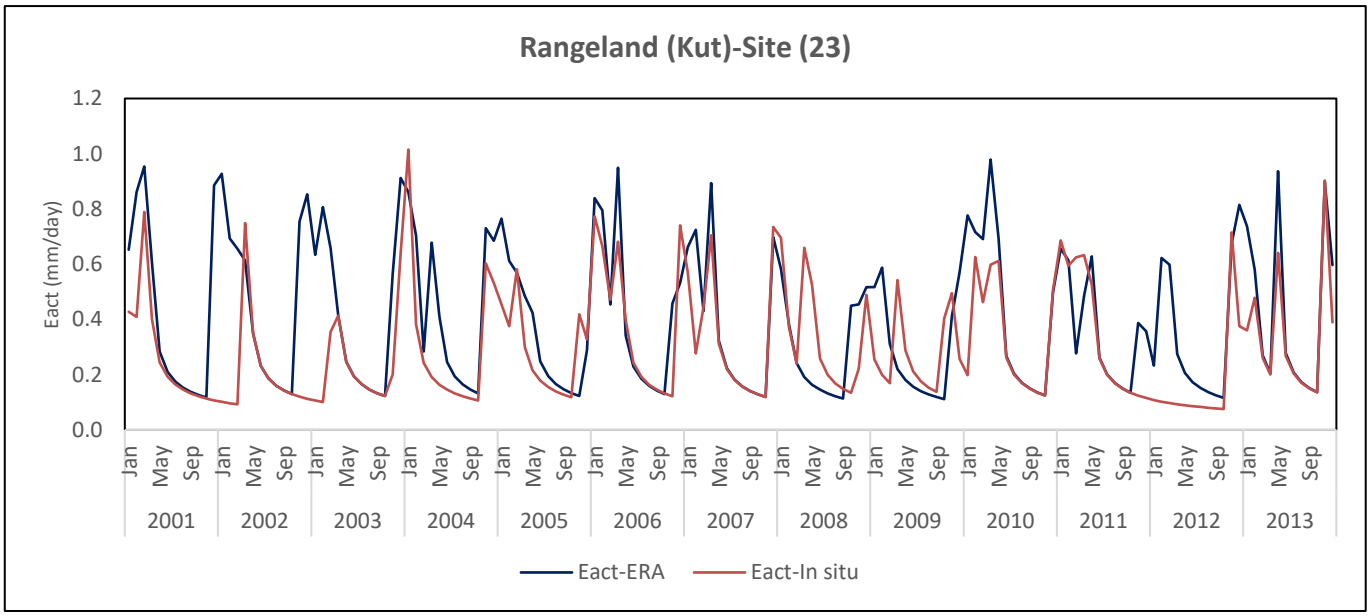

Figure 4.28 Interannual variations in seasonal E_{act} for the rangeland region (as illustrated using site 23) over Iraq during 2001-2013 using measured and ERA interim driving dataset.

4.5.3.6. Actual evapotranspiration (ETact)

Actual evapotranspiration is the sum of $ETact$ and Tact, hence is only shown for rangeland and agricultural sites.

Fig. 4.29 and Appendix H show the variations in $ETact$ predicted by SWAP for rangeland regions, from 2001 to 2013. *Based on measured driving data*, the evolution of $ETact$ for site 23 was very similar, but values were lower than for most other sites. Between 2005 and 2007 values slightly decreased; they were around 0.85$mm\ d^{-1}$ on average. The values of $ETact$ from 2008 to 2012 were low compared with other periods; values increased again in 2013. *Based on ERA interim data*, $ETact$ for site 23 follows a similar evolution as discussed above for in situ data except that values were higher compared with the SWAP output obtained with the measured data, in particular for years 2001-2003 and 2012.

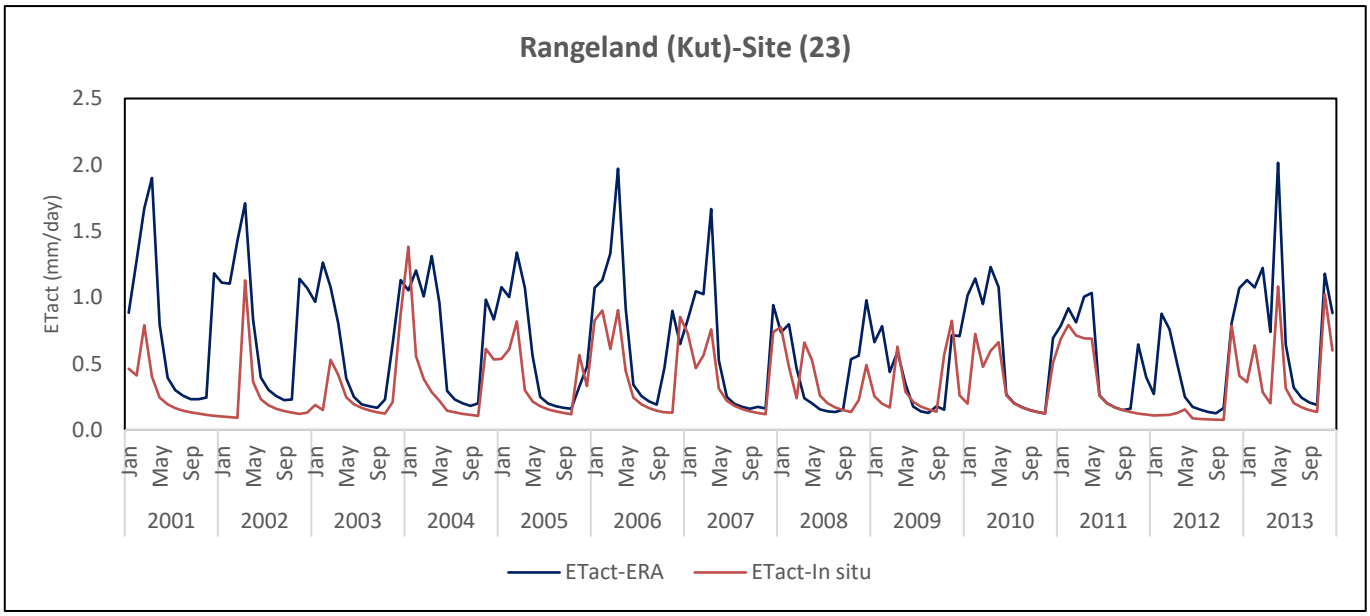

Figure 4.29 Interannual variations in seasonal ET_{act} for rangeland region (Site 23) over Iraq during 2001-2013 using measured and ERA interim driving datasets.

4.5.3.7. Changes in soil water storage

SWAP results based on measured driving data showed that the seasonal fluctuations in water storage for sites 16, 20, and 21 were very low during 2008 to 2010 (see Appendix H). During the wet season, ΔS of was highest in 2013, which was about 131 mm for all 3 Bahgdad sites.

The timeseries of soil water storage change were different for sites 14 and 23 (the latter shown Fig. 4.30). During the period 2003 to 2007 there are a number of extreme peaks during the wet seasons at site 14, see Appendix H, and peaks continue to occur for the remainder of the study period, except for in 2001, 2002, and 2012. The highest(ΔS) was found in 2007 (59 mm) for site 14, and in 2009 (41mm) for site 23, see Fig. 4.30.

ERA interim driven SWAP runs showed similar results, and the highest value was observed in 2013 for all sites (88.5 mm day^{-1}).

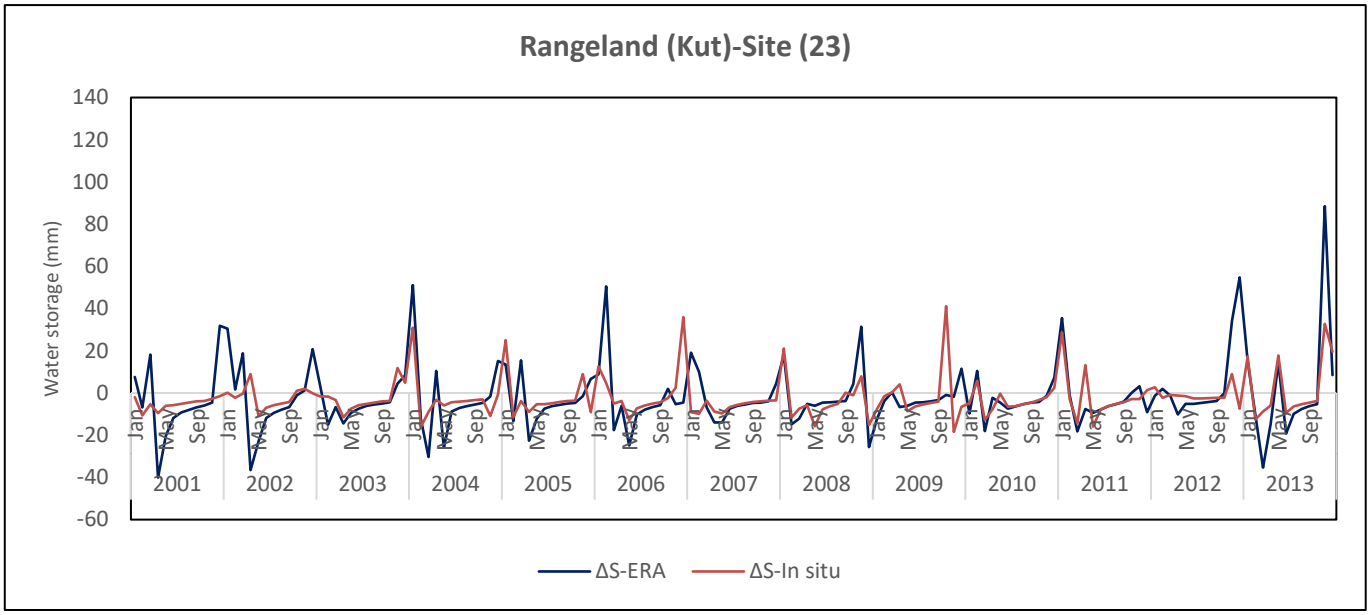

Figure 4.30 Interannual variations in seasonal ΔS for rangeland region over Iraq (site 23 shown as a typical example) during 2001-2013 using measured and ERA interim driving datasets.

Based on measured data, water storage was very low during part of 2001 and 2012, this is because of rain fall shortages, see Figs. 4.31 and 4.32, where the entire water balance for the rangelands is summarised. These figures show that $Eact$ > Tact, in particular for the in-situ data driven runs. For the ERA-Interim runs, Tact is larger and regularly exceeds Eact values, as a result of the considerably larger rainfall inputs. Other loss terms are small or negligible, apart from some interception, in particular in Fig. 4.32.

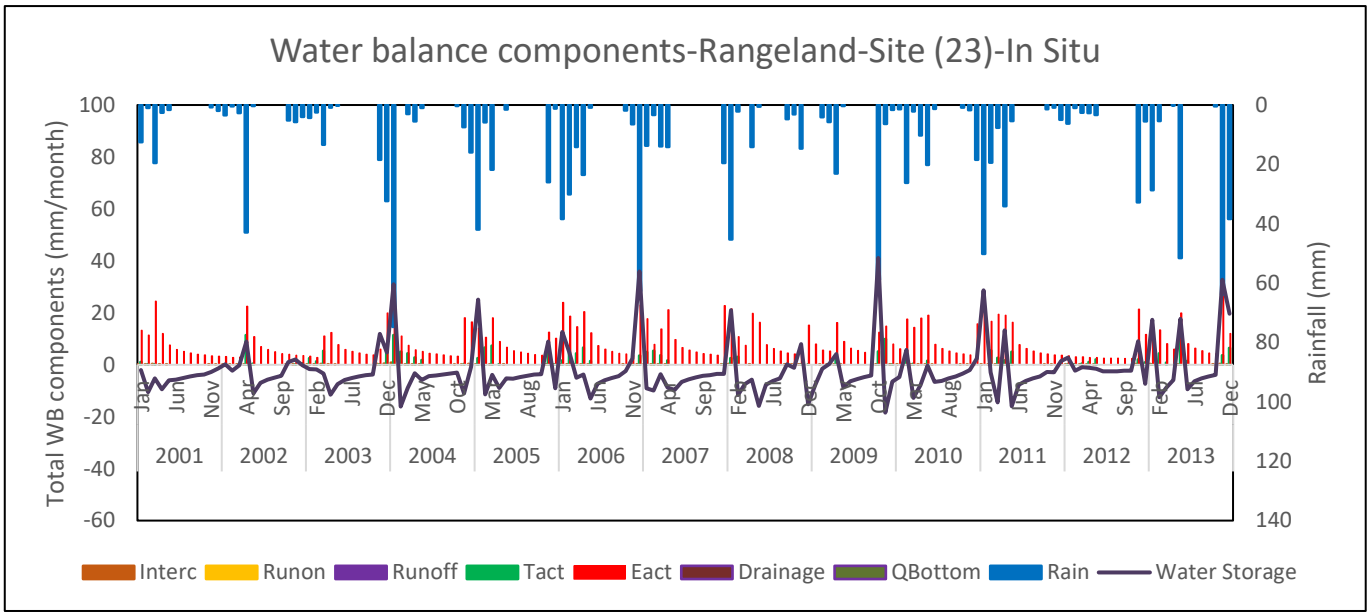

Figure 4.31 Water balance components over site 23 during 2001-2015, based on measured data, and calculated LAI, (QBottom, Drainage, Runoff, and Runon fluxes equal to zero).

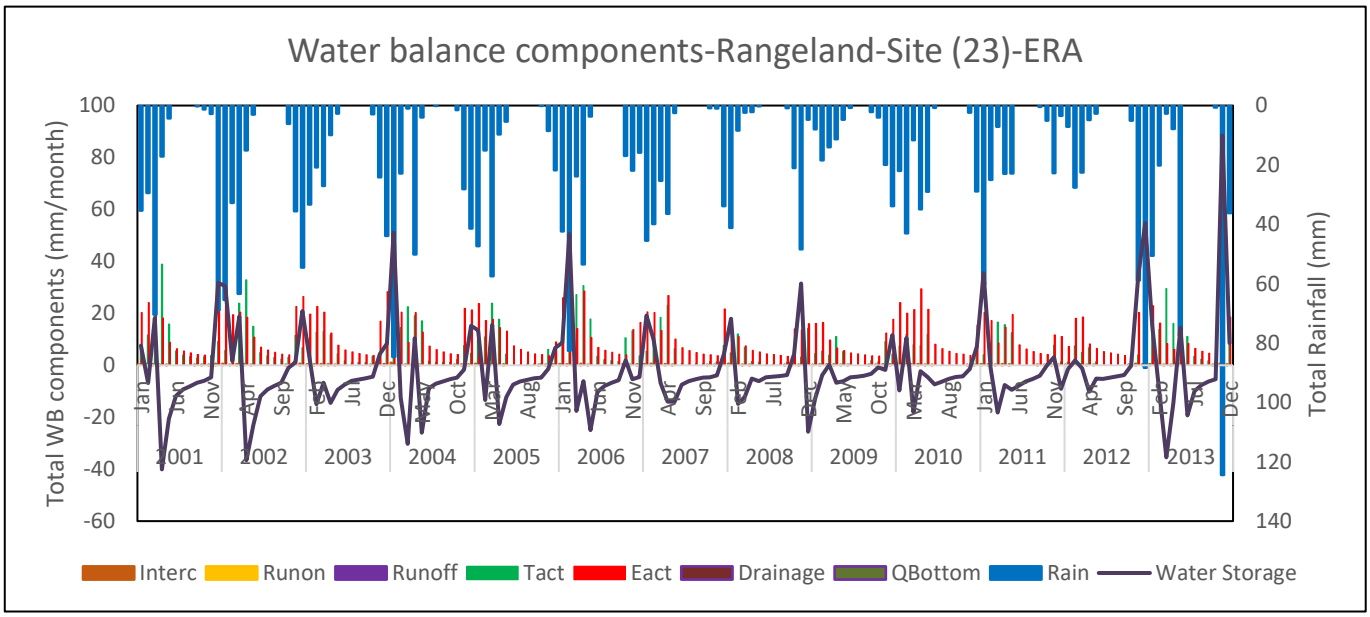

Figure 4.32 Water balance components over site (23) during 2001-2015, based on ERA interim data, and calculated LAI, (QBottom, Drainage, Runoff, and Runon fluxes equal to zero).

4.5.4. Agricultural region

4.5.4.1. Potential transpiration (Tpot)

$Tpot$ strongly depends on LAI. Fig. 4.33 shows the evolution of $Tpot$ between 2001 and 2015, as simulated by SWAP using both in-situ and ERA-Interim driving data (see section 4.5), and calculated and standard LAI values (Fig. 4.34). Firstly, note that for each year there are two peaks in $Tpot$ for all sites. This is caused by the fact that SWAP simulations were conducted for a rotation of two crops (wheat and maize growing between 15 December to 30 April and 15 July to 01 October, respectively, followed by bare soil). The wheat peak in $Tpot$ is smaller than the maize one and reaches peak values of around 4 mm day^{-1} or 8 mm day^{-1}, depending on whether calculated or standard LAI values are used. The second peak in $Tpot$ is much higher and attains values of up to 16 mm day^{-1}. In this case the choice of driving variables plays a much larger role than the selection of LAI approach for a considerable number of years, but particularly for 2001-2002. For some years, differences in wheat peaks between the runs are negligible, e.g. for 2003, 2004 and 2013. The size of both peaks varies somewhat between years, but no real trends are apparent.

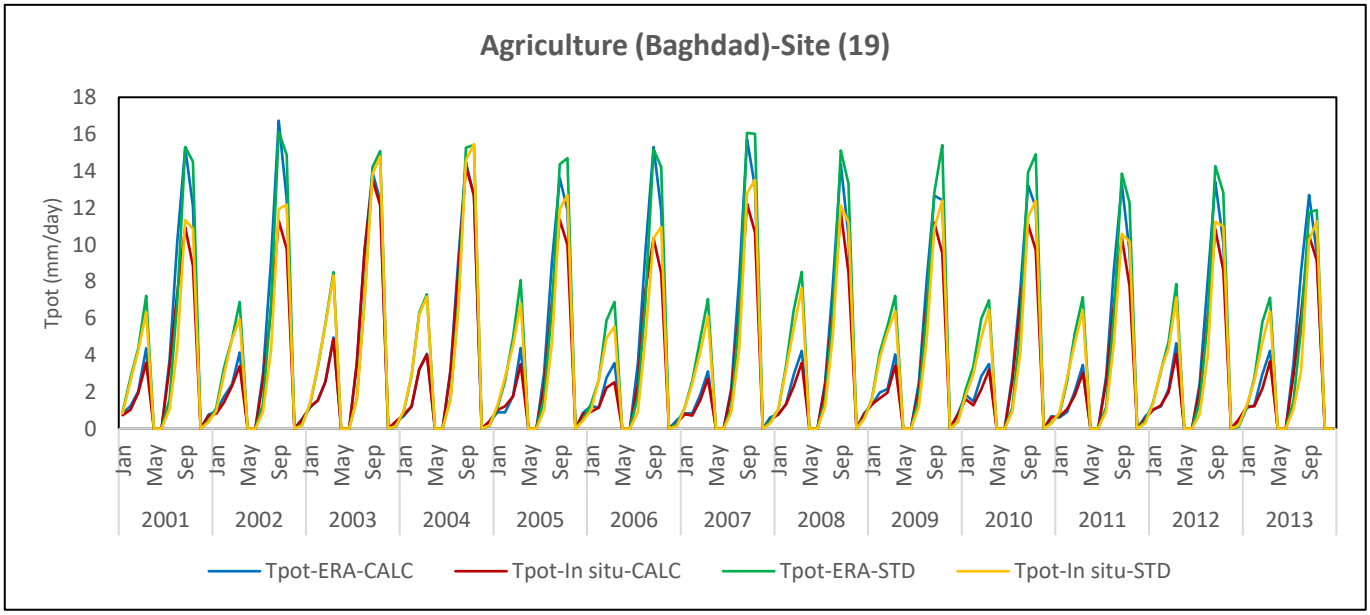

Figure 4.33 Interannual variations in seasonal T_{pot} for agricultural region (represented by site 19) over Iraq during 2001-2013 using measured and ERA interim dataset as driving variables, and LAI of the crops based on NDVI (CALC) and standard LAI (STD).

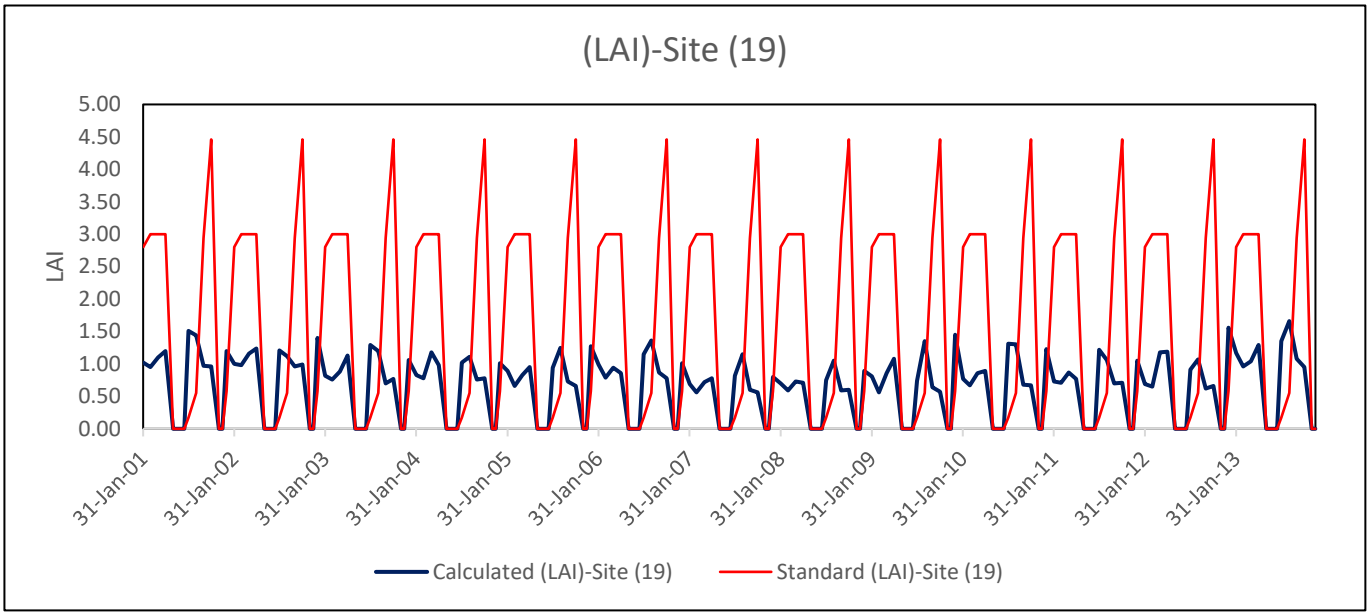

Figure 4.34 LAI of the crops based on calculated LAI (based on NDVI) and standard LAI during 2001-2015.

4.5.4.2. Potential evaporation (Epot)

Fig. 4.35 shows the seasonal and interannual changes of E_{pot} for the agricultural region (with site 19 selected as a typical example) during the study period, again for both sets of driving data and both LAI choices. $Epot$ ranged between 0 and 10 mm day^{-1} and has two peaks, one larger followed by a smaller one, as a result of the fact that the simulations are set up to grow two crops in succession. This means that when LAI is lowest, i.e. in between wheat and maize crop cycles and after the wheat growth during the fallow period (when $Tpot$ is highest, i.e. around May and at end of autumn; see Fig. 4.33), $Epot$ peaks. Also, for the standard LAI we see a pronounced period of zero $Epot$ values before the start of the maize cycle. Again, choice of LAI method appears to be more important that choice of driving data, for most years. SWAP runs for both sets of driving data show that E_{pot} peaks were higher between 2005 to 2008 compared with the period between 2009 to 2012. Dry season E_{pot} decreased between 2009 and 2010, then slightly increased again in 2013 for most sites.

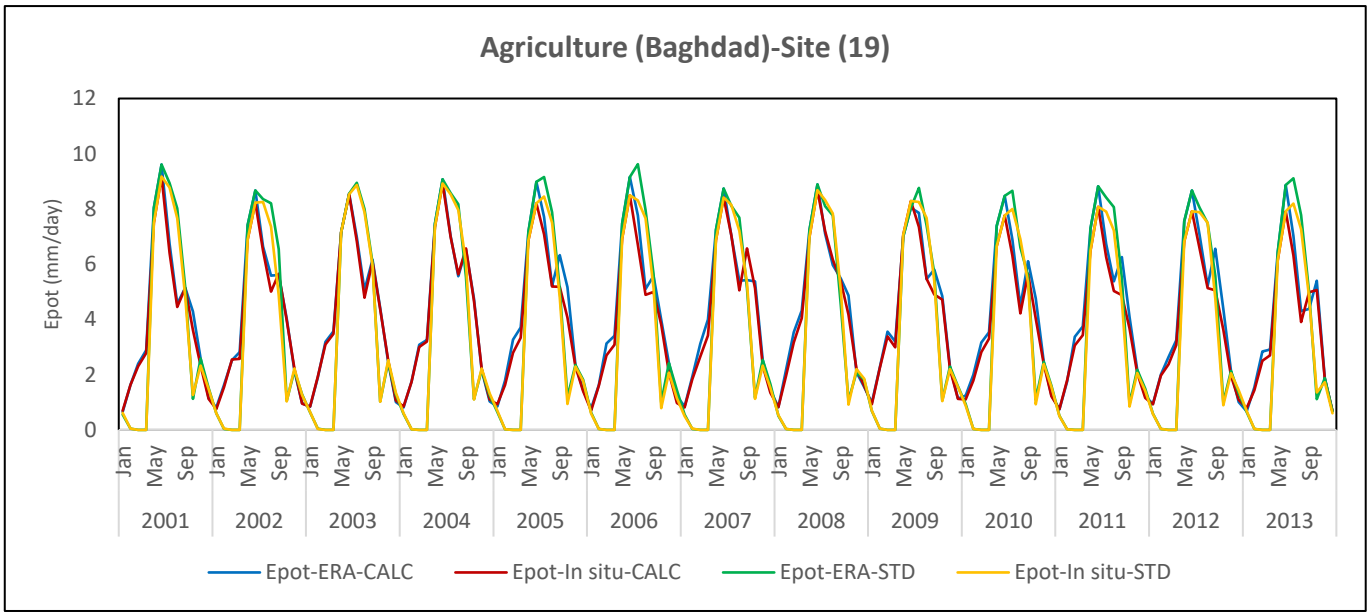

Figure 4.35 Interannual variations in seasonal E_{pot} for agricultural region (site 19 as a typical example) over Iraq during 2001-2013 using measured and ERA interim dataset, and LAI of the crops based on NDVI (CALC) and standard LAI (STD).

4.5.4.3. Potential evapotranspiration (ETpot)

ETpot values are overall higher for the agricultural sites than for the rangeland sites, because of the larger LAI values, leading to particularly large $Tpot$ values. Fig. 4.36 shows the seasonally varying ET_{pot} for site 19 from 2001 to 2013 based on measured and ERA-Interim driving data and LAI derived from NDVI, as well as for standard LAI values as used per default in SWAP. The seasonal ET_{pot} values over this site, as well as for the other agricultural sites, vary from 0 to 20 $mm\ d^{-1}$. The occurrence of the lowest and highest peak (dry season) values depended on the choice of driving data and LAI, but interannual differences were generally within 10% of the maximum $ETpot$ value. The use of ERA-Interim driving data predominantly resulted in higher values of $ETpot$, in particular for years 2001, 2002, 2006, 2011 and 2012. For 2003, differences between the 4 models runs were negligible.

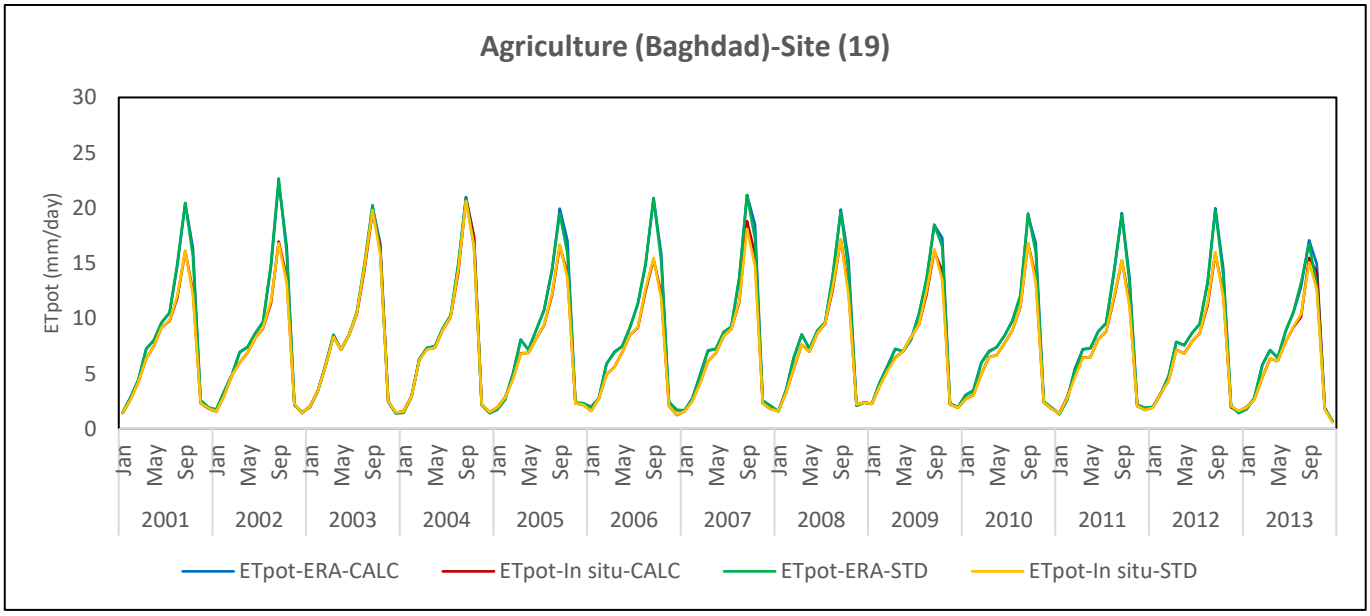

Figure 4.36 Interannual variations in seasonal ET_{pot} for agricultural region (site 19) over Iraq during 2001-2013 using measured and ERA interim dataset to drive SWAP, and LAI of the crops based on NDVI (CALC) and standard LAI (STD).

4.5.4.4. Actual transpiration (Tact)

The multi-year courses of seasonally varying SWAP simulations of actual transpiration ($Tact$), based on measured meteorological data and ERA-Interim, and with NDVI-based and standard LAI, for the agricultural sites (example site 19) is shown in Fig. 4.37. Each year has two peaks, the largest peaks always occurs in the dry season (irrigated maize crop). For site 19 maximum $Tact$ values reached around 12 mm day^{-1} throughout the study period. The first peak (irrigated wheat during rainy season) attained much lower values, generally between 2-3 mm day^{-1}, although some exceptionally high values were found between 2008-2010. Differences between the first peaks in Tact for the 4 model runs were particularly large during those years. When driven with ERA-Interim data the highest dry season $Tact$ values were identified in 2001 and 2002. When using in-situ driving data, SWAP yielded particularly low values of dry season Tact for 2001; differences in Tact between both driving data sets were nearly a factor 2. For other years, in particular 2003/2004, differences were much smaller.

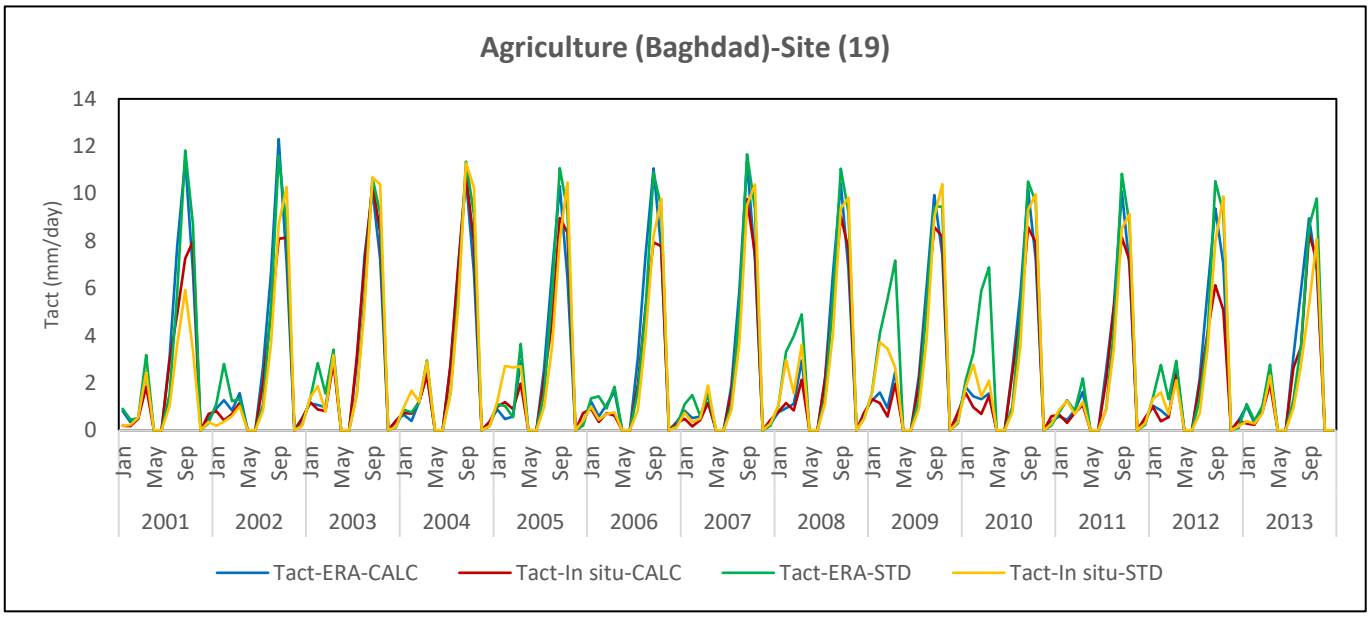

Figure 4.37 Spatiotemporal variations in seasonal T_{act} for site 19 over Iraq during 2001-2013 using measured and ERA interim dataset to drive the SWAP model, and LAI of the crops based on NDVI (CALC) and standard LAI (STD).

4.5.4.5. Actual evaporation (Eact)

Fig 4.38 shows $Eact$ for the agricultural regions (represented by site 19) for 2001 to 2013, with LAI values derived from NDVI or standard, and with in-situ and ERA-Interim driving data being used.

The simulated courses of $Eact$ represented by the red & blue lines (both driving datasets, with LAI derived from NDVI), like those for Tact in Fig. 4.37, also show two peaks per year, again in relation to the two growing seasons of the modelled crop rotation. The results indicate that the values of $Eact$ for the first peak are up to 2 mm day^{-1} and are in fact comparable in size to those for $Tact$. The values for the second peak are larger (maximum of ~ 4 mm day, about 30-50% of the size of maximum $Tact$). Interestingly, when standard LAI is used the first peak occurs in January and is very small, virtually negligible. During the rest of the winter-spring period, $Eact$ values are near zero because of the relatively large standard LAI values (see Fig. 4.34).

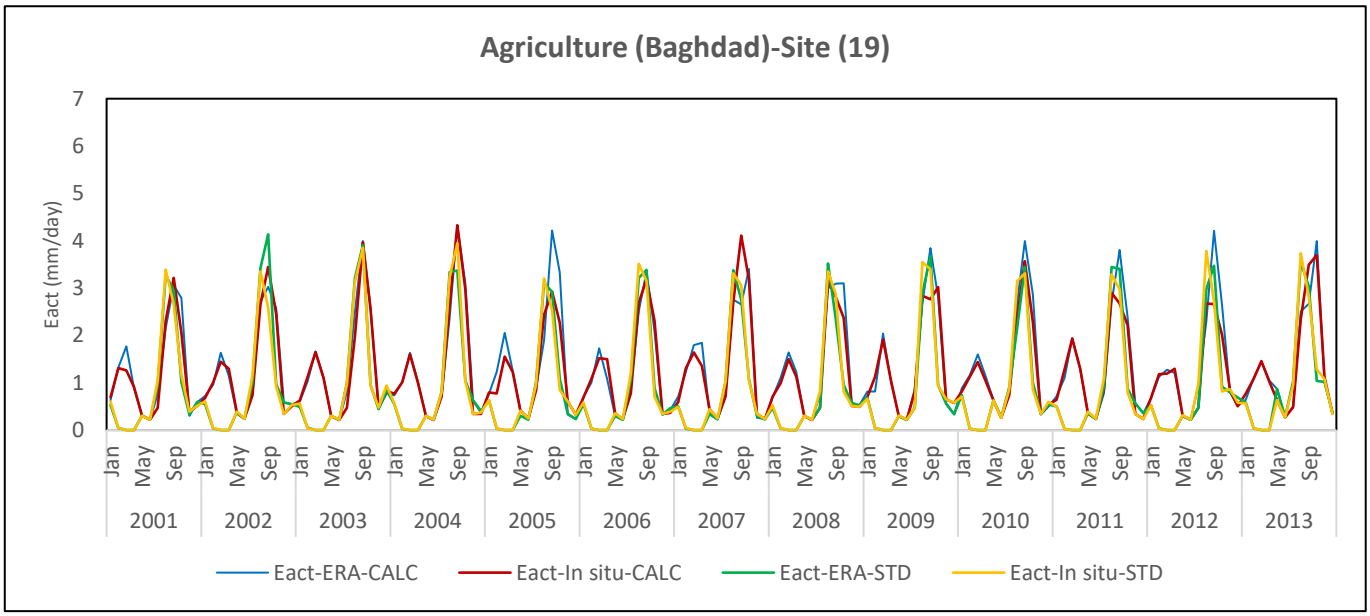

Figure 4.38 Spatiotemporal variations in seasonal E_{act} for agricultural region (site 19) over Iraq during 2001-2013 using measured and ERA interim dataset.

4.5.4.6. Actual evapotranspiration (ETact)

The multi-year evolution of $ETact$, i.e. the sum of $Eact$ and Tact is shown in Fig. 4.39, again for the 4 simulation runs. The smaller first peak (values up to ~ 7 mm day^{-1} in 2008-2009 (ERA-driven, standard LAI), but mostly around 3 mm day^{-1}) and larger second peak (maximum values ranging between ~8 mm day^{-1} (2012; in-situ driving data, NDVI-derived LAI) and 16 mm day^{-1} (2002; ERA driven, both LAIs) are again evident as per Figs. 4.37-4.38. As was the case for Fig. 4.37, the largest differences in the first peak of $ETact$ between the simulations are found for the years 2009-2010. For the second peak, the most prominent differences are for years 2001-2002 and 2011-2012. Differences are very small for 2003- 2004.

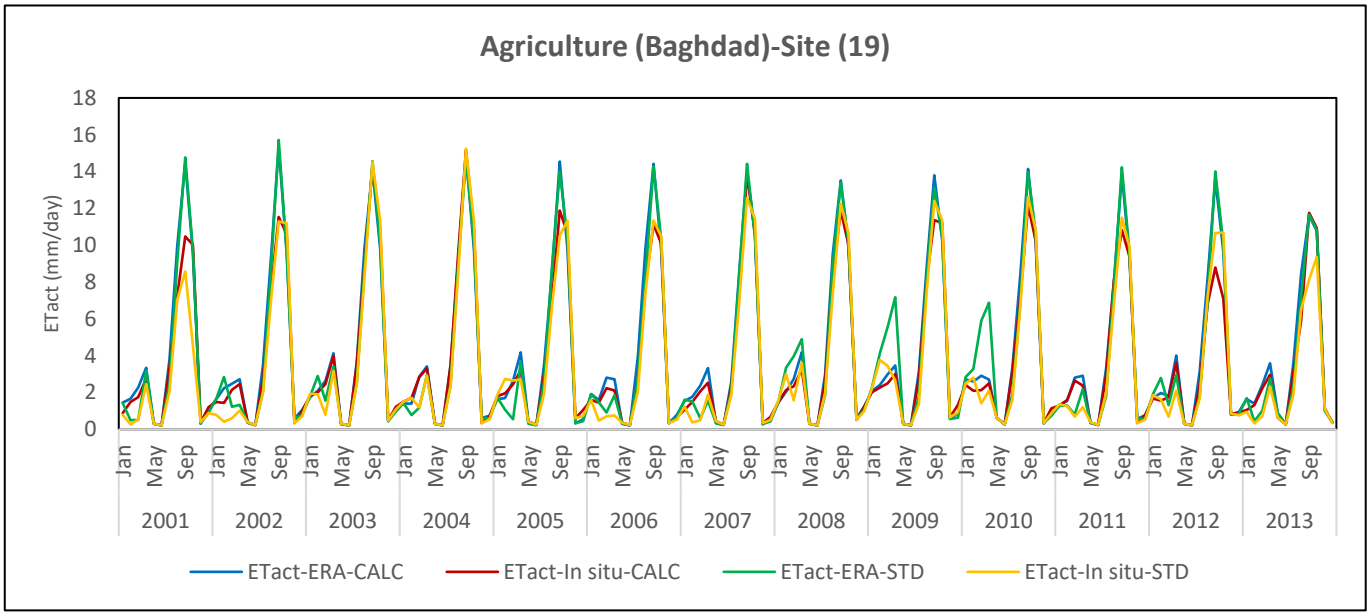

Figure 4.39 Spatiotemporal changes in seasonal ET_{act} for agricultural region over Iraq during 2001-2013 using measured and ERA interim dataset.

4.5.4.7. Changes in soil water storage

The results in Fig. 4.40 present a diagnostic dataset of seasonal variations in water storage for the agricultural region (from 2001-2013) based on measured and ERA-Interim derived driving data and LAI values calculated from NDVI and taken as standard from SWAP (Fig 4.40). ΔS values varied considerably among wet seasons for site 19, that was selected as representative for the agricultural region. Storage of water will depend on the amounts of rainfall during the wet season (when irrigated wheat was grown, causing the first smaller peak in $ETact$) and the amount of irrigation supplied during the dry season (during maize growth, the larger second peak in $ETact$), as well as on the values of $ETact$ itself. Other water balance components appear negligible (see Figs 4.41-4.42). Water storage simulated by SWAP varies between ~ +170 mm (year 2011, wet season, ERA driven) and -160 mm, 2005, dry season (but note that irrigation was supplied). The large *Tpot* for the ERA driven/standard LAI run caused rather negative ΔS values for 2009-2010, compared to the other 3 runs. Considerable differences between the simulations are also visible for the dry seasons of 2001 and 2002 and the end of dry season 2012/ start of wet season of 2013.

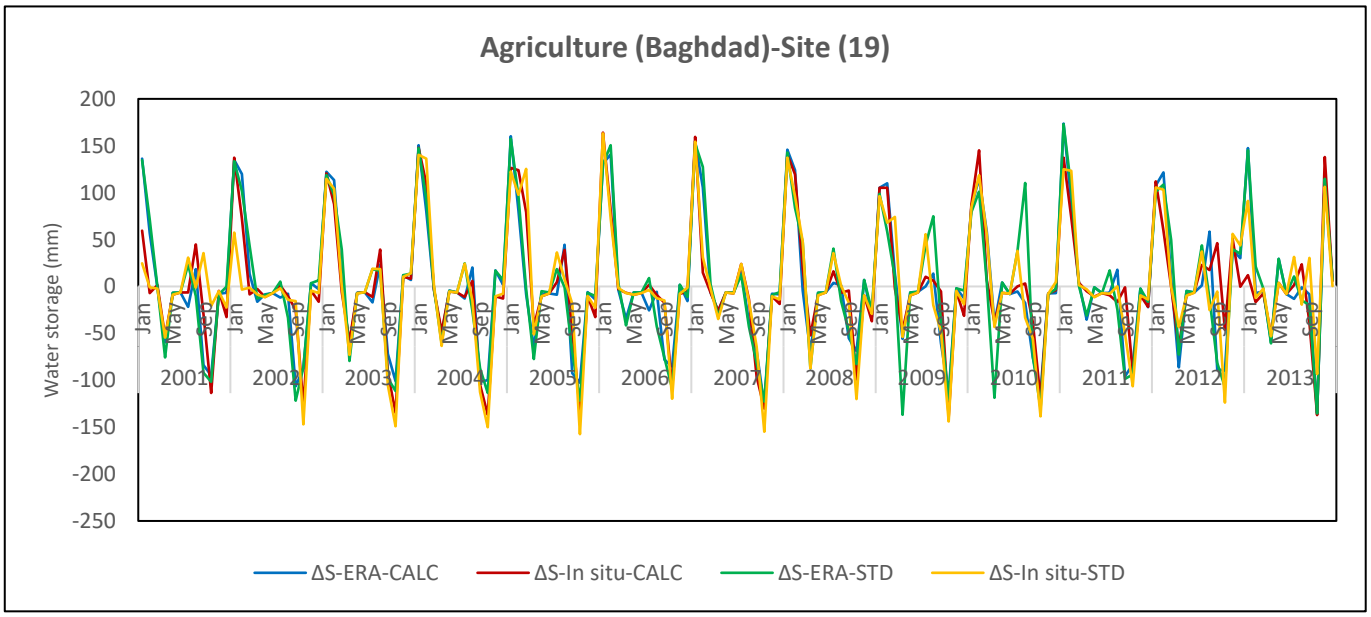

Figure 4.40 The temporal changes in seasonal ΔS for irrigated agricultural region (site 19) over Iraq during 2001-2013 using measured and ERA interim dataset.

Low water storage in 2008 to 2010 is more likely because of lack in the precipitation in these years, see Figs 4.41 and 4.42.

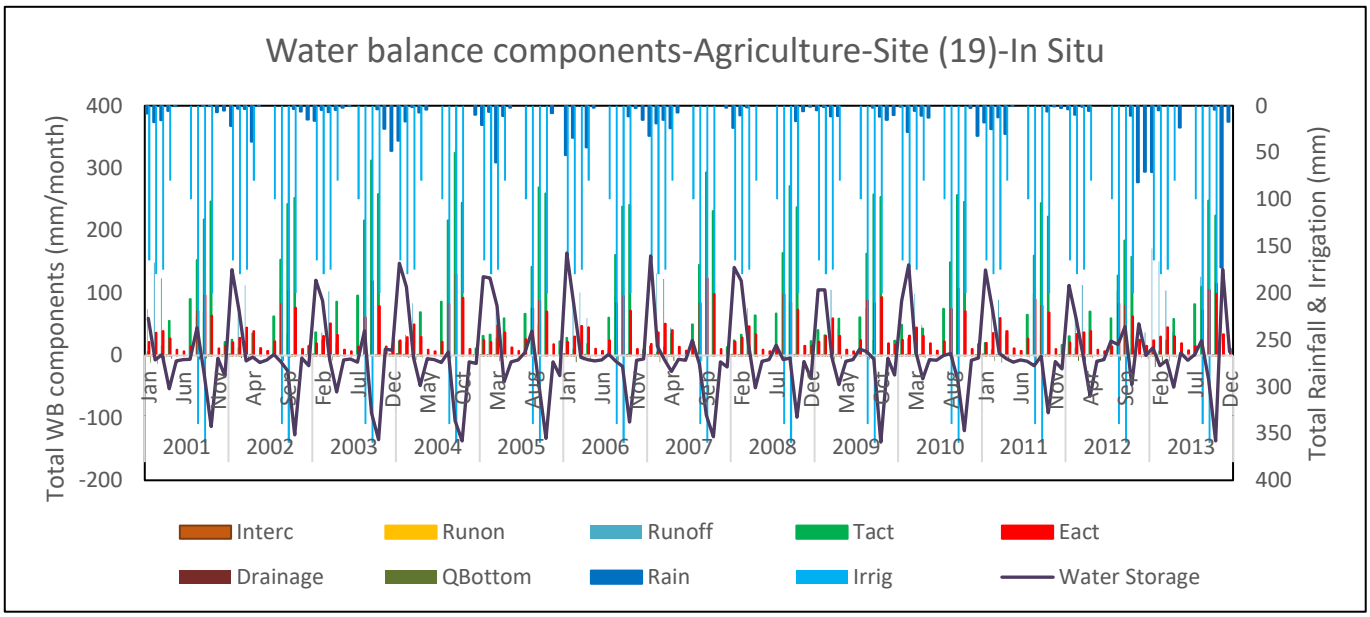

Figure 4.41 Water balance components over site 19 during 2001-2015, based on measured data, and calculated LAI (Drainage and QBottom fluxes equal to zero).

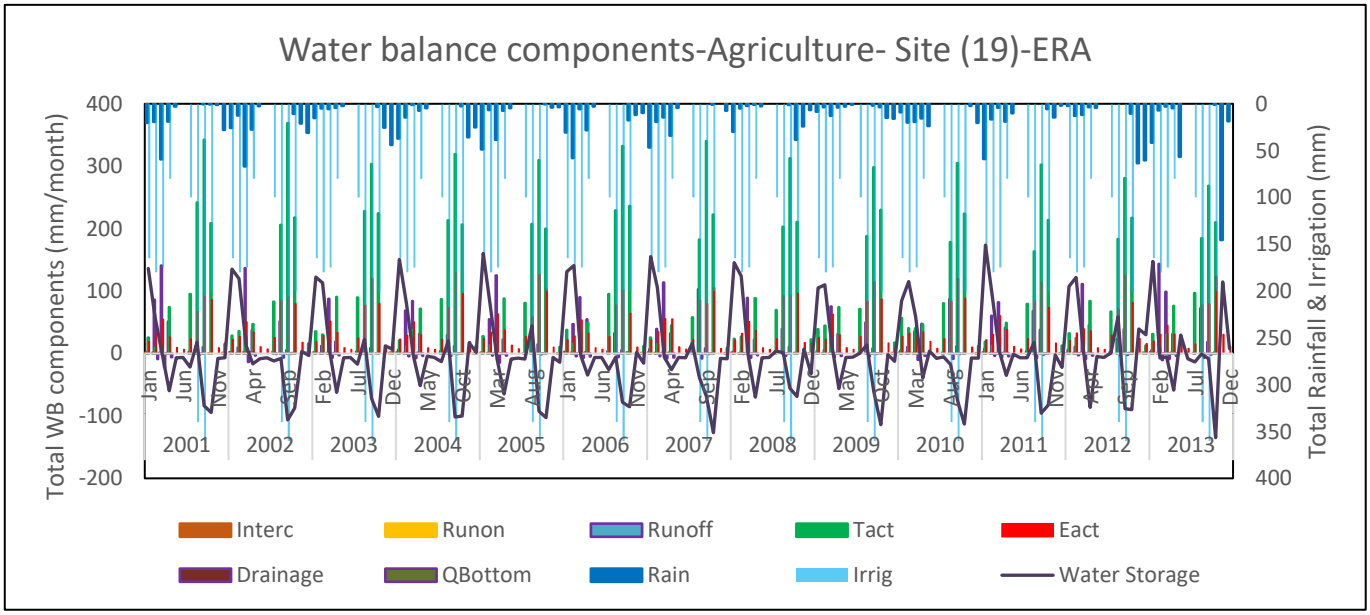

Figure 4.42 Water balance components over site 19 during 2001-2015, based on ERA interim data, and calculated LAI, (Drainage and QBottom fluxes equal to zero).

4.6. Comparison of SWAP for different land surface types

Figs. 4.43-4.49 shows a comparison of all water balance fluxes for the three regions, with the top-plot in each figure representing the SWAP runs driven by in-situ data and the bottom one for the ERA-Interim driving data.

Fig. 4.43 for $Tpot$ illustrates the large differences in absolute values (a factor of about 1.5) between the rangeland and the agricultural sites (note that $Tpot$ is zero for the desert sites), as well as a difference in timing of the peaks. This is mainly caused by differences in LAI (see Figs. 4.21 and 4.34), rather than the values of the driving variables that determine $Tpot$.

Fig. 4.44 shows that values of $Epot$ are in fact pretty similar, and values peak between 8-10 mm day^{-1} for all surface and for both driving sets.

As a result of the considerable differences in the evolution of $Tpot$ between rangeland and agricultural sites and the fact that desert has $Epot$ only, values for $ETpot$ are very different for the three surface types (Fig. 4.45). Peak values are lowest for the desert (between 7-9 mm day^{-1} or so), followed by the rangeland (up to 15 mm day^{-1}) and agricultural site (peak values > 20 mm day^{-1} for ERA-Interim).

Peak values also occur at different times during the season, with the (semi-)natural desert and rangeland sites exhibiting a peak around July, whereas the main agricultural peak is around September. This is the result of the supplementary irrigation for the second crop.

Looking at Tact (Fig. 4.46), large differences are observed between the agricultural and rangeland sites, both in size and timing. Rangeland Tact peaks during the rainy season that occurs during the first 4 months or so of each year. However, the agricultural region exhibits a much larger second peak because SWAP has been given a crop file with an irrigated maize (total irrigation depth = 1000mm) crop being grown after the irrigated wheat (total irrigation depth = 600). As atmospheric conditions (see Figs. 4.16, 4.17) favour high transpiration rates during the maize crop growth season, Tact is particularly high as enough water is available due to the irrigation being added to the SWAP rainfall data.

Whereas $Epot$ peaked roughly at the same time for all three surface types (as dictated largely by the atmospheric conditions), Fig. 4.47 shows that $Eact$ shows a very different behaviour.

Although the values of $Eact$ are very small (maximum around 0.80 (desert) and (rangeland) mm day^{-1}) for the (semi-) natural surfaces, the values for the agricultural site reach values up to 4.5 mm day^{-1}. The peaks for the maize crop occur around the same time as $Tact$ (with values double those of $Tact$) indicating that the crop was still relatively sparse at that time and that $Eact$ contributed considerably to $ETact$ (see Fig. 4.48). As expected from the previous plots the timing in peak and minimum values differed greatly between the regions.

Finally, with regards to, desert values were lowest, as expected. However, for rangeland peak values for certain years were as large as values of $ETact$ for the agricultural region, albeit at very different times.

Based on the discussion above it should come as no surprise that values of ΔS (Fig. 4.49) for the agricultural sites are much larger (positive and negative values) than for the other two sites, and have two pronounced peaks.

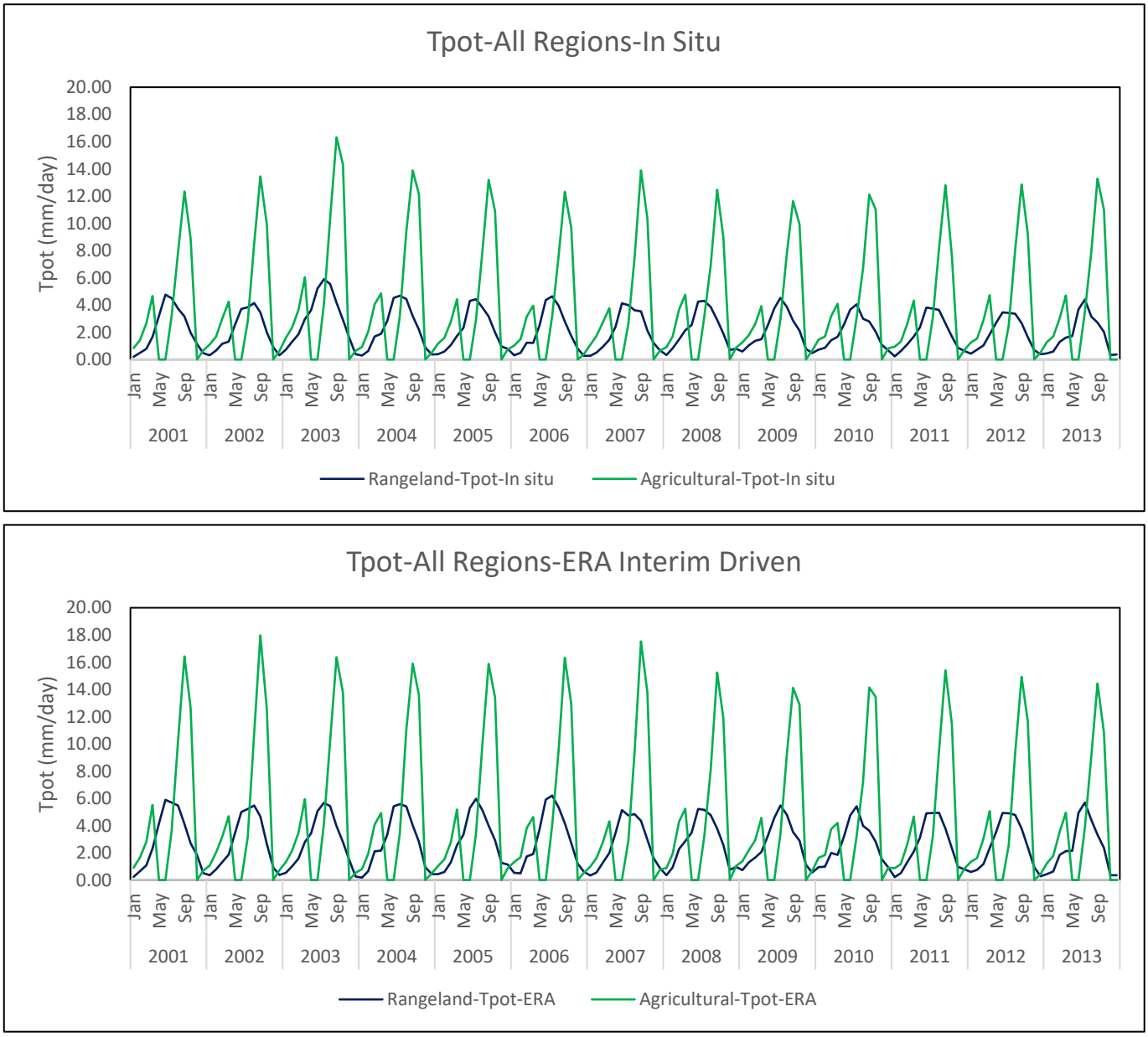

Figure 4.43 The spatiotemporal changes in seasonal $Tpot$ over Iraq during 2001-2013 using measured and ERA interim dataset.

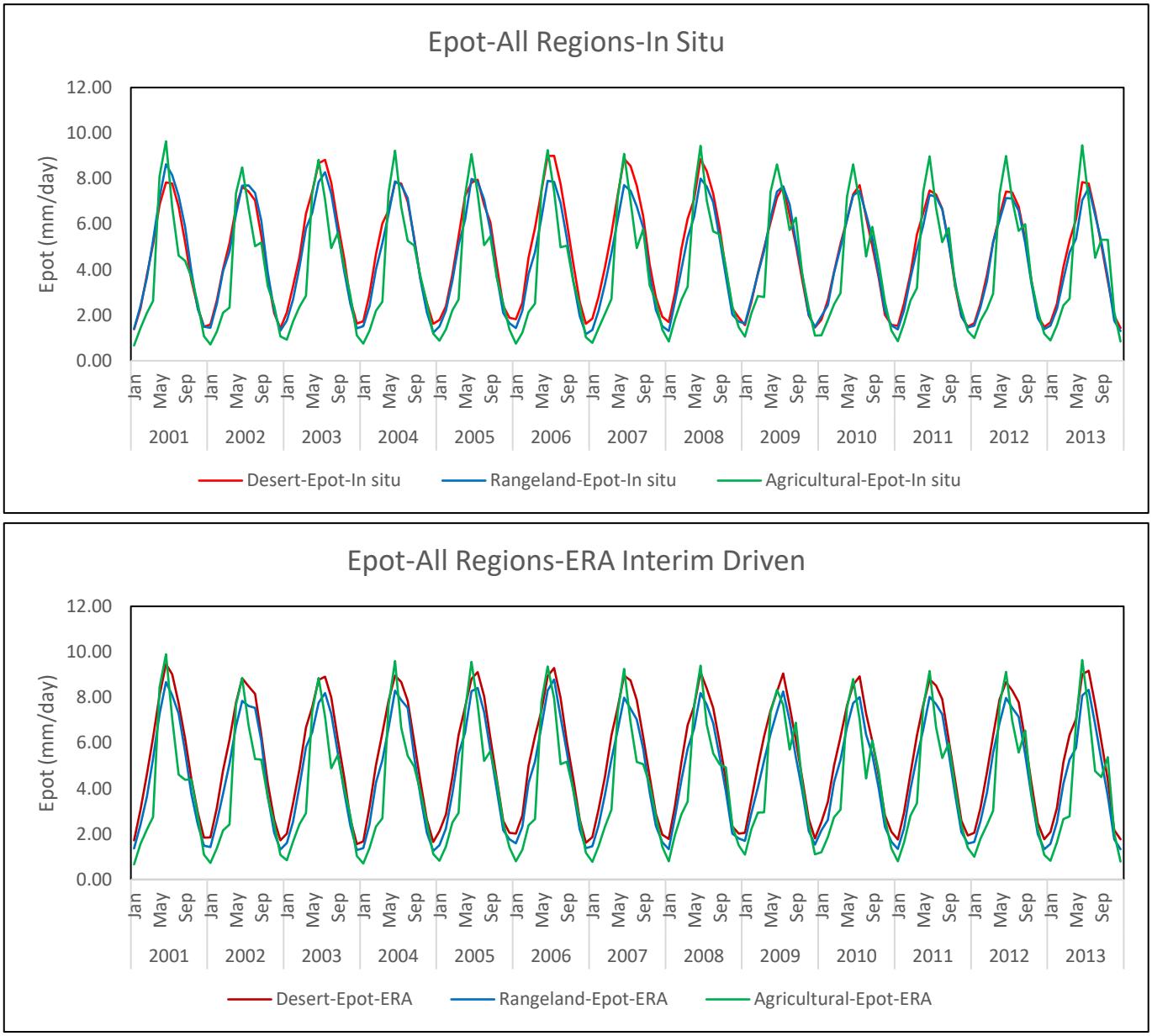

Figure 4.44 The spatiotemporal changes in seasonal *Epot* over Iraq during 2001-2013 using measured and ERA interim dataset.

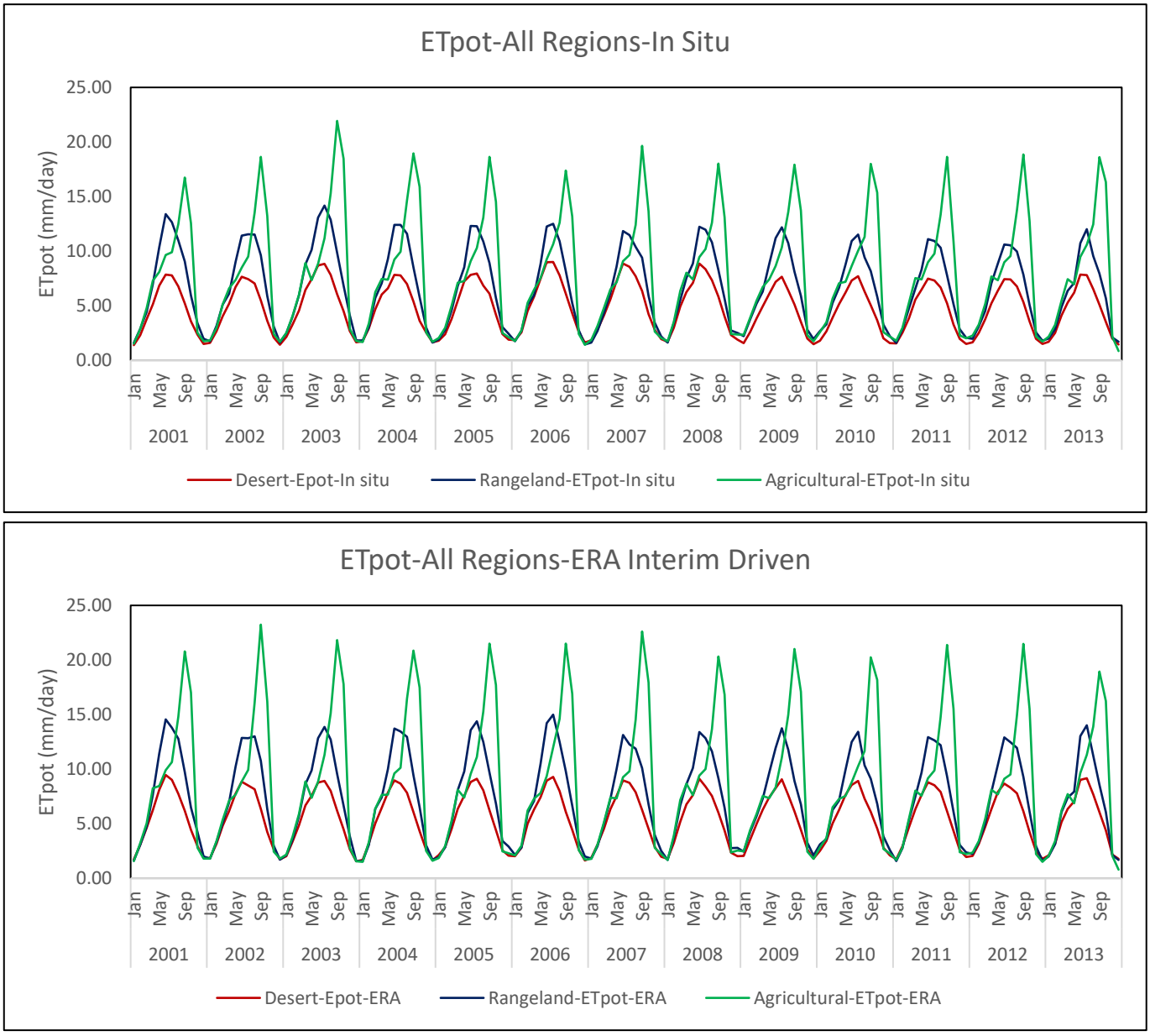

Figure 4.45 The spatiotemporal changes in seasonal $ETpot$ over Iraq during 2001-2013 using measured and ERA interim dataset.

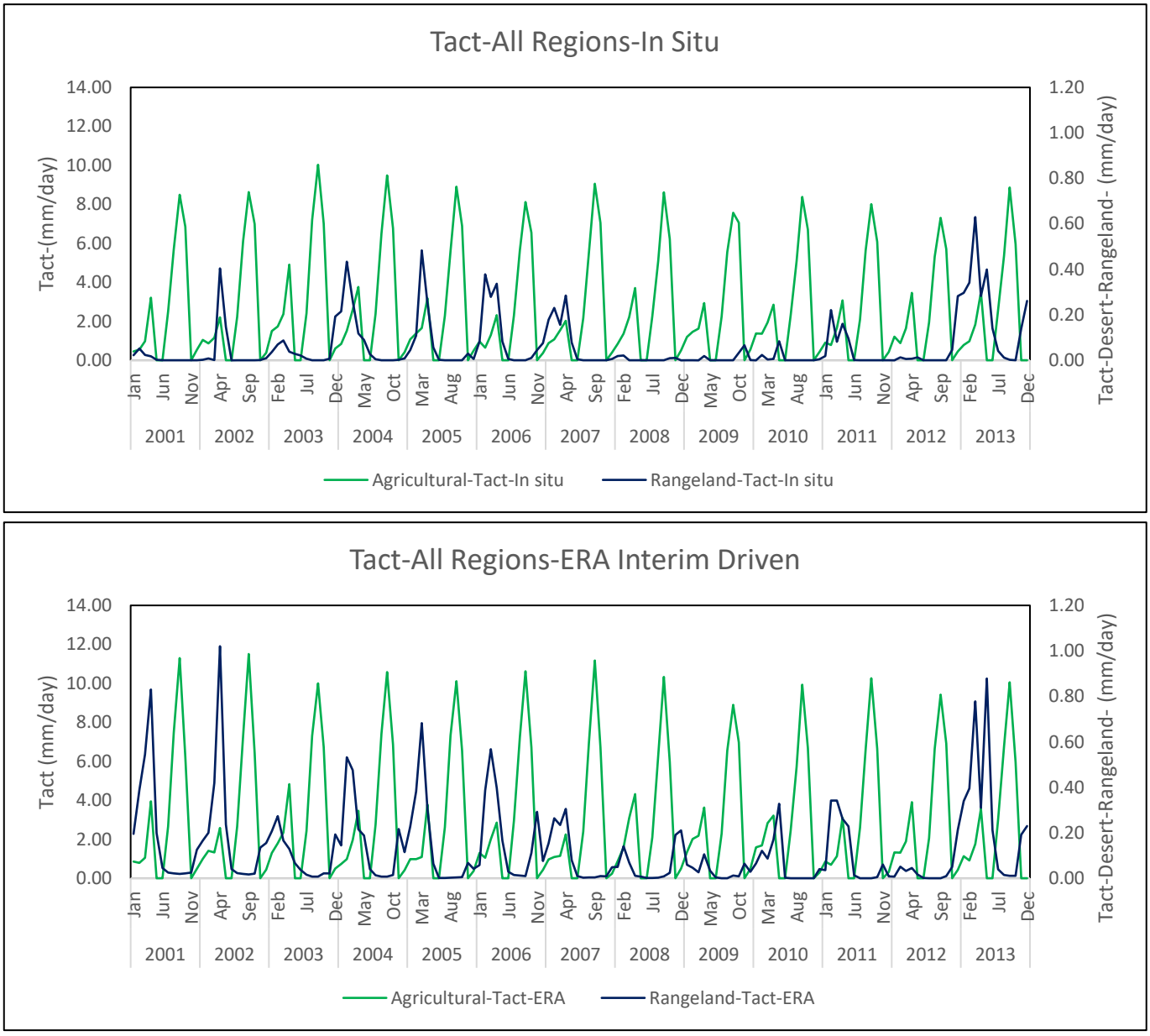

Figure 4.46 The spatiotemporal changes in seasonal $Tact$ over Iraq during 2001-2013 using measured and ERA interim dataset.

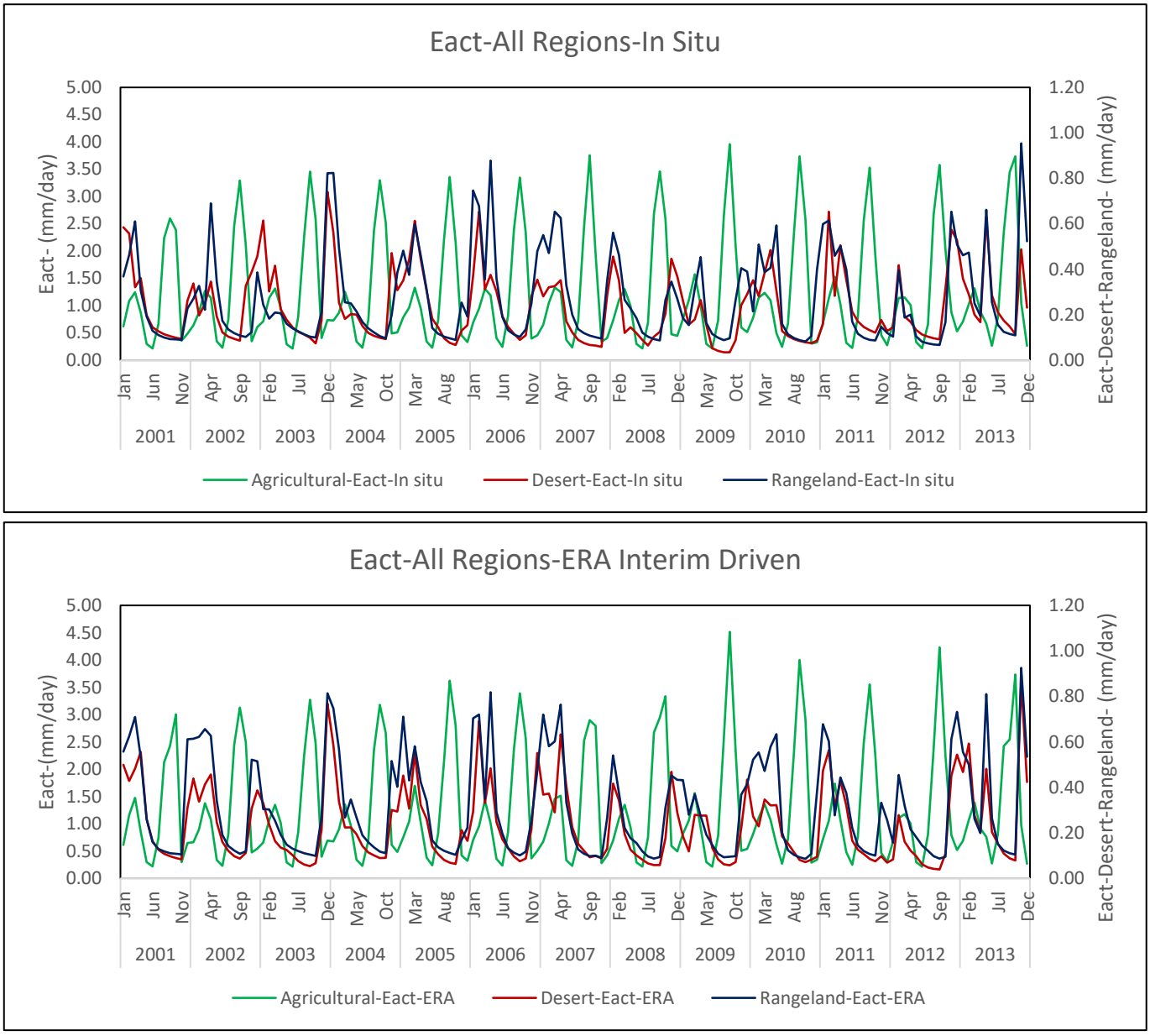

Figure 4.47 The spatiotemporal changes in seasonal $Eact$ over Iraq during 2001-2013 using measured and ERA interim dataset.

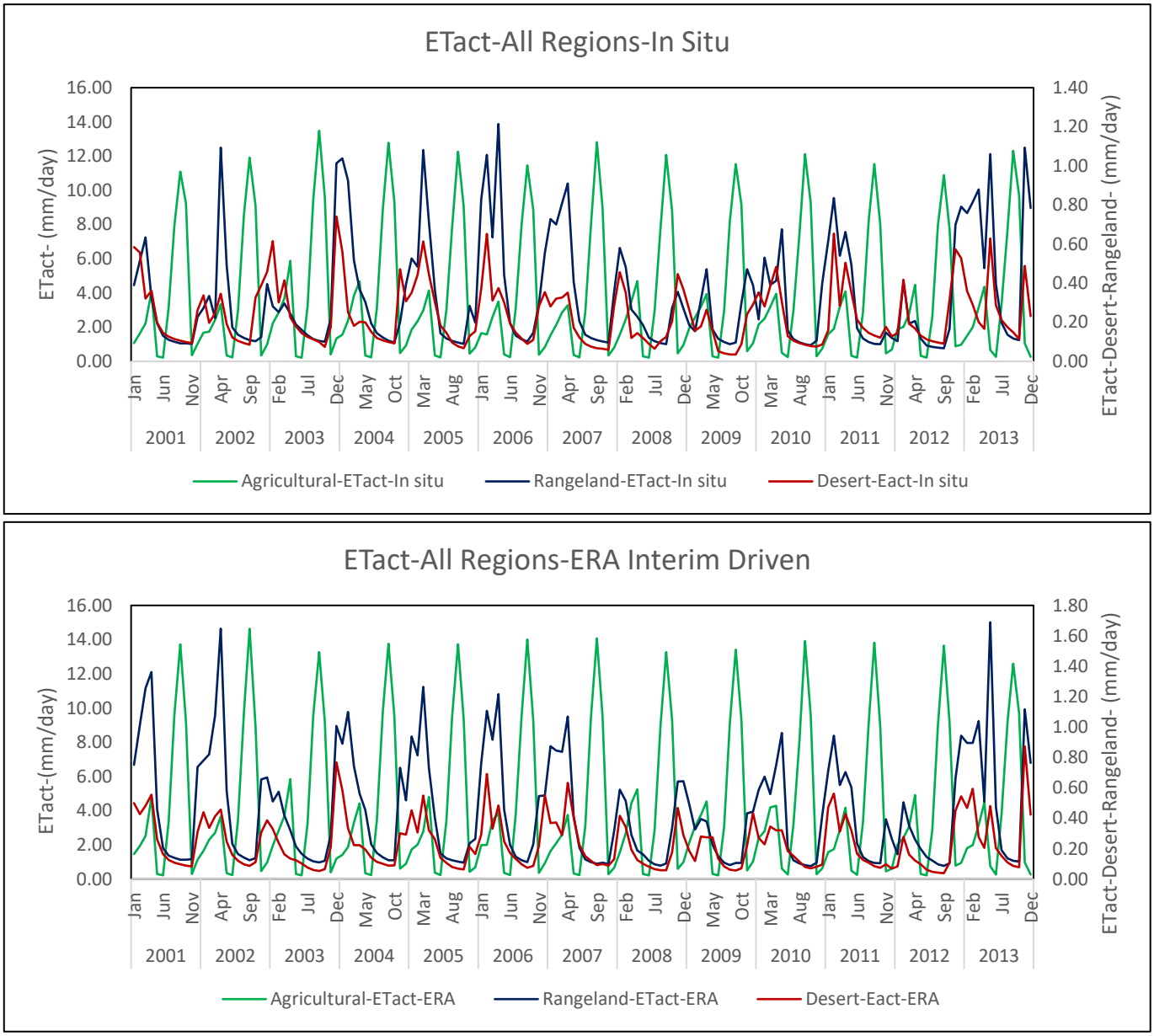

Figure 4.48 The spatiotemporal changes in seasonal $ETact$ over Iraq during 2001-2013 using measured and ERA interim dataset.

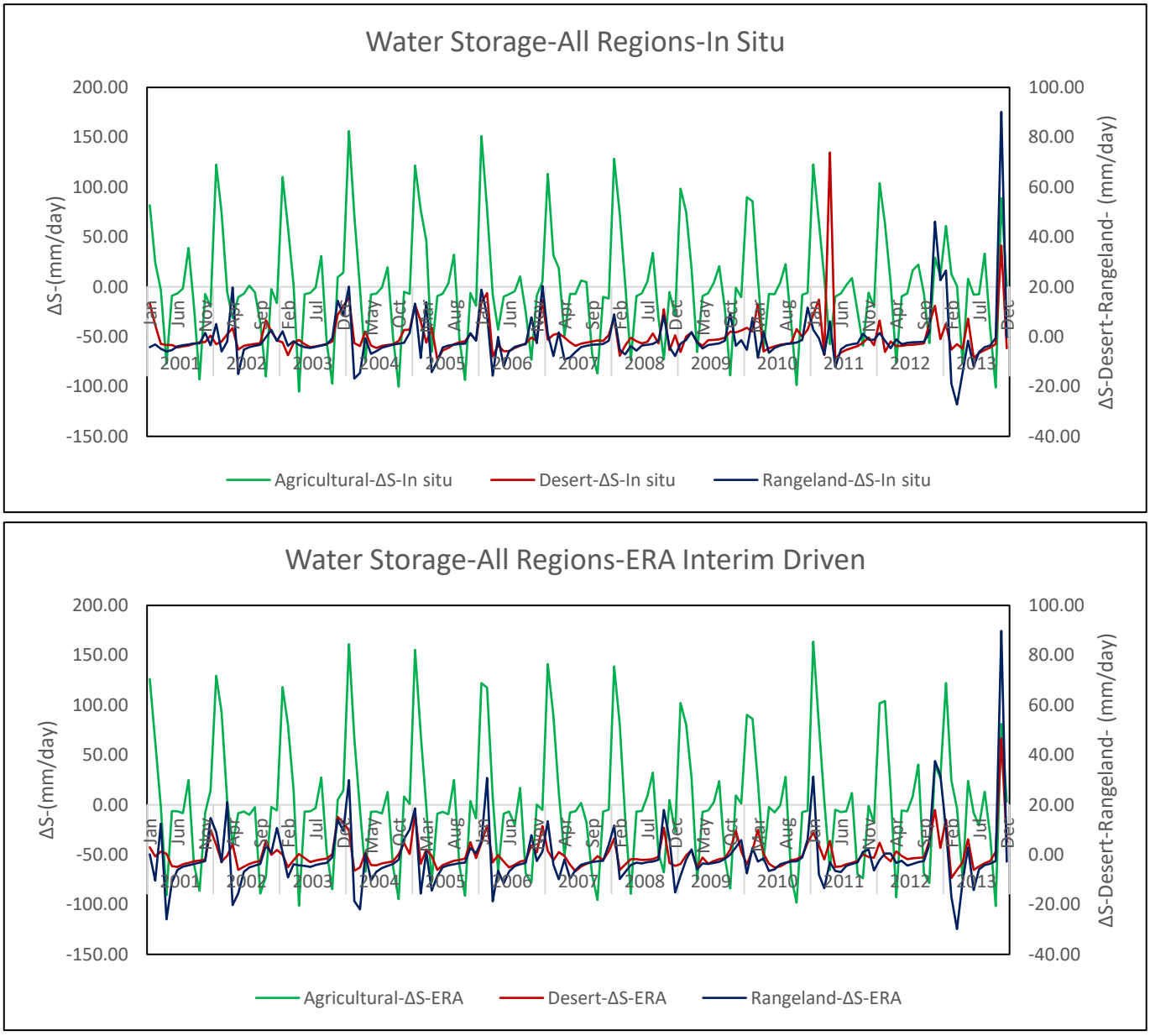

Figure 4.49 The spatiotemporal changes in seasonal ΔS over Iraq during 2001-2013 using measured and ERA interim dataset.

4.7. Comparison of seasonal evolution of regionally-averaged SWAP fluxes

Figs. 4.50-4.52 compare, side by side (i.e. in-situ versus ERA-Interim driven), the regionally (i.e. per surface-type) averaged multi-year average seasonal courses of the SWAP fluxes. Also shown are the standard deviations for each month (15 years, 6 sites for desert, 5 sites for rangeland, and 9 sites for agricultural). For the desert site (Fig. 4.50) both driving data sets show very similar courses although error bars vary throughout the season and between driving data sets. Although $Epot$ peaks around May-August, *Eact* values are in fact the lowest during that period, due to lack of rainfall (see Figs. 4.16 and 4.17). ΔS has negative values during this period. ERA $Epot$ values have much smaller error bars, yet those for Eact are very similar.

For the rangeland (Fig. 4.51), $Tpot$_ERA values peak at a somewhat larger value than $Tpot$_in-situ. Epot shows a very similar peak, whereas $ETpot$ for ERA-runs is ~ 10% larger. Again, ERA error bars are lower, indicating that the driving data are less variable in space and time. The $Tact$ values peak around March, but show large uncertainties, in this in particular for ERA-Interim. The large uncertainties indicate that for both datasets, the timing and occurrence of rainfall in very variable so that peaks in Tact may occur anywhere between February and April. The same goes for $Eact$ and $ETact$.

Finally, both datasets show negative ΔS throughout most of the months and with the largest uncertainties for November. Based on this, it appears that SWAP is predicting a very slow depletion of soil water stores in the rangeland region. Fig. 4.52 shows the monthly water balance flux values representative of the agricultural region. We see the dual-peak shape of $Tpot$ and the single-peaked $Epot$, with the peak in between the $Tpot$ peaks during the fallow period. When the two curves are combined, $ETpot$ peaks in September, after which a steep drop occurs. The shape of $Tact$ mimics that of $Tpot$, but its maximum values are only 60-70% or so of that of $Tpot$, indicating that some water stress occurred during the SWAP model runs.

$Eact$ did not follow the shape of $Epot$ because Epot's peak occured at the end of the winter crop season during the fallow period and start of maize growing season when irrigation amounts were relatively small and the small amounts of water were used by the crop. ΔS for the agricultural region shows a considerable amount of water storage during January-February.

ΔS values indicating soil storage depletion occur during April and September-October, around the time of the peak crop transpiration.

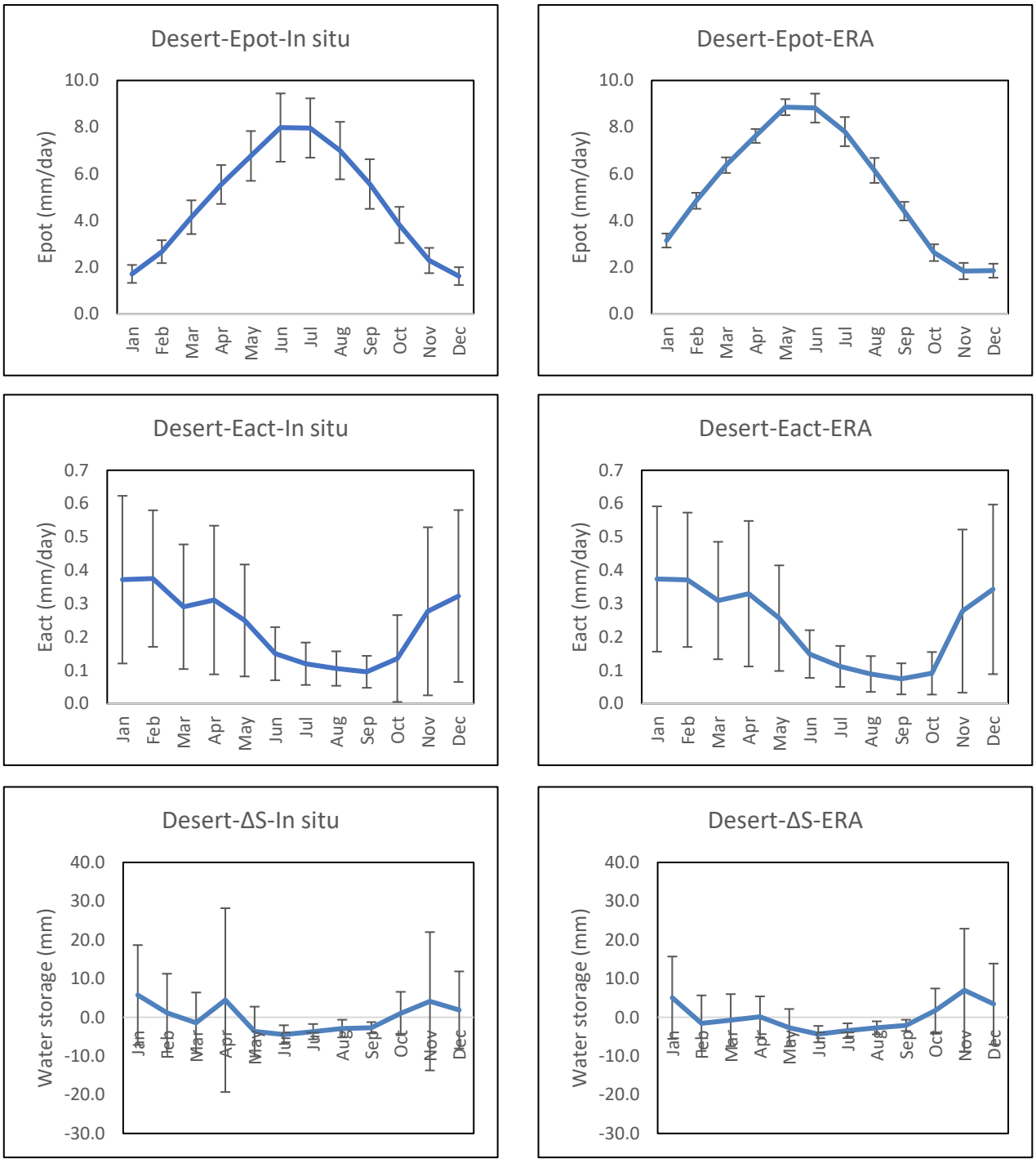

Figure 4.50 The changes in seasonal water balance components for desert region over Iraq during 2001-2013 using measured and ERA interim dataset.

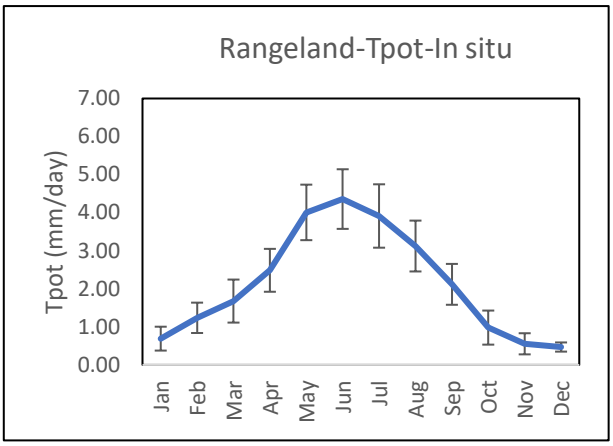
Rangeland-Tpot-In situ
Tpot (mm/day)
7.00
6.00
5.00
4.00
3.00
2.00
1.00
0.00
Jan Feb Mar Apr May Jun Jul Aug Sep Oct Nov Dec

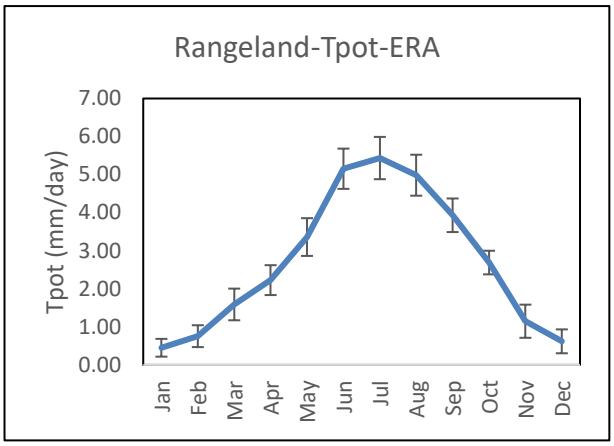
Rangeland-Tpot-ERA
Tpot (mm/day)
7.00
6.00
5.00
4.00
3.00
2.00
1.00
0.00
Jan Feb Mar Apr May Jun Jul Aug Sep Oct Nov Dec

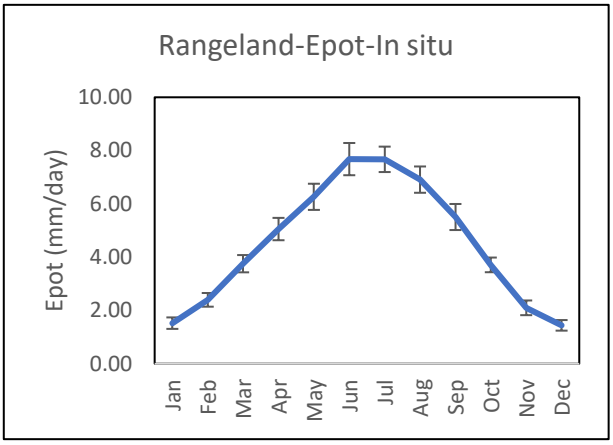
Rangeland-Epot-In situ
Epot (mm/day)
10.00
8.00
6.00
4.00
2.00
0.00
Jan Feb Mar Apr May Jun Jul Aug Sep Oct Nov Dec

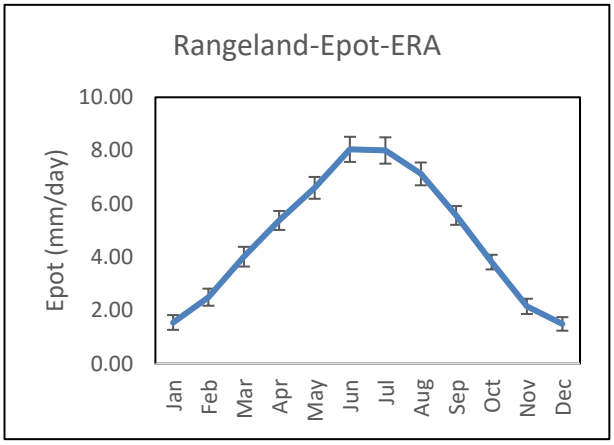
Rangeland-Epot-ERA
Epot (mm/day)
10.00
8.00
6.00
4.00
2.00
0.00
Jan Feb Mar Apr May Jun Jul Aug Sep Oct Nov Dec

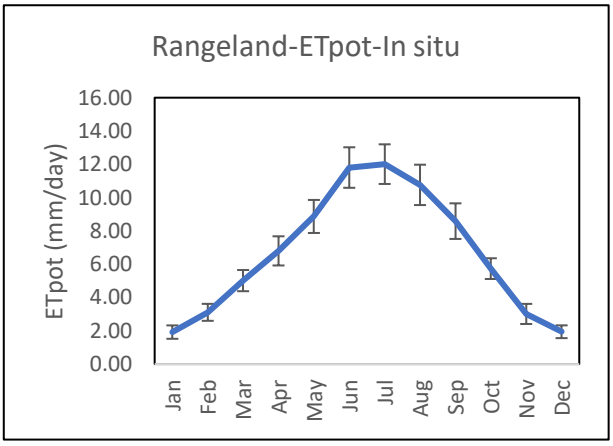
Rangeland-ETpot-In situ
ETpot (mm/day)
16.00
14.00
12.00
10.00
8.00
6.00
4.00
2.00
0.00
Jan Feb Mar Apr May Jun Jul Aug Sep Oct Nov Dec

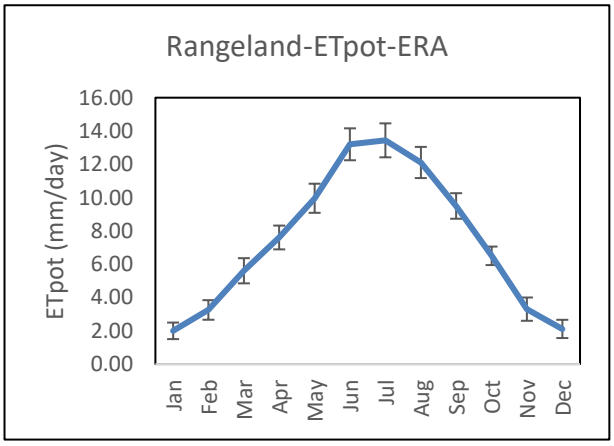
Rangeland-ETpot-ERA
ETpot (mm/day)
16.00
14.00
12.00
10.00
8.00
6.00
4.00
2.00
0.00
Jan Feb Mar Apr May Jun Jul Aug Sep Oct Nov Dec

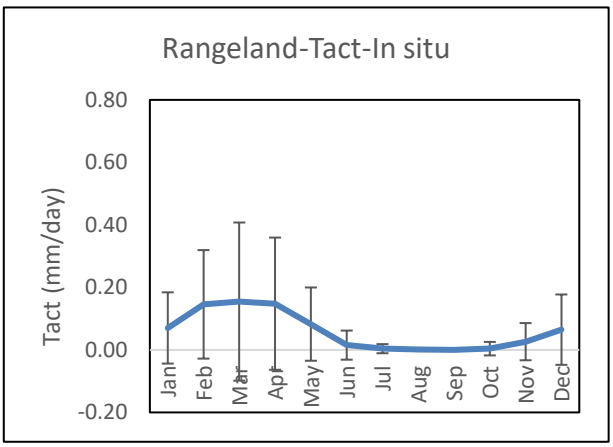
Rangeland-Tact-In situ
Tact (mm/day)
0.80
0.60
0.40
0.20
0.00
-0.20
Jan Feb Mar Apr May Jun Jul Aug Sep Oct Nov Dec

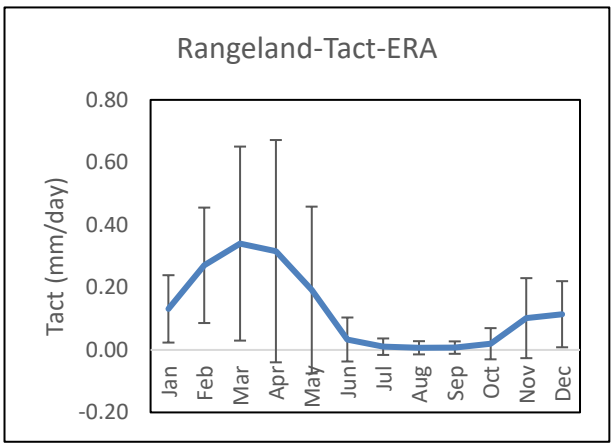
Rangeland-Tact-ERA
Tact (mm/day)
0.80
0.60
0.40
0.20
0.00
-0.20
Jan Feb Mar Apr May Jun Jul Aug Sep Oct Nov Dec

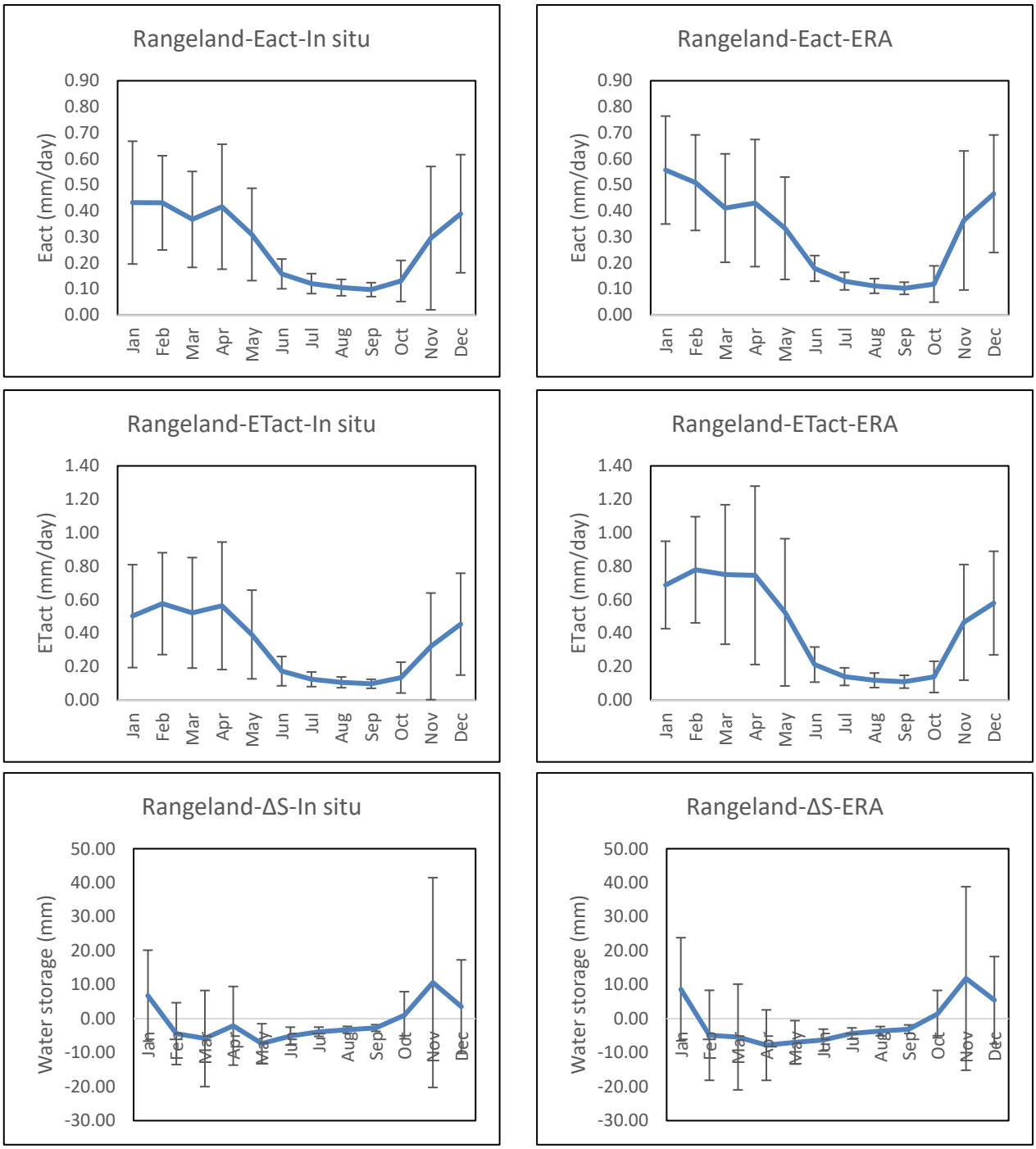

Figure 4.51 The changes in seasonal water balance components for rangeland region over Iraq during 2001-2013 using measured and ERA interim dataset.

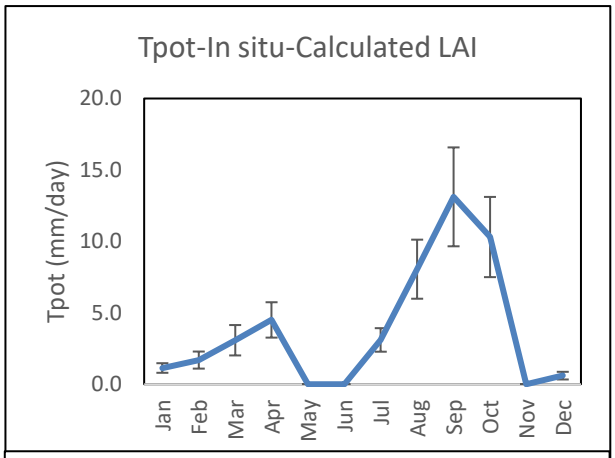
Tpot-In situ-Calculated LAI
Tpot (mm/day)
20.0
15.0
10.0
5.0
0.0
Jan Feb Mar Apr May Jun Jul Aug Sep Oct Nov Dec

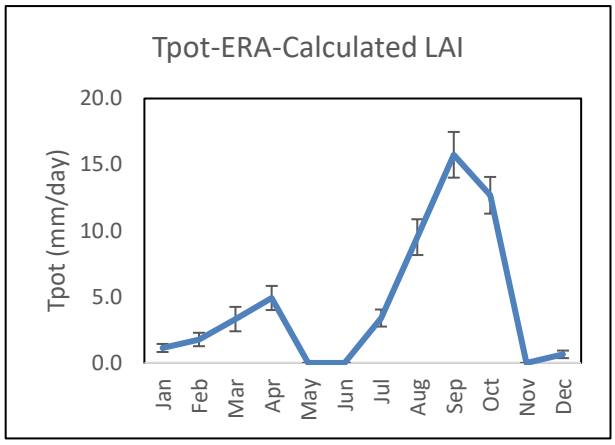
Tpot-ERA-Calculated LAI
Tpot (mm/day)
20.0
15.0
10.0
5.0
0.0
Jan Feb Mar Apr May Jun Jul Aug Sep Oct Nov Dec

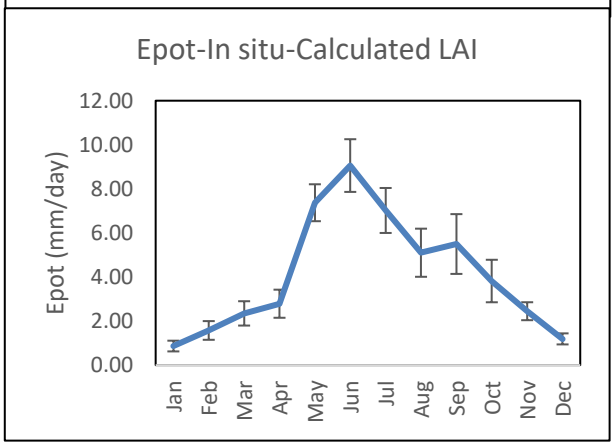
Epot-In situ-Calculated LAI
Epot (mm/day)
12.00
10.00
8.00
6.00
4.00
2.00
0.00
Jan Feb Mar Apr May Jun Jul Aug Sep Oct Nov Dec

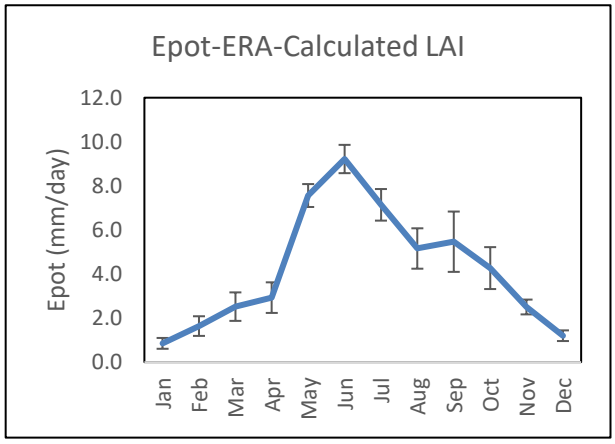
Epot-ERA-Calculated LAI
Epot (mm/day)
12.0
10.0
8.0
6.0
4.0
2.0
0.0
Jan Feb Mar Apr May Jun Jul Aug Sep Oct Nov Dec

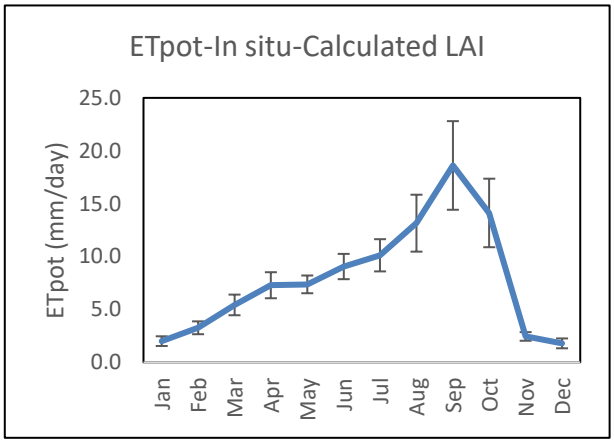
ETpot-In situ-Calculated LAI
ETpot (mm/day)
25.0
20.0
15.0
10.0
5.0
0.0
Jan Feb Mar Apr May Jun Jul Aug Sep Oct Nov Dec

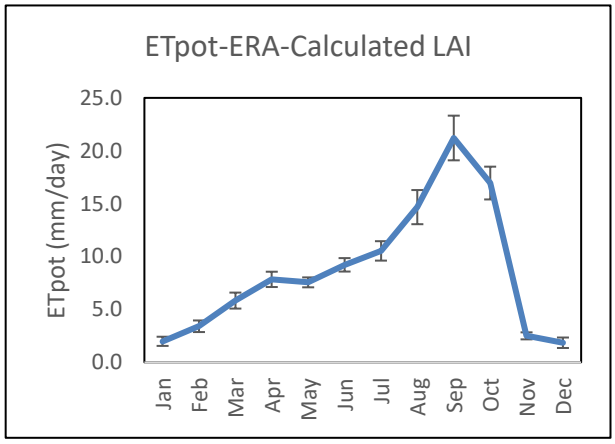
ETpot-ERA-Calculated LAI
ETpot (mm/day)
25.0
20.0
15.0
10.0
5.0
0.0
Jan Feb Mar Apr May Jun Jul Aug Sep Oct Nov Dec

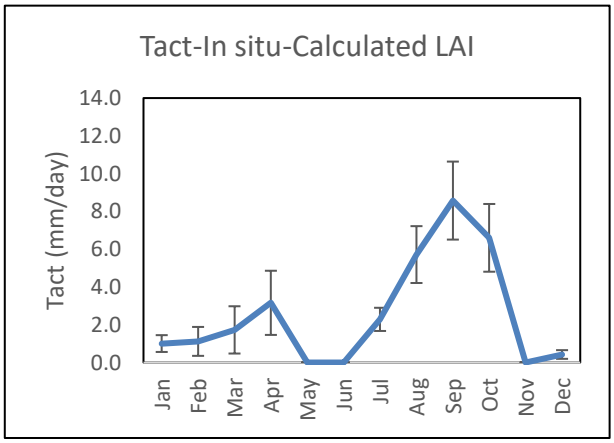
Tact-In situ-Calculated LAI
Tact (mm/day)
14.0
12.0
10.0
8.0
6.0
4.0
2.0
0.0
Jan Feb Mar Apr May Jun Jul Aug Sep Oct Nov Dec

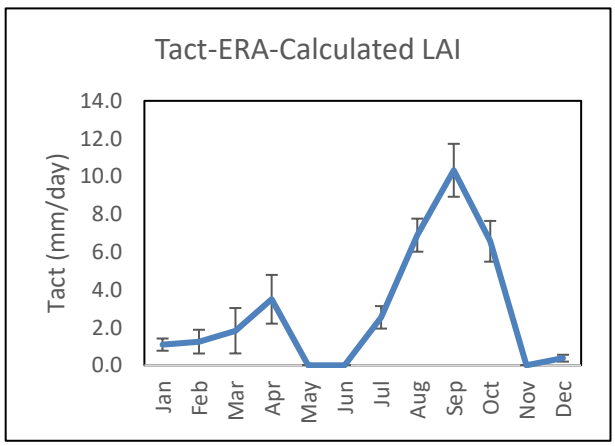
Tact-ERA-Calculated LAI
Tact (mm/day)
14.0
12.0
10.0
8.0
6.0
4.0
2.0
0.0
Jan Feb Mar Apr May Jun Jul Aug Sep Oct Nov Dec

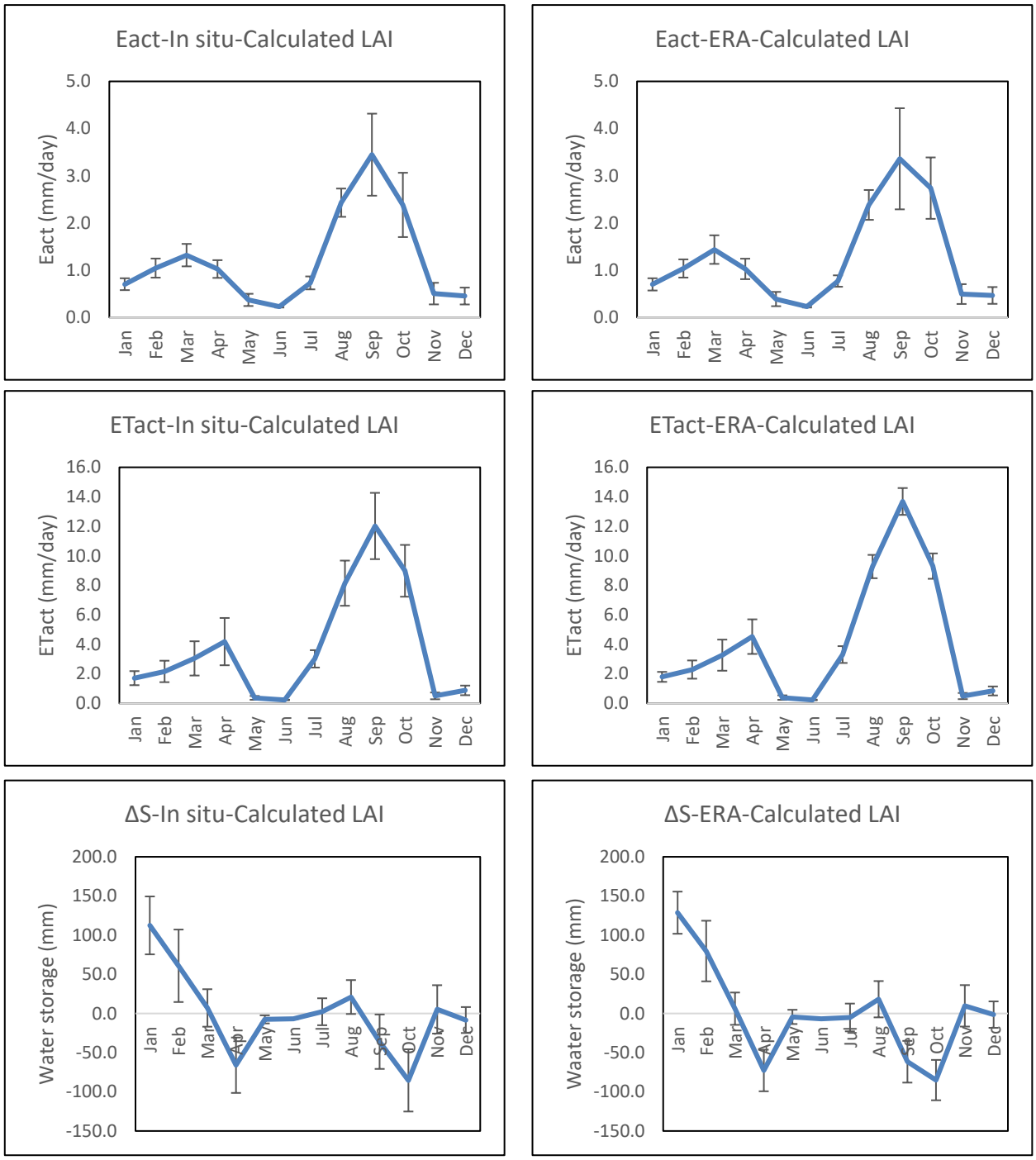

Figure 4.52 The changes in seasonal water balance components for agricultural region over Iraq during 2001-2013 using measured and ERA interim dataset.

4.8. Assessment of energy balance from ERA interim driving data.

Fig. 4.53 shows the full energy balance obtained from ERA-Interim outputs. Annual courses are as expected, i.e. Rn and SSHF are low in winter months and high in summer months (due to the variations in incoming shortwave and longwave, and surface temperatures, respectively.

Ground heat flux (or rather skin layer heat flux, as per the Tessel nomenclature) reaches a positive peak in summer (maximum heat storage and a negative peak in winter (largest heat loss).

Surface latent heat flux peaks before surface sensible heat flux, as a result of the rainy season occulting in the winter/spring months.

In all cases, net radiation is the largest flux, followed by sensible heat flux. For the rangeland and agricultural sites, the next largest flux is the latent heat flux, and the smallest the skin layer heat flux (calculated as the residual of the ERA-Interim energy balance), as expected for vegetated surfaces.

For the desert, latent heat flux and skin layer heat flux are approximately of similar size. Skin layer heat flux seems on the low site, but with high desert albedos, high surface temperatures and low moisture contents (causing low soil thermal conductivity), these values are not implausible. This also caused net radiation in the desert to be lower than those of rangeland and agriculture sites.

Compared to drought years, obvious increases in latent heat flux were observed over the period 2010-2015 and 2013-2015 for agricultural and rangeland sites, respectively. Meanwhile, sensible heat flux decreased for the same period, despite increases in net radiation.

These ERA-Interim reanalyses results fit nicely with the increasing NDVI (see Fig. 4.14), and thus evapotranspiration, when the total precipitation and soil moisture (see Fig. 4.12) were at a high during 2011-2015 (Figs. 4.16 and 4.17).

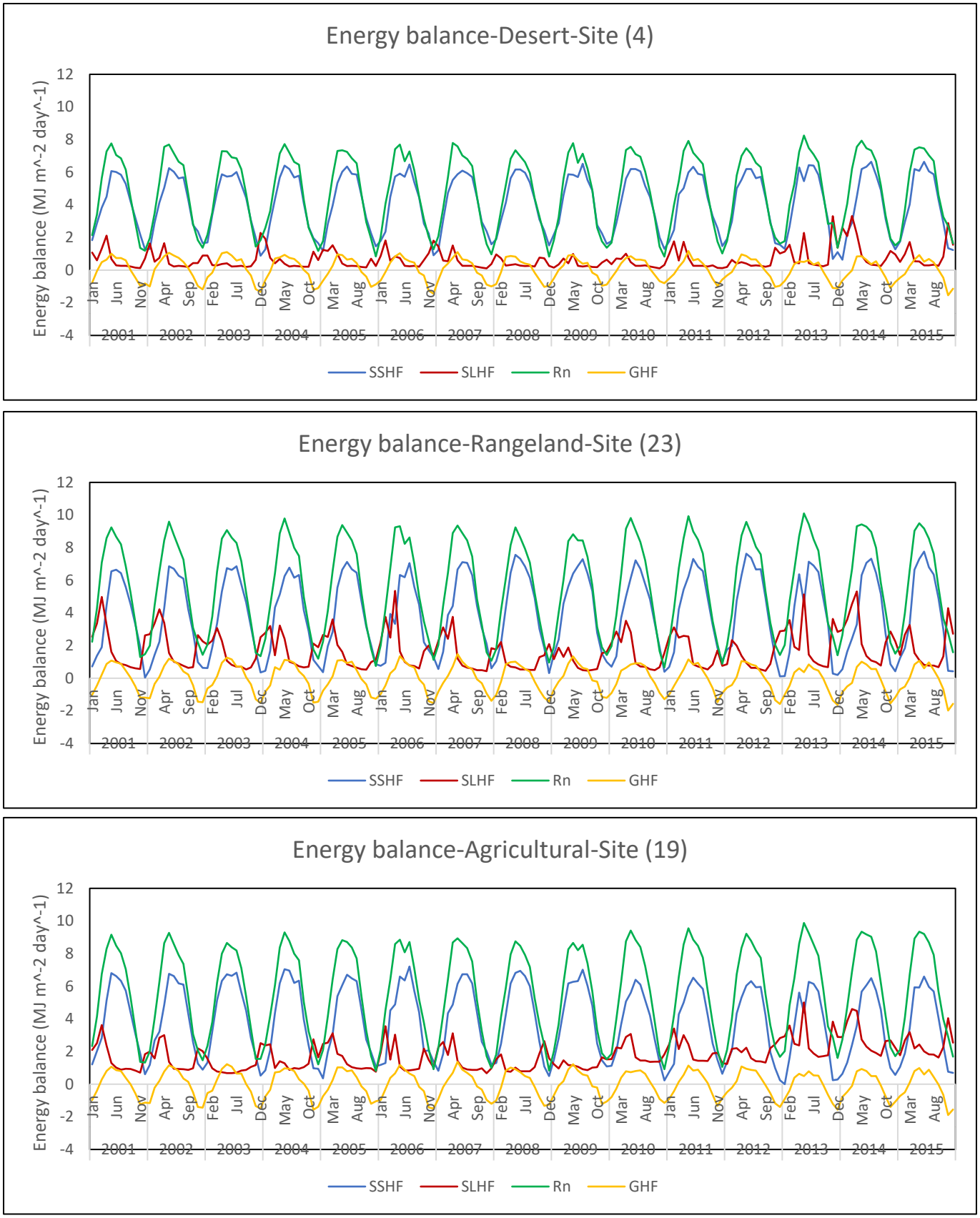

Figure 4.53 Spatiotemporal in energy balance components (SSHF, SLHF, Rn, and GHF) for a reprehensive desert, rangeland, and agricultural sites over Iraq during 2001-2015, using ERA interim driving data.

4.9. Comparison of ERA interim latent heat fluxes and SWAP $ETact$.

Figs. 4.54 show the ERA-Interim surface latent heat flux, together with the SWAP actual evapotranspiration and the evolution of SMC from SMOS for the years 2010-2013. Starting with the desert site we see that both ET fluxes follow each other, in particular when the ERA-Interim driving data are being used to run SWAP. This is encouraging seeing there are considerable differences in scale (field versus degree-scale), underlying model equations (e.g. how to calculate evaporation), bottom boundary conditions etc. Most peaks in the SMOS time series roughly coincide with those in ET, although less so during 2010, which may be due to SMOS teething problems.

Similar observations can be made for the rangeland site, i.e. a remarkably good correspondence between both models, especially when atmospheric data coincide. This also indicates that ERA-Interim's treatment of grass and its assumptions about LAI etc. are comparable to those of SWAP, despite the fact that ERA Interim's land cover data are based on 1 year of AVHHR data only.

Finally, the ET fluxes for the agricultural site are very different. This is not surprising since ERA-Interim does not have dedicated crop routines, nor did it take into account irrigation. Values for ERA-Interim SHLF (i.e. ET) are very low, as if ECMWF assumed desert soils here. The SMOS-based evolutions of SMC generally reach their highest values during the first peak in SWAP $ETact$ (related to the assumed irrigated wheat crop). The second peak SWAP $ETact$ (irrigated maize) generally coincides with the lowest values of $ETact$. This indicates that in reality a second crop was never grown, at least not for these agricultural regions, despite the literature indicating that this is common practice.

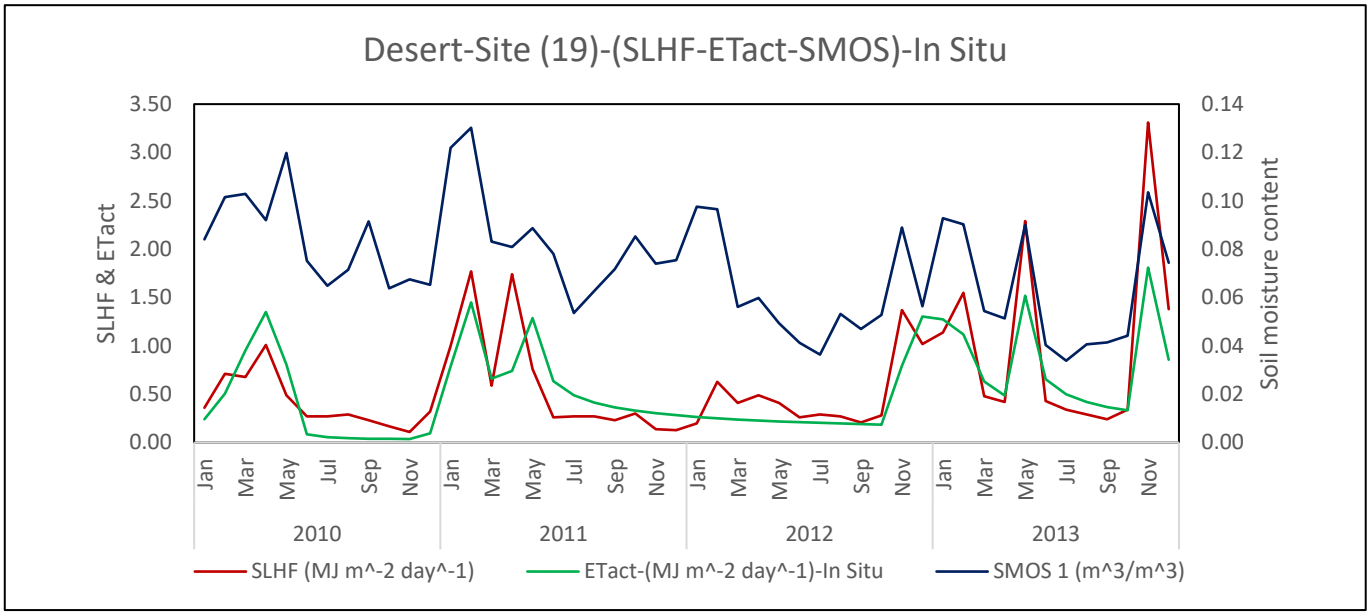
Desert-Site (19)-(SLHF-ETact-SMOS)-In Situ
SLHF & ETact
Soil moisture content
3.50
3.00
2.50
2.00
1.50
1.00
0.50
0.00
0.14
0.12
0.10
0.08
0.06
0.04
0.02
0.00
Jan Mar May Jul Sep Nov Jan Mar May Jul Sep Nov Jan Mar May Jul Sep Nov Jan Mar May Jul Sep Nov
2010
2011
2012
2013
SLHF (MJ m^-2 day^-1)
ETact-(MJ m^-2 day^-1)-In Situ
SMOS 1 (m^3/m^3)

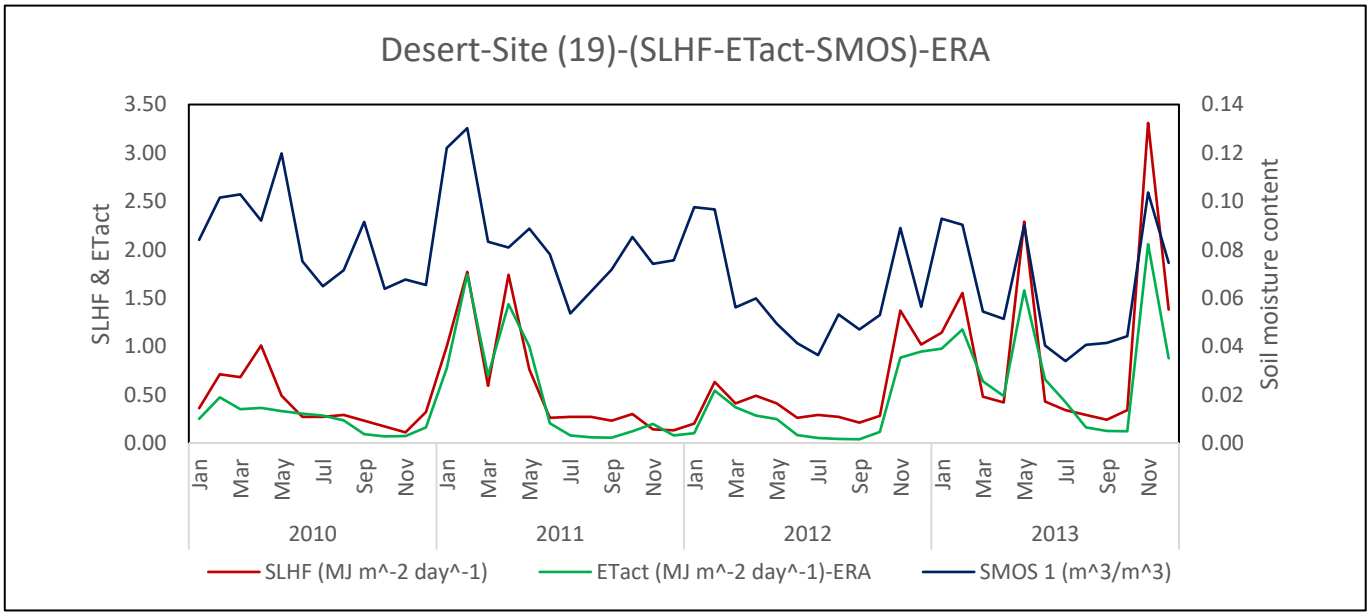
Desert-Site (19)-(SLHF-ETact-SMOS)-ERA
SLHF & ETact
Soil moisture content
3.50
3.00
2.50
2.00
1.50
1.00
0.50
0.00
0.14
0.12
0.10
0.08
0.06
0.04
0.02
0.00
Jan Mar May Jul Sep Nov Jan Mar May Jul Sep Nov Jan Mar May Jul Sep Nov Jan Mar May Jul Sep Nov
2010
2011
2012
2013
SLHF (MJ m^-2 day^-1)
ETact (MJ m^-2 day^-1)-ERA
SMOS 1 (m^3/m^3)

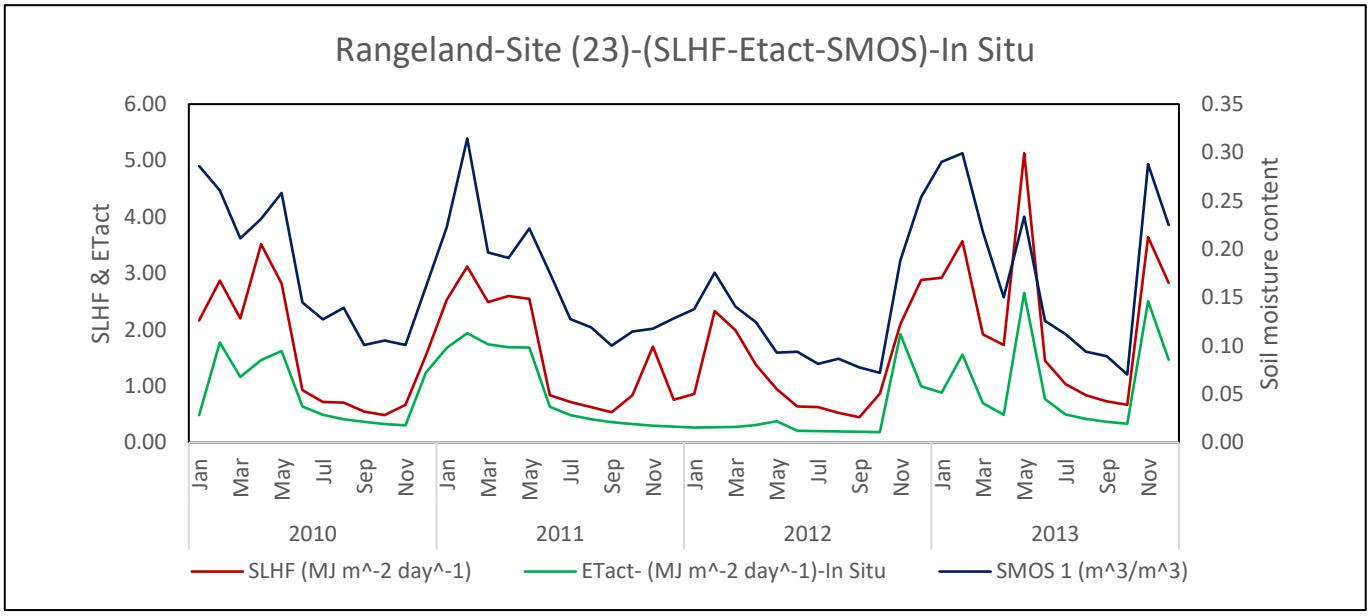
Rangeland-Site (23)-(SLHF-Etact-SMOS)-In Situ
SLHF & ETact
Soil moisture content
6.00
5.00
4.00
3.00
2.00
1.00
0.00
0.35
0.30
0.25
0.20
0.15
0.10
0.05
0.00
Jan Mar May Jul Sep Nov
2010
2011
2012
2013
SLHF (MJ m^-2 day^-1)
ETact- (MJ m^-2 day^-1)-In Situ
SMOS 1 (m^3/m^3)

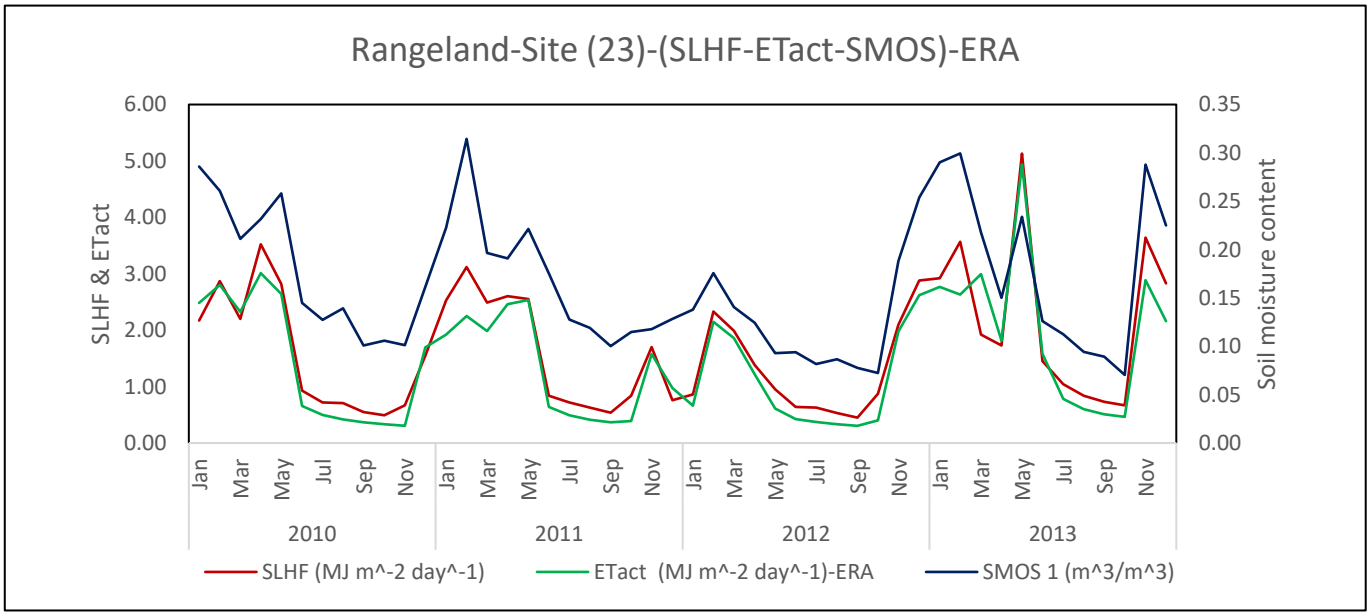
Rangeland-Site (23)-(SLHF-ETact-SMOS)-ERA
SLHF & ETact
Soil moisture content
6.00
5.00
4.00
3.00
2.00
1.00
0.00
0.35
0.30
0.25
0.20
0.15
0.10
0.05
0.00
Jan Mar May Jul Sep Nov
2010
2011
2012
2013
SLHF (MJ m^-2 day^-1)
ETact (MJ m^-2 day^-1)-ERA
SMOS 1 (m^3/m^3)

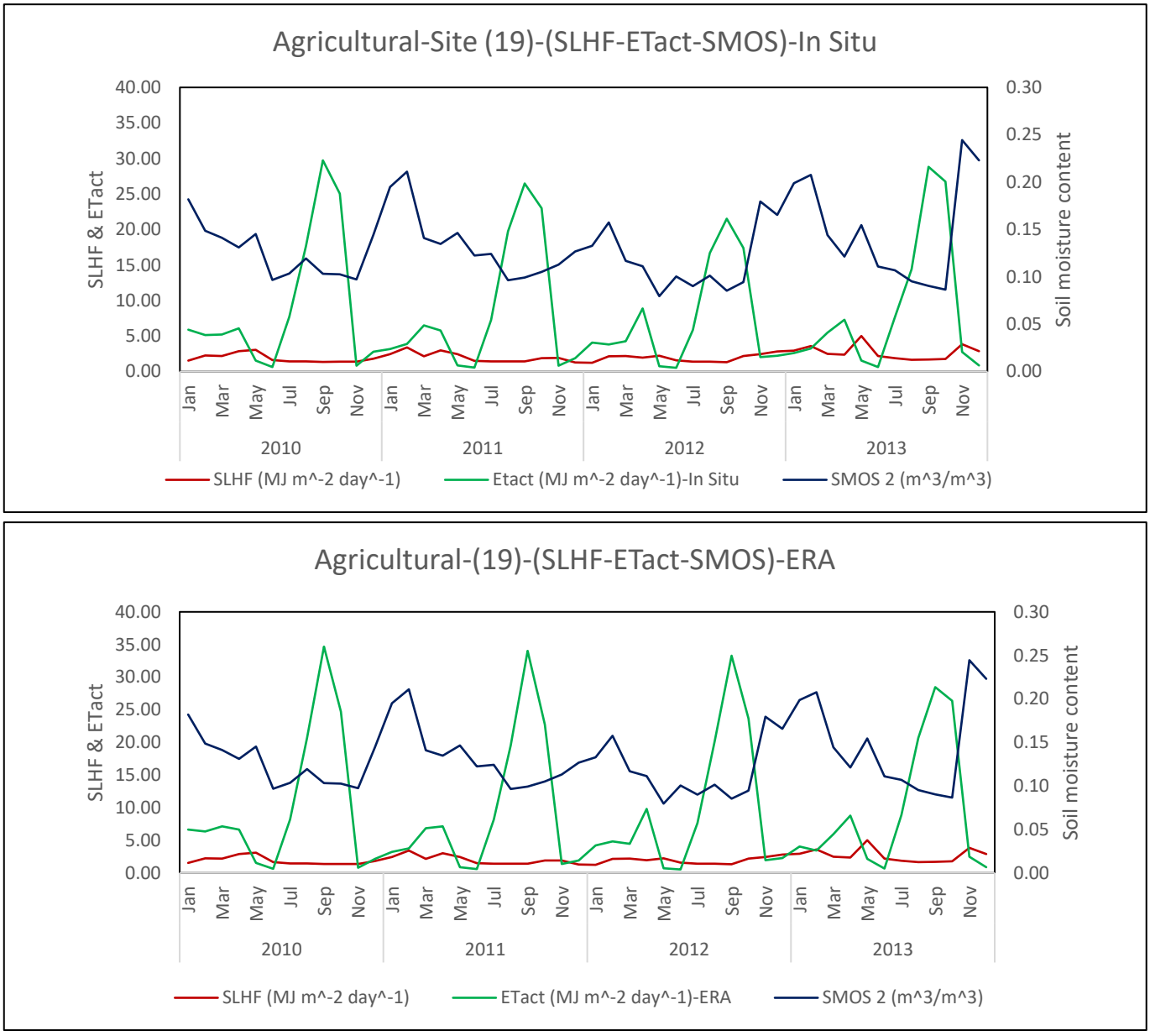

Figure 4.54 The ERA-Interim surface latent heat flux together with the SWAP actual evapotranspiration and the evolution of SMC from SMOS for the years 2010-2013.

5. Chapter five: Discussion

5.1. Monitoring drought based on SPI/SPEI3

Based on in situ data, the spatiotemporal pattern of SPI-3 (see Chapter 4 and Appendix A) shows that there was a prolonged period where drought conditions were near normal to moderately dry during the study period. The SPI values ranged from 0 to 1, indicating the presence of near normal wet conditions during 2001 to 2012, and moderately wet conditions in 2013 and 2014 over regions. The annual SPI-3, which assesses the overall dryness and wetness of the year, shows that 2013 and 2014 were the wettest years experienced in the period according to ERA interim and measured dataset.

Based SPEI-3 it was identified that moderate to severe droughts frequently occurred after 2006. Between 2001-2015, droughts were most extreme during the years 2001, 2008 to 2010, and 2012, with drought conditions the most severe in 2010. The results indicated that the droughts were generally regional phenomena: the moderate 2010 drought in the Mediterranean zone (where the rangeland region is situated), was classified as severe drought in the arid (desert) and semi-arid climate zones (agricultural and marshlands region). The average SPEI-3 value of all regions was found to be less negative in 2011 compared with the period 2008 to 2010, while 2013 was the wettest year during the study period.

The ERA interim data based SPEI-3 showed a similar evolution to that the SPEI-3 that is based on measured data, although the 2010 drought event for the Mediterranean region was more moderate due to the ERA-Interim higher precipitation compared with measured data. It also showed that the wettest years were in 2013 and 2014, when the NDVI values were indeed the highest. Section 4.3 showed that SPEI-3 was a better descriptor of drought than SPI-3 for all 3 surfaces.

The present work agrees with (Mathbout, Lopez-Bustins et al. 2017) in that they analysed the observed spatiotemporal characteristics of drought phenomena in Syria using the Standardised Precipitation Index (SPI) and the Standardised Precipitation Evapotranspiration Index (SPEI). Temporal variability of drought is calculated over the 1961–2012 period for 20 weather station locations. The results revealed the existence of three spatially well-defined regions with different temporal evolution of droughts: Northeastern (inland desert), Southern (mountainous landscape), and Northwestern (Mediterranean coast) regions. The evolutionary characteristics

of drought during 1961-2012 were analysed including spatial and temporal variability of SPI and SPEI, their frequency distribution, and the drought duration. Both drought indices have been correlated both on spatial and temporal scales and they are highly comparable.

They concluded that the spatiotemporal characteristics of SPI and SPEI can be used for developing a drought that assesses the variability of regional droughts in Syria. The analysis of both indices suggests that all three regions experienced the driest period in 2007 to 2010, coinciding with the onset of the recent conflict in Syria.

The temporal evolution of spatially averaged SPI and SPEI during the last five decades showed an increase in drought frequency, severity and duration. These results showed that the longest and most intensely dry drought period was between 2008 to 2012. On a regional scale, there is a clear evidence of a statistically significant increase in the severity and intensity of drought during the last decade (1999-2012). The most recent and severe 2008 to 2012 drought had societal impacts, contributing, according to previous studies, to agricultural failure, rapid economic decline, growing poverty, population displacement and political unrest in the country. The drought in 2008-2012 was particularly long and intense in Syria, it is found that during the last 15–20 years, the droughts have also been longer and more intense than in the past and this is probably due to the temperature rise and precipitation decrease in Syria because of recent evidence of climate change in this area (IPCC 2013), (Evans 2009).

Bussay, Szinell et al. 1998 and Szalai and Szinell 2000 discussed the utility of the precipitation based drought index (SPI) for describing drought in Hungary. This study concluded that SPI was suitable for quantifying agricultural drought, and most successfully when applying SPI on a 3-month time scale. (Hayes, Svoboda et al. 1999) evaluated the advantages and disadvantages of using SPI to assess drought severity. The primary disadvantage is that SPI is not capable to identify drought in regions that may frequently suffer from droughts. In these cases, misleadingly large negative or positive SPI values may result.

Nevertheless, a number of studies have shown that SPI is a useful index when considering droughts that are controlled mainly by the temporal variability in precipitation, while other variables that influence droughts, such evapotranspiration, and its determining variables, such as temperature and relativity, are of negligible importance. Thus, SPI is a useful drought index

in regions where precipitation is much higher than potential evapotranspiration (PET) (Vicente-Serrano, Beguería et al. 2010).

Several studies have explicitly explored the role of temperature on drought conditions. (Hu and Willson 2000) assessed the relative effects of precipitation and temperature on drought conditions; they found that the SPEI index responded equally to changes of similar relative magnitude in both variables. Only where the temperature fluctuation is less than that of precipitation is variability controlled by precipitation.

5.2. The relationship between NDVI and drought indices

Analysis of the evolution of NDVI suggests that vegetation in the study area was stressed during the period 2006 to 2010, the period when drought was more extreme based on the meteorological drought indices. A more obvious decrease in NDVI was observed from 2008 to 2010; this indicates low vegetation cover and is most likely the result of the severe drought during this period. NDVI values recovered to more normal levels in all regions of the study area in 2011, 2013, and 2014, when drought indices were > 0.

For the marshlands region, the NDVI data indicate that vegetation condition returned to normal after the restoration period, roughly from late 2003 onwards. The NDVI time series shows that growth was even more vigorous than the long-term average during the restoration period in all marshes. The vegetation greened up and increased its coverage and vigour from 2004 to 2007 due to increased availability of water. However, there was a series of drought years in the marshlands after 2008. SPEI3 was lower than zero in 2009 and a very severe drought was observed in 2010 for Chibyish and Hammar marshes, whereas SPEI-3 values were near to normal (0.99 to -0.99) at Haweezah. The year 2010 was the most serious drought year; it caused NDVI to decrease sharply so that it reached its lowest point in the time series. For that year the SPEI-3 was nearly –2, indicating that there was a severe deficit in the precipitation and potential evapotranspiration reached its maximum causing the marshes to dry out substantially.

The correlation between NDVI and both drought indices (SPI & SPEI), based on measured data and on ERA interim dataset between 2001 and 2015 (Section 4.3.4. and (Figs. 4.2)) showed that NDVI over Iraq was overall mildly to well correlated with changes in SPI-3 and SPEI-3. It appeared that the strength and sign of their correlation revealed the degree and type of drought, this worked best for rangeland, agricultural and marshland regions but not for the desert sites. NDVI for desert was highly correlated to SPI-3 based on ERA interim data, and less correlation was found based on measured data, this is most likely due to the fact that the desert area was under the control of dissident groups for much of the study period, so that some of the *in situ* data are not sufficiently reliable.

Other studies have addressed the performance of meteorological drought indices via their correlation with vegetation indices; a positive correlation between a vegetation index and drought index carries important information about the drought index' capability of assessing the agricultural response to drought (Ji and Peters 2003), (Quiring and Ganesh 2010), (Vicente-Serrano, Beguería et al. 2012). In this context, NDVI is one of the most used VIs.

The relationship between NDVI and SPI was analysed in Iran during the growing season (Khosravi, Haydari et al. 2017). It was found that NDVI and precipitation index have a strong correlation where water is a major limiting factor for plant growth.

The occurrence of rainfed as opposed to irrigated agriculture affects the relationship between remote sensing indices and meteorological drought indices in arid/semi-arid regions. Compared to positive correlations between SPI and NDVI over rainfed areas, negative correlations were determined over irrigated agricultural areas.

5.3. Drought assessment via remotely-sensed soil moisture content

The results presented in Section 4.3.7 (note: for year 2010-2015 only as SMOS data were not available before then) indicate a switch to a wetting trend in soil moisture for all regions in 2013 and 2014, despite consistent drying trends in 2010, 2012, and 2015. However, there is considerable variability over the whole period. These findings overall fit with the determinations of drought occurrence based on the meteorological drought indices and NDVI.

Note that SMOS-derived SMC represents the soil moisture of the top few cms of soil only. The exact thickness of the near-surface soil layer is unknown as the effective depth observed by the passive microwave instruments depends in fact on the soil moisture status itself, with the depth increasing for drier soils. For the desert and rangeland region the near-surface moisture content is a reasonable indicator of drought as evaporation and relatively shallow-rooting grasses will mostly deplete that layer, and small to medium-rainfall contents will not replenish the soil down to more than 10-20 cm or so. For the agricultural zone, deeper rooting crops, and the addition of irrigation water will cause significant soil moisture changes in the first 50 cm or so. This means that while SMOS data are still useful, they are less representative of the overall soil moisture status of the rootzone.

The relationship between vegetation condition (NDVI) and soil moisture content (from SMOS) are evaluated in this study for the period of 2010 to October 2015. The NDVI data are very effective in indicating ‘thinner’ versus ‘denser’ vegetation periods. For example, the NDVI improved in 2013 and 2014, when the soil moisture was the highest.

In contrast, the increases in soil moisture during rainy periods were most obvious in the Mediterranean regions as a result of sufficient precipitation. Overall, the SMC comparison shows that the semi-arid zone, where most agriculture is practised, also had relatively high SMC, which had a very similar evolution (and magnitude) to that found in the Mediterranean region (rangeland). This is potentially because this region is dominated by agriculture, where irrigation as well as rainfall can cause an increase in soil moisture. However, seeing the time series for both types of land use are so similar, it is more likely that there are issues related to resolution, where the relatively coarse resolution of SMOS (40 by 40 km) is unable to pick up on the small pockets of agriculture within larger semi-urban areas that are in part rangeland or fallow.

SMC was the lowest in the arid zone compared to the semi-arid and Mediterranean regions, because of the lack of rainfall and the high PET.

Other studies have also used SMOS to assess drought. For example, soil moisture product (SMOS) was used to determine drought conditions by taking advantage of its spatial and temporal resolutions. The study investigated the potential relationships between soil moisture two drought indices, the Standardized Precipitation Index (SPI) and the Standardized Precipitation Evapotranspiration Index (SPEI), (Scaini, Sánchez et al. 2015).

5.4. Spatiotemporal variation of latent heat flux (ERA-Interim) changes and NDVI

The changes in latent heat flux (obtained from ERA-Interim outputs) together with vegetation density (NDVI) among the desert, rangeland, and agricultural regions were studied for the years 2001 to 2015. Over all three regions surface latent heat flux showed a downward trend during 2008 to 2010, while NDVI decreased. In other years, both presented upward trends, particularly in 2013 and 2014, when the NDVI was the highest. Although changes in vegetation density (as represented by NDVI) caused by drought resulted in a decreasing in SLHF, this was not the result of a change in (drought-induced) model vegetation density, as land coverage is kept constant over time in the ERA-Interim re-analyses runs.

5.5. Relationship between vegetation-indices, LST, and drought indices

In the present study, land surface temperature (LST) and normalised difference vegetation (NDVI) were studied separately as well as jointly (i.e. by regressing them against each other), to assess their suitability as drought indicators.

The generality of the NDVI and LST relationship over a wide range of climatic regimes encountered over Iraq was studied. For the marshlands region, it was found that the sign and strength of correlations between LST and NDVI vary interannually. For non-drought years, the correlation coefficients for the regression between NDVI and LST are positive. A strong negative correlation between LST and NDVI is only found for drought years (2008 to 2010), when a decrease in vegetation leads to LST increase. Hence, using LST for drought monitoring is feasible, but only when regressed against NDVI. LST time series alone were not useful for inference of drought conditions. Overall differences in LST between regions were apparent (with desert and rangeland having similar LS temperatures that were 4-5 degrees higher than LSTs for the agricultural region), but inter-annual differences were not pronounced enough to warrant using LST data separately as a drought monitoring tool. This is caused by the fact that LST plays a role in all 4 fluxes of the energy balance, and hence in the water balance, via latent heat flux.

A number of studies discuss the strong negative correlations between NDVI and LST resulting from the cooling effects of vegetation transpiration (Goward, Xue et al. 2002). It was also found that a negative slope exists for sparse vegetation cover, whereas the slope of a closed vegetation

canopy is insignificant (Goetz 1997) observed that the slope varies with respect to climatic conditions; steeper slopes are associated with drier situations. It was revealed that the slope is inversely correlated to a crop moisture index (Nemani, Pierce et al. 1993). Other studies concluded that the slope is related to the evapotranspiration rate from the surface (Prihodko and Goward 1997),(Boegh, Soegaard et al. 1999).

The inverse relation between NDVI and LST has also been employed for explicit drought monitoring. 'During drought periods, NDVI at a given pixel will typically be relatively low, whereas LST is expected to be relatively high because of both vegetation deterioration (and hence reduced transpiration, combined with lower soil evaporation) and higher contribution of a 'soil signal' (Kogan 2000).

5.6. Assessment of the water balance

This study investigated the water balance for desert, rangeland, and agricultural regions using the SWAP model for three climatically different zones over Iraq. It provided evidence of significant differences in the water balance between these land surface types/regions under drought and non-drought conditions.

5.6.1. Potential evapotranspiration

Values for $Epot$ for all regions vary between ~1 and 10 mm day^{-1}. The annual course for the agricultural site average exhibits two peaks, a smaller one (wheat) followed by larger one (maize), as shown in Fig 4.44. These peaks are sharper than the ones for desert and rangeland. $Epot$_Agriculture falls below that of desert and agricultural regions during the months of January-April when wheat was grown. When driven with in-situ meteorological data, the differences between the surface types are more pronounced.

The results clearly indicate that the $Tpot$ values in the agriculture-dominated semi-arid region are generally higher than those in Mediterranean for rangeland region. Also, it shows that the $Tpot$ values for irrigated crop lands are high during growing season. Despite the higher precipitation and soil moisture availability, the rangeland areas generally have lower $Tpot$ values because of their lower vegetation density.

These results indicate that the spatial distribution of $ETpot$ for the semi-arid region, particularly irrigated area had the highest values of $ETpot$. Meanwhile, the highest peaks were found in

September, as a result of the high transpiration for summer maize crops. In contrast, the $ETpot$ was found lower for rangelands that are situated Mediterranean regions, and the lowest in the desert region, which is located in the arid region, due to the sparse vegetation in the rangeland and desert regions.

5.6.2. Actual evapotranspiration

In general, the agricultural region has higher average $Tact$ values than the rangeland region. The values of $Tact$ show a rapid decrease between 2008 to 2010, and during 2012 based on measured and ERA interim data. This could be mainly due to the fact that the NDVI (used to determine LAI) was affected by drought as shown by SPEI-3 (as a result of increasing evapotranspiration) and lack of precipitation (SPI-3) during rainy seasons. $Tact$ values obtained using ERA interim driving data are higher than those predicted by the measured data, due higher precipitation values compared with measured data. Higher P resulted in generally less water-stress vegetation and hence higher Tact.

$ETact$ peaks were detected over rangeland and desert regions during the rainy seasons. At the beginning (January-April) and the end of the year (November-December), where the vegetation activity was strongly linked to the precipitation. Likewise, the temporal variations of $ETact$ were strongly linked with the occurrence of drought and non-drought years. $ETact$ was found to be very low for the rangeland region during the years that vegetation that was affected by drought (2008-2010), and was relatively high in 2006; this is more likely due to the increased rainfall in this year. However, the relation between drought and the $ETact$ for the region of irrigated crops did not show any relationship. The transpiration based on standard LAI of agricultural region showed lower values in the rainy season compared with calculated LAI. On the contrary, evaporation under the maize crop was consistently higher with standard LAI than calculated LAI based on NDVI. In general, all water balance components based on ERA interim data had slightly higher $ETact$ than those obtained with the measured driving data, because they were characterized by higher rainfall levels.

Leaf area index (LAI) is a key factor determining the size of the evapotranspiration flux; however, it is a difficult and labor-intensive variable to measure, making its measurement impractical for large-scale and long-term studies. In general, calculated LAI (derived from NDVI) exhibited a similar course compared with standard LAI despite the slight differences in

their influence on the water balance fluxes. Using MODIS LAI resulted in estimated evapotranspiration fluxes that had a more realistic evolution. In addition, ET obtained using satellite-derived estimates of LAI also appeared to respond more realistically to environmental variations than those derived from standard LAI standard, for all regions.

5.6.3. Water storage

Based on both measured and ERA interim data, water storage, (ΔS), was found to be low during the drought years (2008 to 2010) for all regions in their entirety. (ΔS) was increased in the wet years of 2011, and 2013 to 2014 in particular. More positive peaks were seen in the southern region in the arid zone (e.g. site 10) compared with those sites in the western region (Site 1, 2, 3, 4).

The positive ΔS values of the agricultural region were higher than those calculated for the rangeland and desert regions, this is because irrigation was one of the major recharge sources to water storage for the agricultural region. More pronounced variations in ΔS for SWAP runs based on ERA interim driving data were for all regions, as caused by higher ERA precipitation values compared with in situ data.

5.7. The comparison between SLHF, SWAP ETact, and soil moisture

Fig. 4.54 plots the evolution of the SMOS SMC between 2010-2015, together with ERA-interim's evapotranspiration (SHLF) and that predicted by SWAP, driven by ERA-Interim data. For the rangeland and agricultural areas SMOS overall tracks very well with the time series of SHLF and $ETact$. While for the desert sites the correspondence between variations in SMOS SMC and ET is reasonable for the last 3 years of the 2010-2015 period, it is quite poor for the first two years, when overall relatively high SMC levels do not seem to coincide with higher ET values. The potential reasons for this are not immediately apparent, but it could have to do with SMOS post-processing algorithms or radio-signal interference.

6. Chapter six: Conclusions

6.1. Research key findings

This study set out to determine the following:

- What has been the recent evolution of droughts over Iraq, for a range of land surface types, namely desert, rangeland, agricultural, and marshlands.
- Which drought indices are best suited for analysing the extent and severity of drought in Iraq and similar areas?
- How can remote sensing help to assess drought in Iraq?
- How can land surface modelling be used to further our understanding of droughts in Iraq?
- How will the findings inform water resources management in Iraq?

The key findings of this research are:

- The findings based on the meteorological drought indices indicated that major droughts occured for/between the following years, for the following regions; desert (arid climate): 2008, and 2010; rangeland (mediterranean climate): 2001, 2008, and 2010; agricultural region (semi-arid climate, often irrigated): 2008, and 2010
- SPEI was more useful in indicating drought than SPI, in particular for the agricultural region region(s), based on measured data.
- There is a considerable difference between the droughts depicted by the temperature (as well as precpitation) influenced SPEI and the precipitation-only based SPI, primarily because of the high variability of the temperature and precipitation. SPEI also captures the influence of potential evaporation (via temperature) and it depicted more severe and longer duration droughts in the study area. These results provide support for the notion that the SPEI is a relatively better index for evaluating droughts in Iraq than SPI because it incorporates the influence of temperature on multi-temporal droughts.
- Near-surface soil moisture estimates obtained from SMOS satellite data corresponds fairly well with the drought indices, the modelled latent heat flux (ERA-Interim output and SWAP output, the latter model both driven with ERA-Interim and in-situ data), and NDVI in the study area, for the desert and rangelands region, but not for the agriculture regions.

- Frequent drought from 2006 to 2010 affected vegetation vigour and hence NDVI negatively (NDVI decreased). The vegetation being more water-stressed and sparse would result in an increase in LST, largely due to reduced transpiration and a larger percentage of exposed bare soil. This increase in LST was picked up by satellite imagery, but the LST data became more powerful as drought predictors when regressed against NDVI, see below.
- The relationship between LST and NDVI data varies between different land surface types. The analysis shows a negative relationship between LST and NDVI during drought years within the marshlands region, but this was not the same for other land surface types. According to the results, the LST and NDVI relationship can make an effective tool in evaluating drought with remote sensing and geographical information systems.
- As well as the occurrence of temporal drought variability; there is also a strong spatial gradient across the study area. The Mediterranean climate zone experienced higher precipitation totals and less negative meteorological drought indices compared to arid and semi-arid zones; this is reflected in the spatial distribution of soil moisture (from SMOS) and NDVI data of the study area.
- The SWAP model was found to be useful for predicting the water balance over the different climatic regions in Iraq and it was able to pick out the key drought periods via reduced evapotranspiration and stored soil moisture content, partly as a result of driving data, but also because of reduced NDVI-dependent LAI values.
- A comparison SWAP $ETact$ and ERA-Interim SHLF shows that for the desert and rangeland regions these fluxes compare very well, especially when using ERA-Interim driving data. This illustrates that the ERA-Interim land-cover map used was reliable, as well as the other vegetation properties, such as height, LAI etc. For the agricultural simulation runs the biggest differences were found, especially for the high peak (irrigated wheat) in $ETact$. This could be because the ECMWF Tessel model is not able to simulate crops, including rotations. There is also the fact that SWAP rainfall driving data were supplemented with irrigation.
- The effect of re-flooding was further increased, causing a significant and rapid environmental change in the Iraqi marshlands during 2003-2005. In November 2005, marshlands extent decreased due to the high evapotranspiration rates in the preceding hot summer months. Due to drought events in 2008-2009, marshlands extent started shrinking

again. And only very slightly recovered during the winter months of 2009/2010. The recovery rate from January 2010 to January 2011 was highest and positively reflected on NDVI and LST.

- Drought can be identified by estimating NDVI and land surface temperature together. This paper explored the spatial and temporal relationship between NDVI and LST. It was found that in the marshes a combination of a decrease in vegetation cover caused a direct increase in surface temperature. By comparing three different periods: 2001 to 2003, 2004 to 2007, and 2008 to 2010, it was concluded that the average land surface temperature of the marshes has risen during drought, and draining periods. Considering the impacts of vegetation cover decrease on the increase in surface temperature, the role of human activities becomes more and more evident. According to the results, simultaneous analysis of NDVI and LST is ideal for the study of marshland environment how it is affected by anthropogenic interventions and climate variations. The correlation between LST and NDVI is negative during draining and drought periods. Hereby LST, when correlated with a vegetation index, can be used to detect drought of marshland areas.
- As demonstrated in this work, NDVI can be used successfully as a tool to analyse drought and non-drought conditions. This strongly supports the feasibility of a drought assessment tool based on NDVI and SPI/SPEI in these regions. The NDVI values of non-drought years were higher when compared to that of the drought years indicating healthy growth of vegetation during the non-drought year when compared to the drought years. This indicates that the real time NDVI data extracted can be a good indicator of vegetation health and ultimately drought.

6.2. Research implications and future directions

This project has presented a methodology for integrating remote sensing and *in situ* data with land surface models and re-analysis data for the monitoring and assessment of droughts in areas with spatiotemporally variable climatic conditions. This approach has worked well for Iraq, but the same methodology could be adapted for other regions too, particularly in dryland regions and in Developing countries, where there is a paucity of previous research, and *in situ* data are unreliable or absent (e.g. due to remote conditions, lack of funding or the political situation. Most of the data used in this study are freely available from global archives and the models are widely used in the research literature. Land surface models are particularly useful to improve our understanding of biophysical systems, and so the methodology used here holds great potential for less-studied parts of the world.

Furthermore, land surface models are increasingly being used to explore the potential impacts of future climate change scenarios. These data could be invaluable for decision makers to propose adaptation strategies and improve preparedness and sustainability of agriculture in the Middle East, and elsewhere. There is a great deal of scope for further research on this topic.

6.3. Research limitations

It is recognised that there are several limitations of this study:

- In situ meteorological data were missing in 2003 and 2004 because of the political conflict and instability at that time. This is a common problem for researchers in many parts of the world, but this study has explored the extent to which other data (such as ERA-Interim or RS data) can be used in these circumstances
- A significant part of the study area, in particular the western desert close to the borders of Jordan and Syria, was under the control of dissident groups for much of the study period, so some of the in situ data are not sufficiently reliable. This may explain why the relationships between NDVI and SPI/SPEI were higher with ERA interim data compared to in situ data in these circumstances
- The confounding effect of irrigation systems, which are widespread in the Tigris Euphrates basin, complicates determining the relationship between NDVI and drought in the study area. Irrigated agricultural systems are common, especially in drylands, so further research is needed to find a robust solution to this problem. Water losses in irrigation schemes, throughout Iraq, are a major issue. By and large, water is transferred to farmers' fields through very poorly maintained distribution systems made of earth canals and ditches due to widespread deterioration of irrigation infrastructure which suffer significant water losses because of seepage or leakage, and infiltration. Likewise, most of the pump stations are severely run down, and some can no longer be repaired, which in turn affects the crops. Moreover, on-farm field application efficiency using the traditional surface gravity systems is assumed to be between 30–40 percent but is probably near 20 percent or less (Lucani 2012), (Water 2006). The SWAP analyses presented in Chapter 4 does not take account of these losses.
- Land use change is often rapid in countries like Iraq, and can confound the use of land cover maps over the exended periods of time required for hydrometeorological studies of this kind. Note that the ERA-Interim reanalysis uses the same land cover for each year, and for the SWAP runs, the same crop rotation was used for each year. In real life, there would be much more inter-annual variability, which would have affected the model water balance calculations. Some agricultural areas were lost due to urban expansion, and

conflict and instability in the region has led to some abandonment of farmland in some areas.

- Suitable in situ soil moisture and land surface temperature data were unavailable to attempt a calibration of the SMOS and remote LST retrievals. The same goes for verification of NDVI and water balance or energy balance fluxes. For example, there are no FLUXNET sites in Iraq.
- Different spatial resolutions are used for all the data sources used in this study, ranging from 30m pixels in the case of Landsat data, to degree squares for some meteorological data. There is a mismatch between the requirements for modelling agricultural systems and the data provided by climate models. There are geostatistical considerations when combining data at different spatial resolutions in models. Further research is required, firstly to identify the optimum spatial resolution for modelling these types of environmental systems (especially in the light of massive improvements in computer processing power and data storage), and secondly to develop robust downscaling methods to retrieve climate parameters at the appropriate resolutions.

7. References

Atyah, L.,et al. (2012). "Integration Study of Vegetation cover in Babil governorate By using Remote Sensing data and GIS."

Al-Ansari, N. and S. Knutsson (2011). Possibilities of restoring the Iraqi marshes known as the Garden of Eden. Water and Climate Change in the MENA-Region Adaptation, Mitigation, and Best Practices International Conference April.

Al-Ansari, N. A. (2013). "Management of water resources in Iraq: perspectives and prognoses."

Al-Haboby, A., et al. (2014). Agriculture for development in Iraq? Estimating the impacts of achieving the agricultural targets of the national development plan 2013 2017 on economic growth, incomes, and gender equality, Intl Food Policy Res Inst.

Al-Maliki, A. S. a. D. (2005). "Report climatic water balance in Iraq - a study in Applied Climatology." Journal of Basra.

Al-Qinna, M. I., et al. (2011). "Drought analysis in Jordan under current and future climates." Climatic Change 106(3): 421-440.

Al-Shamaa, I. and B. Ali (2011). "Hydrological Conditions of Badra-Jassan Basin." Diyala Journal of Agricultural Sciences 3(2): 693-702.

Al-Timimi, Y. K. and M. H. Al-Jiboori (2013). "Assessment of spatial and temporal drought in Iraq during the period 1980–2010." Int J Energy Environ 4(2): 291-302.

Al Qatrani, F. S. (2012). "Environmental and Economic Impacts of Drought in Iraq." Zeszyty Naukowe Uniwersytetu Szczecińskiego. Studia i Prace Wydziału Nauk Ekonomicznych i Zarządzania(29 Climate change, economy and society-interactions in the Baltic See Region): 5-17.

Ali, M. F. (2008). "Geographical analysis of the reality of drought and climate water deficit and the potential for the proposed addressed: case study Najaf governorate." Journal of Kufa.

Allen, R. G., et al. (1998). "Crop evapotranspiration-Guidelines for computing crop water requirements-FAO Irrigation and drainage paper 56." FAO, Rome 300(9): D05109.

Almamalachy, Y. (2017). Utilization of Remote Sensing in Drought Monitoring Over Iraq, Portland State University.

Alsdorf, D. E. and D. P. Lettenmaier (2003). "Tracking fresh water from space." Science 301(5639): 1491-1494.

Anderson, M. C., et al. (2007). "A climatological study of evapotranspiration and moisture stress across the continental United States based on thermal remote sensing: 2. Surface moisture climatology." Journal of Geophysical Research: Atmospheres 112(D11).

Anderson, R. G., et al. (2012). "Assessing regional evapotranspiration and water balance across a Mediterranean montane climate gradient." Agricultural and Forest Meteorology 166: 10-22.

Bank, U. U. N. a. W. (2003). " "Joint Iraq Needs Assessment." http://go.worldbank.org/I0L3C1CEQ0.".

Beaumont, P. (1998). Restructuring of water usage in the upper Euphrates catchment of Turkey and Syria and their political and economic implications. Transformations of Middle Eastern Natural Environments: Legacies and Lessons. J. Coppock and JA Miller, New Haven, Yale University Press.

Belmans, C., et al. (1983). "Simulation model of the water balance of a cropped soil: SWATRE." Journal of Hydrology 63(3-4): 271-286.

Bierkens, M. F., et al. (2008). Climate and the hydrological cycle, International Association of Hydrological Sciences.

Bishay, F. K. (2003). "Towards sustainable agricultural development in Iraq. The transition from relief, rehabilitation and reconstruction to development."

Black, T., et al. (1969). "The prediction of evaporation, drainage, and soil water storage for a bare soil." Soil Science Society of America Journal 33(5): 655-660.

Boegh, E., et al. (1999). "A remote sensing study of the NDVI–Ts relationship and the transpiration from sparse vegetation in the Sahel based on high-resolution satellite data." Remote Sensing of Environment 69(3): 224-240.

Boesten, J. and L. Stroosnijder (1986). "Simple model for daily evaporation from fallow tilled soil under spring conditions in a temperate climate." Netherlands Journal of Agricultural Science 34: 75-90.

Boken, V. K., et al. (2005). Monitoring and predicting agricultural drought: a global study, Oxford University Press Cary^ eNC NC.

Braden, H. (1985). "Ein energiehaushalts-und verdunstungsmodell for wasser und stoffhaushaltsuntersuchungen landwirtschaftlich genutzer einzugsgebiete." Mittelungen Deutsche Bodenkundliche Geselschaft 42(S): 294-299.

Bronk Ramsey, C. (2009). Bayesian analysis of radiocarbon dates. Radiocarbon 51, 337e360.

Buringh, P. (1960). "Soils and soil conditions in Iraq." Ministry of Agriculture, Baghdad 322.

Bussay, A., et al. (1998). Monitoring drought in Hungary using the standardized precipitation index. Annales Geophysicae, Supplement.

Campbell, J. (2002). "Introduction to Remote Sensing, CORINE Land Cover Technical Guide." (European Commission, Luxemburg): pp. 21-53.

Chen, H., et al. (2006). "Surface pollen in the east of Qaidam Basin." Journal of Geographical Sciences 16(4): 439-446.

Dehghan, A. (2011). "Status and potentials of renewable energies in Yazd Province-Iran." Renewable and Sustainable Energy Reviews 15(3): 1491-1496.

Dempster, C. (2010). Resilience of social-ecological systems (SESs): A case study of water management in the Iraqi Marshlands.

Djaman, K., et al. (2015). "Evaluation of sixteen reference evapotranspiration methods under sahelian conditions in the Senegal River Valley." Journal of Hydrology: Regional Studies 3: 139-159.

EDEN, U. (2012). "DROUGHT ASSESSMENT BY EVAPOTRANSPIRATION MAPPING IN TWENTE, THE NETHERLANDS."

Eklund, L. and J. Seaquist (2015). "Meteorological, agricultural and socioeconomic drought in the Duhok Governorate, Iraqi Kurdistan." Natural Hazards 76(1): 421-441.

Entekhabi, D., et al. (1996). "Mutual interaction of soil moisture state and atmospheric processes." Journal of Hydrology 184(1): 3-17.

Evans, J. P. (2009). "century climate change in the Middle East. Journal of Climate Chang."

Evensen, G. (2003). "The ensemble Kalman filter: Theoretical formulation and practical implementation." Ocean dynamics 53(4): 343-367.

Fan, L.-y., et al. (2009). "Investigating the relationship between NDVI and LAI in semi-arid grassland in Inner Mongolia using in-situ measurements." Theoretical and applied climatology 95(1-2): 151-156.

FAO (2009). "(Food and Agriculture Organization of the United Nations). 2009. Agricultural Overview. Rome: FAO. www.faoiraq.org/images/word/Agriculture.".

FAO (2012). ".Iraq Agriculture Sector Note. Rome: FAO Investment Centre. www.fao.org/docrep/017/i2877e/i2877e.pdf.".

FAOSTAT (2013). "FAOSTAT database. http://faostat.fao.org. Accessed December 4, 2013."

Fish, R. E. (2011). Using water balance models to approximate the effects of climate change on spring catchment discharge: Mt. Hanang, Tanzania, Michigan Technological University.

Forootan, E., et al. (2017). "Large-Scale Total Water Storage and Water Flux Changes over the Arid and Semiarid Parts of the Middle East from GRACE and Reanalysis Products." Surveys in Geophysics 38(3): 591-615.

Gallo, K., et al. (2004). "Comparison of MODIS and AVHRR 16-day normalized difference vegetation index composite data." Geophysical Research Letters 31(7).

Gigante, V., et al. (2009). "Influences of Leaf Area Index estimations on water balance modeling in a Mediterranean semi-arid basin." Natural Hazards and Earth System Sciences 9(3): 979.

Goetz, S. (1997). "Multi-sensor analysis of NDVI, surface temperature and biophysical variables at a mixed grassland site." International Journal of Remote Sensing 18(1): 71-94.

Goward, S. N., et al. (2002). "Evaluating land surface moisture conditions from the remotely sensed temperature/vegetation index measurements: An exploration with the simplified simple biosphere model." Remote Sensing of Environment 79(2): 225-242.

Haied, N., et al. (2017). "Drought assessment and monitoring using meteorological indices in a semi-arid region." Energy Procedia 119: 518-529.

Hargreaves, G. H. and Z. A. Samani (1985). "Reference crop evapotranspiration from temperature." Applied engineering in agriculture 1(2): 96-99.

Haverkamp, R., et al. (1977). "A comparison of numerical simulation models for one-dimensional infiltration." Soil Science Society of America Journal 41(2): 285-294.

Hayes, M. J., et al. (1999). "Monitoring the 1996 drought using the standardized precipitation index." Bulletin of the American Meteorological Society 80(3): 429-438.

Held, C. C. (2000). "Middle East Patterns: Places, People, and Politics." Boulder: Westview Press(3rd ed).

Henderson, A. (2012). "The Future of the World's Climate (Second Edition). Henderson-Sellers, A. and McGuffie, K. (eds), pp. 531-621, Elsevier, Boston.".

Hijmans, R. J., et al. (1994). WOFOST 6.0: User's guide for the WOFOST 6.0 crop growth simulation model, DLO Winand Staring Centre.

Hoerling, M. and A. Kumar (2003). "The perfect ocean for drought." Science 299(5607): 691-694.

Hu, Q. S. and G. D. Willson (2000). "Effects of temperature anomalies on the Palmer Drought Severity Index in the central United States."

Huffman, G. J., et al. (2007). "The TRMM Multisatellite Precipitation Analysis (TMPA): Quasi-global, multiyear, combined-sensor precipitation estimates at fine scales." Journal of Hydrometeorology 8(1): 38-55.

Ibrahim, O. S., Salih, S.A. and Ali, N.H (2012). "Using of Climatic Water Balance to Assess The Reality of Groundwater Recharge in Baiji – Tikrit Sub Basin North West of Iraq." Journal of Kirkuk University For scientific studies 7(1), 79-107.

IPCC (2013). "Summary for Policymakers, in Climate Change. The Physical Science Basis. Contribution of Working Group I to the Fifth Assessment Report of the Intergovernmental Panel on Climate Change."

Jang, J. D., et al. (2006). "Thermal-water stress index from satellite images." International Journal of Remote Sensing 27(8): 1619-1639.

Jaradat, A. (2003). "Agriculture in Iraq: Resources, potentials, constraints, research needs and priorities." Food, Agriculture & Environment 1(2): 160-166.

Ji, L. and A. J. Peters (2003). "Assessing vegetation response to drought in the northern Great Plains using vegetation and drought indices." Remote Sensing of Environment 87(1): 85-98.

Jouhari Nadiah, S. A.-S., Sudipto Mukerjee (2012). "Development of National Framework for Integrated Drought Risk Management (DRM) in Iraq." programme number P3 – 01.

Kafle, H. K. and H. J. Bruins (2009). "Climatic trends in Israel 1970–2002: warmer and increasing aridity inland." Climatic Change 96(1): 63-77.

Kalnay, E., et al. (1996). "The NCEP/NCAR 40-year reanalysis project." Bulletin of the American Meteorological Society 77(3): 437-471.

Kamil, M. (2002a). "Iraq's Economic Predicament. Exeter Arab and Islamic Studies Series." Ithaca Press.

Kaniewski, D., et al. (2012). "Drought is a recurring challenge in the Middle East." Proceedings of the National Academy of Sciences 109(10): 3862-3867.

Kerr, Y. H., et al. (2004). "Land surface temperature retrieval techniques and applications." Thermal remote sensing in land surface processes: 33-109.

Khosravi, H., et al. (2017). "Assessment the Effect of Drought on Vegetation in Desert Area using Landsat Data." The Egyptian Journal of Remote Sensing and Space Science 20: S3-S12.

Knutson, T. R., et al. (2007). "Simulation of the recent multidecadal increase of Atlantic hurricane activity using an 18-km-grid regional model." Bulletin of the American Meteorological Society 88(10): 1549-1565.

Kogan, F. N. (2000). "Satellite-observed sensitivity of world land ecosystems to El Nino/La Nina." Remote Sensing of Environment 74(3): 445-462.

Kroes, J., et al. (2008). SWAP version 3.2: Theory description and user manual, Alterra Wageningen, The Netherlands.

Liou, Y.-A. and S. K. Kar (2014). "Evapotranspiration estimation with remote sensing and various surface energy balance algorithms—A review." Energies 7(5): 2821-2849.

Liu, H. Q. and A. Huete (1995). "A feedback based modification of the NDVI to minimize canopy background and atmospheric noise." IEEE Transactions on Geoscience and Remote Sensing 33(2): 457-465.

Lloyd-Hughes, B. and M. A. Saunders (2002). "A drought climatology for Europe." International journal of climatology 22(13): 1571-1592.

Lucani, P. (2012). "Iraq Agriculture sector note."

Mathbout, S., et al. (2017). "Spatial and temporal analysis of drought variability at several time scales in Syria during 1961–2012." Atmospheric Research.

McKee, T. B. (2000). A history of drought in Colorado: lessons learned and what lies ahead, Colorado State University, Colorado Water Resources Research Institute.

McKee, T. B., et al. (1993). The relationship of drought frequency and duration to time scales. Proceedings of the 8th Conference on Applied Climatology, American Meteorological Society Boston, MA.

Mesinger, F., et al. (2006). "North American regional reanalysis." Bulletin of the American Meteorological Society 87(3): 343-360.

Mishra, A. K. and V. P. Singh (2010). "A review of drought concepts." Journal of Hydrology 391(1): 202-216.

Mitchell, K. E., et al. (2004). "The multi-institution North American Land Data Assimilation System (NLDAS): Utilizing multiple GCIP products and partners in a continental distributed hydrological modeling system." Journal of Geophysical Research 109(D7): D07S90.

Mohammad, T. R. S. (2008). "Locational Discrepancy in the Values of the Water Losses by the Potential Evapotranspiration Process in Iraq - A critical Comparative Study of the Khosla and Thornthwaite Equations " Journal of Basra Research For Human Sciences.

Mualem, Y. (1976). "A new model for predicting the hydraulic conductivity of unsaturated porous media." Water Resources Research 12(3): 513-522.

Muchoney, D., et al. (1999). "The IGBP DISCover confidence sites and the system for terrestrial ecosystem parameterization: Tools for validating global land-cover data." Photogrammetric engineering and remote sensing 65(9): 1061-1067.

Nagarajan, R. (2009). Drought assessment, Springer.

Naresh Kumar, M., et al. (2009). "On the use of Standardized Precipitation Index (SPI) for drought intensity assessment." Meteorological applications 16(3): 381-389.

Nemani, R., et al. (1993). "Developing satellite-derived estimates of surface moisture status." Journal of Applied Meteorology 32(3): 548-557.

NOAA (2008). "Drought[Fact sheet] (Tech. Rep.). Retrieved from http://www.nws.noaa.gov/os/brochures/climate/DroughtPublic2.pdf."

Obid, K. R., et al. (2013). "The comparison between different methods for estimating consumptive use of water in Iraq." Journal of Babylon University/Engineering Sciences 21: 27-36.

Omer, T. M. A. (2011). "Country pasture/forage resource profiles." FAO, available on: http://www. fao. org/ag/AGP/AGPC/doc/Counprof/PDF% 20files/iraq. pdf.

Orth, R., et al. (2016). "Improving weather predictability by including land surface model parameter uncertainty." Monthly Weather Review 144(4): 1551-1569.

Otgonjargal, N. (2012). Assessment of drought hazard: a case study in Sehoul area, Morocco, University of Twente Faculty of Geo-Information and Earth Observation (ITC).

Pala, M., et al. (2011). "Assessment of wheat yield gap in the Mediterranean: case studies from Morocco, Syria and Turkey." International Center for Agricultural Research in the Dry Areas (ICARDA), Aleppo, Syria. iv: 963-921.

Patel, N., et al. (2012). "Analysis of agricultural drought using vegetation temperature condition index (VTCI) from Terra/MODIS satellite data." Environmental monitoring and assessment 184(12): 7153-7163.

Petach, A. R., et al. (2014). "Monitoring vegetation phenology using an infrared-enabled security camera." Agricultural and Forest Meteorology 195: 143-151.

Prihodko, L. and S. N. Goward (1997). "Estimation of air temperature from remotely sensed surface observations." Remote Sensing of Environment 60(3): 335-346.

Quiring, S. M. and S. Ganesh (2010). "Evaluating the utility of the Vegetation Condition Index (VCI) for monitoring meteorological drought in Texas." Agricultural and Forest Meteorology 150(3): 330-339.

Qureshi, A. S. and A. A. Al-Falahi (2015). "Modeling the effects of different irrigation schedules and drain depths for soil salinity management: A case study from Southern Iraq." African Journal of Agricultural Research 10(32): 3178-3188.

Rossi, G., et al. (1992). "On regional drought estimation and analysis." Water Resources Management 6(4): 249-277.

Saud, A., et al. (2014). "Temporal and Spatial variability of Potential Evapotranspiration in Semi-Arid Region: Case Study the Valleys of Western Region of Iraq." International Journal of Engineering Science and Technology 6(9): 653.

Saud, A., et al. (2016). "Investigation of Water Balance Methods of Haqlan Basin in the Western Region of Iraq." World Applied Sciences Journal 34(5): 652-656.

Scaini, A., et al. (2015). "SMOS-derived soil moisture anomalies and drought indices: a comparative analysis using in situ measurements." Hydrological processes 29(3): 373-383.

Schnepf, R. (2004). Iraq agriculture and food supply: Background and issues, Congressional Research Service Report for Congress. Library of Congress.

Schnepf, R. D. (2004). Iraq agriculture and food supply: Background and issues, Congressional Research Service, Library of Congress.

Schowengerdt, R. A. (2006). Remote sensing: models and methods for image processing, Academic press.

Sheffield, J., et al. (2009). "Global and continental drought in the second half of the twentieth century: Severity-area-duration analysis and temporal variability of large-scale events." Journal of Climate 22(8): 1962-1981.

Sheffield, J. and E. F. Wood (2012). Drought: past problems and future scenarios, Routledge.

Shrestha, D. P. (2012). "NATSAGDORJ OTGONJARGAL February, 2012."

Shubbar, R. M., et al. (2017). "Characteristics of climate variation indices in Iraq using a statistical factor analysis." International journal of climatology 37(2): 918-927.

Solomon, S. (2007). Climate change 2007-the physical science basis: Working group I contribution to the fourth assessment report of the IPCC, Cambridge University Press.

Soltani, S., et al. (2012). "Rainfall and rainy days trend in Iran." Climatic Change 110(1-2): 187-213.

Sowers, J., et al. (2011). "Climate change, water resources, and the politics of adaptation in the Middle East and North Africa." Climatic Change 104(3): 599-627.

Stagge, J. H., et al. (2014). "Standardized precipitation-evapotranspiration index (SPEI): Sensitivity to potential evapotranspiration model and parameters." Proceedings of FRIEND-Water: 367-373.

Su, H., et al. (2005). "Modeling evapotranspiration during SMACEX: Comparing two approaches for local-and regional-scale prediction." Journal of Hydrometeorology 6(6): 910-922.

Svoboda, M., et al. (2012). "Standardized precipitation index user guide." World Meteorological Organization (WMO-No. 1090), Geneva 16.

Szalai, S. and C. Szinell (2000). Comparison of two drought indices for drought monitoring in Hungary—a case study. Drought and drought mitigation in Europe, Springer: 161-166.

Tayanç, M., et al. (2009). "Climate change in Turkey for the last half century." Climatic Change 94(3): 483-502.

Thornthwaite, C. W. (1948). "An approach toward a rational classification of climate." Geographical review 38(1): 55-94.

Trenberth, K. E., et al. (2007). "Estimates of the global water budget and its annual cycle using observational and model data." Journal of Hydrometeorology 8(4): 758-769.

Trigo, R. M., et al. (2010). "The intense 2007–2009 drought in the Fertile Crescent: Impacts and associated atmospheric circulation." Agricultural and Forest Meteorology 150(9): 1245-1257.

Tucker, C. J. (1979). "Red and photographic infrared linear combinations for monitoring vegetation." Remote Sensing of Environment 8(2): 127-150.

UNEP . Nairobi (2010). "Support for Environmental Management of the Iraqi Marshlands 2004 - 2009." 104 pp.

UNESCO (2014). "Integrated drought risk management, DRM: national framework for Iraq, an analysis report (Tech. Rep.). Amman: UNESCO Office Iraq (Jordan)."

van Dam, J. C. (2000). Field-scale water flow and solute transport: SWAP model concepts, parameter estimation and case studies, [sn].

Van Genuchten, M. T. (1980). "A closed-form equation for predicting the hydraulic conductivity of unsaturated soils." Soil Science Society of America Journal 44(5): 892-898.

van Genuchten, M. T. (1987). "A numerical model for water and solute movement in and below the root zone. United States Department of Agriculture." Agricultural Research Service, US Salinity Laboratory, Riverside, California, US.

Van Loon, A. F. (2015). "Hydrological drought explained." Wiley Interdisciplinary Reviews: Water 2(4): 359-392.

Verhoef, A., et al. (1999). "Seasonal variation of surface energy balance over two Sahelian surfaces." International journal of climatology 19(11): 1267-1277.

Vicente-Serrano, S. M., et al. (2010). "A multiscalar drought index sensitive to global warming: the standardized precipitation evapotranspiration index." Journal of Climate 23(7): 1696-1718.

Vicente-Serrano, S. M., et al. (2012). "Performance of drought indices for ecological, agricultural, and hydrological applications." Earth Interactions 16(10): 1-27.

Vicente-Serrano, S. M., et al. (2011). "Effects of warming processes on droughts and water resources in the NW Iberian Peninsula (1930-2006)." Climate research 48: 203-212.

Wang, K., et al. (2005). "Estimation of surface long wave radiation and broadband emissivity using Moderate Resolution Imaging Spectroradiometer (MODIS) land surface temperature/emissivity products." Journal of Geophysical Research: Atmospheres 110(D11).

Water, E., Social and Rural Development Department Middle East and North Africa Region (2006). "Iraq: Country Water Resource Assistance Strategy: Addressing Major Threats to People's Livelihoods."

Weiss, H., et al. (1993). "The genesis and collapse of third millennium north Mesopotamian civilization." SCIENCE-NEW YORK THEN WASHINGTON- 261: 995-995.

Wild, M., et al. (2015). "The energy balance over land and oceans: an assessment based on direct observations and CMIP5 climate models." Climate dynamics 44(11-12): 3393-3429.

Wilhite, D. A., et al. (2007). "Understanding the complex impacts of drought: a key to enhancing drought mitigation and preparedness." Water Resources Management 21(5): 763-774.

Wösten, J., et al. (1998). Using existing soil data to derive hydraulic parameters for simulation models in environmental studies and in land use planning, Report.

Wright Jr, H., et al. (1967). "Modern pollen rain in western Iran, and its relation to plant geography and Quaternary vegetational history." The Journal of Ecology: 415-443.

APPENDICES

APPENDIX A: Yearly averaged SPI-3 and SPEI-3 values over the period 2001–2015, and NDVI

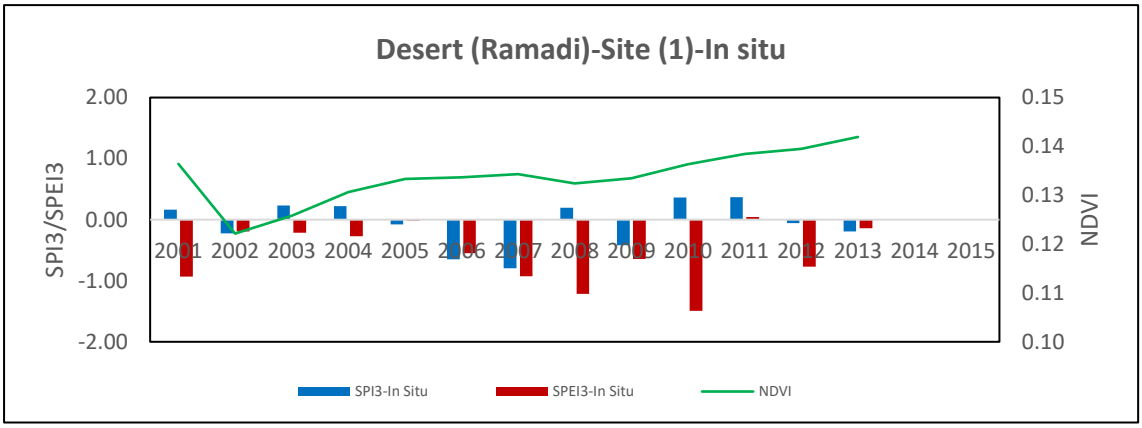

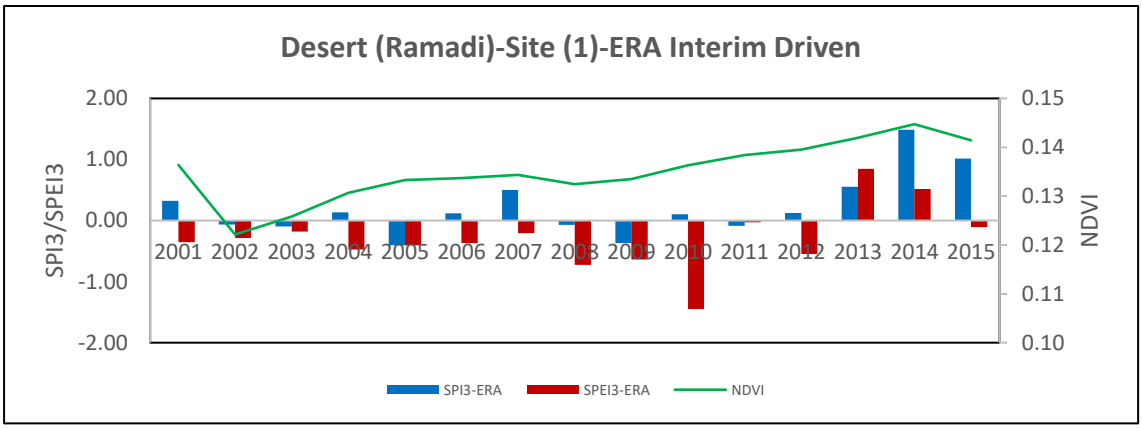

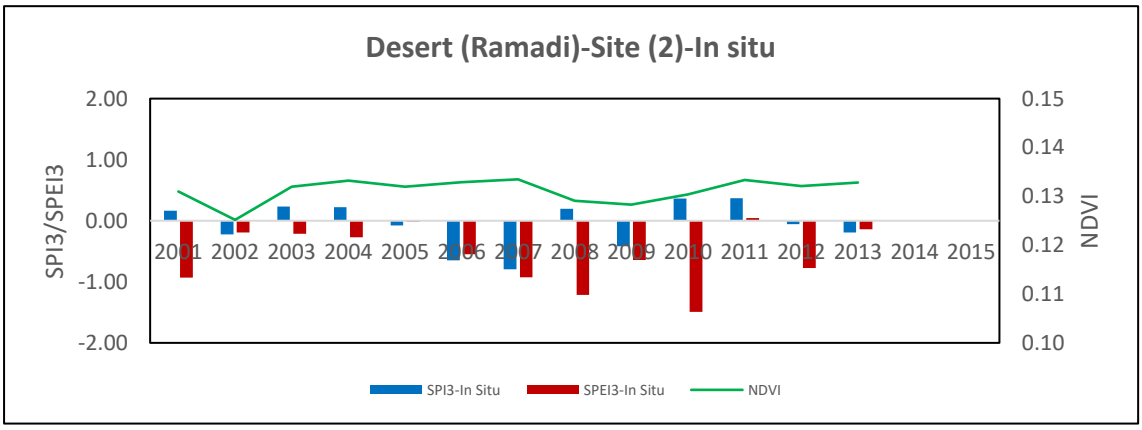

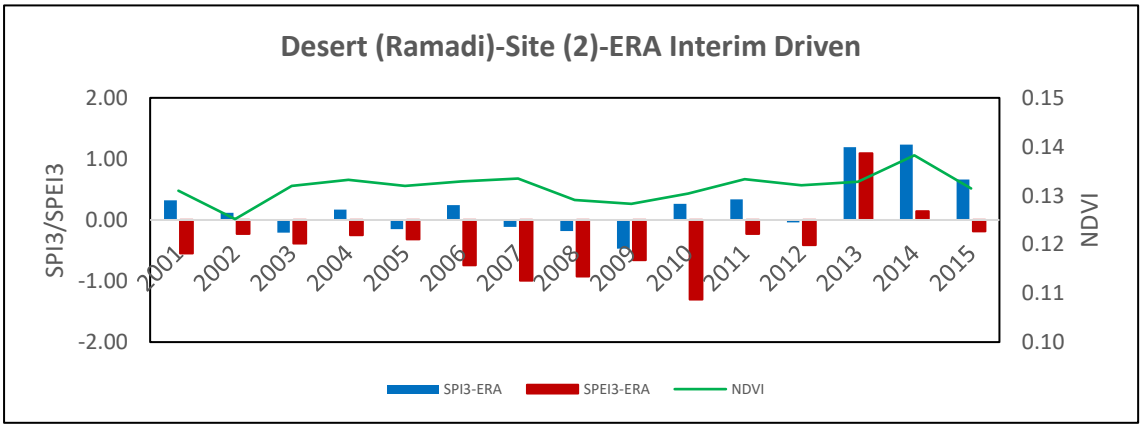

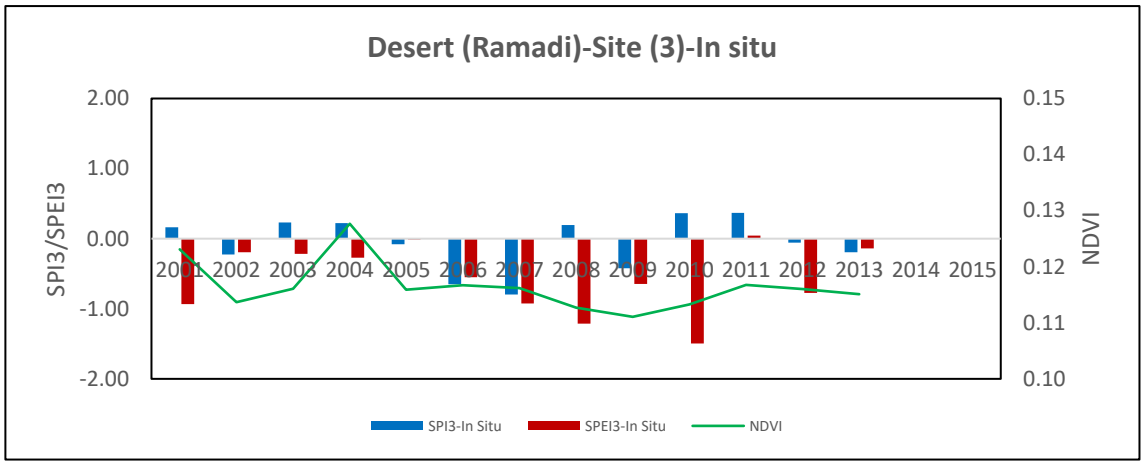
Desert (Ramadi)-Site (3)-In situ
SPI3/SPEI3
NDVI
2.00
1.00
0.00
-1.00
-2.00
0.15
0.14
0.13
0.12
0.11
0.10
2001 2002 2003 2004 2005 2006 2007 2008 2009 2010 2011 2012 2013 2014 2015
SPI3-In Situ
SPEI3-In Situ
NDVI

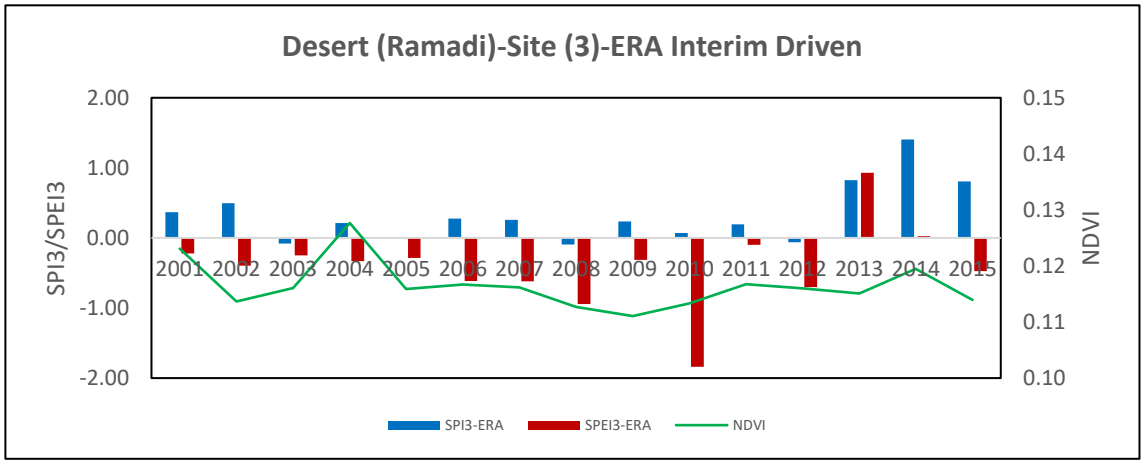
Desert (Ramadi)-Site (3)-ERA Interim Driven
SPI3/SPEI3
NDVI
2.00
1.00
0.00
-1.00
-2.00
0.15
0.14
0.13
0.12
0.11
0.10
2001 2002 2003 2004 2005 2006 2007 2008 2009 2010 2011 2012 2013 2014 2015
SPI3-ERA
SPEI3-ERA
NDVI

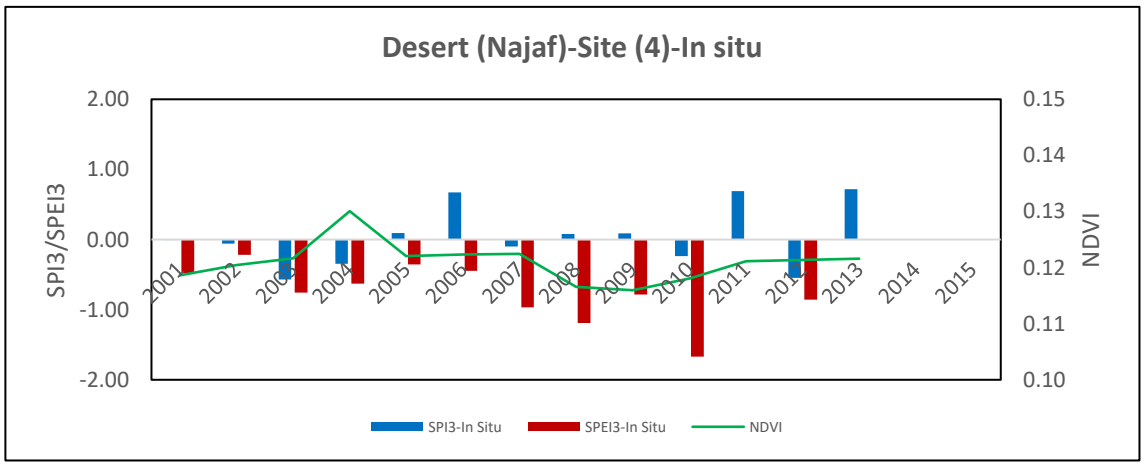
Desert (Najaf)-Site (4)-In situ
SPI3/SPEI3
NDVI
2.00
1.00
0.00
-1.00
-2.00
0.15
0.14
0.13
0.12
0.11
0.10
2001 2002 2003 2004 2005 2006 2007 2008 2009 2010 2011 2012 2013 2014 2015
SPI3-In Situ
SPEI3-In Situ
NDVI

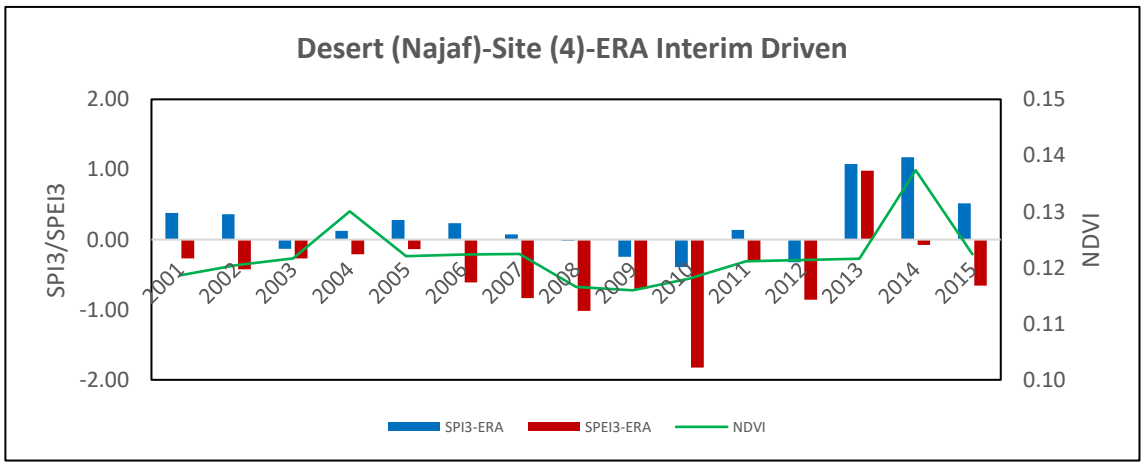
Desert (Najaf)-Site (4)-ERA Interim Driven
SPI3/SPEI3
NDVI
2.00
1.00
0.00
-1.00
-2.00
0.15
0.14
0.13
0.12
0.11
0.10
2001 2002 2003 2004 2005 2006 2007 2008 2009 2010 2011 2012 2013 2014 2015
SPI3-ERA
SPEI3-ERA
NDVI

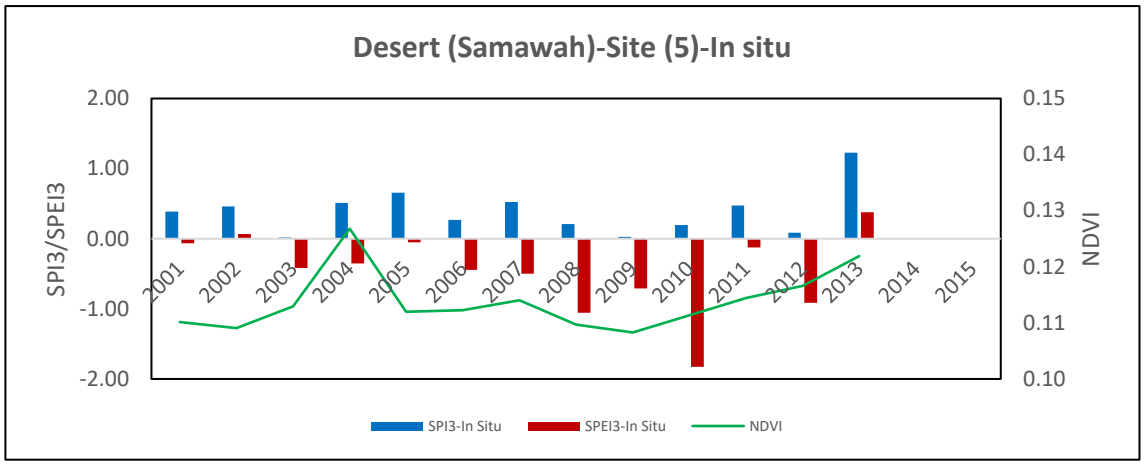
Desert (Samawah)-Site (5)-In situ
SPI3/SPEI3
NDVI
2.00
1.00
0.00
-1.00
-2.00
0.15
0.14
0.13
0.12
0.11
0.10
2001
2002
2003
2004
2005
2006
2007
2008
2009
2010
2011
2012
2013
2014
2015
SPI3-In Situ
SPEI3-In Situ
NDVI

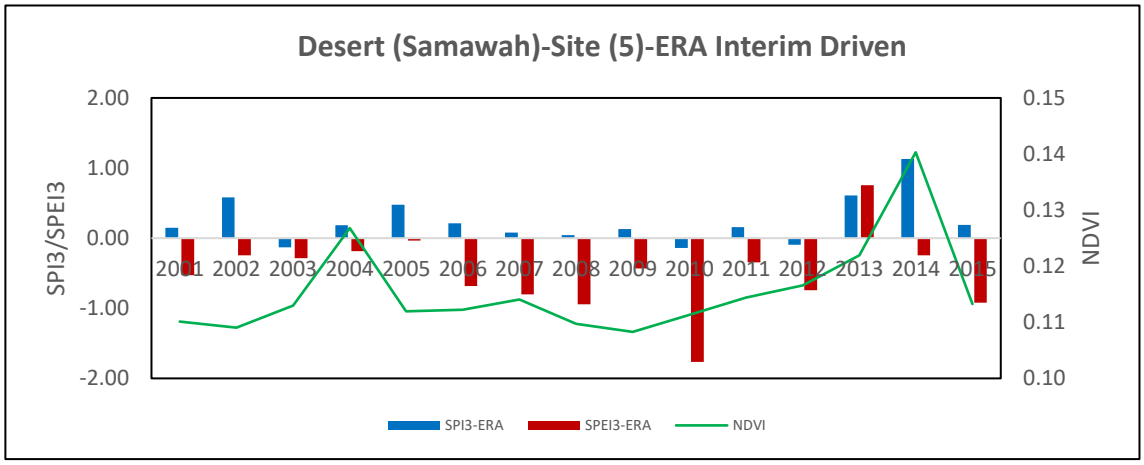
Desert (Samawah)-Site (5)-ERA Interim Driven
SPI3/SPEI3
NDVI
2.00
1.00
0.00
-1.00
-2.00
0.15
0.14
0.13
0.12
0.11
0.10
2001
2002
2003
2004
2005
2006
2007
2008
2009
2010
2011
2012
2013
2014
2015
SPI3-ERA
SPEI3-ERA
NDVI

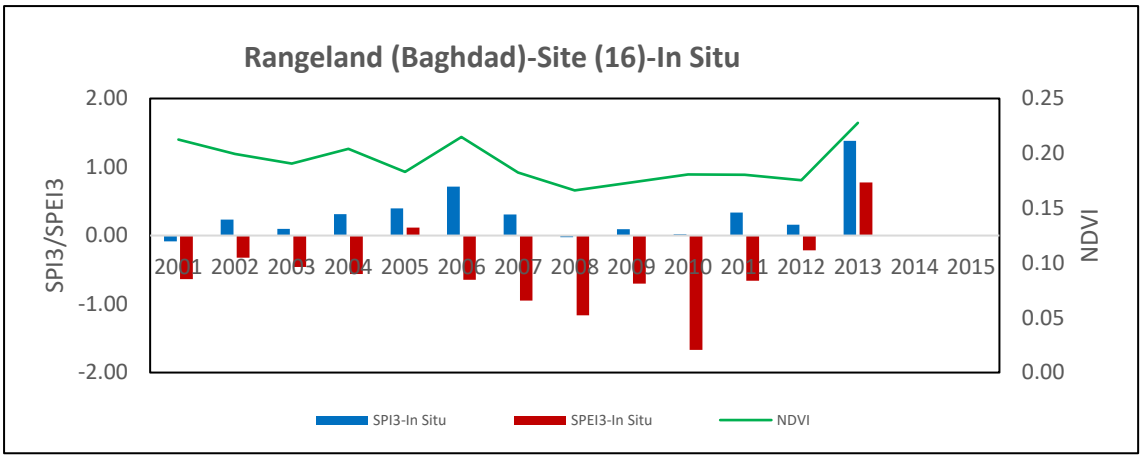
Rangeland (Baghdad)-Site (16)-In Situ
SPI3/SPEI3
NDVI
2.00
1.00
0.00
-1.00
-2.00
0.25
0.20
0.15
0.10
0.05
0.00
2001 2002 2003 2004 2005 2006 2007 2008 2009 2010 2011 2012 2013 2014 2015
SPI3-In Situ
SPEI3-In Situ
NDVI

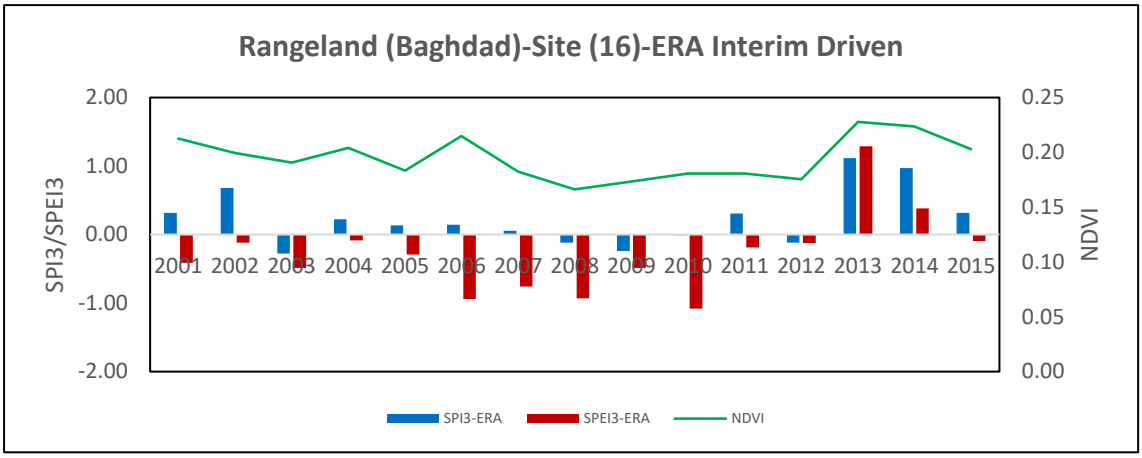
Rangeland (Baghdad)-Site (16)-ERA Interim Driven
SPI3/SPEI3
NDVI
2.00
1.00
0.00
-1.00
-2.00
0.25
0.20
0.15
0.10
0.05
0.00
2001 2002 2003 2004 2005 2006 2007 2008 2009 2010 2011 2012 2013 2014 2015
SPI3-ERA
SPEI3-ERA
NDVI

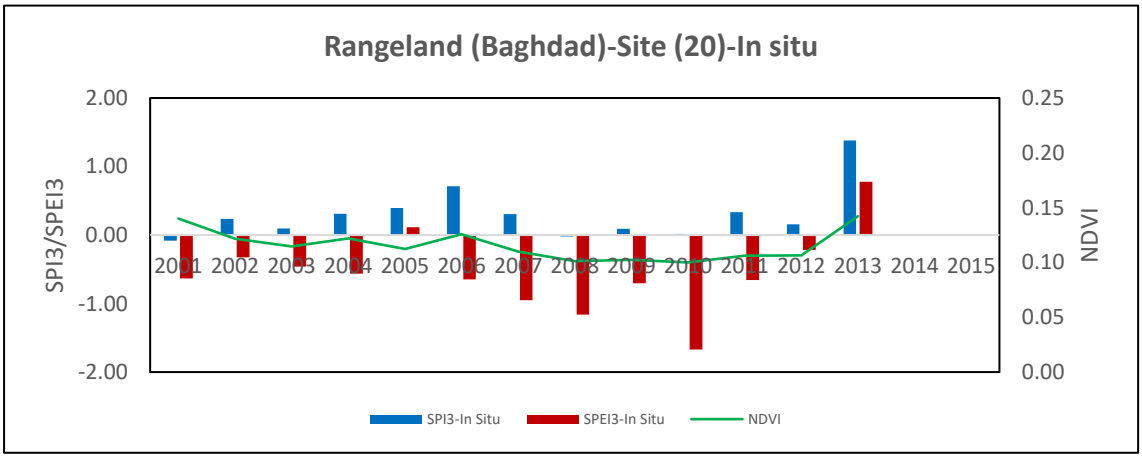
Rangeland (Baghdad)-Site (20)-In situ
SPI3/SPEI3
NDVI
2.00
1.00
0.00
-1.00
-2.00
0.25
0.20
0.15
0.10
0.05
0.00
2001 2002 2003 2004 2005 2006 2007 2008 2009 2010 2011 2012 2013 2014 2015
SPI3-In Situ
SPEI3-In Situ
NDVI

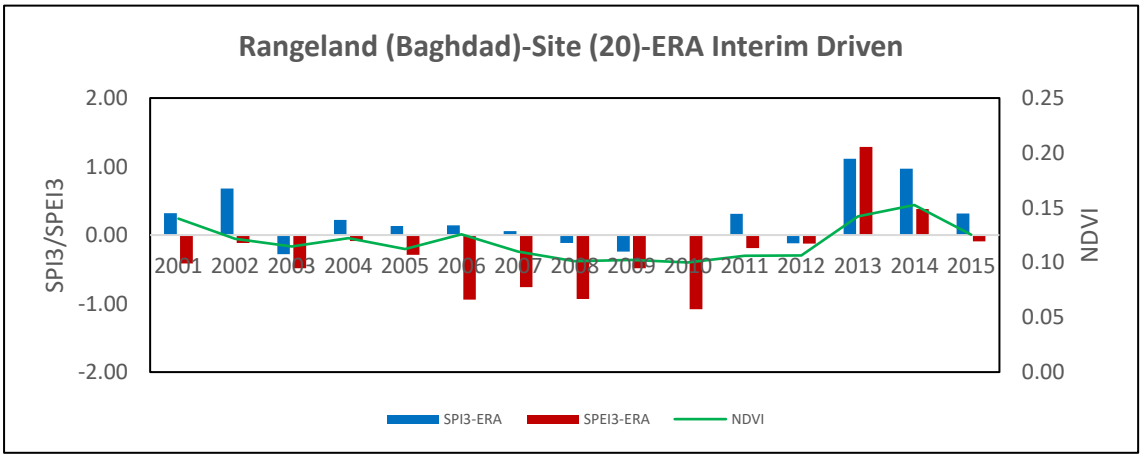
Rangeland (Baghdad)-Site (20)-ERA Interim Driven
SPI3/SPEI3
NDVI
2.00
1.00
0.00
-1.00
-2.00
0.25
0.20
0.15
0.10
0.05
0.00
2001 2002 2003 2004 2005 2006 2007 2008 2009 2010 2011 2012 2013 2014 2015
SPI3-ERA
SPEI3-ERA
NDVI

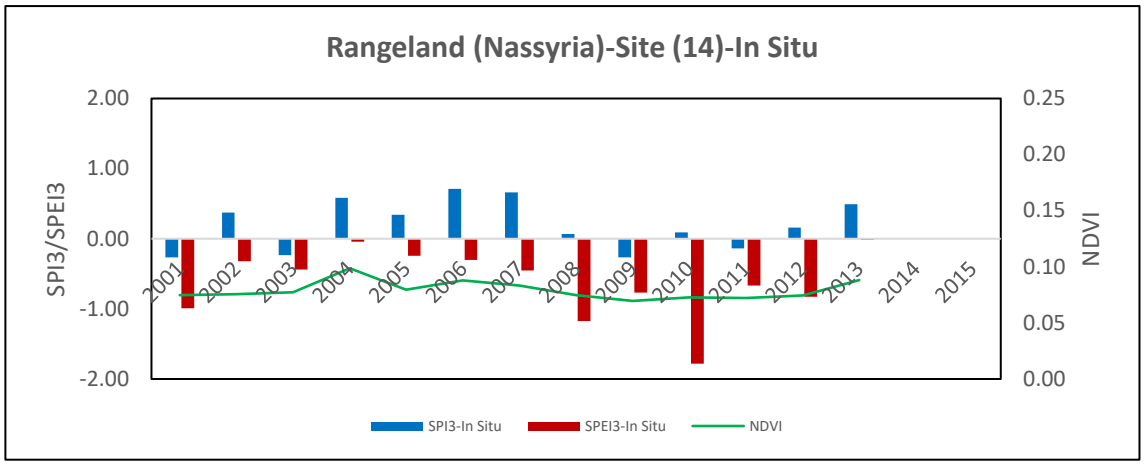
Rangeland (Nassyria)-Site (14)-In Situ
SPI3/SPEI3
NDVI
2.00
1.00
0.00
-1.00
-2.00
0.25
0.20
0.15
0.10
0.05
0.00
2001 2002 2003 2004 2005 2006 2007 2008 2009 2010 2011 2012 2013 2014 2015
SPI3-In Situ
SPEI3-In Situ
NDVI

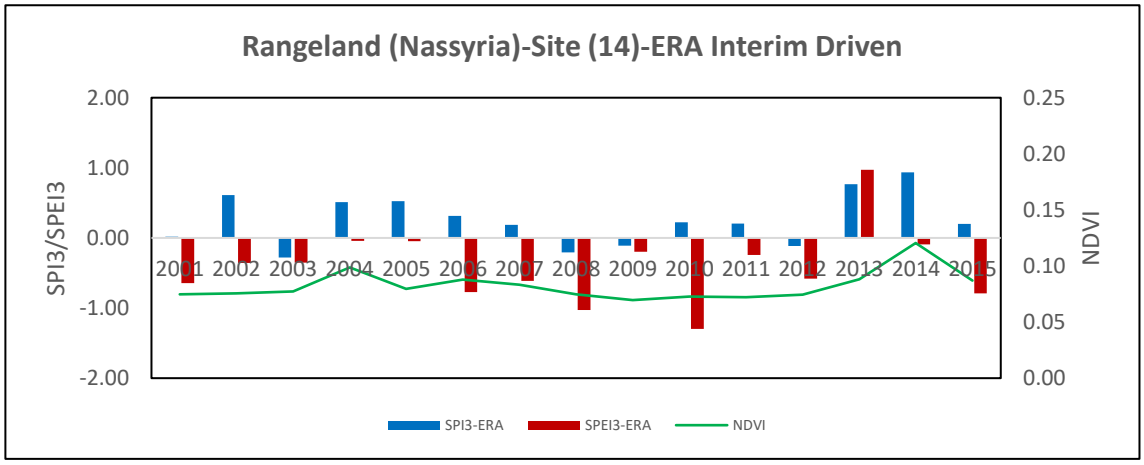
Rangeland (Nassyria)-Site (14)-ERA Interim Driven
SPI3/SPEI3
NDVI
2.00
1.00
0.00
-1.00
-2.00
0.25
0.20
0.15
0.10
0.05
0.00
2001 2002 2003 2004 2005 2006 2007 2008 2009 2010 2011 2012 2013 2014 2015
SPI3-ERA
SPEI3-ERA
NDVI

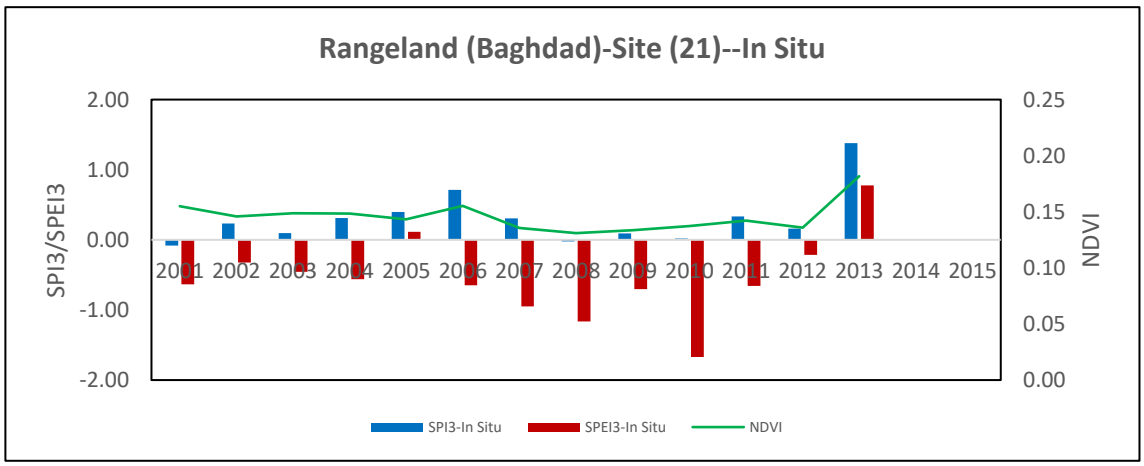
Rangeland (Baghdad)-Site (21)--In Situ
SPI3/SPEI3
NDVI
2.00
1.00
0.00
-1.00
-2.00
0.25
0.20
0.15
0.10
0.05
0.00
2001 2002 2003 2004 2005 2006 2007 2008 2009 2010 2011 2012 2013 2014 2015
SPI3-In Situ
SPEI3-In Situ
NDVI

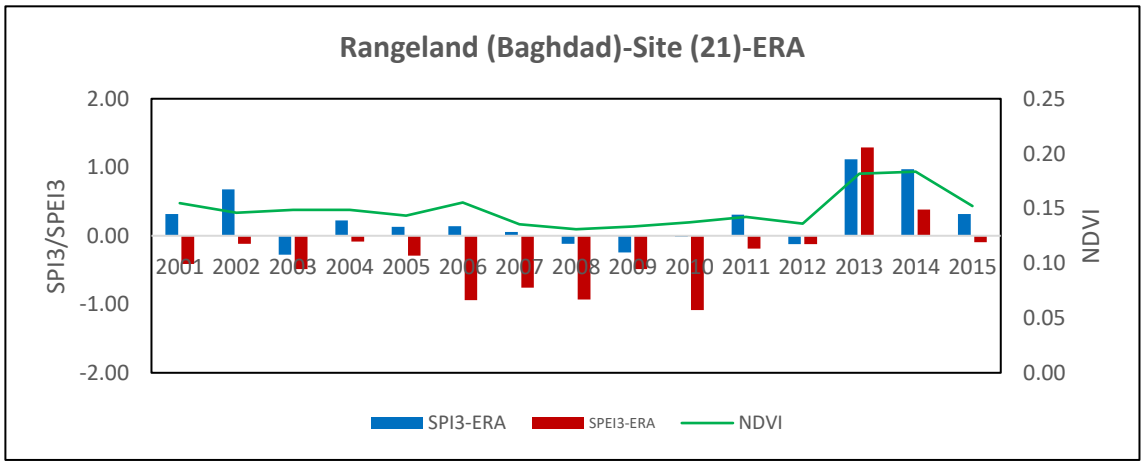
Rangeland (Baghdad)-Site (21)-ERA
SPI3/SPEI3
NDVI
2.00
1.00
0.00
-1.00
-2.00
0.25
0.20
0.15
0.10
0.05
0.00
2001 2002 2003 2004 2005 2006 2007 2008 2009 2010 2011 2012 2013 2014 2015
SPI3-ERA
SPEI3-ERA
NDVI

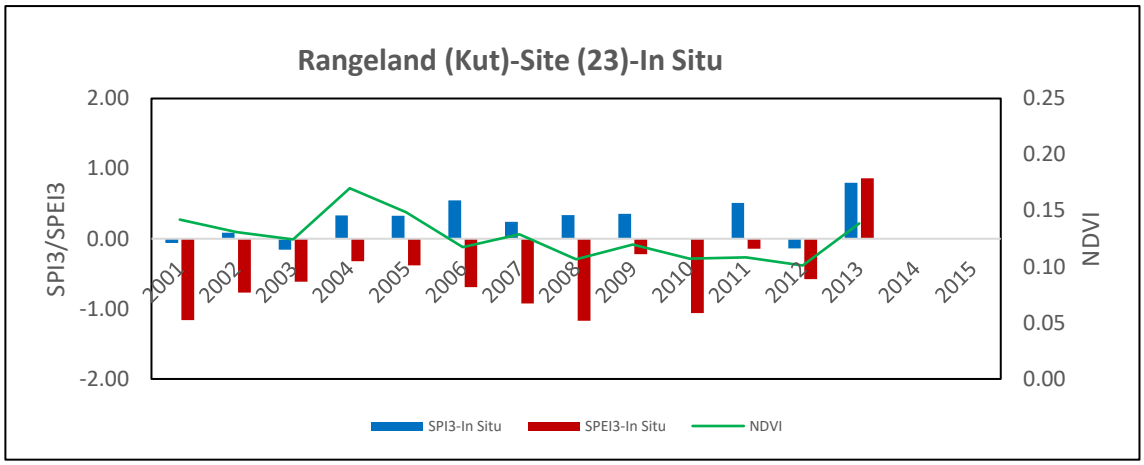
Rangeland (Kut)-Site (23)-In Situ
SPI3/SPEI3
NDVI
2.00
1.00
0.00
-1.00
-2.00
0.25
0.20
0.15
0.10
0.05
0.00
2001
2002
2003
2004
2005
2006
2007
2008
2009
2010
2011
2012
2013
2014
2015
SPI3-In Situ
SPEI3-In Situ
NDVI

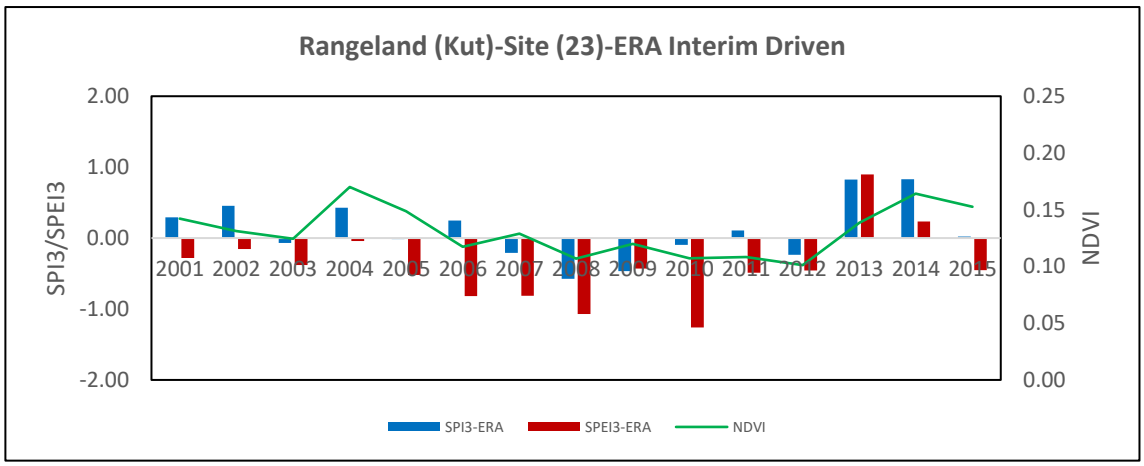
Rangeland (Kut)-Site (23)-ERA Interim Driven
SPI3/SPEI3
NDVI
2.00
1.00
0.00
-1.00
-2.00
0.25
0.20
0.15
0.10
0.05
0.00
2001 2002 2003 2004 2005 2006 2007 2008 2009 2010 2011 2012 2013 2014 2015
SPI3-ERA
SPEI3-ERA
NDVI

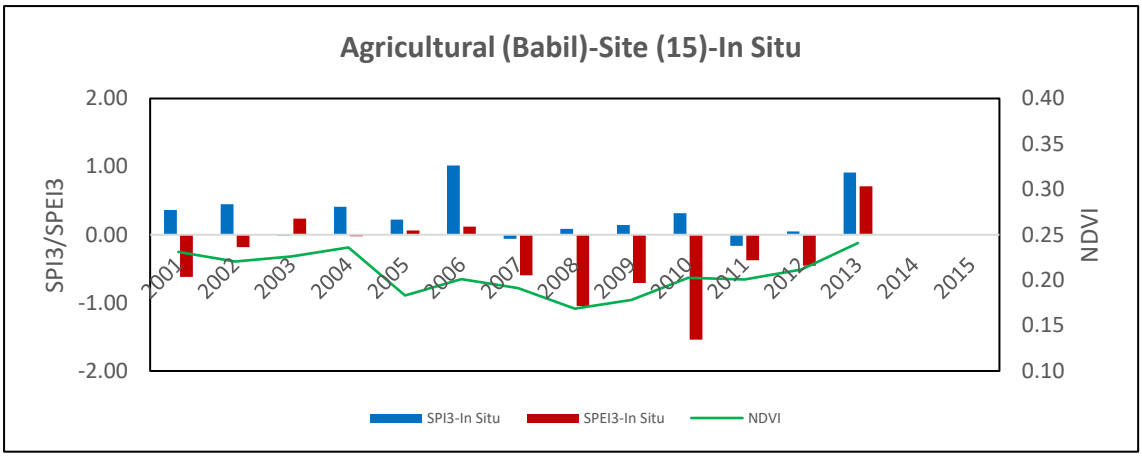
Agricultural (Babil)-Site (15)-In Situ
SPI3/SPEI3
NDVI
2.00
1.00
0.00
-1.00
-2.00
0.40
0.35
0.30
0.25
0.20
0.15
0.10
2001
2002
2003
2004
2005
2006
2007
2008
2009
2010
2011
2012
2013
2014
2015
SPI3-In Situ
SPEI3-In Situ
NDVI

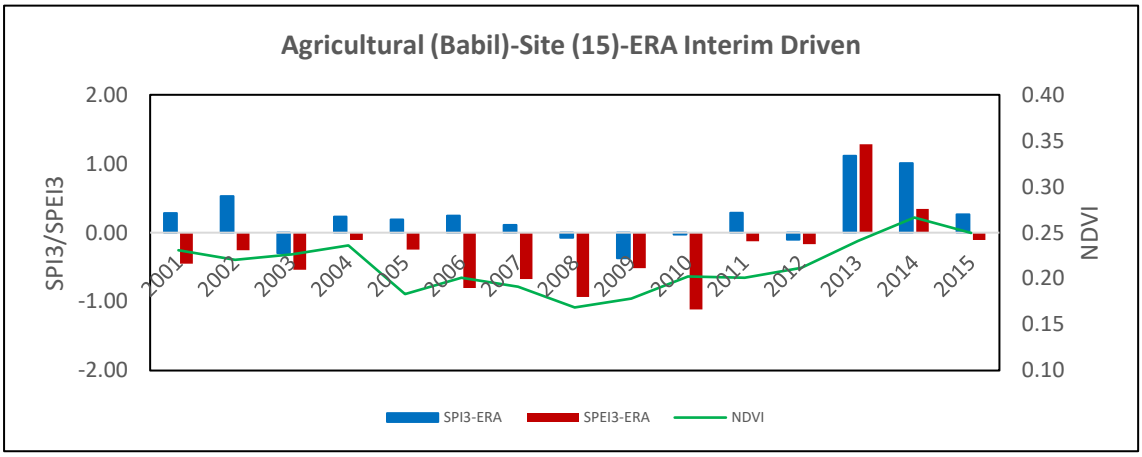
Agricultural (Babil)-Site (15)-ERA Interim Driven
SPI3/SPEI3
NDVI
2.00
1.00
0.00
-1.00
-2.00
0.40
0.35
0.30
0.25
0.20
0.15
0.10
2001
2002
2003
2004
2005
2006
2007
2008
2009
2010
2011
2012
2013
2014
2015
SPI3-ERA
SPEI3-ERA
NDVI

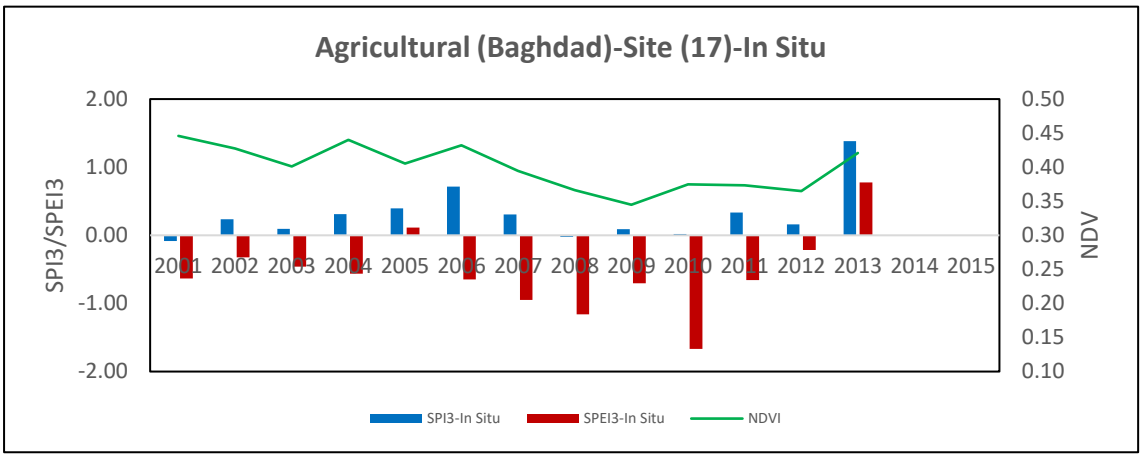
Agricultural (Baghdad)-Site (17)-In Situ
SPI3/SPEI3
NDV
2.00
1.00
0.00
-1.00
-2.00
0.50
0.45
0.40
0.35
0.30
0.25
0.20
0.15
0.10
2001 2002 2003 2004 2005 2006 2007 2008 2009 2010 2011 2012 2013 2014 2015
SPI3-In Situ
SPEI3-In Situ
NDVI

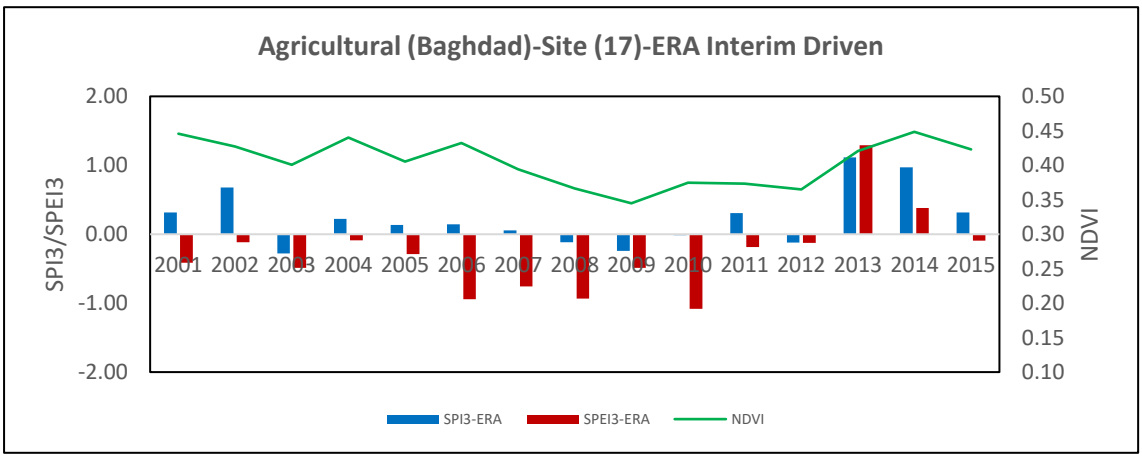
Agricultural (Baghdad)-Site (17)-ERA Interim Driven
SPI3/SPEI3
NDVI
2.00
1.00
0.00
-1.00
-2.00
0.50
0.45
0.40
0.35
0.30
0.25
0.20
0.15
0.10
2001 2002 2003 2004 2005 2006 2007 2008 2009 2010 2011 2012 2013 2014 2015
SPI3-ERA
SPEI3-ERA
NDVI

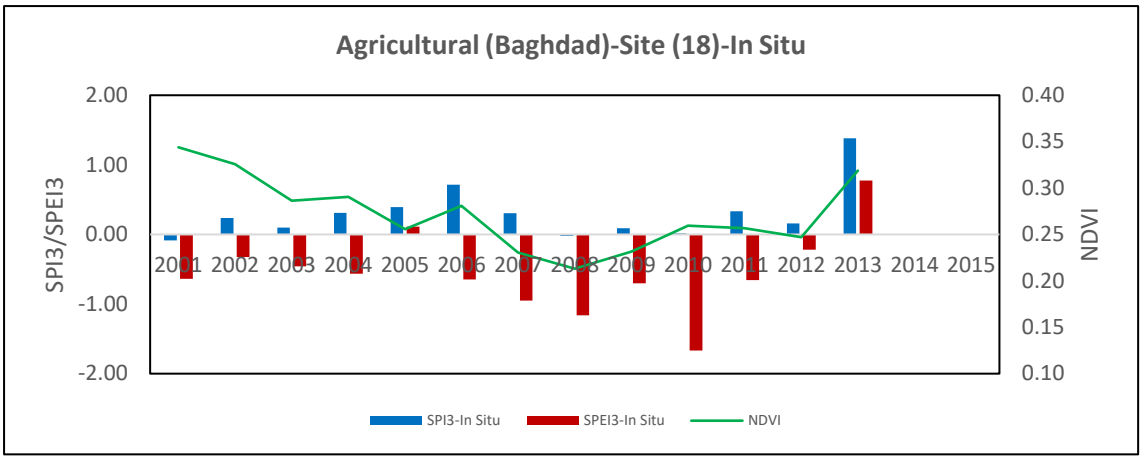
Agricultural (Baghdad)-Site (18)-In Situ
SPI3/SPEI3
NDVI
2.00
1.00
0.00
-1.00
-2.00
0.40
0.35
0.30
0.25
0.20
0.15
0.10
2001 2002 2003 2004 2005 2006 2007 2008 2009 2010 2011 2012 2013 2014 2015
SPI3-In Situ
SPEI3-In Situ
NDVI

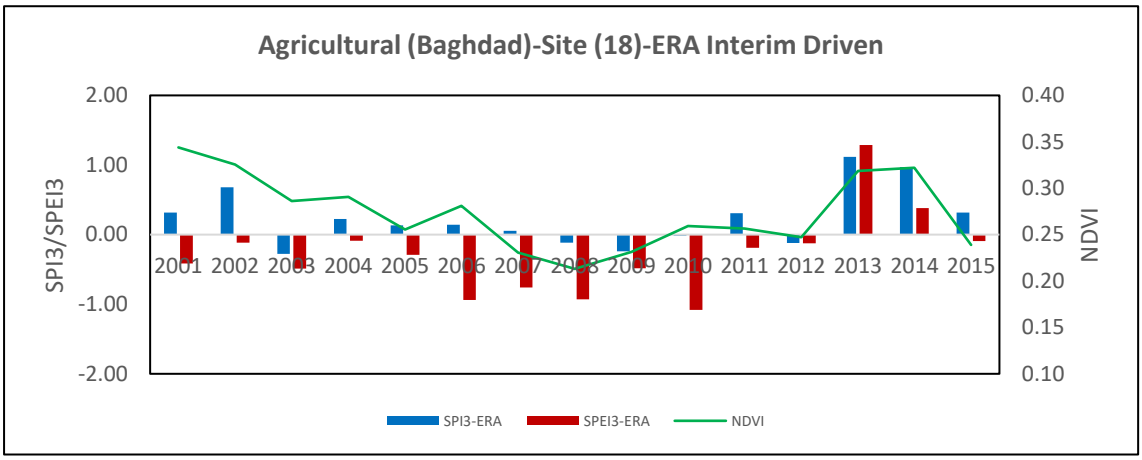
Agricultural (Baghdad)-Site (18)-ERA Interim Driven
SPI3/SPEI3
NDVI
2.00
1.00
0.00
-1.00
-2.00
0.40
0.35
0.30
0.25
0.20
0.15
0.10
2001 2002 2003 2004 2005 2006 2007 2008 2009 2010 2011 2012 2013 2014 2015
SPI3-ERA
SPEI3-ERA
NDVI

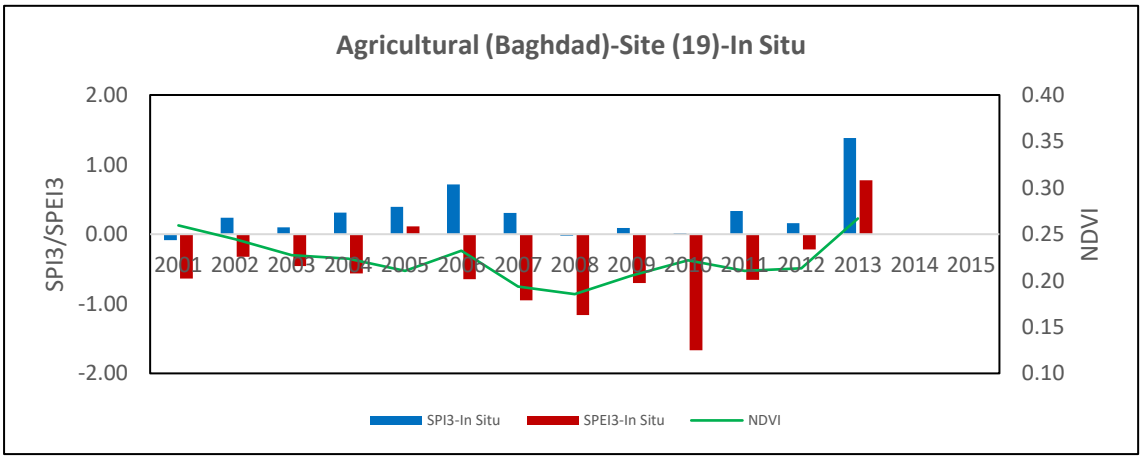
Agricultural (Baghdad)-Site (19)-In Situ
SPI3/SPEI3
NDVI
2.00
1.00
0.00
-1.00
-2.00
0.40
0.35
0.30
0.25
0.20
0.15
0.10
2001 2002 2003 2004 2005 2006 2007 2008 2009 2010 2011 2012 2013 2014 2015
SPI3-In Situ
SPEI3-In Situ
NDVI

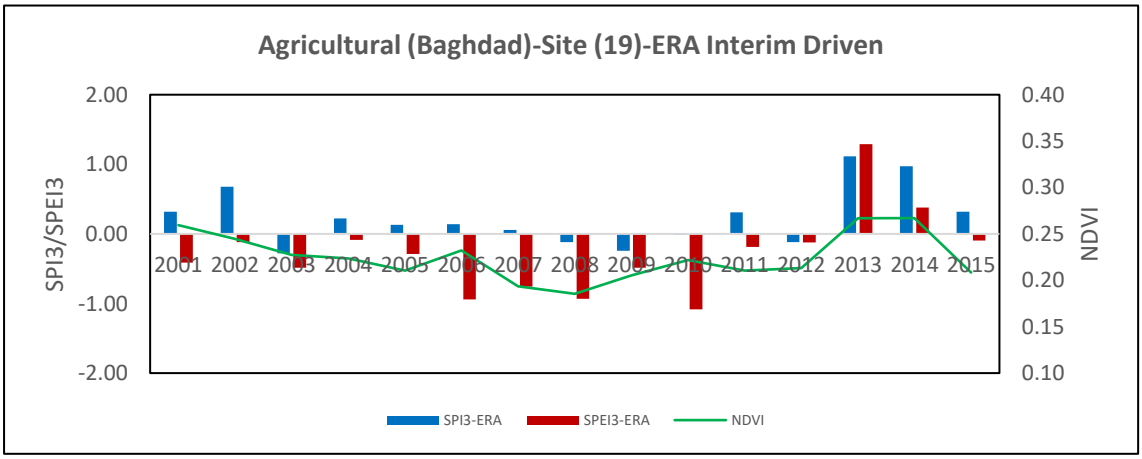
Agricultural (Baghdad)-Site (19)-ERA Interim Driven
SPI3/SPEI3
NDVI
2.00
1.00
0.00
-1.00
-2.00
0.40
0.35
0.30
0.25
0.20
0.15
0.10
2001 2002 2003 2004 2005 2006 2007 2008 2009 2010 2011 2012 2013 2014 2015
SPI3-ERA
SPEI3-ERA
NDVI

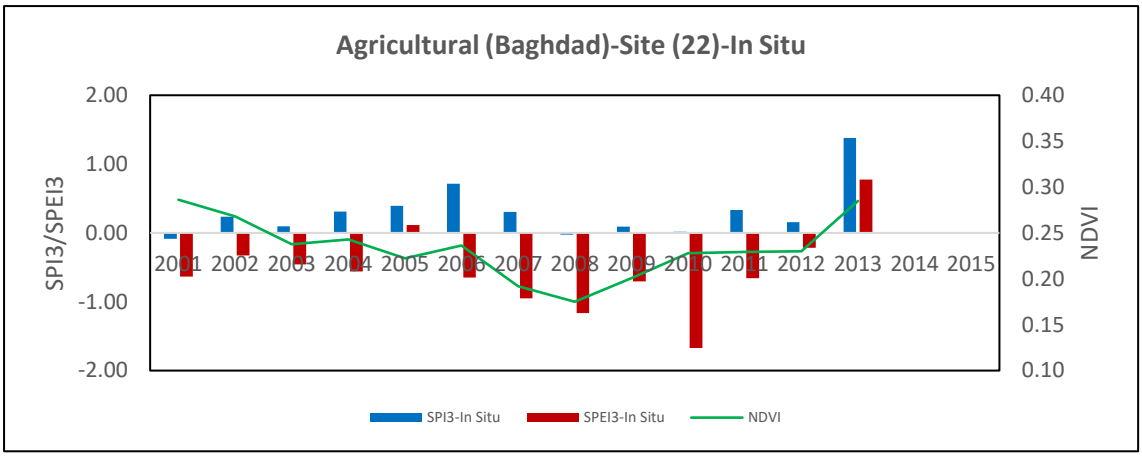
Agricultural (Baghdad)-Site (22)-In Situ
SPI3/SPEI3
NDVI
2.00
1.00
0.00
-1.00
-2.00
0.40
0.35
0.30
0.25
0.20
0.15
0.10
2001 2002 2003 2004 2005 2006 2007 2008 2009 2010 2011 2012 2013 2014 2015
SPI3-In Situ
SPEI3-In Situ
NDVI

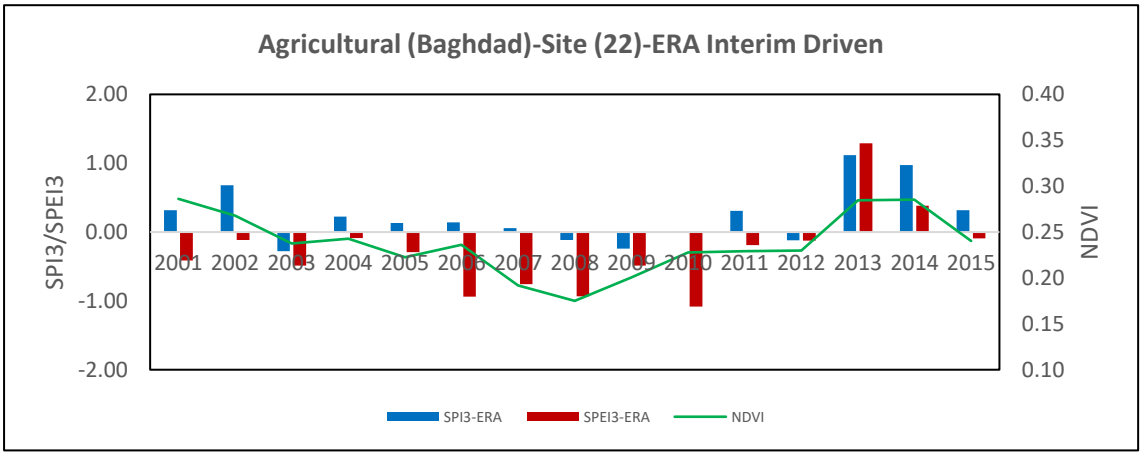
Agricultural (Baghdad)-Site (22)-ERA Interim Driven
SPI3/SPEI3
NDVI
2.00
1.00
0.00
-1.00
-2.00
0.40
0.35
0.30
0.25
0.20
0.15
0.10
2001 2002 2003 2004 2005 2006 2007 2008 2009 2010 2011 2012 2013 2014 2015
SPI3-ERA
SPEI3-ERA
NDVI

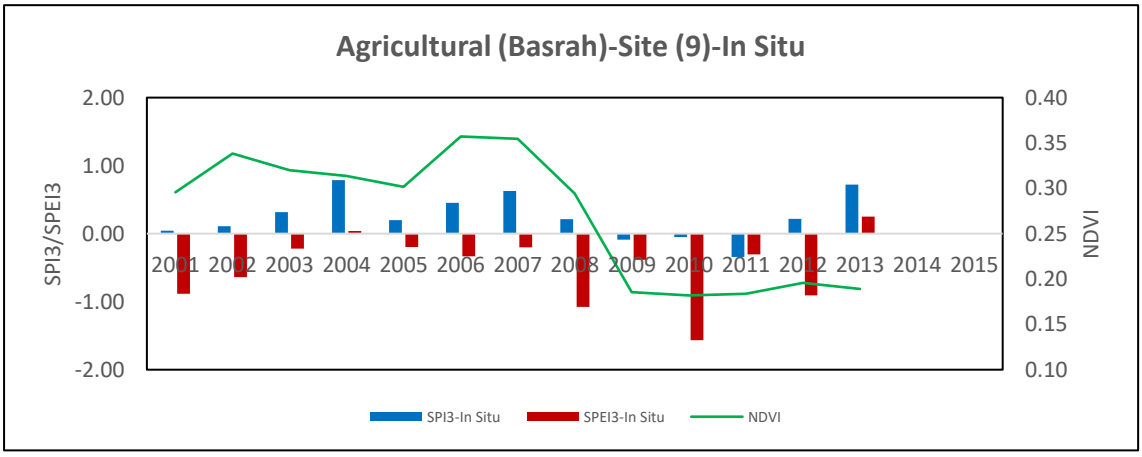
Agricultural (Basrah)-Site (9)-In Situ
SPI3/SPEI3
NDVI
2.00
1.00
0.00
-1.00
-2.00
0.40
0.35
0.30
0.25
0.20
0.15
0.10
2001 2002 2003 2004 2005 2006 2007 2008 2009 2010 2011 2012 2013 2014 2015
SPI3-In Situ
SPEI3-In Situ
NDVI

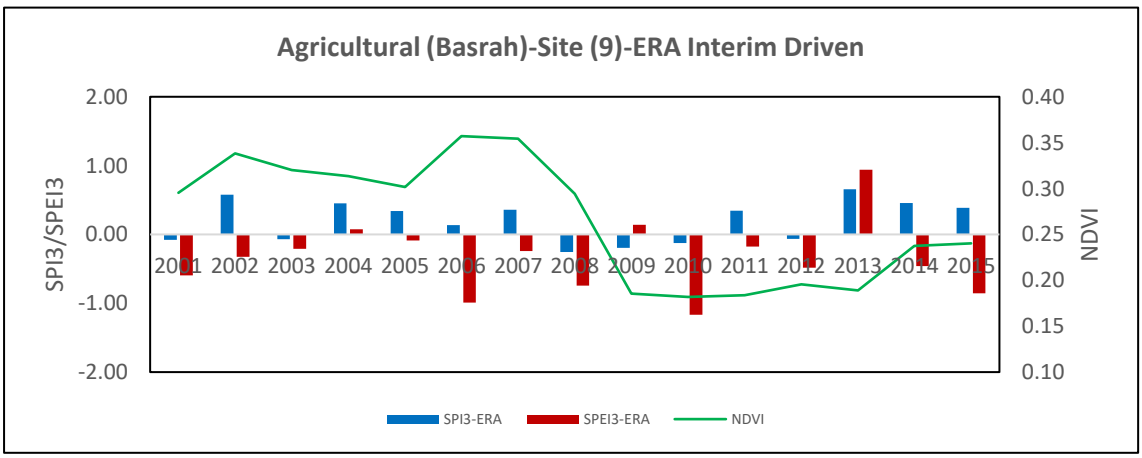
Agricultural (Basrah)-Site (9)-ERA Interim Driven
SPI3/SPEI3
NDVI
2.00
1.00
0.00
-1.00
-2.00
0.40
0.35
0.30
0.25
0.20
0.15
0.10
2001 2002 2003 2004 2005 2006 2007 2008 2009 2010 2011 2012 2013 2014 2015
SPI3-ERA
SPEI3-ERA
NDVI

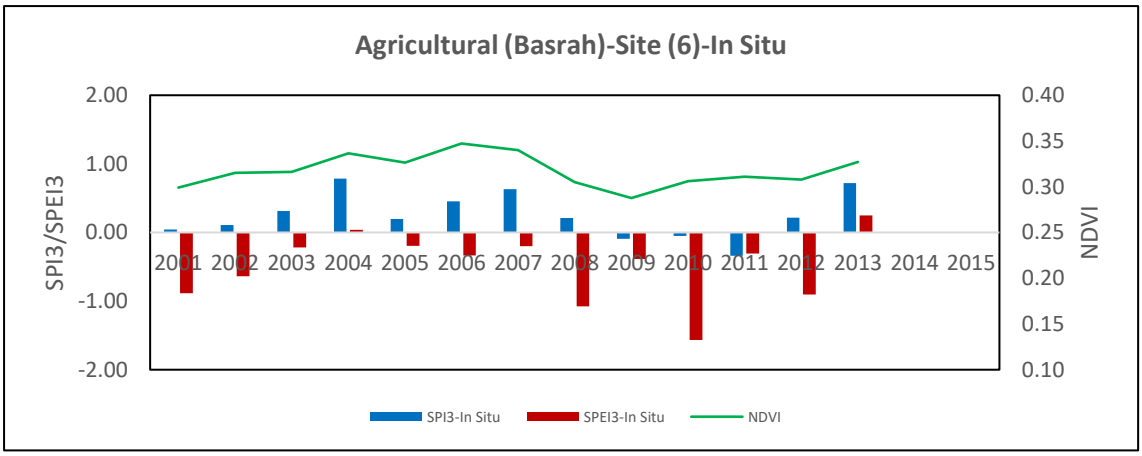
Agricultural (Basrah)-Site (6)-In Situ
SPI3/SPEI3
NDVI
2.00
1.00
0.00
-1.00
-2.00
0.40
0.35
0.30
0.25
0.20
0.15
0.10
2001 2002 2003 2004 2005 2006 2007 2008 2009 2010 2011 2012 2013 2014 2015
SPI3-In Situ
SPEI3-In Situ
NDVI

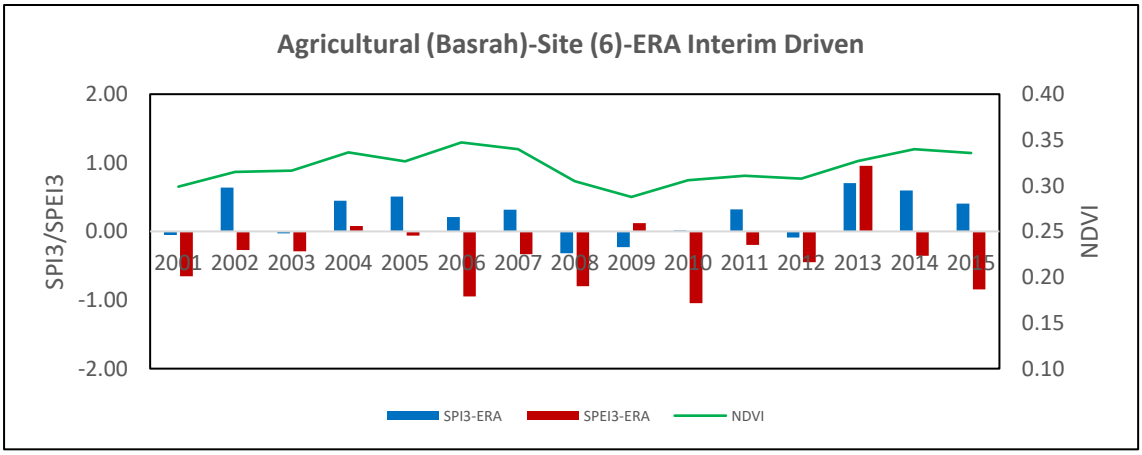
Agricultural (Basrah)-Site (6)-ERA Interim Driven
SPI3/SPEI3
NDVI
2.00
1.00
0.00
-1.00
-2.00
0.40
0.35
0.30
0.25
0.20
0.15
0.10
2001 2002 2003 2004 2005 2006 2007 2008 2009 2010 2011 2012 2013 2014 2015
SPI3-ERA
SPEI3-ERA
NDVI

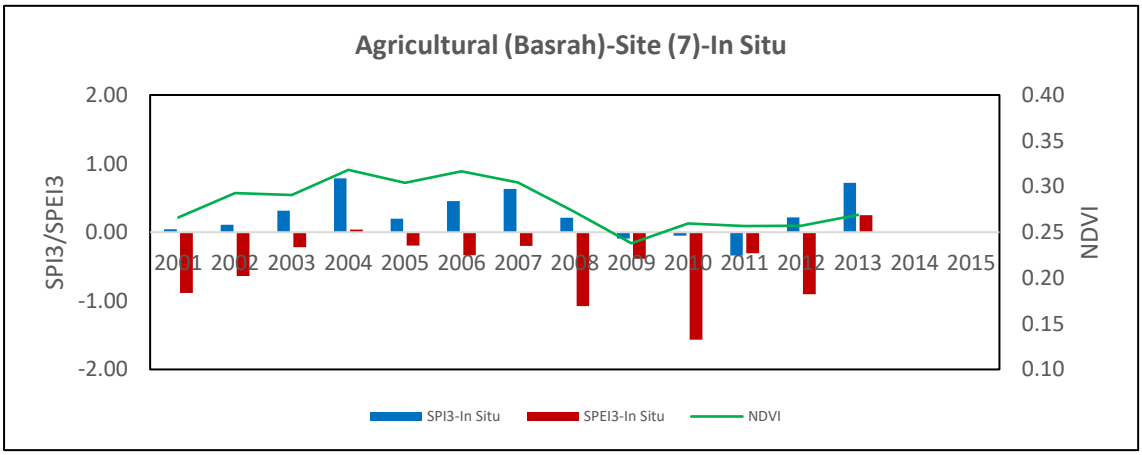
Agricultural (Basrah)-Site (7)-In Situ
SPI3/SPEI3
NDVI
2.00
1.00
0.00
-1.00
-2.00
0.40
0.35
0.30
0.25
0.20
0.15
0.10
2001 2002 2003 2004 2005 2006 2007 2008 2009 2010 2011 2012 2013 2014 2015
SPI3-In Situ
SPEI3-In Situ
NDVI

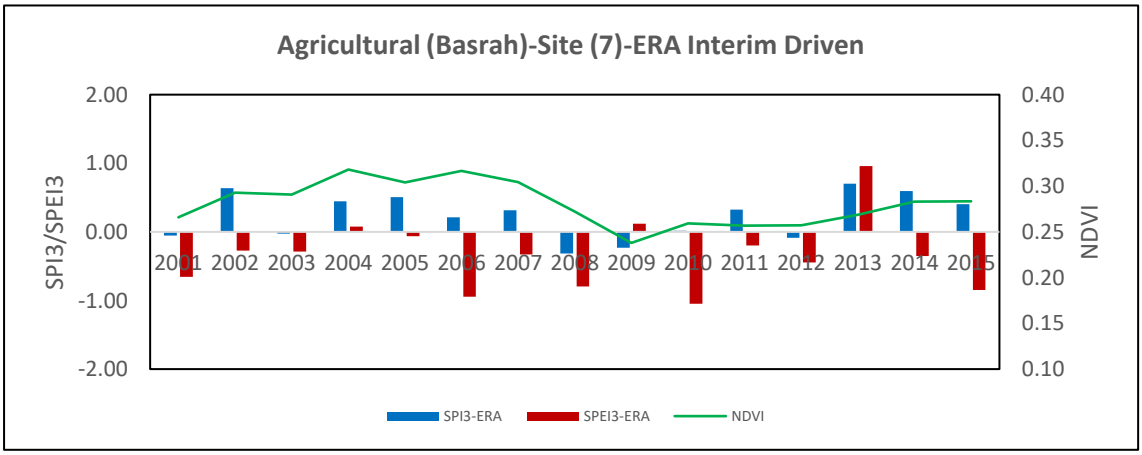
Agricultural (Basrah)-Site (7)-ERA Interim Driven
SPI3/SPEI3
NDVI
2.00
1.00
0.00
-1.00
-2.00
0.40
0.35
0.30
0.25
0.20
0.15
0.10
2001 2002 2003 2004 2005 2006 2007 2008 2009 2010 2011 2012 2013 2014 2015
SPI3-ERA
SPEI3-ERA
NDVI

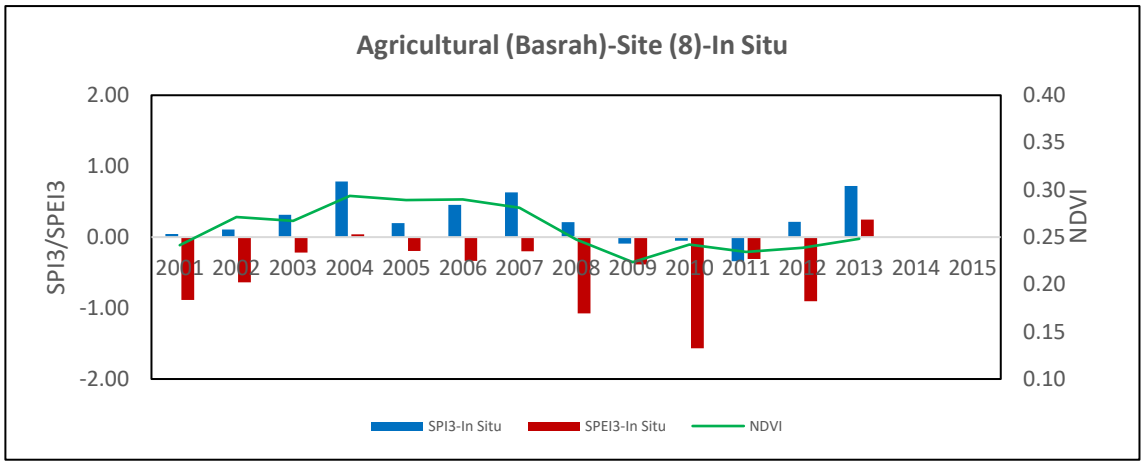
Agricultural (Basrah)-Site (8)-In Situ
SPI3/SPEI3
NDVI
2.00
1.00
0.00
-1.00
-2.00
0.40
0.35
0.30
0.25
0.20
0.15
0.10
2001 2002 2003 2004 2005 2006 2007 2008 2009 2010 2011 2012 2013 2014 2015
SPI3-In Situ
SPEI3-In Situ
NDVI

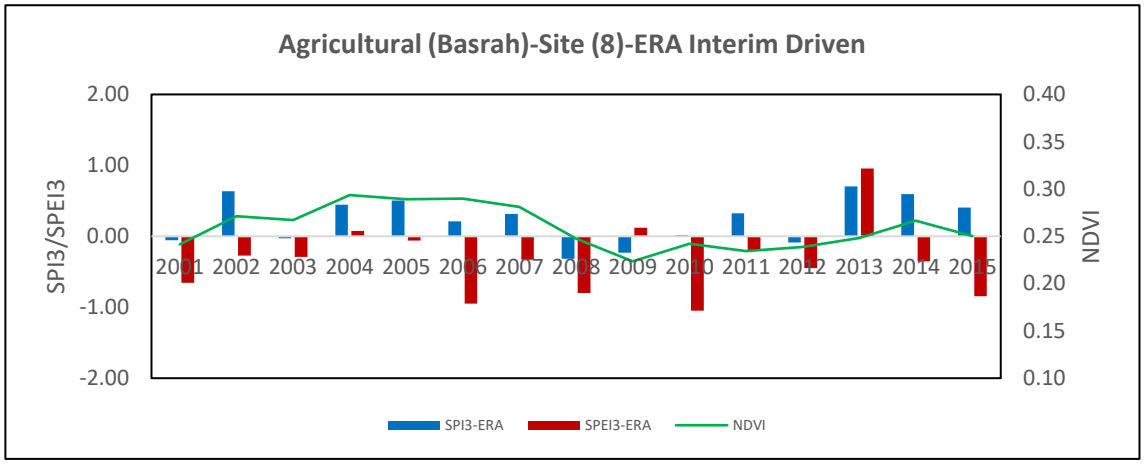
Agricultural (Basrah)-Site (8)-ERA Interim Driven
SPI3/SPEI3
NDVI
2.00
1.00
0.00
-1.00
-2.00
0.40
0.35
0.30
0.25
0.20
0.15
0.10
2001 2002 2003 2004 2005 2006 2007 2008 2009 2010 2011 2012 2013 2014 2015
SPI3-ERA
SPEI3-ERA
NDVI

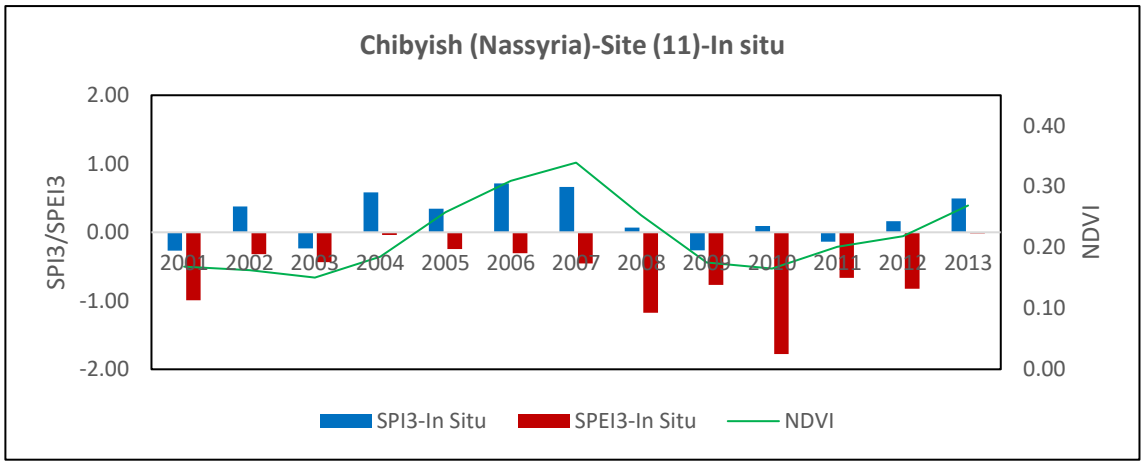
Chibyish (Nassyria)-Site (11)-In situ
SPI3/SPEI3
NDVI
2.00
1.00
0.00
-1.00
-2.00
0.40
0.30
0.20
0.10
0.00
2001 2002 2003 2004 2005 2006 2007 2008 2009 2010 2011 2012 2013
SPI3-In Situ
SPEI3-In Situ
NDVI

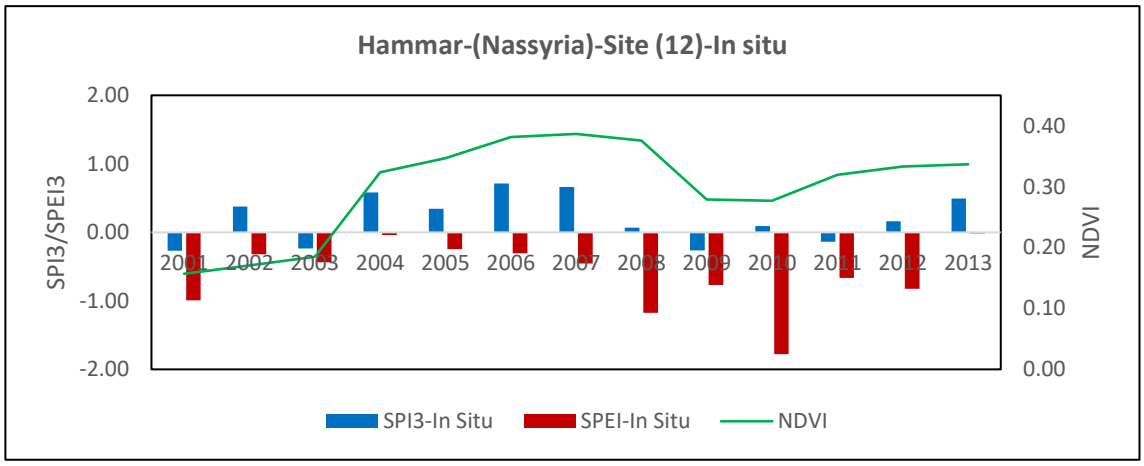
Hammar-(Nassyria)-Site (12)-In situ
SPI3/SPEI3
NDVI
2.00
1.00
0.00
-1.00
-2.00
0.40
0.30
0.20
0.10
0.00
2001 2002 2003 2004 2005 2006 2007 2008 2009 2010 2011 2012 2013
SPI3-In Situ
SPEI-In Situ
NDVI

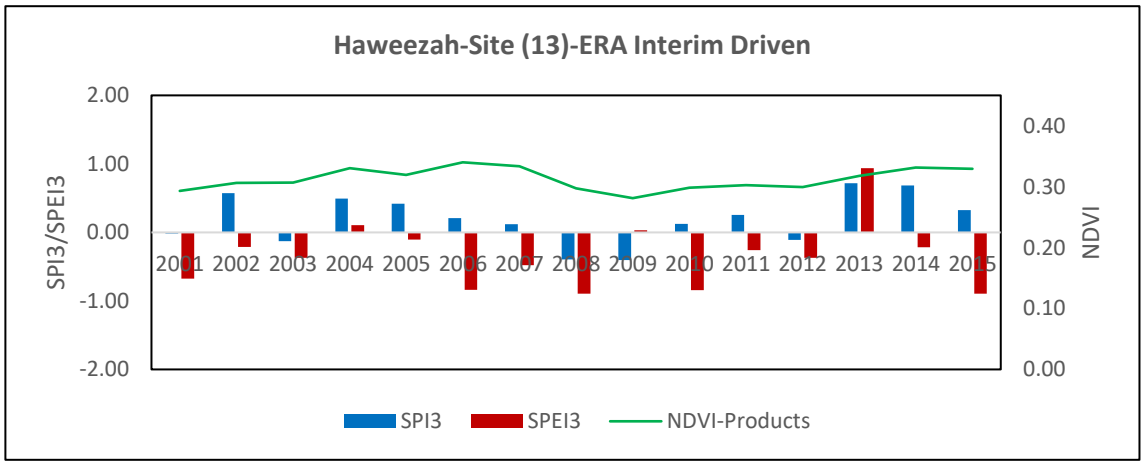
Haweezah-Site (13)-ERA Interim Driven
SPI3/SPEI3
NDVI
2.00
1.00
0.00
-1.00
-2.00
0.40
0.30
0.20
0.10
0.00
2001 2002 2003 2004 2005 2006 2007 2008 2009 2010 2011 2012 2013 2014 2015
SPI3
SPEI3
NDVI-Products

APPENDIX B: Spatiotemporal seasonal and interannual variation in the NDVI for three surface types in Iraq during 2001–2015.

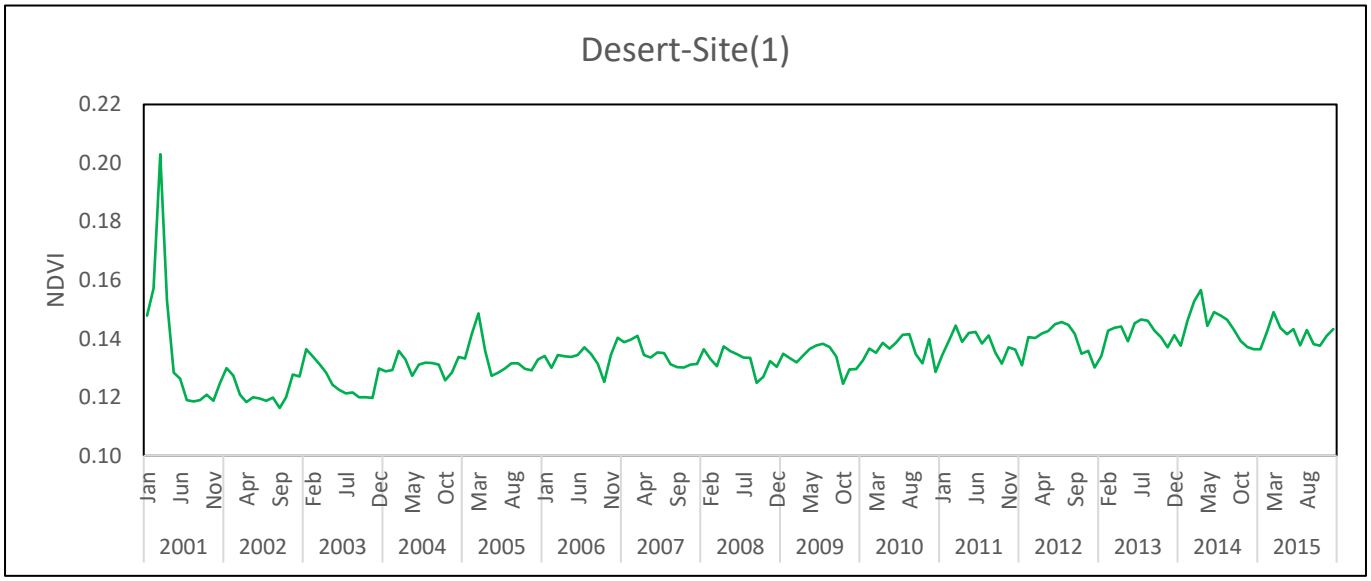

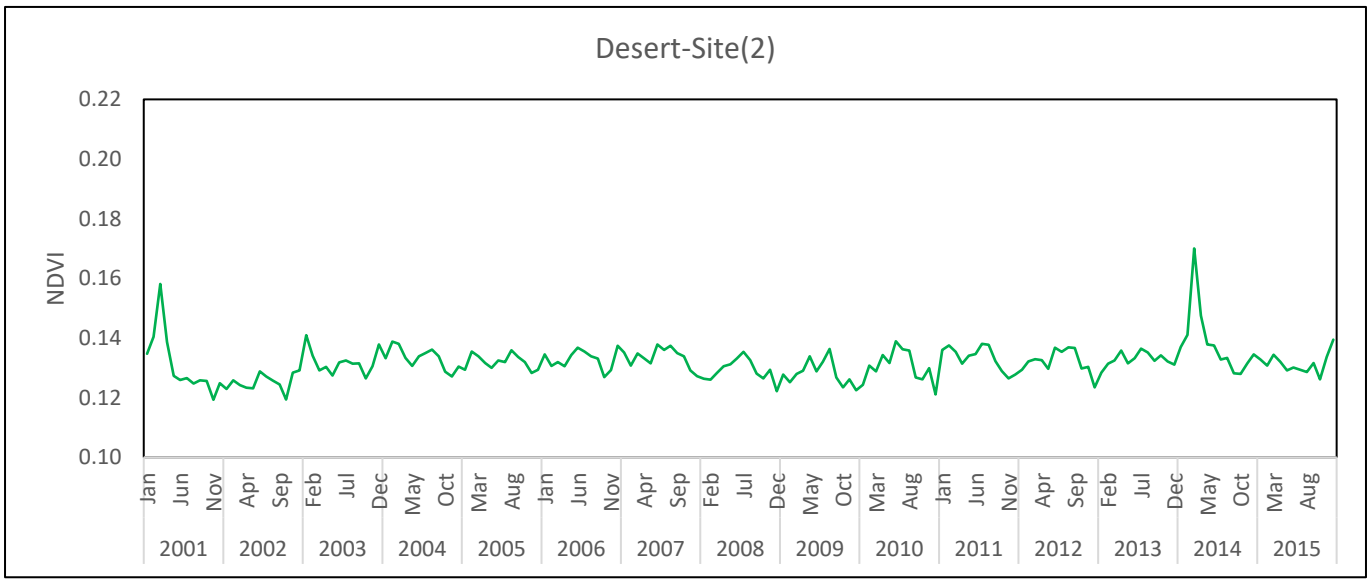

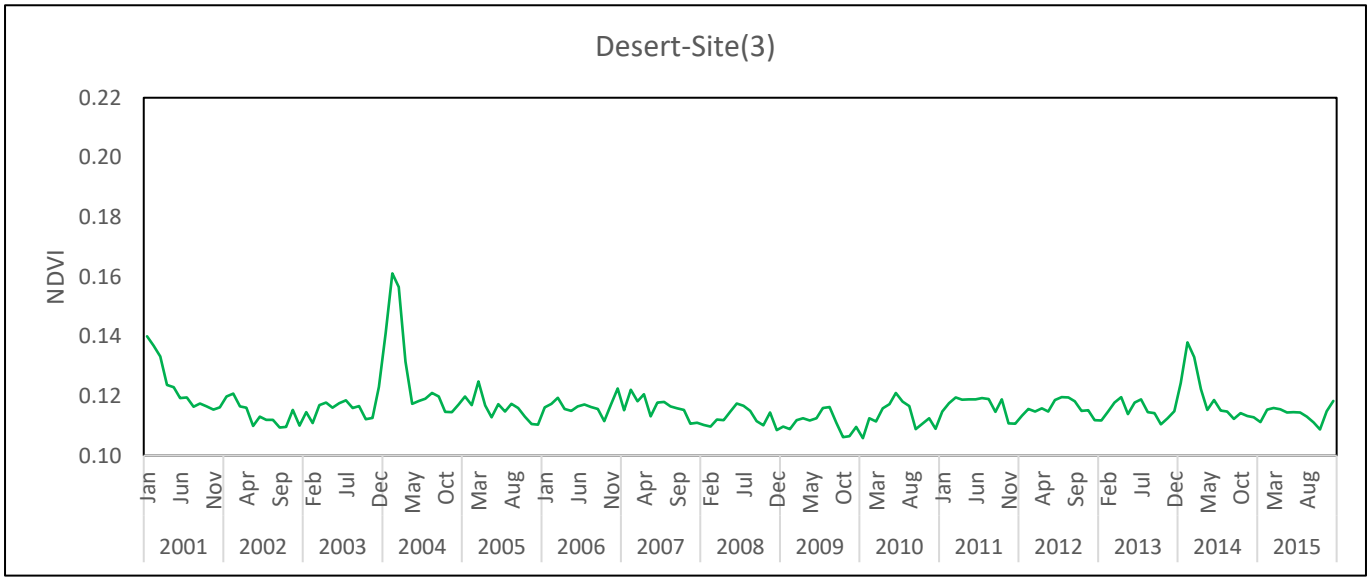

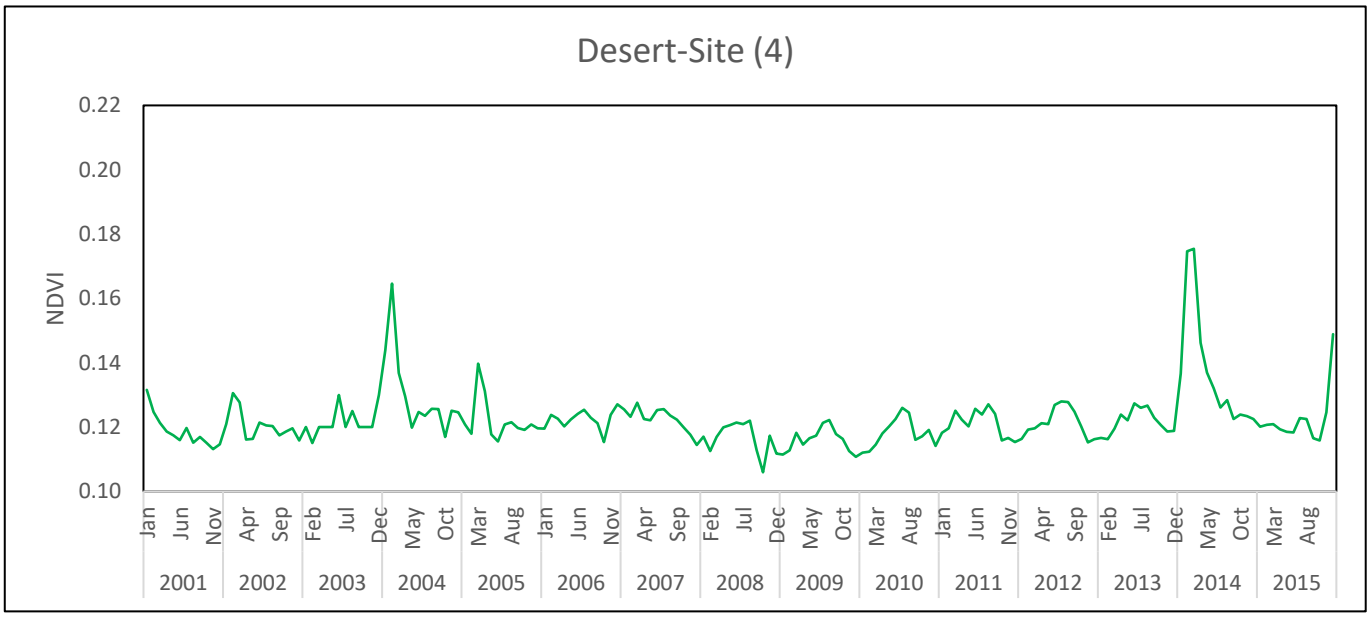
Desert-Site (4)
NDVI
0.22
0.20
0.18
0.16
0.14
0.12
0.10
Jan Jun Nov Apr Sep Feb Jul Dec May Oct Mar Aug Jan Jun Nov Apr Sep Feb Jul Dec May Oct Mar Aug Jan Jun Nov Apr Sep Feb Jul Dec May Oct Mar Aug Jan Jun Nov Apr Sep Feb Jul Dec May Oct Mar Aug
2001 2002 2003 2004 2005 2006 2007 2008 2009 2010 2011 2012 2013 2014 2015

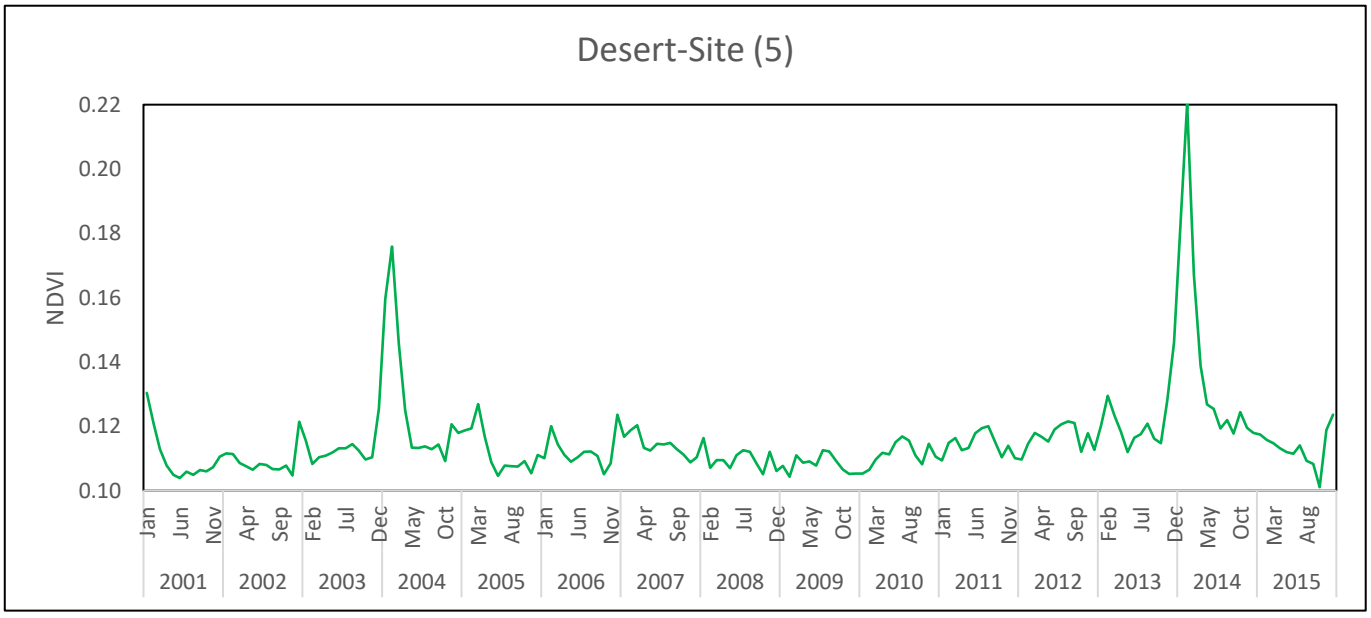
Desert-Site (5)
NDVI
0.22
0.20
0.18
0.16
0.14
0.12
0.10
Jan Jun Nov Apr Sep Feb Jul Dec May Oct Mar Aug Jan Jun Nov Apr Sep Feb Jul Dec May Oct Mar Aug Jan Jun Nov Apr Sep Feb Jul Dec May Oct Mar Aug Jan Jun Nov Apr Sep Feb Jul Dec May Oct Mar Aug
2001 2002 2003 2004 2005 2006 2007 2008 2009 2010 2011 2012 2013 2014 2015

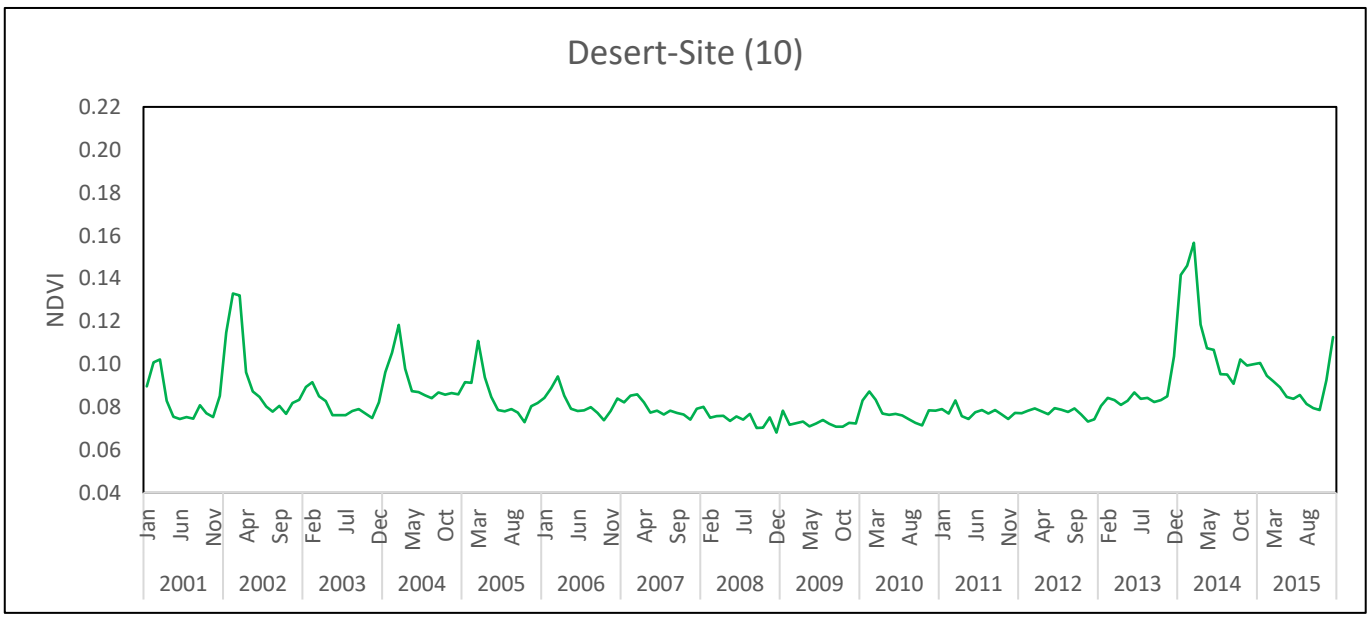
Desert-Site (10)
NDVI
0.22
0.20
0.18
0.16
0.14
0.12
0.10
0.08
0.06
0.04
Jan Jun Nov Apr Sep Feb Jul Dec May Oct Mar Aug Jan Jun Nov Apr Sep Feb Jul Dec May Oct Mar Aug Jan Jun Nov Apr Sep Feb Jul Dec May Oct Mar Aug Jan Jun Nov Apr Sep Feb Jul Dec May Oct Mar Aug
2001 2002 2003 2004 2005 2006 2007 2008 2009 2010 2011 2012 2013 2014 2015

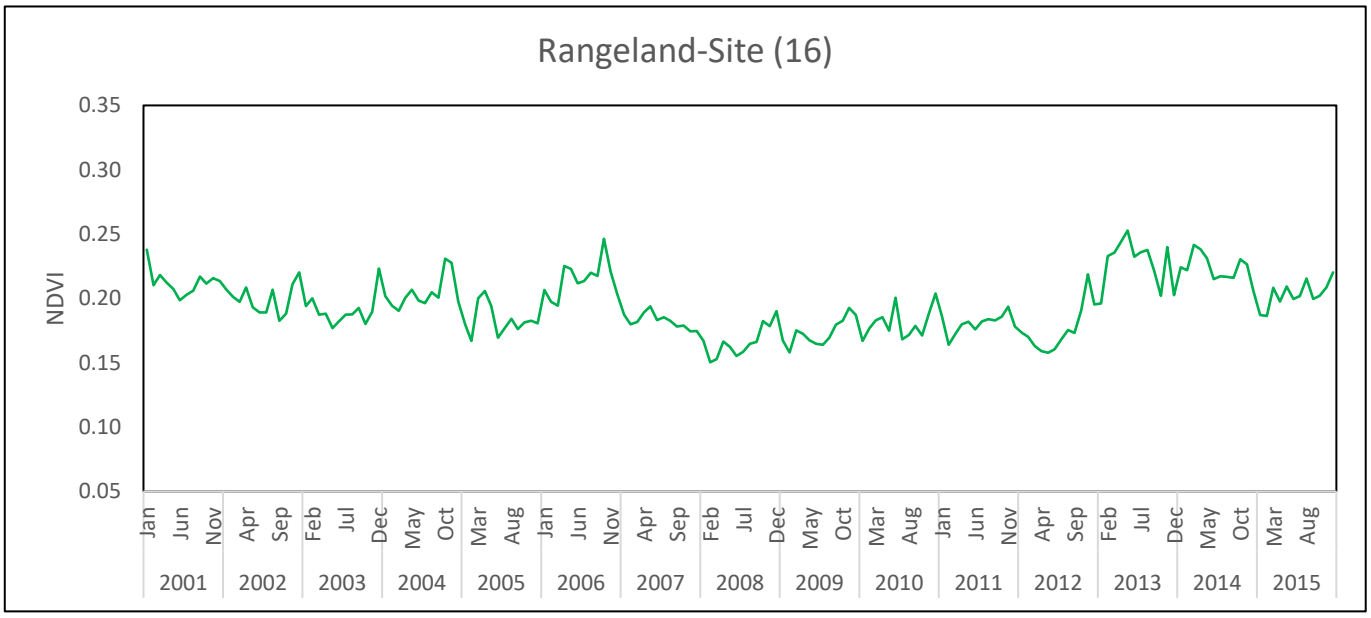
Rangeland-Site (16)
NDVI
0.35
0.30
0.25
0.20
0.15
0.10
0.05
Jan Jun Nov Apr Sep Feb Jul Dec May Oct Mar Aug Jan Jun Nov Apr Sep Feb Jul Dec May Oct Mar Aug Jan Jun Nov Apr Sep Feb Jul Dec May Oct Mar Aug Jan Jun Nov Apr Sep Feb Jul Dec May Oct Mar Aug
2001 2002 2003 2004 2005 2006 2007 2008 2009 2010 2011 2012 2013 2014 2015

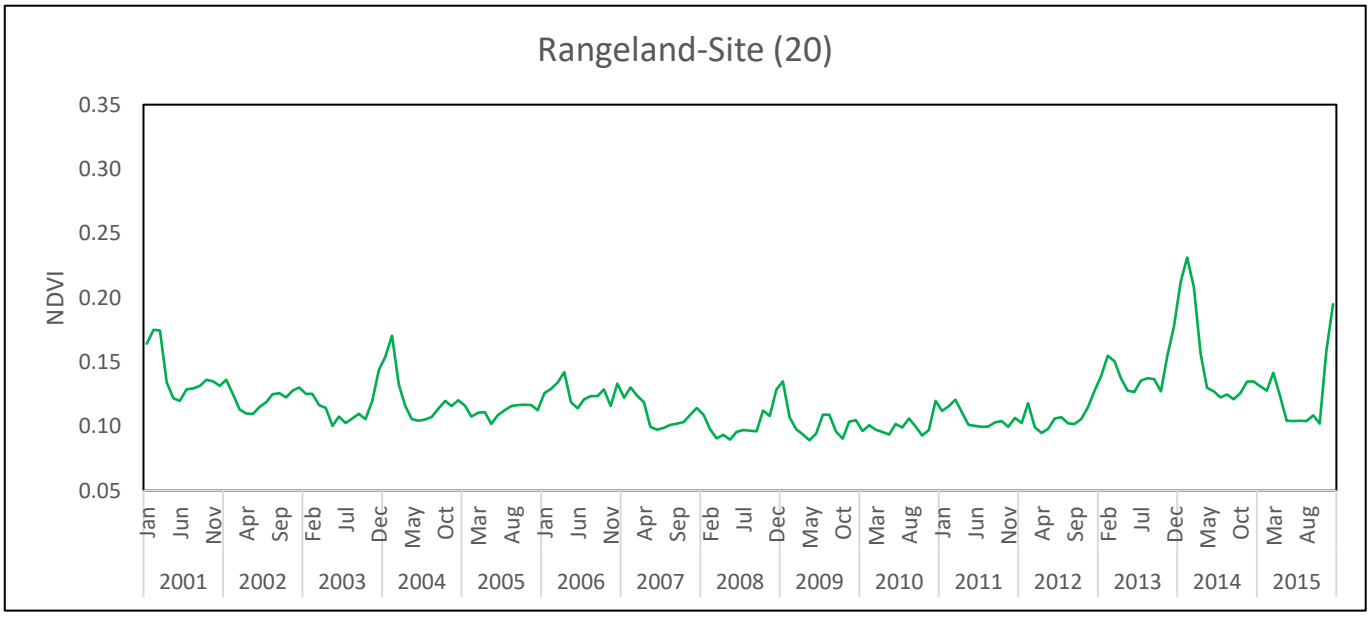
Rangeland-Site (20)
NDVI
0.35
0.30
0.25
0.20
0.15
0.10
0.05
Jan Jun Nov Apr Sep Feb Jul Dec May Oct Mar Aug Jan Jun Nov Apr Sep Feb Jul Dec May Oct Mar Aug Jan Jun Nov Apr Sep Feb Jul Dec May Oct Mar Aug Jan Jun Nov Apr Sep Feb Jul Dec May Oct Mar Aug
2001 2002 2003 2004 2005 2006 2007 2008 2009 2010 2011 2012 2013 2014 2015

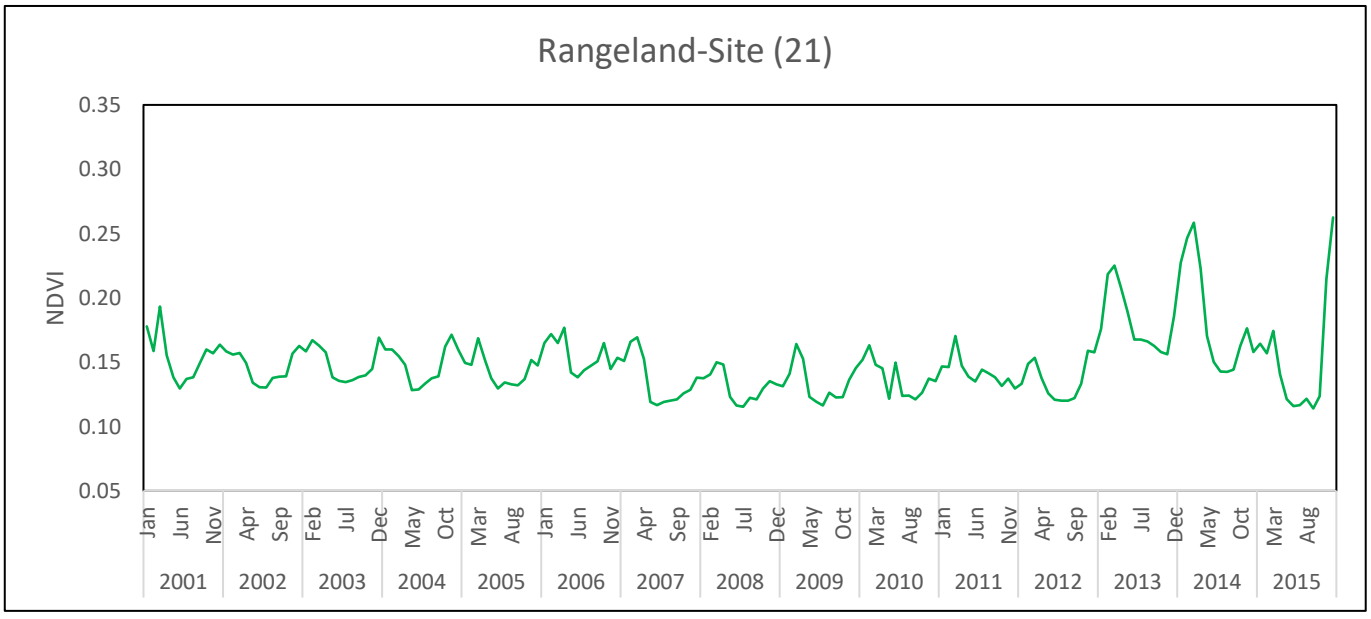
Rangeland-Site (21)
NDVI
0.35
0.30
0.25
0.20
0.15
0.10
0.05
Jan Jun Nov Apr Sep Feb Jul Dec May Oct Mar Aug Jan Jun Nov Apr Sep Feb Jul Dec May Oct Mar Aug Jan Jun Nov Apr Sep Feb Jul Dec May Oct Mar Aug Jan Jun Nov Apr Sep Feb Jul Dec May Oct Mar Aug
2001 2002 2003 2004 2005 2006 2007 2008 2009 2010 2011 2012 2013 2014 2015

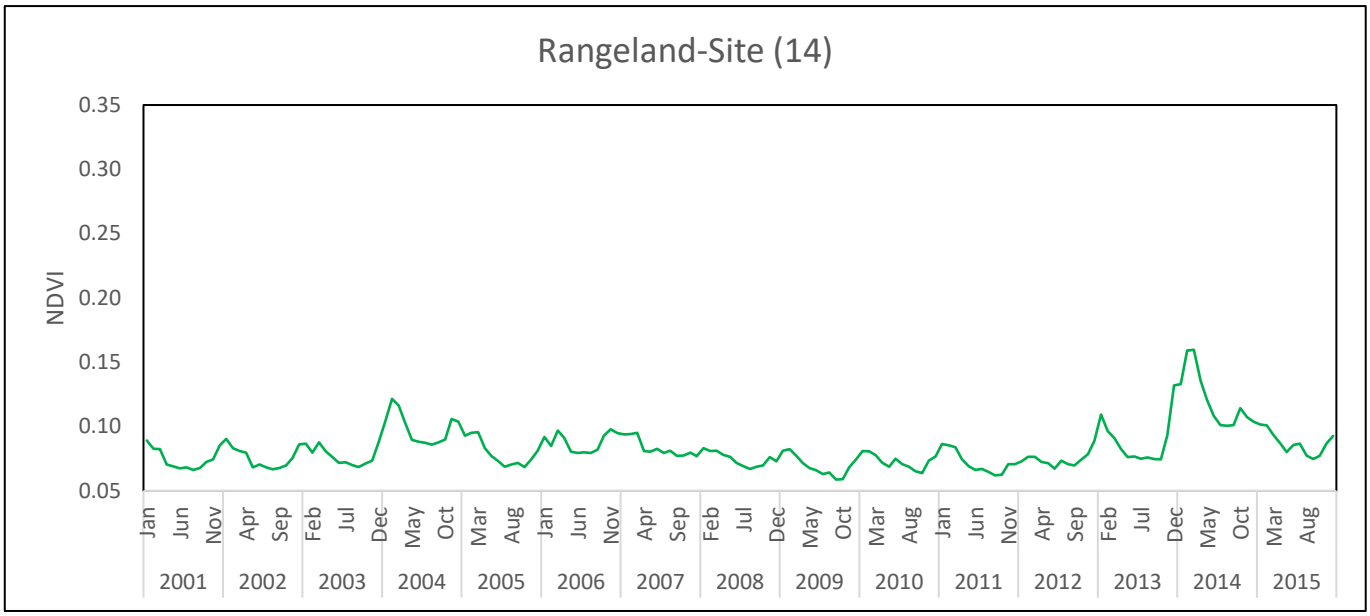
Rangeland-Site (14)
NDVI
0.35
0.30
0.25
0.20
0.15
0.10
0.05
Jan Jun Nov Apr Sep Feb Jul Dec May Oct Mar Aug Jan Jun Nov Apr Sep Feb Jul Dec May Oct Mar Aug Jan Jun Nov Apr Sep Feb Jul Dec May Oct Mar Aug Jan Jun Nov Apr Sep Feb Jul Dec May Oct Mar Aug
2001 2002 2003 2004 2005 2006 2007 2008 2009 2010 2011 2012 2013 2014 2015

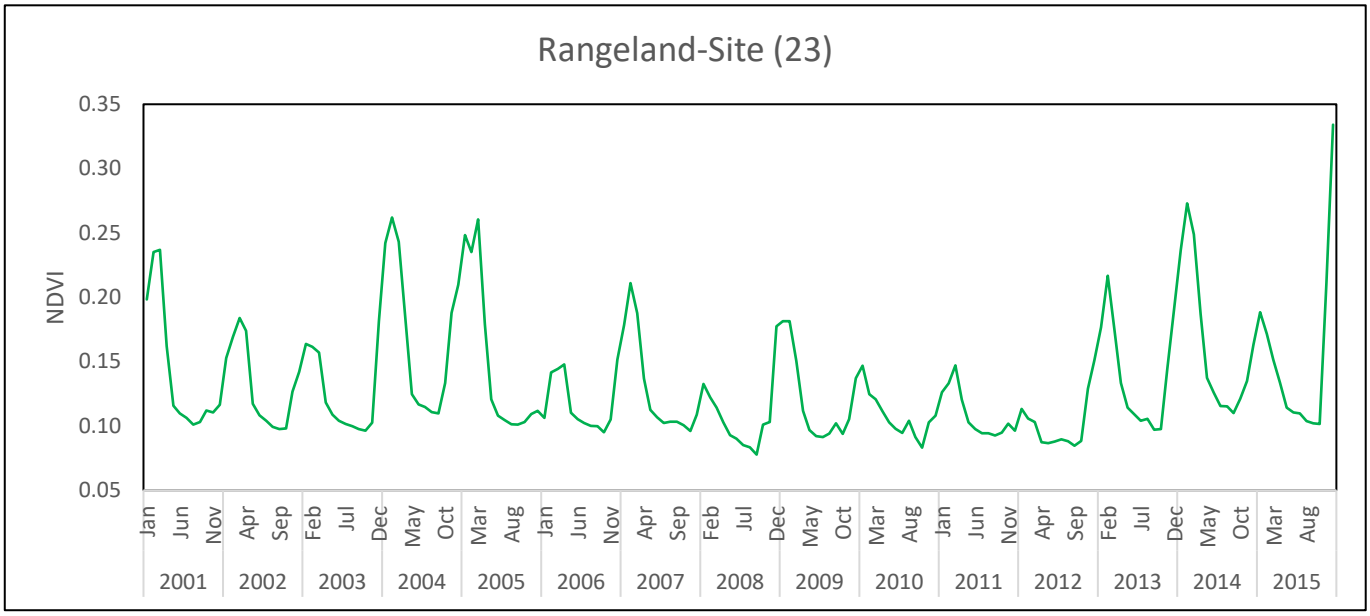
Rangeland-Site (23)
NDVI
0.35
0.30
0.25
0.20
0.15
0.10
0.05
Jan Jun Nov Apr Sep Feb Jul Dec May Oct Mar Aug Jan Jun Nov Apr Sep Feb Jul Dec May Oct Mar Aug Jan Jun Nov Apr Sep Feb Jul Dec May Oct Mar Aug Jan Jun Nov Apr Sep Feb Jul Dec May Oct Mar Aug
2001 2002 2003 2004 2005 2006 2007 2008 2009 2010 2011 2012 2013 2014 2015

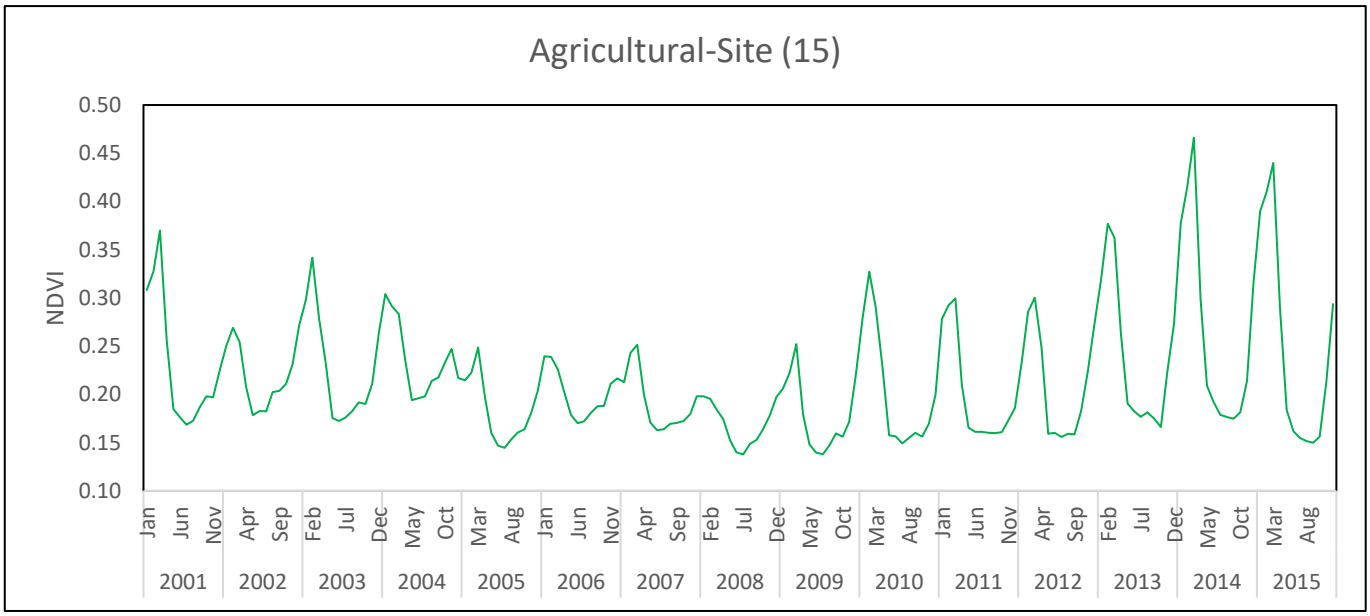
Agricultural-Site (15)
NDVI
0.50
0.45
0.40
0.35
0.30
0.25
0.20
0.15
0.10
Jan Jun Nov Apr Sep Feb Jul Dec May Oct Mar Aug
2001 2002 2003 2004 2005 2006 2007 2008 2009 2010 2011 2012 2013 2014 2015

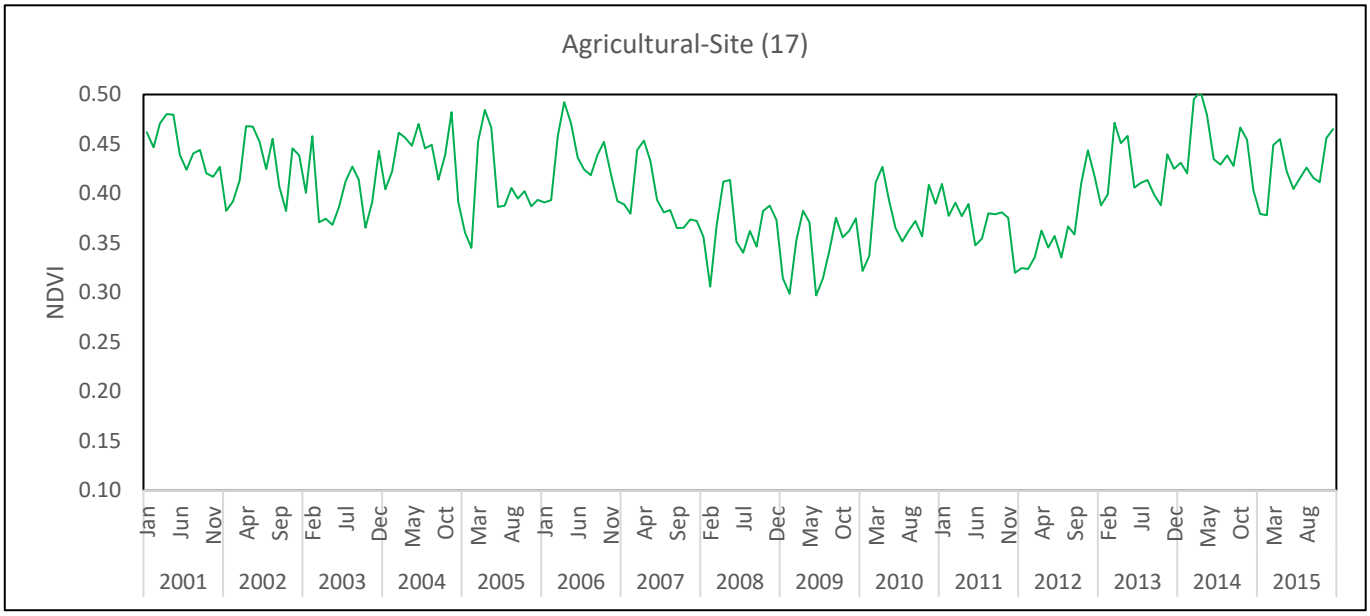
Agricultural-Site (17)
NDVI
0.50
0.45
0.40
0.35
0.30
0.25
0.20
0.15
0.10
Jan Jun Nov Apr Sep Feb Jul Dec May Oct Mar Aug
2001 2002 2003 2004 2005 2006 2007 2008 2009 2010 2011 2012 2013 2014 2015

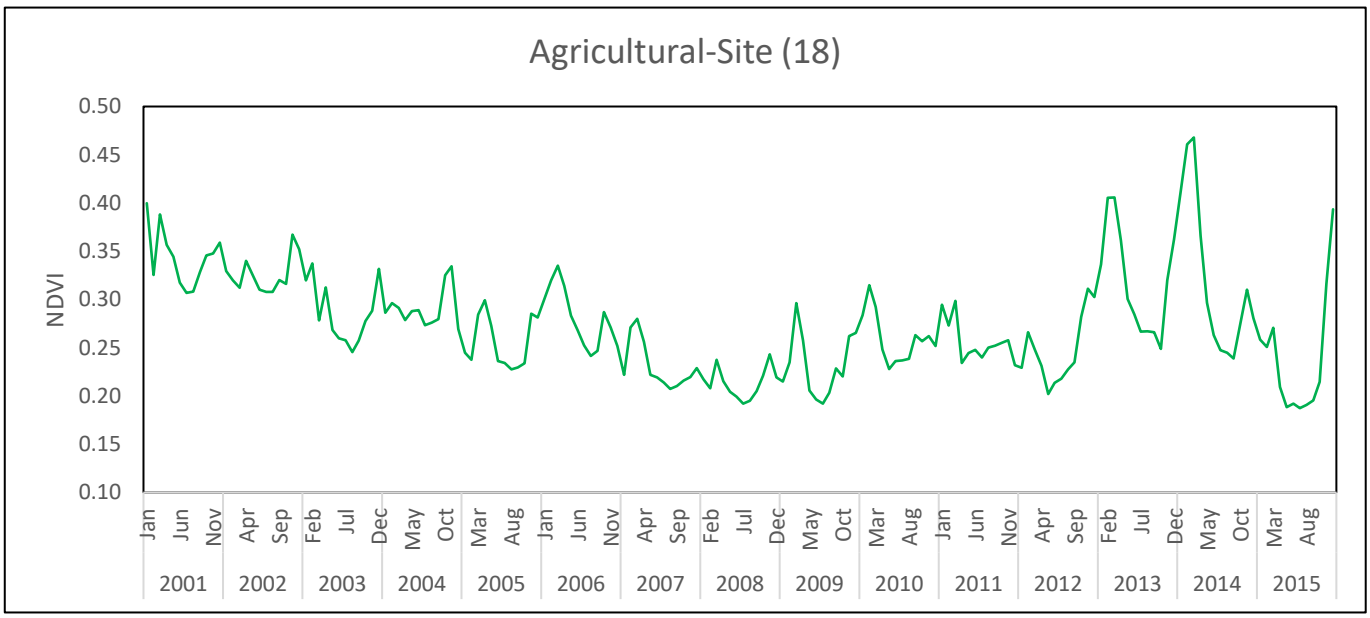
Agricultural-Site (18)
NDVI
0.50
0.45
0.40
0.35
0.30
0.25
0.20
0.15
0.10
Jan Jun Nov Apr Sep Feb Jul Dec May Oct Mar Aug
2001 2002 2003 2004 2005 2006 2007 2008 2009 2010 2011 2012 2013 2014 2015

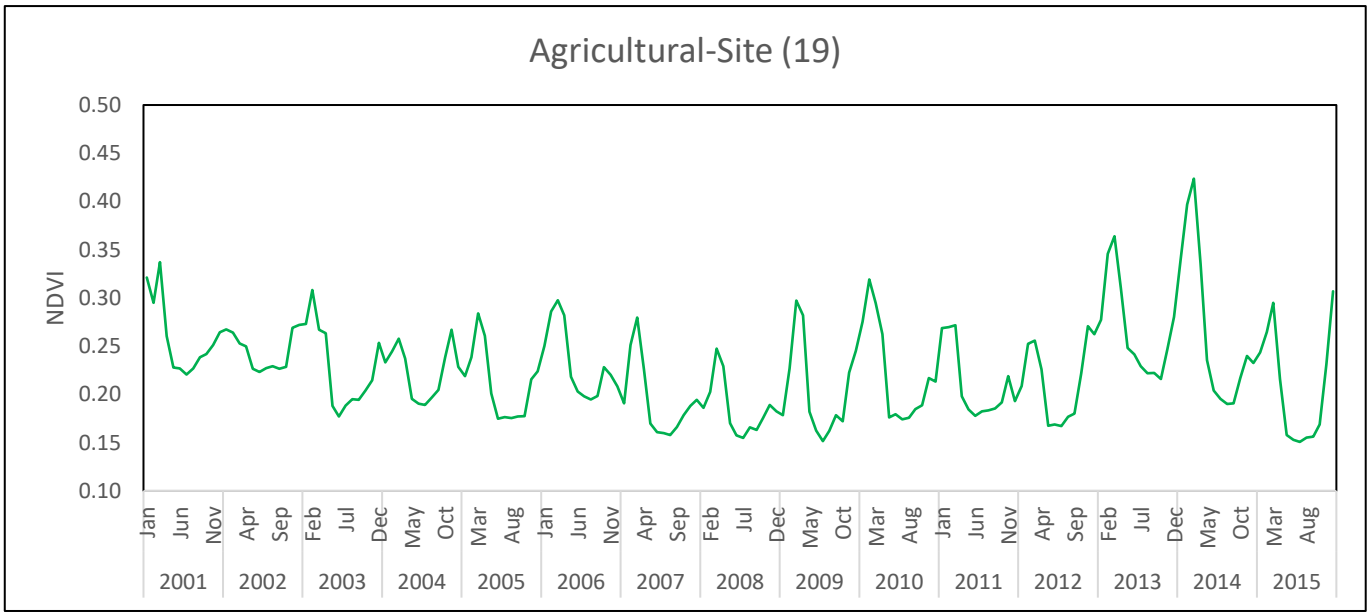
Agricultural-Site (19)
NDVI
0.50
0.45
0.40
0.35
0.30
0.25
0.20
0.15
0.10
Jan Jun Nov Apr Sep Feb Jul Dec May Oct Mar Aug Jan Jun Nov Apr Sep Feb Jul Dec May Oct Mar Aug Jan Jun Nov Apr Sep Feb Jul Dec May Oct Mar Aug
2001 2002 2003 2004 2005 2006 2007 2008 2009 2010 2011 2012 2013 2014 2015

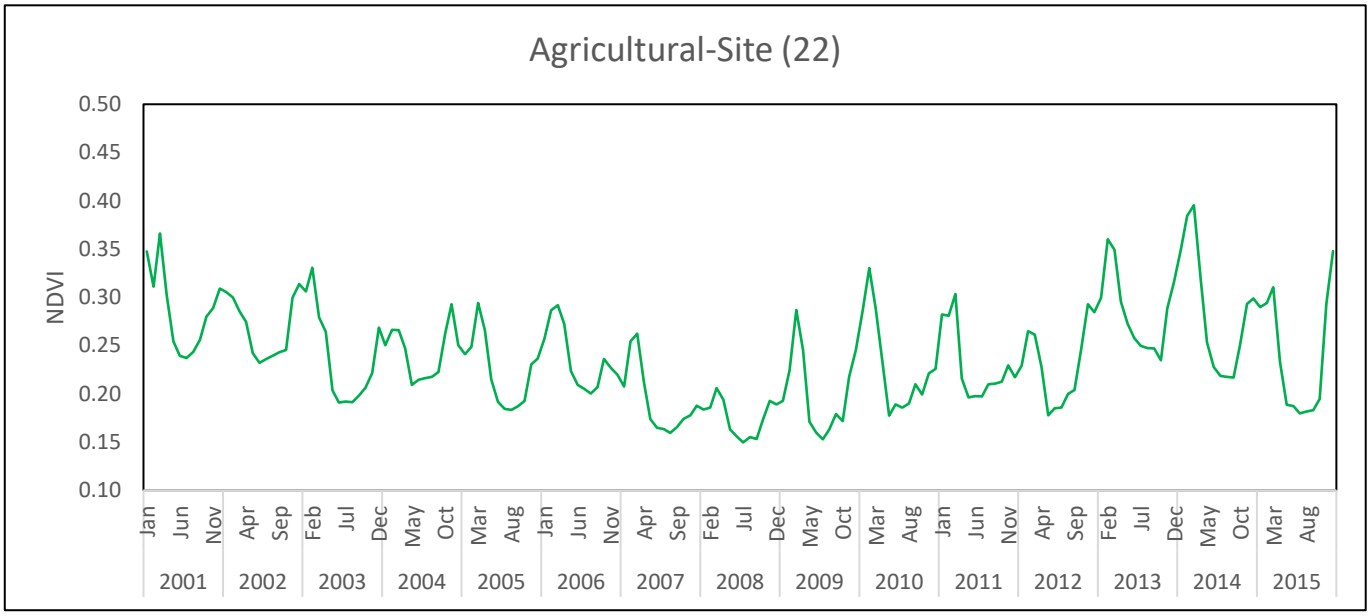
Agricultural-Site (22)
NDVI
0.50
0.45
0.40
0.35
0.30
0.25
0.20
0.15
0.10
Jan Jun Nov Apr Sep Feb Jul Dec May Oct Mar Aug Jan Jun Nov Apr Sep Feb Jul Dec May Oct Mar Aug Jan Jun Nov Apr Sep Feb Jul Dec May Oct Mar Aug
2001 2002 2003 2004 2005 2006 2007 2008 2009 2010 2011 2012 2013 2014 2015

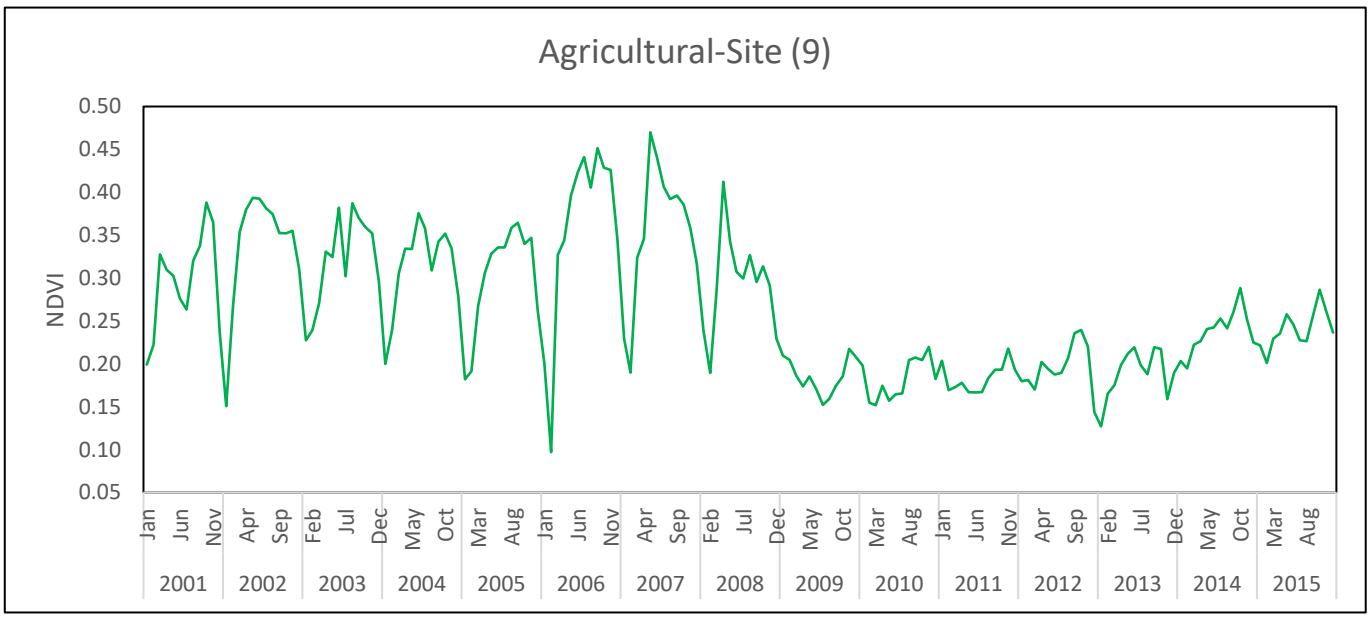
Agricultural-Site (9)
NDVI
0.50
0.45
0.40
0.35
0.30
0.25
0.20
0.15
0.10
0.05
Jan Jun Nov Apr Sep Feb Jul Dec May Oct Mar Aug Jan Jun Nov Apr Sep Feb Jul Dec May Oct Mar Aug Jan Jun Nov Apr Sep Feb Jul Dec May Oct Mar Aug
2001 2002 2003 2004 2005 2006 2007 2008 2009 2010 2011 2012 2013 2014 2015

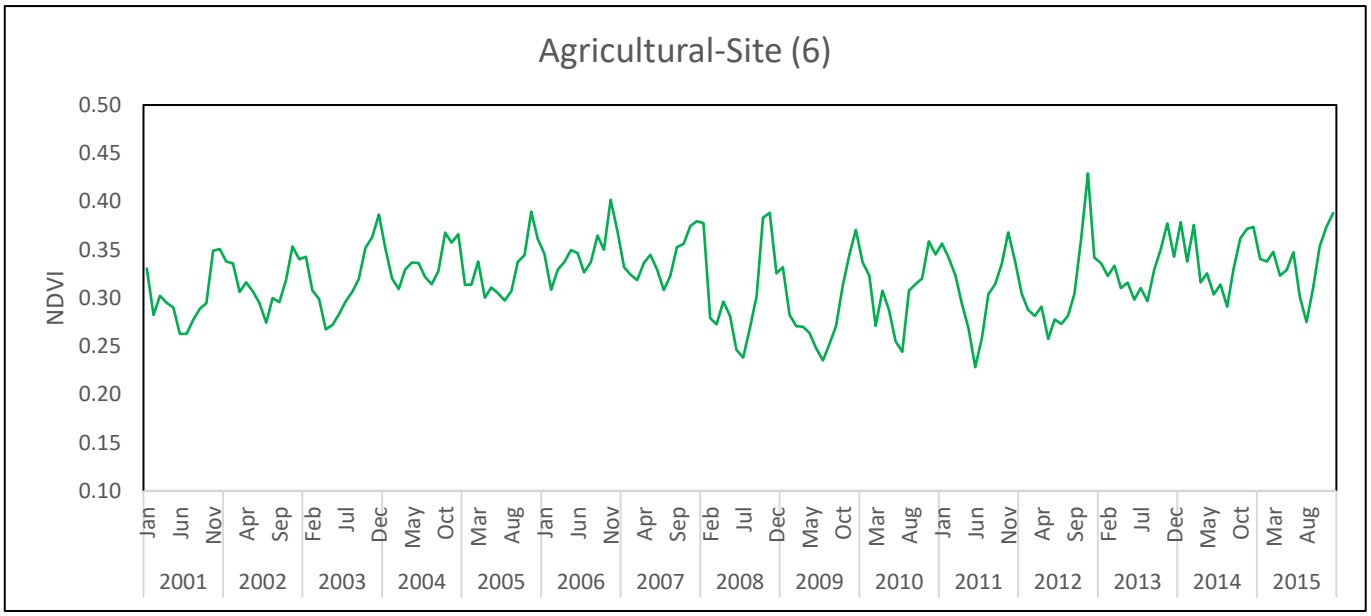
Agricultural-Site (6)
NDVI
0.50
0.45
0.40
0.35
0.30
0.25
0.20
0.15
0.10
Jan Jun Nov Apr Sep Feb Jul Dec May Oct Mar Aug Jan Jun Nov Apr Sep Feb Jul Dec May Oct Mar Aug Jan Jun Nov Apr Sep Feb Jul Dec May Oct Mar Aug
2001 2002 2003 2004 2005 2006 2007 2008 2009 2010 2011 2012 2013 2014 2015

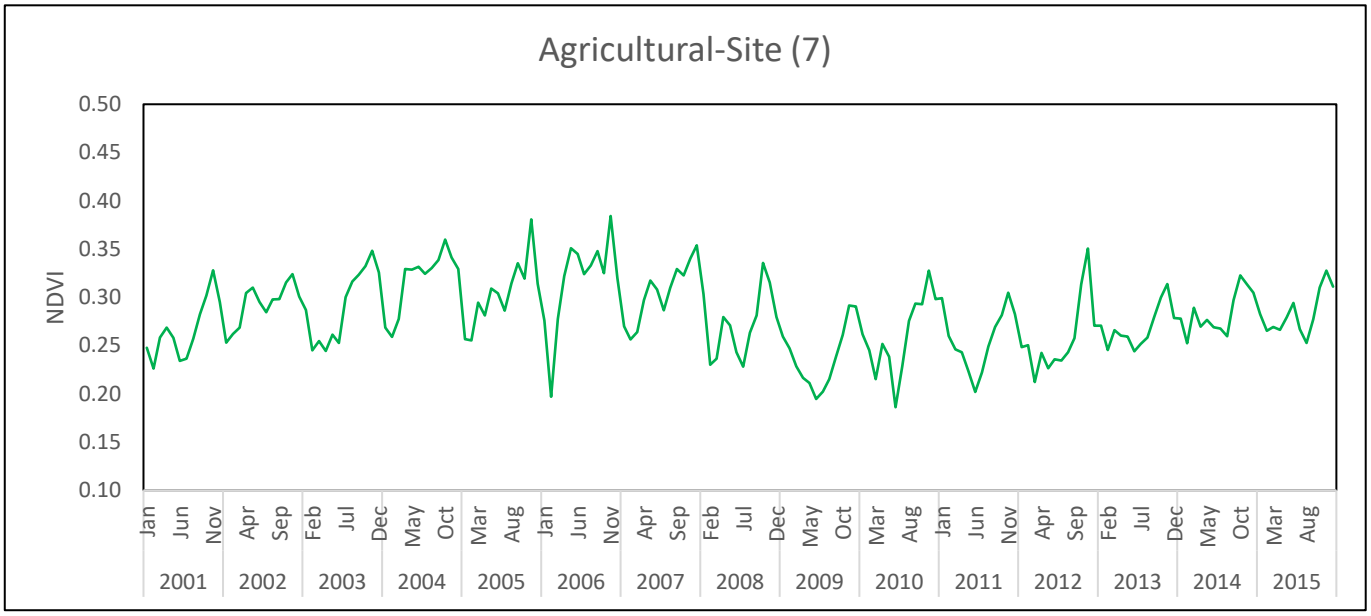
Agricultural-Site (7)
NDVI
0.50
0.45
0.40
0.35
0.30
0.25
0.20
0.15
0.10
Jan Jun Nov Apr Sep Feb Jul Dec May Oct Mar Aug Jan Jun Nov Apr Sep Feb Jul Dec May Oct Mar Aug Jan Jun Nov Apr Sep Feb Jul Dec May Oct Mar Aug
2001 2002 2003 2004 2005 2006 2007 2008 2009 2010 2011 2012 2013 2014 2015

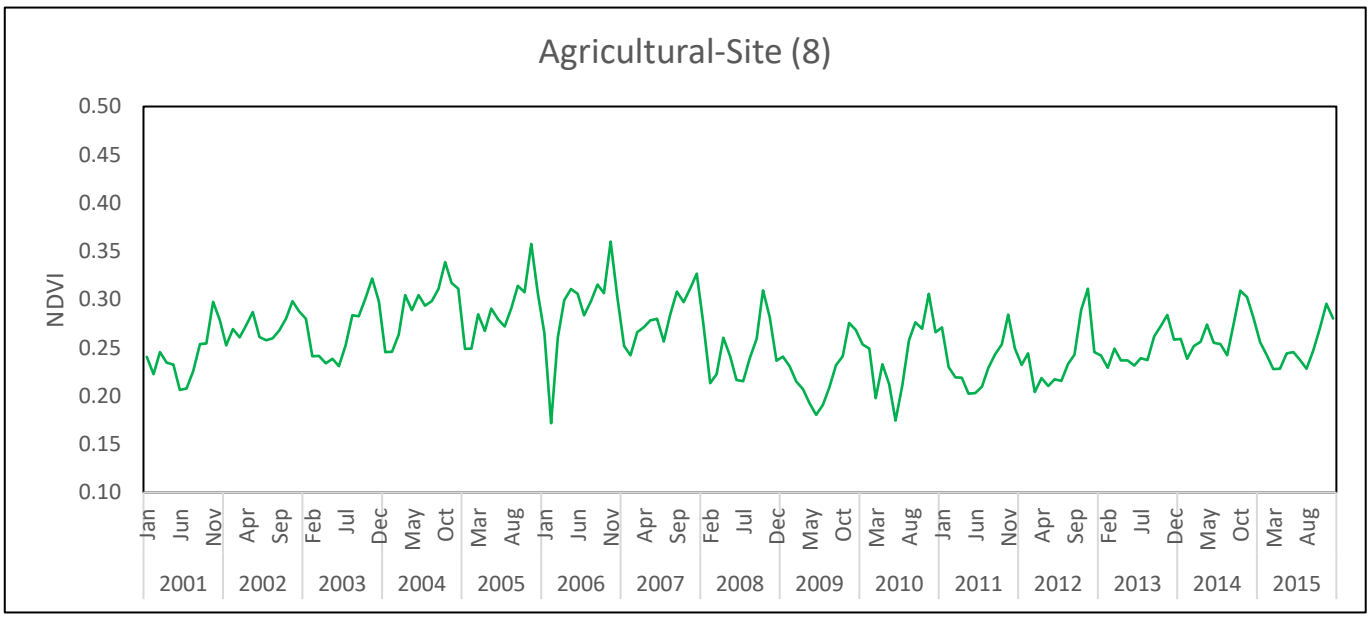
Agricultural-Site (8)
NDVI
0.50
0.45
0.40
0.35
0.30
0.25
0.20
0.15
0.10
Jan Jun Nov Apr Sep Feb Jul Dec May Oct Mar Aug Jan Jun Nov Apr Sep Feb Jul Dec May Oct Mar Aug Jan Jun Nov Apr Sep Feb Jul Dec May Oct Mar Aug
2001 2002 2003 2004 2005 2006 2007 2008 2009 2010 2011 2012 2013 2014 2015

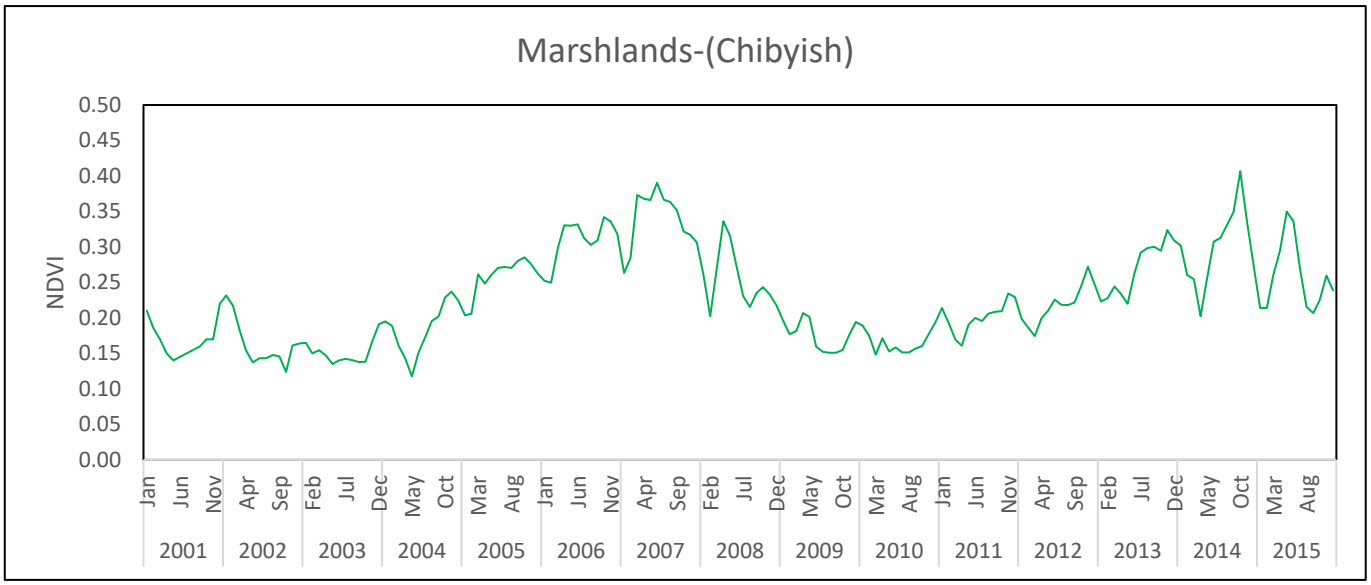
Marshlands-(Chibyish)
NDVI
0.50
0.45
0.40
0.35
0.30
0.25
0.20
0.15
0.10
0.05
0.00
Jan Jun Nov Apr Sep Feb Jul Dec May Oct Mar Aug Jan Jun Nov Apr Sep Feb Jul Dec May Oct Mar Aug Jan Jun Nov Apr Sep Feb Jul Dec May Oct Mar Aug
2001 2002 2003 2004 2005 2006 2007 2008 2009 2010 2011 2012 2013 2014 2015

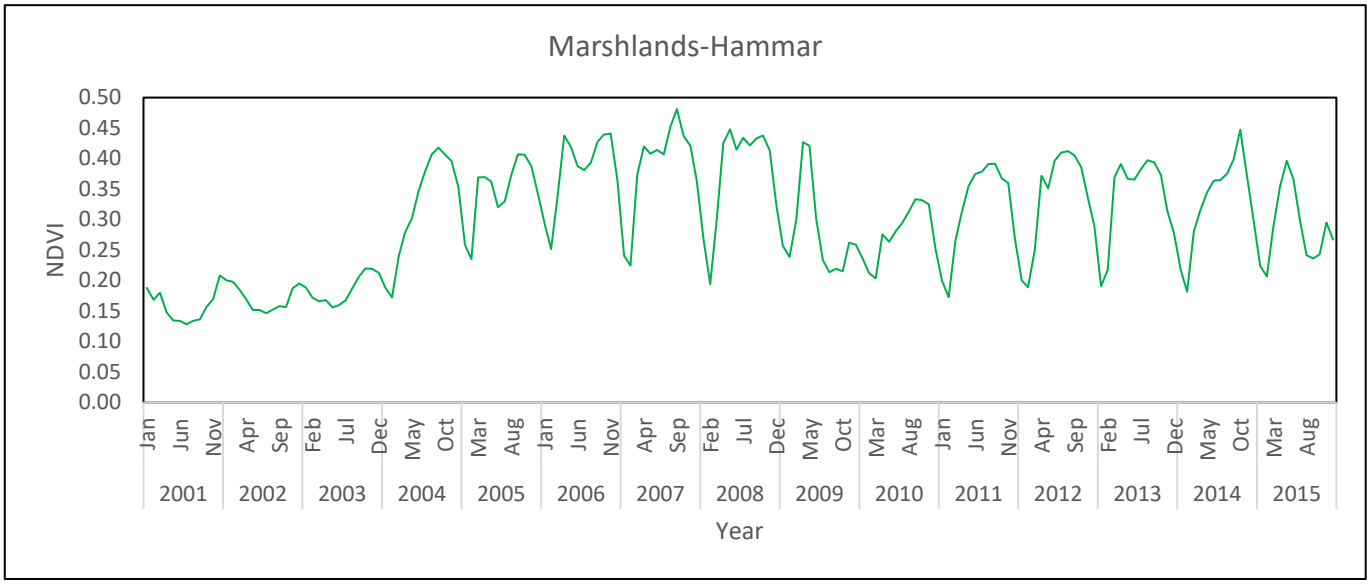
Marshlands-Hammar
NDVI
0.50
0.45
0.40
0.35
0.30
0.25
0.20
0.15
0.10
0.05
0.00
Jan Jun Nov Apr Sep Feb Jul Dec May Oct Mar Aug Jan Jun Nov Apr Sep Feb Jul Dec May Oct Mar Aug Jan Jun Nov Apr Sep Feb Jul Dec May Oct Mar Aug
2001 2002 2003 2004 2005 2006 2007 2008 2009 2010 2011 2012 2013 2014 2015
Year

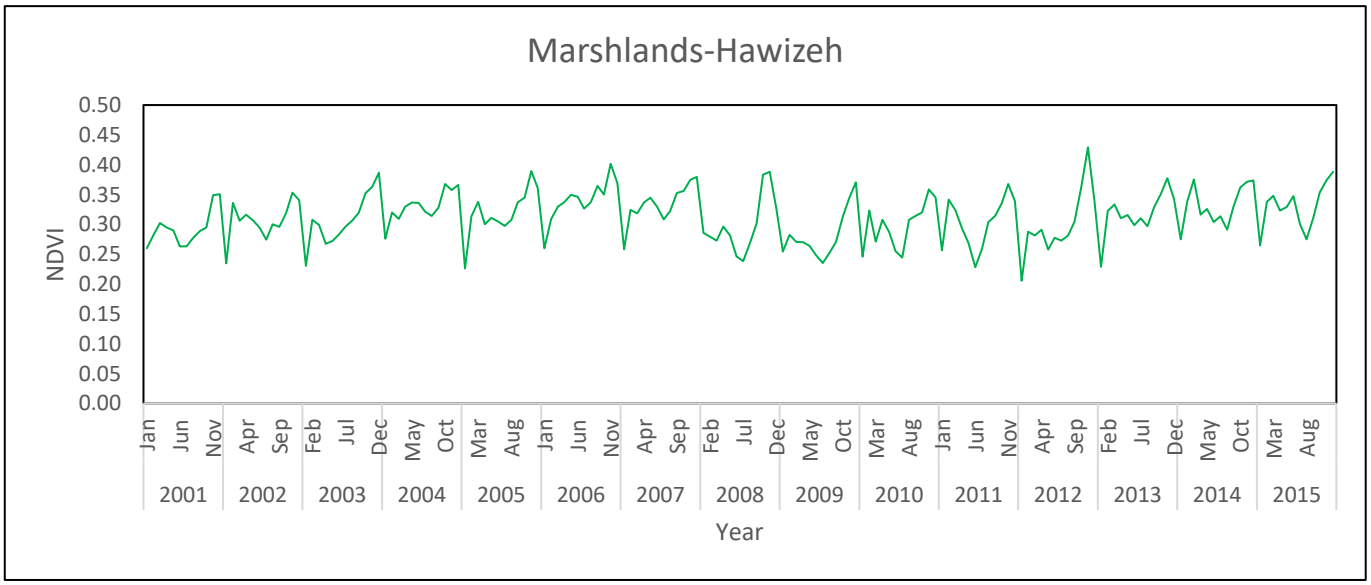
Marshlands-Hawizeh
NDVI
0.50
0.45
0.40
0.35
0.30
0.25
0.20
0.15
0.10
0.05
0.00
Jan Jun Nov Apr Sep Feb Jul Dec May Oct Mar Aug Jan Jun Nov Apr Sep Feb Jul Dec May Oct Mar Aug Jan Jun Nov Apr Sep Feb Jul Dec May Oct Mar Aug
2001 2002 2003 2004 2005 2006 2007 2008 2009 2010 2011 2012 2013 2014 2015
Year

APPENDIX C: Spatiotemporal seasonal variation in the LST (°C) throughout desert, rangeland, agriculture during 2001–2015.

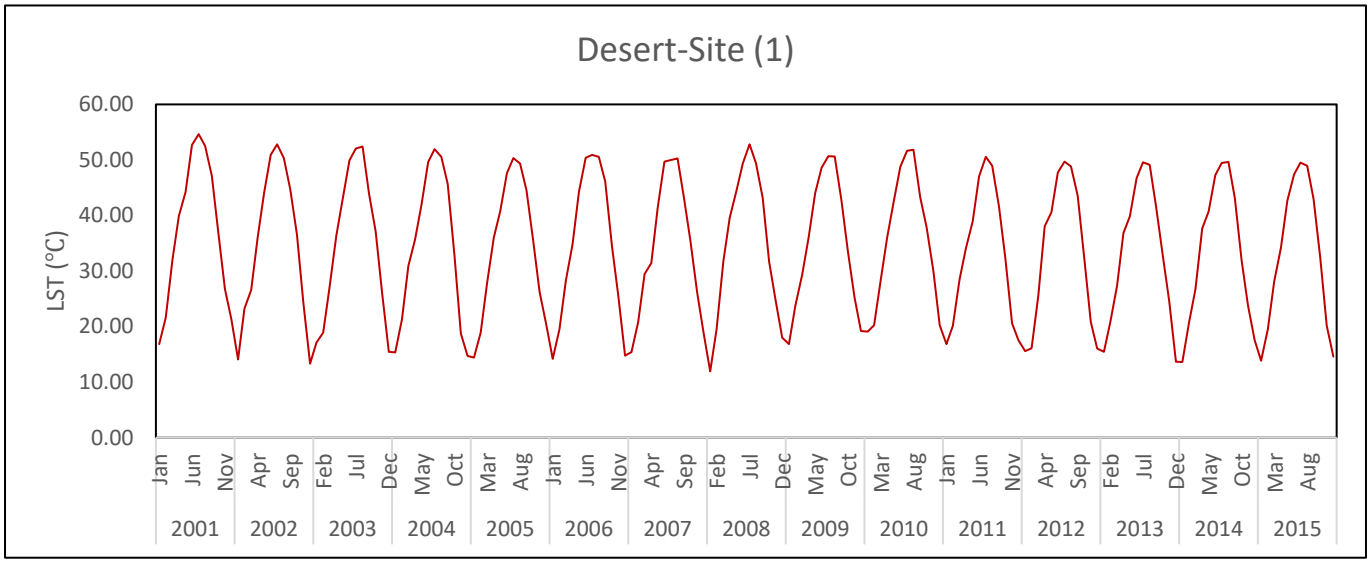

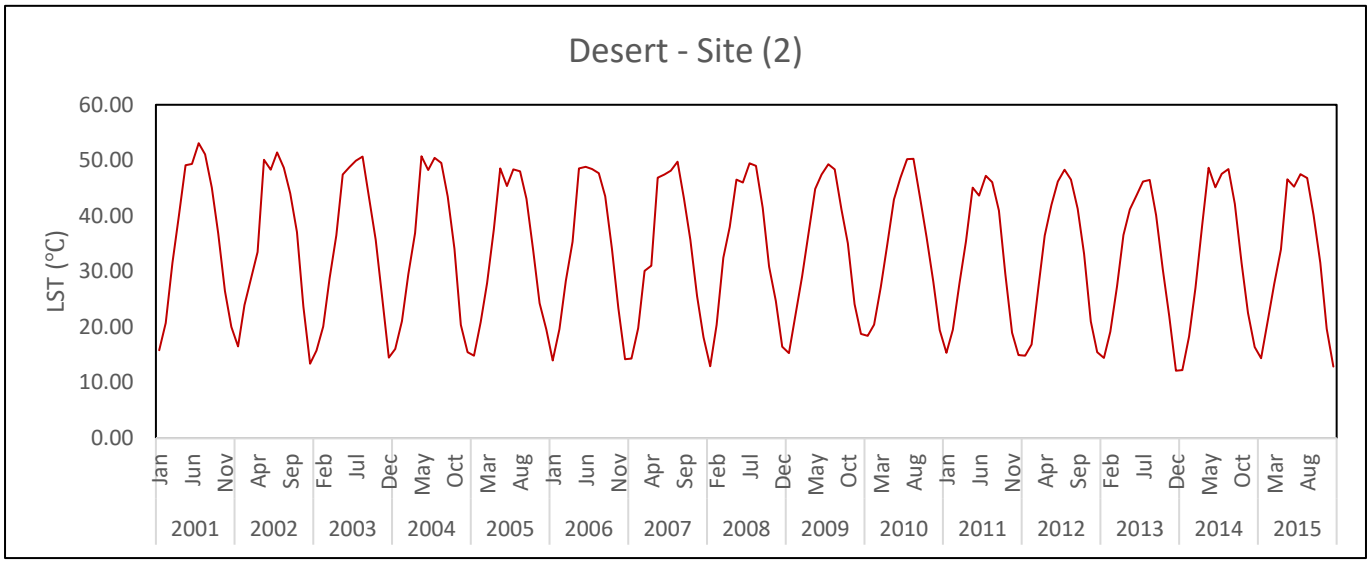

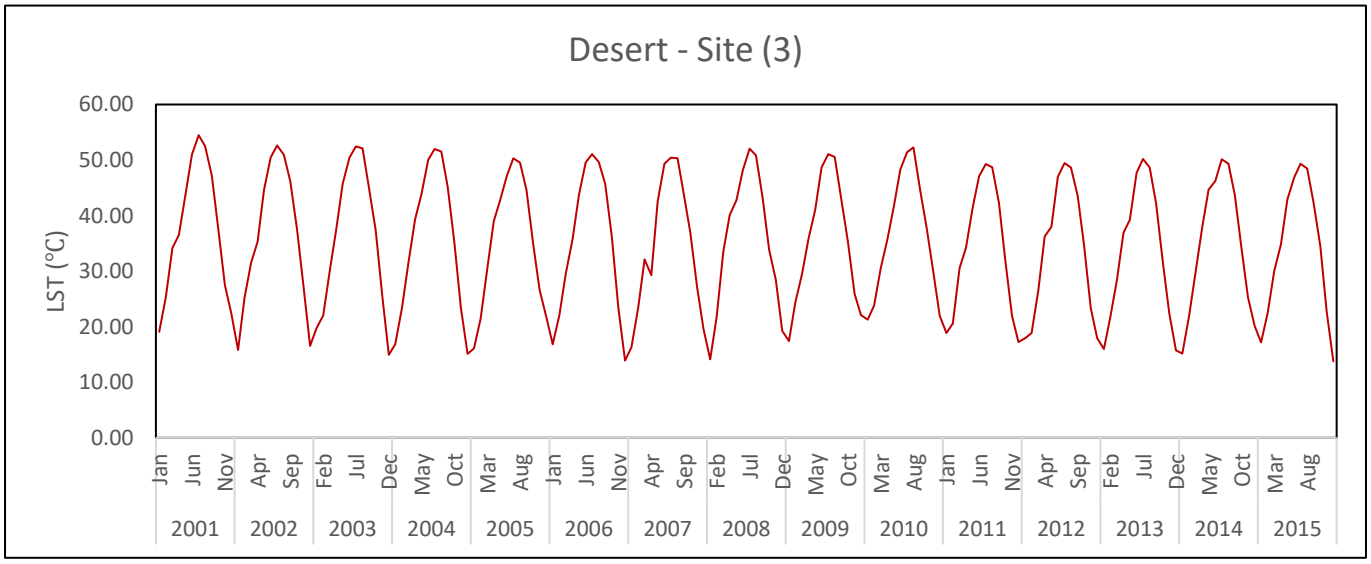

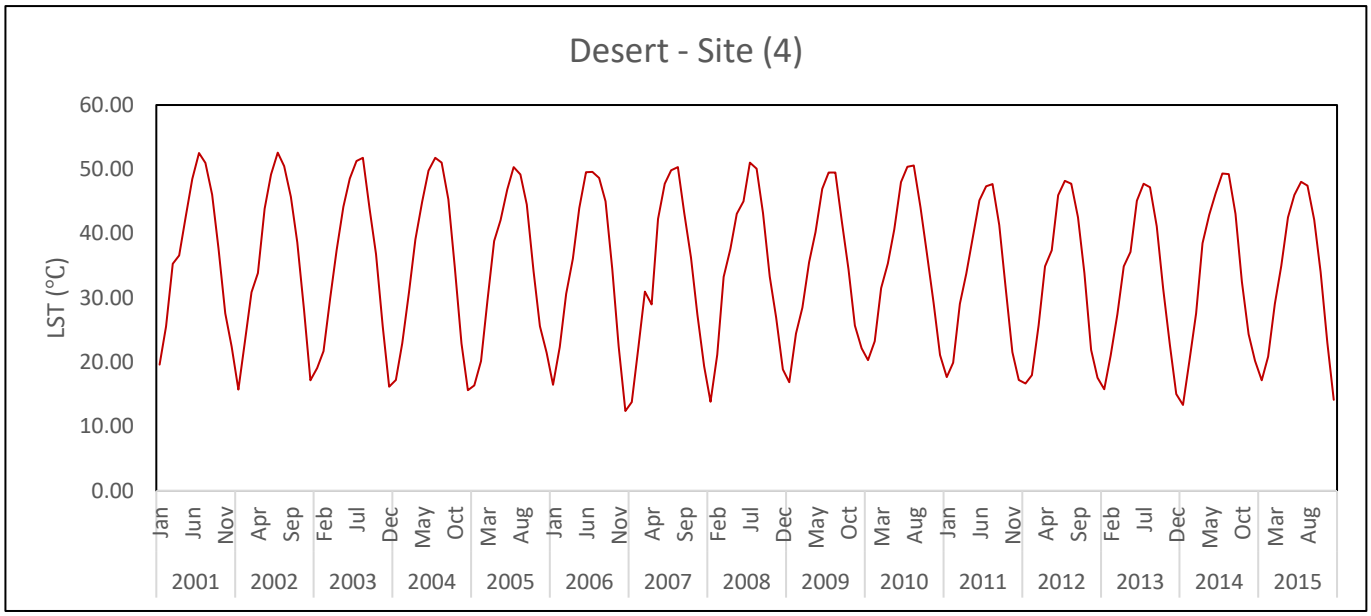
Desert - Site (4)
LST (°C)
60.00
50.00
40.00
30.00
20.00
10.00
0.00
Jan Jun Nov Apr Sep Feb Jul Dec May Oct Mar Aug
2001 2002 2003 2004 2005 2006 2007 2008 2009 2010 2011 2012 2013 2014 2015

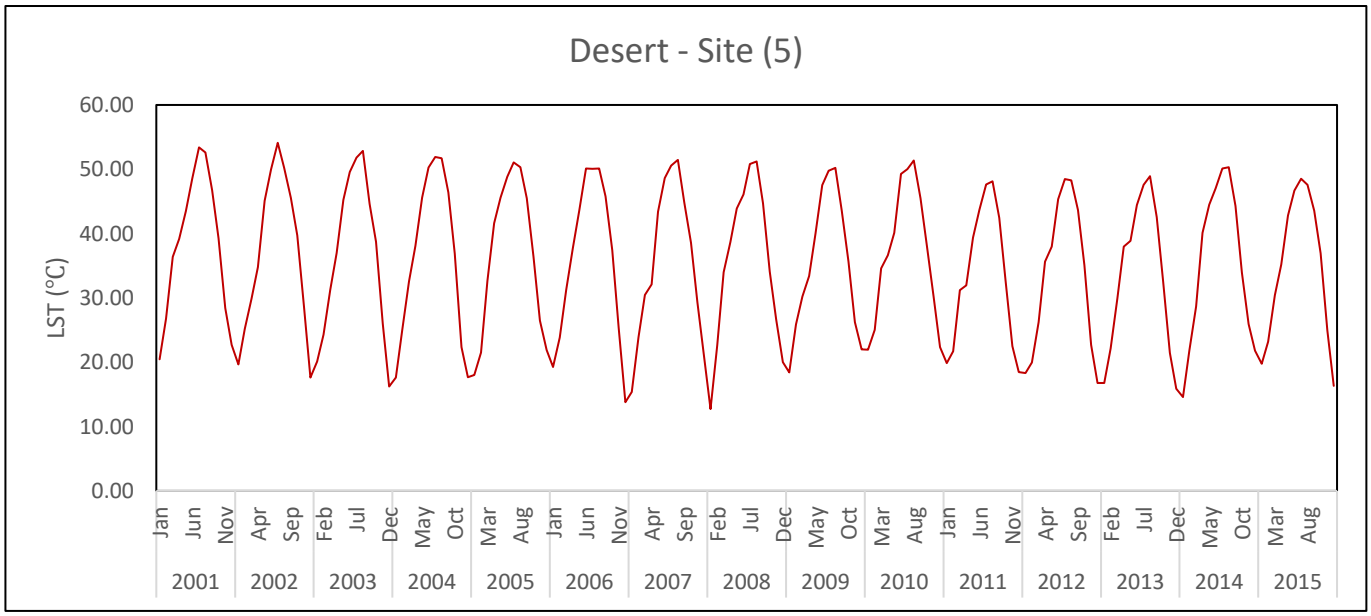
Desert - Site (5)
LST (°C)
60.00
50.00
40.00
30.00
20.00
10.00
0.00
Jan Jun Nov Apr Sep Feb Jul Dec May Oct Mar Aug
2001 2002 2003 2004 2005 2006 2007 2008 2009 2010 2011 2012 2013 2014 2015

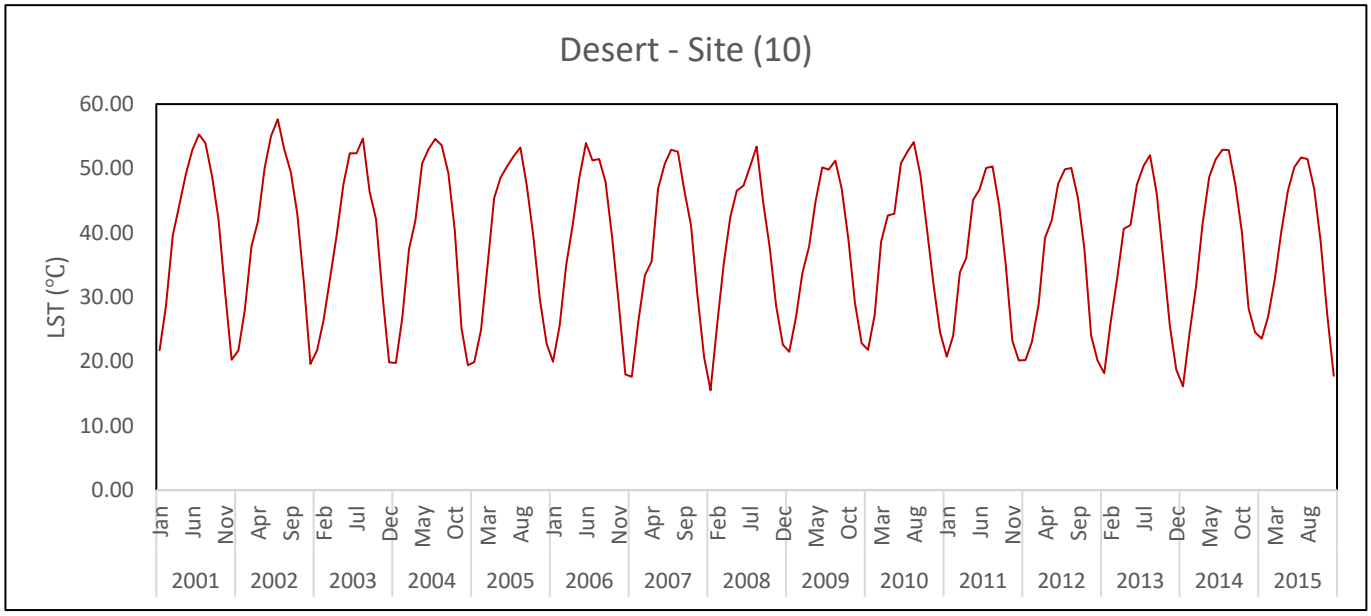
Desert - Site (10)
LST (°C)
60.00
50.00
40.00
30.00
20.00
10.00
0.00
Jan Jun Nov Apr Sep Feb Jul Dec May Oct Mar Aug
2001 2002 2003 2004 2005 2006 2007 2008 2009 2010 2011 2012 2013 2014 2015

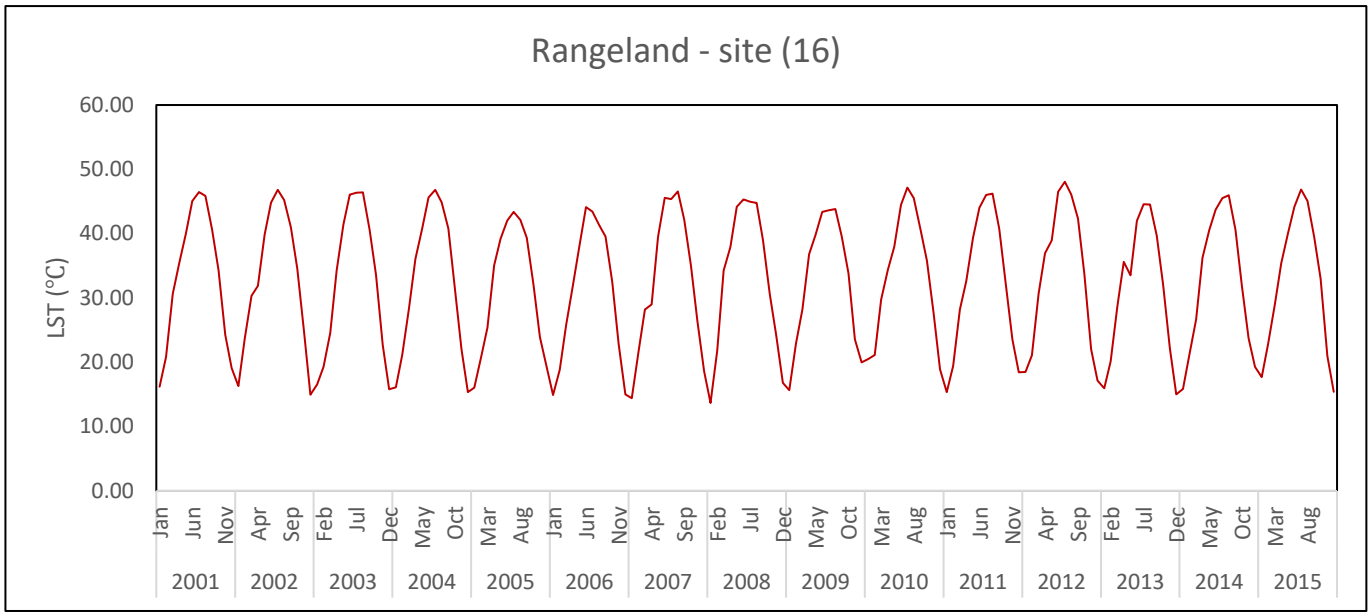
Rangeland - site (16)
LST (°C)
60.00
50.00
40.00
30.00
20.00
10.00
0.00
Jan Jun Nov Apr Sep Feb Jul Dec May Oct Mar Aug
2001 2002 2003 2004 2005 2006 2007 2008 2009 2010 2011 2012 2013 2014 2015

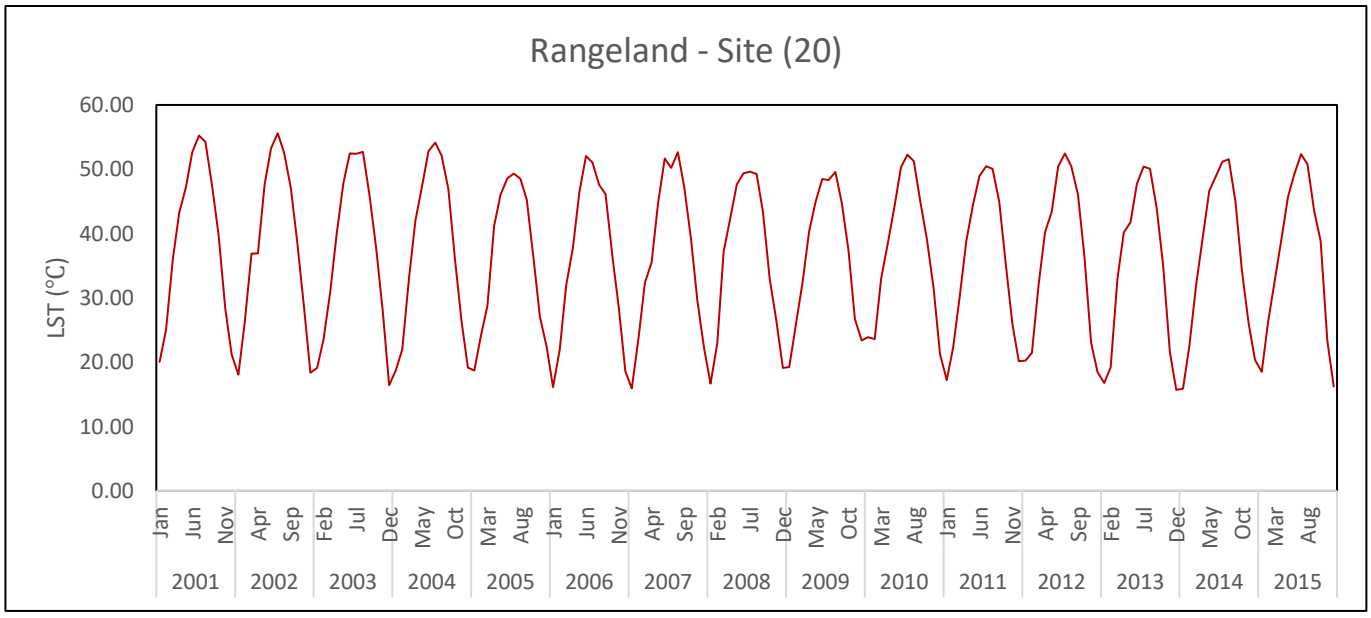
Rangeland - Site (20)
LST (°C)
60.00
50.00
40.00
30.00
20.00
10.00
0.00
Jan Jun Nov Apr Sep Feb Jul Dec May Oct Mar Aug
2001 2002 2003 2004 2005 2006 2007 2008 2009 2010 2011 2012 2013 2014 2015

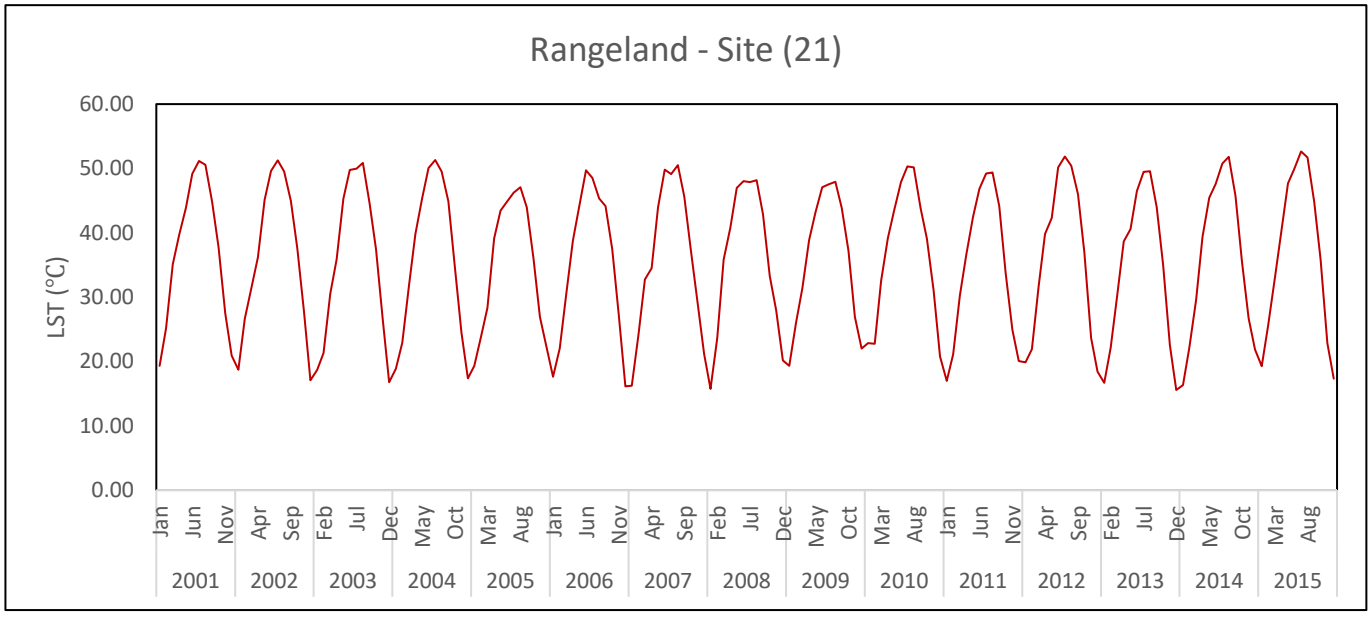
Rangeland - Site (21)
LST (°C)
60.00
50.00
40.00
30.00
20.00
10.00
0.00
Jan Jun Nov Apr Sep Feb Jul Dec May Oct Mar Aug
2001 2002 2003 2004 2005 2006 2007 2008 2009 2010 2011 2012 2013 2014 2015

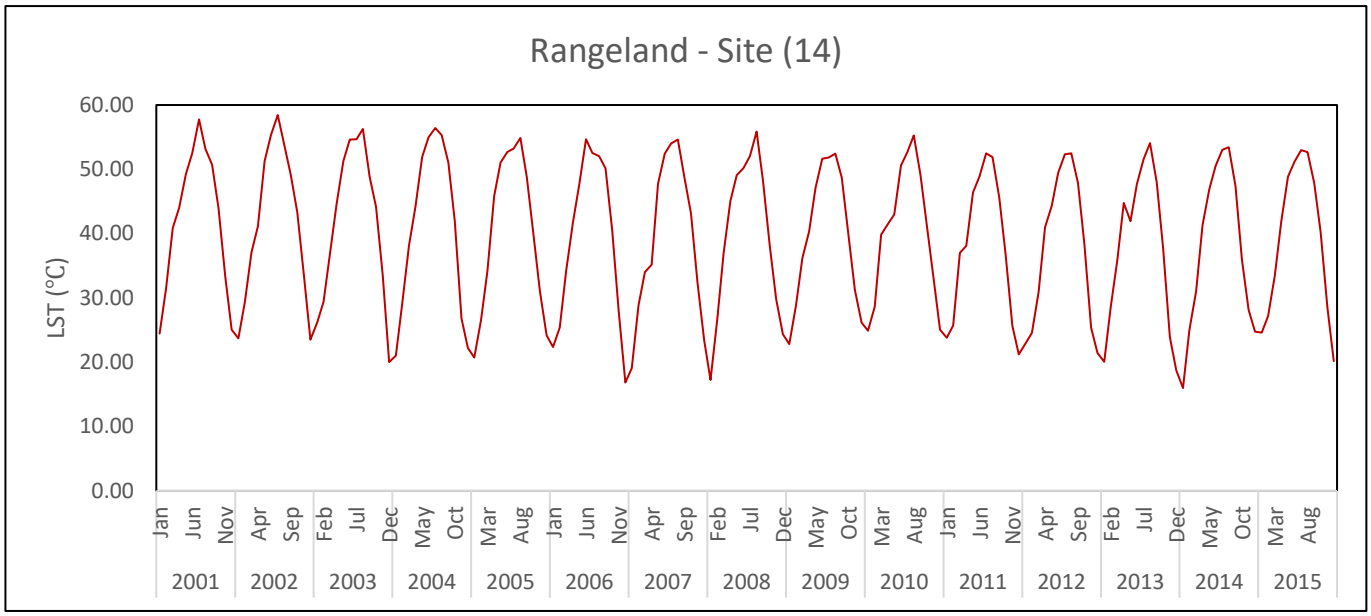
Rangeland - Site (14)
LST (°C)
60.00
50.00
40.00
30.00
20.00
10.00
0.00
Jan Jun Nov Apr Sep Feb Jul Dec May Oct Mar Aug Jan Jun Nov Apr Sep Feb Jul Dec May Oct Mar Aug Jan Jun Nov Apr Sep Feb Jul Dec May Oct Mar Aug Jan Jun Nov Apr Sep Feb Jul Dec May Oct Mar Aug
2001 2002 2003 2004 2005 2006 2007 2008 2009 2010 2011 2012 2013 2014 2015

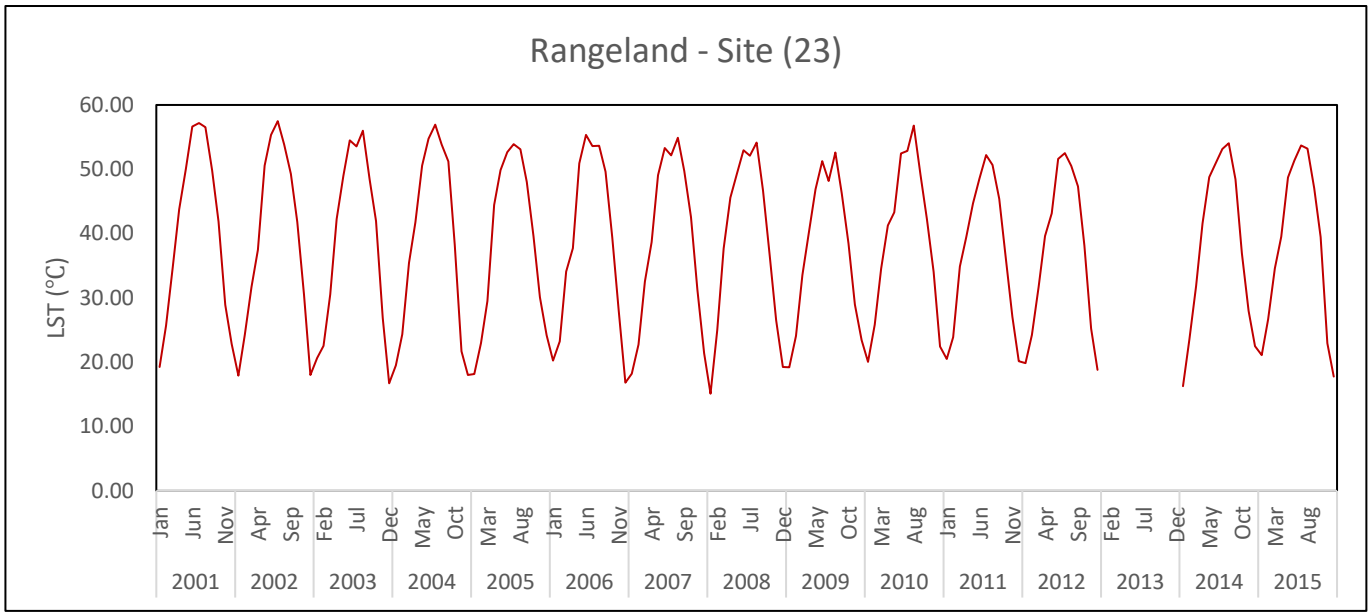
Rangeland - Site (23)
LST (°C)
60.00
50.00
40.00
30.00
20.00
10.00
0.00
Jan Jun Nov Apr Sep Feb Jul Dec May Oct Mar Aug Jan Jun Nov Apr Sep Feb Jul Dec May Oct Mar Aug Jan Jun Nov Apr Sep Feb Jul Dec May Oct Mar Aug Jan Jun Nov Apr Sep Feb Jul Dec May Oct Mar Aug
2001 2002 2003 2004 2005 2006 2007 2008 2009 2010 2011 2012 2013 2014 2015

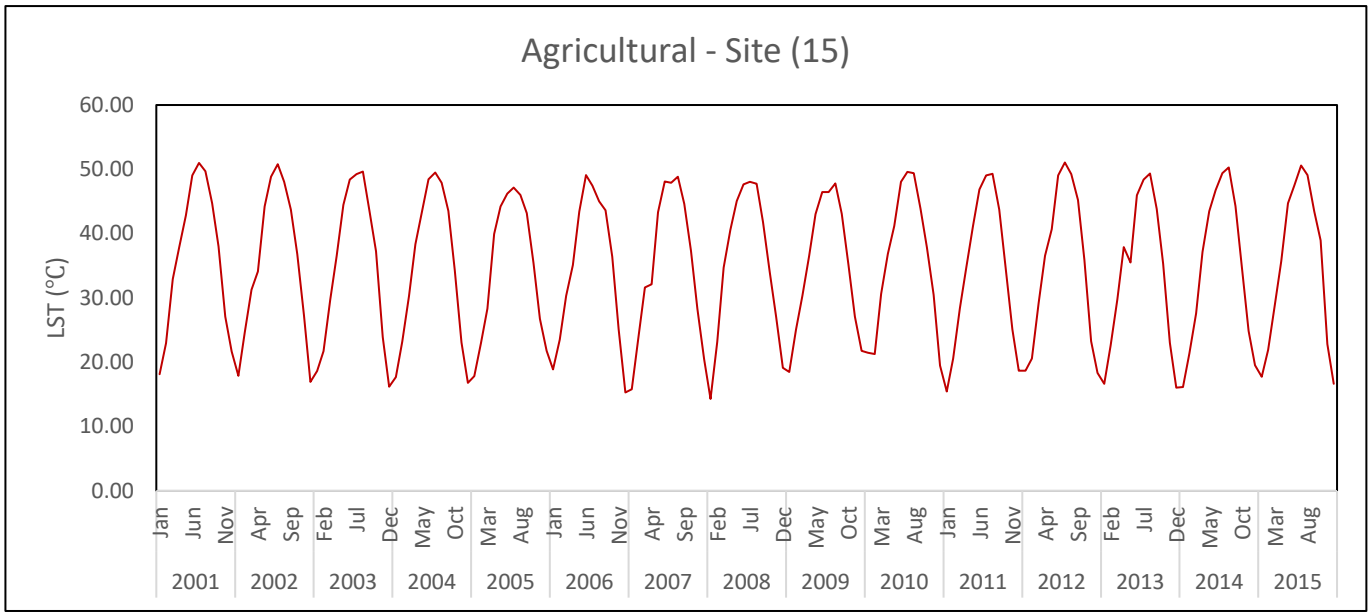
Agricultural - Site (15)
LST (°C)
60.00
50.00
40.00
30.00
20.00
10.00
0.00
Jan Jun Nov Apr Sep Feb Jul Dec May Oct Mar Aug Jan Jun Nov Apr Sep Feb Jul Dec May Oct Mar Aug Jan Jun Nov Apr Sep Feb Jul Dec May Oct Mar Aug
2001 2002 2003 2004 2005 2006 2007 2008 2009 2010 2011 2012 2013 2014 2015

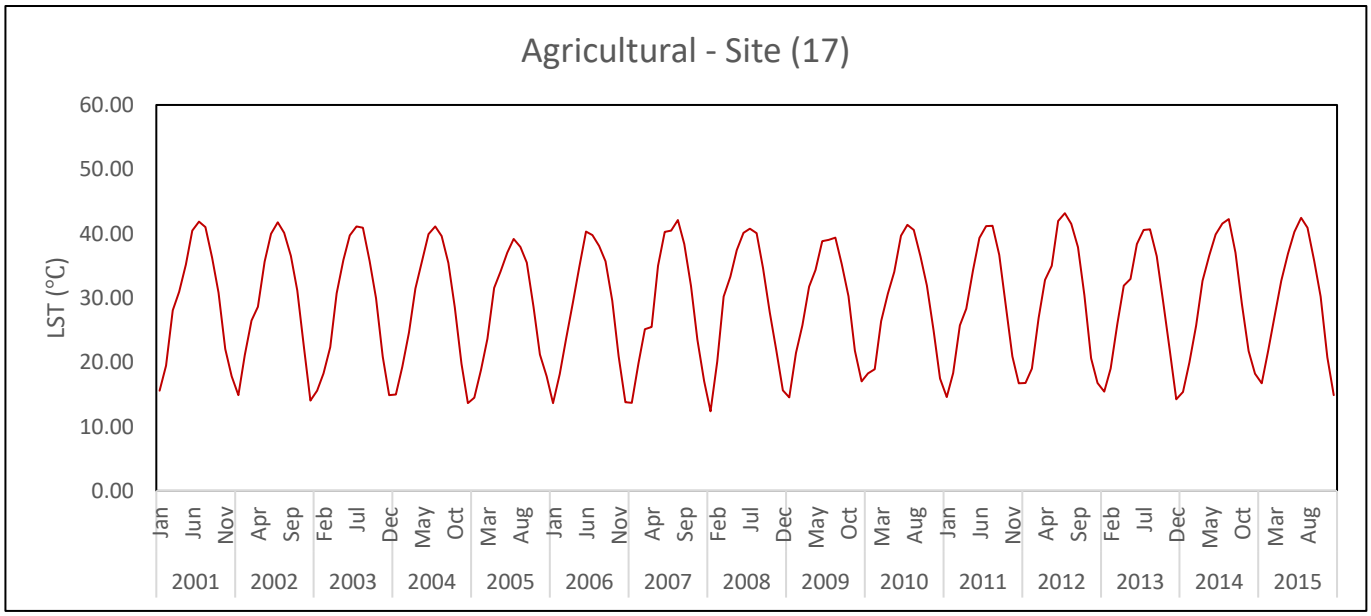
Agricultural - Site (17)
LST (°C)
60.00
50.00
40.00
30.00
20.00
10.00
0.00
Jan Jun Nov Apr Sep Feb Jul Dec May Oct Mar Aug Jan Jun Nov Apr Sep Feb Jul Dec May Oct Mar Aug Jan Jun Nov Apr Sep Feb Jul Dec May Oct Mar Aug
2001 2002 2003 2004 2005 2006 2007 2008 2009 2010 2011 2012 2013 2014 2015

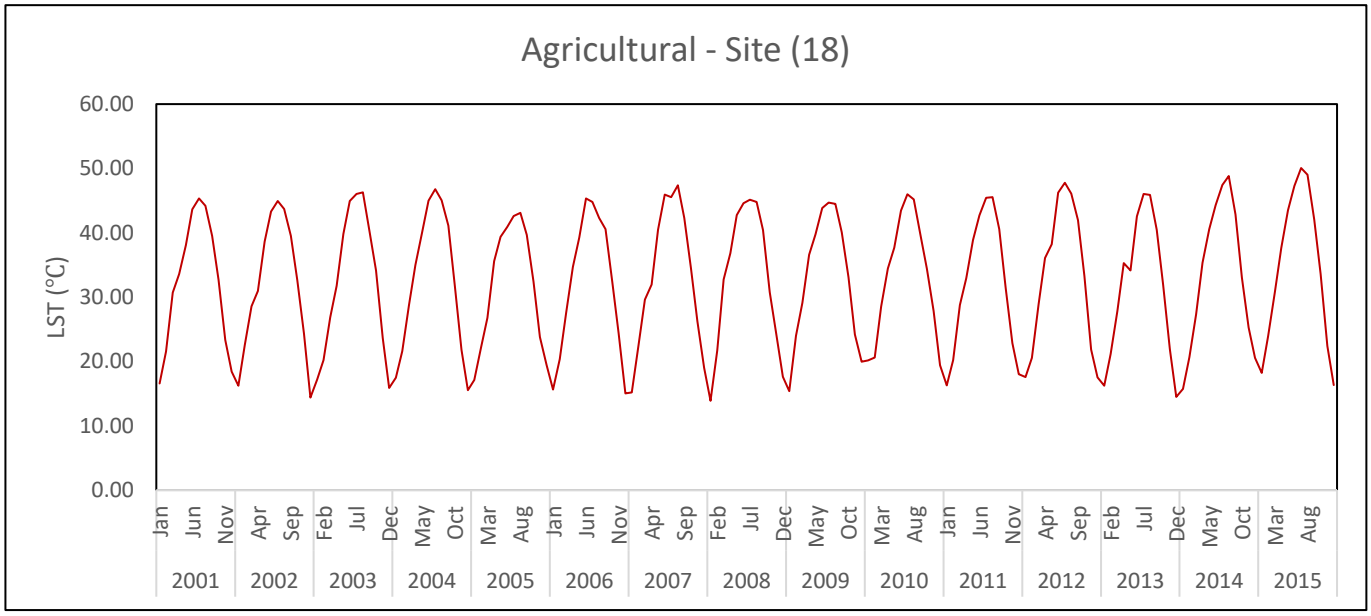
Agricultural - Site (18)
LST (°C)
60.00
50.00
40.00
30.00
20.00
10.00
0.00
Jan Jun Nov Apr Sep Feb Jul Dec May Oct Mar Aug Jan Jun Nov Apr Sep Feb Jul Dec May Oct Mar Aug Jan Jun Nov Apr Sep Feb Jul Dec May Oct Mar Aug
2001 2002 2003 2004 2005 2006 2007 2008 2009 2010 2011 2012 2013 2014 2015

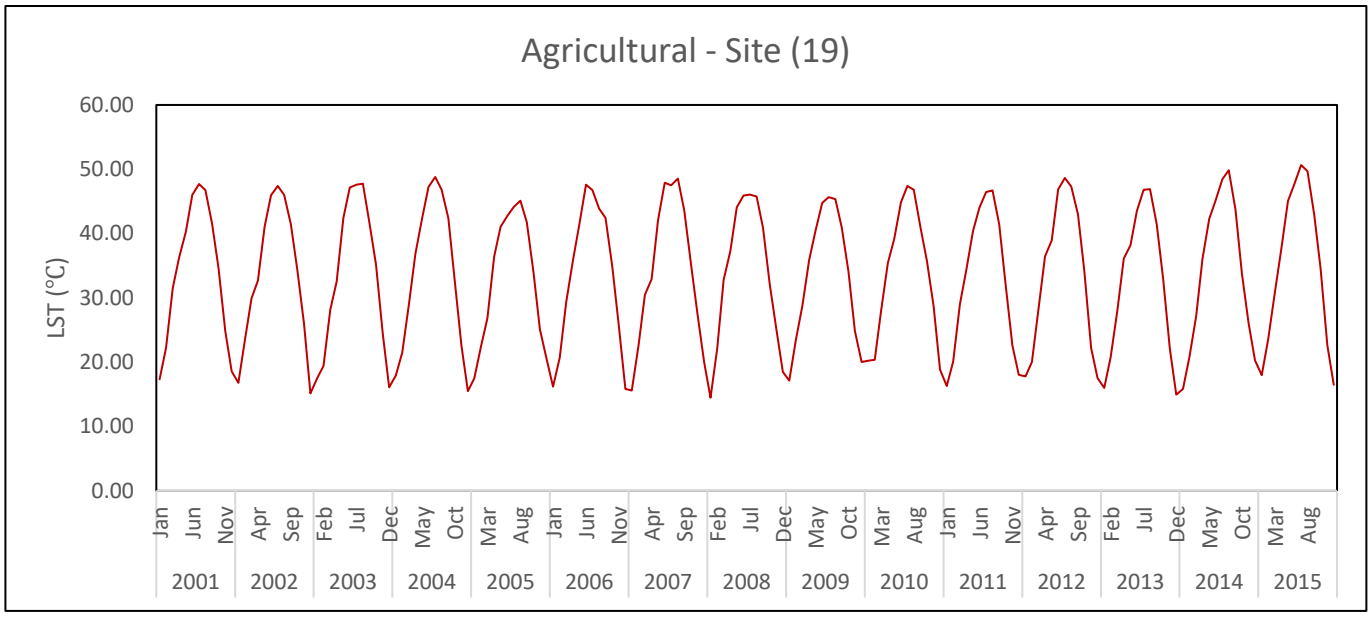
Agricultural - Site (19)
LST (°C)
60.00
50.00
40.00
30.00
20.00
10.00
0.00
Jan Jun Nov Apr Sep Feb Jul Dec May Oct Mar Aug Jan Jun Nov Apr Sep Feb Jul Dec May Oct Mar Aug Jan Jun Nov Apr Sep Feb Jul Dec May Oct Mar Aug
2001 2002 2003 2004 2005 2006 2007 2008 2009 2010 2011 2012 2013 2014 2015

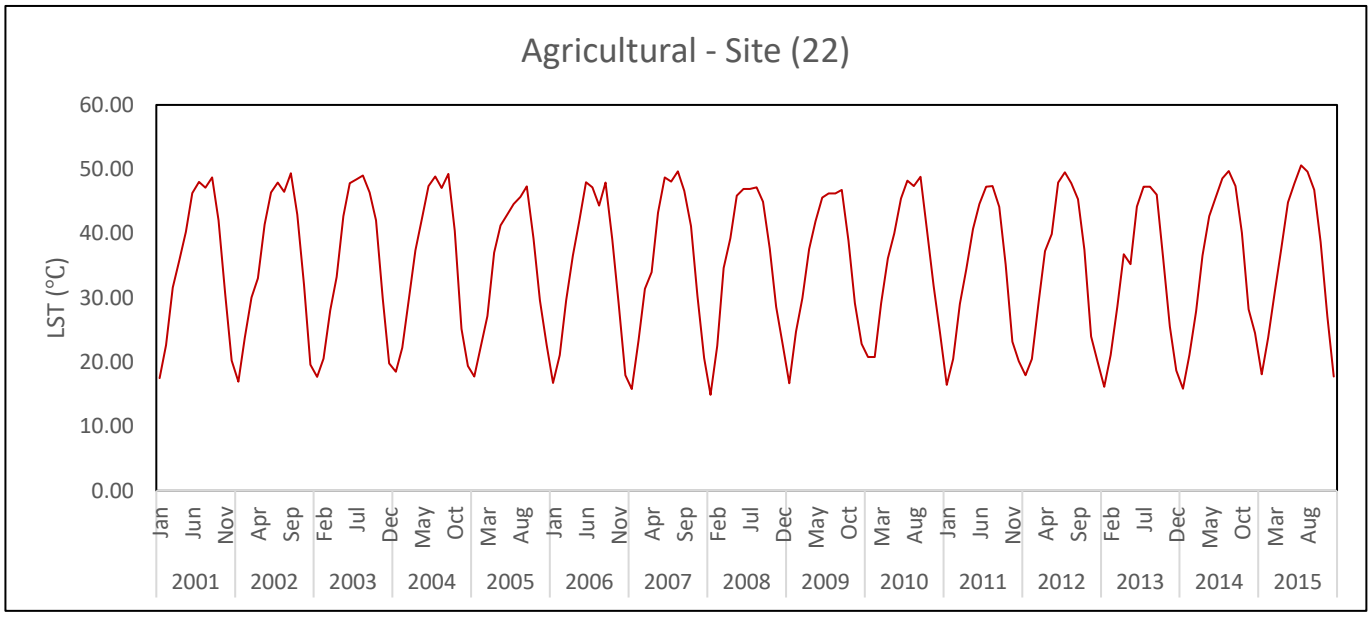
Agricultural - Site (22)
LST (°C)
60.00
50.00
40.00
30.00
20.00
10.00
0.00
Jan Jun Nov Apr Sep Feb Jul Dec May Oct Mar Aug Jan Jun Nov Apr Sep Feb Jul Dec May Oct Mar Aug Jan Jun Nov Apr Sep Feb Jul Dec May Oct Mar Aug
2001 2002 2003 2004 2005 2006 2007 2008 2009 2010 2011 2012 2013 2014 2015

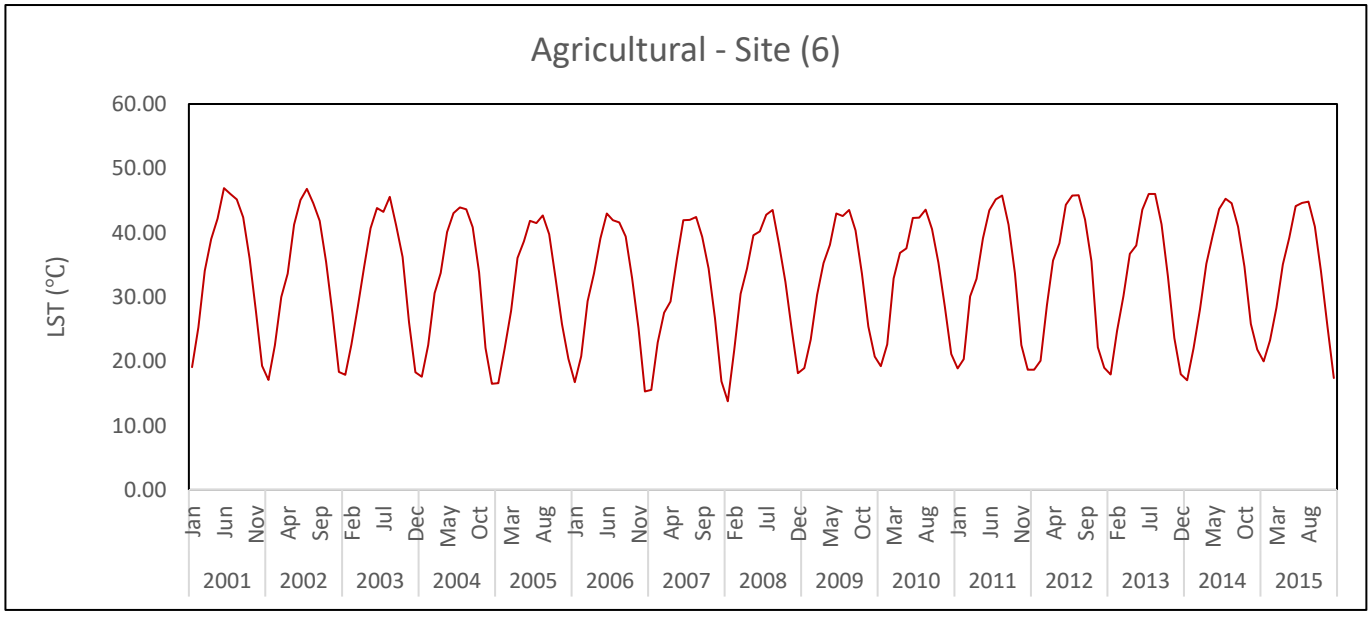
Agricultural - Site (6)
LST (°C)
60.00
50.00
40.00
30.00
20.00
10.00
0.00
Jan Jun Nov Apr Sep Feb Jul Dec May Oct Mar Aug Jan Jun Nov Apr Sep Feb Jul Dec May Oct Mar Aug Jan Jun Nov Apr Sep Feb Jul Dec May Oct Mar Aug
2001 2002 2003 2004 2005 2006 2007 2008 2009 2010 2011 2012 2013 2014 2015

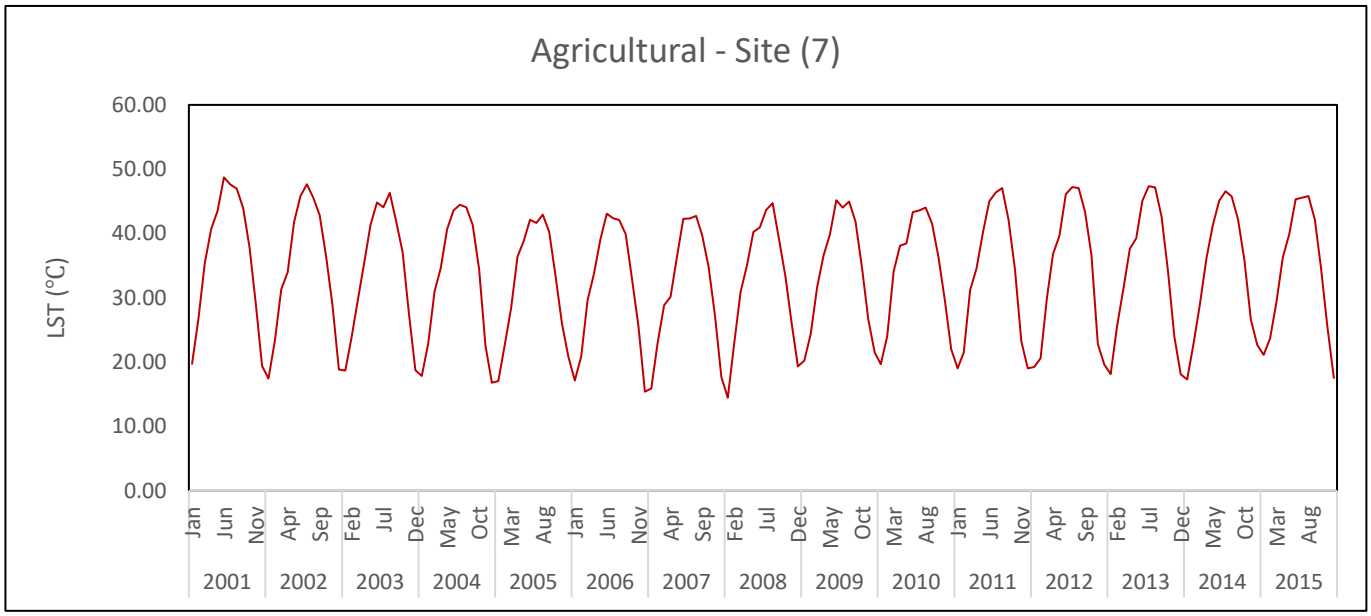
Agricultural - Site (7)
LST (°C)
60.00
50.00
40.00
30.00
20.00
10.00
0.00
Jan Jun Nov Apr Sep Feb Jul Dec May Oct Mar Aug Jan Jun Nov Apr Sep Feb Jul Dec May Oct Mar Aug Jan Jun Nov Apr Sep Feb Jul Dec May Oct Mar Aug
2001 2002 2003 2004 2005 2006 2007 2008 2009 2010 2011 2012 2013 2014 2015

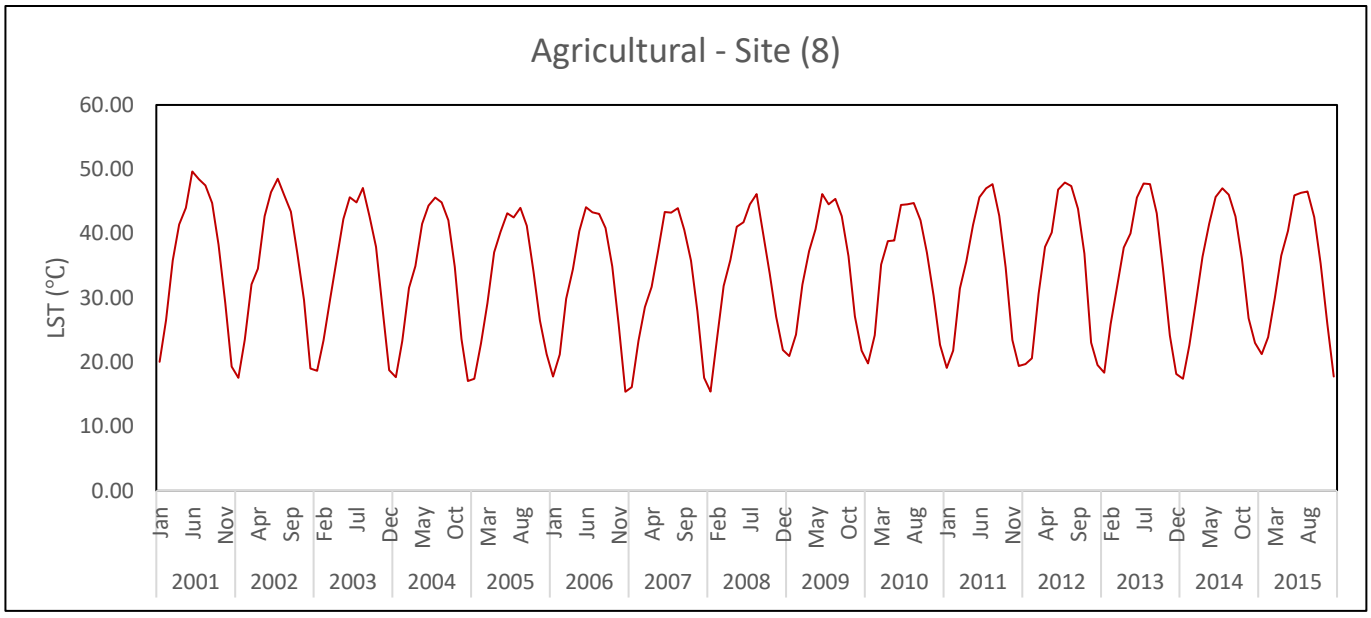
Agricultural - Site (8)
LST (°C)
60.00
50.00
40.00
30.00
20.00
10.00
0.00
Jan Jun Nov Apr Sep Feb Jul Dec May Oct Mar Aug Jan Jun Nov Apr Sep Feb Jul Dec May Oct Mar Aug Jan Jun Nov Apr Sep Feb Jul Dec May Oct Mar Aug
2001 2002 2003 2004 2005 2006 2007 2008 2009 2010 2011 2012 2013 2014 2015

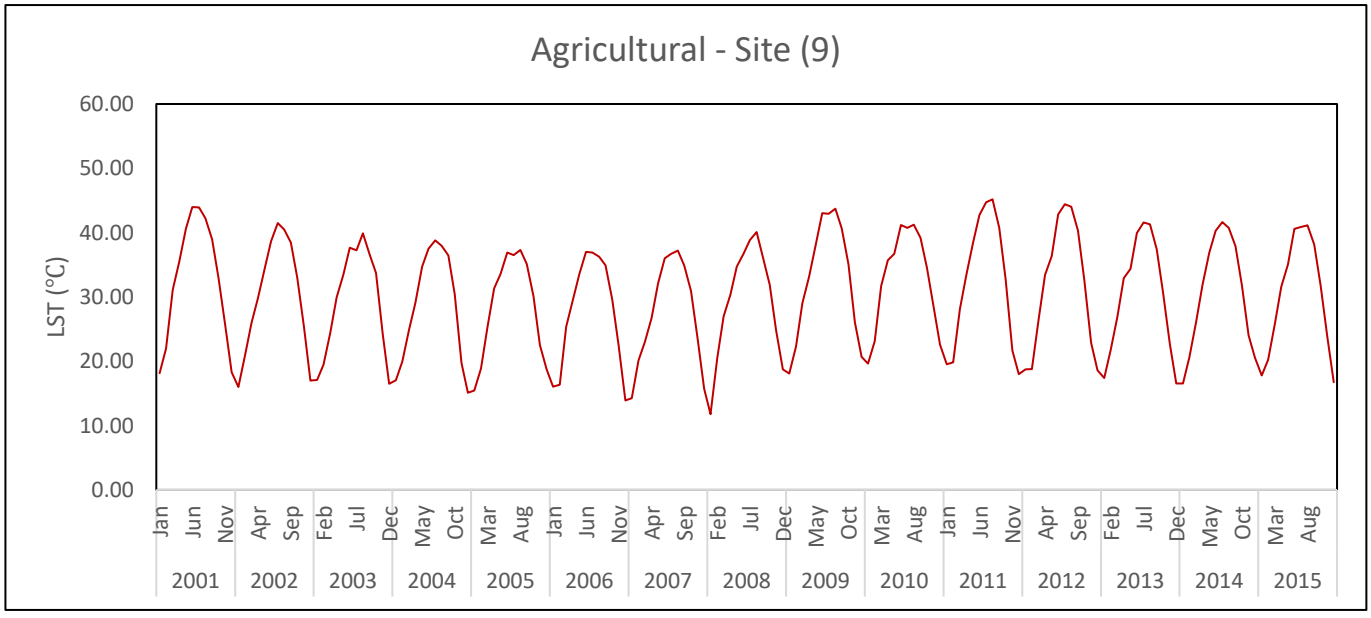
Agricultural - Site (9)
LST (°C)
60.00
50.00
40.00
30.00
20.00
10.00
0.00
Jan Jun Nov Apr Sep Feb Jul Dec May Oct Mar Aug Jan Jun Nov Apr Sep Feb Jul Dec May Oct Mar Aug Jan Jun Nov Apr Sep Feb Jul Dec May Oct Mar Aug
2001 2002 2003 2004 2005 2006 2007 2008 2009 2010 2011 2012 2013 2014 2015

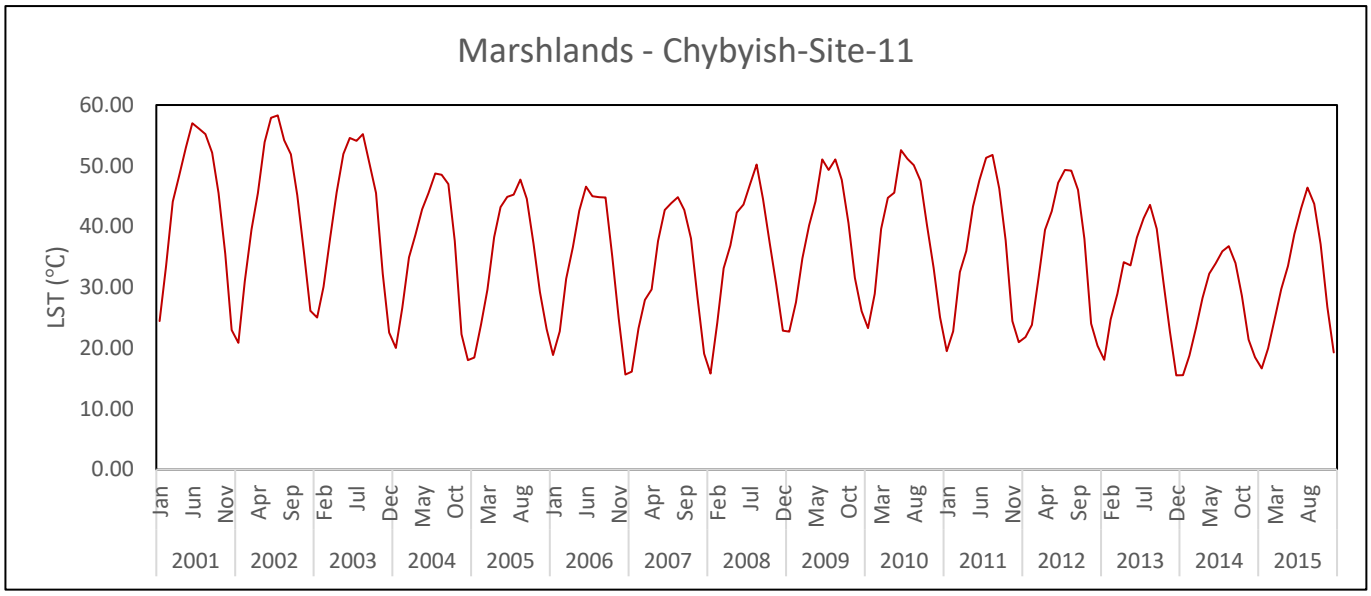
Marshlands - Chybyish-Site-11
LST (°C)
60.00
50.00
40.00
30.00
20.00
10.00
0.00
Jan Jun Nov Apr Sep Feb Jul Dec May Oct Mar Aug Jan Jun Nov Apr Sep Feb Jul Dec May Oct Mar Aug Jan Jun Nov Apr Sep Feb Jul Dec May Oct Mar Aug Jan Jun Nov Apr Sep Feb Jul Dec May Oct Mar Aug
2001 2002 2003 2004 2005 2006 2007 2008 2009 2010 2011 2012 2013 2014 2015

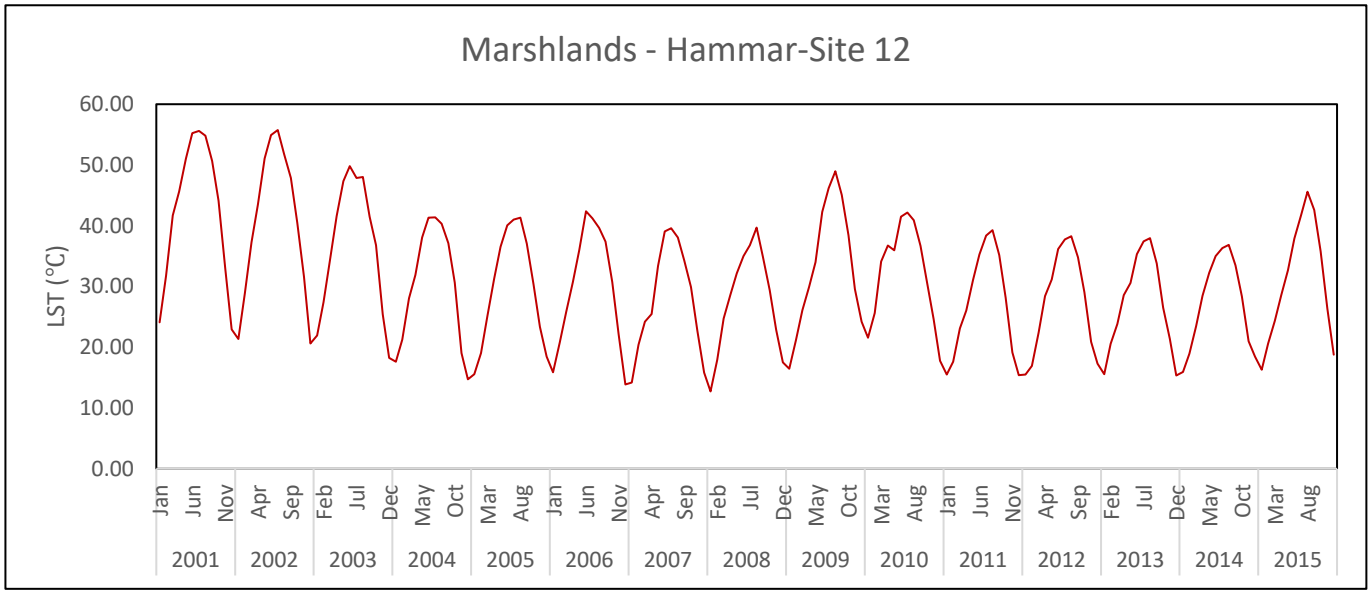
Marshlands - Hammar-Site 12
LST (°C)
60.00
50.00
40.00
30.00
20.00
10.00
0.00
Jan Jun Nov Apr Sep Feb Jul Dec May Oct Mar Aug Jan Jun Nov Apr Sep Feb Jul Dec May Oct Mar Aug Jan Jun Nov Apr Sep Feb Jul Dec May Oct Mar Aug Jan Jun Nov Apr Sep Feb Jul Dec May Oct Mar Aug
2001 2002 2003 2004 2005 2006 2007 2008 2009 2010 2011 2012 2013 2014 2015

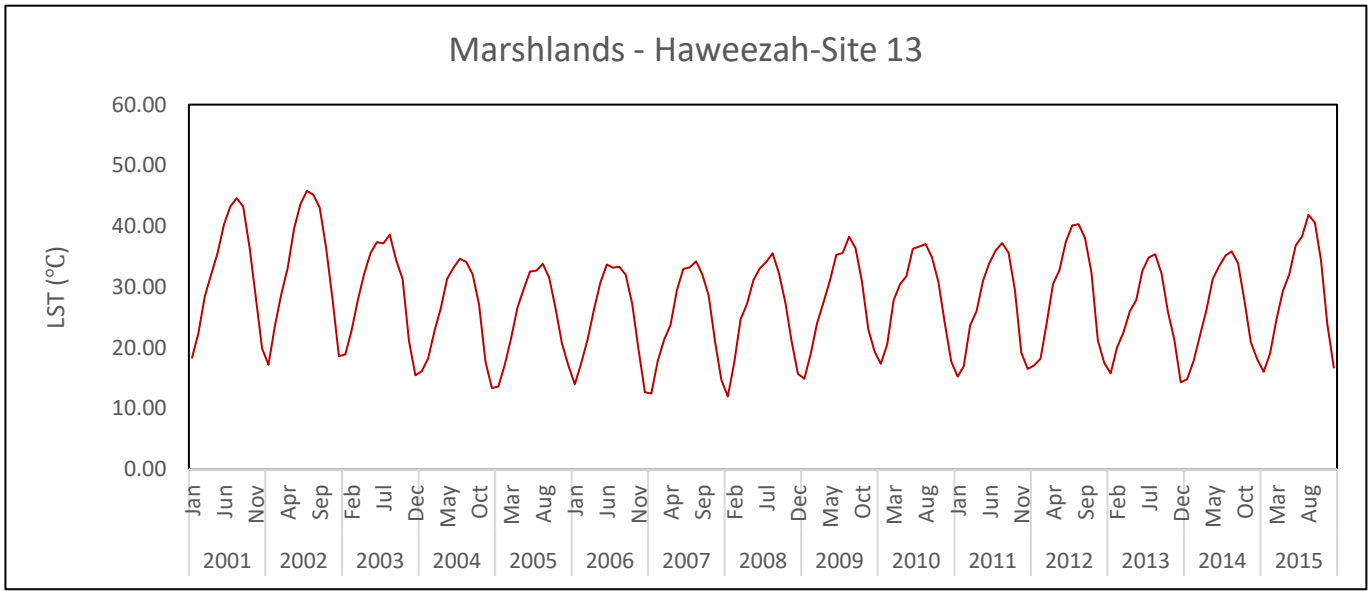
Marshlands - Haweezah-Site 13
LST (°C)
60.00
50.00
40.00
30.00
20.00
10.00
0.00
Jan Jun Nov Apr Sep Feb Jul Dec May Oct Mar Aug Jan Jun Nov Apr Sep Feb Jul Dec May Oct Mar Aug Jan Jun Nov Apr Sep Feb Jul Dec May Oct Mar Aug Jan Jun Nov Apr Sep Feb Jul Dec May Oct Mar Aug
2001 2002 2003 2004 2005 2006 2007 2008 2009 2010 2011 2012 2013 2014 2015

APPENDIX D: The spatial correlation analyses between LST and NDVI over Iraq.

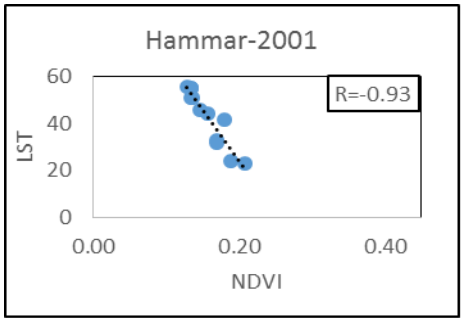

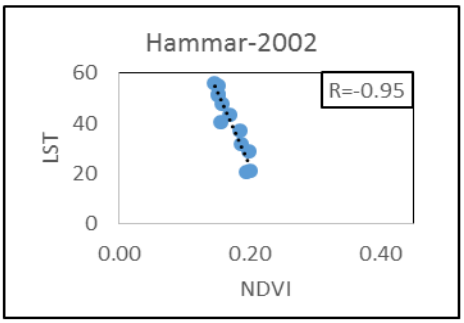

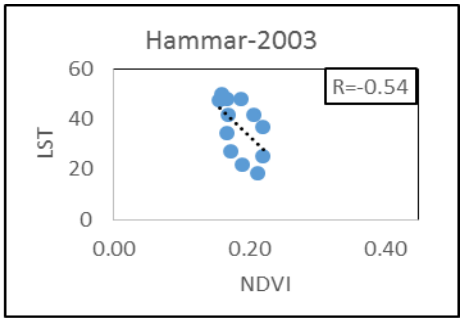

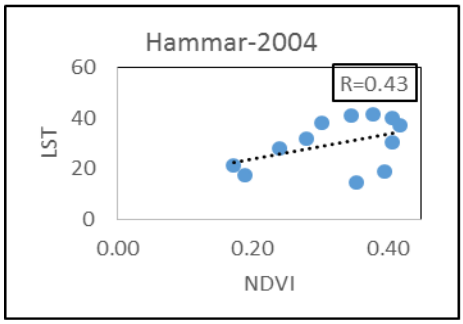

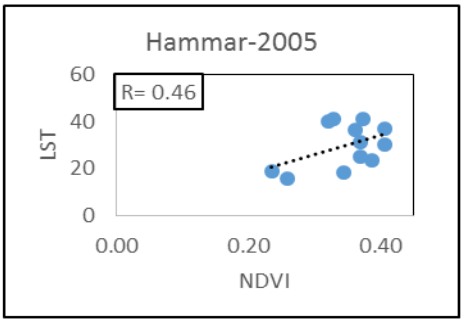

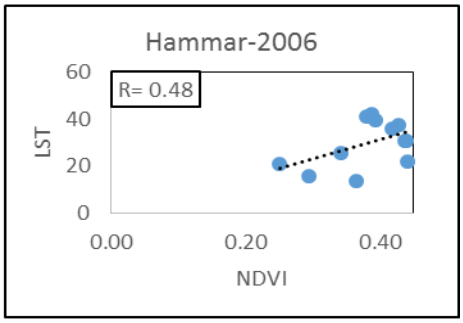

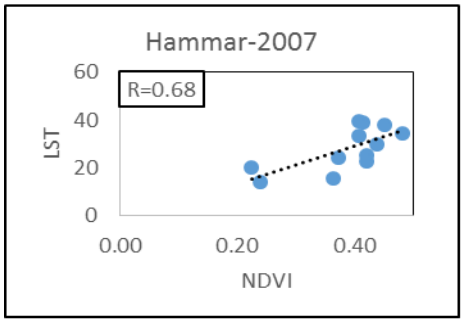

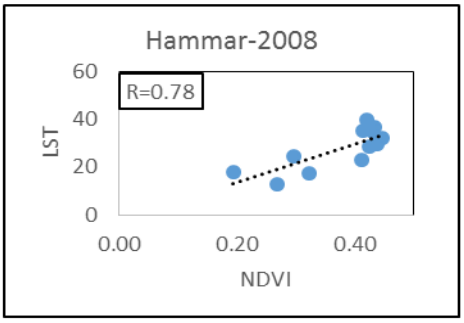

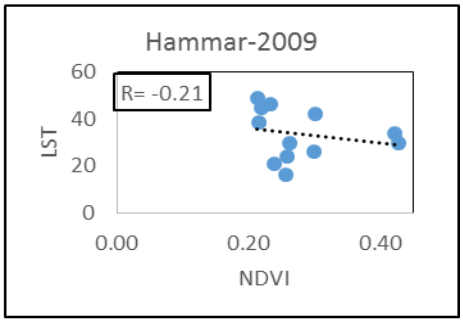

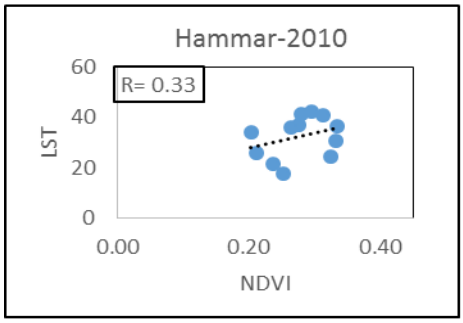

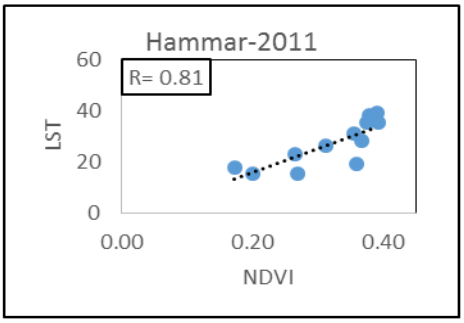

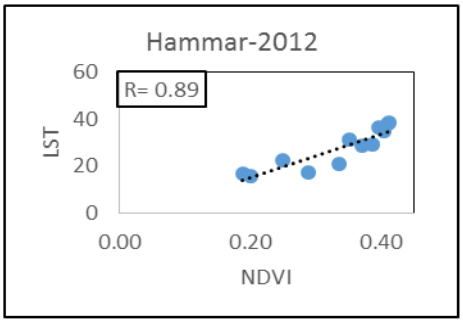

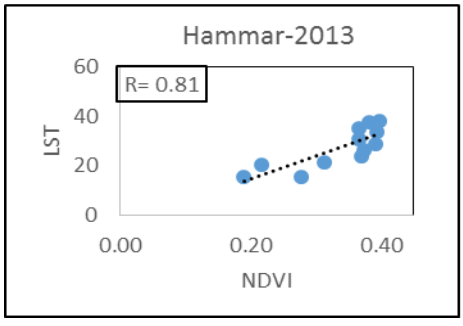

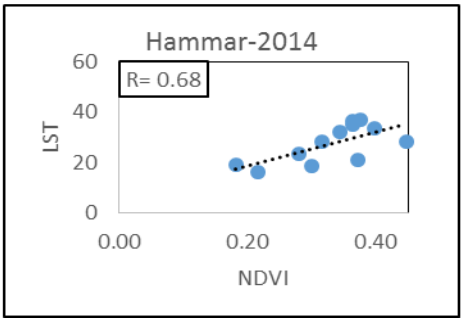

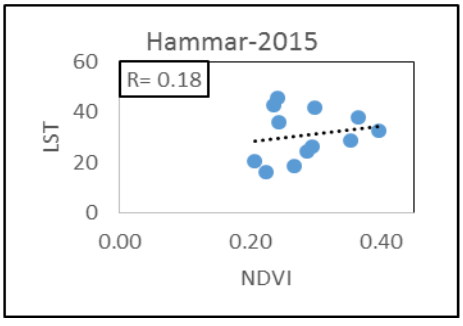

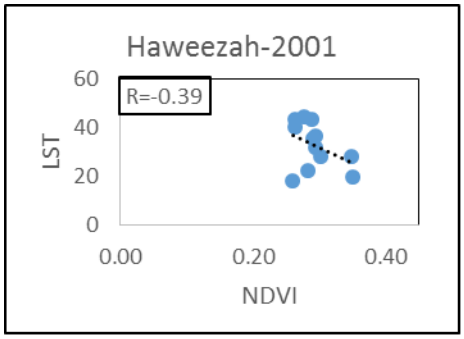
Haweezah-2001
R=-0.39
LST
NDVI
0
20
40
60
0.00
0.20
0.40

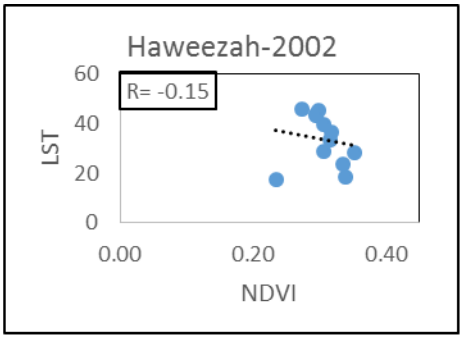
Haweezah-2002
R= -0.15
LST
NDVI
0
20
40
60
0.00
0.20
0.40

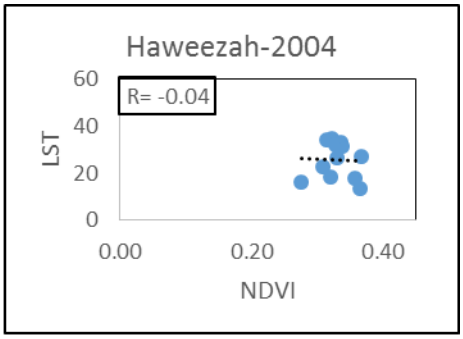
Haweezah-2004
R= -0.04
LST
NDVI
0
20
40
60
0.00
0.20
0.40

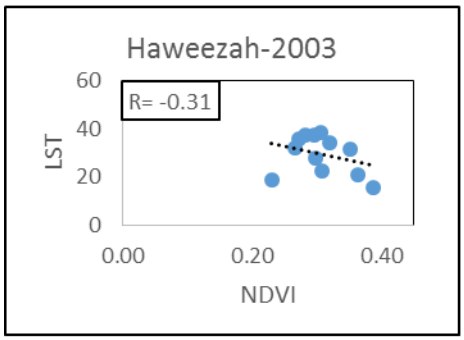
Haweezah-2003
R= -0.31
LST
NDVI
0
20
40
60
0.00
0.20
0.40

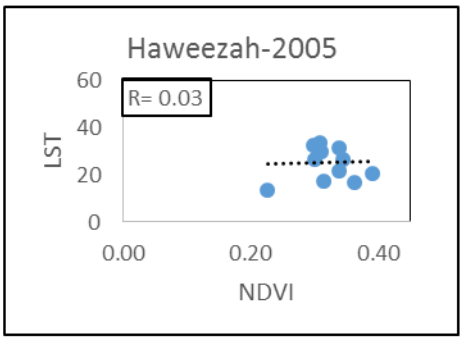
Haweezah-2005
R= 0.03
LST
NDVI
0
20
40
60
0.00
0.20
0.40

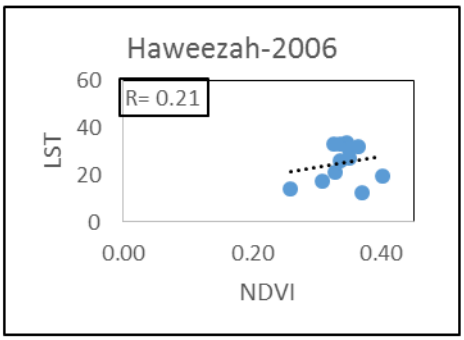
Haweezah-2006
R= 0.21
LST
NDVI
0
20
40
60
0.00
0.20
0.40

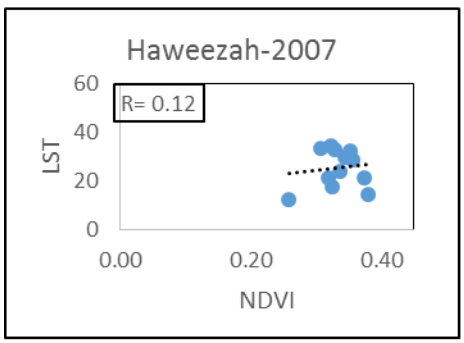
Haweezah-2007
R= 0.12
LST
NDVI
0
20
40
60
0.00
0.20
0.40

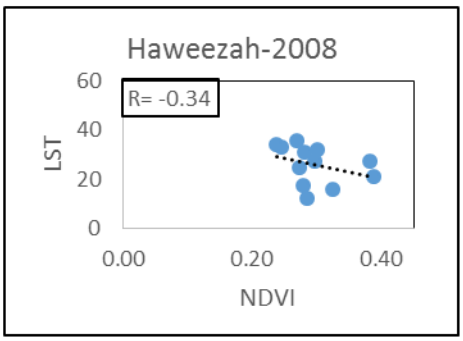
Haweezah-2008
R= -0.34
LST
NDVI
0
20
40
60
0.00
0.20
0.40

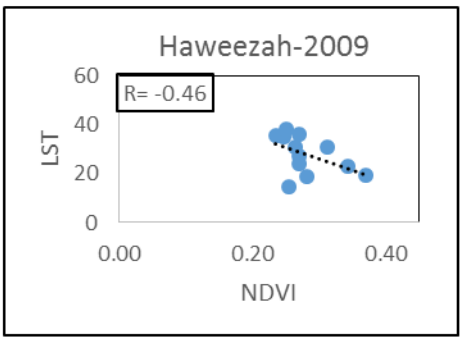
Haweezah-2009
R= -0.46
LST
NDVI
0
20
40
60
0.00
0.20
0.40

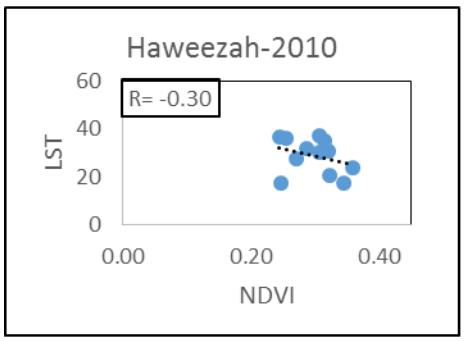
Haweezah-2010
R= -0.30
LST
NDVI
0
20
40
60
0.00
0.20
0.40

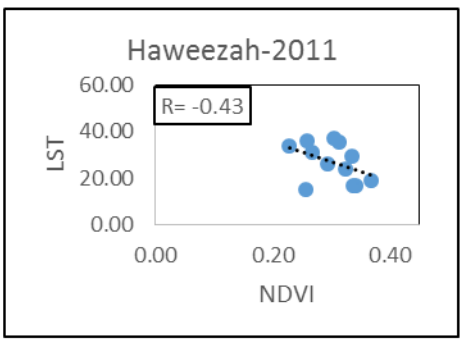
Haweezah-2011
R= -0.43
LST
NDVI
0.00
20.00
40.00
60.00
0.00
0.20
0.40

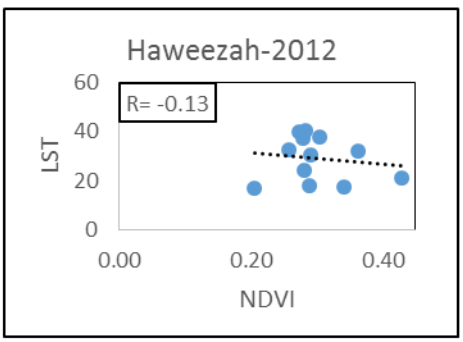
Haweezah-2012
R= -0.13
LST
NDVI
0
20
40
60
0.00
0.20
0.40

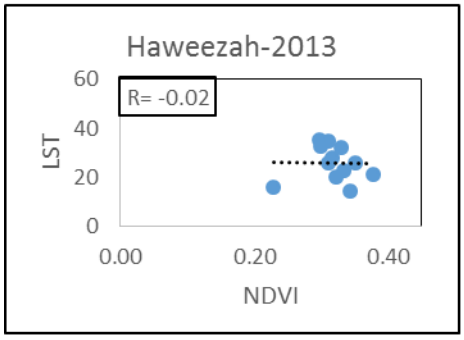
Haweezah-2013
R= -0.02
LST
NDVI
0
20
40
60
0.00
0.20
0.40

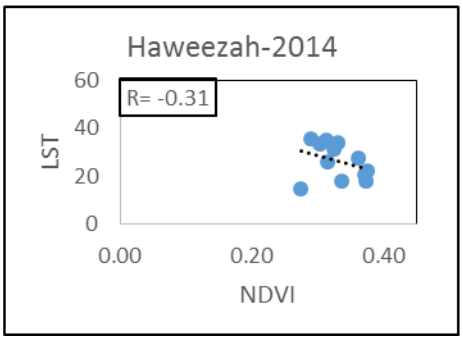
Haweezah-2014
R= -0.31
LST
NDVI
0
20
40
60
0.00
0.20
0.40

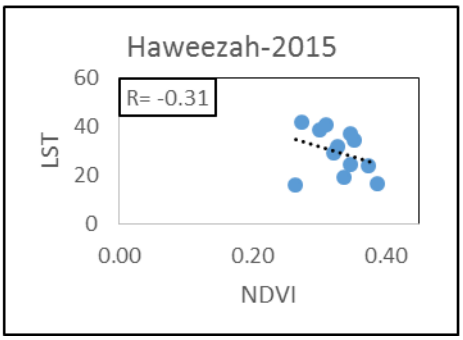
Haweezah-2015
R= -0.31
LST
NDVI
0
20
40
60
0.00
0.20
0.40

P-Values between NDVI and LST in Chibyish, Hammar and Haweezah marshes from 2001 to 2003

Year	P-Value (Chibyish)	P-Value (Hammar)	P-Value (Haweezah)
2001	0.000	0.000	0.195
2002	0.002	0.000	0.637
2003	0.000	0.063	0.312
2004	0.103	0.151	0.882
2005	0.015	0.126	0.920
2006	0.140	0.103	0.503
2007	0.003	0.011	0.691
2008	0.666	0.002	0.260
2009	0.032	0.498	0.120
2010	0.000	0.282	0.323
2011	0.368	0.001	0.155
2012	0.855	0.000	0.673
2013	0.727	0.001	0.934
2014	0.435	0.011	0.308
2015	0.661	0.569	0.317

A spatial correlation analyses between NDVI and LST over desert region

Year	Site (1)	Site (2)	Site (3)	Site (4)	Site (5)	Site (10)
2001	-0.39	-0.28	-0.51	-0.43	-0.74	-0.54
2002	-0.85	-0.10	-0.53	-0.20	-0.62	-0.49
2003	-0.74	-0.59	0.09	0.14	-0.30	-0.68
2004	0.10	0.16	-0.38	-0.49	-0.59	-0.31
2005	-0.45	0.33	-0.02	-0.10	-0.51	-0.35
2006	-0.07	0.17	-0.46	-0.06	-0.51	-0.47
2007	-0.36	0.61	0.15	0.32	-0.13	-0.47
2008	0.04	0.86	0.78	0.52	-0.04	-0.08
2009	0.59	0.70	0.71	0.88	0.69	-0.41
2010	0.63	0.72	0.72	0.87	0.73	-0.66
2011	0.33	0.42	0.64	0.77	0.76	0.02
2012	0.82	0.73	0.87	0.94	0.73	0.53
2013	0.68	0.73	0.46	0.94	-0.68	-0.37
2014	0.50	-0.16	-0.43	-0.33	-0.61	-0.61
2015	-0.04	-0.68	-0.27	-0.52	-0.67	-0.86

A spatial correlation analyses between NDVI and LST over rangeland region

Year	Site (16)	Site (20)	Site (21)	Site (14)	Site (23)
2001	-0.71	-0.62	-0.70	-0.91	-0.58
2002	-0.71	-0.58	-0.95	-0.92	-0.71
2003	-0.64	-0.89	-0.88	-0.77	-0.84
2004	-0.10	-0.76	-0.88	-0.74	-0.84
2005	0.04	-0.18	-0.71	-0.69	-0.66
2006	0.43	-0.43	-0.51	-0.76	-0.57
2007	0.22	-0.84	-0.71	-0.49	-0.63
2008	-0.44	-0.71	-0.56	-0.67	-0.82
2009	-0.29	-0.52	-0.55	-0.76	-0.84
2010	-0.21	-0.24	-0.61	-0.66	-0.71
2011	0.12	-0.60	-0.10	-0.60	-0.46
2012	-0.51	-0.58	-0.84	-0.73	-0.83
2013	0.49	-0.72	-0.29	-0.86	---
2014	-0.09	-0.65	-0.64	-0.51	-0.71
2015	0.10	-0.83	-0.83	-0.73	-0.84

A spatial correlation analyses between NDVI and LST over agricultural region

Year	Site (15)	Site (17)	Site (18)	Site (19)	Site (22)	Site (6)	Site (7)	Site (8)	Site (9)
2001	-0.66	-0.02	-0.69	-0.71	-0.81	-0.82	-0.27	-0.58	0.41
2002	-0.91	0.35	-0.65	-0.94	-0.95	-0.87	0.38	-0.20	0.76
2003	-0.83	-0.25	-0.90	-0.84	-0.92	-0.61	-0.03	-0.28	0.79
2004	-0.73	0.45	-0.29	-0.78	-0.74	-0.51	0.46	0.34	0.73
2005	-0.80	0.35	-0.36	-0.60	-0.72	-0.46	0.23	0.10	0.83
2006	-0.90	0.50	-0.41	-0.49	-0.60	-0.16	0.49	0.34	0.73
2007	-0.69	-0.07	-0.45	-0.57	-0.64	-0.37	0.14	0.04	0.81
2008	-0.93	0.12	-0.59	-0.38	-0.69	-0.64	-0.32	-0.26	0.63
2009	-0.79	-0.03	-0.54	-0.49	-0.62	-0.84	-0.81	-0.76	-0.90
2010	-0.74	0.04	-0.71	-0.75	-0.83	-0.68	-0.33	-0.40	-0.04
2011	-0.68	-0.11	-0.44	-0.71	-0.70	-0.80	-0.73	-0.67	-0.49
2012	-0.82	-0.23	-0.68	-0.84	-0.81	-0.47	-0.34	-0.37	0.44
2013	-0.70	0.01	-0.66	-0.53	-0.75	-0.70	-0.42	-0.34	0.70
2014	-0.74	0.16	-0.70	-0.66	-0.87	-0.83	-0.24	-0.12	0.60
2015	-0.76	-0.09	-0.85	-0.86	-0.94	-0.73	-0.43	-0.55	0.28

APPENDIX E: Spatiotemporal variability in soil moisture contents (SMOS) and NDVI in Iraq during (2010-2015).

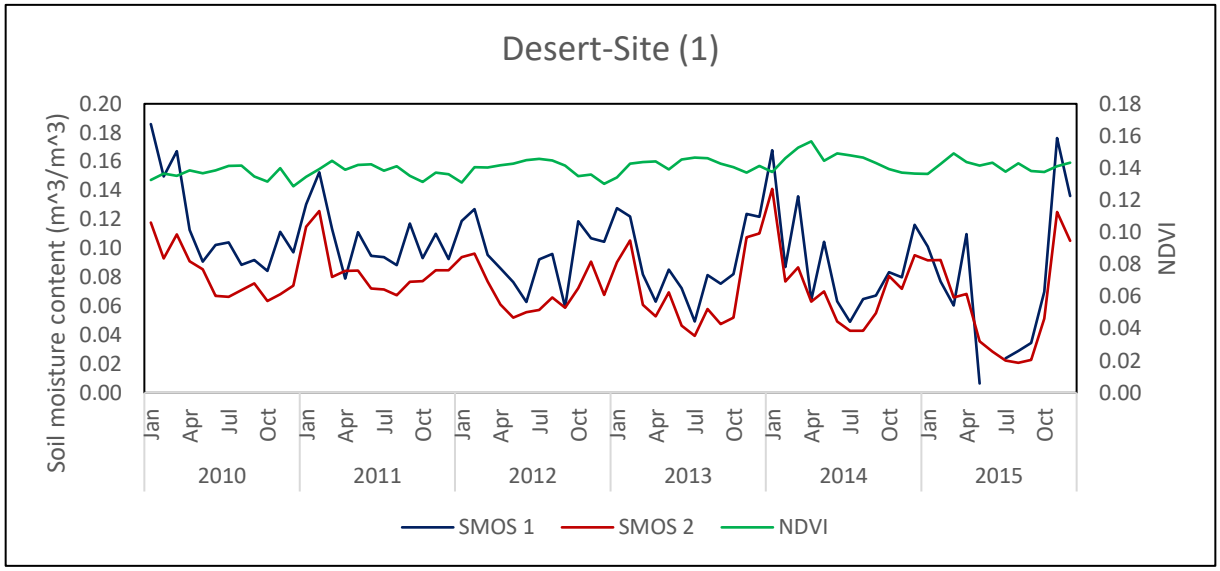

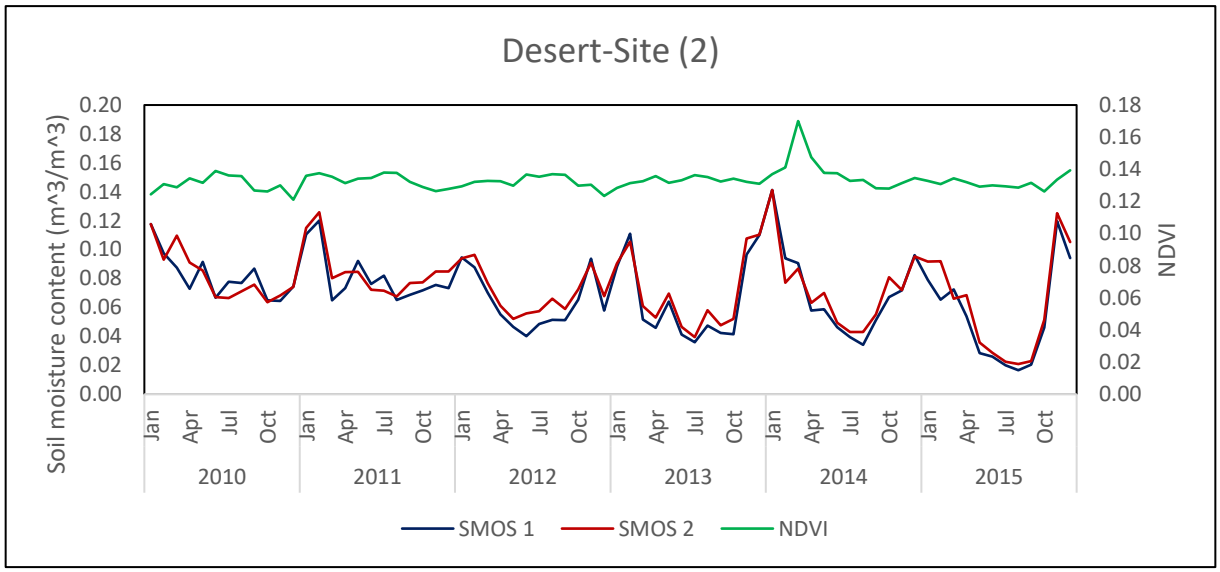

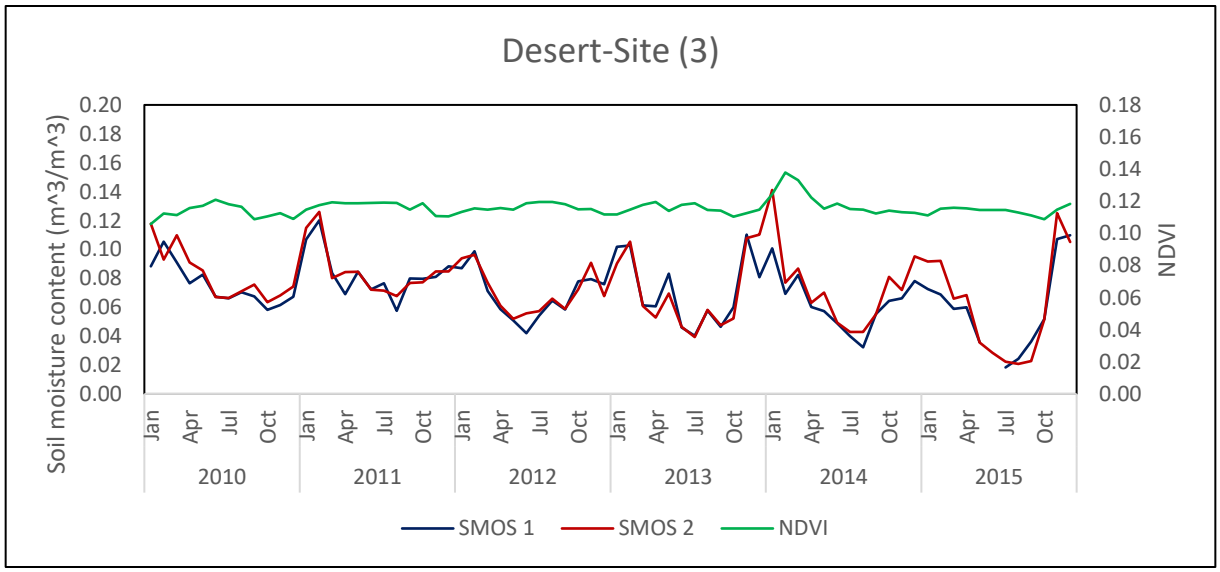

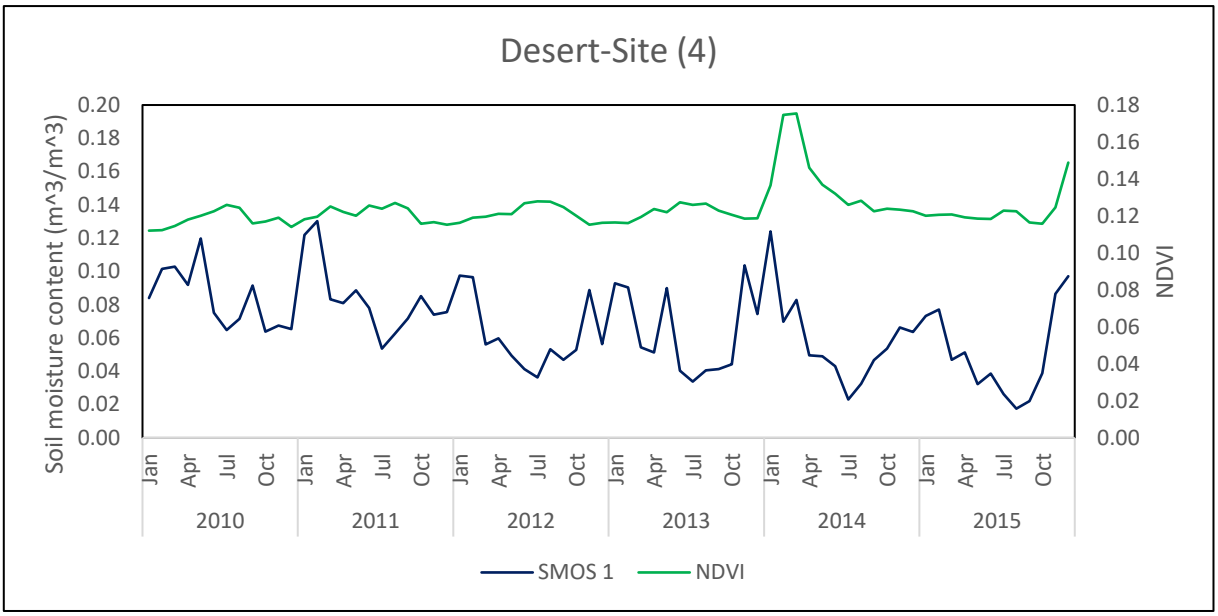
Desert-Site (4)
Soil moisture content (m^3/m^3)
NDVI
0.20
0.18
0.16
0.14
0.12
0.10
0.08
0.06
0.04
0.02
0.00
Jan Apr Jul Oct
2010 2011 2012 2013 2014 2015
SMOS 1
NDVI

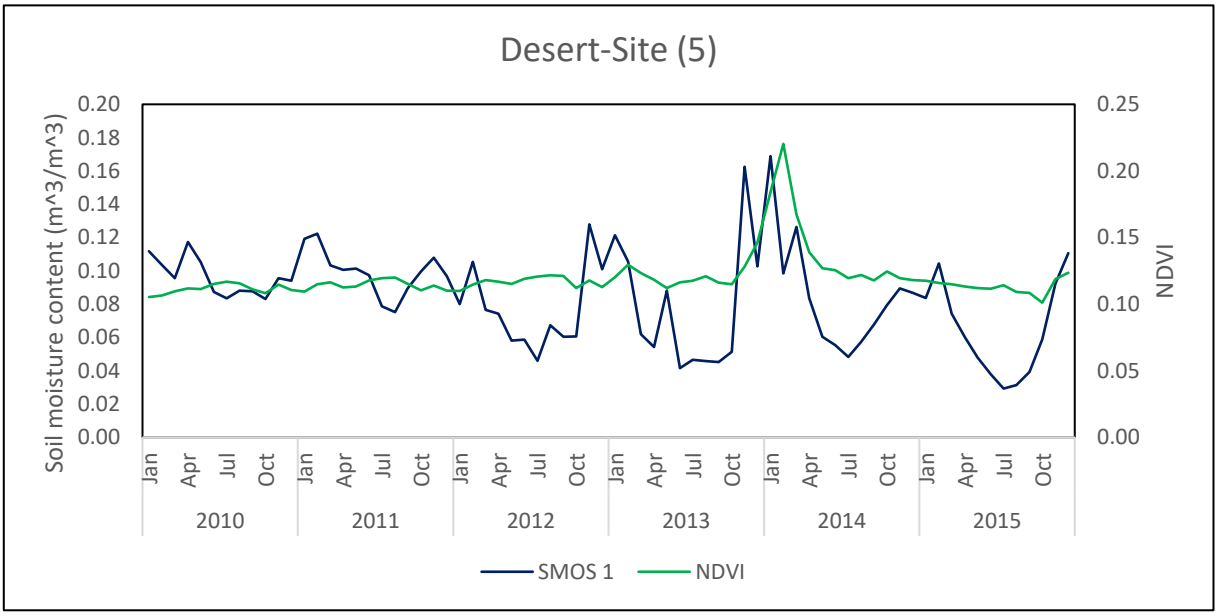
Desert-Site (5)
Soil moisture content (m^3/m^3)
NDVI
0.25
0.20
0.15
0.10
0.05
0.00
Jan Apr Jul Oct
2010 2011 2012 2013 2014 2015
SMOS 1
NDVI

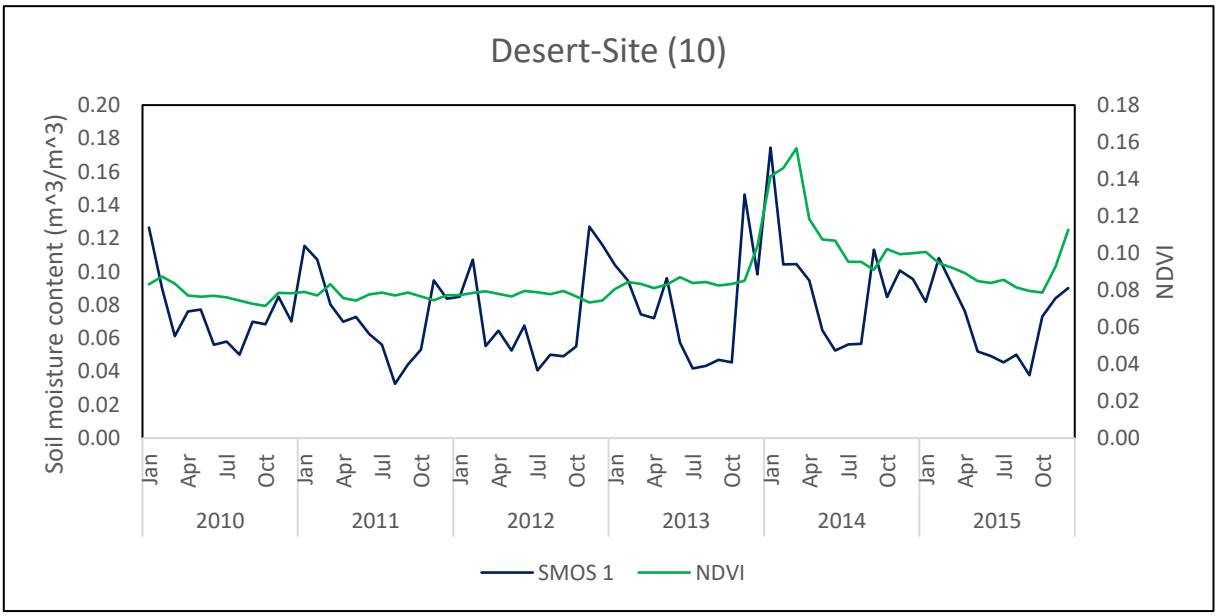
Desert-Site (10)
Soil moisture content (m^3/m^3)
NDVI
Jan Apr Jul Oct
2010 2011 2012 2013 2014 2015
SMOS 1
NDVI

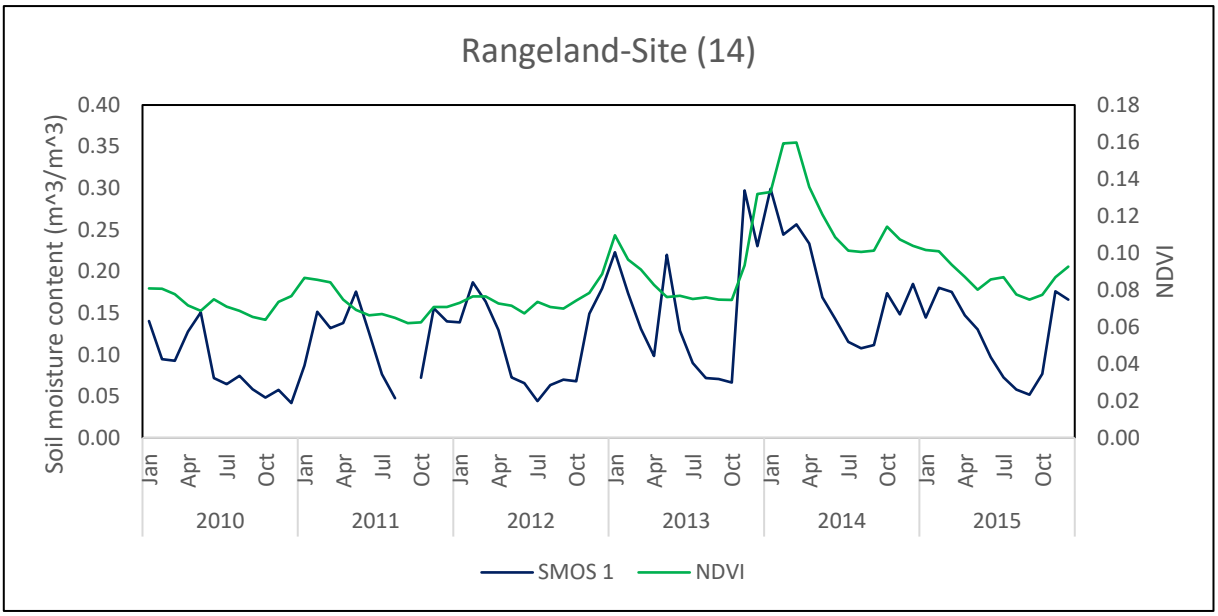
Rangeland-Site (14)
Soil moisture content (m^3/m^3)
NDVI
0.40
0.35
0.30
0.25
0.20
0.15
0.10
0.05
0.00
0.18
0.16
0.14
0.12
0.10
0.08
0.06
0.04
0.02
0.00
Jan Apr Jul Oct
2010
2011
2012
2013
2014
2015
SMOS 1
NDVI

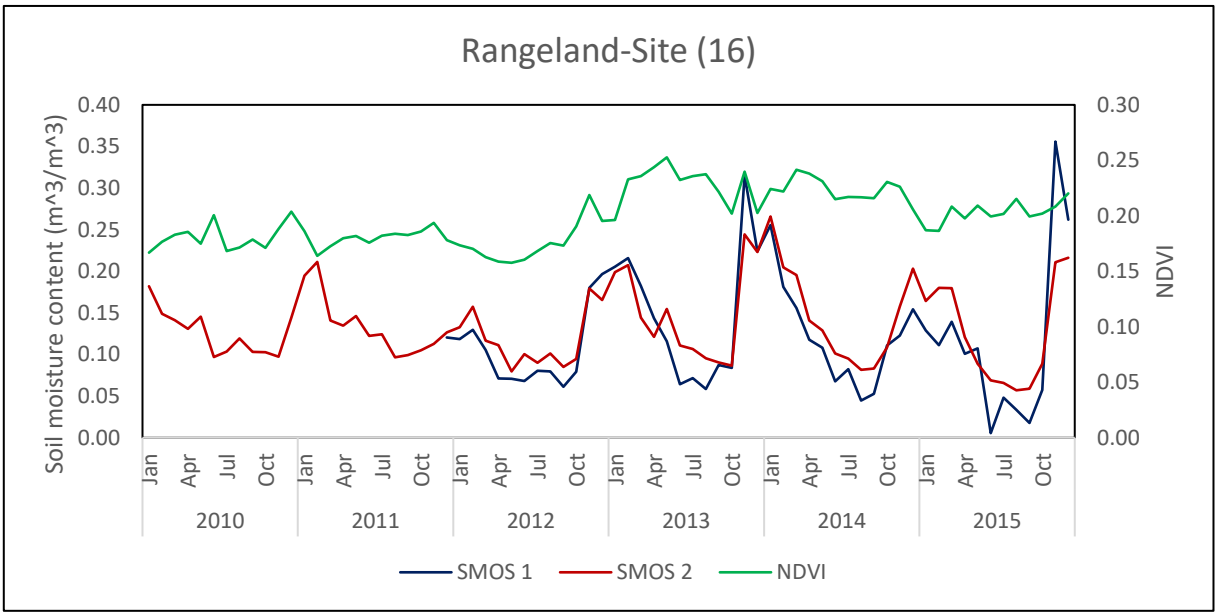
Rangeland-Site (16)
Soil moisture content (m^3/m^3)
NDVI
0.40
0.35
0.30
0.25
0.20
0.15
0.10
0.05
0.00
0.30
0.25
0.20
0.15
0.10
0.05
0.00
Jan Apr Jul Oct
2010
2011
2012
2013
2014
2015
SMOS 1
SMOS 2
NDVI

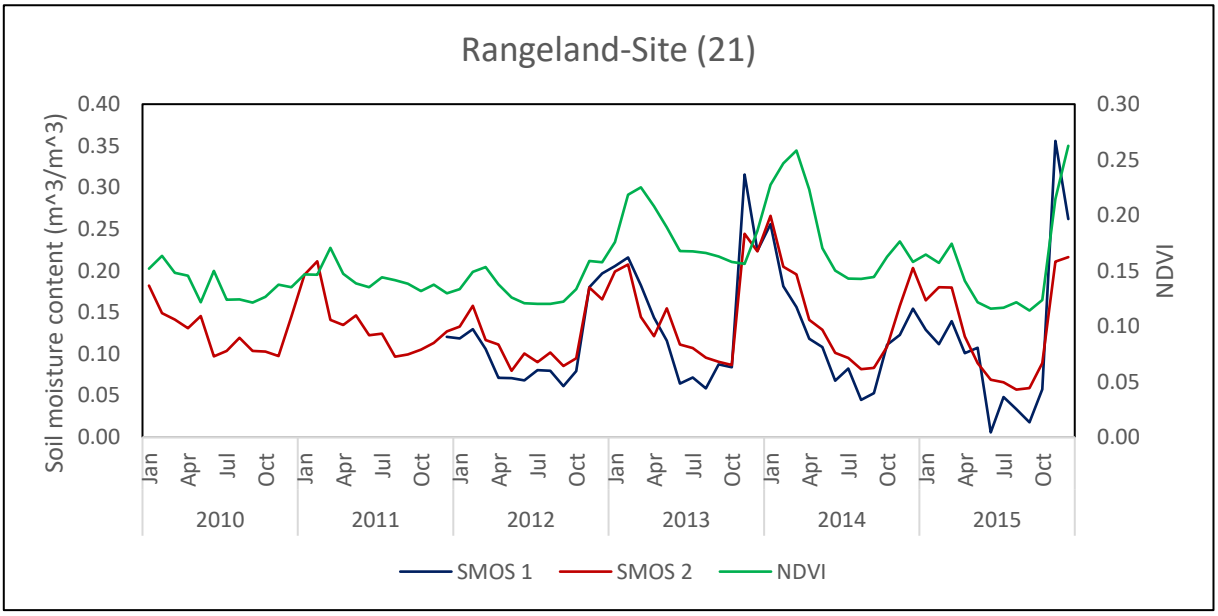
Rangeland-Site (21)
Soil moisture content (m^3/m^3)
NDVI
0.40
0.35
0.30
0.25
0.20
0.15
0.10
0.05
0.00
0.30
0.25
0.20
0.15
0.10
0.05
0.00
Jan Apr Jul Oct
2010
2011
2012
2013
2014
2015
SMOS 1
SMOS 2
NDVI

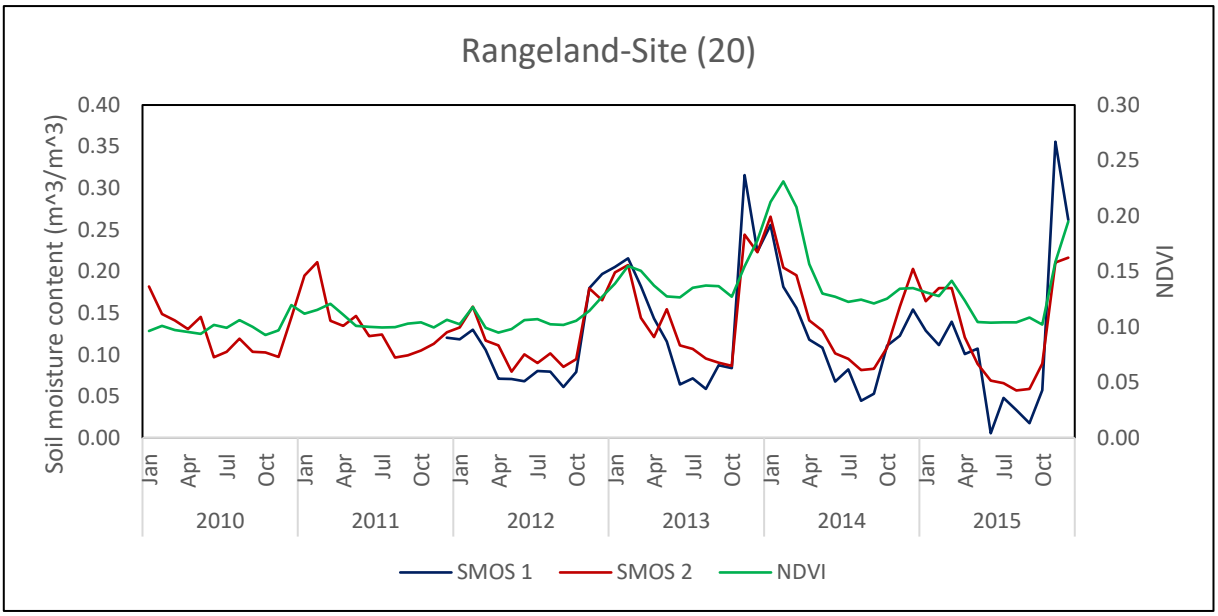
Rangeland-Site (20)
Soil moisture content (m^3/m^3)
NDVI
0.40
0.35
0.30
0.25
0.20
0.15
0.10
0.05
0.00
Jan
Apr
Jul
Oct
2010
2011
2012
2013
2014
2015
SMOS 1
SMOS 2
NDVI

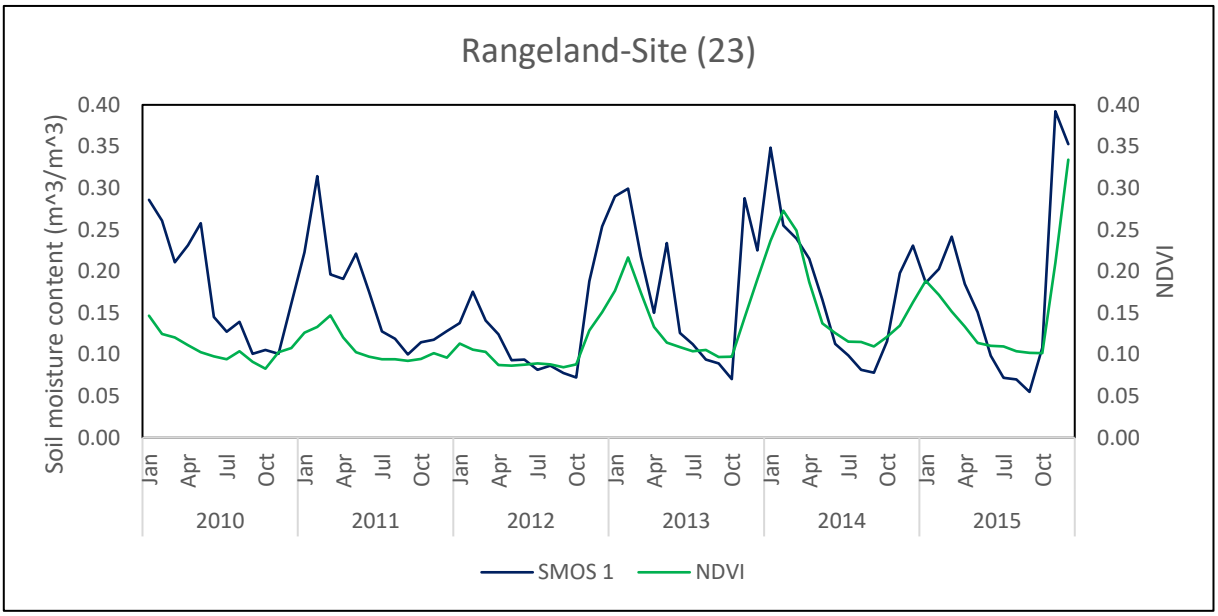
Rangeland-Site (23)
Soil moisture content (m^3/m^3)
NDVI
0.40
0.35
0.30
0.25
0.20
0.15
0.10
0.05
0.00
Jan
Apr
Jul
Oct
2010
2011
2012
2013
2014
2015
SMOS 1
NDVI

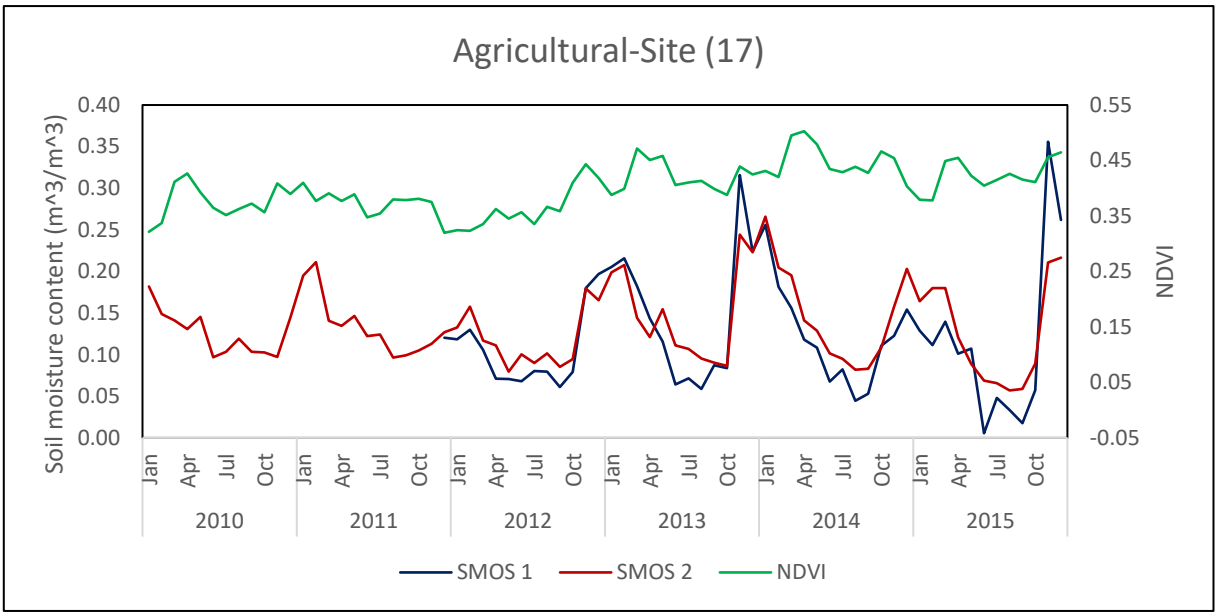
Agricultural-Site (17)
Soil moisture content (m^3/m^3)
0.40
0.35
0.30
0.25
0.20
0.15
0.10
0.05
0.00
0.55
0.45
0.35
0.25
0.15
0.05
-0.05
NDVI
Jan Apr Jul Oct Jan Apr Jul Oct Jan Apr Jul Oct Jan Apr Jul Oct Jan Apr Jul Oct Jan Apr Jul Oct
2010 2011 2012 2013 2014 2015
SMOS 1
SMOS 2
NDVI

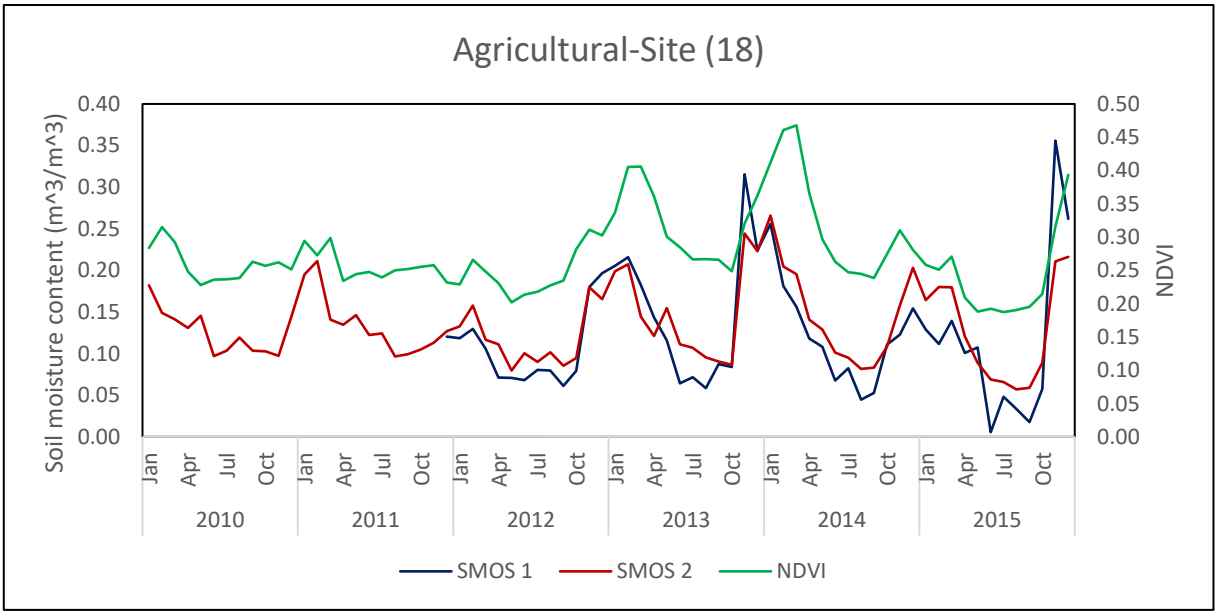
Agricultural-Site (18)
Soil moisture content (m^3/m^3)
0.40
0.35
0.30
0.25
0.20
0.15
0.10
0.05
0.00
0.50
0.45
0.40
0.35
0.30
0.25
0.20
0.15
0.10
0.05
0.00
NDVI
Jan Apr Jul Oct Jan Apr Jul Oct Jan Apr Jul Oct Jan Apr Jul Oct Jan Apr Jul Oct Jan Apr Jul Oct
2010 2011 2012 2013 2014 2015
SMOS 1
SMOS 2
NDVI

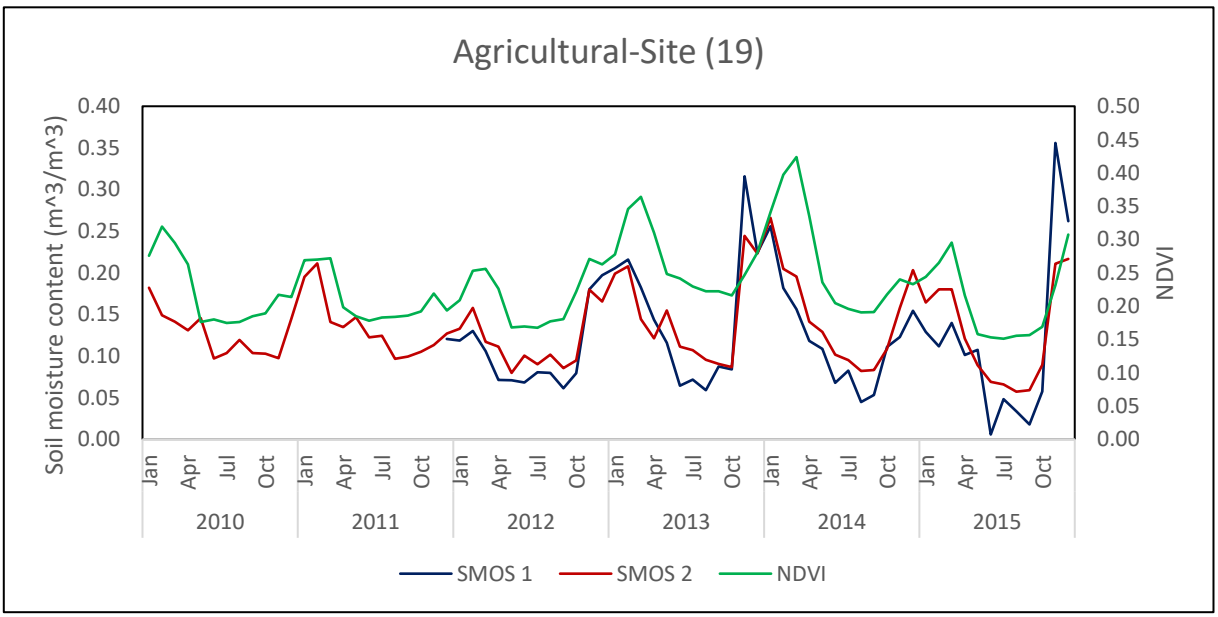
Agricultural-Site (19)
Soil moisture content (m^3/m^3)
0.40
0.35
0.30
0.25
0.20
0.15
0.10
0.05
0.00
0.50
0.45
0.40
0.35
0.30
0.25
0.20
0.15
0.10
0.05
0.00
NDVI
Jan Apr Jul Oct Jan Apr Jul Oct Jan Apr Jul Oct Jan Apr Jul Oct Jan Apr Jul Oct Jan Apr Jul Oct
2010 2011 2012 2013 2014 2015
SMOS 1
SMOS 2
NDVI

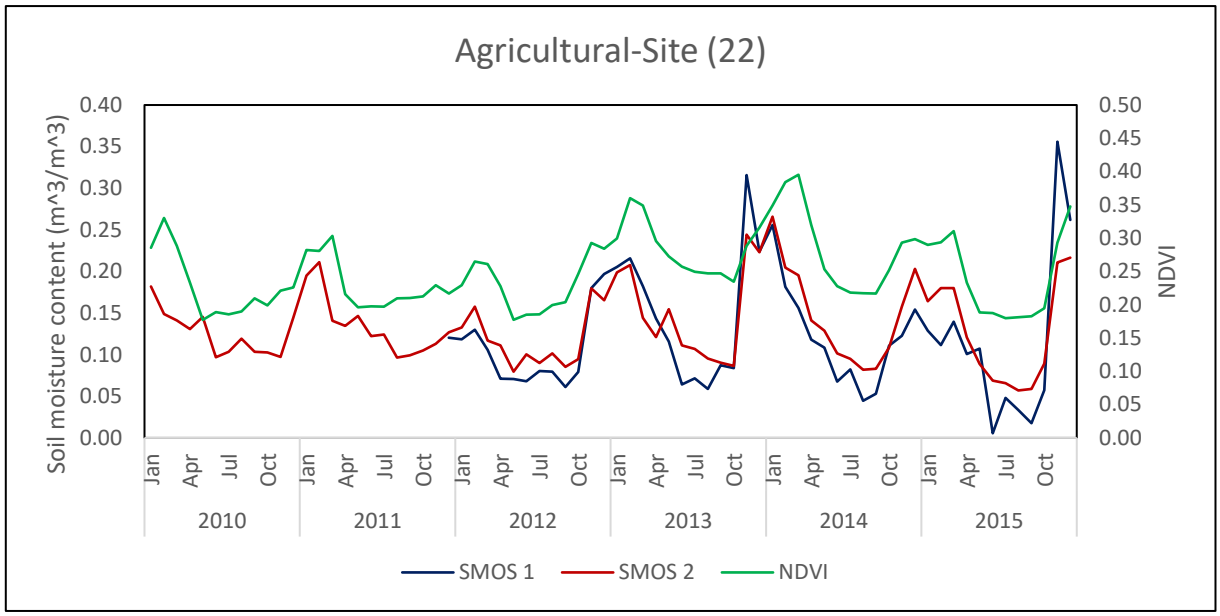
Agricultural-Site (22)
Soil moisture content (m^3/m^3)
NDVI
0.40
0.35
0.30
0.25
0.20
0.15
0.10
0.05
0.00
0.50
0.45
0.40
0.35
0.30
0.25
0.20
0.15
0.10
0.05
0.00
Jan Apr Jul Oct
2010
2011
2012
2013
2014
2015
SMOS 1
SMOS 2
NDVI

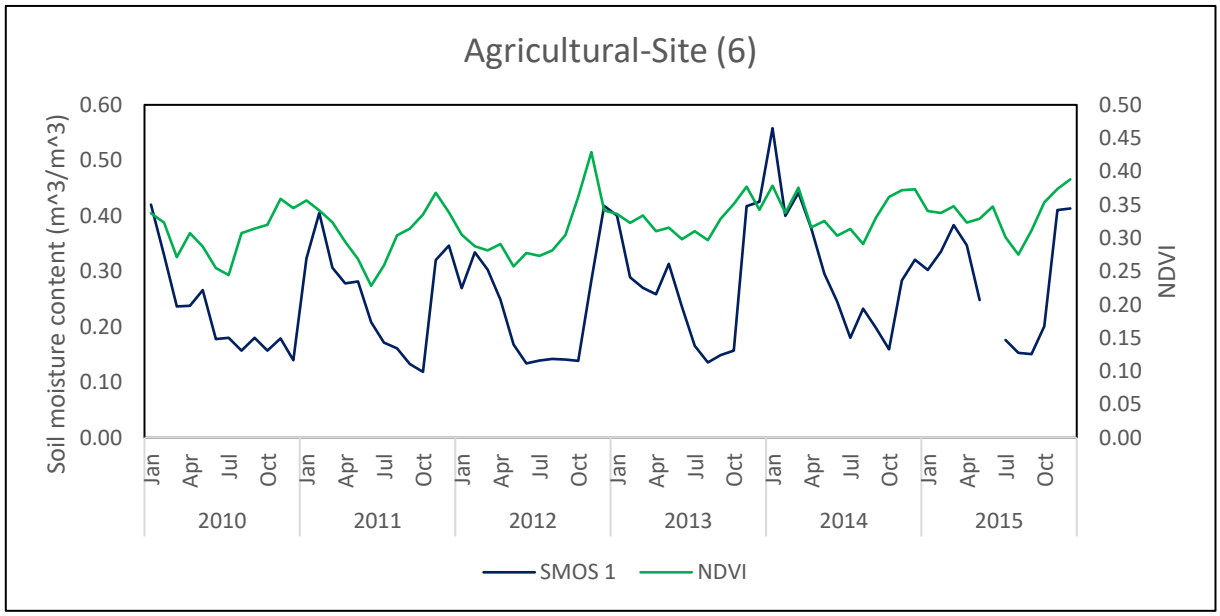
Agricultural-Site (6)
Soil moisture content (m^3/m^3)
NDVI
0.60
0.50
0.40
0.30
0.20
0.10
0.00
0.50
0.45
0.40
0.35
0.30
0.25
0.20
0.15
0.10
0.05
0.00
Jan Apr Jul Oct
2010
2011
2012
2013
2014
2015
SMOS 1
NDVI

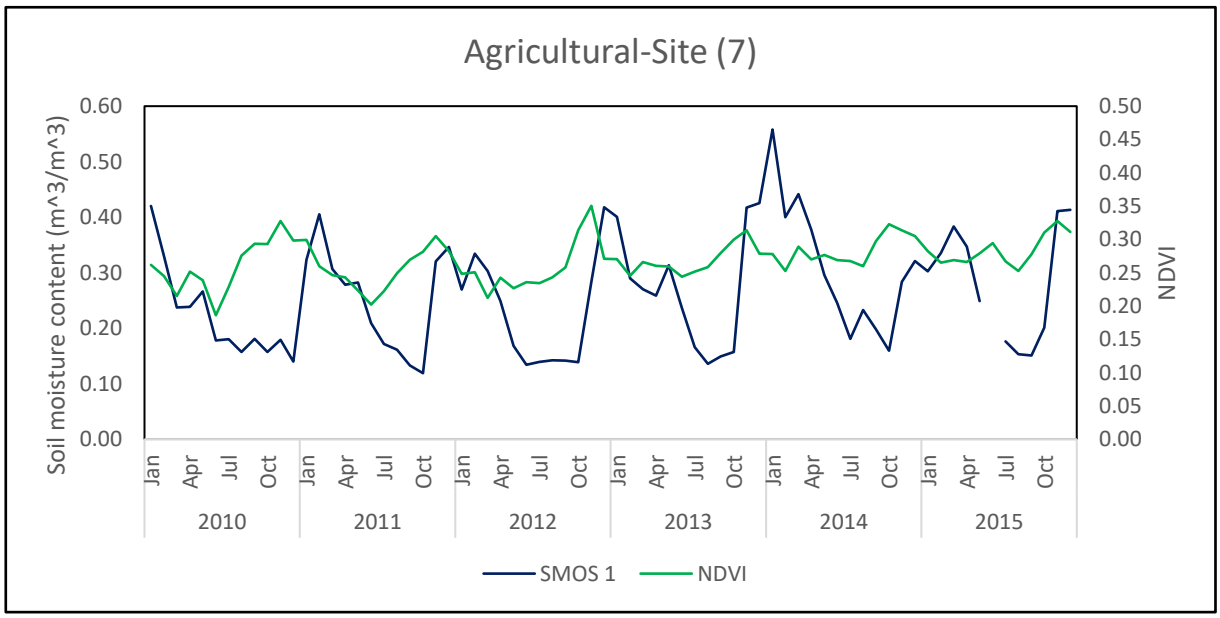
Agricultural-Site (7)
Soil moisture content (m^3/m^3)
NDVI
0.60
0.50
0.40
0.30
0.20
0.10
0.00
0.50
0.45
0.40
0.35
0.30
0.25
0.20
0.15
0.10
0.05
0.00
Jan Apr Jul Oct
2010
2011
2012
2013
2014
2015
SMOS 1
NDVI

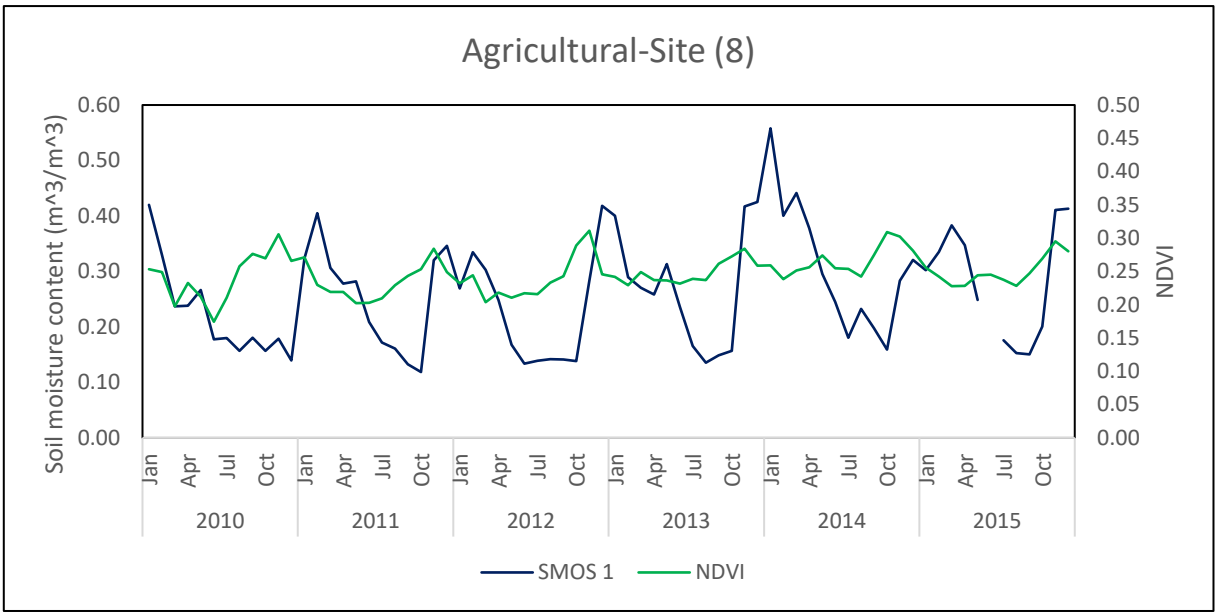
Agricultural-Site (8)
Soil moisture content (m^3/m^3)
NDVI
0.60
0.50
0.40
0.30
0.20
0.10
0.00
0.50
0.45
0.40
0.35
0.30
0.25
0.20
0.15
0.10
0.05
0.00
Jan Apr Jul Oct
2010
2011
2012
2013
2014
2015
SMOS 1
NDVI

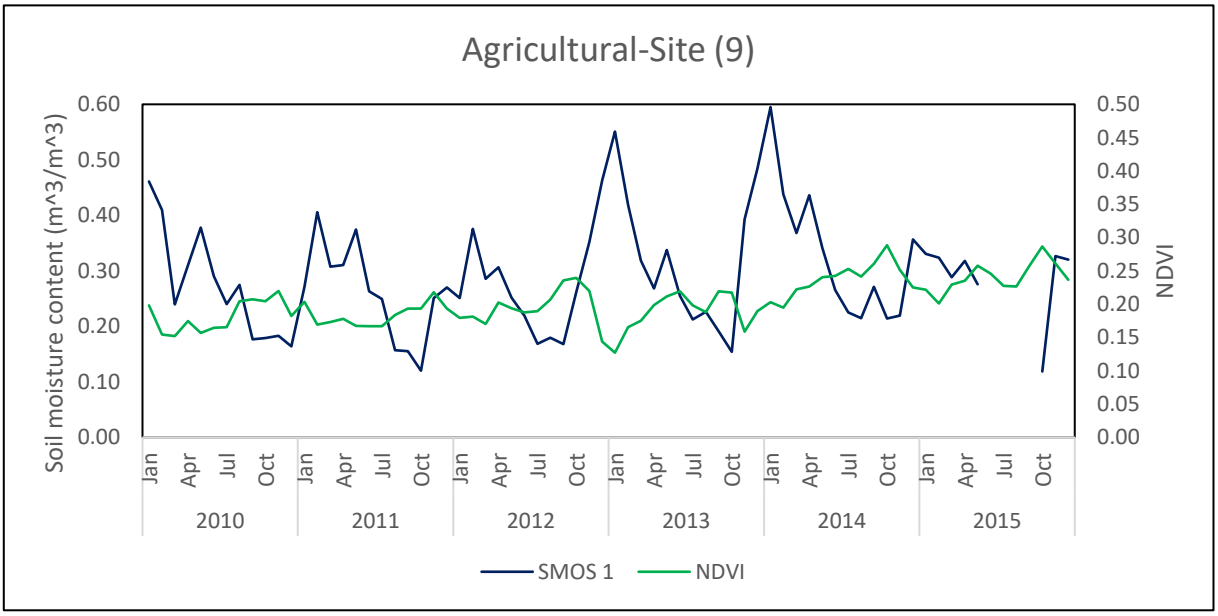
Agricultural-Site (9)
Soil moisture content (m^3/m^3)
NDVI
0.60
0.50
0.40
0.30
0.20
0.10
0.00
0.50
0.45
0.40
0.35
0.30
0.25
0.20
0.15
0.10
0.05
0.00
Jan Apr Jul Oct
2010
2011
2012
2013
2014
2015
SMOS 1
NDVI

APPENDIX F: Interannual and seasonal variation in the SLHF as obtained from ERA-Interim and measured data, with NDVI throughout desert, rangeland, agricultural, and marshes sites

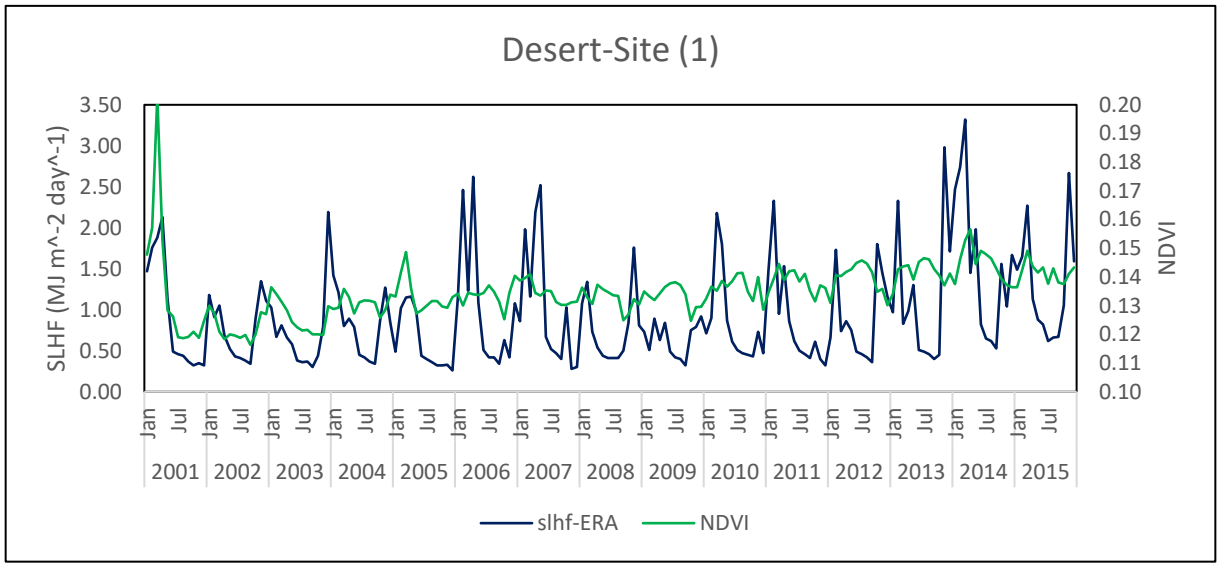

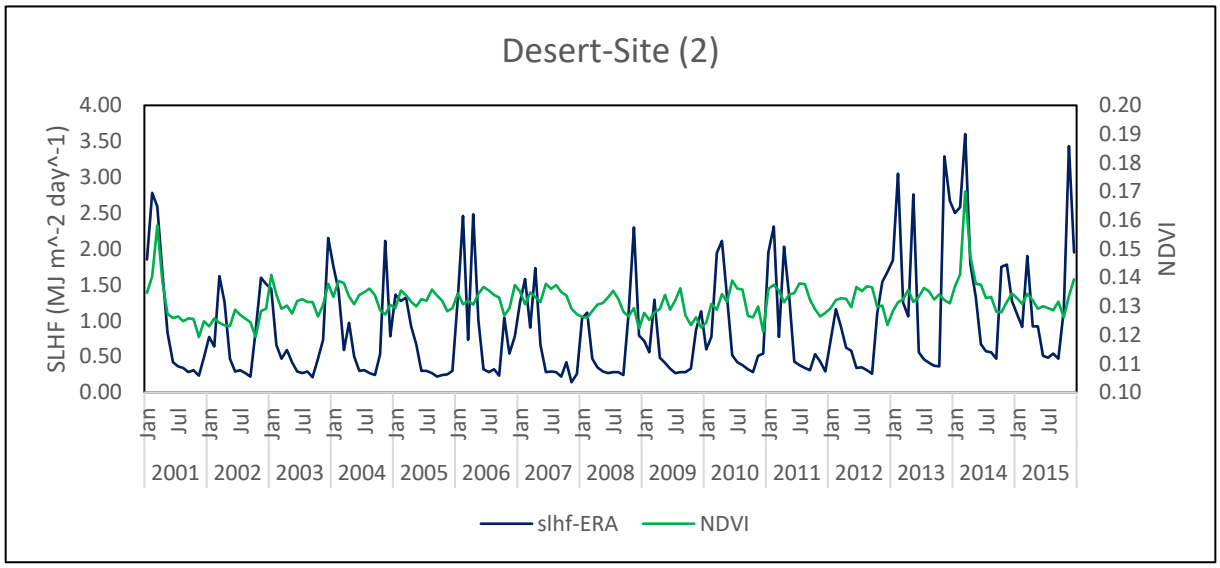

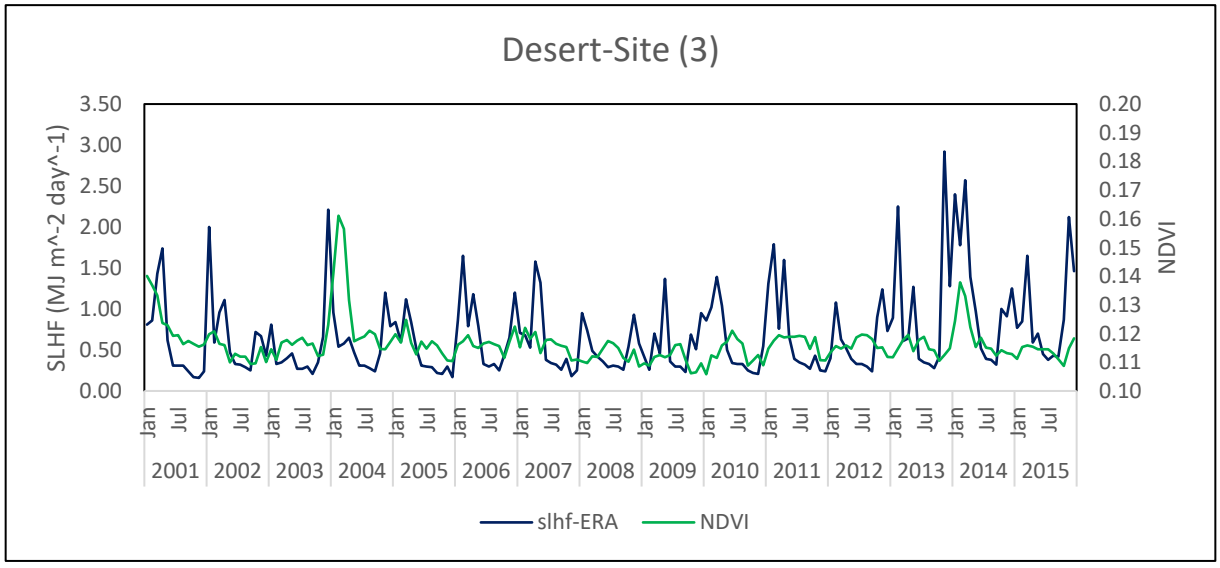

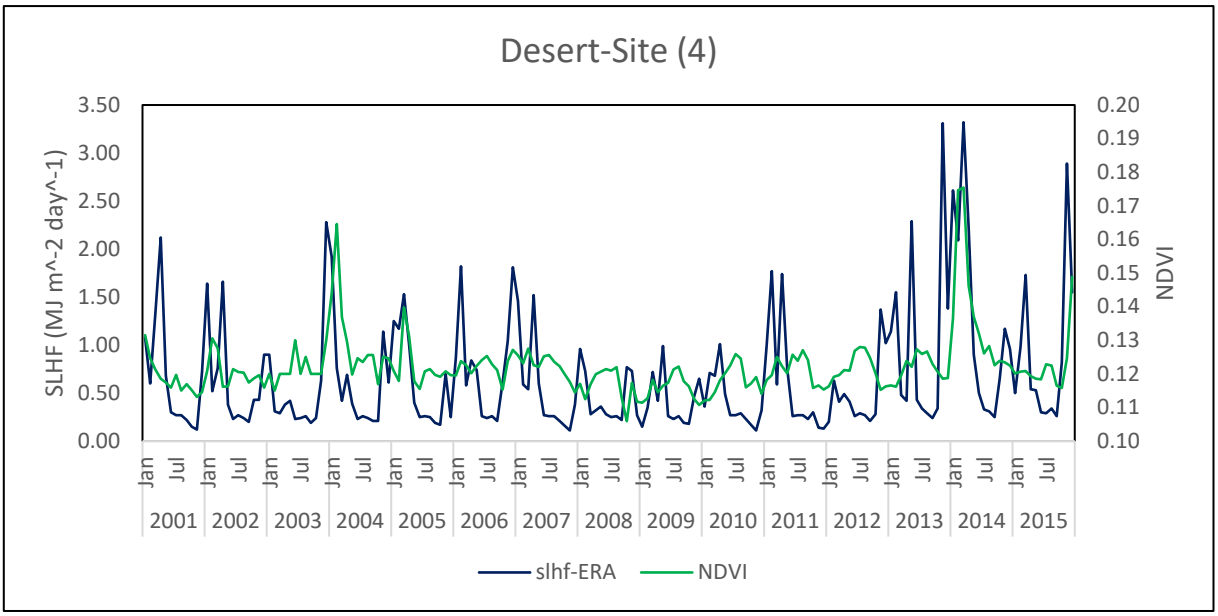
Desert-Site (4)
SLHF (MJ m^-2 day^-1)
NDVI
3.50
3.00
2.50
2.00
1.50
1.00
0.50
0.00
0.20
0.19
0.18
0.17
0.16
0.15
0.14
0.13
0.12
0.11
0.10
Jan Jul
2001 2002 2003 2004 2005 2006 2007 2008 2009 2010 2011 2012 2013 2014 2015
slhf-ERA
NDVI

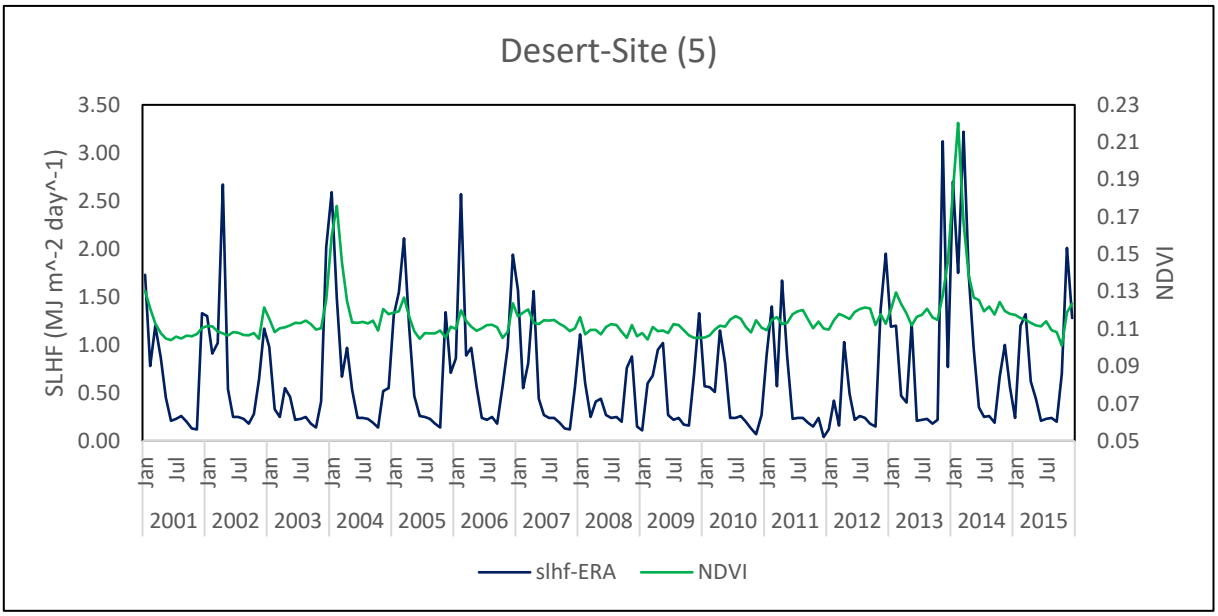
Desert-Site (5)
SLHF (MJ m^-2 day^-1)
NDVI
3.50
3.00
2.50
2.00
1.50
1.00
0.50
0.00
0.23
0.21
0.19
0.17
0.15
0.13
0.11
0.09
0.07
0.05
Jan Jul
2001 2002 2003 2004 2005 2006 2007 2008 2009 2010 2011 2012 2013 2014 2015
slhf-ERA
NDVI

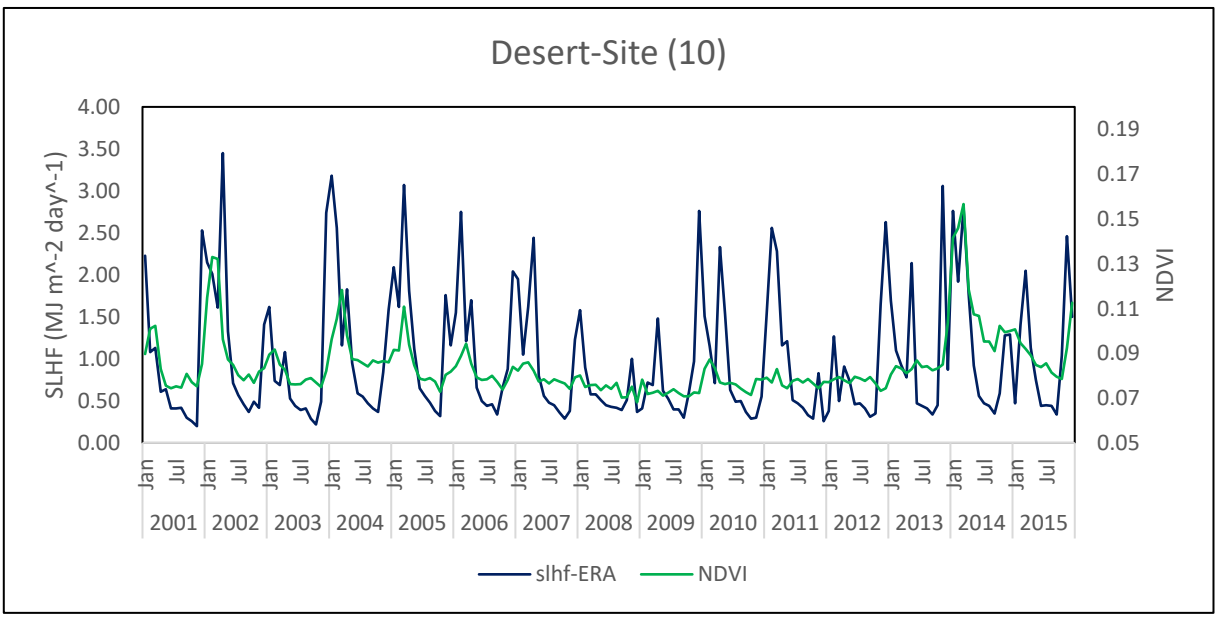
Desert-Site (10)
SLHF (MJ m^-2 day^-1)
NDVI
4.00
3.50
3.00
2.50
2.00
1.50
1.00
0.50
0.00
0.19
0.17
0.15
0.13
0.11
0.09
0.07
0.05
Jan Jul
2001 2002 2003 2004 2005 2006 2007 2008 2009 2010 2011 2012 2013 2014 2015
slhf-ERA
NDVI

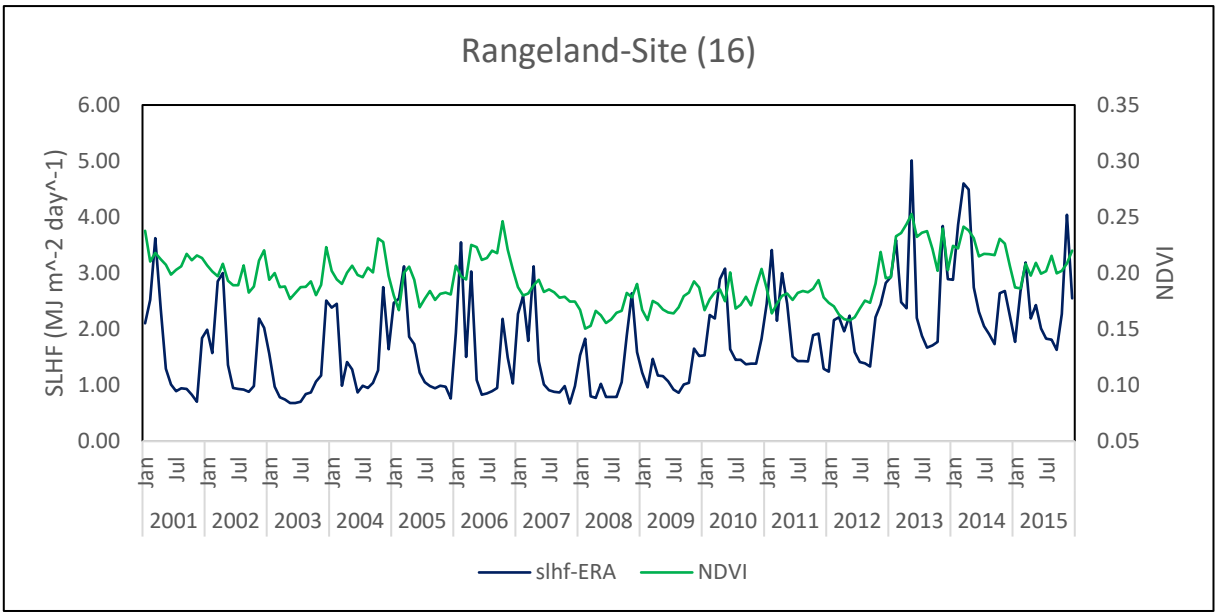
Rangeland-Site (16)
SLHF (MJ m^-2 day^-1)
NDVI
6.00
5.00
4.00
3.00
2.00
1.00
0.00
0.35
0.30
0.25
0.20
0.15
0.10
0.05
Jan Jul Jan Jul Jan Jul Jan Jul Jan Jul Jan Jul Jan Jul Jan Jul Jan Jul Jan Jul Jan Jul Jan Jul Jan Jul Jan Jul Jan Jul Jan Jul
2001 2002 2003 2004 2005 2006 2007 2008 2009 2010 2011 2012 2013 2014 2015
slhf-ERA
NDVI

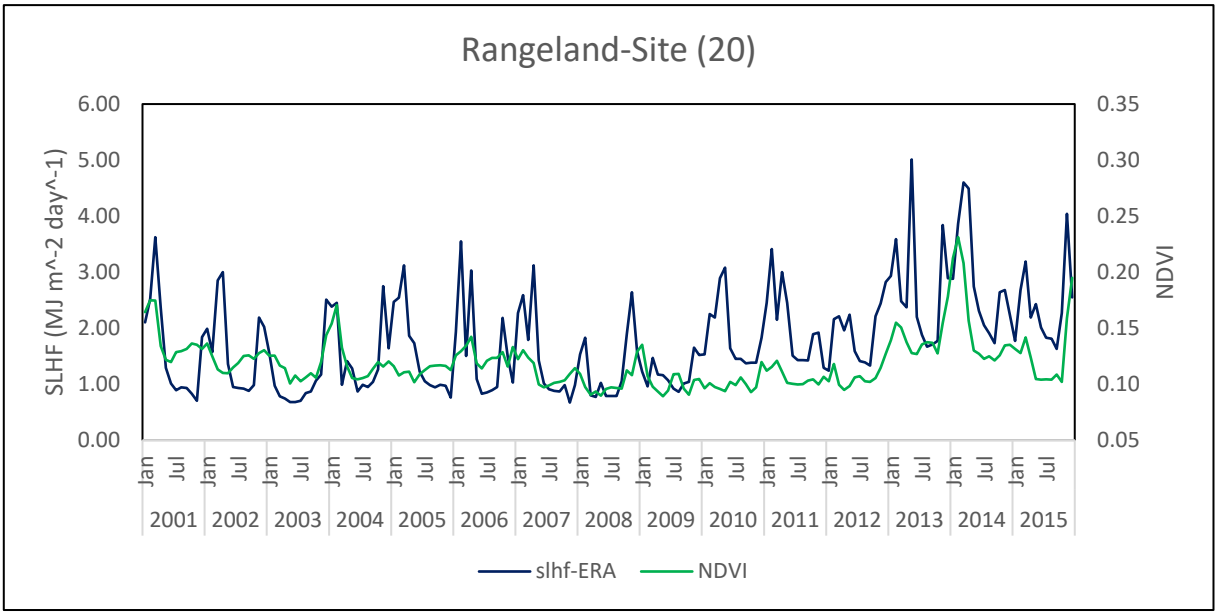
Rangeland-Site (20)
SLHF (MJ m^-2 day^-1)
NDVI
6.00
5.00
4.00
3.00
2.00
1.00
0.00
0.35
0.30
0.25
0.20
0.15
0.10
0.05
Jan Jul Jan Jul Jan Jul Jan Jul Jan Jul Jan Jul Jan Jul Jan Jul Jan Jul Jan Jul Jan Jul Jan Jul Jan Jul Jan Jul Jan Jul Jan Jul
2001 2002 2003 2004 2005 2006 2007 2008 2009 2010 2011 2012 2013 2014 2015
slhf-ERA
NDVI

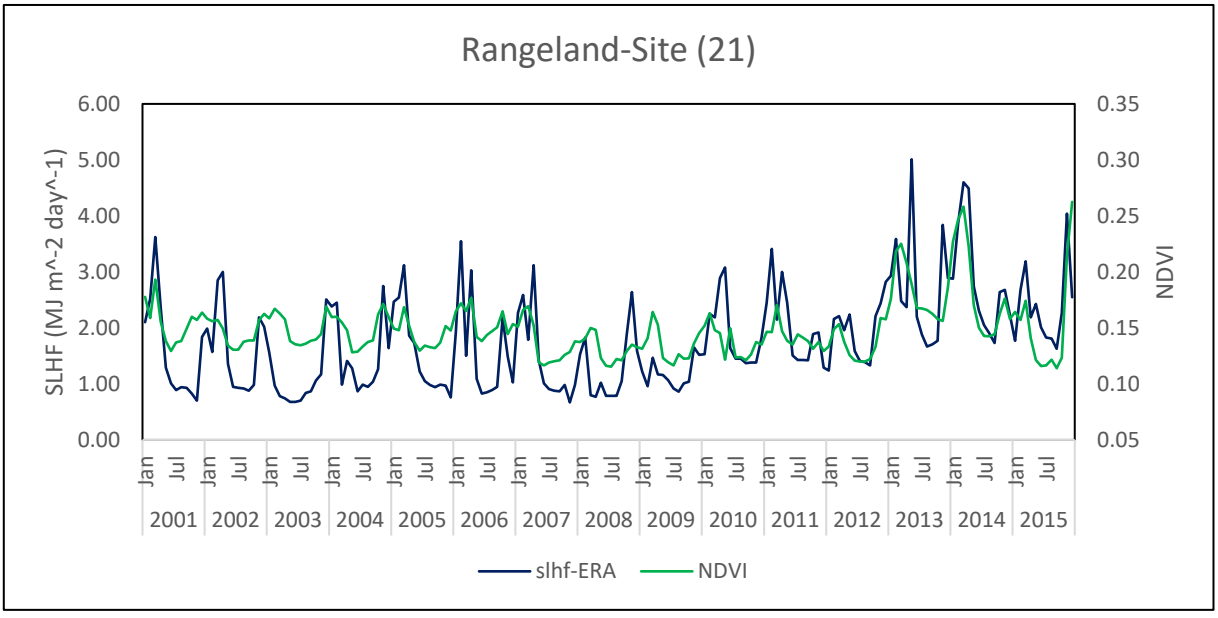
Rangeland-Site (21)
SLHF (MJ m^-2 day^-1)
NDVI
6.00
5.00
4.00
3.00
2.00
1.00
0.00
0.35
0.30
0.25
0.20
0.15
0.10
0.05
Jan Jul Jan Jul Jan Jul Jan Jul Jan Jul Jan Jul Jan Jul Jan Jul Jan Jul Jan Jul Jan Jul Jan Jul Jan Jul Jan Jul Jan Jul Jan Jul
2001 2002 2003 2004 2005 2006 2007 2008 2009 2010 2011 2012 2013 2014 2015
slhf-ERA
NDVI

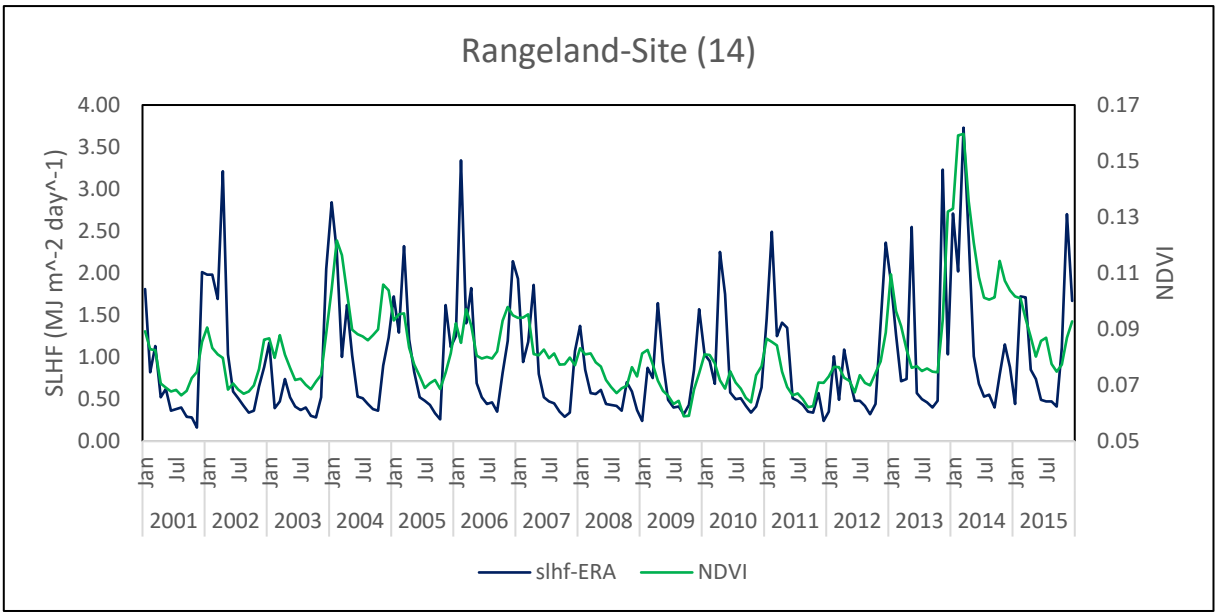
Rangeland-Site (14)
SLHF (MJ m^-2 day^-1)
NDVI
4.00
3.50
3.00
2.50
2.00
1.50
1.00
0.50
0.00
0.17
0.15
0.13
0.11
0.09
0.07
0.05
Jan Jul Jan Jul Jan Jul Jan Jul Jan Jul Jan Jul Jan Jul Jan Jul Jan Jul Jan Jul Jan Jul Jan Jul Jan Jul Jan Jul Jan Jul Jan Jul
2001 2002 2003 2004 2005 2006 2007 2008 2009 2010 2011 2012 2013 2014 2015
slhf-ERA
NDVI

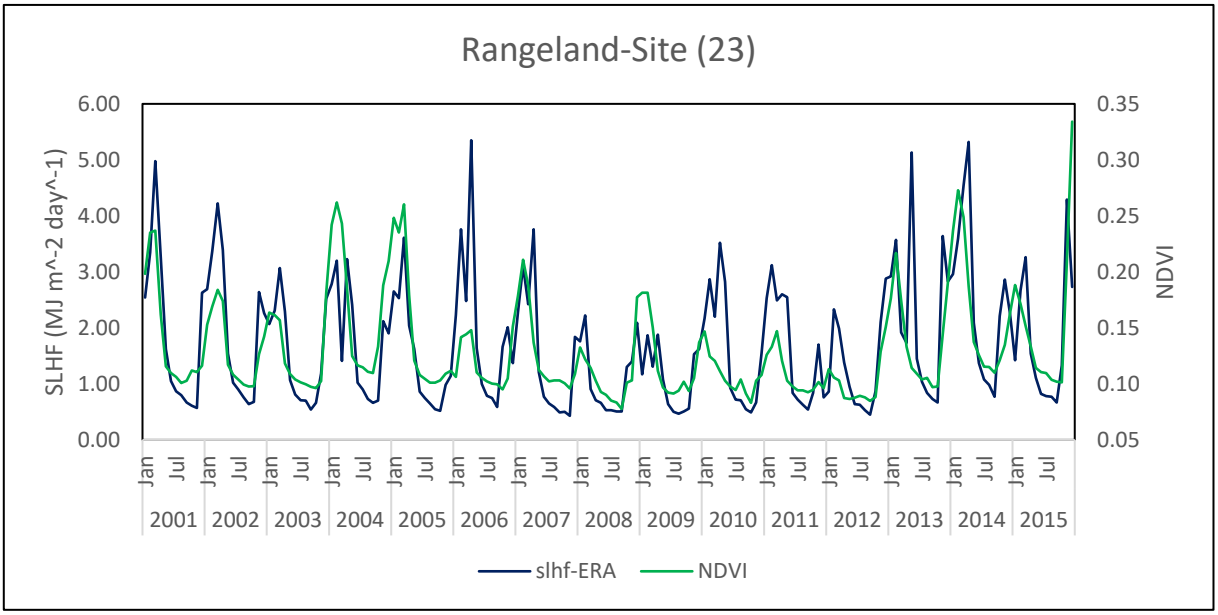
Rangeland-Site (23)
SLHF (MJ m^-2 day^-1)
NDVI
6.00
5.00
4.00
3.00
2.00
1.00
0.00
0.35
0.30
0.25
0.20
0.15
0.10
0.05
Jan Jul Jan Jul Jan Jul Jan Jul Jan Jul Jan Jul Jan Jul Jan Jul Jan Jul Jan Jul Jan Jul Jan Jul Jan Jul Jan Jul Jan Jul Jan Jul
2001 2002 2003 2004 2005 2006 2007 2008 2009 2010 2011 2012 2013 2014 2015
slhf-ERA
NDVI

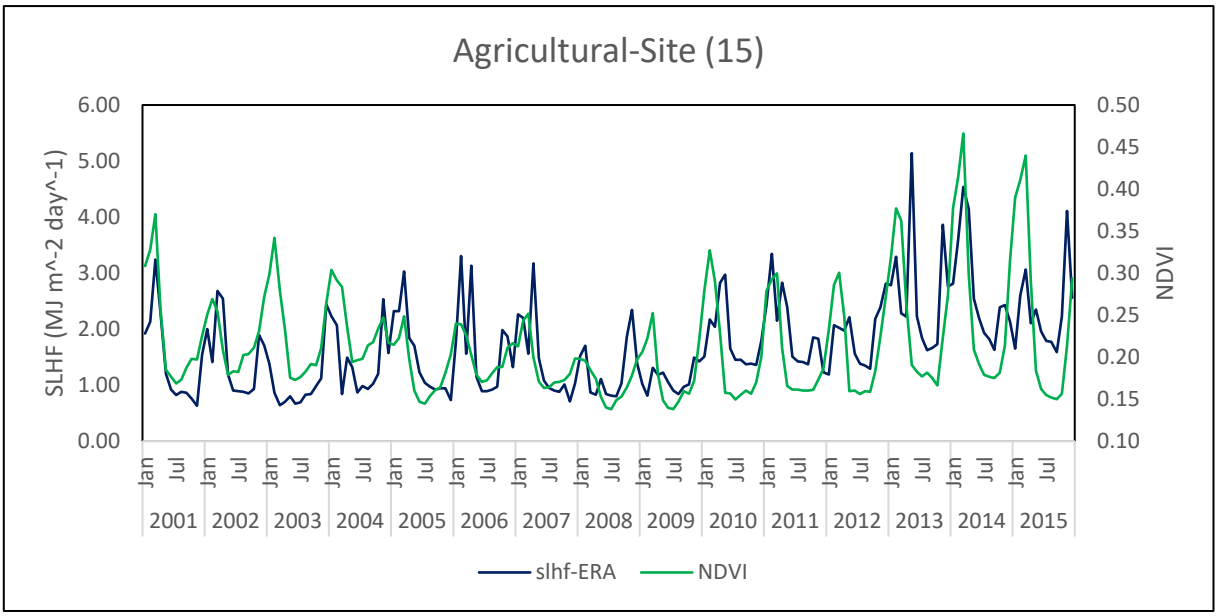
Agricultural-Site (15)
SLHF (MJ m^-2 day^-1)
NDVI
6.00
5.00
4.00
3.00
2.00
1.00
0.00
0.50
0.45
0.40
0.35
0.30
0.25
0.20
0.15
0.10
Jan Jul Jan Jul Jan Jul Jan Jul Jan Jul Jan Jul Jan Jul Jan Jul Jan Jul Jan Jul Jan Jul Jan Jul Jan Jul Jan Jul Jan Jul
2001 2002 2003 2004 2005 2006 2007 2008 2009 2010 2011 2012 2013 2014 2015
slhf-ERA
NDVI

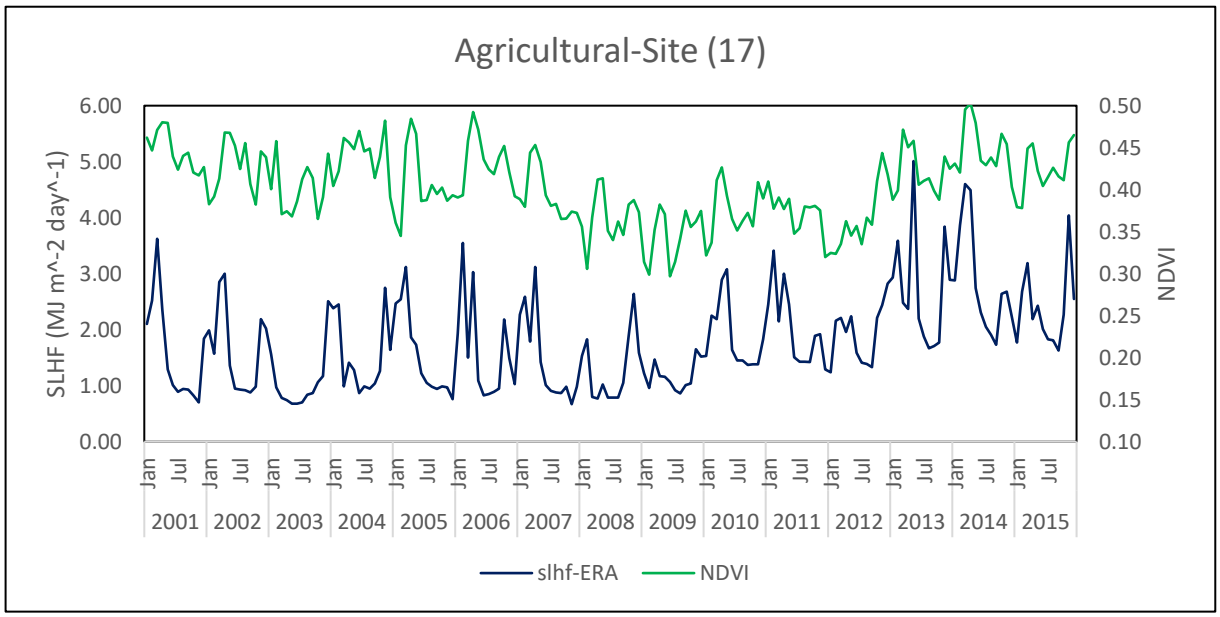
Agricultural-Site (17)
SLHF (MJ m^-2 day^-1)
NDVI
6.00
5.00
4.00
3.00
2.00
1.00
0.00
0.50
0.45
0.40
0.35
0.30
0.25
0.20
0.15
0.10
Jan Jul Jan Jul Jan Jul Jan Jul Jan Jul Jan Jul Jan Jul Jan Jul Jan Jul Jan Jul Jan Jul Jan Jul Jan Jul Jan Jul Jan Jul
2001 2002 2003 2004 2005 2006 2007 2008 2009 2010 2011 2012 2013 2014 2015
slhf-ERA
NDVI

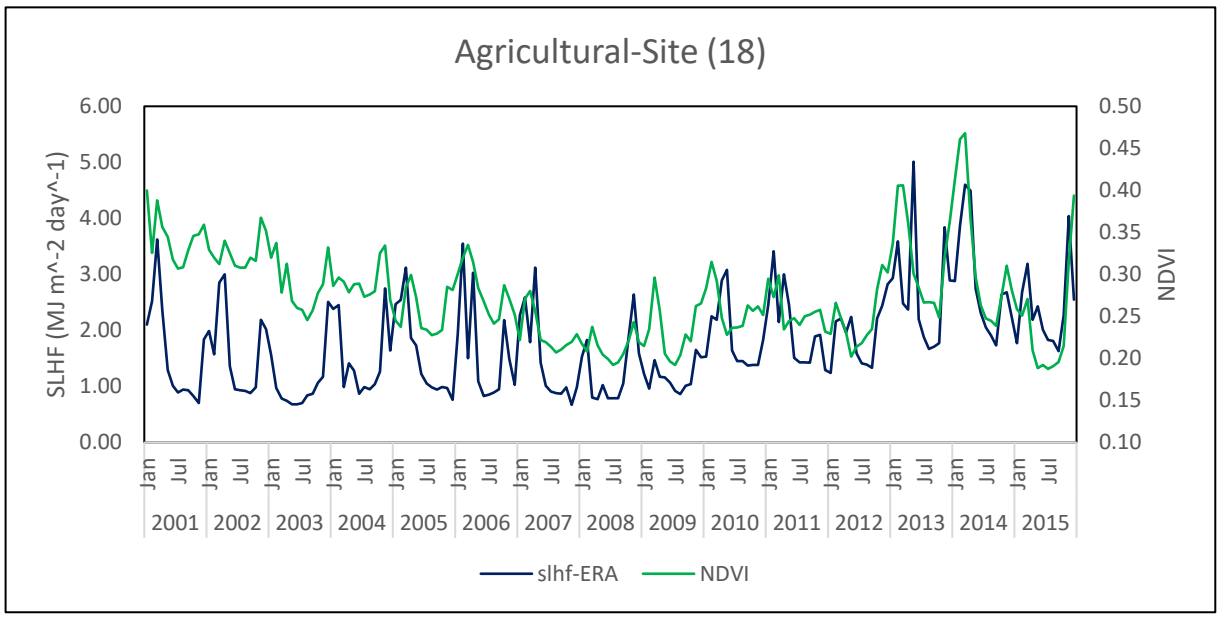
Agricultural-Site (18)
SLHF (MJ m^-2 day^-1)
NDVI
6.00
5.00
4.00
3.00
2.00
1.00
0.00
0.50
0.45
0.40
0.35
0.30
0.25
0.20
0.15
0.10
Jan Jul Jan Jul Jan Jul Jan Jul Jan Jul Jan Jul Jan Jul Jan Jul Jan Jul Jan Jul Jan Jul Jan Jul Jan Jul Jan Jul Jan Jul
2001 2002 2003 2004 2005 2006 2007 2008 2009 2010 2011 2012 2013 2014 2015
slhf-ERA
NDVI

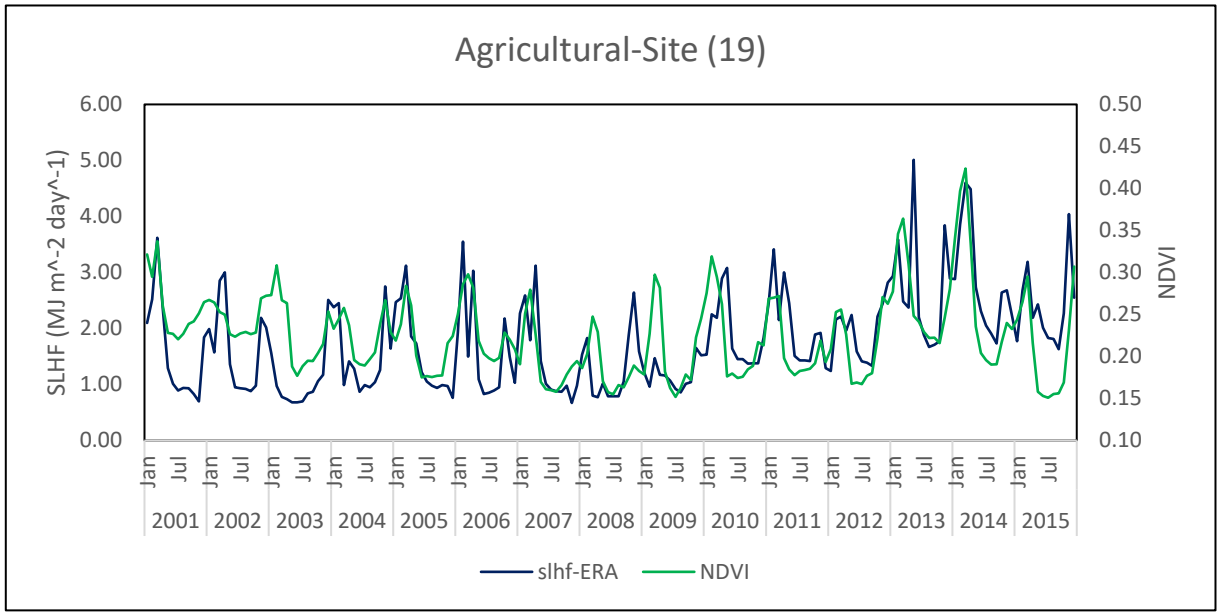
Agricultural-Site (19)
SLHF (MJ m^-2 day^-1)
NDVI
6.00
5.00
4.00
3.00
2.00
1.00
0.00
0.50
0.45
0.40
0.35
0.30
0.25
0.20
0.15
0.10
Jan Jul
2001 2002 2003 2004 2005 2006 2007 2008 2009 2010 2011 2012 2013 2014 2015
slhf-ERA
NDVI

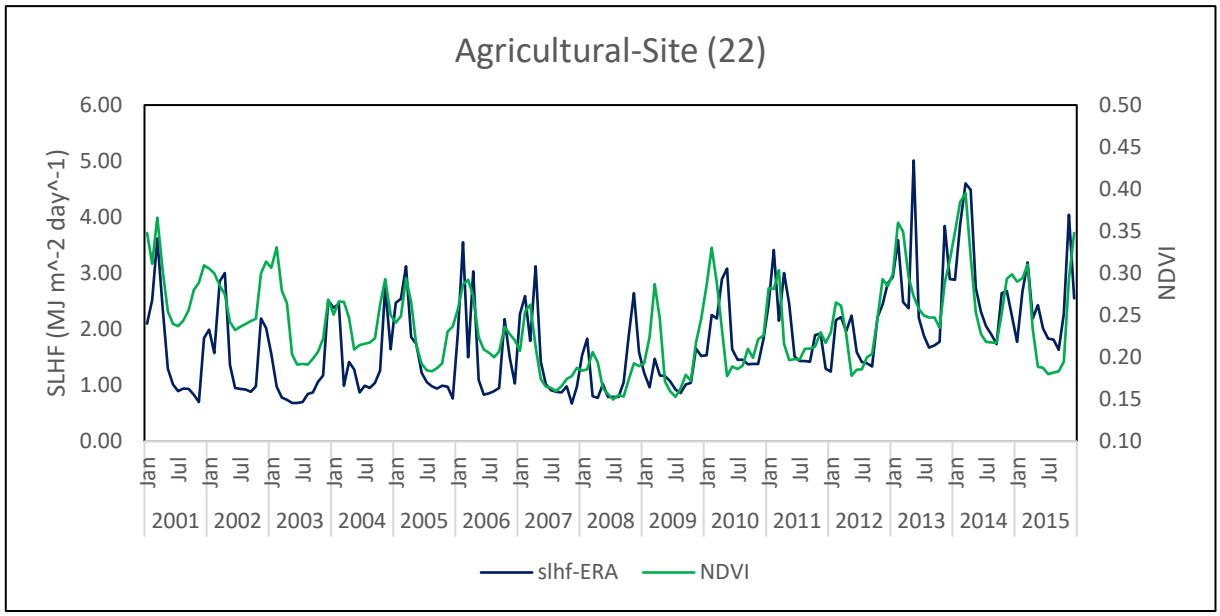
Agricultural-Site (22)
SLHF (MJ m^-2 day^-1)
NDVI
6.00
5.00
4.00
3.00
2.00
1.00
0.00
0.50
0.45
0.40
0.35
0.30
0.25
0.20
0.15
0.10
Jan Jul
2001 2002 2003 2004 2005 2006 2007 2008 2009 2010 2011 2012 2013 2014 2015
slhf-ERA
NDVI

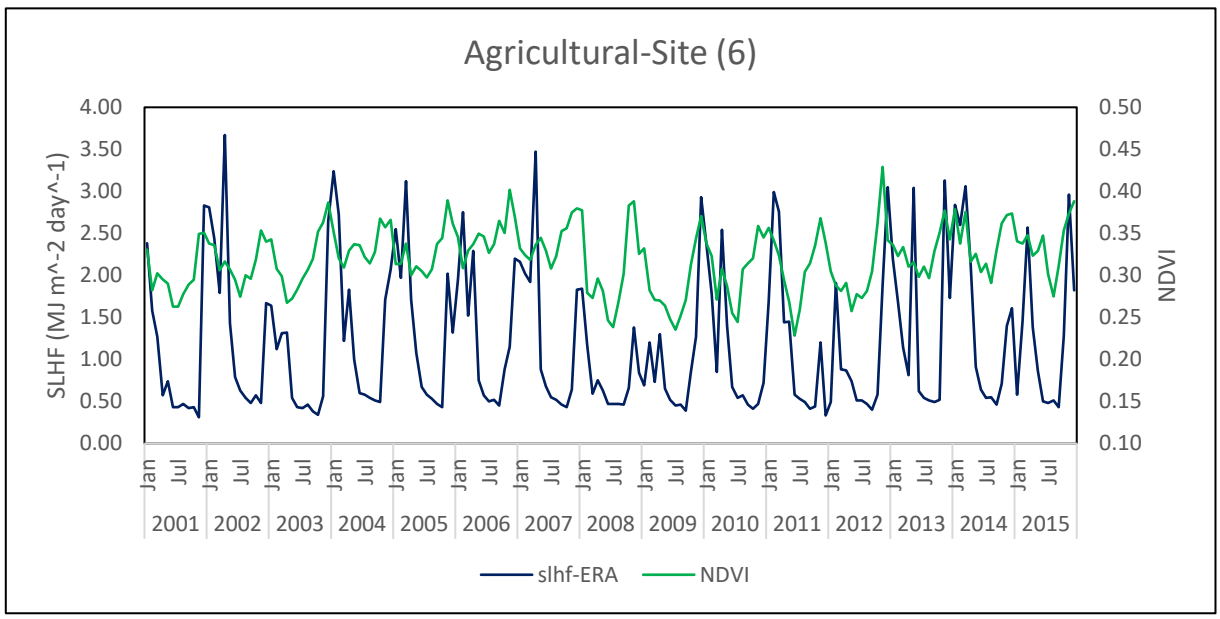
Agricultural-Site (6)
SLHF (MJ m^-2 day^-1)
NDVI
4.00
3.50
3.00
2.50
2.00
1.50
1.00
0.50
0.00
0.50
0.45
0.40
0.35
0.30
0.25
0.20
0.15
0.10
Jan Jul
2001 2002 2003 2004 2005 2006 2007 2008 2009 2010 2011 2012 2013 2014 2015
slhf-ERA
NDVI

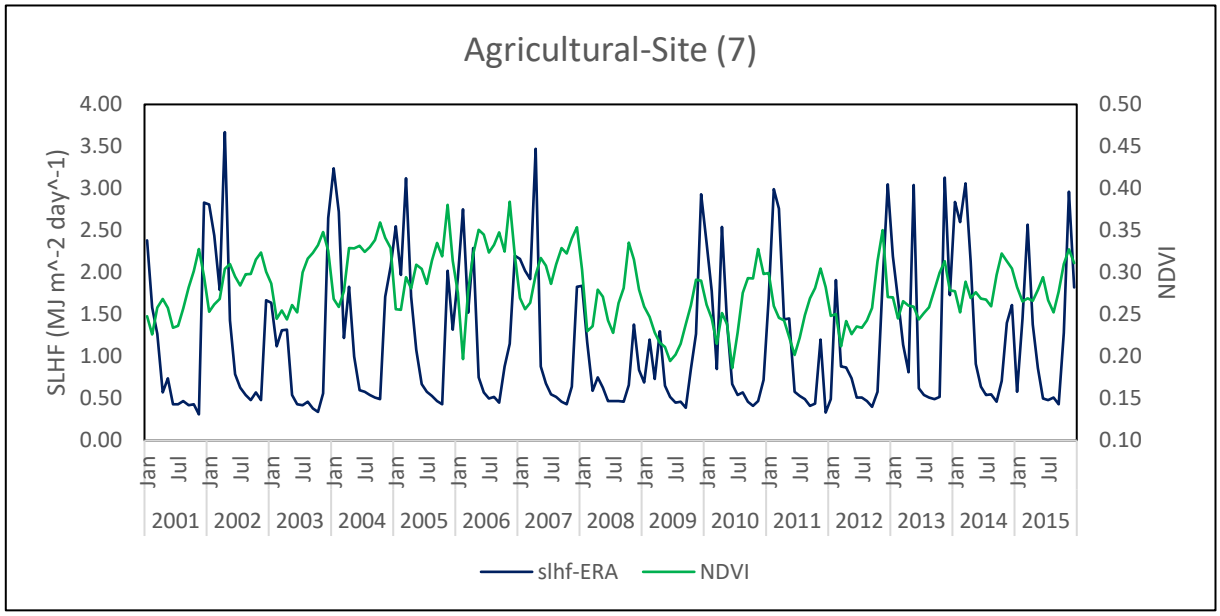
Agricultural-Site (7)
SLHF (MJ m^-2 day^-1)
NDVI
4.00
3.50
3.00
2.50
2.00
1.50
1.00
0.50
0.00
0.50
0.45
0.40
0.35
0.30
0.25
0.20
0.15
0.10
Jan Jul Jan Jul Jan Jul Jan Jul Jan Jul Jan Jul Jan Jul Jan Jul Jan Jul Jan Jul Jan Jul Jan Jul Jan Jul Jan Jul Jan Jul
2001 2002 2003 2004 2005 2006 2007 2008 2009 2010 2011 2012 2013 2014 2015
slhf-ERA
NDVI

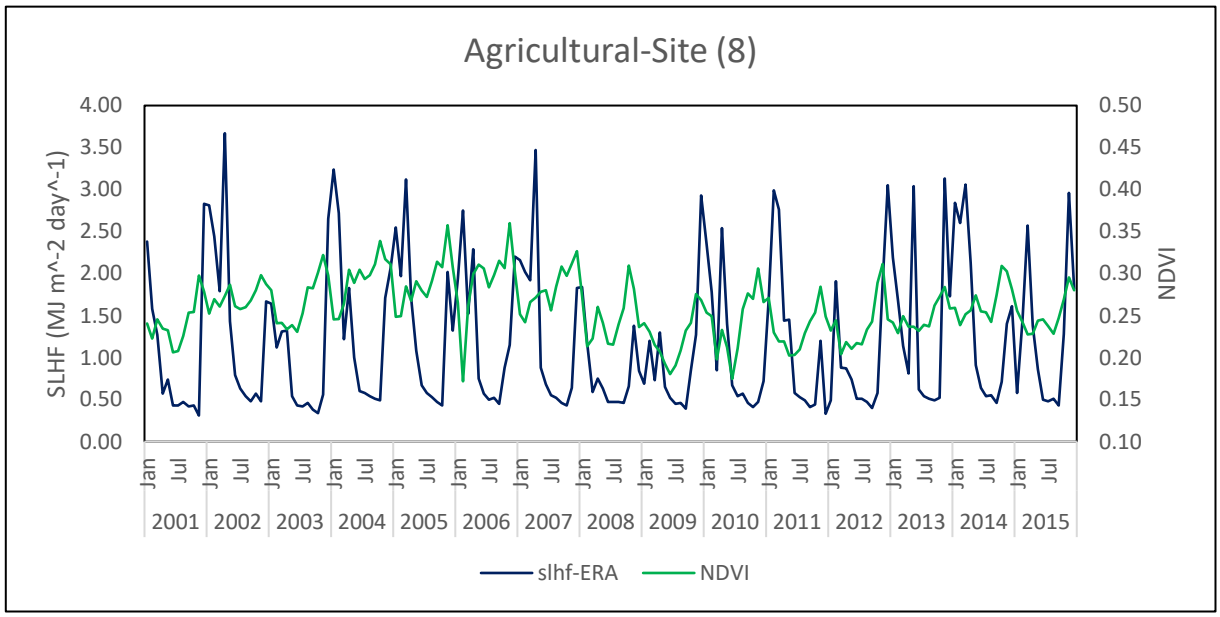
Agricultural-Site (8)
SLHF (MJ m^-2 day^-1)
NDVI
4.00
3.50
3.00
2.50
2.00
1.50
1.00
0.50
0.00
0.50
0.45
0.40
0.35
0.30
0.25
0.20
0.15
0.10
Jan Jul Jan Jul Jan Jul Jan Jul Jan Jul Jan Jul Jan Jul Jan Jul Jan Jul Jan Jul Jan Jul Jan Jul Jan Jul Jan Jul Jan Jul
2001 2002 2003 2004 2005 2006 2007 2008 2009 2010 2011 2012 2013 2014 2015
slhf-ERA
NDVI

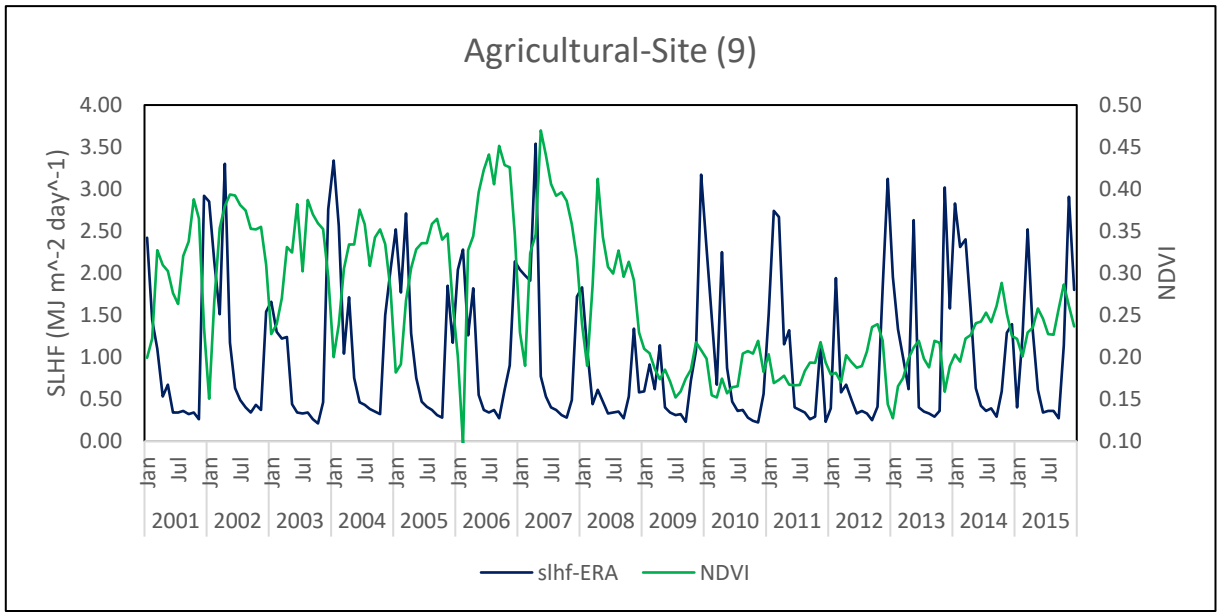
Agricultural-Site (9)
SLHF (MJ m^-2 day^-1)
NDVI
4.00
3.50
3.00
2.50
2.00
1.50
1.00
0.50
0.00
0.50
0.45
0.40
0.35
0.30
0.25
0.20
0.15
0.10
Jan Jul Jan Jul Jan Jul Jan Jul Jan Jul Jan Jul Jan Jul Jan Jul Jan Jul Jan Jul Jan Jul Jan Jul Jan Jul Jan Jul Jan Jul
2001 2002 2003 2004 2005 2006 2007 2008 2009 2010 2011 2012 2013 2014 2015
slhf-ERA
NDVI

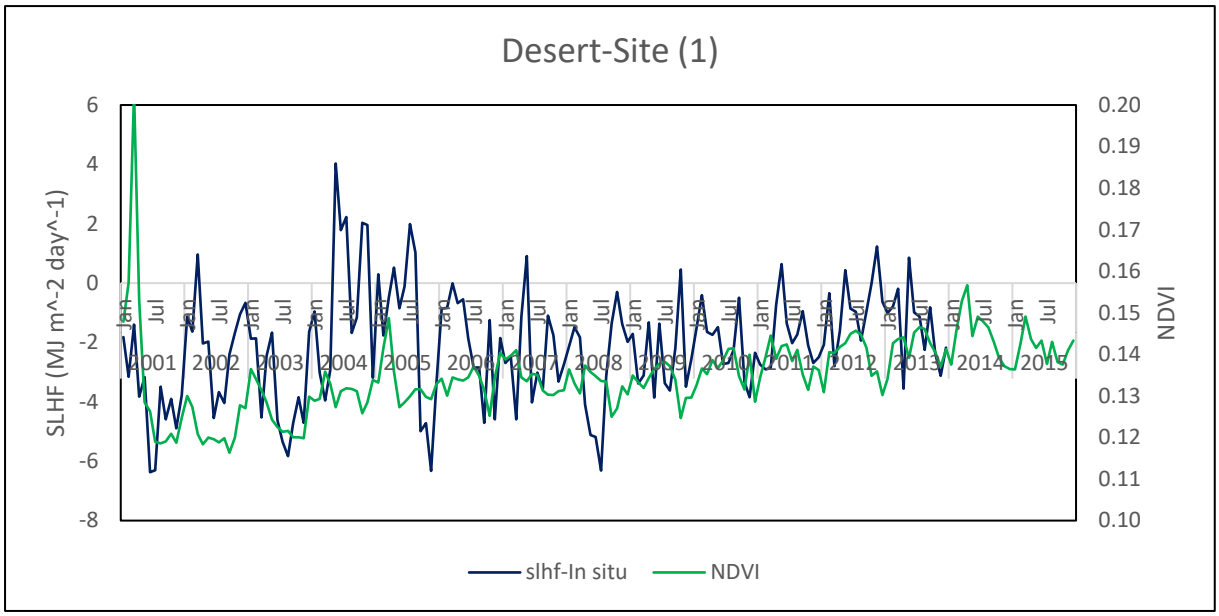
Desert-Site (1)
SLHF (MJ m^-2 day^-1)
NDVI
slhf-In situ
NDVI

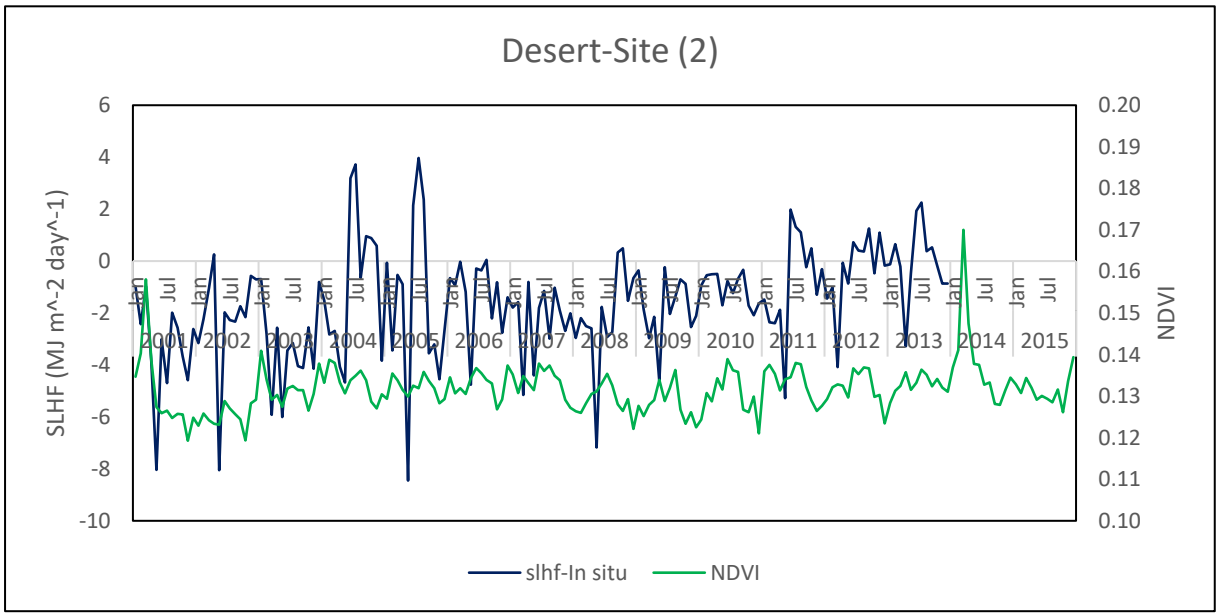
Desert-Site (2)
SLHF (MJ m^-2 day^-1)
NDVI
slhf-In situ
NDVI

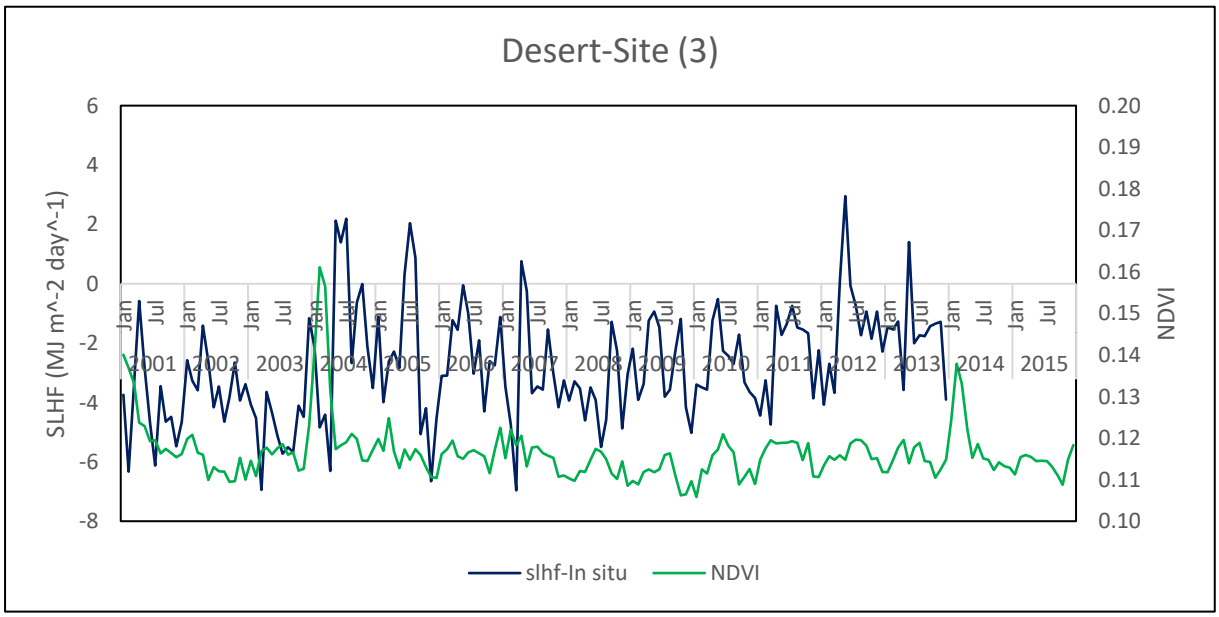
Desert-Site (3)
SLHF (MJ m^-2 day^-1)
NDVI
slhf-In situ
NDVI

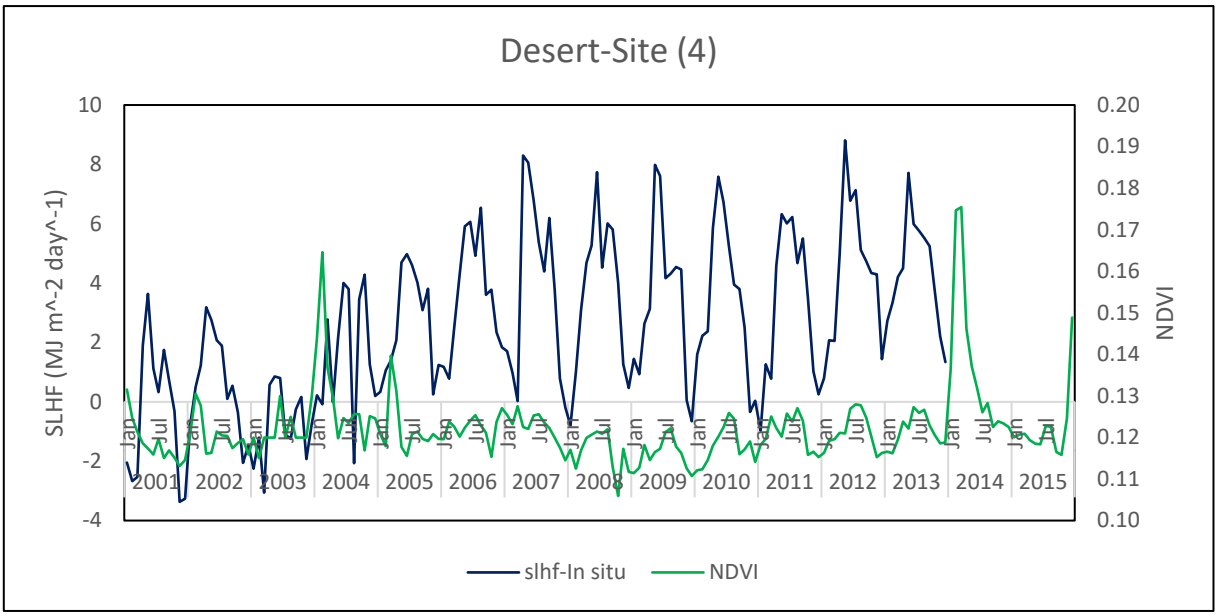
Desert-Site (4)
SLHF (MJ m^-2 day^-1)
NDVI
slhf-In situ
NDVI

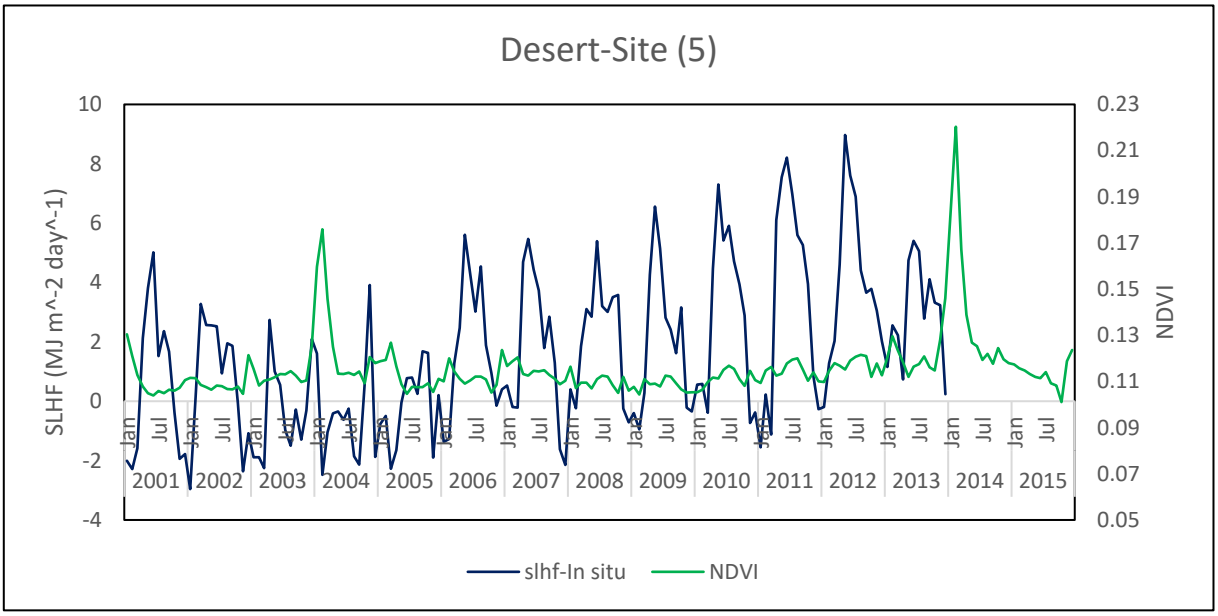
Desert-Site (5)
SLHF (MJ m^-2 day^-1)
NDVI
slhf-In situ
NDVI

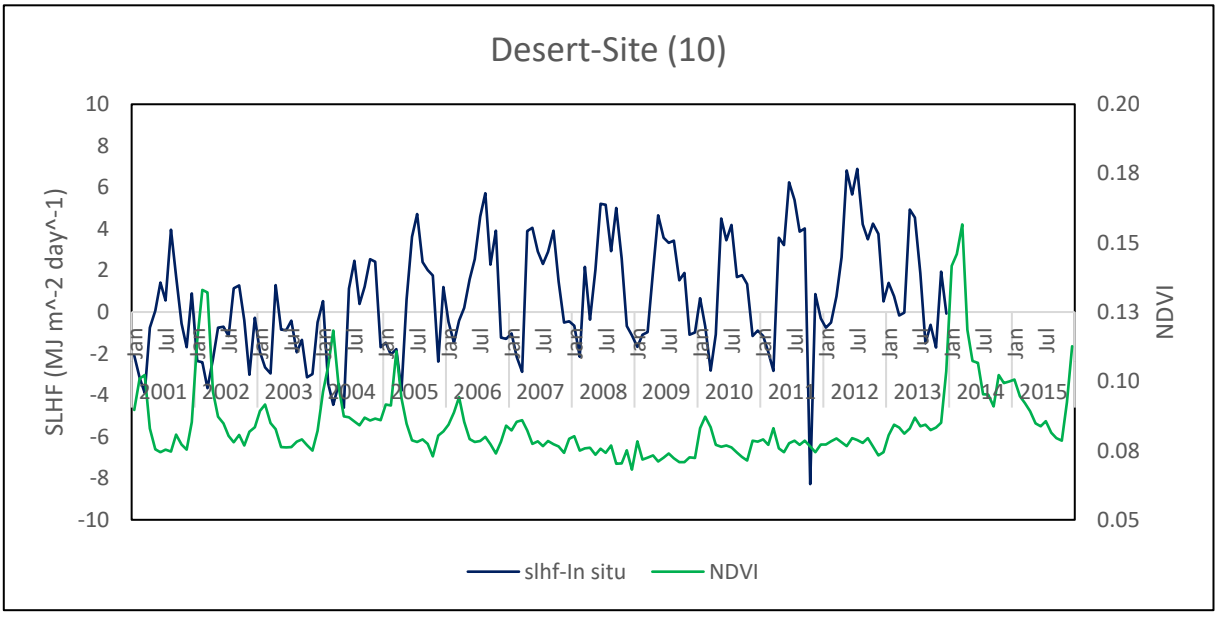
Desert-Site (10)
SLHF (MJ m^-2 day^-1)
NDVI
slhf-In situ
NDVI

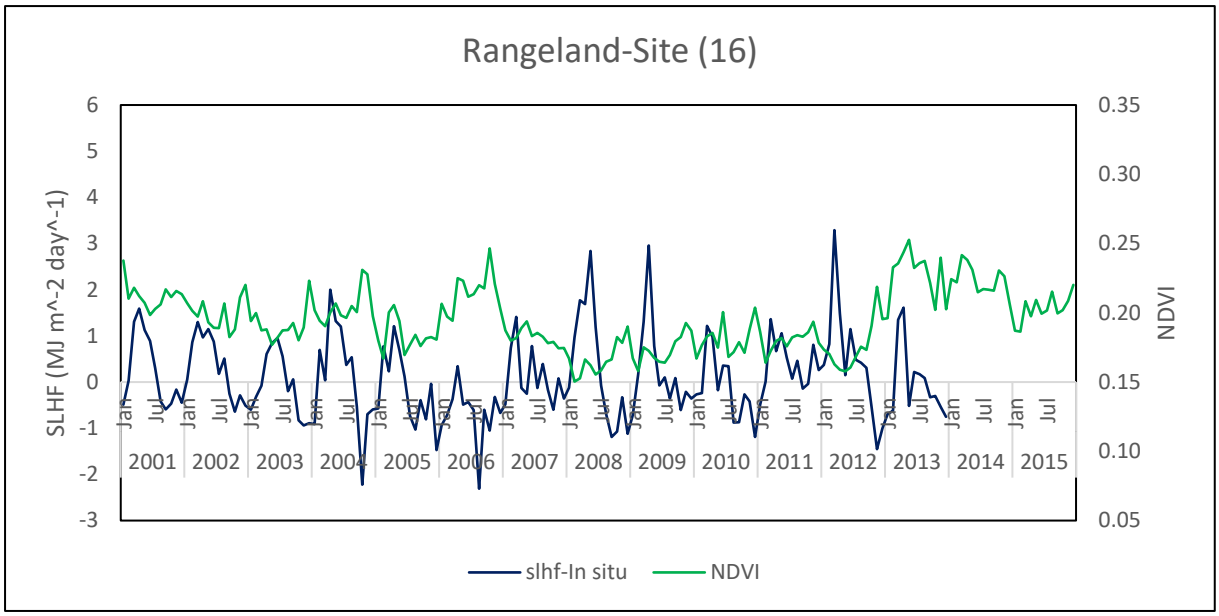
Rangeland-Site (16)
SLHF (MJ m^-2 day^-1)
NDVI
6
5
4
3
2
1
0
-1
-2
-3
0.35
0.30
0.25
0.20
0.15
0.10
0.05
Jan Jul
2001 2002 2003 2004 2005 2006 2007 2008 2009 2010 2011 2012 2013 2014 2015
slhf-In situ
NDVI

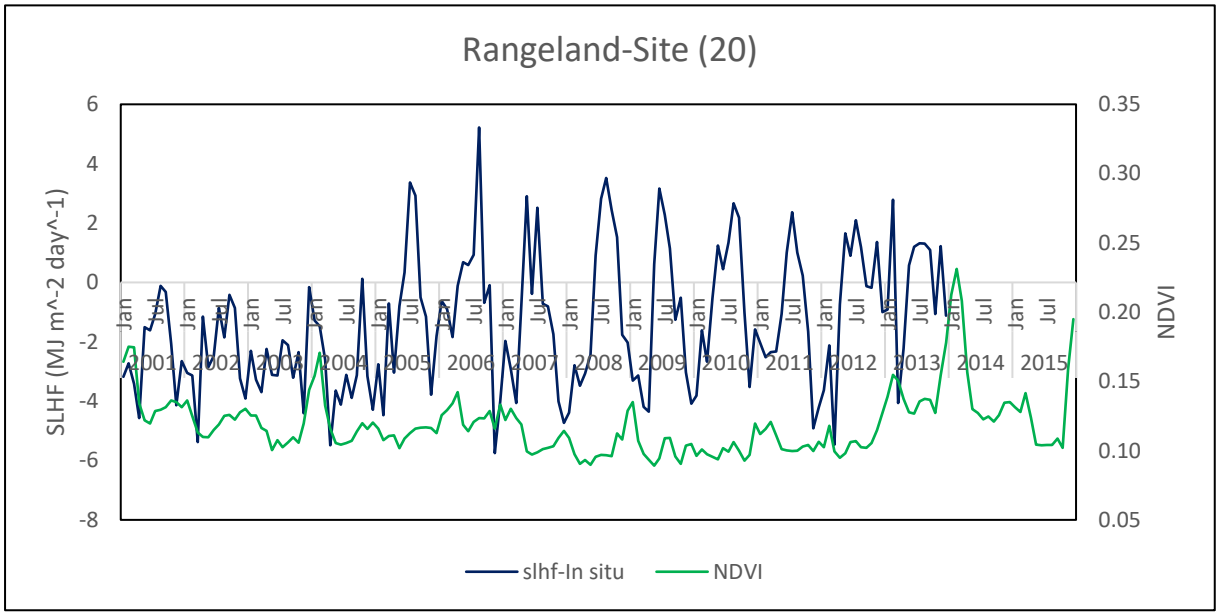
Rangeland-Site (20)
SLHF (MJ m^-2 day^-1)
NDVI
6
4
2
0
-2
-4
-6
-8
0.35
0.30
0.25
0.20
0.15
0.10
0.05
Jan Jul
2001 2002 2003 2004 2005 2006 2007 2008 2009 2010 2011 2012 2013 2014 2015
slhf-In situ
NDVI

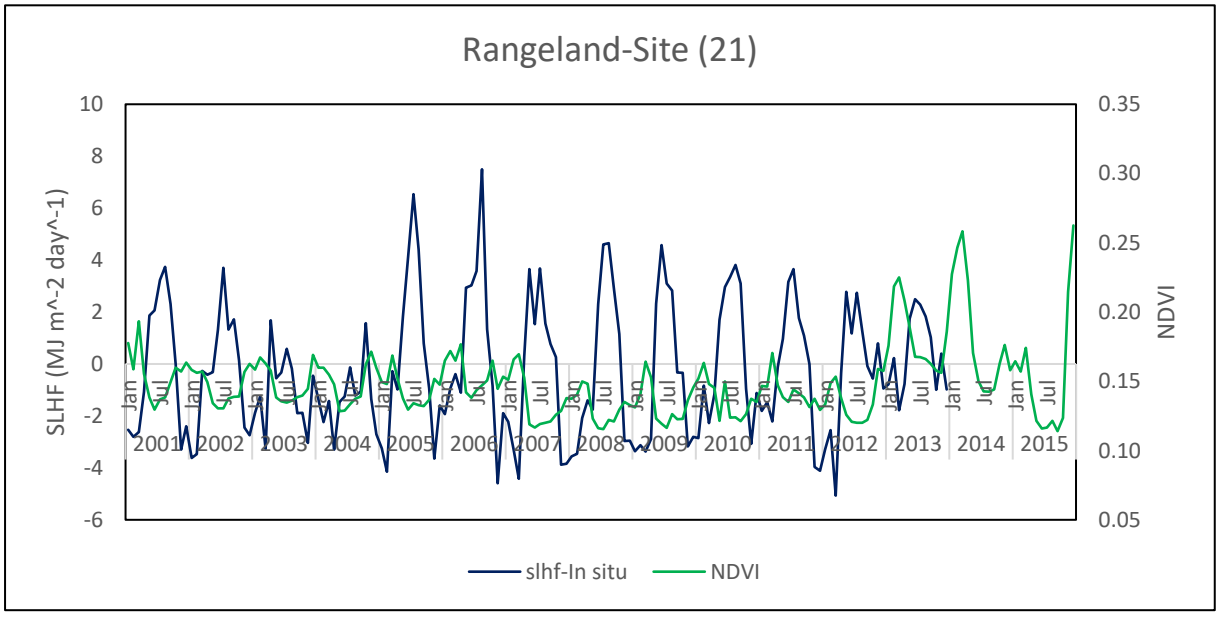
Rangeland-Site (21)
SLHF (MJ m^-2 day^-1)
NDVI
10
8
6
4
2
0
-2
-4
-6
0.35
0.30
0.25
0.20
0.15
0.10
0.05
Jan Jul
2001 2002 2003 2004 2005 2006 2007 2008 2009 2010 2011 2012 2013 2014 2015
slhf-In situ
NDVI

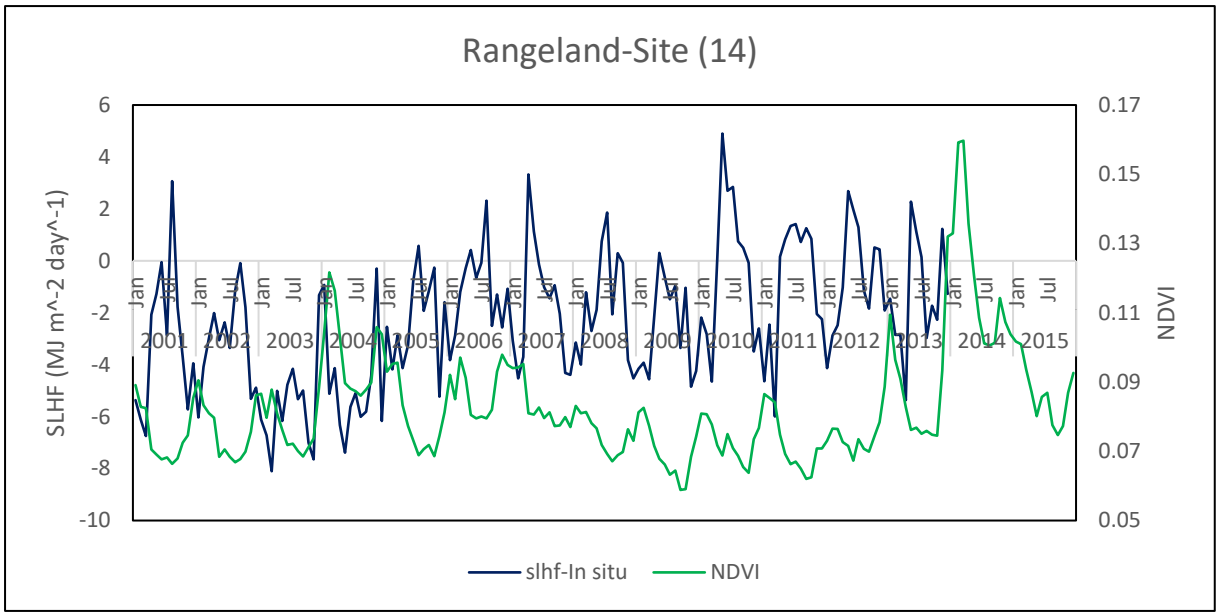
Rangeland-Site (14)
SLHF (MJ m^-2 day^-1)
NDVI
6
4
2
0
-2
-4
-6
-8
-10
0.17
0.15
0.13
0.11
0.09
0.07
0.05
2001
2002
2003
2004
2005
2006
2007
2008
2009
2010
2011
2012
2013
2014
2015
slhf-In situ
NDVI

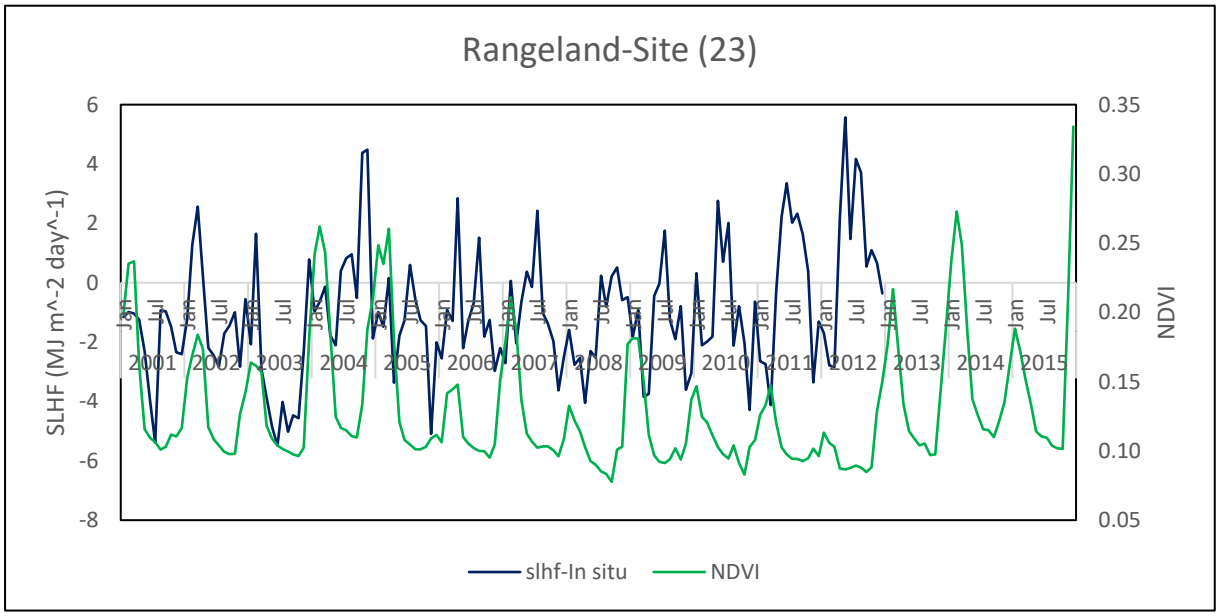
Rangeland-Site (23)
SLHF (MJ m^-2 day^-1)
NDVI
6
4
2
0
-2
-4
-6
-8
0.35
0.30
0.25
0.20
0.15
0.10
0.05
2001
2002
2003
2004
2005
2006
2007
2008
2009
2010
2011
2012
2013
2014
2015
slhf-In situ
NDVI

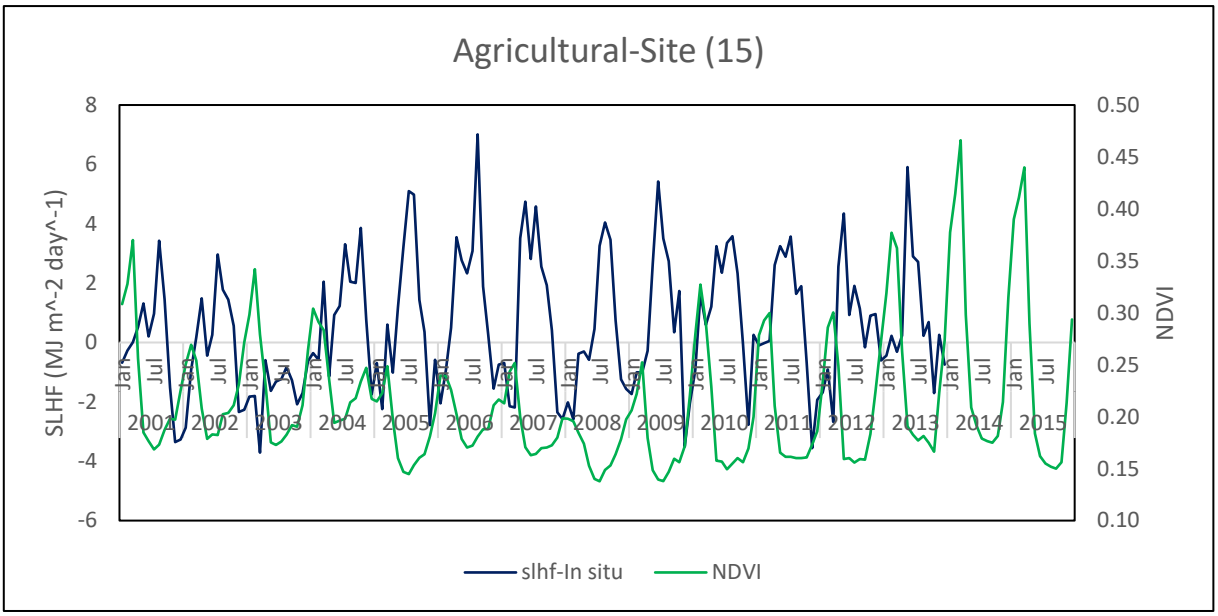
Agricultural-Site (15)
SLHF (MJ m^-2 day^-1)
NDVI
slhf-In situ
NDVI

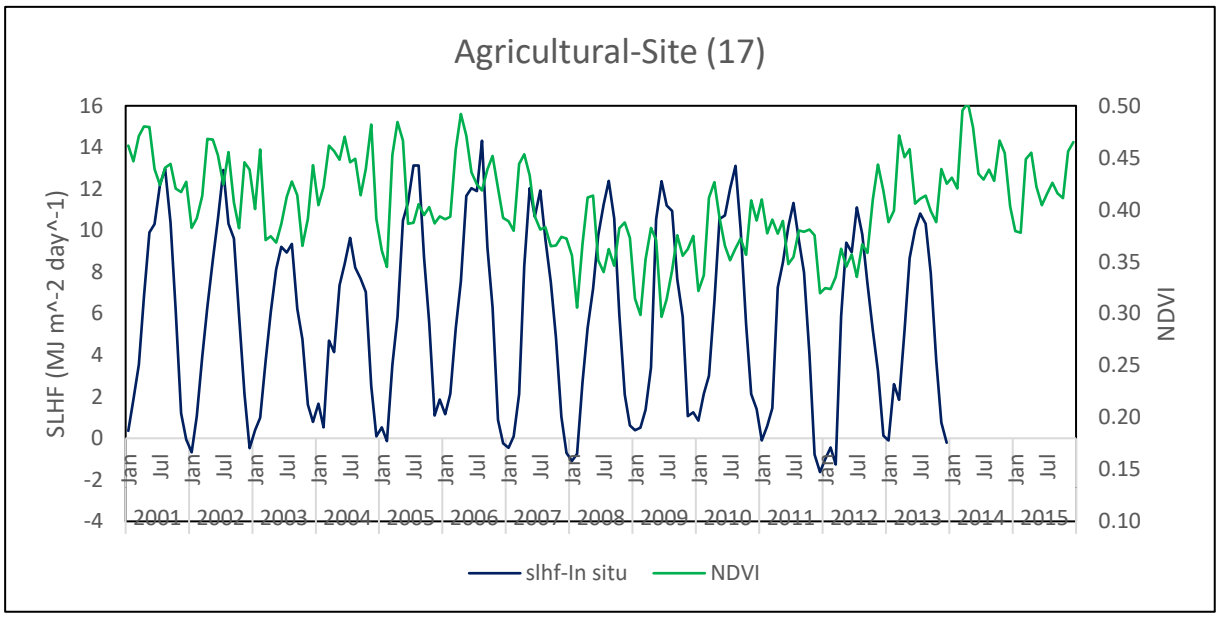
Agricultural-Site (17)
SLHF (MJ m^-2 day^-1)
NDVI
slhf-In situ
NDVI

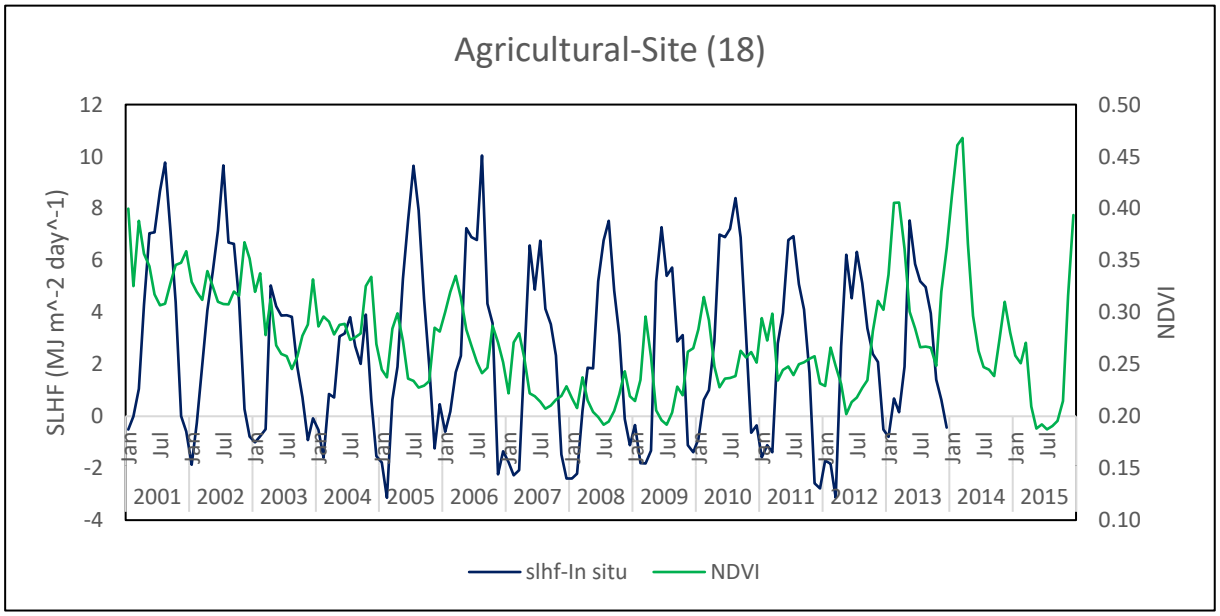
Agricultural-Site (18)
SLHF (MJ m^-2 day^-1)
NDVI
slhf-In situ
NDVI

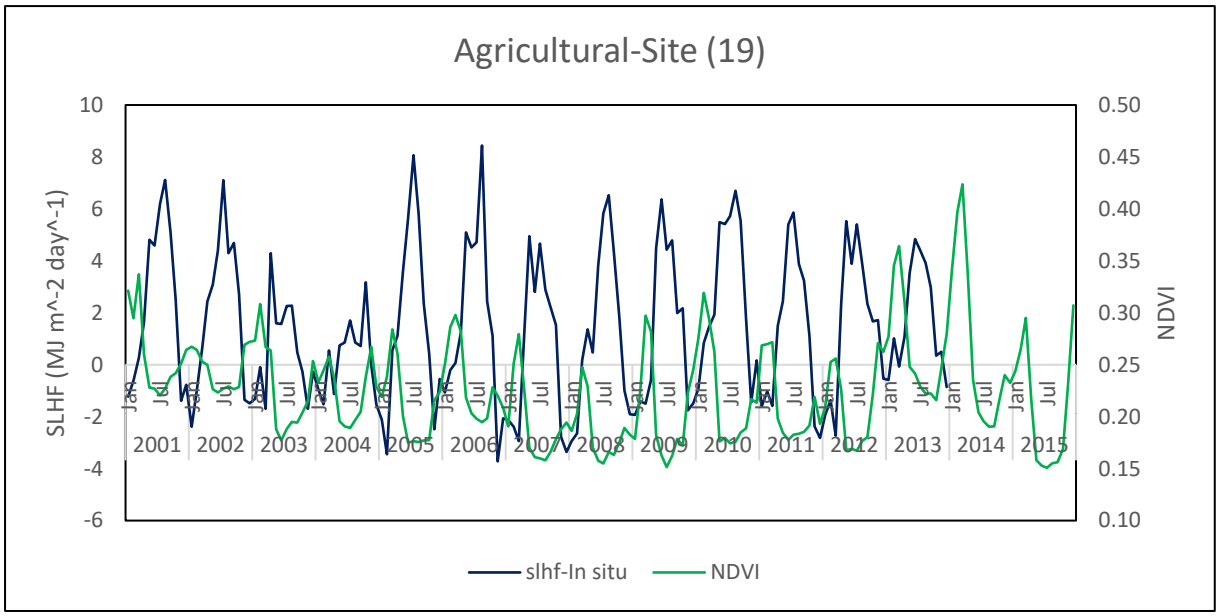
Agricultural-Site (19)
SLHF (MJ m^-2 day^-1)
NDVI
slhf-In situ
NDVI

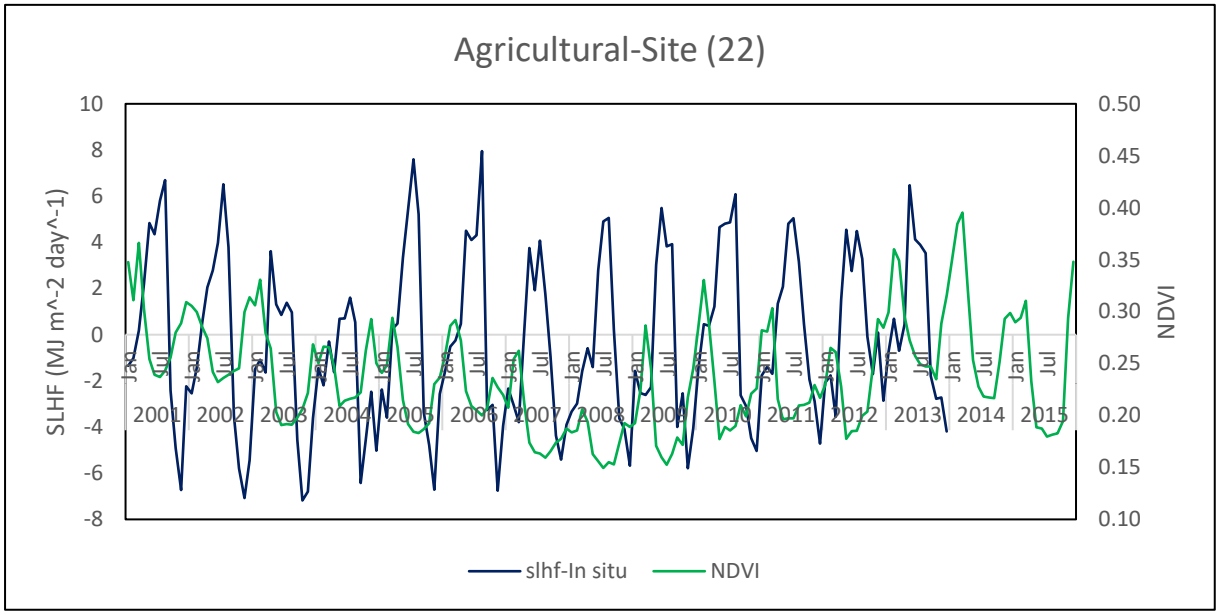
Agricultural-Site (22)
SLHF (MJ m^-2 day^-1)
NDVI
slhf-In situ
NDVI

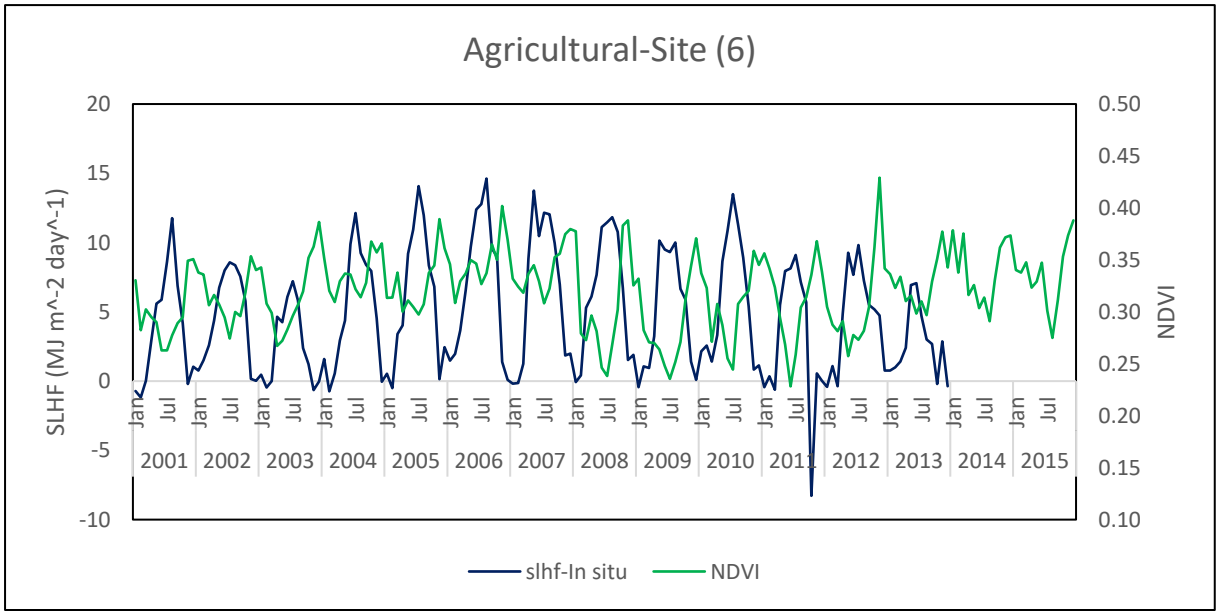
Agricultural-Site (6)
SLHF (MJ m^-2 day^-1)
NDVI
slhf-In situ
NDVI

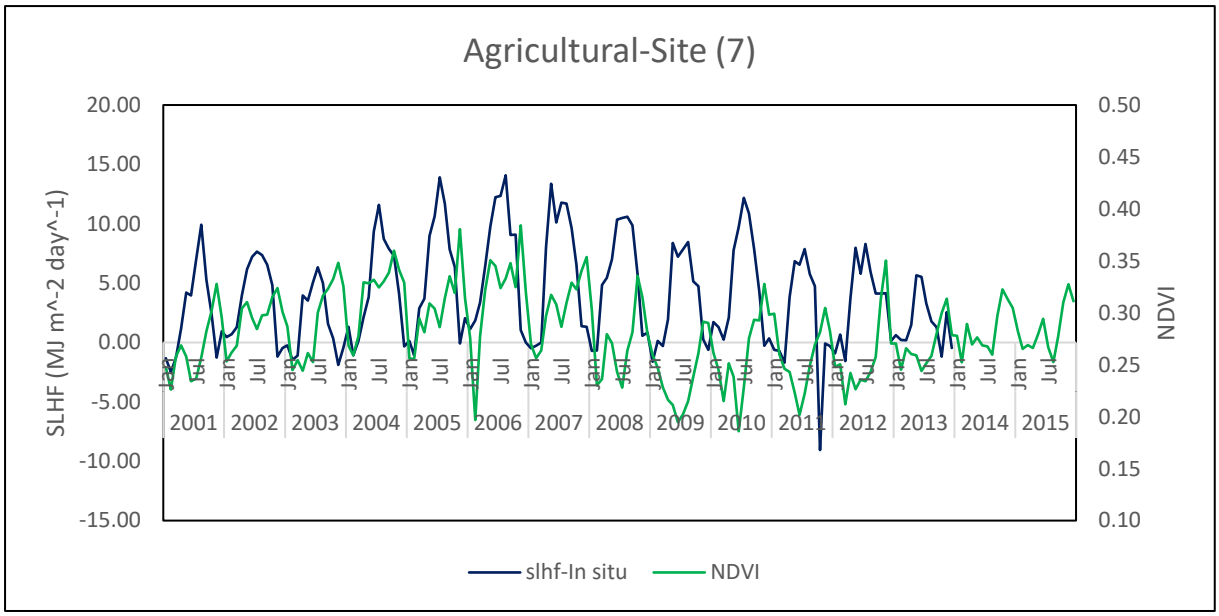
Agricultural-Site (7)
SLHF (MJ m^-2 day^-1)
NDVI
20.00
15.00
10.00
5.00
0.00
-5.00
-10.00
-15.00
0.50
0.45
0.40
0.35
0.30
0.25
0.20
0.15
0.10
Jan Jul
2001 2002 2003 2004 2005 2006 2007 2008 2009 2010 2011 2012 2013 2014 2015
slhf-In situ
NDVI

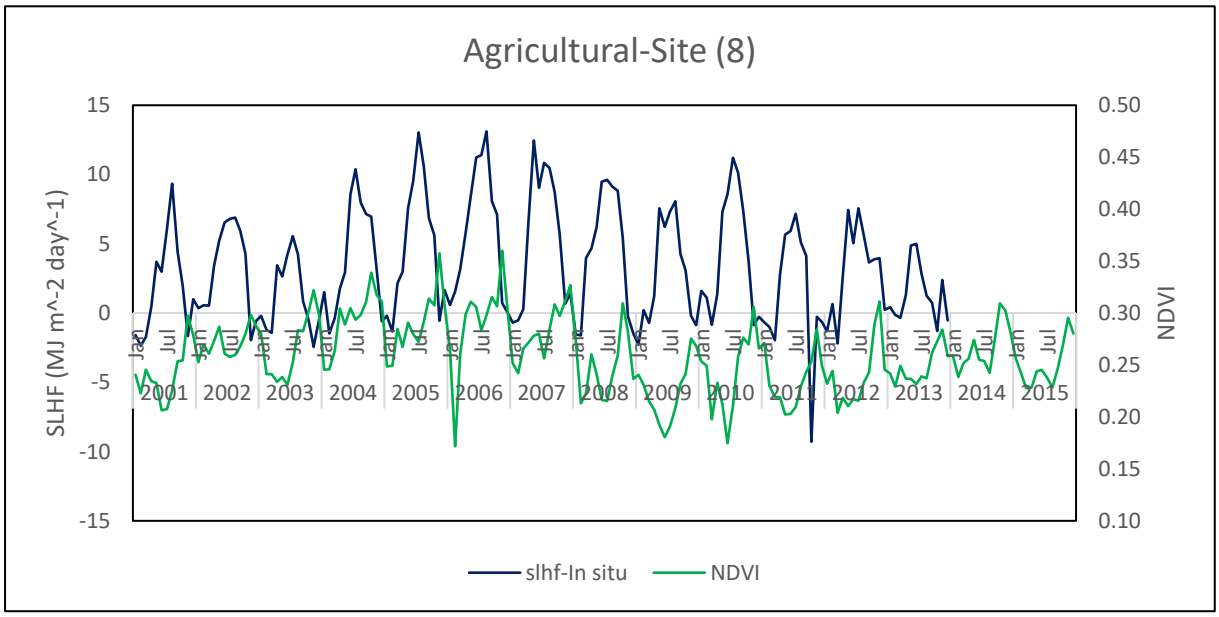
Agricultural-Site (8)
SLHF (MJ m^-2 day^-1)
NDVI
15
10
5
0
-5
-10
-15
0.50
0.45
0.40
0.35
0.30
0.25
0.20
0.15
0.10
Jan Jul
2001 2002 2003 2004 2005 2006 2007 2008 2009 2010 2011 2012 2013 2014 2015
slhf-In situ
NDVI

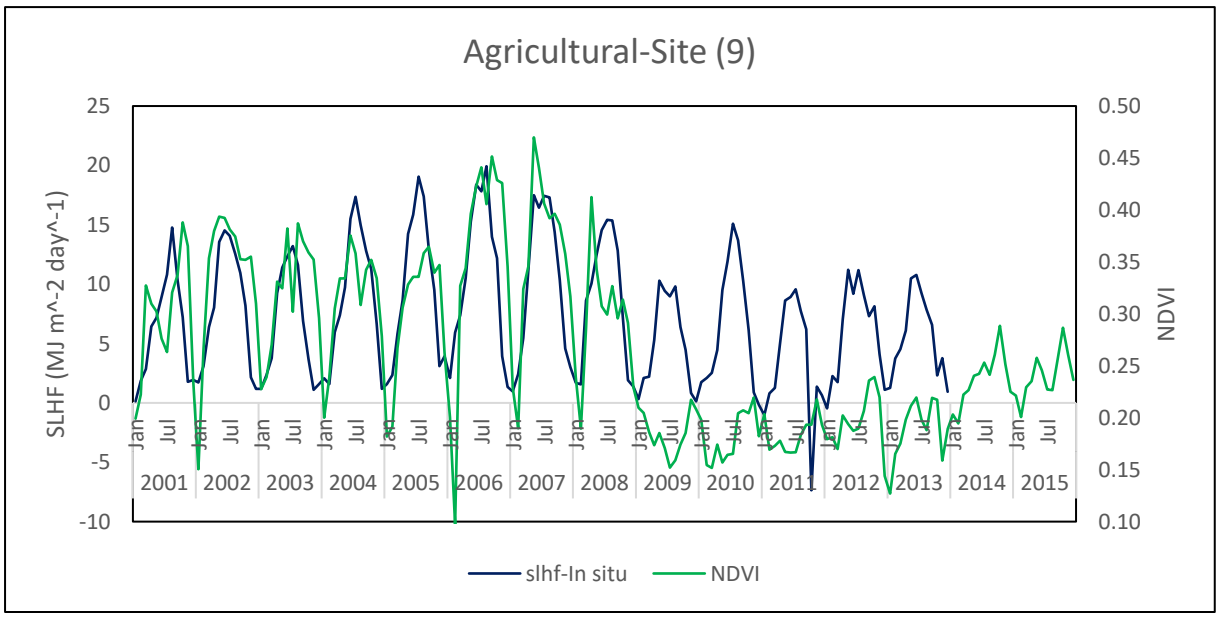
Agricultural-Site (9)
SLHF (MJ m^-2 day^-1)
NDVI
25
20
15
10
5
0
-5
-10
0.50
0.45
0.40
0.35
0.30
0.25
0.20
0.15
0.10
Jan Jul
2001 2002 2003 2004 2005 2006 2007 2008 2009 2010 2011 2012 2013 2014 2015
slhf-In situ
NDVI

APPENDIX G: Assessment of water balance components from SWAP runs during (2001-2015) for the desert region.

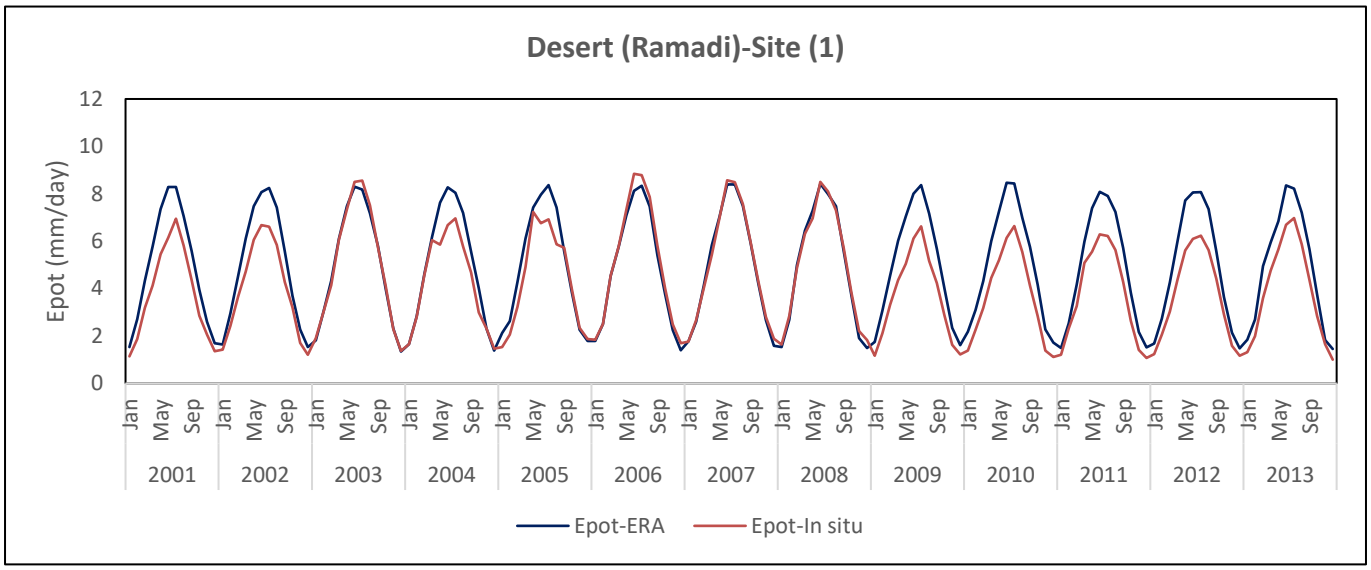

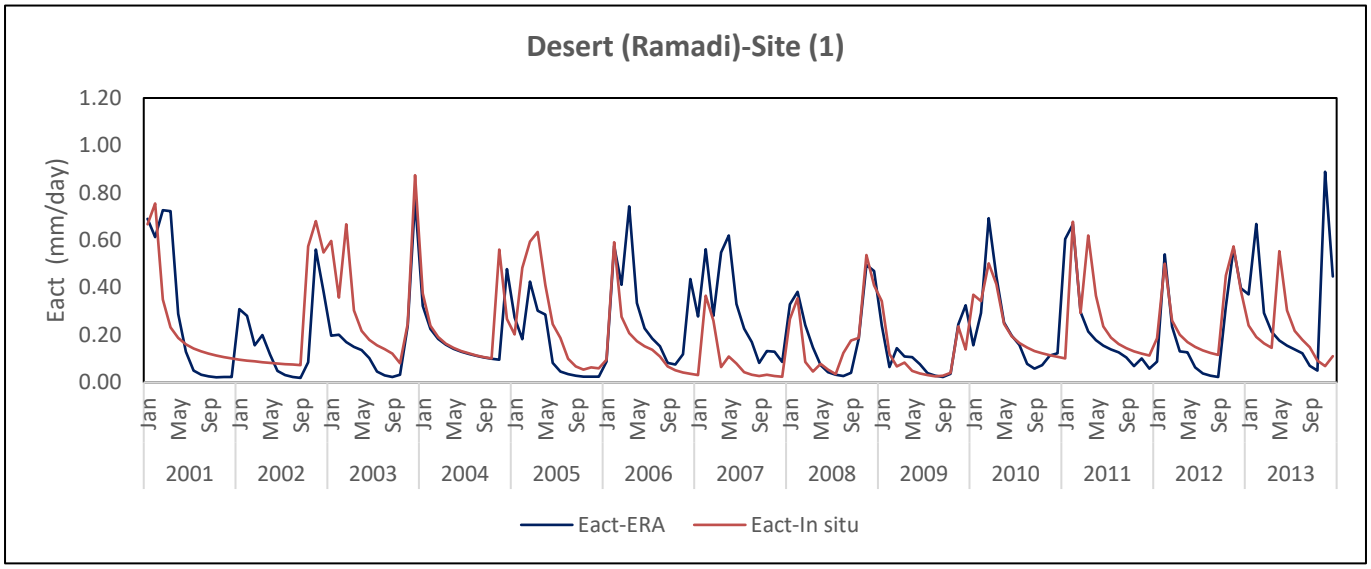

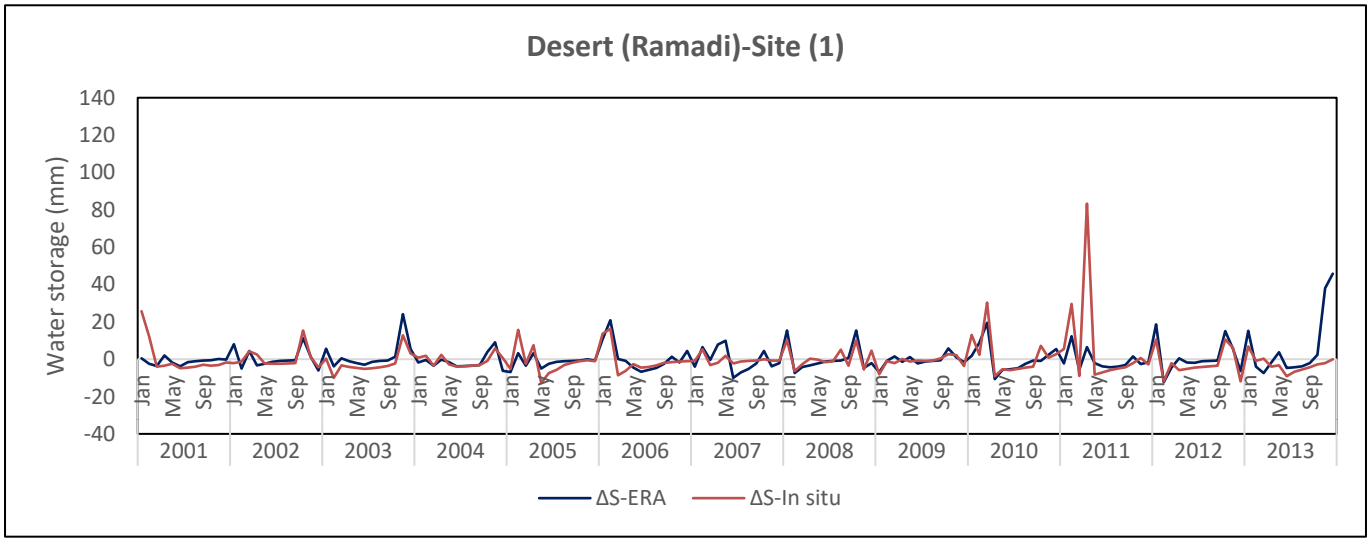

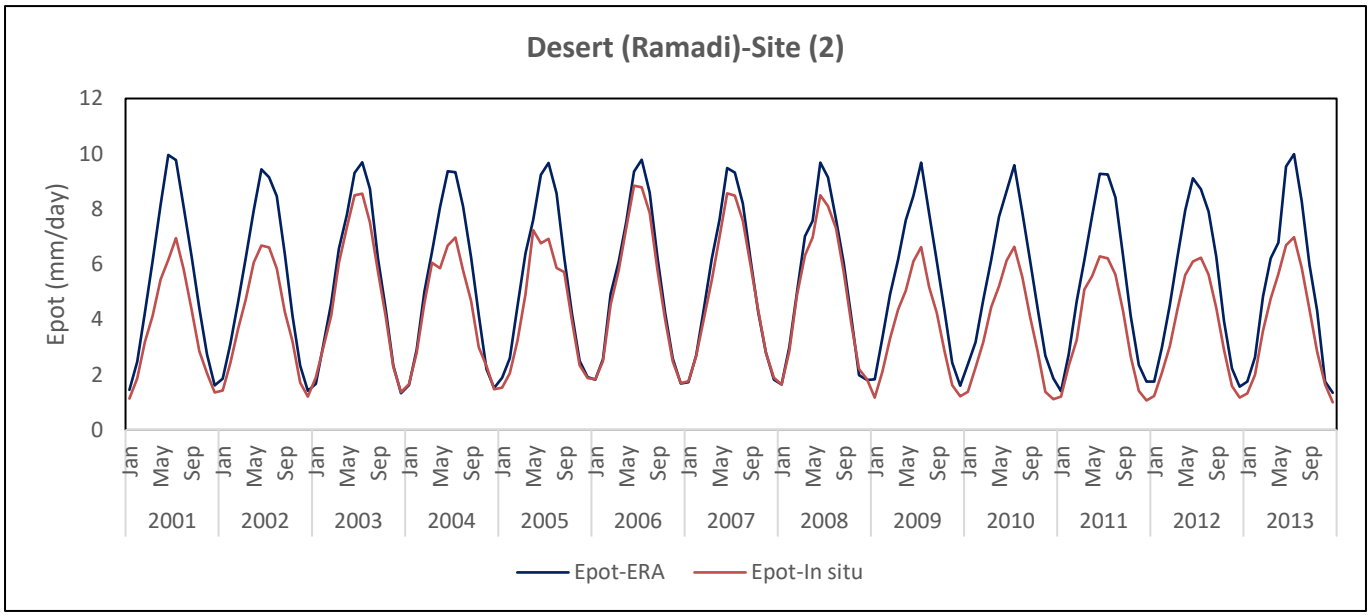
Desert (Ramadi)-Site (2)
Epot (mm/day)
0
2
4
6
8
10
12
Jan May Sep
2001 2002 2003 2004 2005 2006 2007 2008 2009 2010 2011 2012 2013
Epot-ERA
Epot-In situ

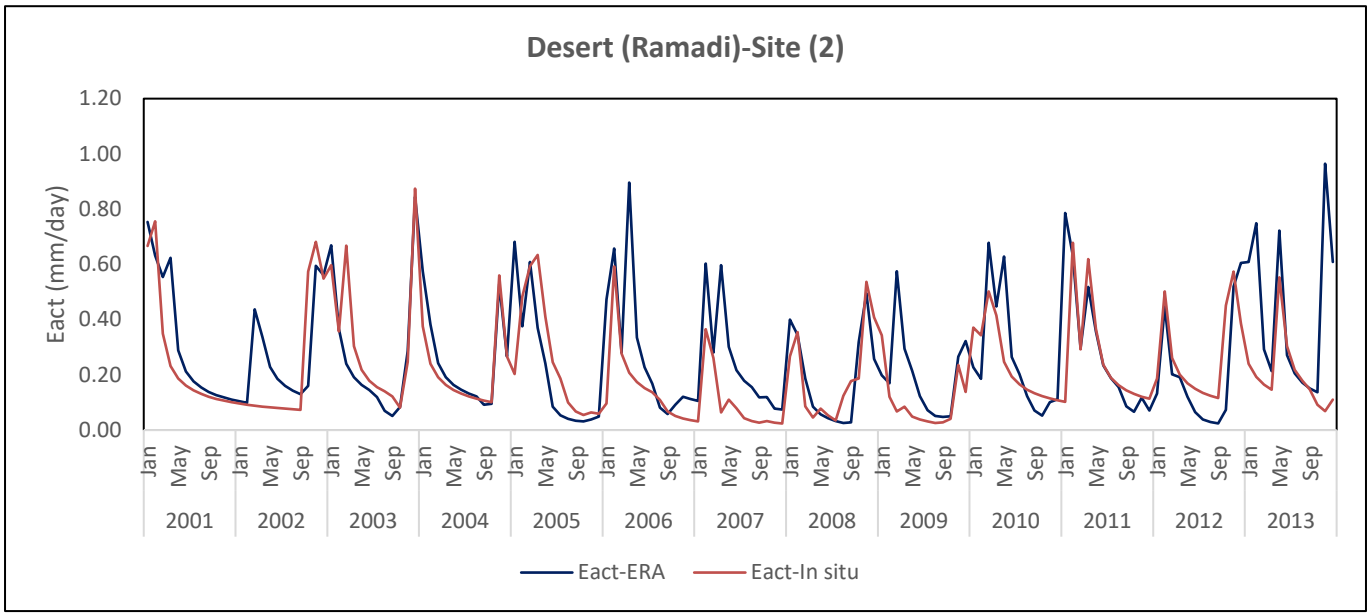
Desert (Ramadi)-Site (2)
Eact (mm/day)
0.00
0.20
0.40
0.60
0.80
1.00
1.20
Jan May Sep
2001 2002 2003 2004 2005 2006 2007 2008 2009 2010 2011 2012 2013
Eact-ERA
Eact-In situ

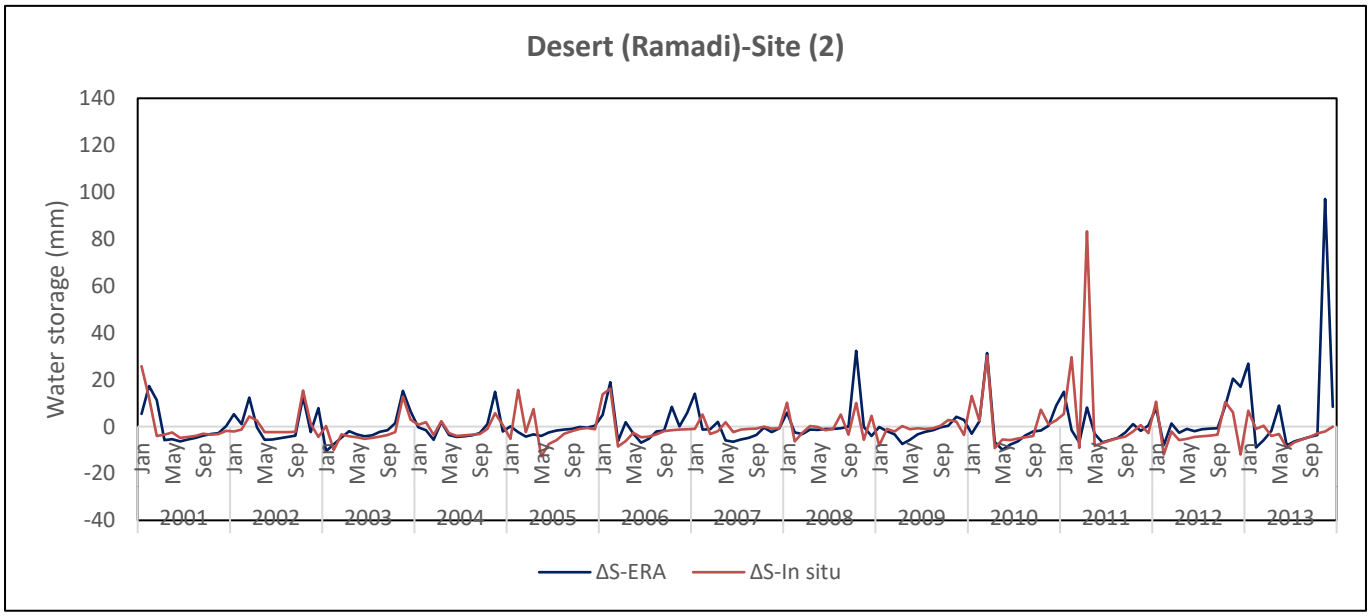
Desert (Ramadi)-Site (2)
Water storage (mm)
-40
-20
0
20
40
60
80
100
120
140
Jan May Sep
2001 2002 2003 2004 2005 2006 2007 2008 2009 2010 2011 2012 2013
ΔS-ERA
ΔS-In situ

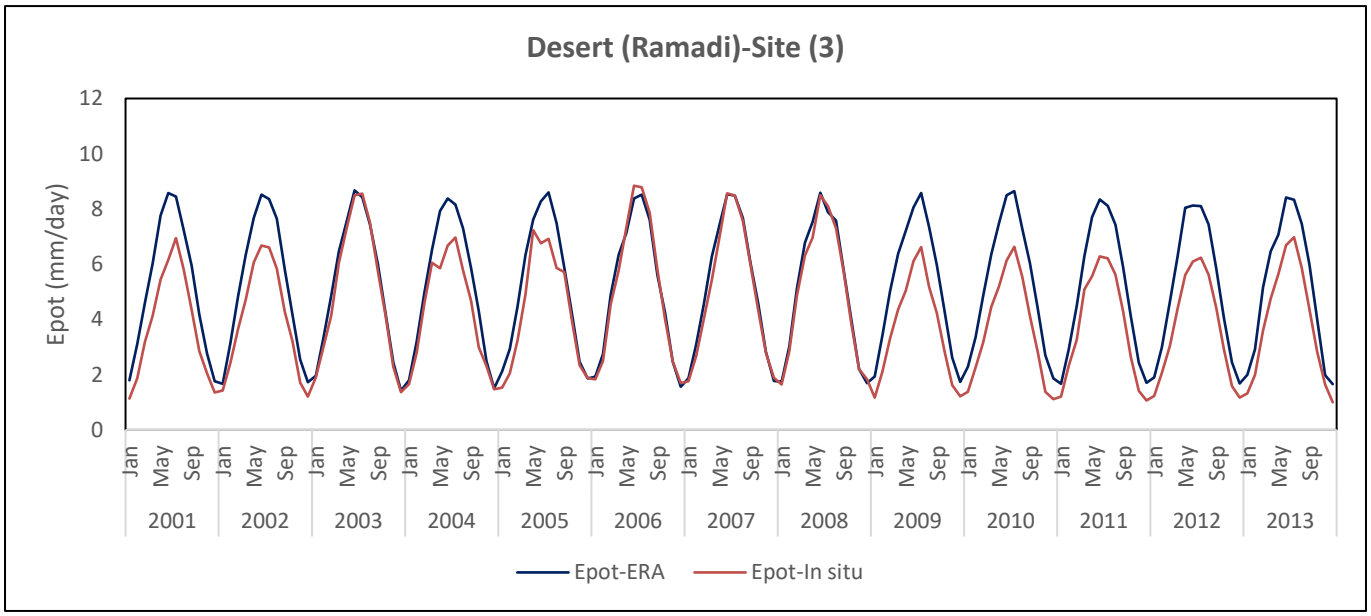
Desert (Ramadi)-Site (3)
Epot (mm/day)
12
10
8
6
4
2
0
Jan May Sep
2001 2002 2003 2004 2005 2006 2007 2008 2009 2010 2011 2012 2013
Epot-ERA
Epot-In situ

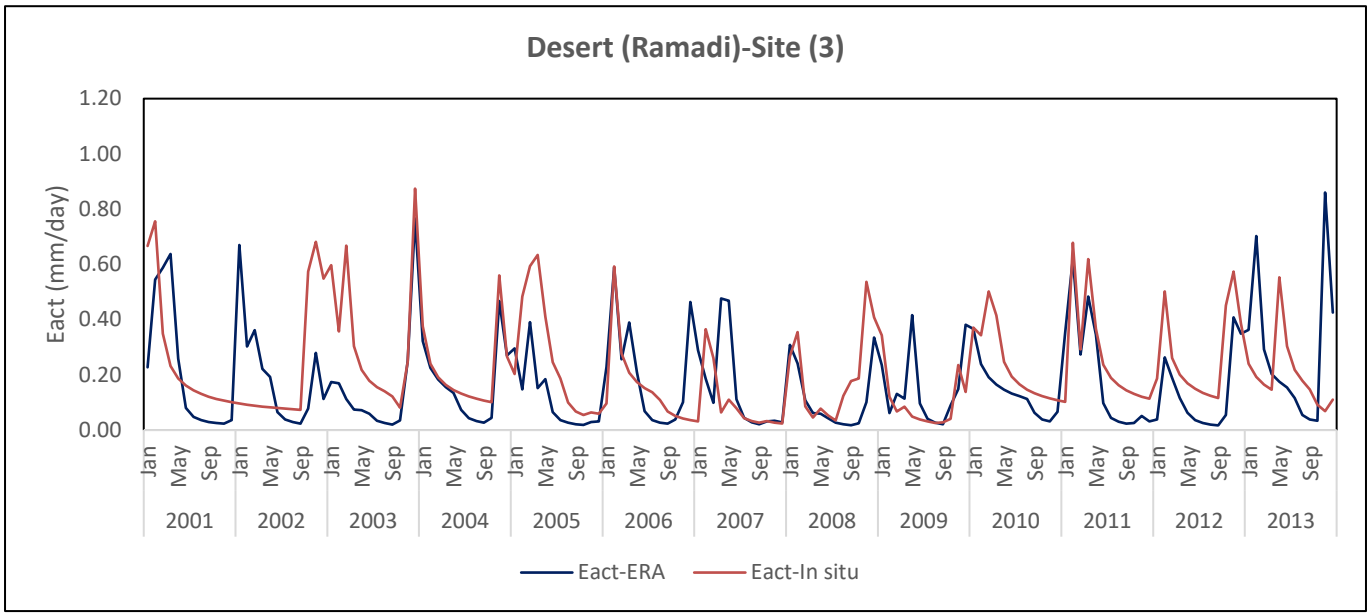
Desert (Ramadi)-Site (3)
Eact (mm/day)
1.20
1.00
0.80
0.60
0.40
0.20
0.00
Jan May Sep
2001 2002 2003 2004 2005 2006 2007 2008 2009 2010 2011 2012 2013
Eact-ERA
Eact-In situ

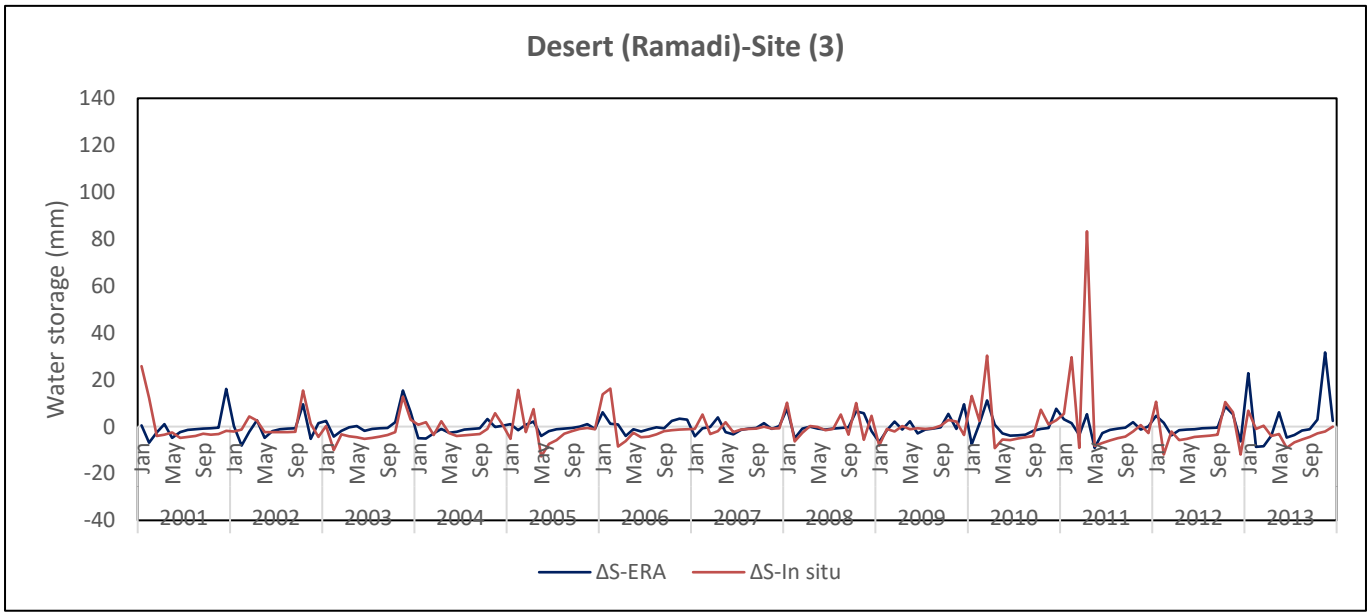
Desert (Ramadi)-Site (3)
Water storage (mm)
140
120
100
80
60
40
20
0
-20
-40
Jan May Sep
2001 2002 2003 2004 2005 2006 2007 2008 2009 2010 2011 2012 2013
ΔS-ERA
ΔS-In situ

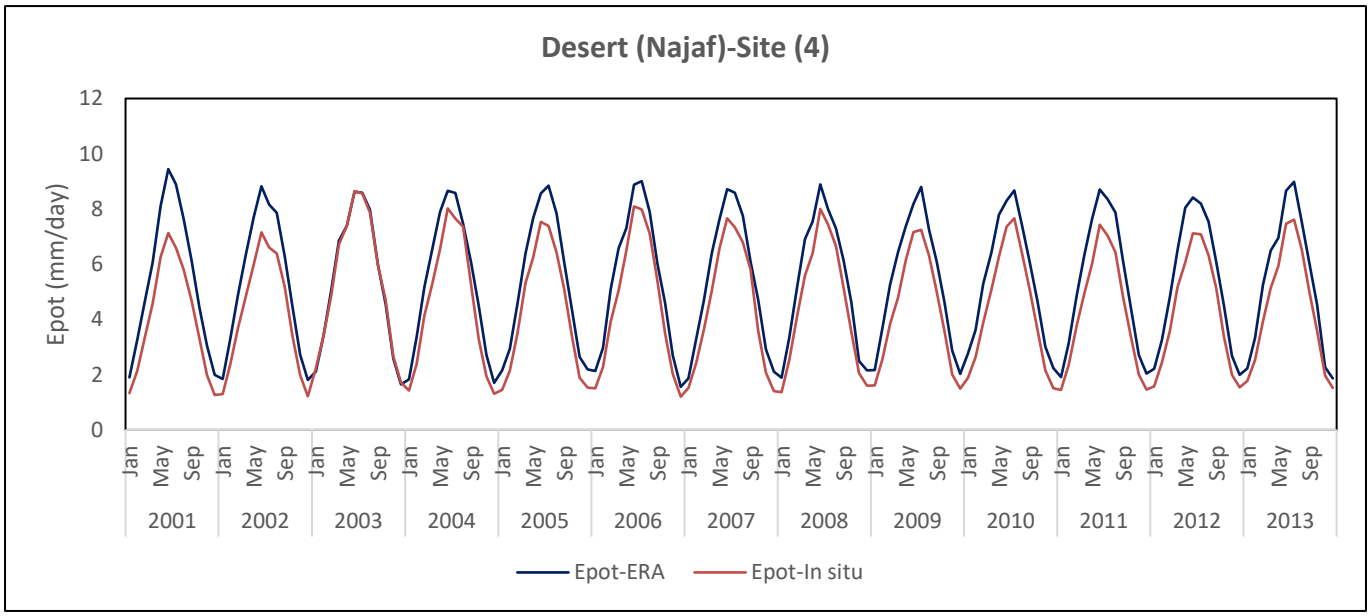
Desert (Najaf)-Site (4)
Epot (mm/day)
0
2
4
6
8
10
12
Jan May Sep
2001 2002 2003 2004 2005 2006 2007 2008 2009 2010 2011 2012 2013
Epot-ERA
Epot-In situ

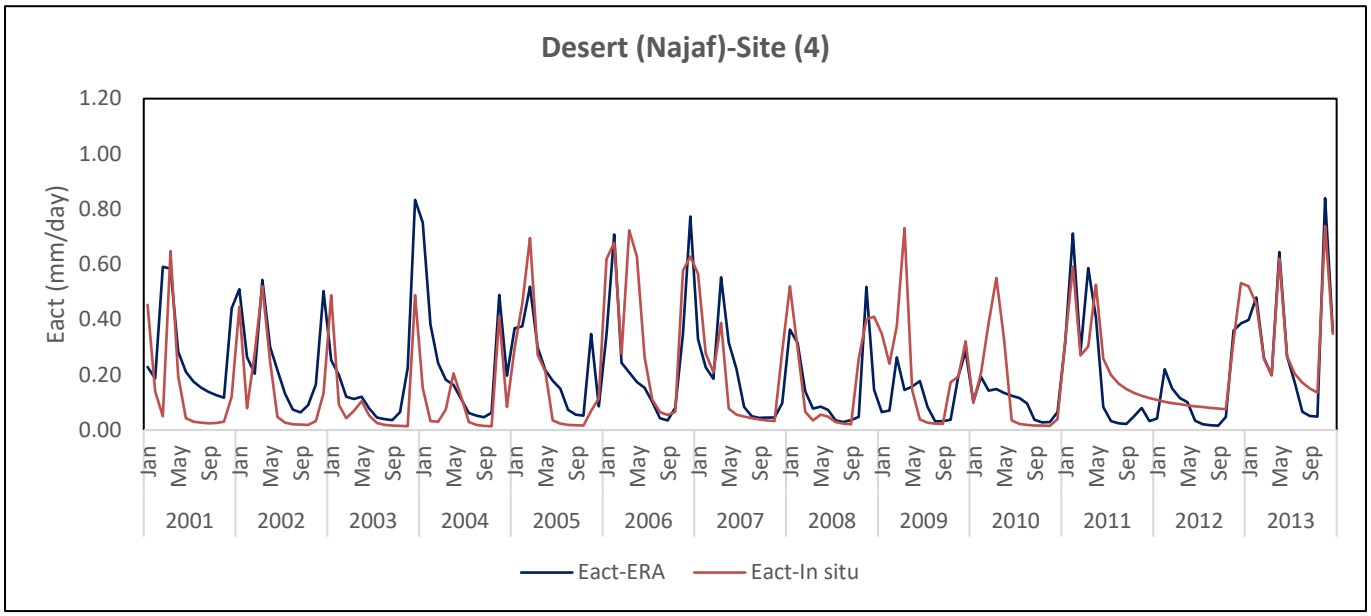
Desert (Najaf)-Site (4)
Eact (mm/day)
0.00
0.20
0.40
0.60
0.80
1.00
1.20
Jan May Sep
2001 2002 2003 2004 2005 2006 2007 2008 2009 2010 2011 2012 2013
Eact-ERA
Eact-In situ

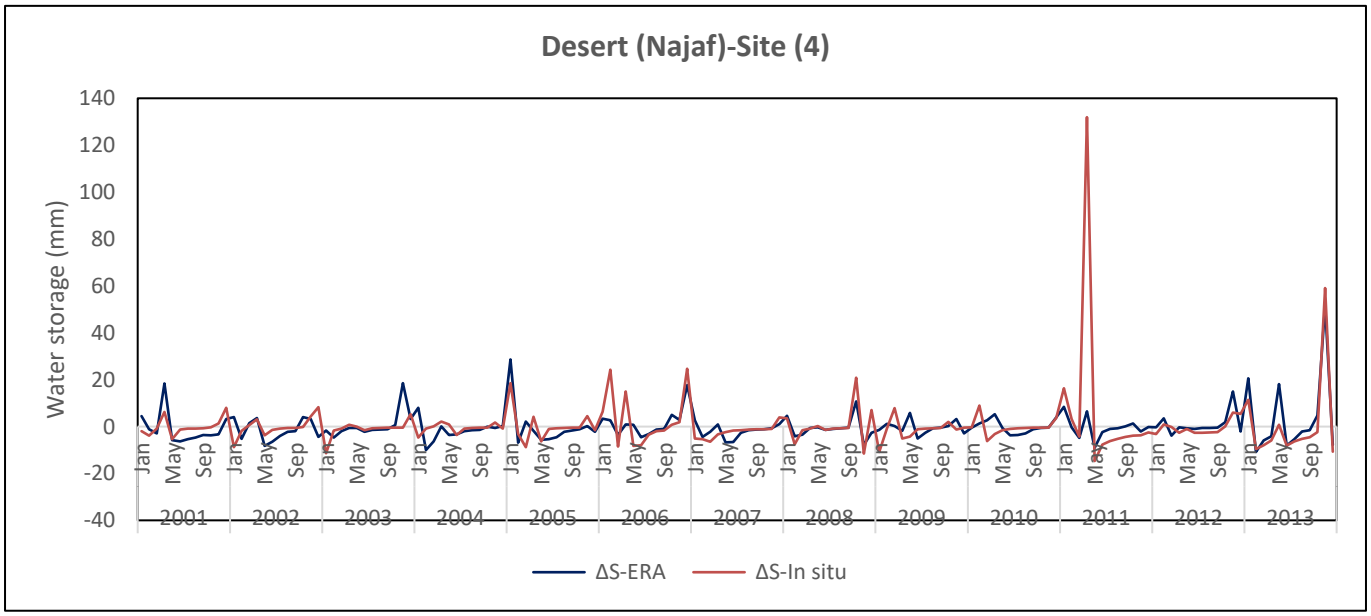
Desert (Najaf)-Site (4)
Water storage (mm)
-40
-20
0
20
40
60
80
100
120
140
Jan May Sep
2001 2002 2003 2004 2005 2006 2007 2008 2009 2010 2011 2012 2013
ΔS-ERA
ΔS-In situ

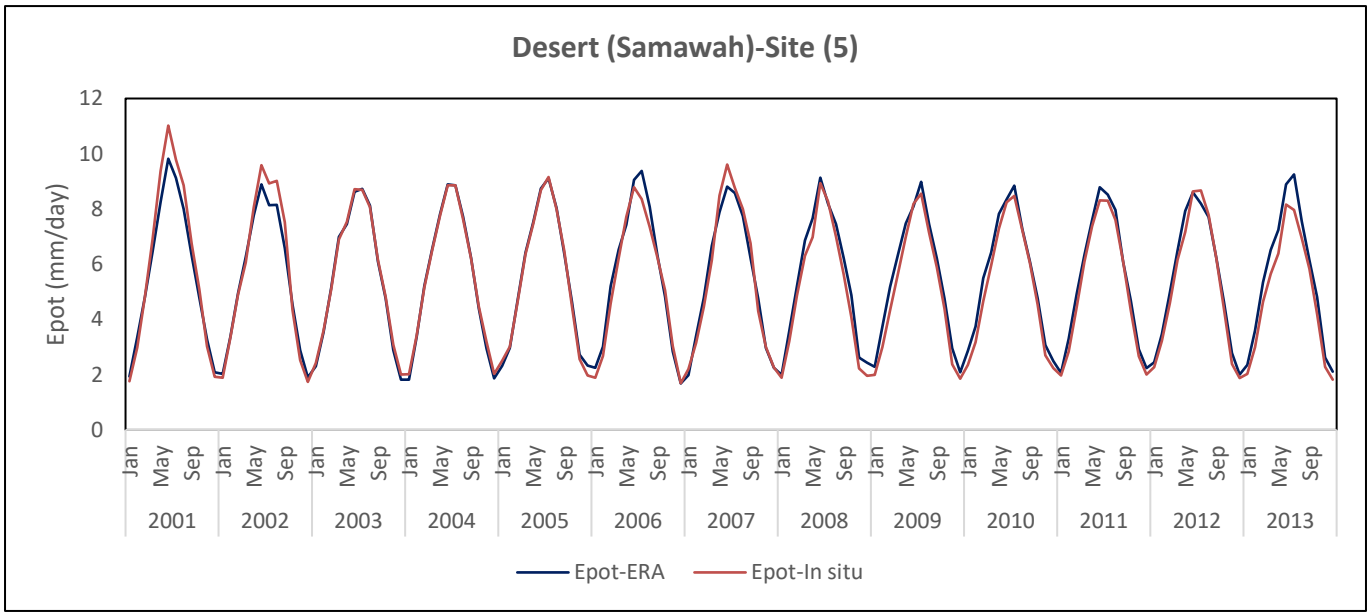
Desert (Samawah)-Site (5)
Epot (mm/day)
0
2
4
6
8
10
12
Jan May Sep
2001 2002 2003 2004 2005 2006 2007 2008 2009 2010 2011 2012 2013
Epot-ERA
Epot-In situ

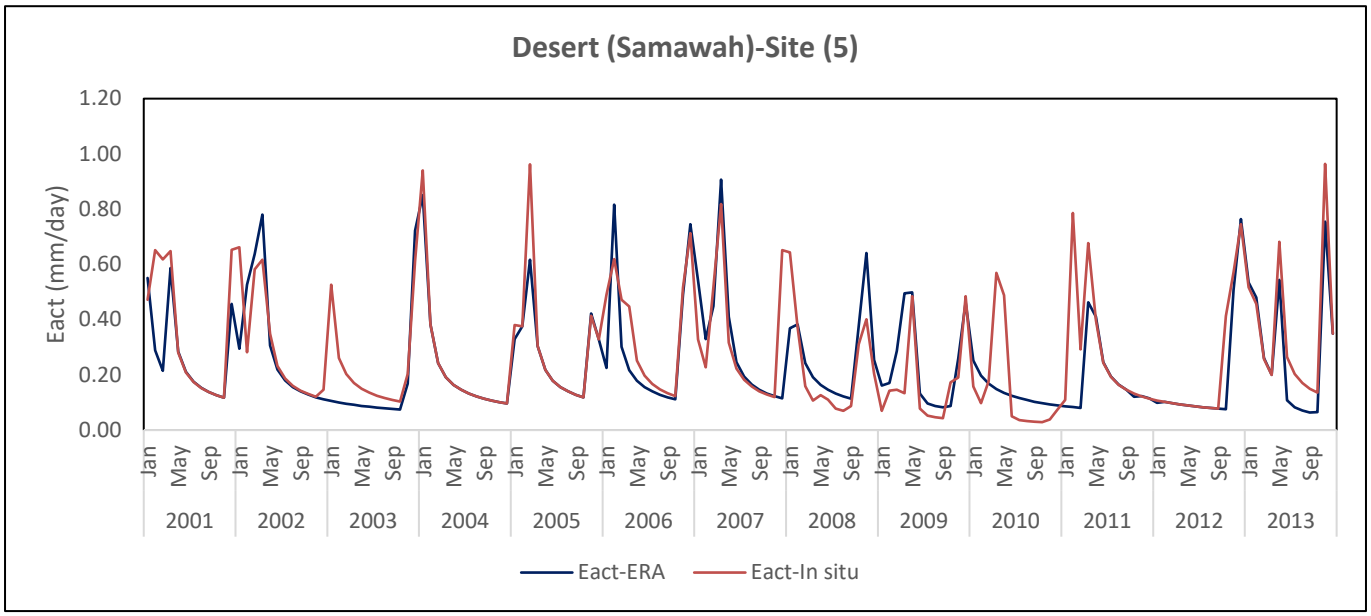
Desert (Samawah)-Site (5)
Eact (mm/day)
0.00
0.20
0.40
0.60
0.80
1.00
1.20
Jan May Sep
2001 2002 2003 2004 2005 2006 2007 2008 2009 2010 2011 2012 2013
Eact-ERA
Eact-In situ

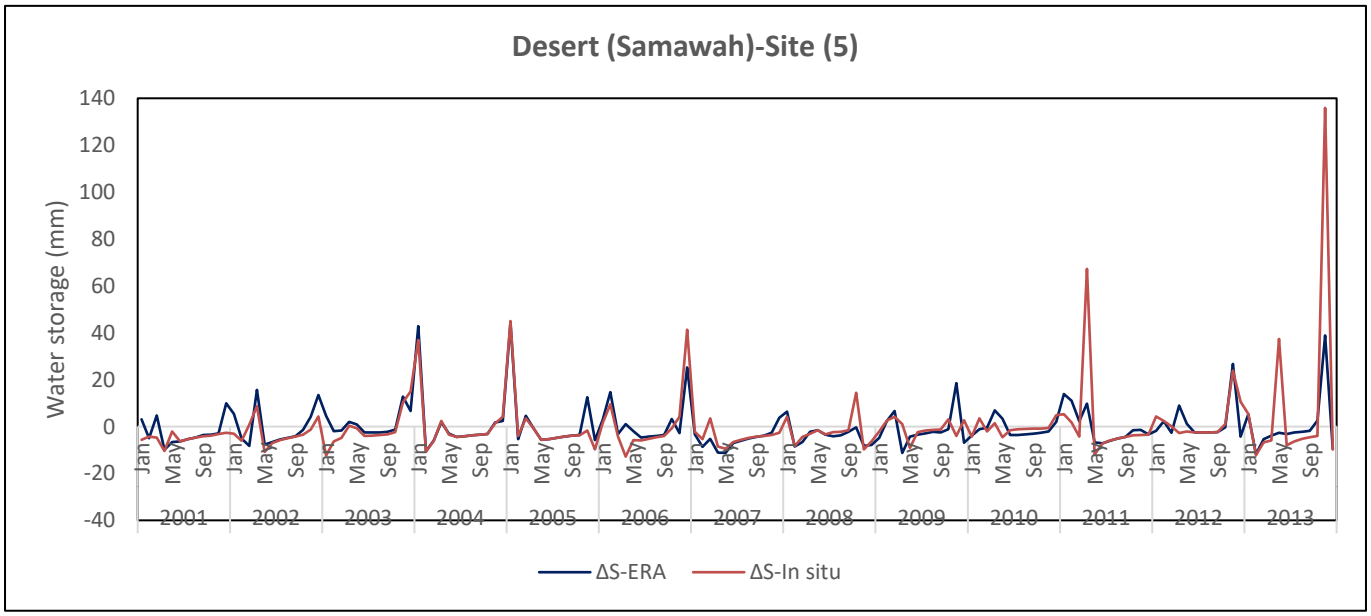
Desert (Samawah)-Site (5)
Water storage (mm)
-40
-20
0
20
40
60
80
100
120
140
Jan May Sep
2001 2002 2003 2004 2005 2006 2007 2008 2009 2010 2011 2012 2013
ΔS-ERA
ΔS-In situ

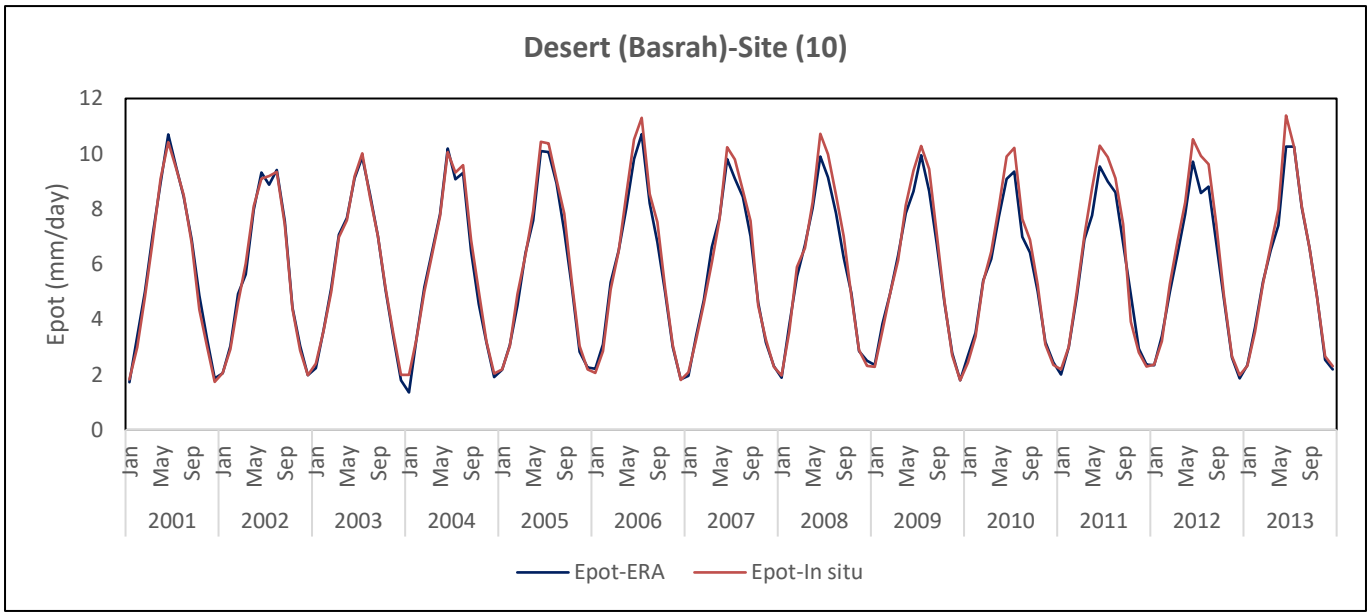
Desert (Basrah)-Site (10)
Epot (mm/day)
0
2
4
6
8
10
12
Jan May Sep
2001 2002 2003 2004 2005 2006 2007 2008 2009 2010 2011 2012 2013
Epot-ERA
Epot-In situ

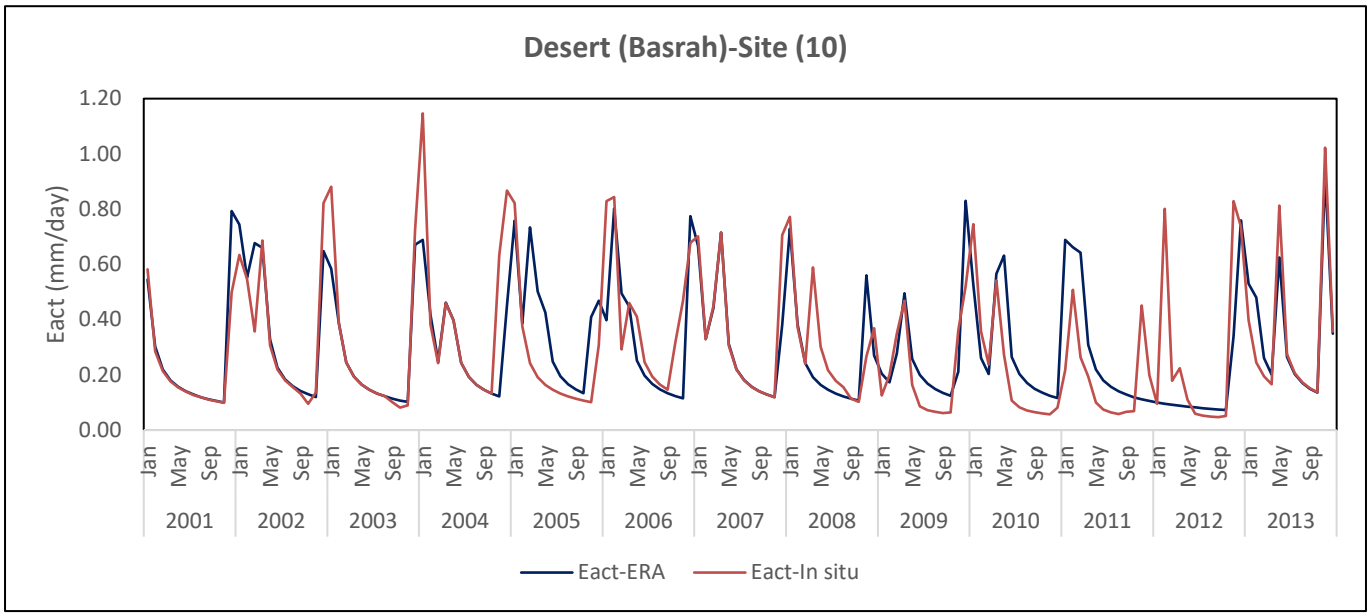
Desert (Basrah)-Site (10)
Eact (mm/day)
0.00
0.20
0.40
0.60
0.80
1.00
1.20
Jan May Sep
2001 2002 2003 2004 2005 2006 2007 2008 2009 2010 2011 2012 2013
Eact-ERA
Eact-In situ

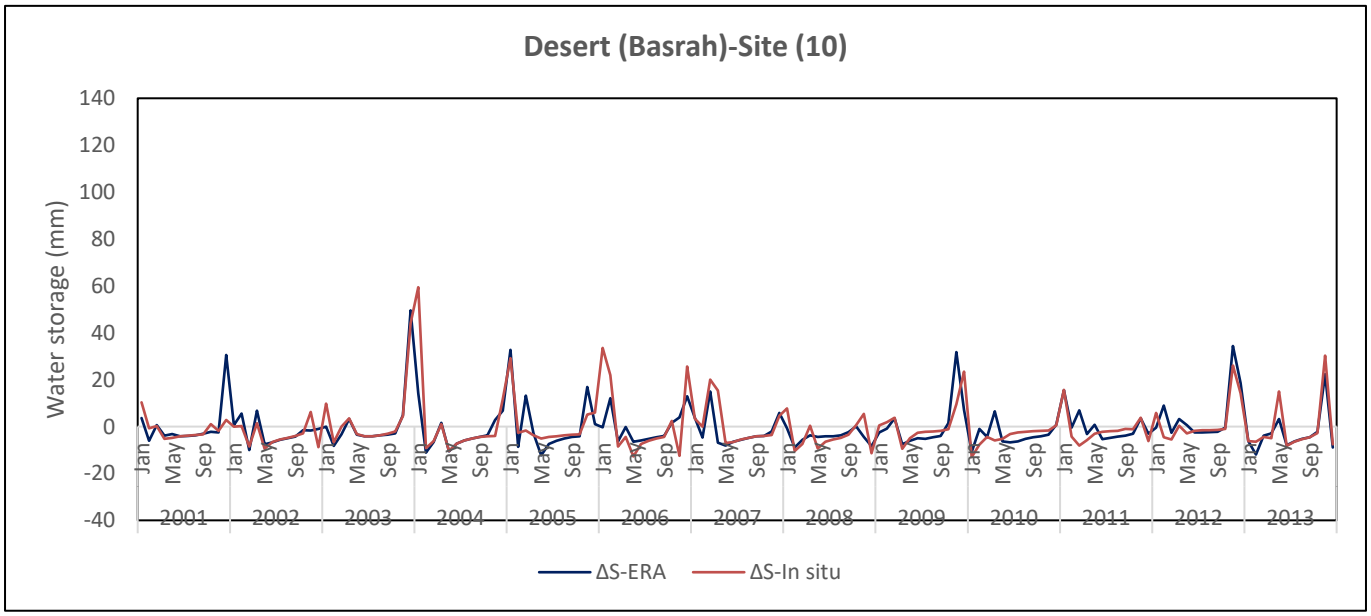
Desert (Basrah)-Site (10)
Water storage (mm)
-40
-20
0
20
40
60
80
100
120
140
Jan May Sep
2001 2002 2003 2004 2005 2006 2007 2008 2009 2010 2011 2012 2013
ΔS-ERA
ΔS-In situ

APPENDIX H: Assessment of water balance components from SWAP runs during (2001-2015) for the rangeland region.

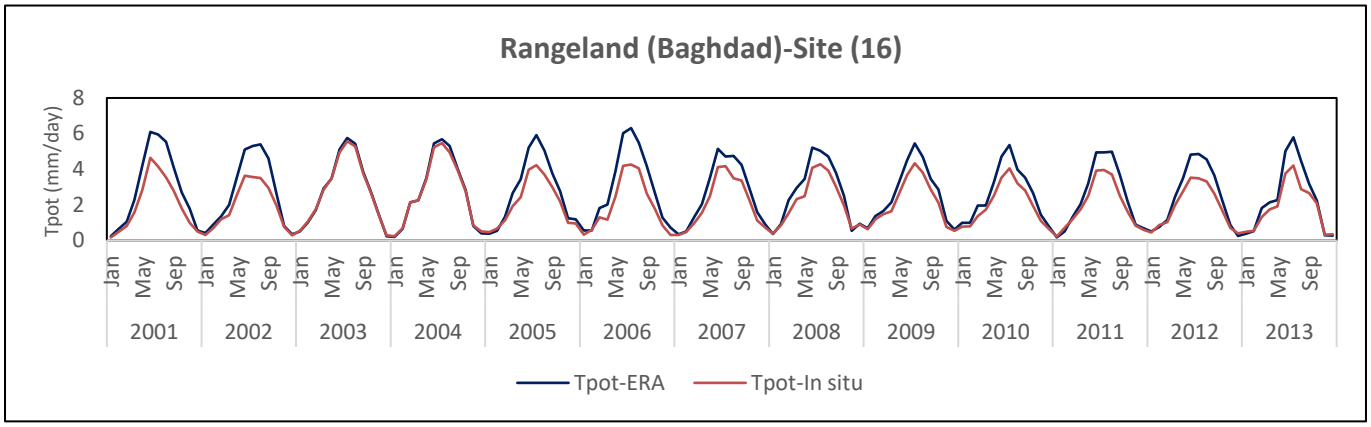

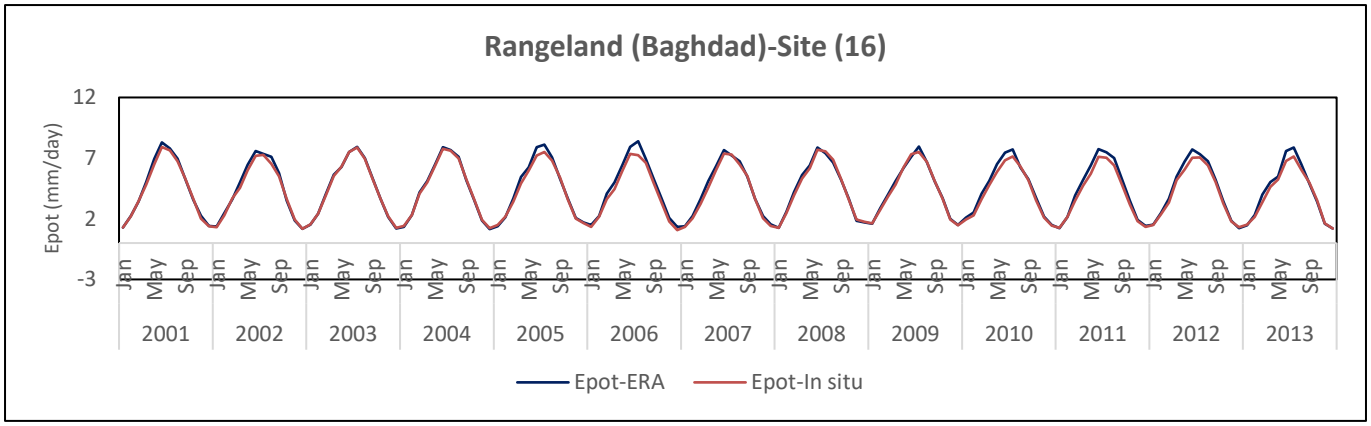

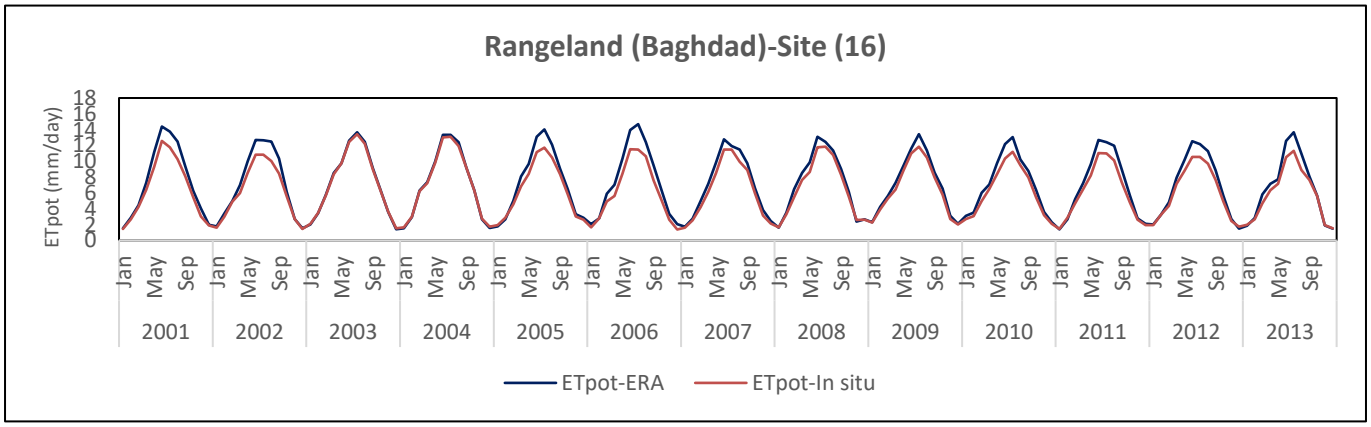

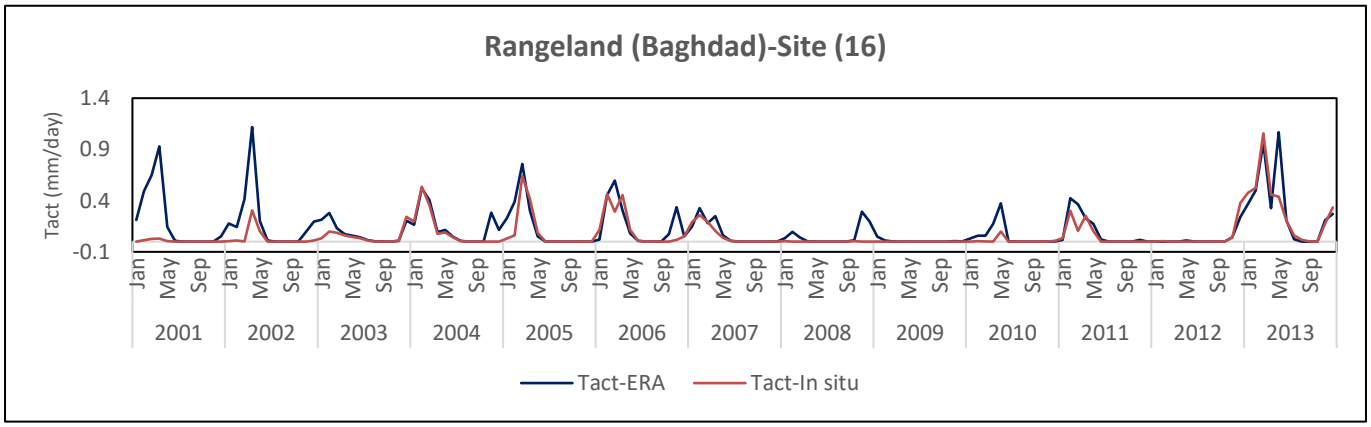

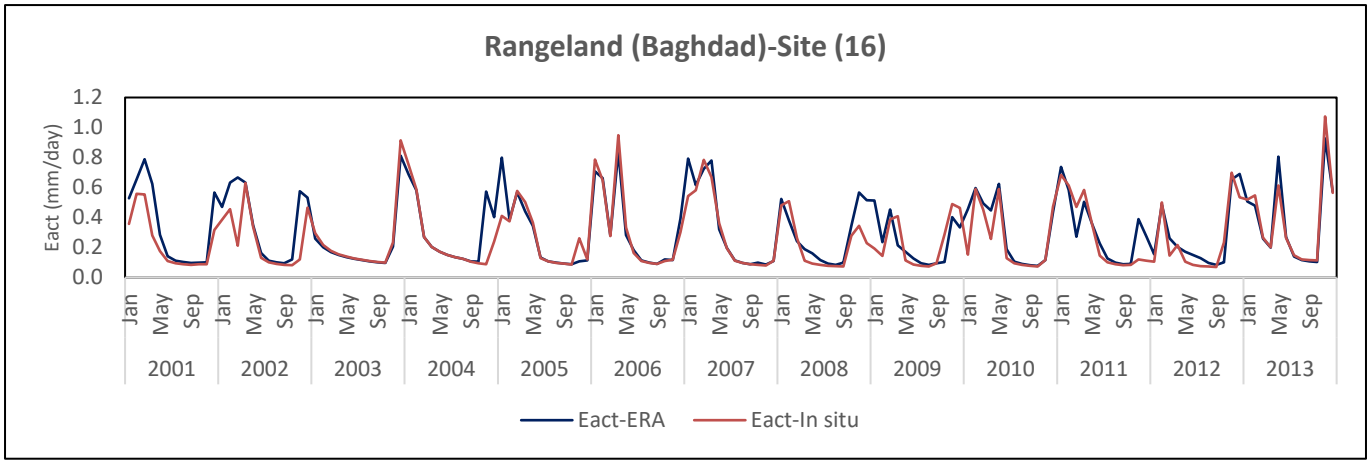
Rangeland (Baghdad)-Site (16)
Eact (mm/day)
1.2
1.0
0.8
0.6
0.4
0.2
0.0
Jan May Sep
2001 2002 2003 2004 2005 2006 2007 2008 2009 2010 2011 2012 2013
Eact-ERA
Eact-In situ

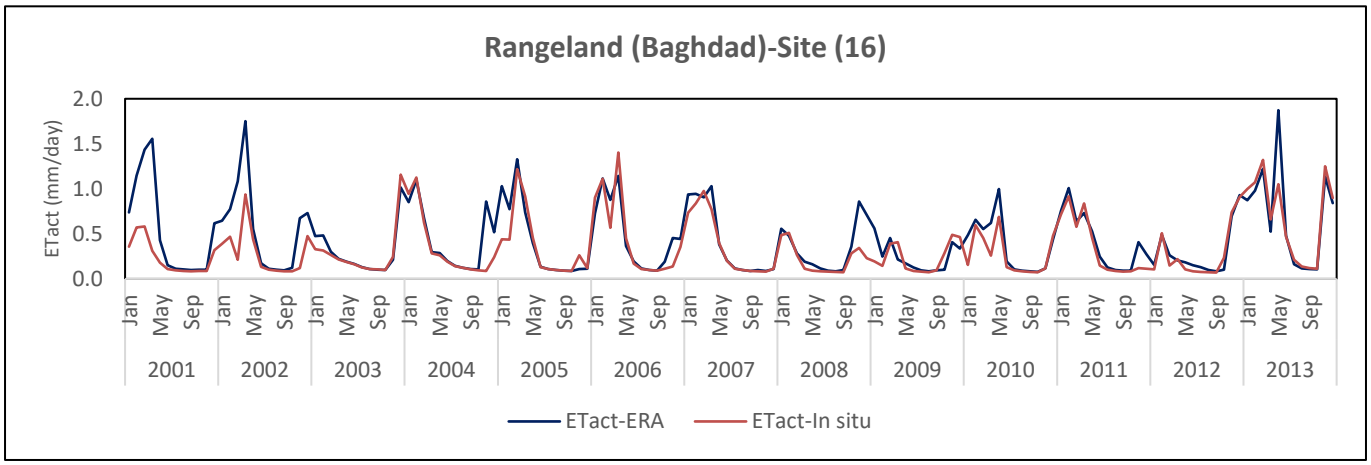
Rangeland (Baghdad)-Site (16)
ETact (mm/day)
2.0
1.5
1.0
0.5
0.0
Jan May Sep
2001 2002 2003 2004 2005 2006 2007 2008 2009 2010 2011 2012 2013
ETact-ERA
ETact-In situ

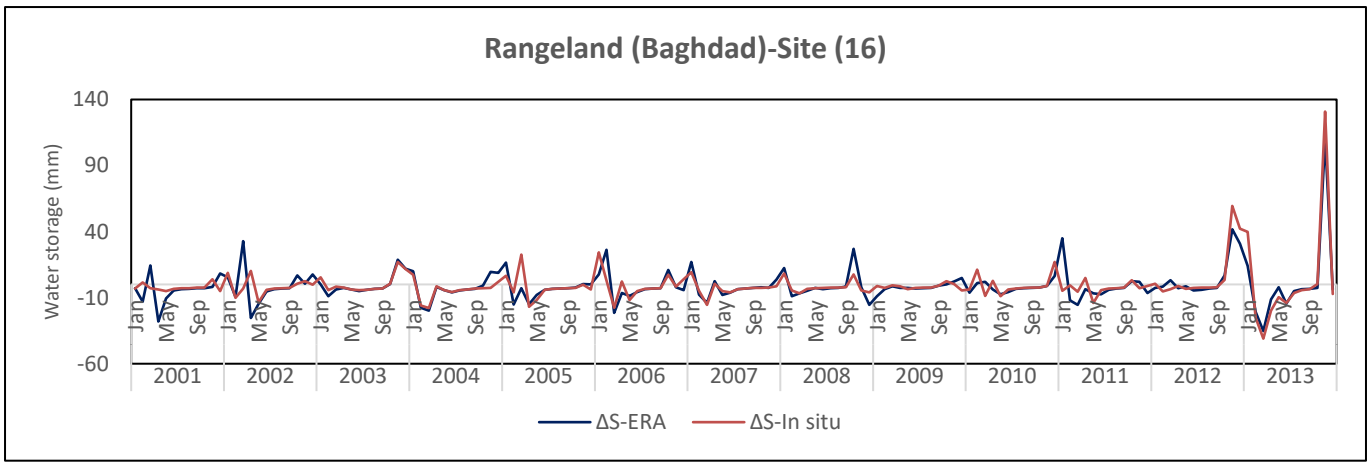
Rangeland (Baghdad)-Site (16)
Water storage (mm)
140
90
40
-10
-60
Jan May Sep
2001 2002 2003 2004 2005 2006 2007 2008 2009 2010 2011 2012 2013
ΔS-ERA
ΔS-In situ

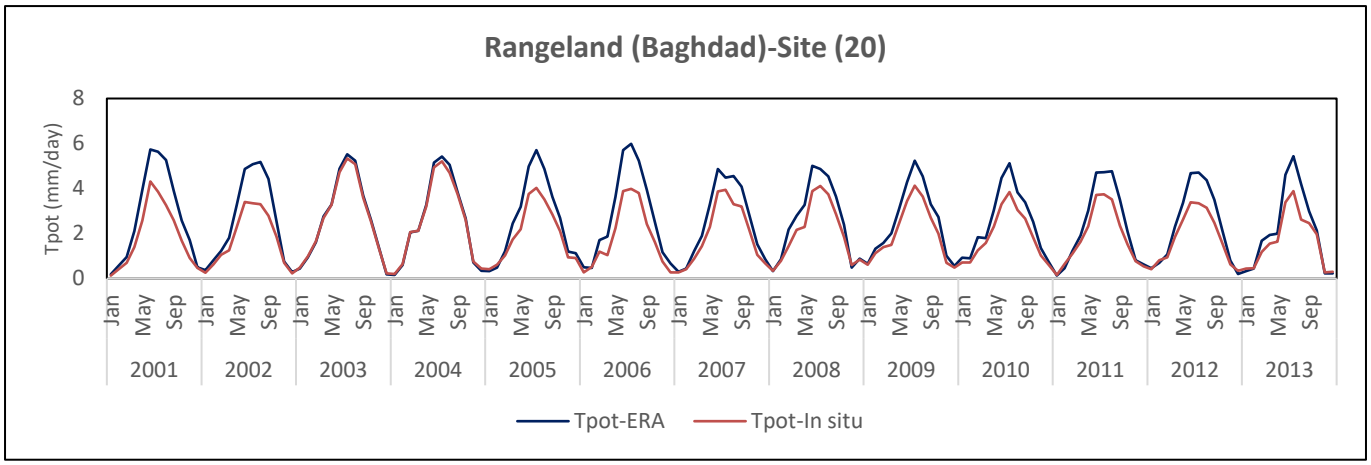
Rangeland (Baghdad)-Site (20)
Tpot (mm/day)
0
2
4
6
8
Jan May Sep
2001 2002 2003 2004 2005 2006 2007 2008 2009 2010 2011 2012 2013
Tpot-ERA
Tpot-In situ

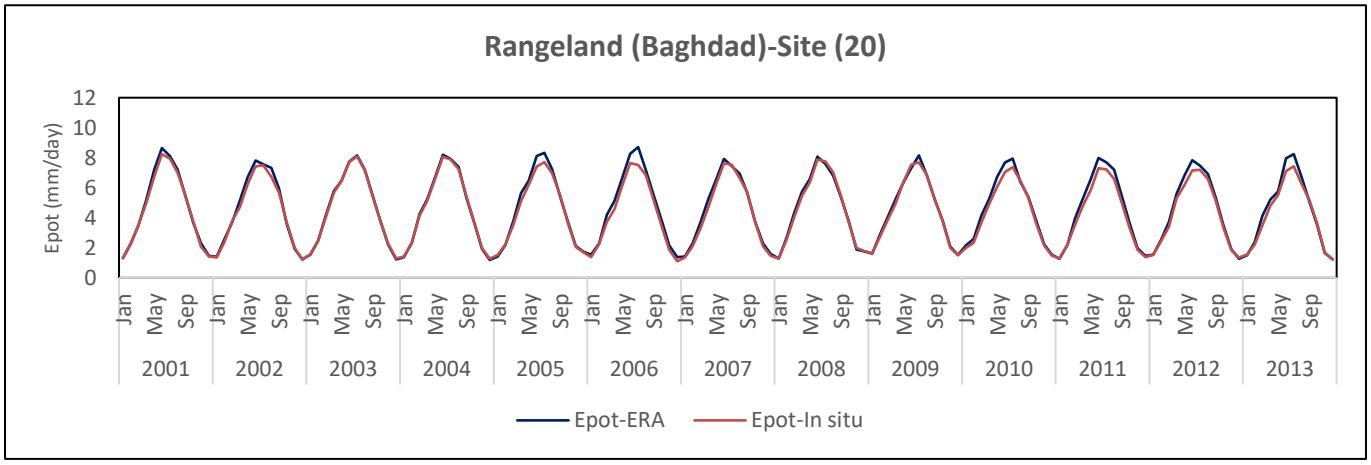
Rangeland (Baghdad)-Site (20)
Epot (mm/day)
0
2
4
6
8
10
12
Jan May Sep
2001 2002 2003 2004 2005 2006 2007 2008 2009 2010 2011 2012 2013
Epot-ERA
Epot-In situ

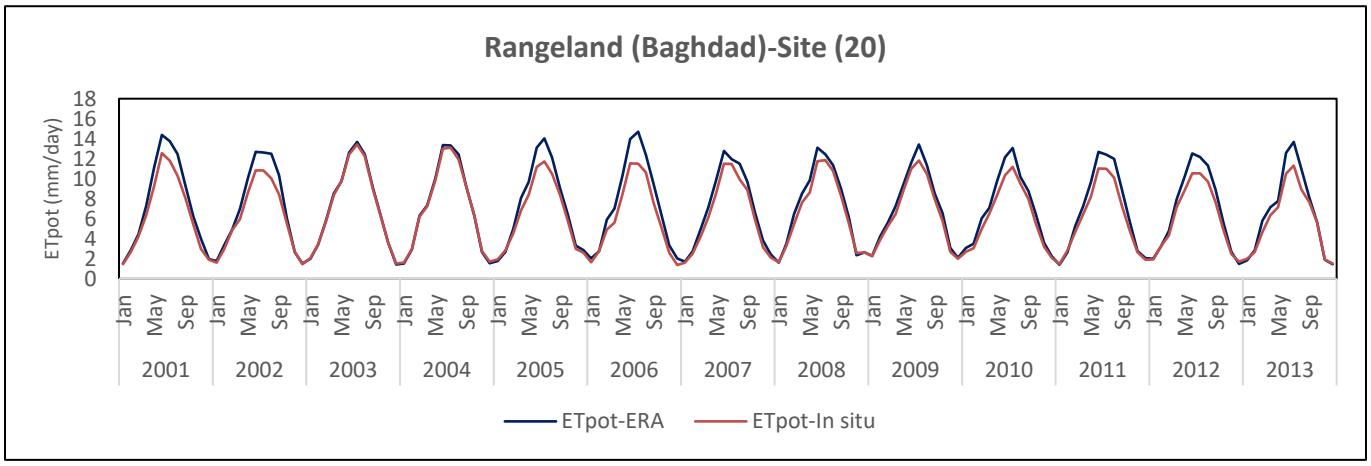
Rangeland (Baghdad)-Site (20)
ETpot (mm/day)
0
2
4
6
8
10
12
14
16
18
Jan May Sep
2001 2002 2003 2004 2005 2006 2007 2008 2009 2010 2011 2012 2013
ETpot-ERA
ETpot-In situ

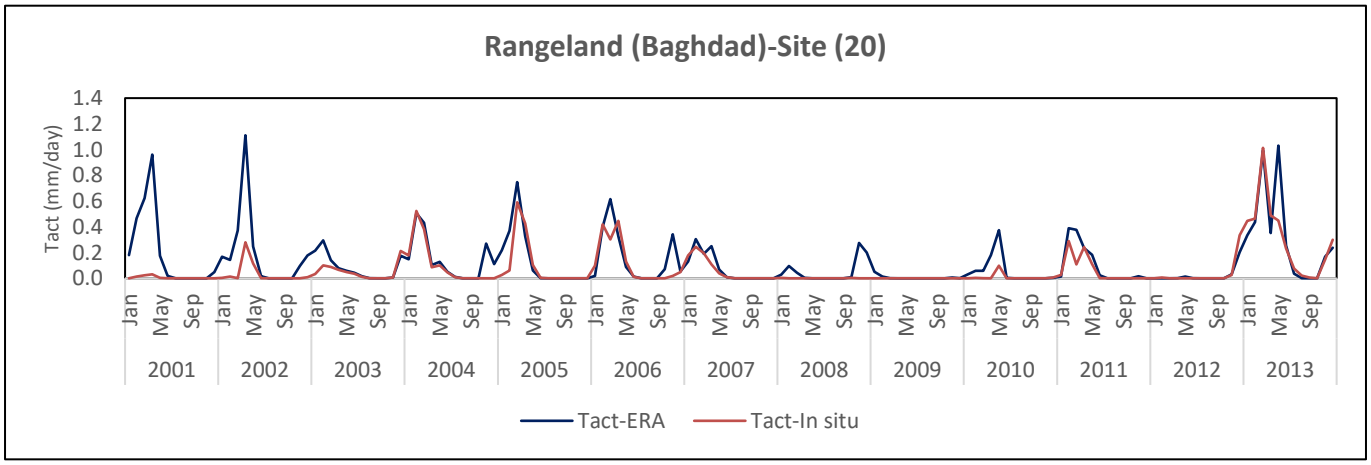
Rangeland (Baghdad)-Site (20)
Tact (mm/day)
0.0
0.2
0.4
0.6
0.8
1.0
1.2
1.4
Jan May Sep
2001 2002 2003 2004 2005 2006 2007 2008 2009 2010 2011 2012 2013
Tact-ERA
Tact-In situ

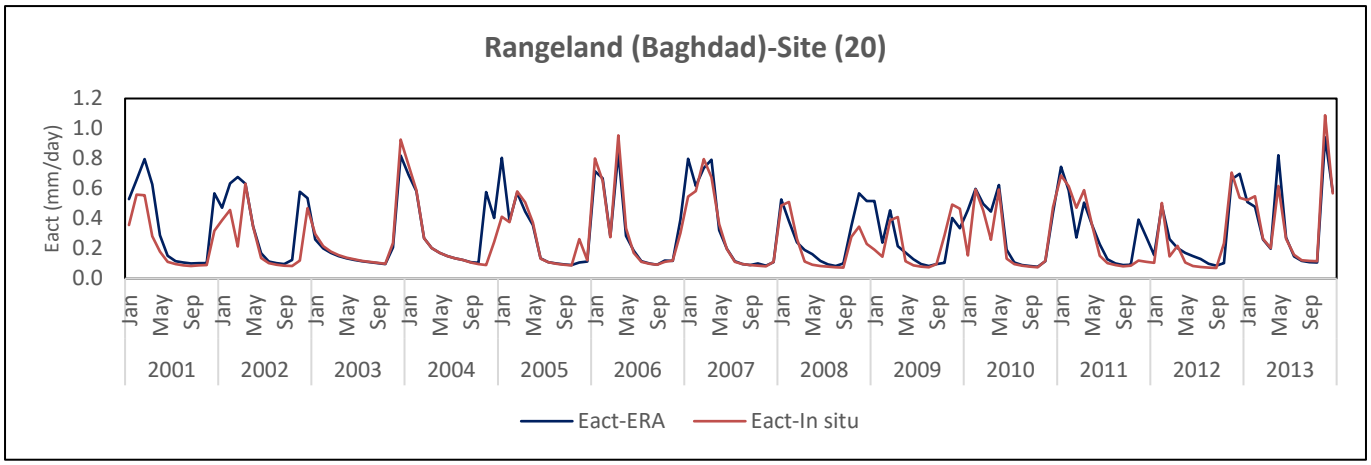
Rangeland (Baghdad)-Site (20)
Eact (mm/day)
1.2
1.0
0.8
0.6
0.4
0.2
0.0
Jan May Sep
2001 2002 2003 2004 2005 2006 2007 2008 2009 2010 2011 2012 2013
Eact-ERA
Eact-In situ

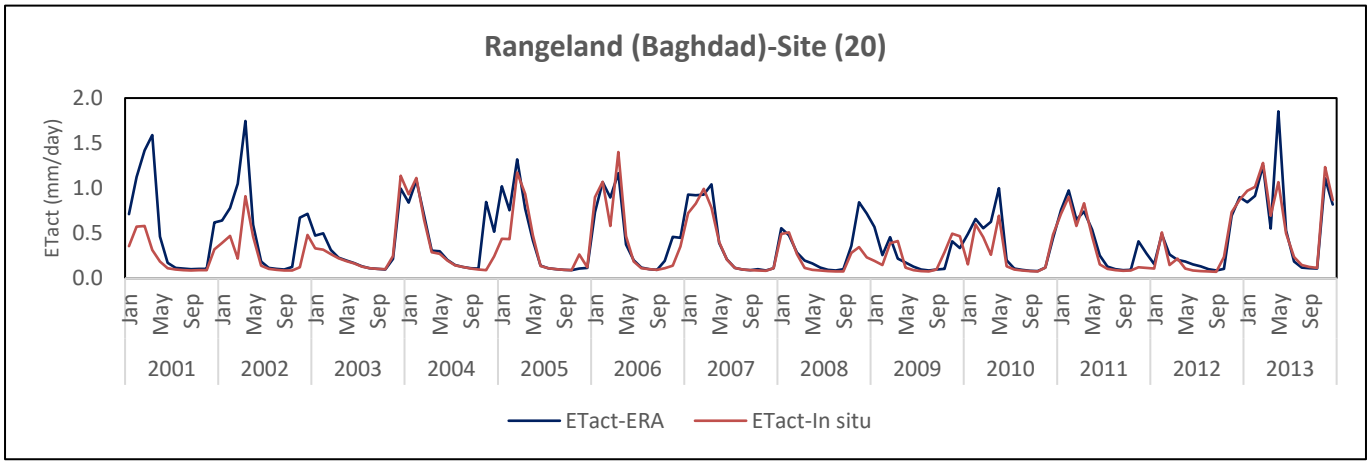
Rangeland (Baghdad)-Site (20)
ETact (mm/day)
2.0
1.5
1.0
0.5
0.0
Jan May Sep
2001 2002 2003 2004 2005 2006 2007 2008 2009 2010 2011 2012 2013
ETact-ERA
ETact-In situ

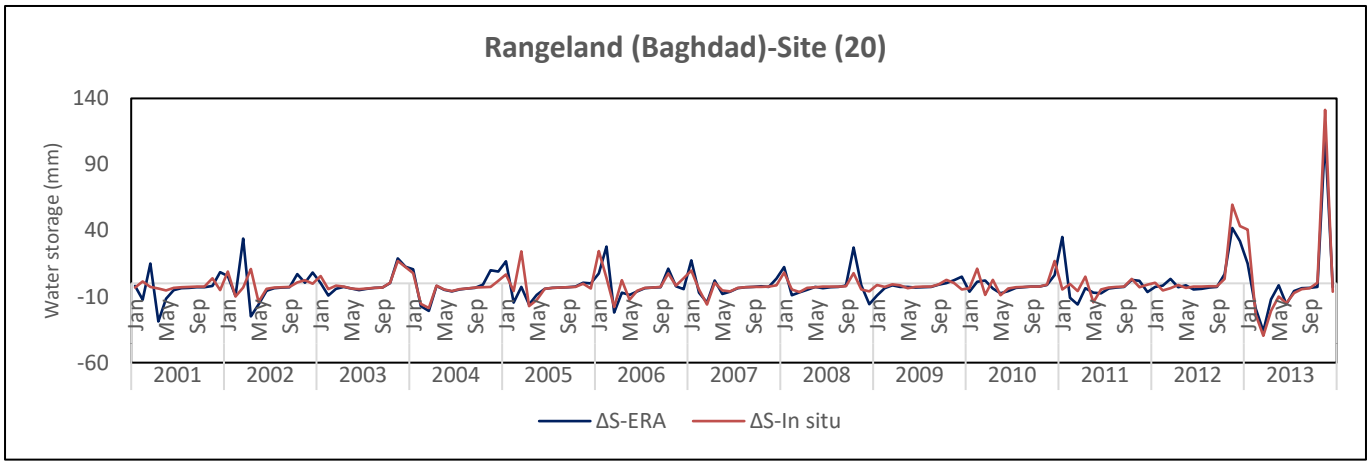
Rangeland (Baghdad)-Site (20)
Water storage (mm)
140
90
40
-10
-60
Jan May Sep
2001 2002 2003 2004 2005 2006 2007 2008 2009 2010 2011 2012 2013
ΔS-ERA
ΔS-In situ

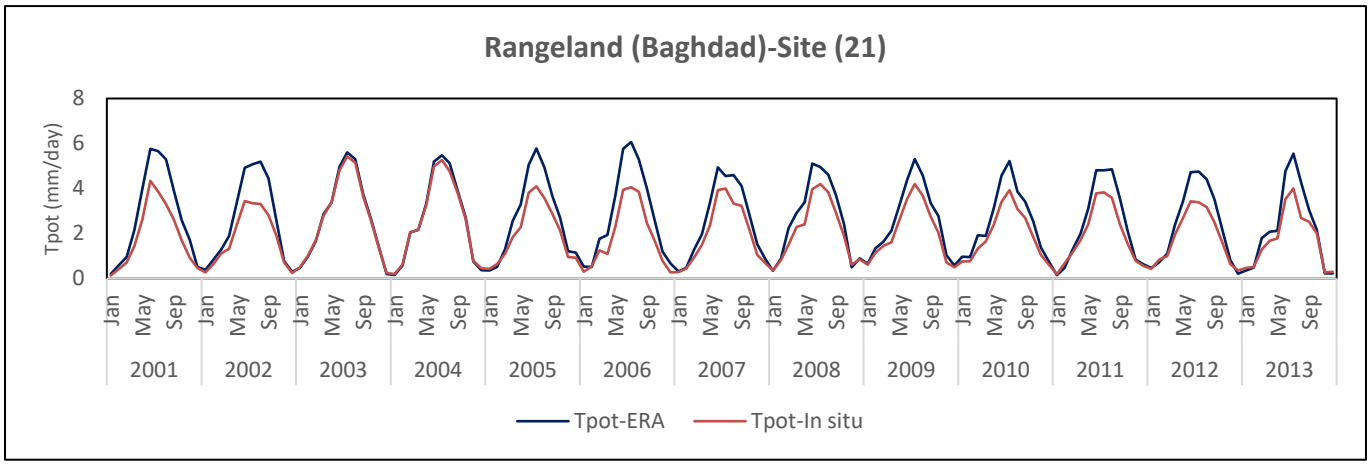
Rangeland (Baghdad)-Site (21)
Tpot (mm/day)
0
2
4
6
8
Jan May Sep
2001 2002 2003 2004 2005 2006 2007 2008 2009 2010 2011 2012 2013
Tpot-ERA
Tpot-In situ

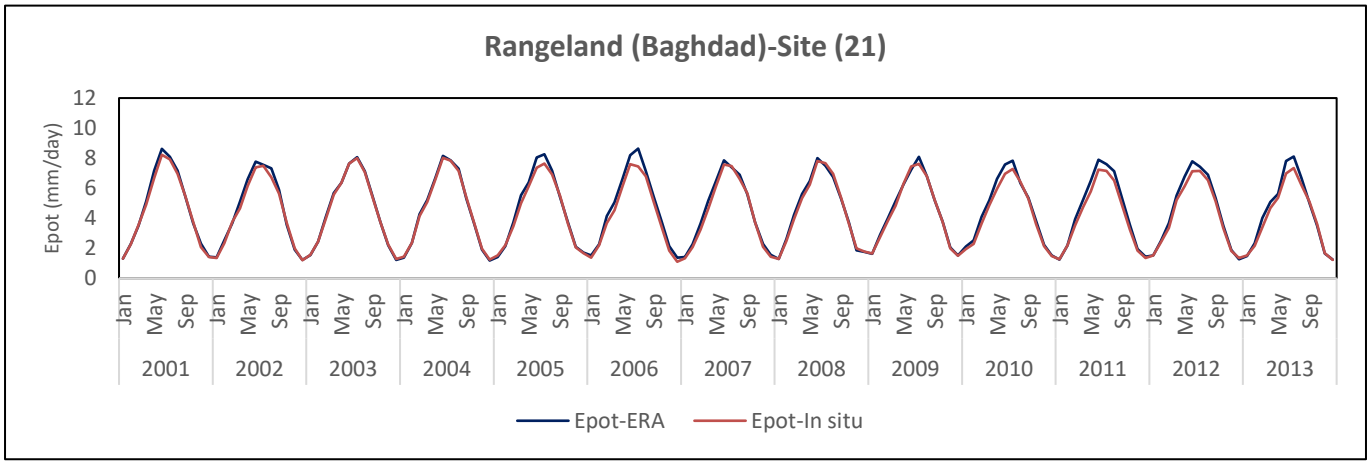
Rangeland (Baghdad)-Site (21)
Epot (mm/day)
0
2
4
6
8
10
12
Jan May Sep
2001 2002 2003 2004 2005 2006 2007 2008 2009 2010 2011 2012 2013
Epot-ERA
Epot-In situ

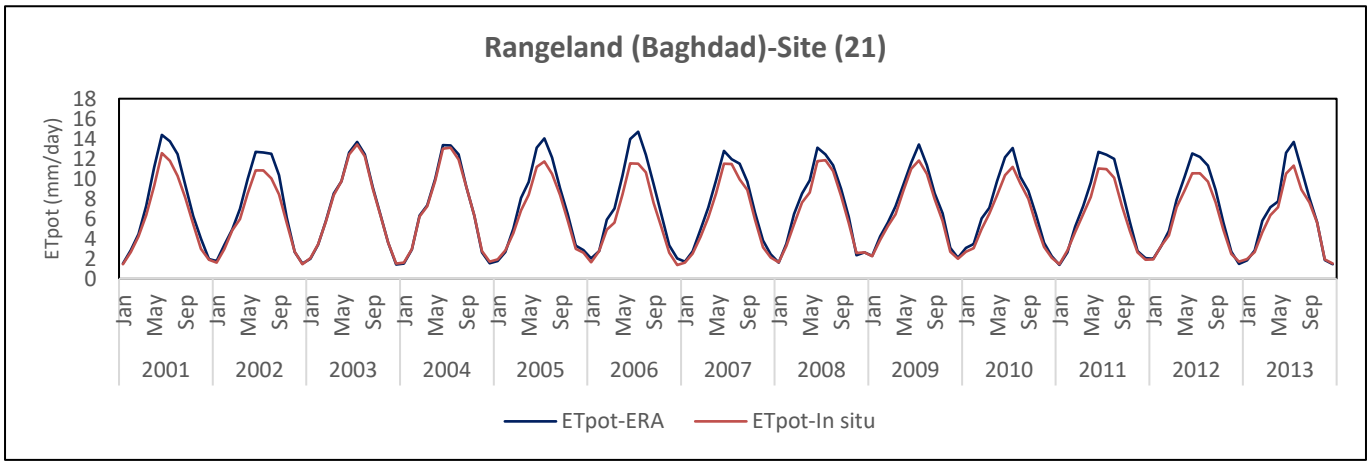
Rangeland (Baghdad)-Site (21)
ETpot (mm/day)
0
2
4
6
8
10
12
14
16
18
Jan May Sep
2001 2002 2003 2004 2005 2006 2007 2008 2009 2010 2011 2012 2013
ETpot-ERA
ETpot-In situ

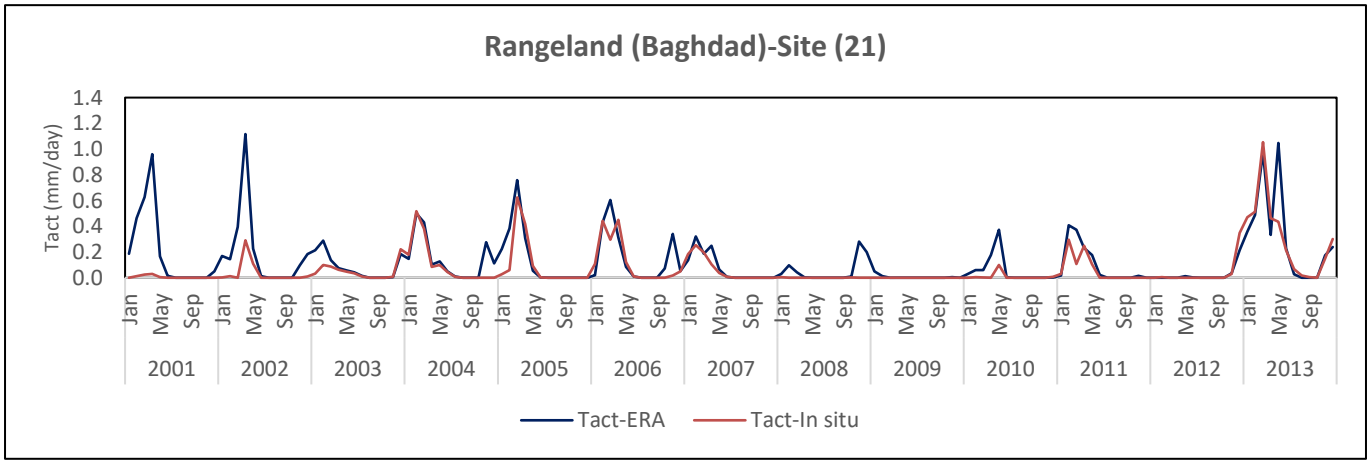
Rangeland (Baghdad)-Site (21)
Tact (mm/day)
0.0
0.2
0.4
0.6
0.8
1.0
1.2
1.4
Jan May Sep
2001 2002 2003 2004 2005 2006 2007 2008 2009 2010 2011 2012 2013
Tact-ERA
Tact-In situ

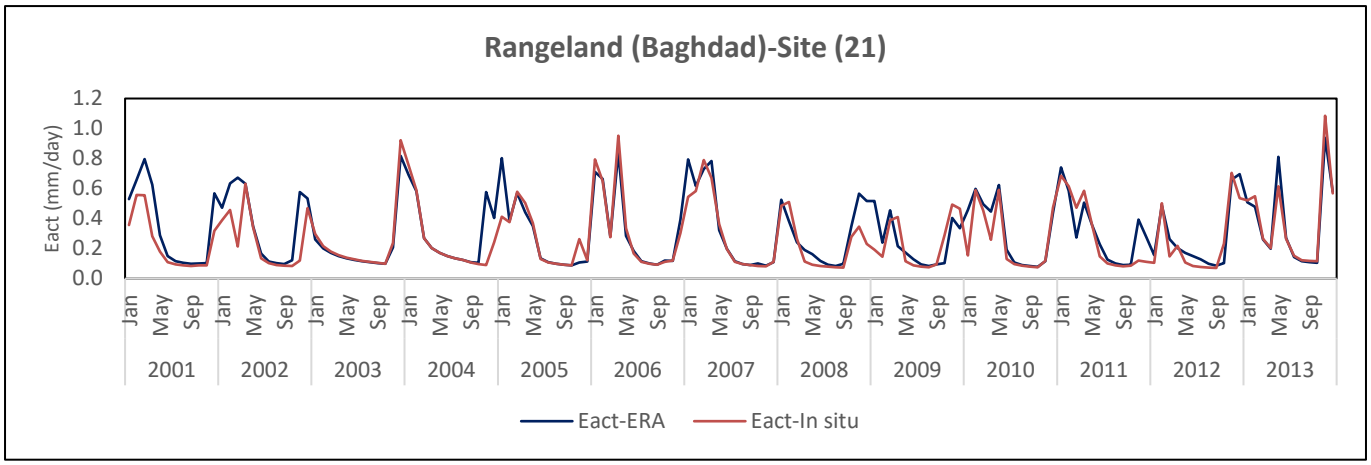
Rangeland (Baghdad)-Site (21)
Eact (mm/day)
1.2
1.0
0.8
0.6
0.4
0.2
0.0
Jan May Sep
2001 2002 2003 2004 2005 2006 2007 2008 2009 2010 2011 2012 2013
Eact-ERA
Eact-In situ

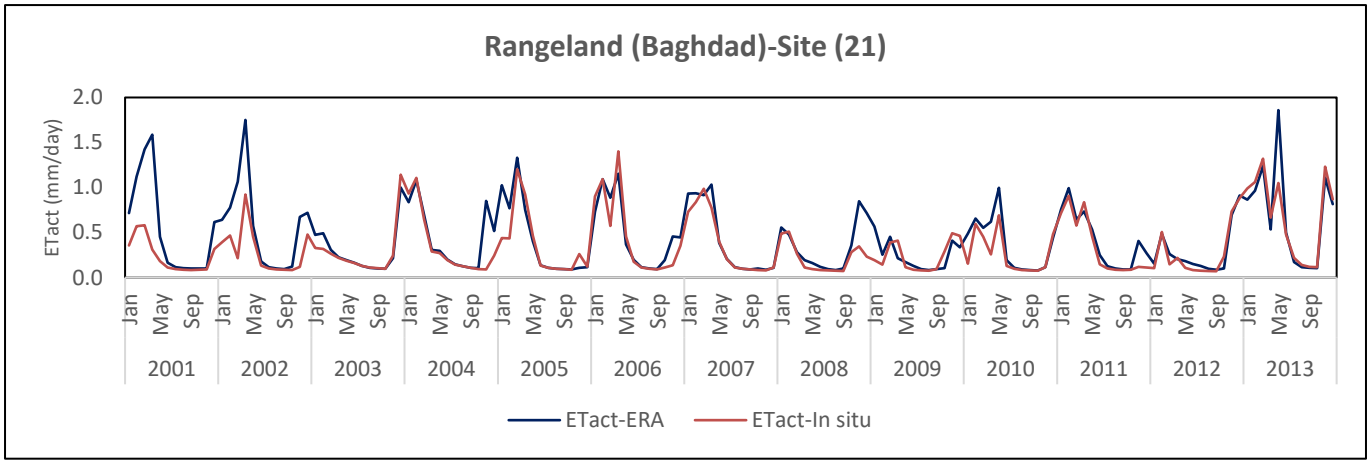
Rangeland (Baghdad)-Site (21)
ETact (mm/day)
2.0
1.5
1.0
0.5
0.0
Jan May Sep
2001 2002 2003 2004 2005 2006 2007 2008 2009 2010 2011 2012 2013
ETact-ERA
ETact-In situ

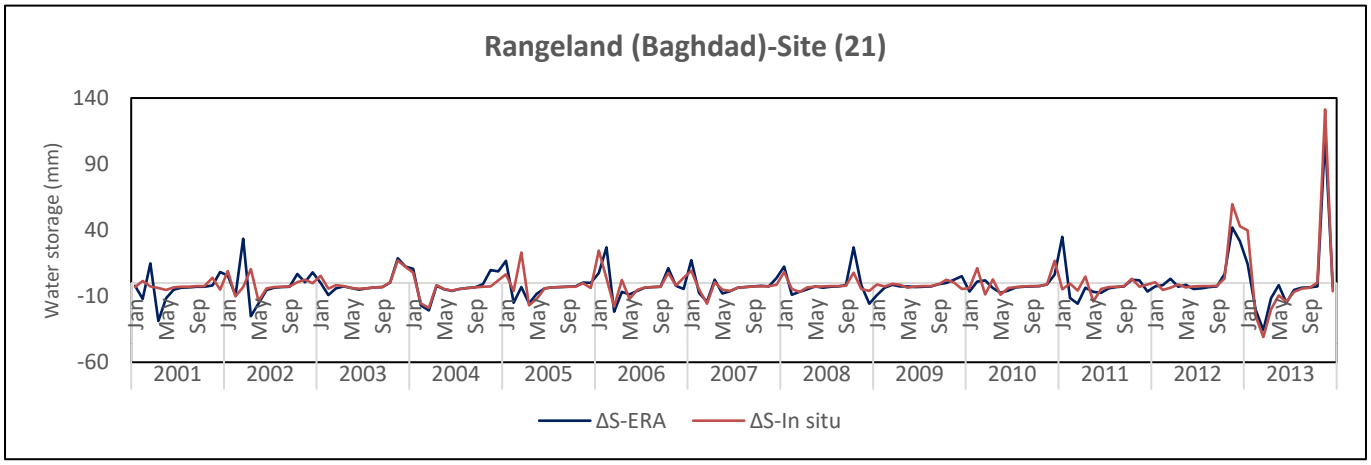
Rangeland (Baghdad)-Site (21)
Water storage (mm)
140
90
40
-10
-60
Jan May Sep
2001 2002 2003 2004 2005 2006 2007 2008 2009 2010 2011 2012 2013
ΔS-ERA
ΔS-In situ

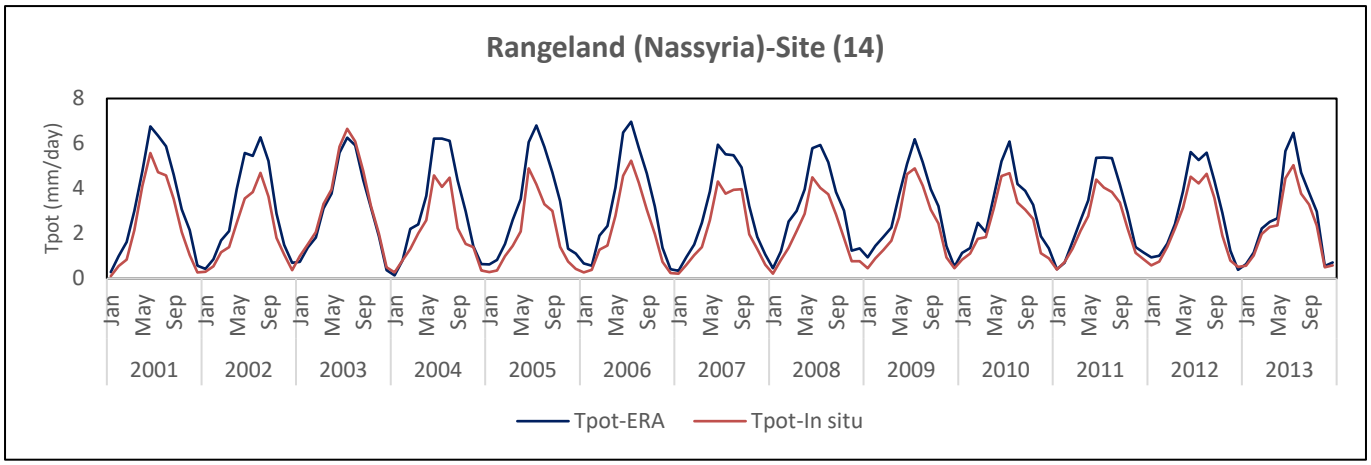
Rangeland (Nassyria)-Site (14)
Tpot (mm/day)
0
2
4
6
8
Jan May Sep
2001 2002 2003 2004 2005 2006 2007 2008 2009 2010 2011 2012 2013
Tpot-ERA
Tpot-In situ

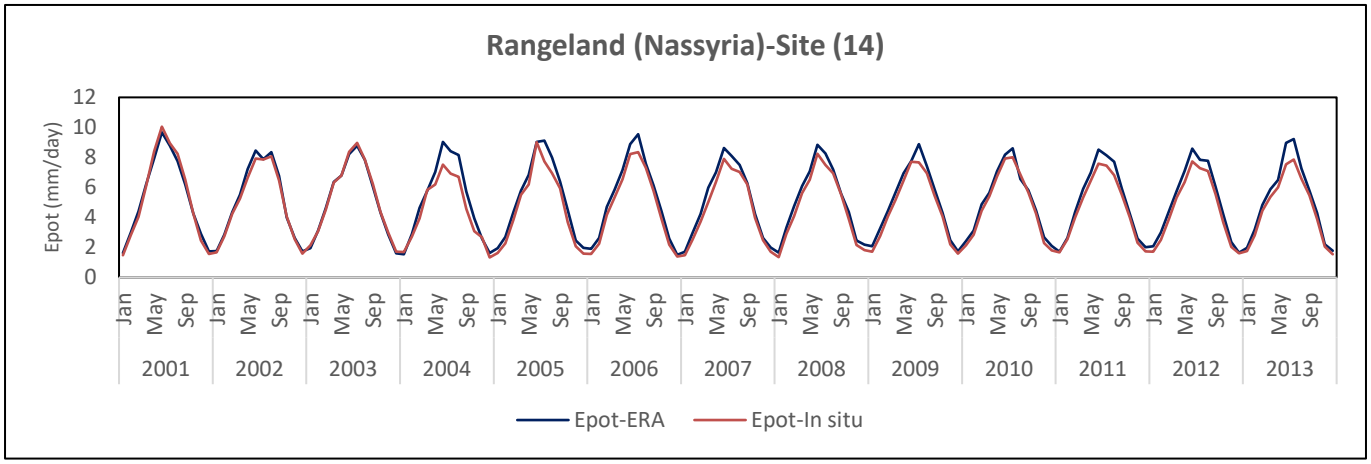
Rangeland (Nassyria)-Site (14)
Epot (mm/day)
0
2
4
6
8
10
12
Jan May Sep
2001 2002 2003 2004 2005 2006 2007 2008 2009 2010 2011 2012 2013
Epot-ERA
Epot-In situ

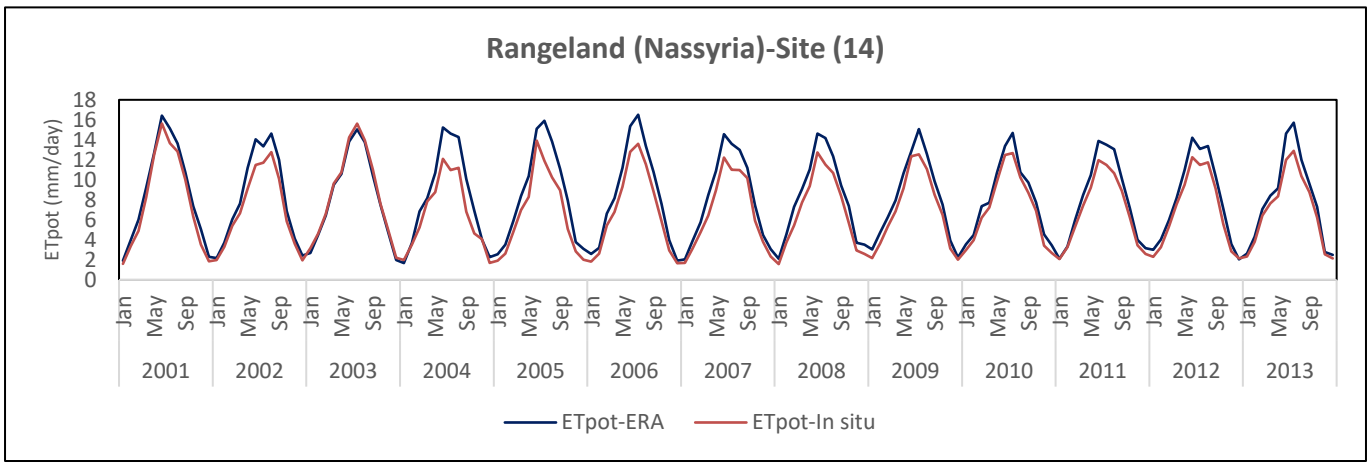
Rangeland (Nassyria)-Site (14)
ETpot (mm/day)
0
2
4
6
8
10
12
14
16
18
Jan May Sep
2001 2002 2003 2004 2005 2006 2007 2008 2009 2010 2011 2012 2013
ETpot-ERA
ETpot-In situ

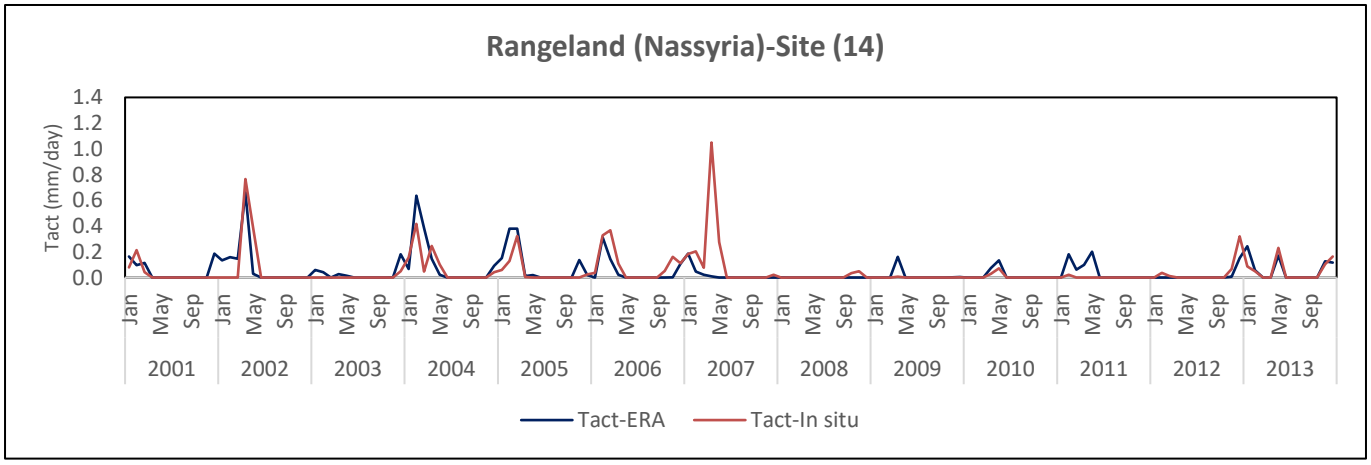
Rangeland (Nassyria)-Site (14)
Tact (mm/day)
0.0
0.2
0.4
0.6
0.8
1.0
1.2
1.4
Jan May Sep
2001 2002 2003 2004 2005 2006 2007 2008 2009 2010 2011 2012 2013
Tact-ERA
Tact-In situ

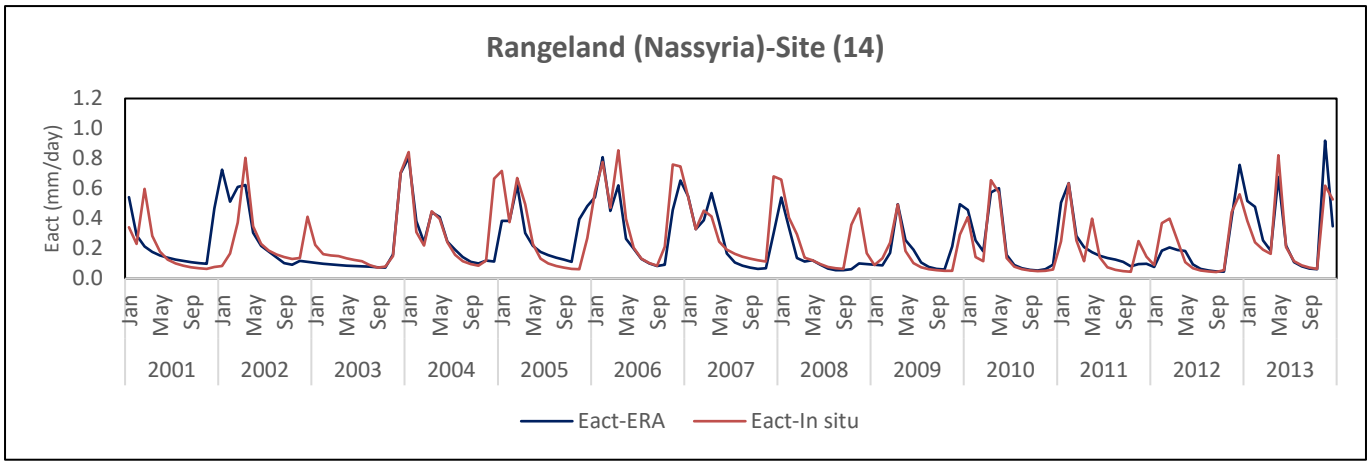
Rangeland (Nassyria)-Site (14)
Eact (mm/day)
1.2
1.0
0.8
0.6
0.4
0.2
0.0
Jan May Sep
2001 2002 2003 2004 2005 2006 2007 2008 2009 2010 2011 2012 2013
Eact-ERA
Eact-In situ

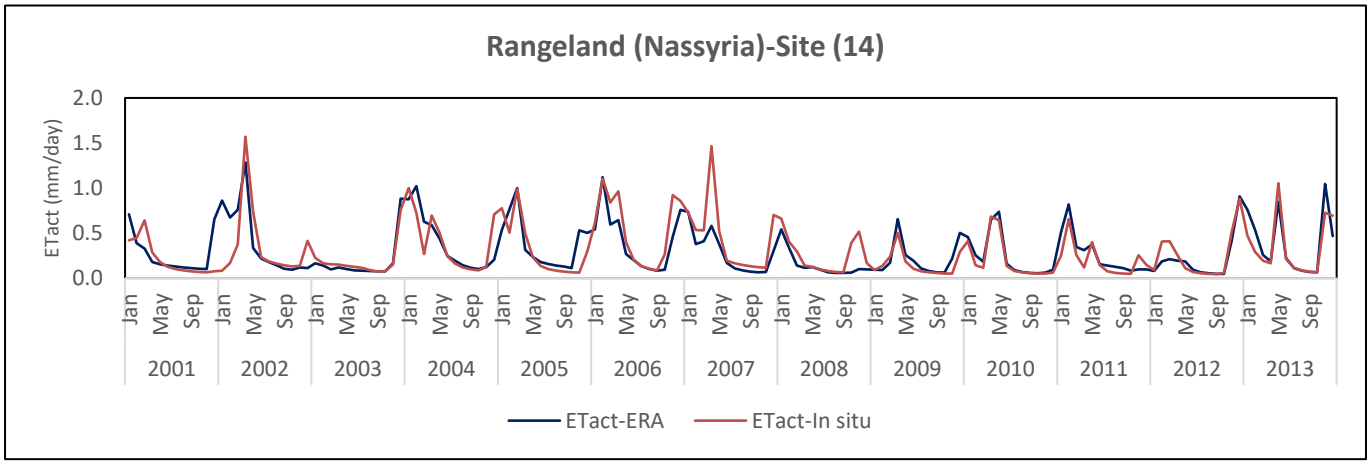
Rangeland (Nassyria)-Site (14)
ETact (mm/day)
2.0
1.5
1.0
0.5
0.0
Jan May Sep
2001 2002 2003 2004 2005 2006 2007 2008 2009 2010 2011 2012 2013
ETact-ERA
ETact-In situ

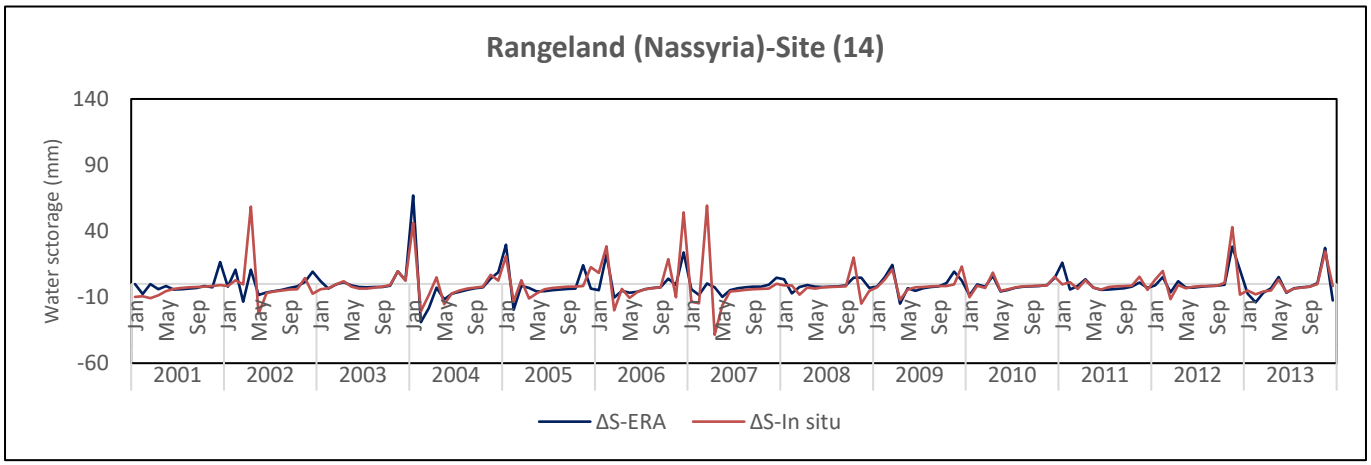
Rangeland (Nassyria)-Site (14)
Water sctorage (mm)
140
90
40
-10
-60
Jan May Sep
2001 2002 2003 2004 2005 2006 2007 2008 2009 2010 2011 2012 2013
ΔS-ERA
ΔS-In situ

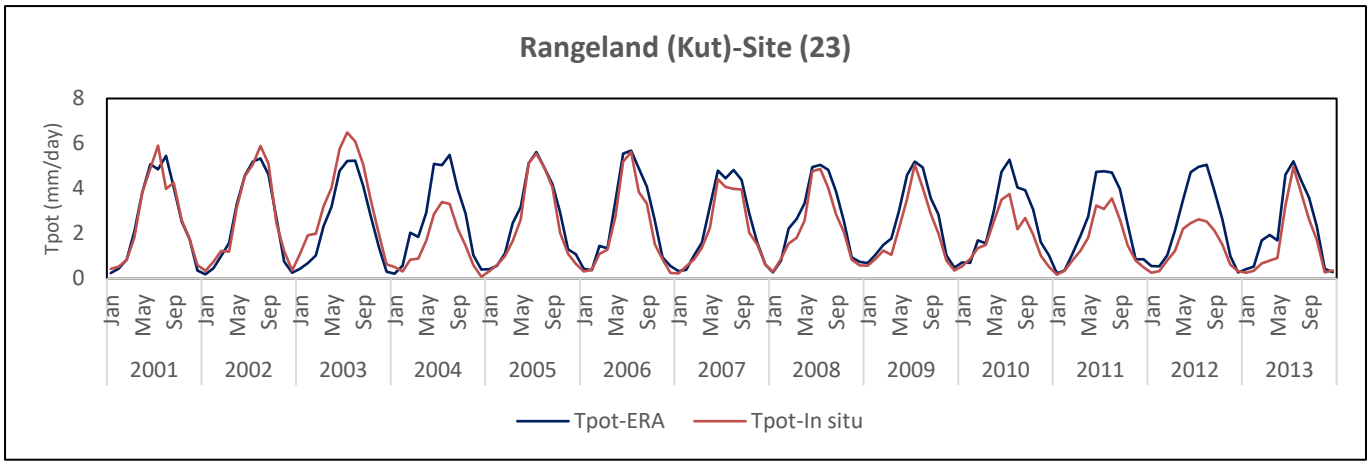
Rangeland (Kut)-Site (23)
Tpot (mm/day)
0
2
4
6
8
Jan May Sep
2001 2002 2003 2004 2005 2006 2007 2008 2009 2010 2011 2012 2013
Tpot-ERA
Tpot-In situ

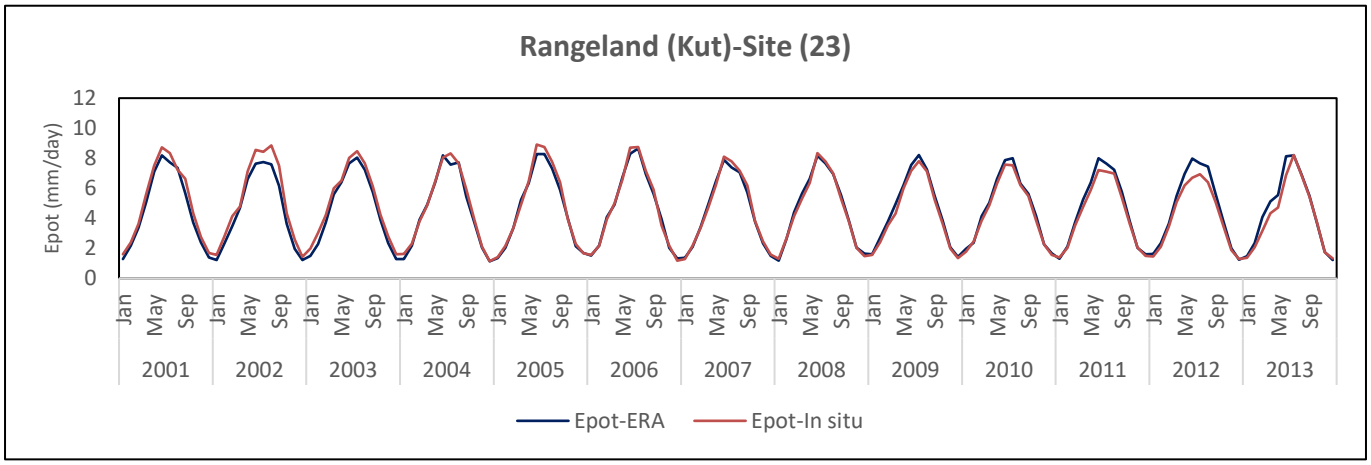
Rangeland (Kut)-Site (23)
Epot (mm/day)
0
2
4
6
8
10
12
Jan May Sep
2001 2002 2003 2004 2005 2006 2007 2008 2009 2010 2011 2012 2013
Epot-ERA
Epot-In situ

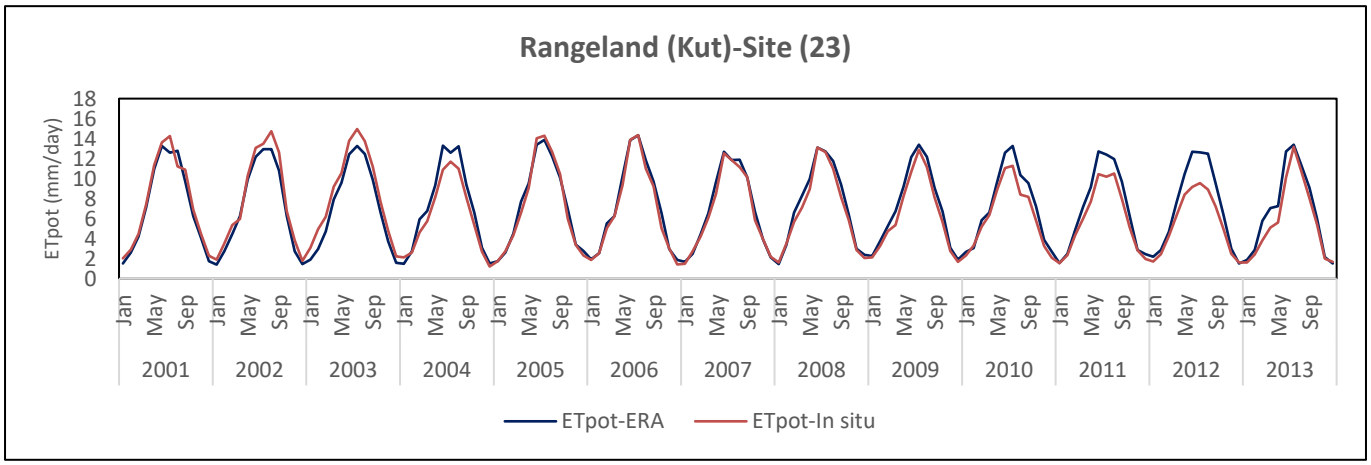
Rangeland (Kut)-Site (23)
ETpot (mm/day)
0
2
4
6
8
10
12
14
16
18
Jan May Sep
2001 2002 2003 2004 2005 2006 2007 2008 2009 2010 2011 2012 2013
ETpot-ERA
ETpot-In situ

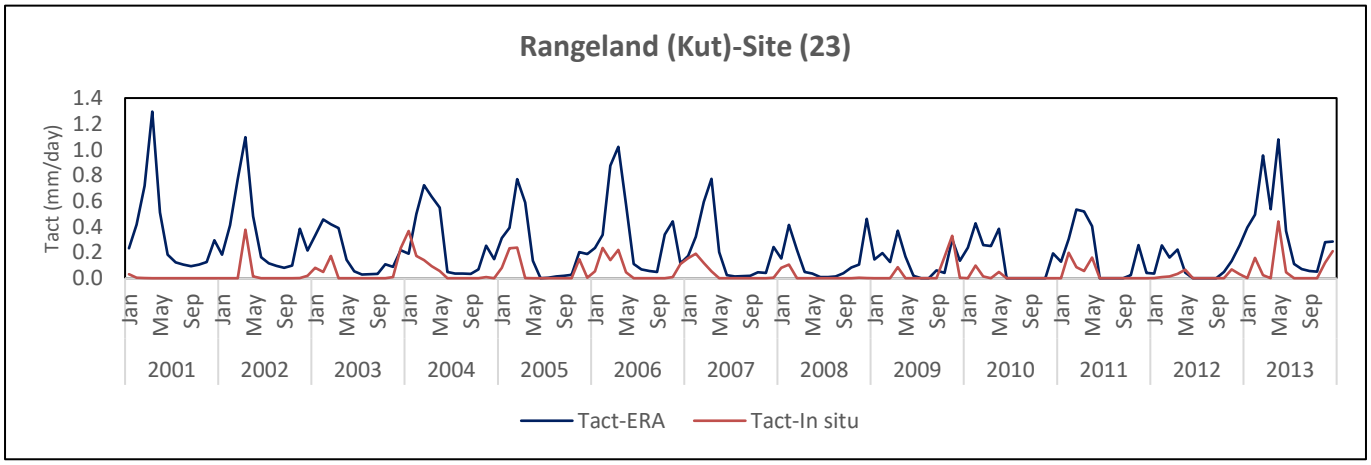
Rangeland (Kut)-Site (23)
Tact (mm/day)
0.0
0.2
0.4
0.6
0.8
1.0
1.2
1.4
Jan May Sep
2001 2002 2003 2004 2005 2006 2007 2008 2009 2010 2011 2012 2013
Tact-ERA
Tact-In situ

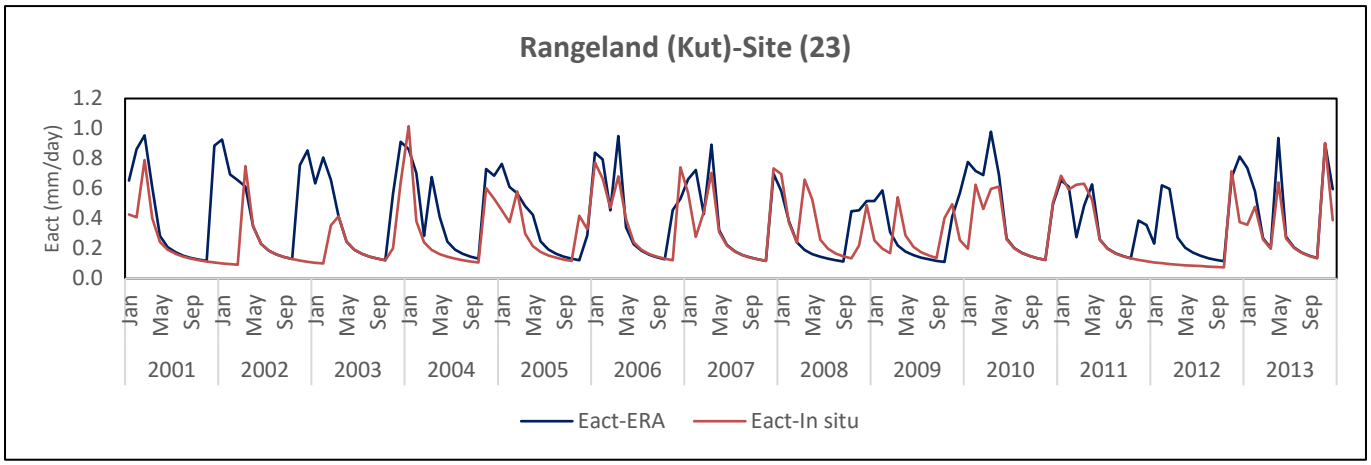
Rangeland (Kut)-Site (23)
Eact (mm/day)
1.2
1.0
0.8
0.6
0.4
0.2
0.0
Jan May Sep
2001 2002 2003 2004 2005 2006 2007 2008 2009 2010 2011 2012 2013
Eact-ERA
Eact-In situ

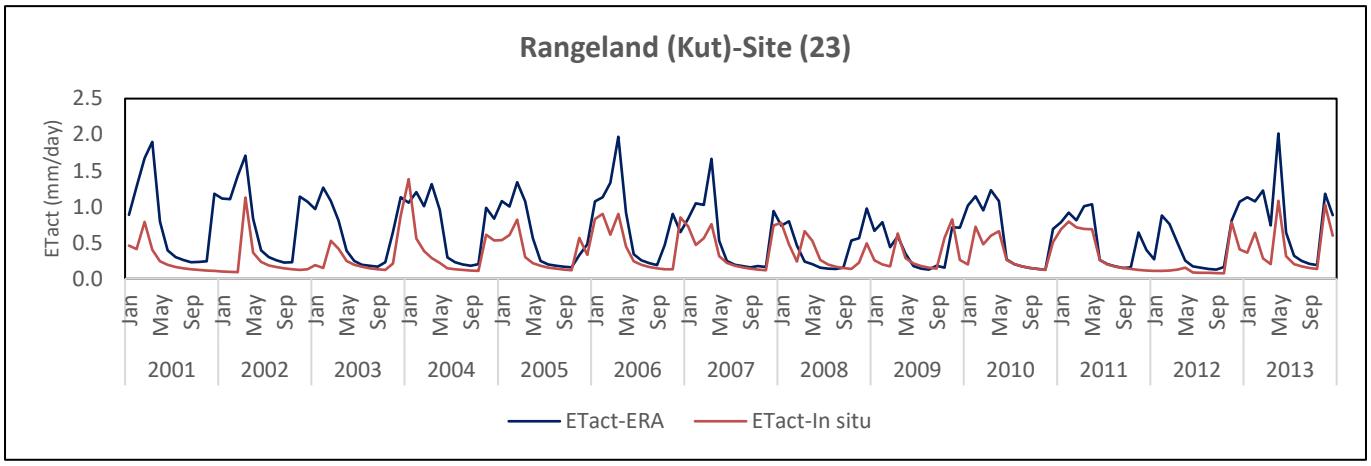
Rangeland (Kut)-Site (23)
ETact (mm/day)
2.5
2.0
1.5
1.0
0.5
0.0
Jan May Sep
2001 2002 2003 2004 2005 2006 2007 2008 2009 2010 2011 2012 2013
ETact-ERA
ETact-In situ

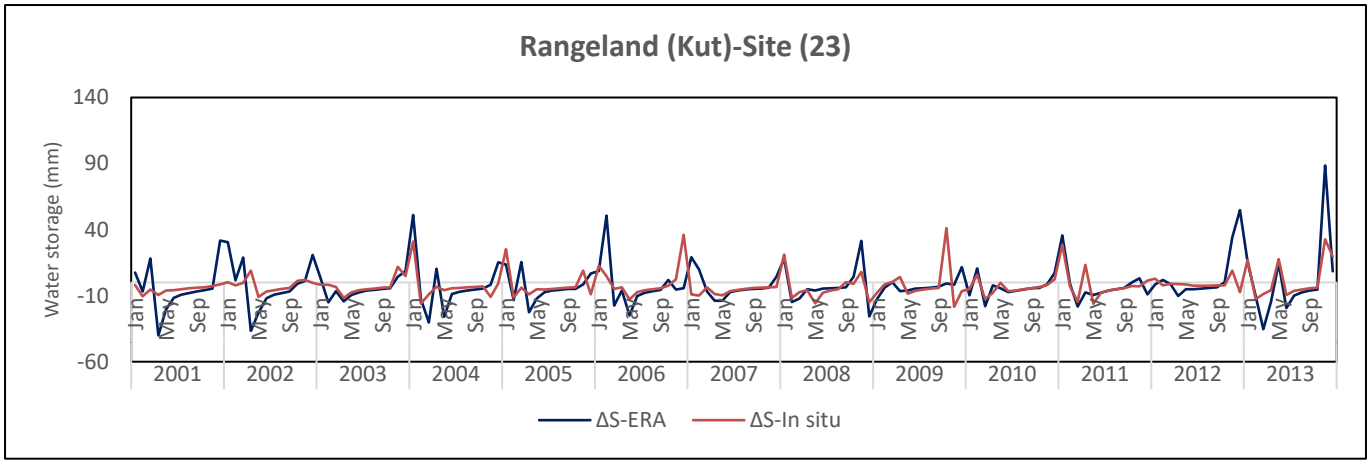
Rangeland (Kut)-Site (23)
Water storage (mm)
140
90
40
-10
-60
Jan May Sep
2001 2002 2003 2004 2005 2006 2007 2008 2009 2010 2011 2012 2013
ΔS-ERA
ΔS-In situ

APPENDIX I: Assessment of water balance components from SWAP runs during (2001-2015) for the agricultural region.

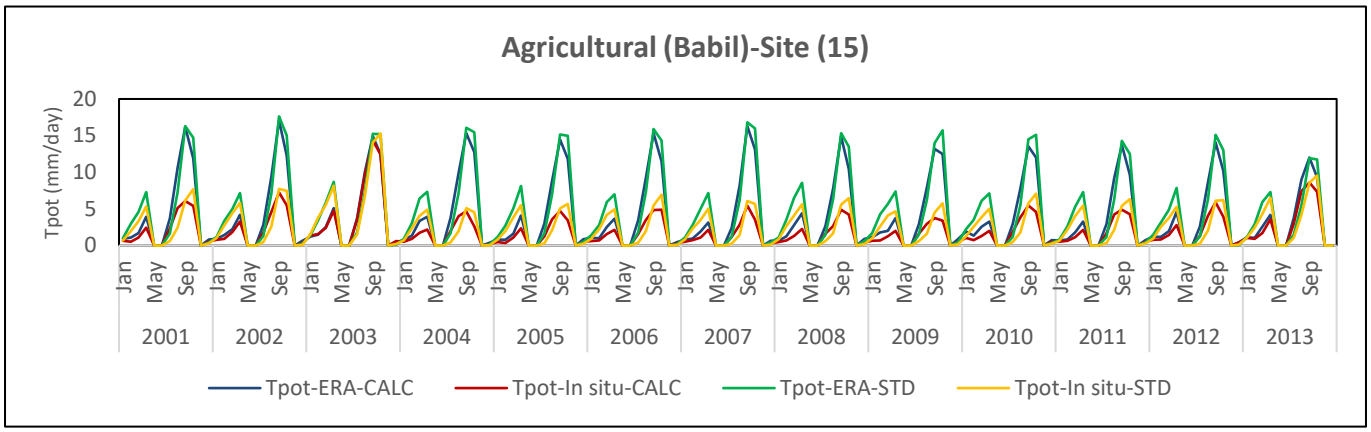

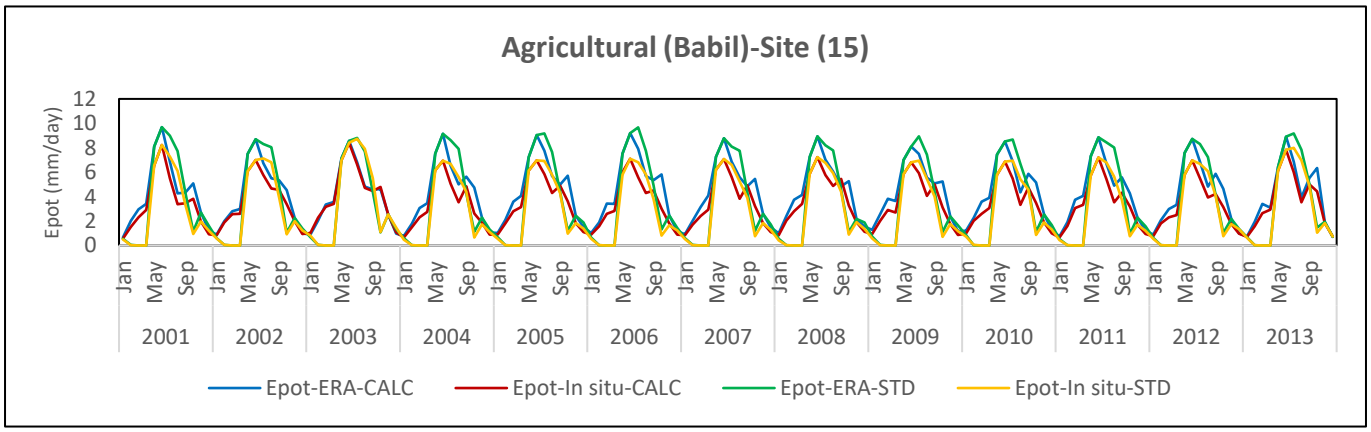

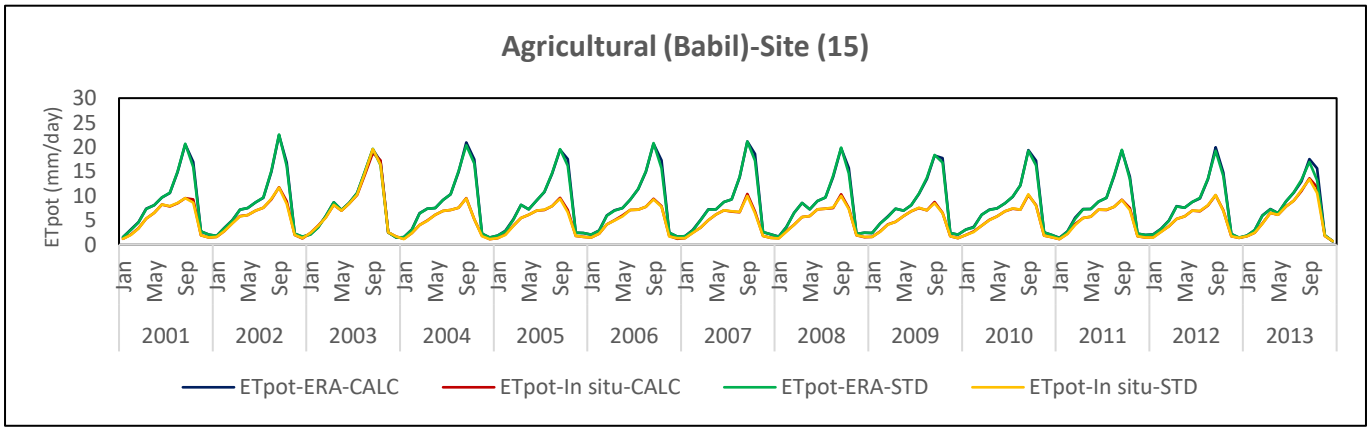

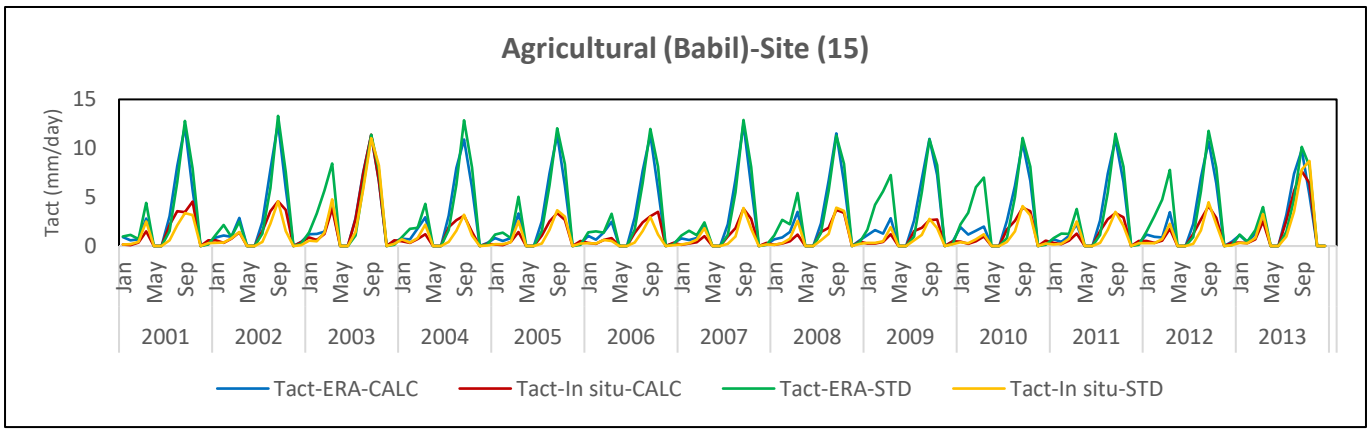

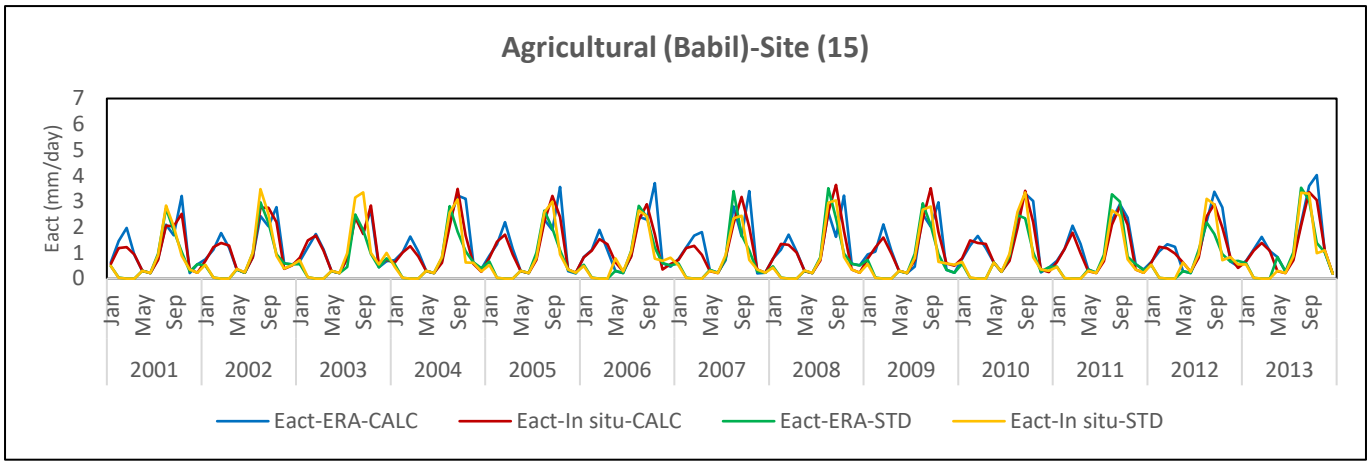
Agricultural (Babil)-Site (15)
Eact (mm/day)
0
1
2
3
4
5
6
7
Jan May Sep
2001 2002 2003 2004 2005 2006 2007 2008 2009 2010 2011 2012 2013
Eact-ERA-CALC
Eact-In situ-CALC
Eact-ERA-STD
Eact-In situ-STD

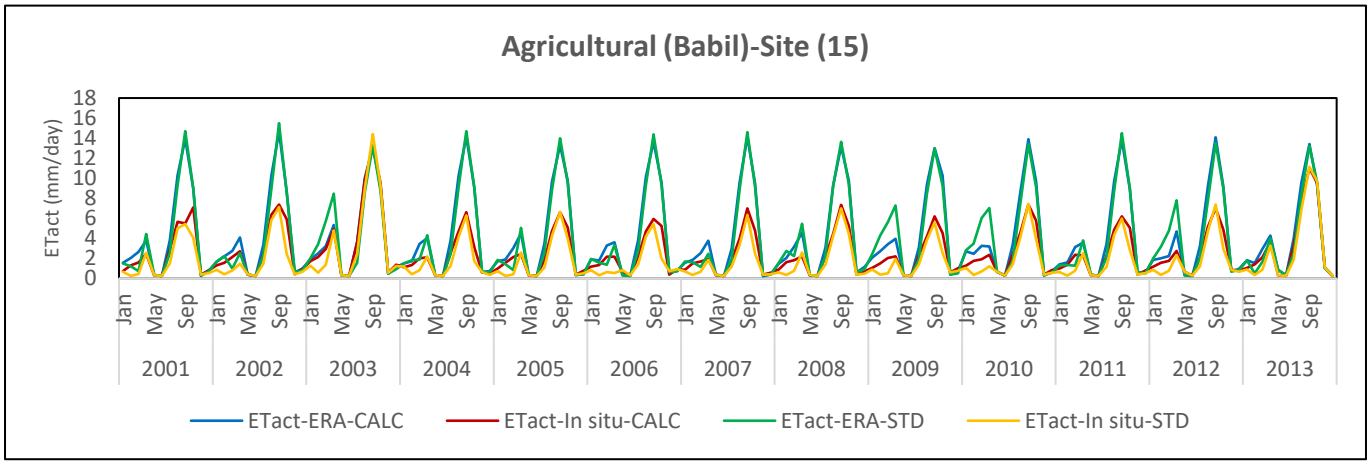
Agricultural (Babil)-Site (15)
ETact (mm/day)
0
2
4
6
8
10
12
14
16
18
Jan May Sep
2001 2002 2003 2004 2005 2006 2007 2008 2009 2010 2011 2012 2013
ETact-ERA-CALC
ETact-In situ-CALC
ETact-ERA-STD
ETact-In situ-STD

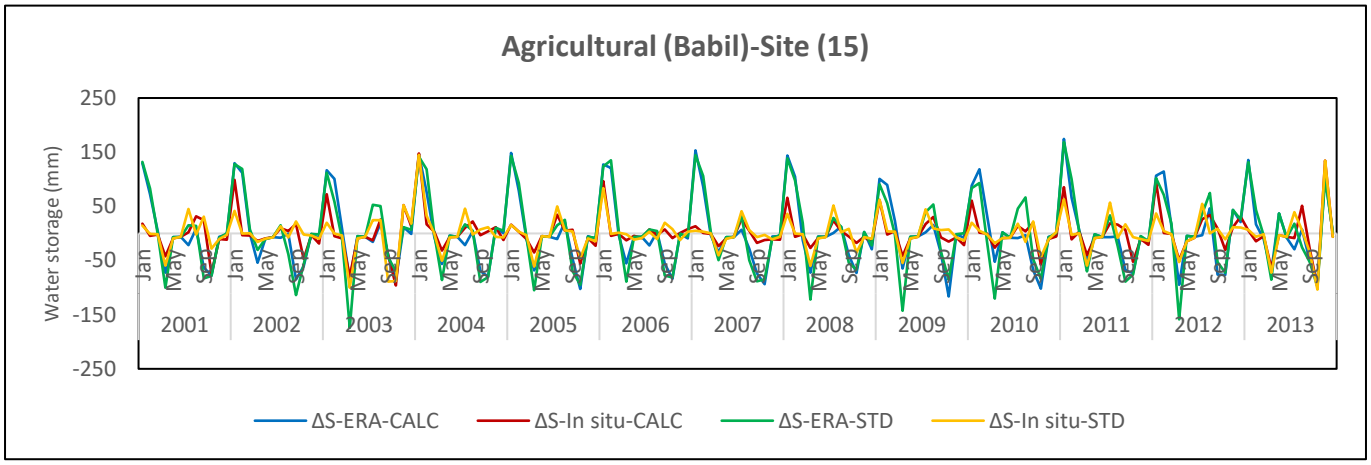
Agricultural (Babil)-Site (15)
Water storage (mm)
250
150
50
-50
-150
-250
Jan May Sep
2001 2002 2003 2004 2005 2006 2007 2008 2009 2010 2011 2012 2013
ΔS-ERA-CALC
ΔS-In situ-CALC
ΔS-ERA-STD
ΔS-In situ-STD

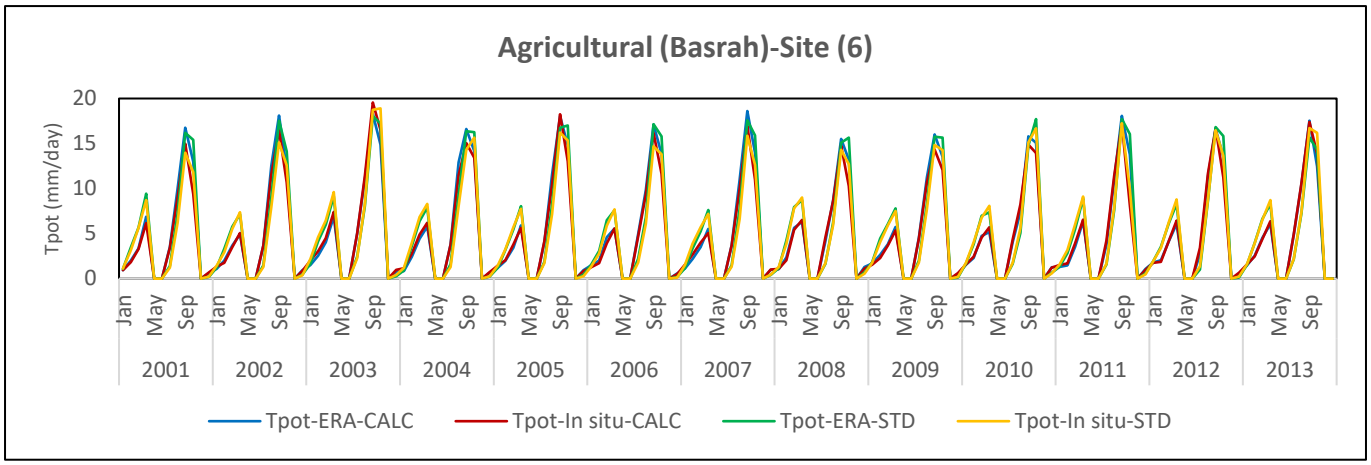
Agricultural (Basrah)-Site (6)
Tpot (mm/day)
0
5
10
15
20
Jan May Sep
2001 2002 2003 2004 2005 2006 2007 2008 2009 2010 2011 2012 2013
Tpot-ERA-CALC
Tpot-In situ-CALC
Tpot-ERA-STD
Tpot-In situ-STD

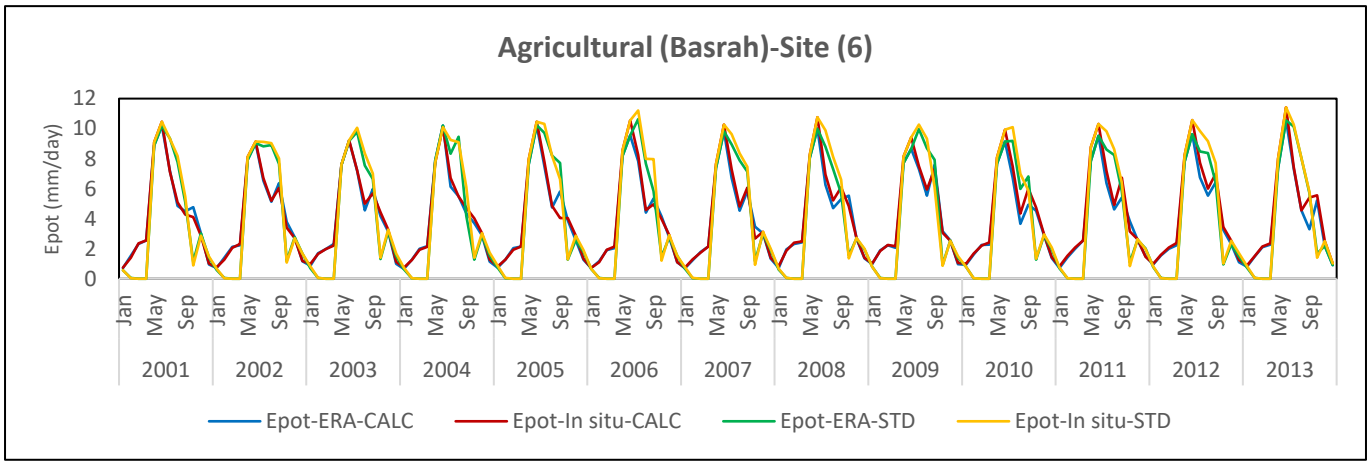
Agricultural (Basrah)-Site (6)
Epot (mm/day)
0
2
4
6
8
10
12
Jan May Sep
2001 2002 2003 2004 2005 2006 2007 2008 2009 2010 2011 2012 2013
Epot-ERA-CALC
Epot-In situ-CALC
Epot-ERA-STD
Epot-In situ-STD

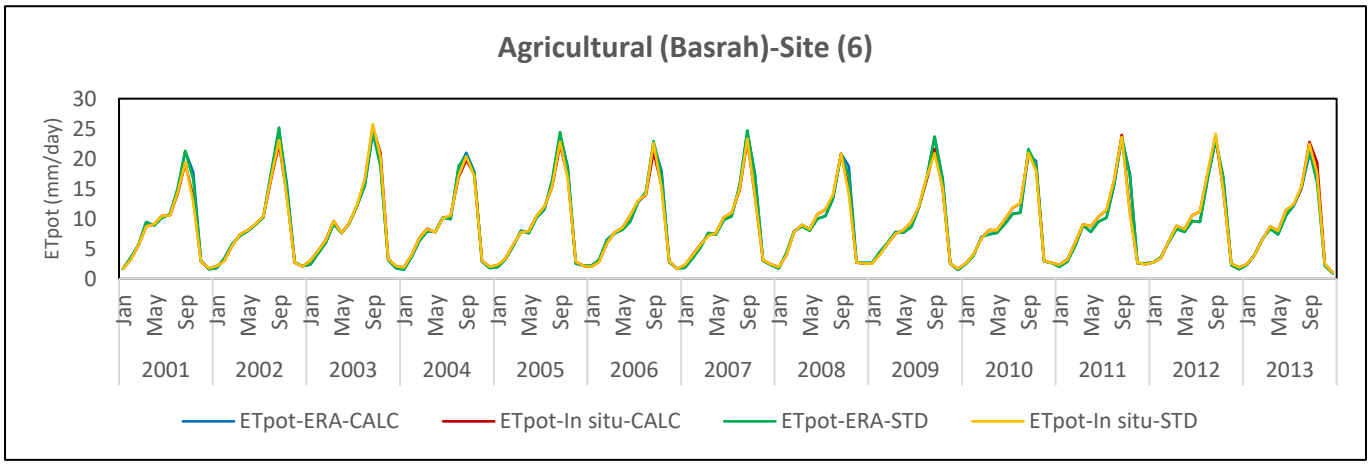
Agricultural (Basrah)-Site (6)
ETpot (mm/day)
0
5
10
15
20
25
30
Jan May Sep
2001 2002 2003 2004 2005 2006 2007 2008 2009 2010 2011 2012 2013
ETpot-ERA-CALC
ETpot-In situ-CALC
ETpot-ERA-STD
ETpot-In situ-STD

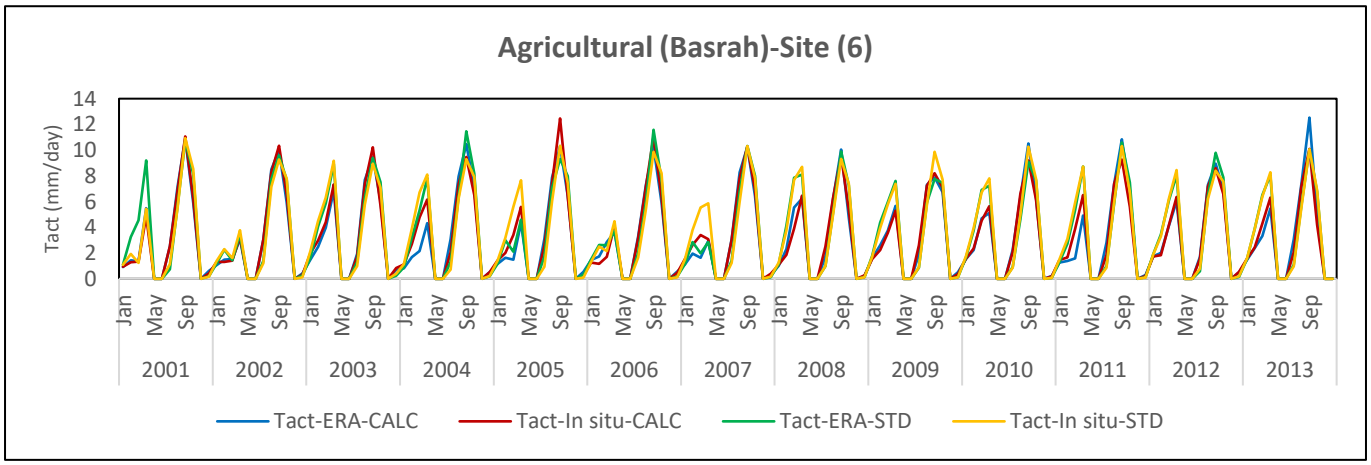
Agricultural (Basrah)-Site (6)
Tact (mm/day)
0
2
4
6
8
10
12
14
Jan May Sep
2001 2002 2003 2004 2005 2006 2007 2008 2009 2010 2011 2012 2013
Tact-ERA-CALC
Tact-In situ-CALC
Tact-ERA-STD
Tact-In situ-STD

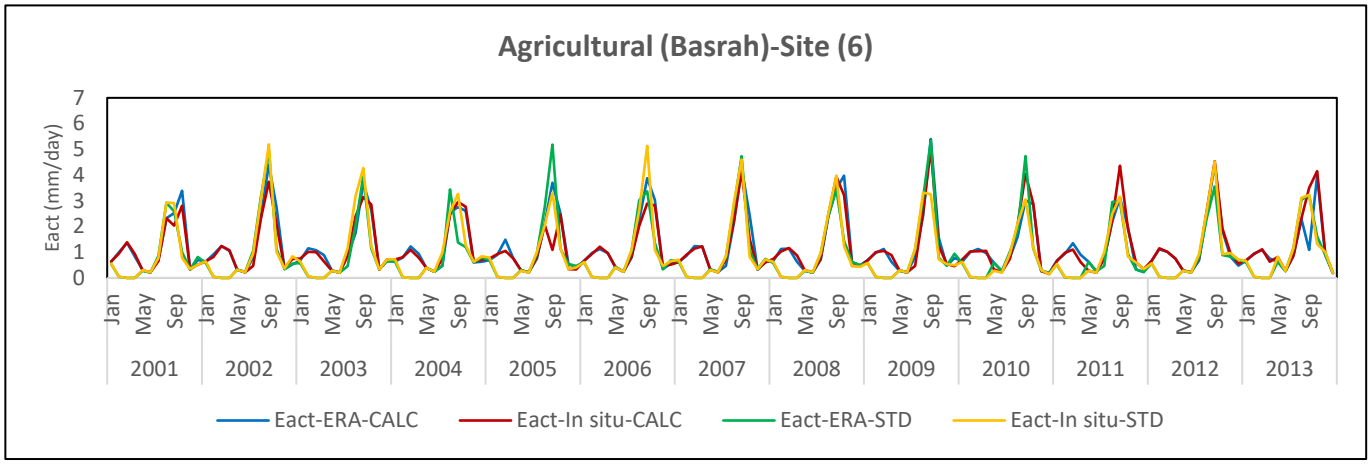
Agricultural (Basrah)-Site (6)
Eact (mm/day)
0
1
2
3
4
5
6
7
Jan May Sep
2001 2002 2003 2004 2005 2006 2007 2008 2009 2010 2011 2012 2013
Eact-ERA-CALC
Eact-In situ-CALC
Eact-ERA-STD
Eact-In situ-STD

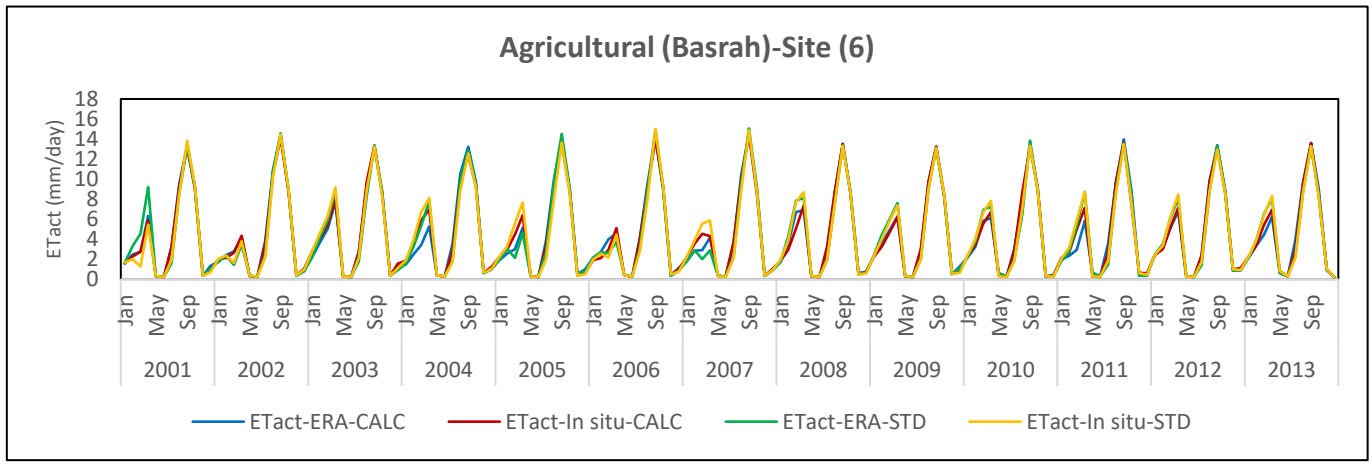
Agricultural (Basrah)-Site (6)
ETact (mm/day)
0
2
4
6
8
10
12
14
16
18
Jan May Sep
2001 2002 2003 2004 2005 2006 2007 2008 2009 2010 2011 2012 2013
ETact-ERA-CALC
ETact-In situ-CALC
ETact-ERA-STD
ETact-In situ-STD

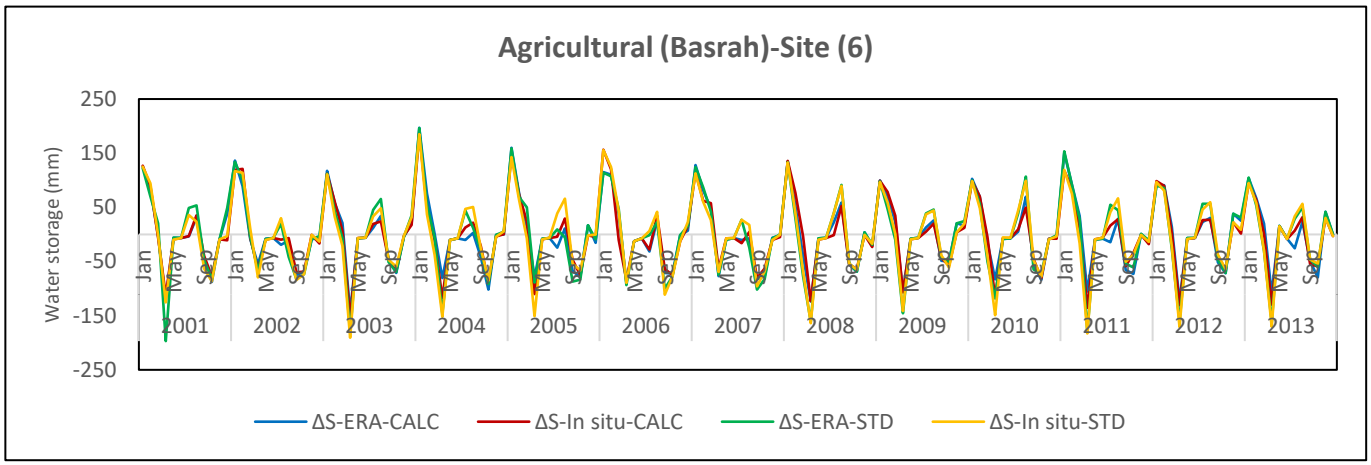
Agricultural (Basrah)-Site (6)
Water storage (mm)
250
150
50
-50
-150
-250
Jan May Sep
2001 2002 2003 2004 2005 2006 2007 2008 2009 2010 2011 2012 2013
ΔS-ERA-CALC
ΔS-In situ-CALC
ΔS-ERA-STD
ΔS-In situ-STD

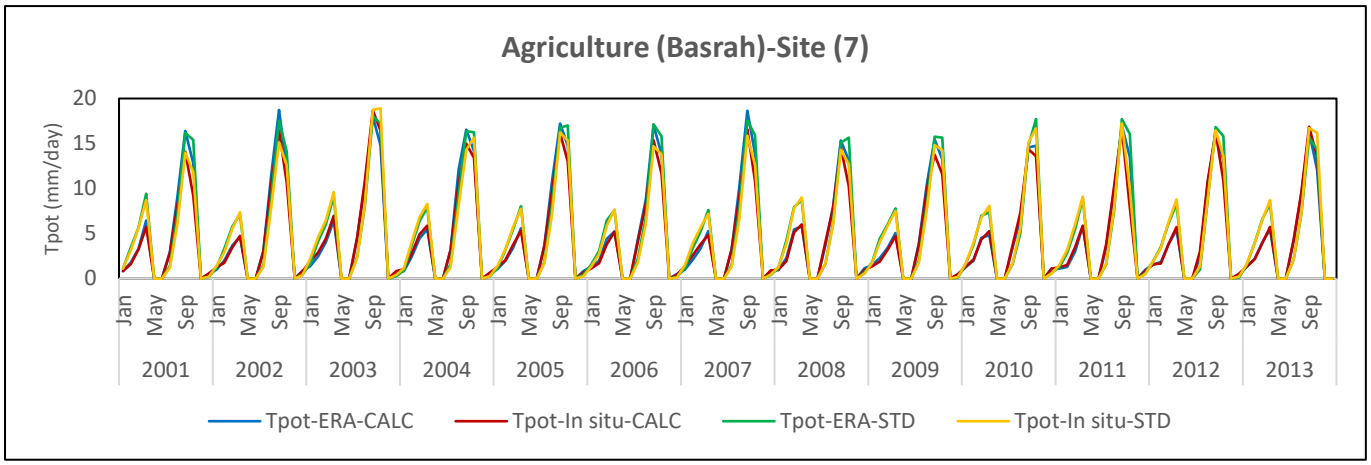
Agriculture (Basrah)-Site (7)
Tpot (mm/day)
0
5
10
15
20
Jan May Sep
2001 2002 2003 2004 2005 2006 2007 2008 2009 2010 2011 2012 2013
Tpot-ERA-CALC
Tpot-In situ-CALC
Tpot-ERA-STD
Tpot-In situ-STD

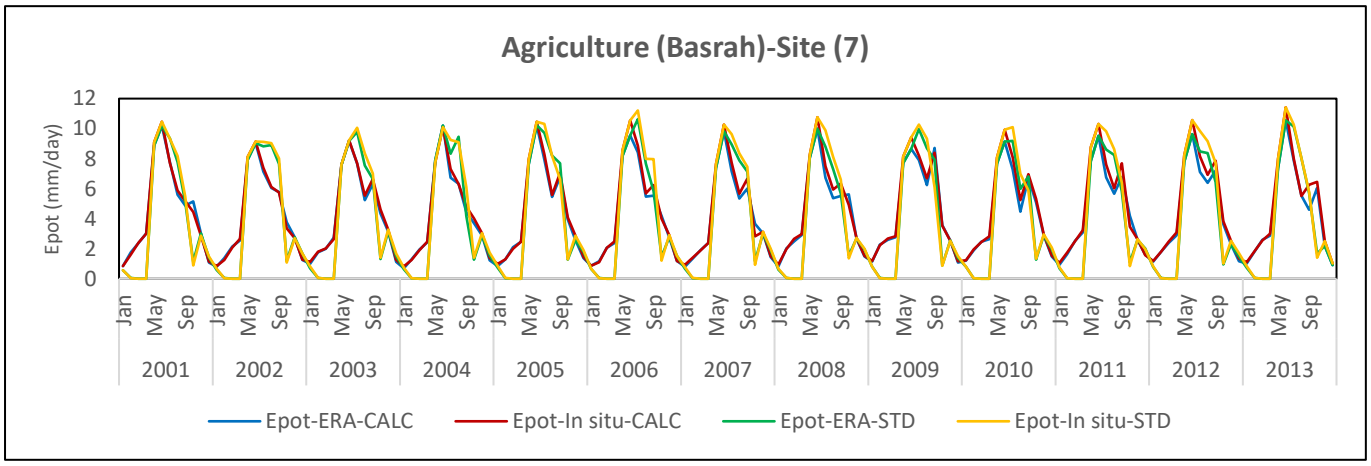
Agriculture (Basrah)-Site (7)
Epot (mm/day)
0
2
4
6
8
10
12
Jan May Sep
2001 2002 2003 2004 2005 2006 2007 2008 2009 2010 2011 2012 2013
Epot-ERA-CALC
Epot-In situ-CALC
Epot-ERA-STD
Epot-In situ-STD

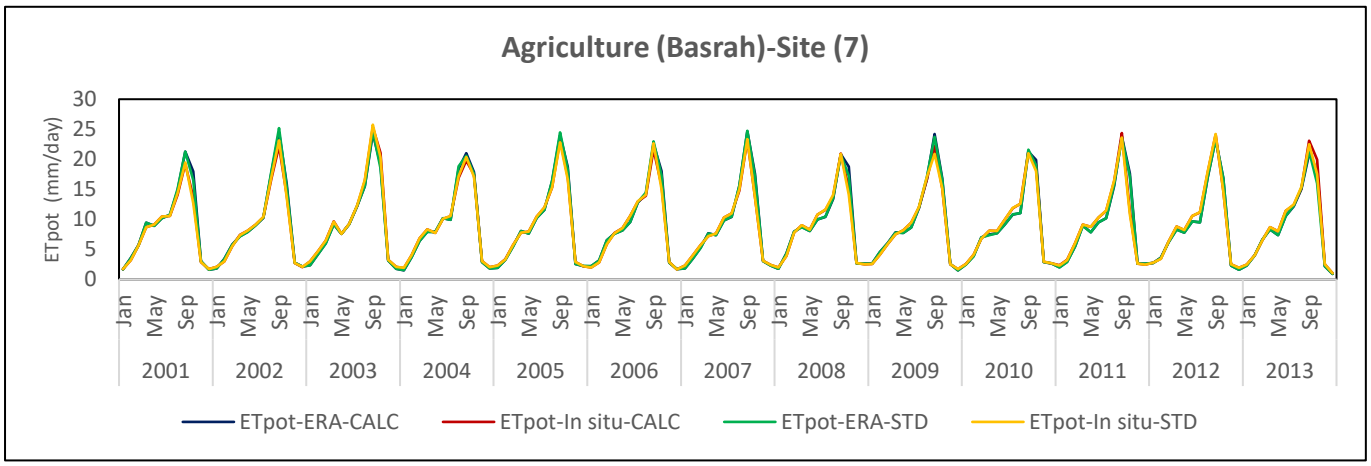
Agriculture (Basrah)-Site (7)
ETpot (mm/day)
0
5
10
15
20
25
30
Jan May Sep
2001 2002 2003 2004 2005 2006 2007 2008 2009 2010 2011 2012 2013
ETpot-ERA-CALC
ETpot-In situ-CALC
ETpot-ERA-STD
ETpot-In situ-STD

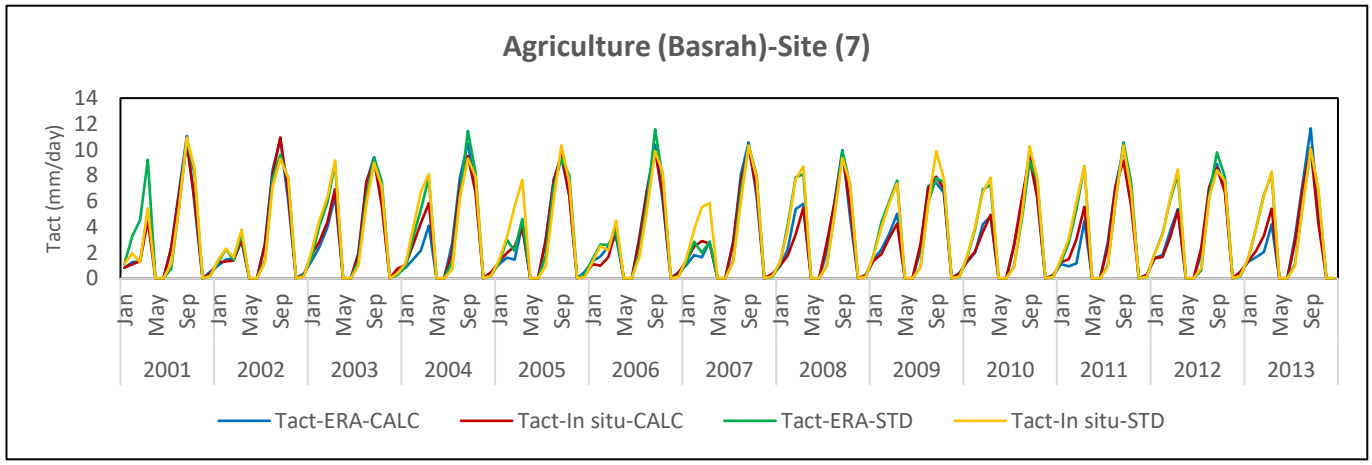
Agriculture (Basrah)-Site (7)
Tact (mm/day)
0
2
4
6
8
10
12
14
Jan May Sep
2001 2002 2003 2004 2005 2006 2007 2008 2009 2010 2011 2012 2013
Tact-ERA-CALC
Tact-In situ-CALC
Tact-ERA-STD
Tact-In situ-STD

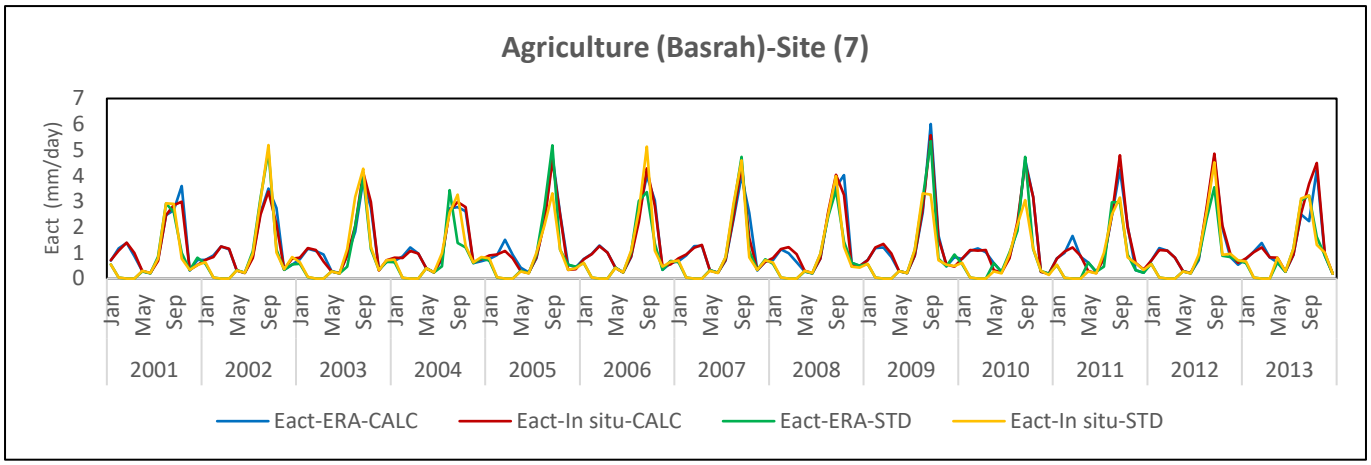
Agriculture (Basrah)-Site (7)
Eact (mm/day)
0
1
2
3
4
5
6
7
Jan May Sep
2001 2002 2003 2004 2005 2006 2007 2008 2009 2010 2011 2012 2013
Eact-ERA-CALC
Eact-In situ-CALC
Eact-ERA-STD
Eact-In situ-STD

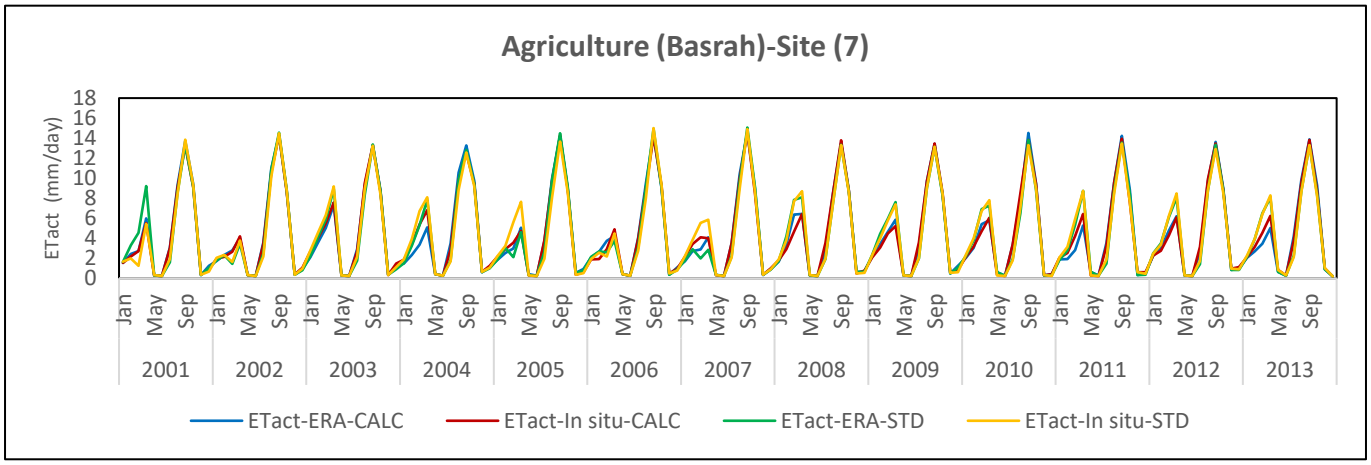
Agriculture (Basrah)-Site (7)
ETact (mm/day)
0
2
4
6
8
10
12
14
16
18
Jan May Sep
2001 2002 2003 2004 2005 2006 2007 2008 2009 2010 2011 2012 2013
ETact-ERA-CALC
ETact-In situ-CALC
ETact-ERA-STD
ETact-In situ-STD

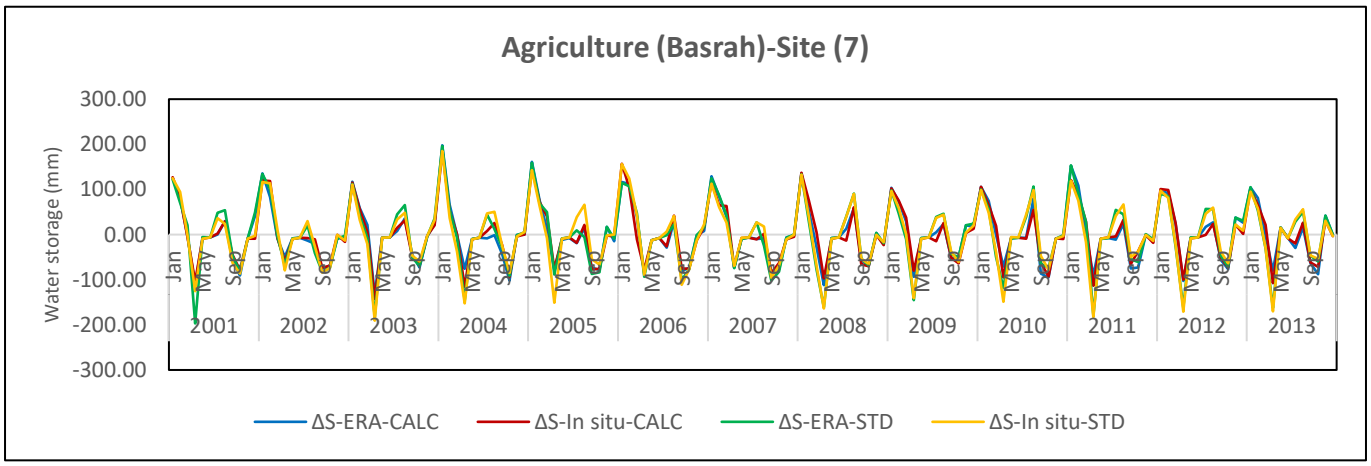
Agriculture (Basrah)-Site (7)
Water storage (mm)
300.00
200.00
100.00
0.00
-100.00
-200.00
-300.00
Jan May Sep
2001 2002 2003 2004 2005 2006 2007 2008 2009 2010 2011 2012 2013
ΔS-ERA-CALC
ΔS-In situ-CALC
ΔS-ERA-STD
ΔS-In situ-STD

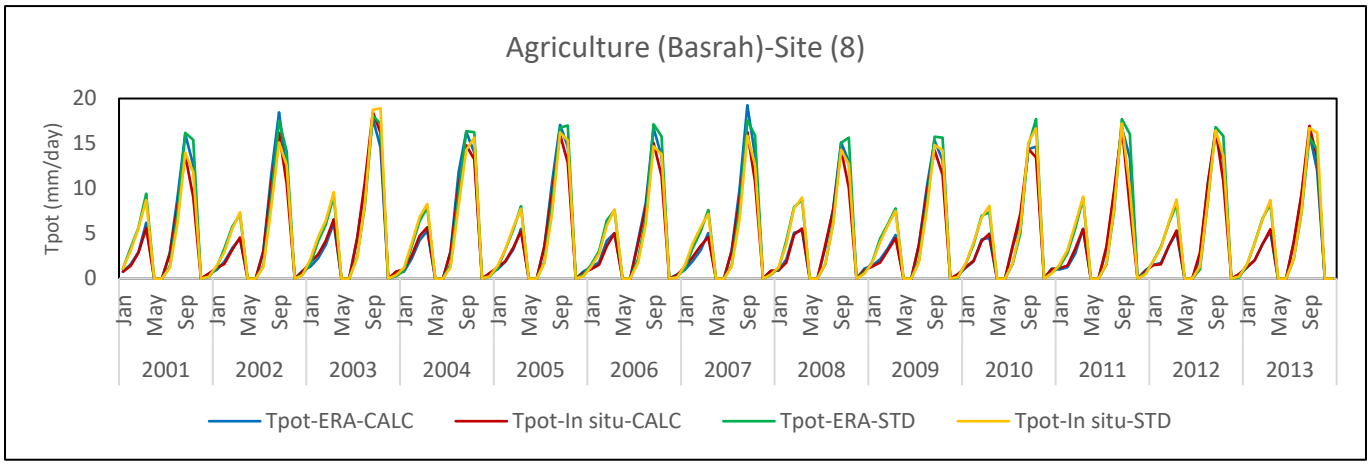
Agriculture (Basrah)-Site (8)
Tpot (mm/day)
0
5
10
15
20
Jan May Sep
2001 2002 2003 2004 2005 2006 2007 2008 2009 2010 2011 2012 2013
Tpot-ERA-CALC
Tpot-In situ-CALC
Tpot-ERA-STD
Tpot-In situ-STD

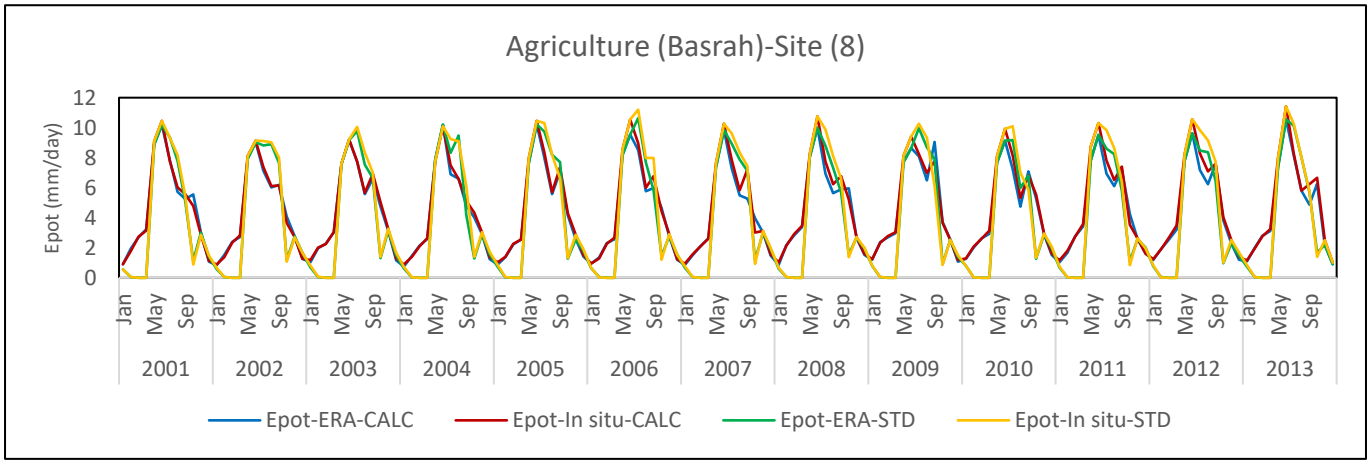
Agriculture (Basrah)-Site (8)
Epot (mm/day)
0
2
4
6
8
10
12
Jan May Sep
2001 2002 2003 2004 2005 2006 2007 2008 2009 2010 2011 2012 2013
Epot-ERA-CALC
Epot-In situ-CALC
Epot-ERA-STD
Epot-In situ-STD

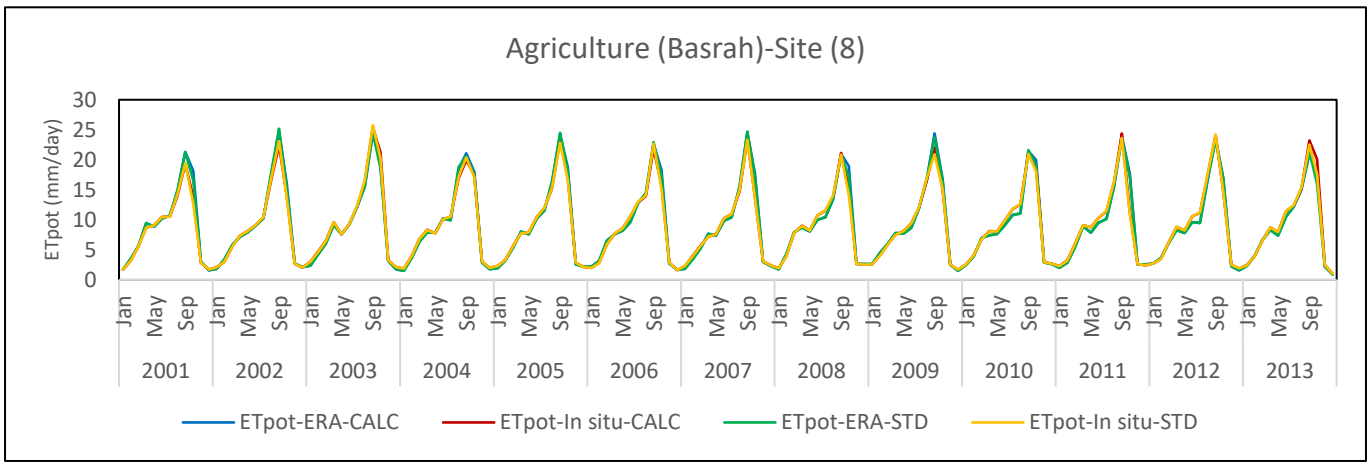
Agriculture (Basrah)-Site (8)
ETpot (mm/day)
0
5
10
15
20
25
30
Jan May Sep
2001 2002 2003 2004 2005 2006 2007 2008 2009 2010 2011 2012 2013
ETpot-ERA-CALC
ETpot-In situ-CALC
ETpot-ERA-STD
ETpot-In situ-STD

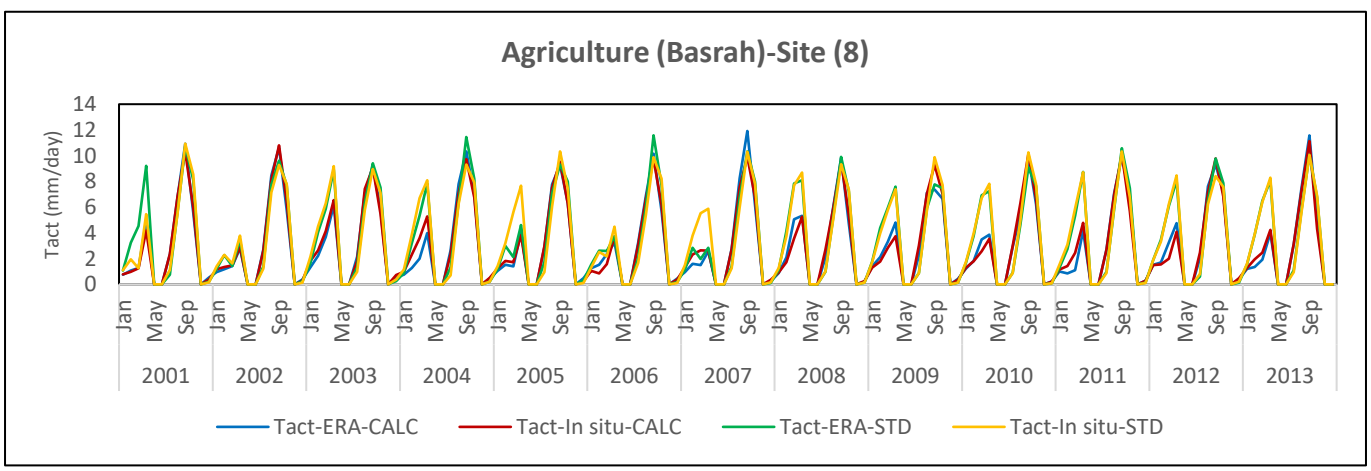
Agriculture (Basrah)-Site (8)
Tact (mm/day)
0
2
4
6
8
10
12
14
Jan May Sep
2001 2002 2003 2004 2005 2006 2007 2008 2009 2010 2011 2012 2013
Tact-ERA-CALC
Tact-In situ-CALC
Tact-ERA-STD
Tact-In situ-STD

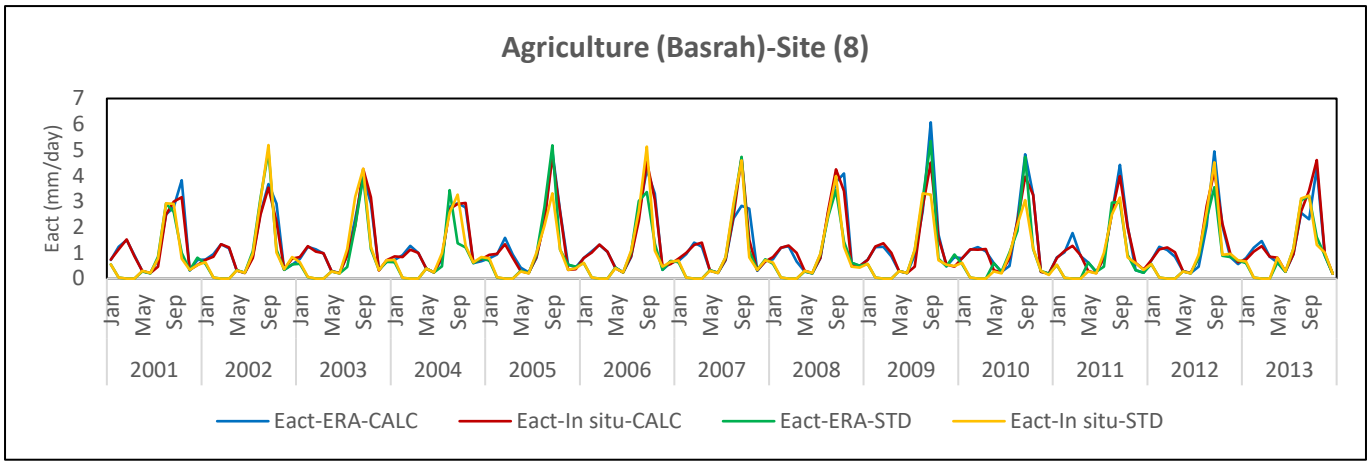
Agriculture (Basrah)-Site (8)
Eact (mm/day)
0
1
2
3
4
5
6
7
Jan May Sep
2001 2002 2003 2004 2005 2006 2007 2008 2009 2010 2011 2012 2013
Eact-ERA-CALC
Eact-In situ-CALC
Eact-ERA-STD
Eact-In situ-STD

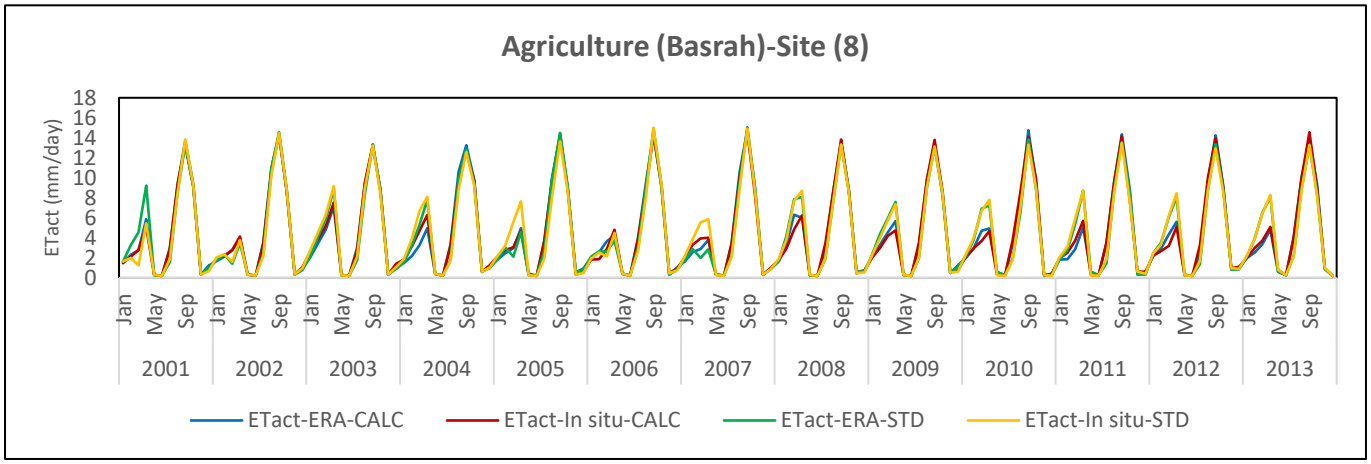
Agriculture (Basrah)-Site (8)
ETact (mm/day)
0
2
4
6
8
10
12
14
16
18
Jan May Sep
2001 2002 2003 2004 2005 2006 2007 2008 2009 2010 2011 2012 2013
ETact-ERA-CALC
ETact-In situ-CALC
ETact-ERA-STD
ETact-In situ-STD

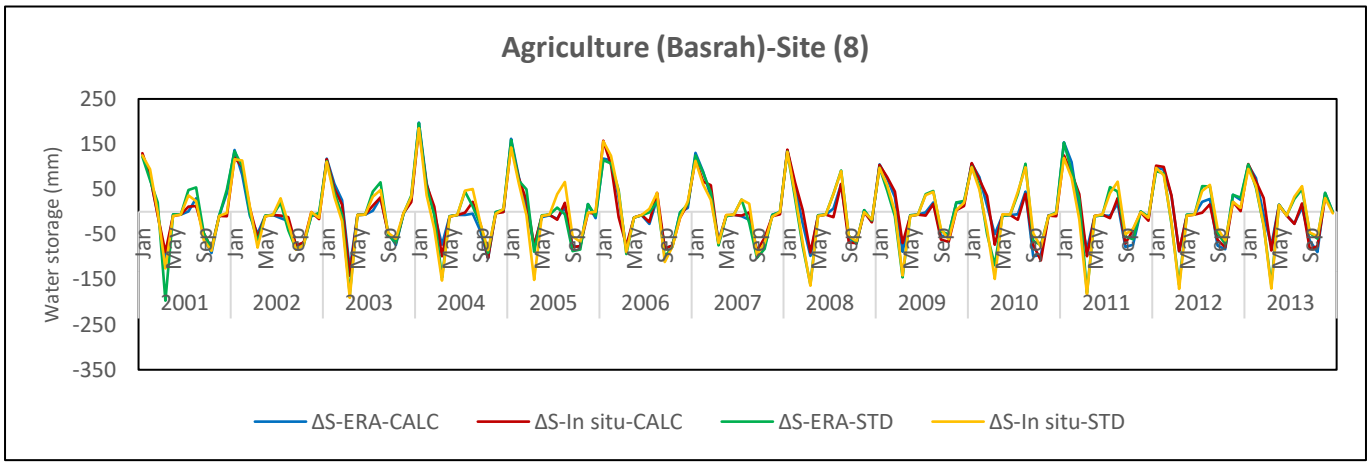
Agriculture (Basrah)-Site (8)
Water storage (mm)
250
150
50
-50
-150
-250
-350
Jan May Sep
2001 2002 2003 2004 2005 2006 2007 2008 2009 2010 2011 2012 2013
ΔS-ERA-CALC
ΔS-In situ-CALC
ΔS-ERA-STD
ΔS-In situ-STD

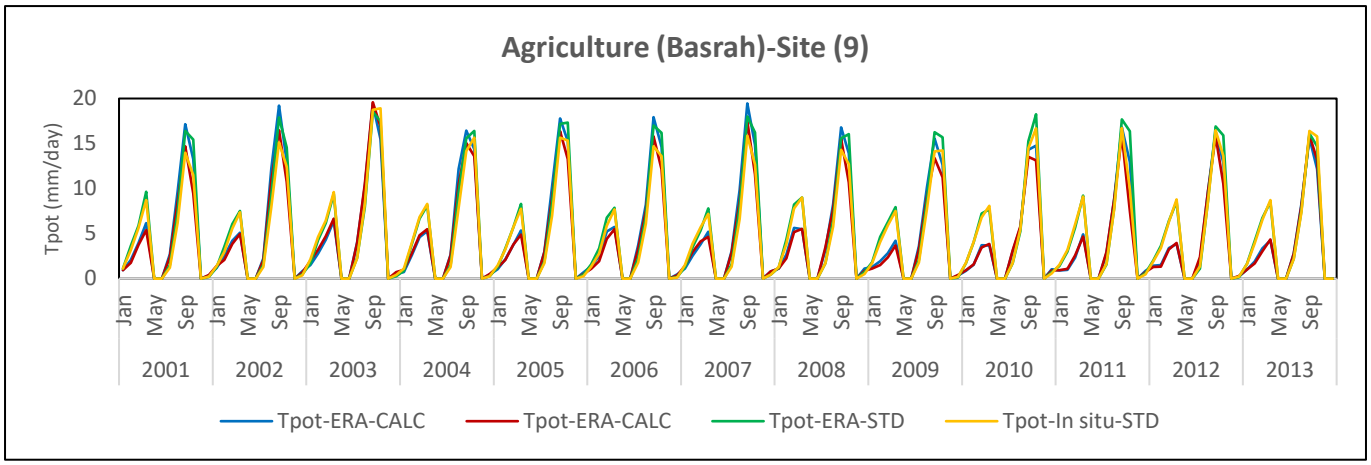
Agriculture (Basrah)-Site (9)
Tpot (mm/day)
0
5
10
15
20
Jan May Sep
2001 2002 2003 2004 2005 2006 2007 2008 2009 2010 2011 2012 2013
Tpot-ERA-CALC
Tpot-ERA-CALC
Tpot-ERA-STD
Tpot-In situ-STD

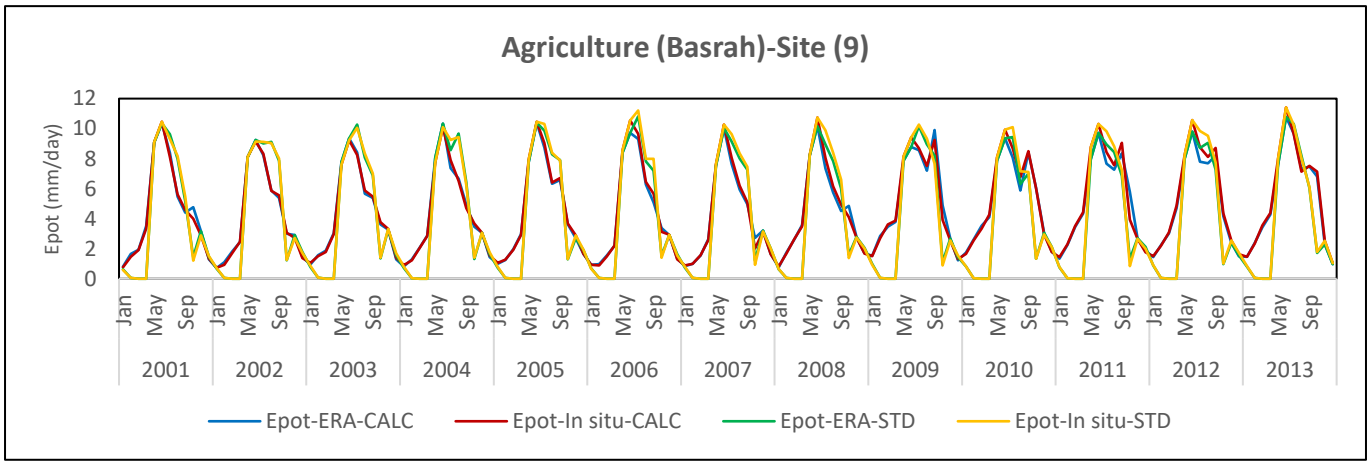
Agriculture (Basrah)-Site (9)
Epot (mm/day)
0
2
4
6
8
10
12
Jan May Sep
2001 2002 2003 2004 2005 2006 2007 2008 2009 2010 2011 2012 2013
Epot-ERA-CALC
Epot-In situ-CALC
Epot-ERA-STD
Epot-In situ-STD

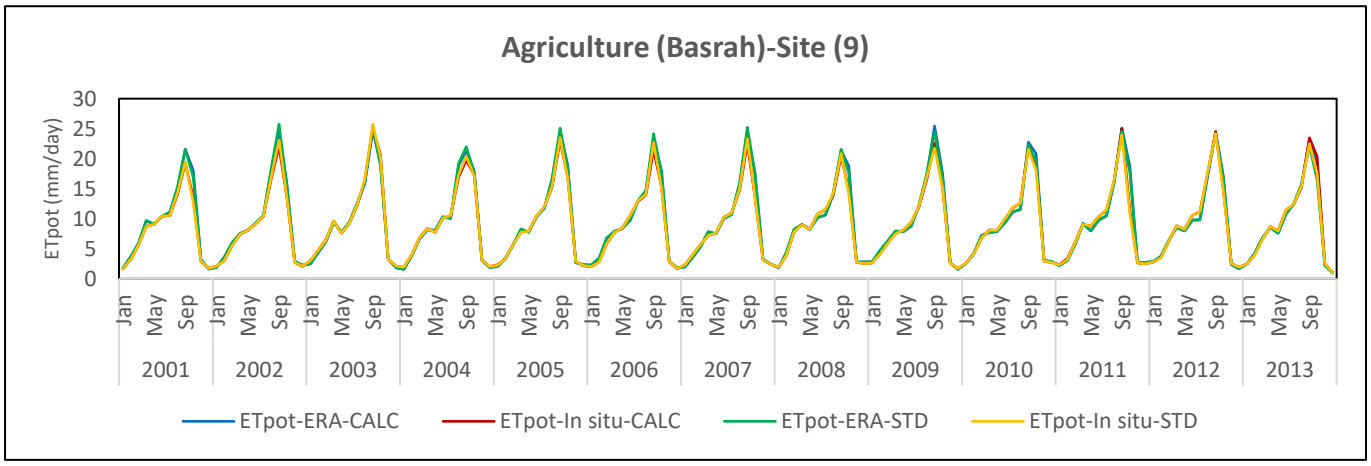
Agriculture (Basrah)-Site (9)
ETpot (mm/day)
0
5
10
15
20
25
30
Jan May Sep
2001 2002 2003 2004 2005 2006 2007 2008 2009 2010 2011 2012 2013
ETpot-ERA-CALC
ETpot-In situ-CALC
ETpot-ERA-STD
ETpot-In situ-STD

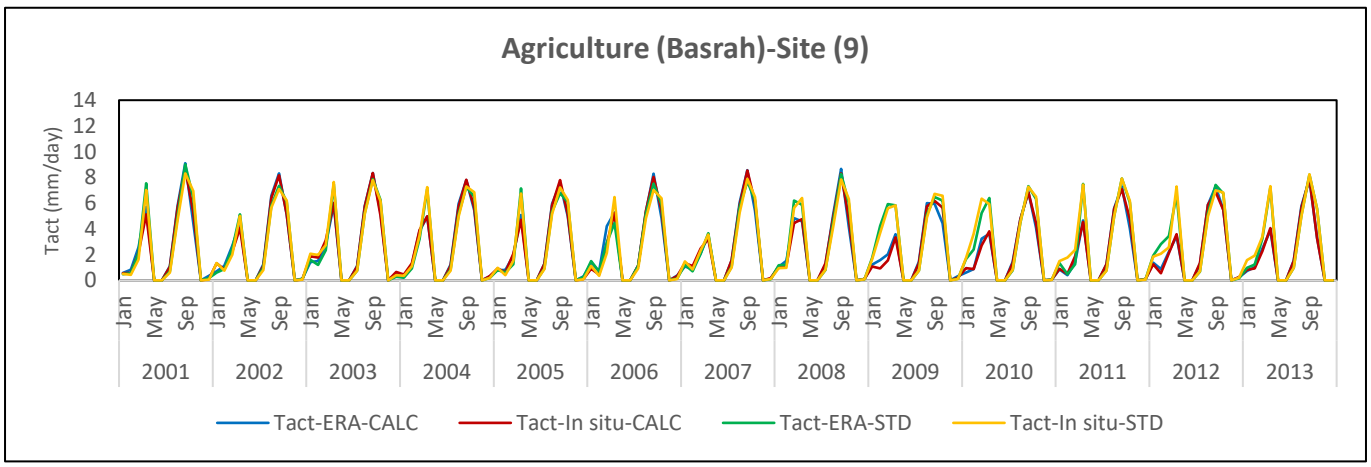
Agriculture (Basrah)-Site (9)
Tact (mm/day)
0
2
4
6
8
10
12
14
Jan May Sep
2001 2002 2003 2004 2005 2006 2007 2008 2009 2010 2011 2012 2013
Tact-ERA-CALC
Tact-In situ-CALC
Tact-ERA-STD
Tact-In situ-STD

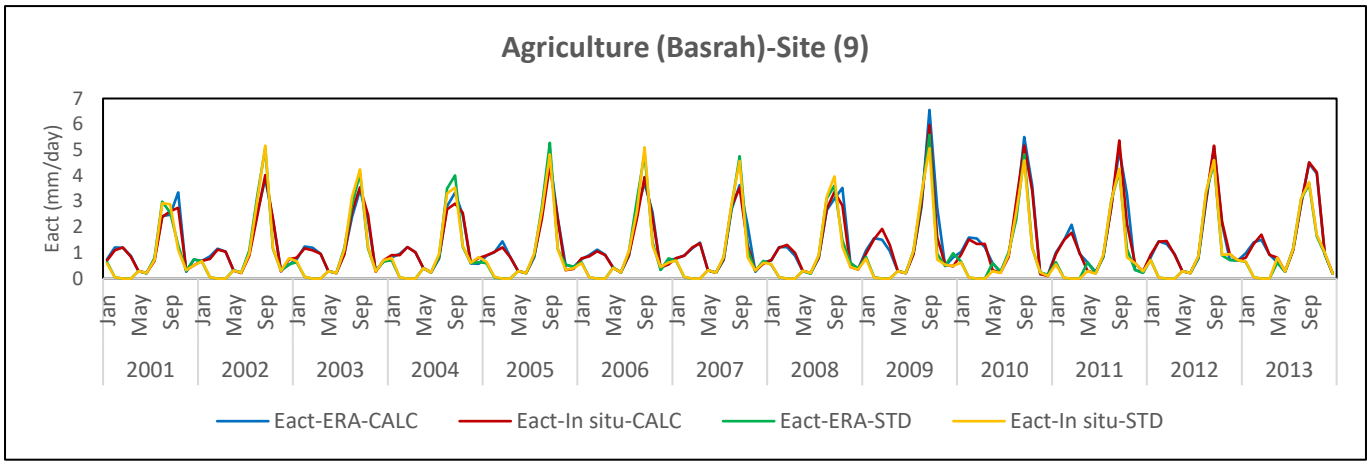
Agriculture (Basrah)-Site (9)
Eact (mm/day)
0
1
2
3
4
5
6
7
Jan May Sep
2001 2002 2003 2004 2005 2006 2007 2008 2009 2010 2011 2012 2013
Eact-ERA-CALC
Eact-In situ-CALC
Eact-ERA-STD
Eact-In situ-STD

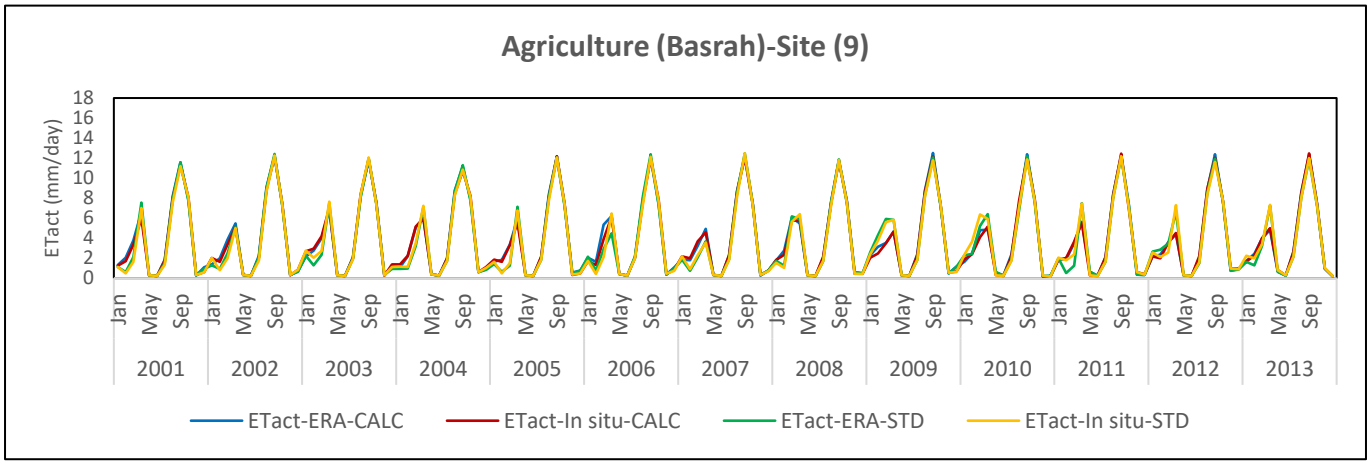
Agriculture (Basrah)-Site (9)
ETact (mm/day)
0
2
4
6
8
10
12
14
16
18
Jan May Sep
2001 2002 2003 2004 2005 2006 2007 2008 2009 2010 2011 2012 2013
ETact-ERA-CALC
ETact-In situ-CALC
ETact-ERA-STD
ETact-In situ-STD

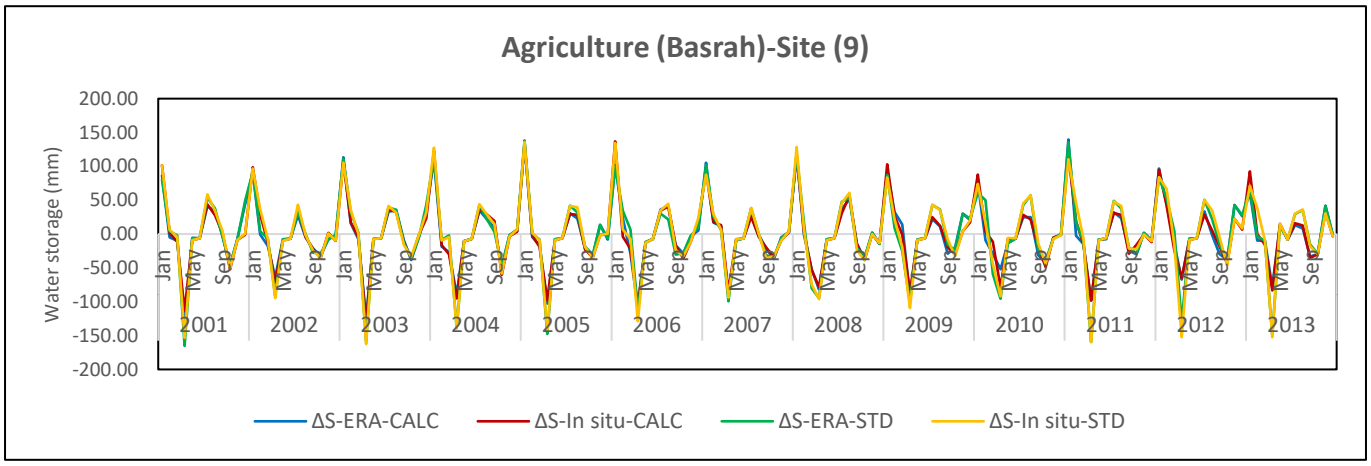
Agriculture (Basrah)-Site (9)
Water storage (mm)
200.00
150.00
100.00
50.00
0.00
-50.00
-100.00
-150.00
-200.00
Jan May Sep
2001 2002 2003 2004 2005 2006 2007 2008 2009 2010 2011 2012 2013
ΔS-ERA-CALC
ΔS-In situ-CALC
ΔS-ERA-STD
ΔS-In situ-STD

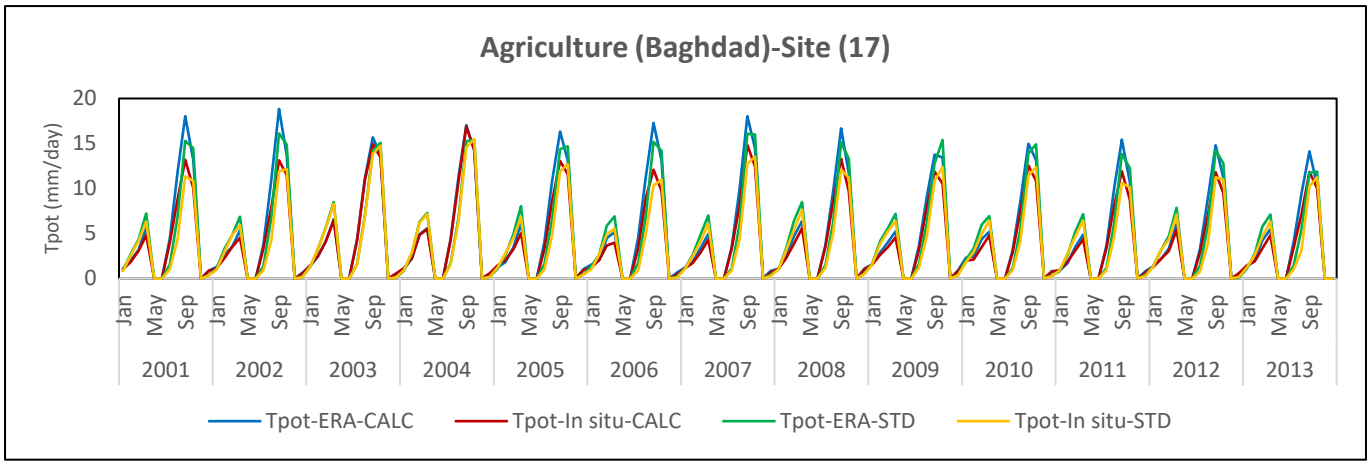
Agriculture (Baghdad)-Site (17)
Tpot (mm/day)
0
5
10
15
20
Jan May Sep
2001 2002 2003 2004 2005 2006 2007 2008 2009 2010 2011 2012 2013
Tpot-ERA-CALC
Tpot-In situ-CALC
Tpot-ERA-STD
Tpot-In situ-STD

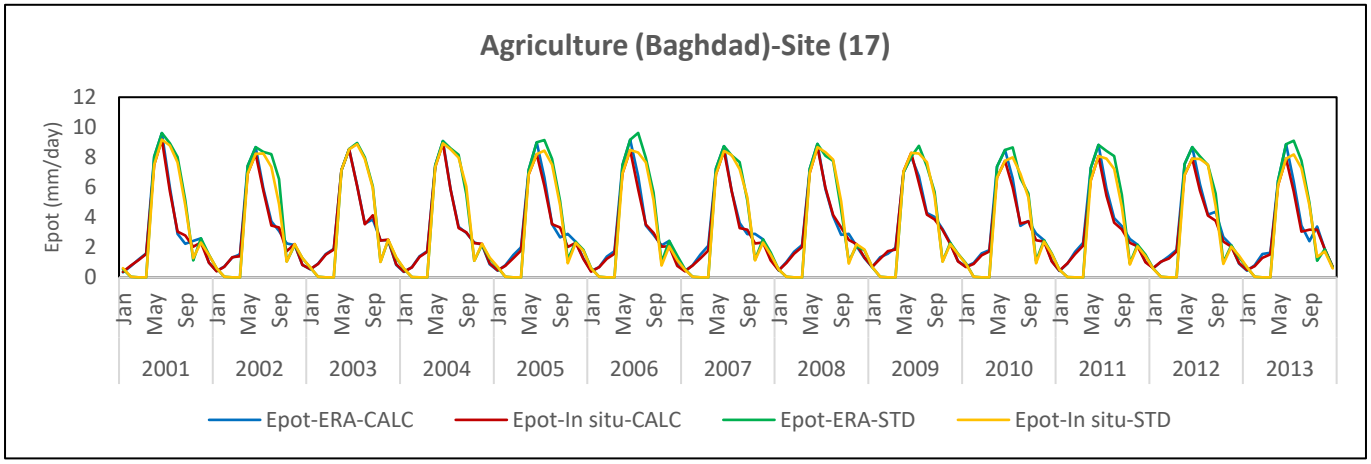
Agriculture (Baghdad)-Site (17)
Epot (mm/day)
0
2
4
6
8
10
12
Jan May Sep
2001 2002 2003 2004 2005 2006 2007 2008 2009 2010 2011 2012 2013
Epot-ERA-CALC
Epot-In situ-CALC
Epot-ERA-STD
Epot-In situ-STD

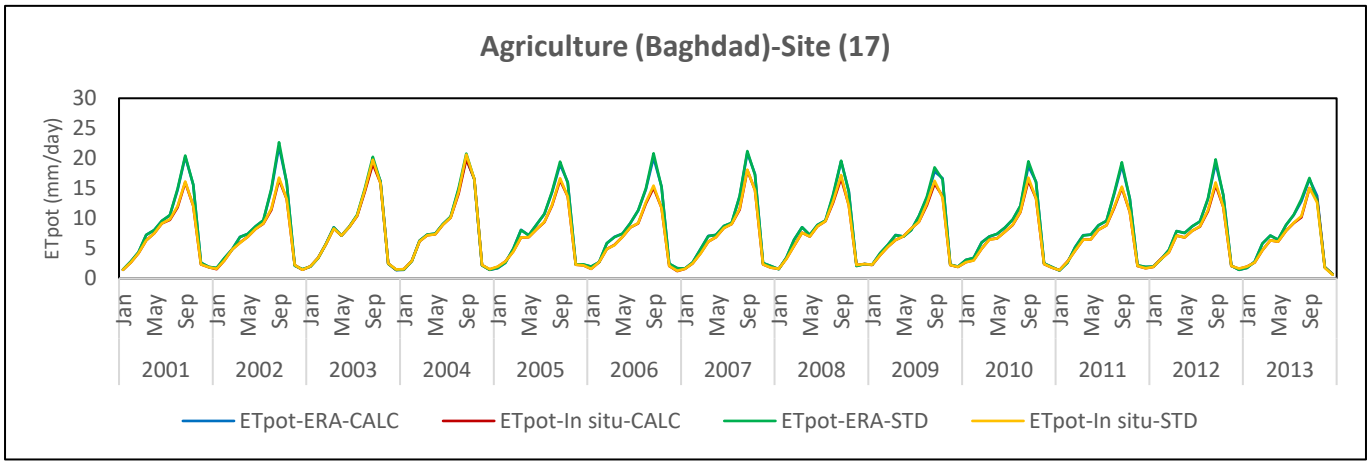
Agriculture (Baghdad)-Site (17)
ETpot (mm/day)
0
5
10
15
20
25
30
Jan May Sep
2001 2002 2003 2004 2005 2006 2007 2008 2009 2010 2011 2012 2013
ETpot-ERA-CALC
ETpot-In situ-CALC
ETpot-ERA-STD
ETpot-In situ-STD

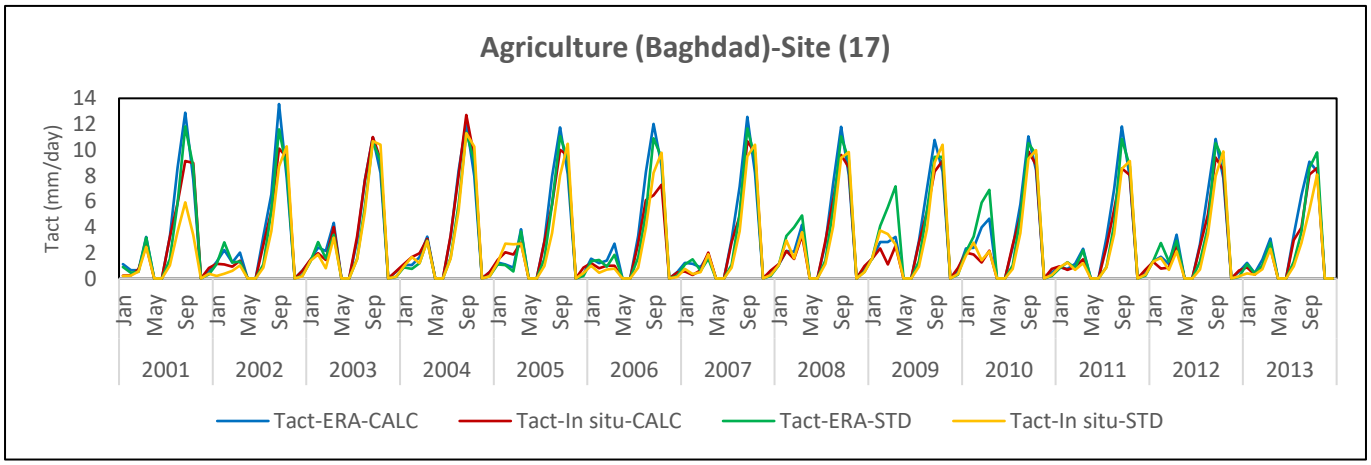
Agriculture (Baghdad)-Site (17)
Tact (mm/day)
0
2
4
6
8
10
12
14
Jan May Sep
2001 2002 2003 2004 2005 2006 2007 2008 2009 2010 2011 2012 2013
Tact-ERA-CALC
Tact-In situ-CALC
Tact-ERA-STD
Tact-In situ-STD

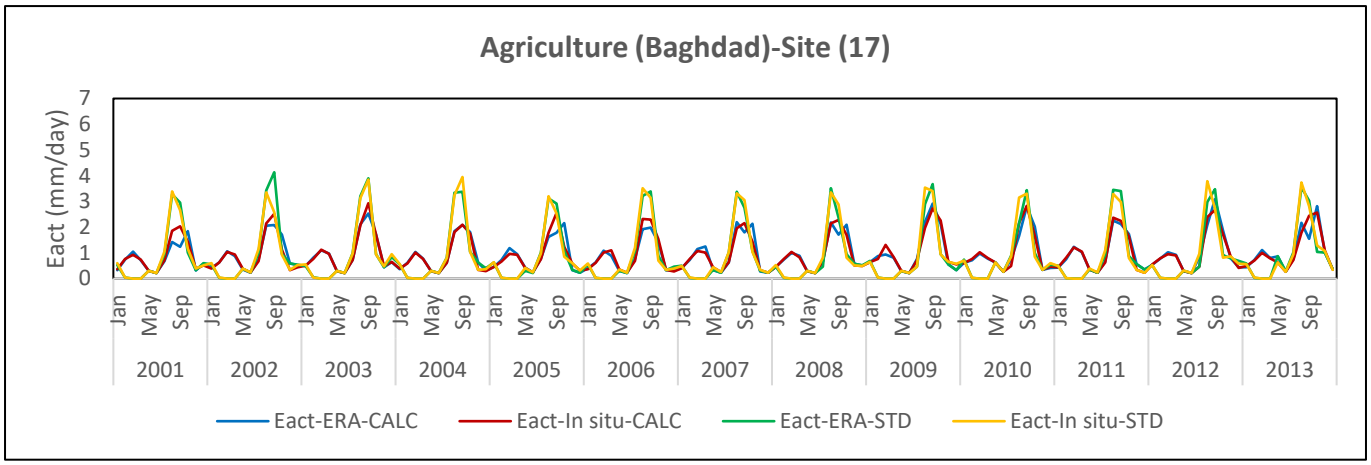
Agriculture (Baghdad)-Site (17)
Eact (mm/day)
0
1
2
3
4
5
6
7
Jan May Sep
2001 2002 2003 2004 2005 2006 2007 2008 2009 2010 2011 2012 2013
Eact-ERA-CALC
Eact-In situ-CALC
Eact-ERA-STD
Eact-In situ-STD

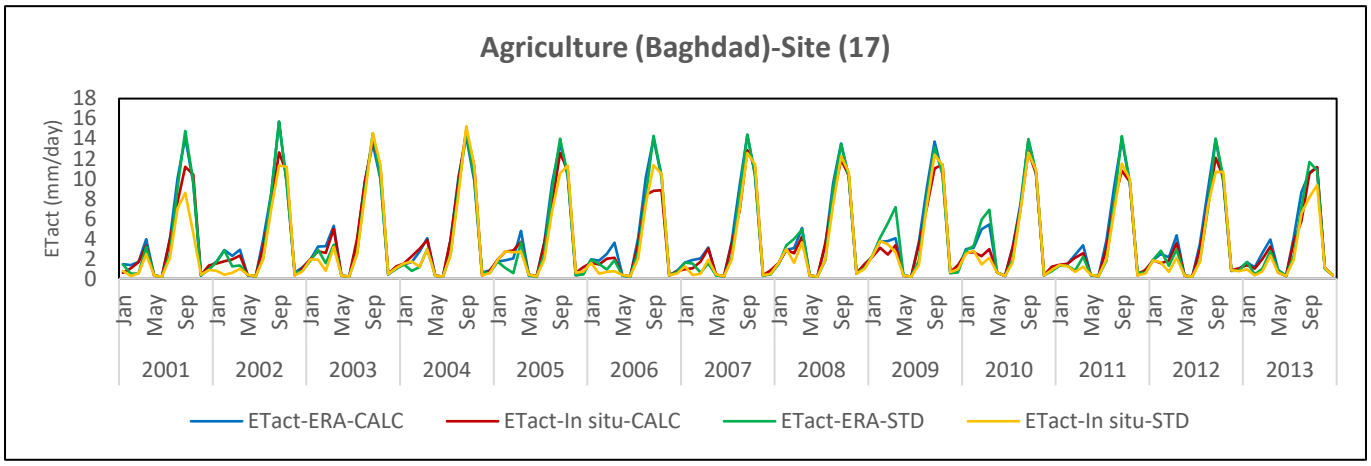
Agriculture (Baghdad)-Site (17)
ETact (mm/day)
0
2
4
6
8
10
12
14
16
18
Jan May Sep
2001 2002 2003 2004 2005 2006 2007 2008 2009 2010 2011 2012 2013
ETact-ERA-CALC
ETact-In situ-CALC
ETact-ERA-STD
ETact-In situ-STD

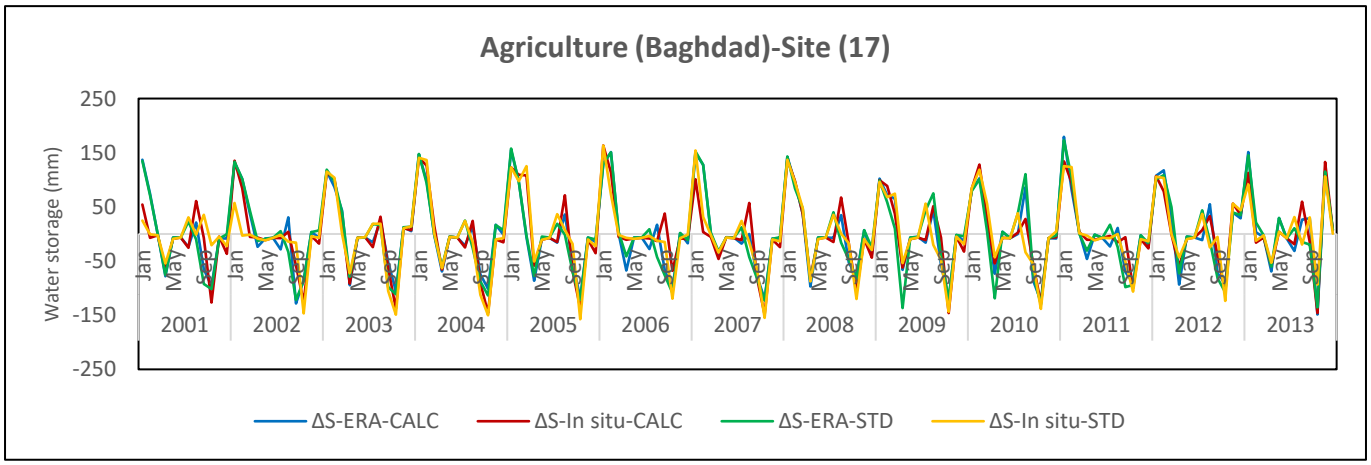
Agriculture (Baghdad)-Site (17)
Water storage (mm)
250
150
50
-50
-150
-250
Jan May Sep
2001 2002 2003 2004 2005 2006 2007 2008 2009 2010 2011 2012 2013
ΔS-ERA-CALC
ΔS-In situ-CALC
ΔS-ERA-STD
ΔS-In situ-STD

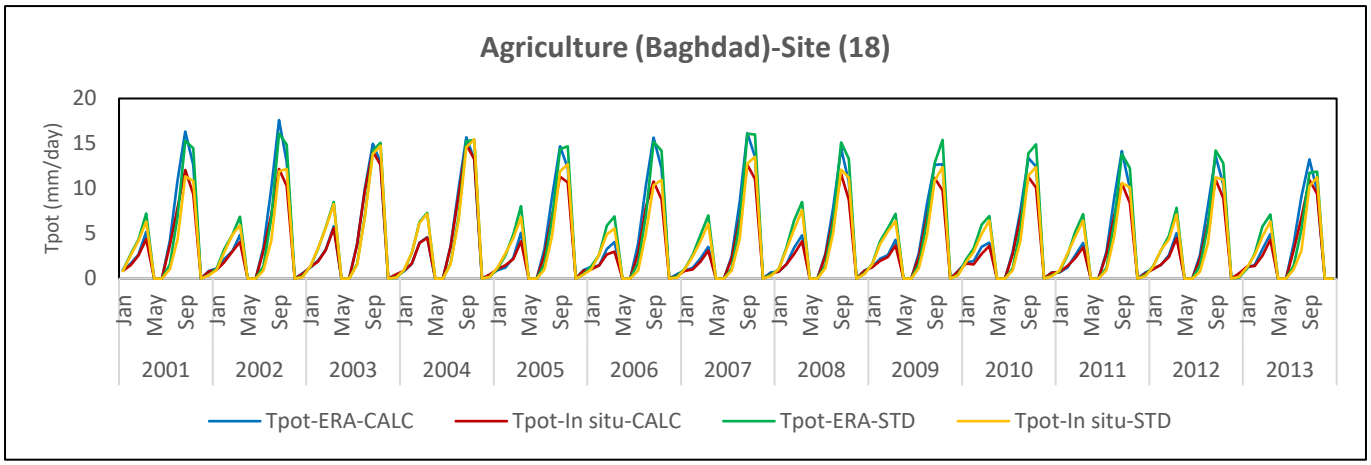
Agriculture (Baghdad)-Site (18)
Tpot (mm/day)
0
5
10
15
20
Jan May Sep
2001 2002 2003 2004 2005 2006 2007 2008 2009 2010 2011 2012 2013
Tpot-ERA-CALC
Tpot-In situ-CALC
Tpot-ERA-STD
Tpot-In situ-STD

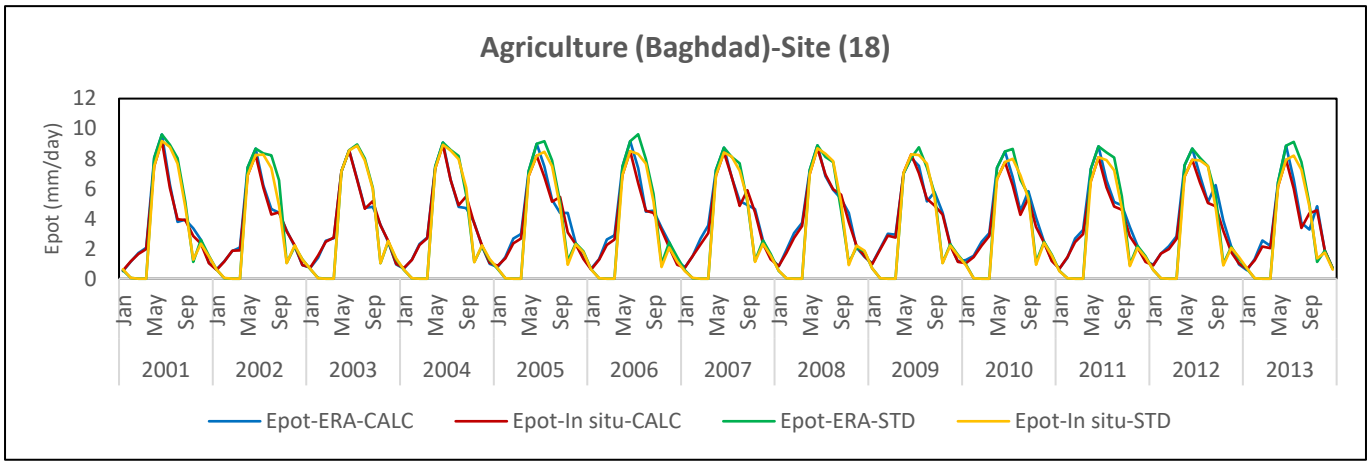
Agriculture (Baghdad)-Site (18)
Epot (mm/day)
0
2
4
6
8
10
12
Jan May Sep
2001 2002 2003 2004 2005 2006 2007 2008 2009 2010 2011 2012 2013
Epot-ERA-CALC
Epot-In situ-CALC
Epot-ERA-STD
Epot-In situ-STD

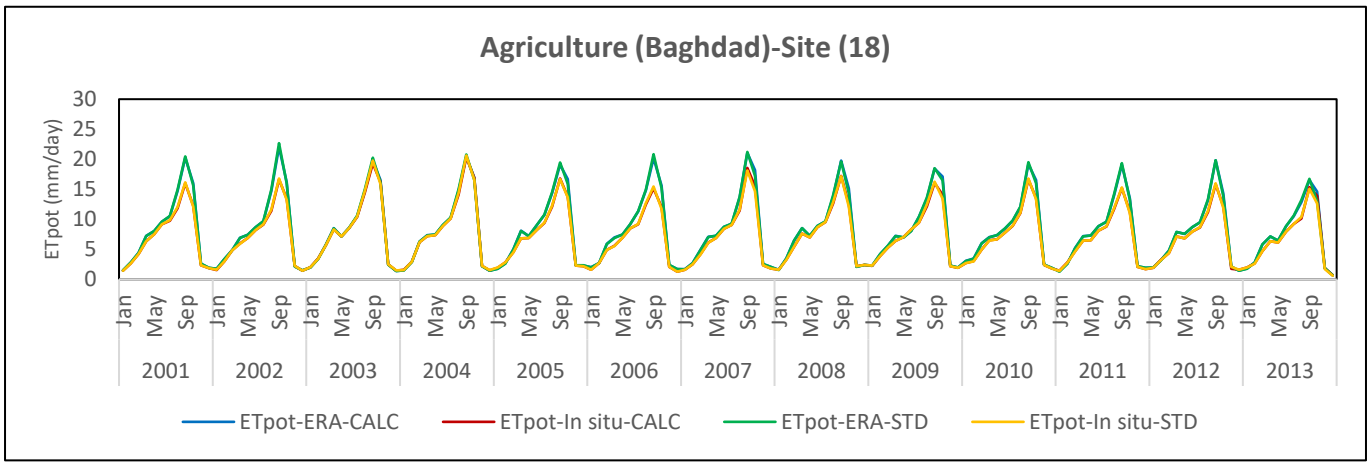
Agriculture (Baghdad)-Site (18)
ETpot (mm/day)
0
5
10
15
20
25
30
Jan May Sep
2001 2002 2003 2004 2005 2006 2007 2008 2009 2010 2011 2012 2013
ETpot-ERA-CALC
ETpot-In situ-CALC
ETpot-ERA-STD
ETpot-In situ-STD

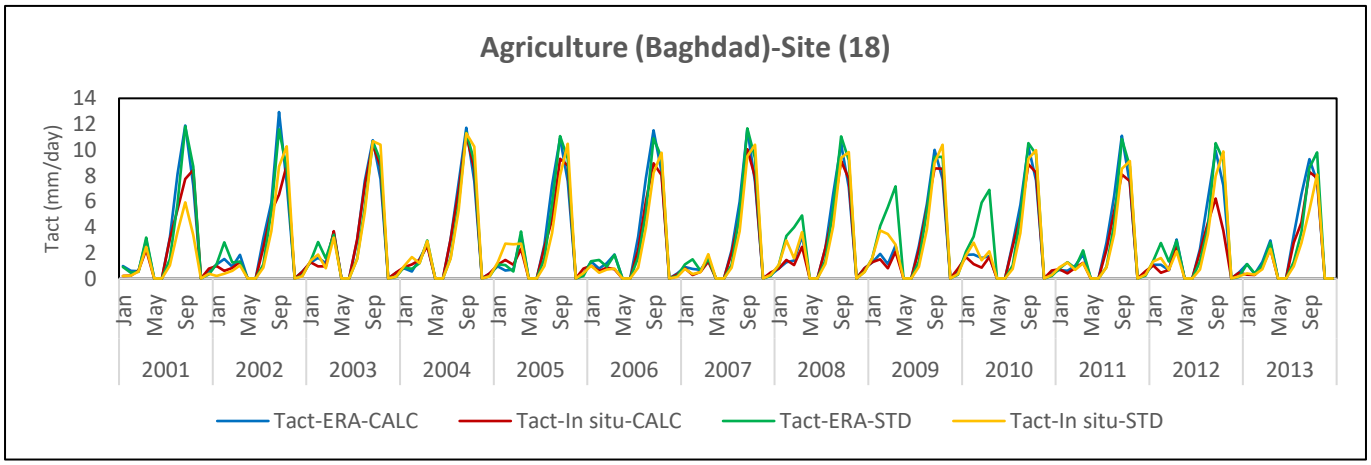
Agriculture (Baghdad)-Site (18)
Tact (mm/day)
0
2
4
6
8
10
12
14
Jan May Sep
2001 2002 2003 2004 2005 2006 2007 2008 2009 2010 2011 2012 2013
Tact-ERA-CALC
Tact-In situ-CALC
Tact-ERA-STD
Tact-In situ-STD

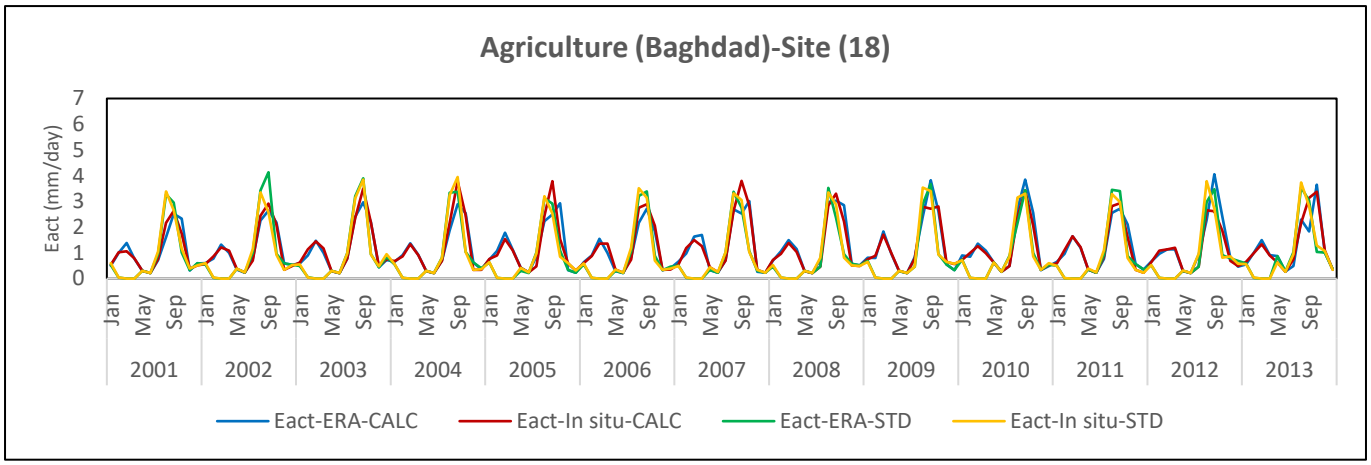
Agriculture (Baghdad)-Site (18)
Eact (mm/day)
0
1
2
3
4
5
6
7
Jan May Sep
2001 2002 2003 2004 2005 2006 2007 2008 2009 2010 2011 2012 2013
Eact-ERA-CALC
Eact-In situ-CALC
Eact-ERA-STD
Eact-In situ-STD

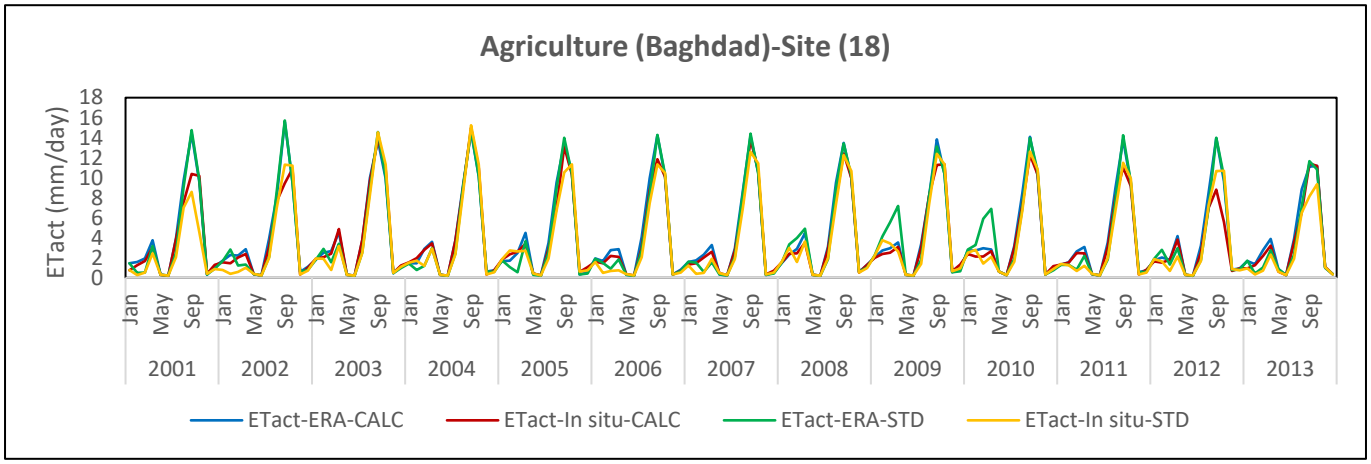
Agriculture (Baghdad)-Site (18)
ETact (mm/day)
0
2
4
6
8
10
12
14
16
18
Jan May Sep
2001 2002 2003 2004 2005 2006 2007 2008 2009 2010 2011 2012 2013
ETact-ERA-CALC
ETact-In situ-CALC
ETact-ERA-STD
ETact-In situ-STD

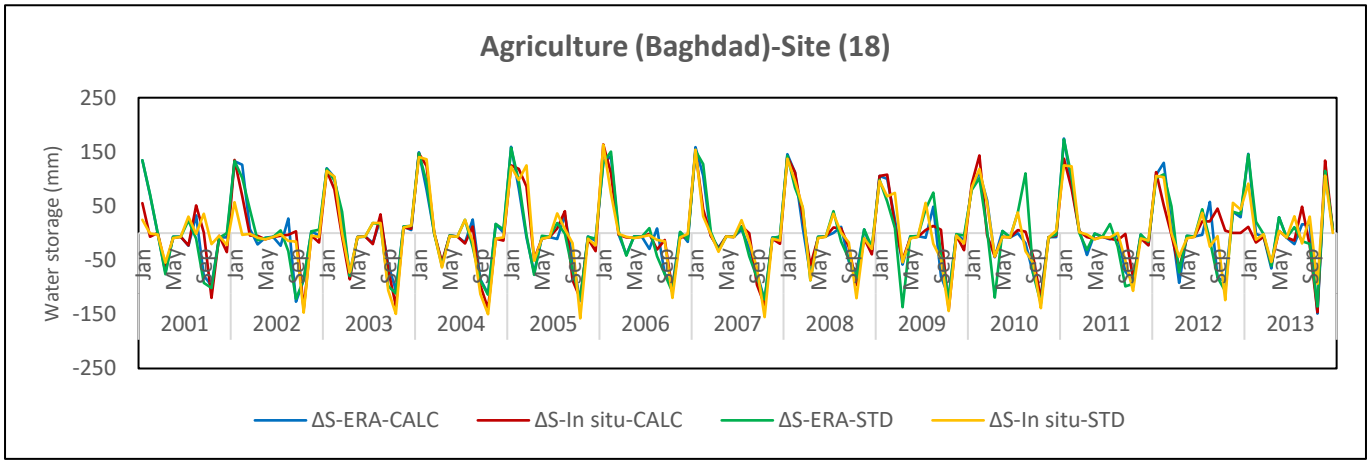
Agriculture (Baghdad)-Site (18)
Water storage (mm)
250
150
50
-50
-150
-250
Jan May Sep
2001 2002 2003 2004 2005 2006 2007 2008 2009 2010 2011 2012 2013
ΔS-ERA-CALC
ΔS-In situ-CALC
ΔS-ERA-STD
ΔS-In situ-STD

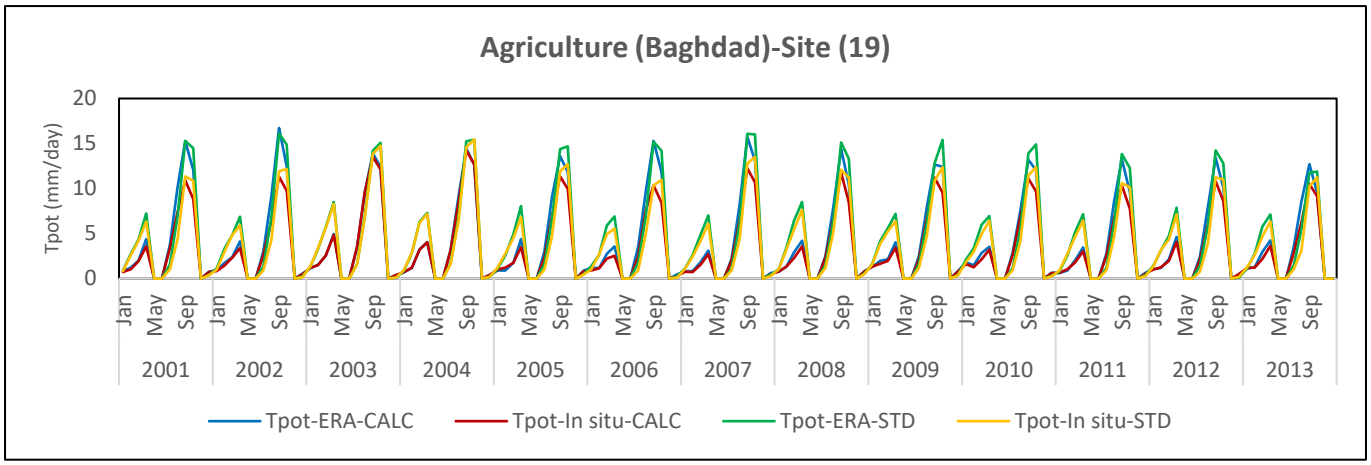
Agriculture (Baghdad)-Site (19)
Tpot (mm/day)
0
5
10
15
20
Jan May Sep
2001 2002 2003 2004 2005 2006 2007 2008 2009 2010 2011 2012 2013
Tpot-ERA-CALC
Tpot-In situ-CALC
Tpot-ERA-STD
Tpot-In situ-STD

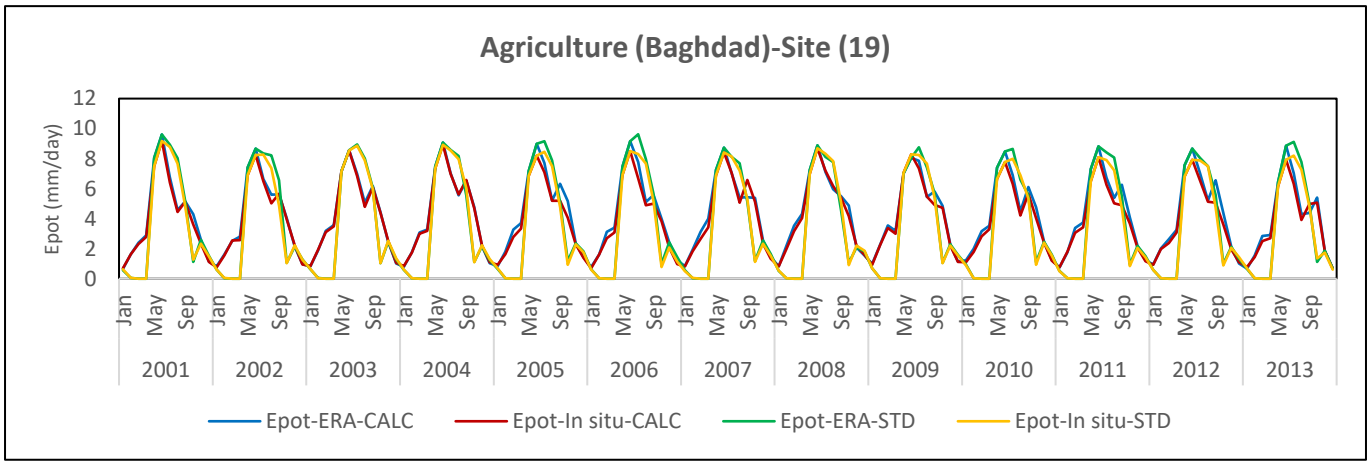
Agriculture (Baghdad)-Site (19)
Epot (mm/day)
0
2
4
6
8
10
12
Jan May Sep
2001 2002 2003 2004 2005 2006 2007 2008 2009 2010 2011 2012 2013
Epot-ERA-CALC
Epot-In situ-CALC
Epot-ERA-STD
Epot-In situ-STD

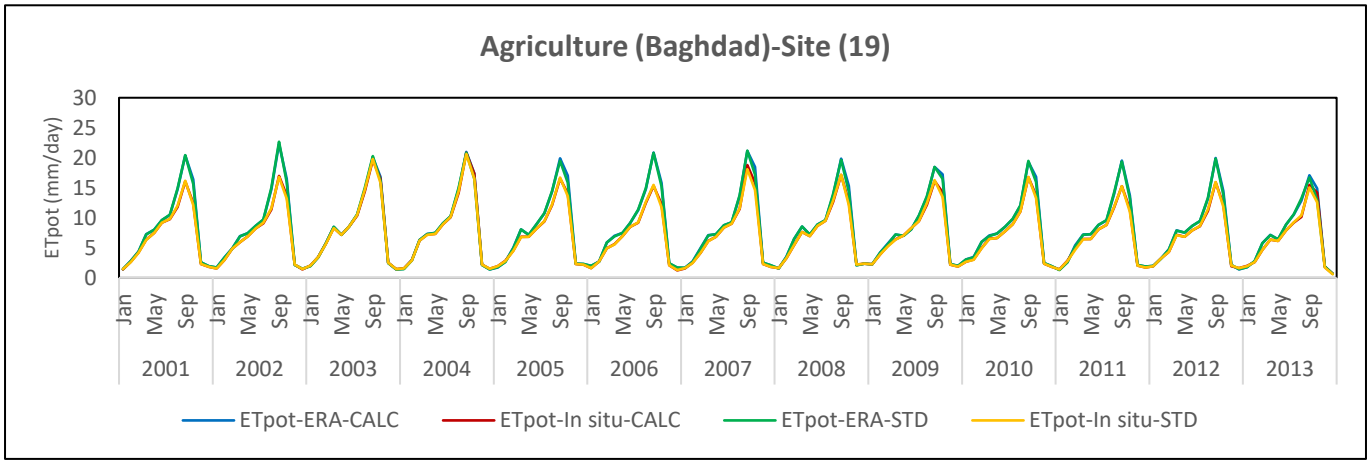
Agriculture (Baghdad)-Site (19)
ETpot (mm/day)
0
5
10
15
20
25
30
Jan May Sep
2001 2002 2003 2004 2005 2006 2007 2008 2009 2010 2011 2012 2013
ETpot-ERA-CALC
ETpot-In situ-CALC
ETpot-ERA-STD
ETpot-In situ-STD

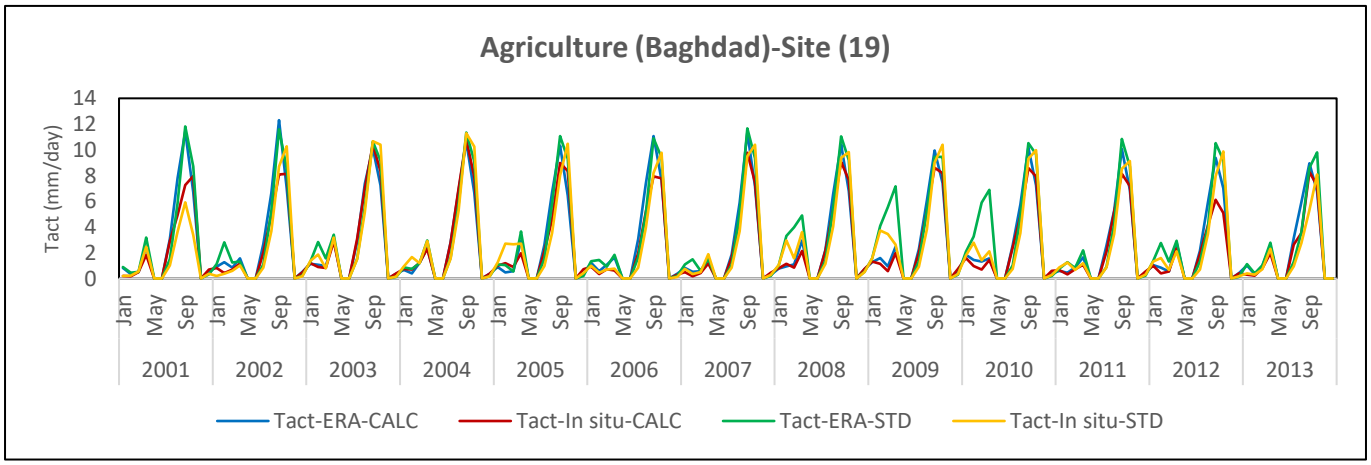
Agriculture (Baghdad)-Site (19)
Tact (mm/day)
0
2
4
6
8
10
12
14
Jan May Sep
2001 2002 2003 2004 2005 2006 2007 2008 2009 2010 2011 2012 2013
Tact-ERA-CALC
Tact-In situ-CALC
Tact-ERA-STD
Tact-In situ-STD

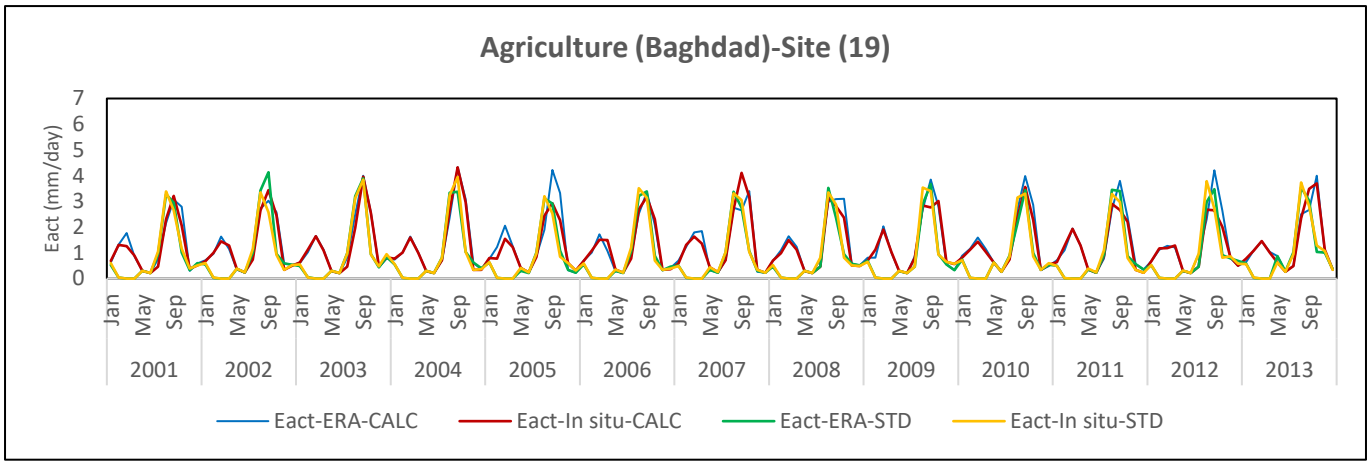
Agriculture (Baghdad)-Site (19)
Eact (mm/day)
0
1
2
3
4
5
6
7
Jan May Sep
2001 2002 2003 2004 2005 2006 2007 2008 2009 2010 2011 2012 2013
Eact-ERA-CALC
Eact-In situ-CALC
Eact-ERA-STD
Eact-In situ-STD

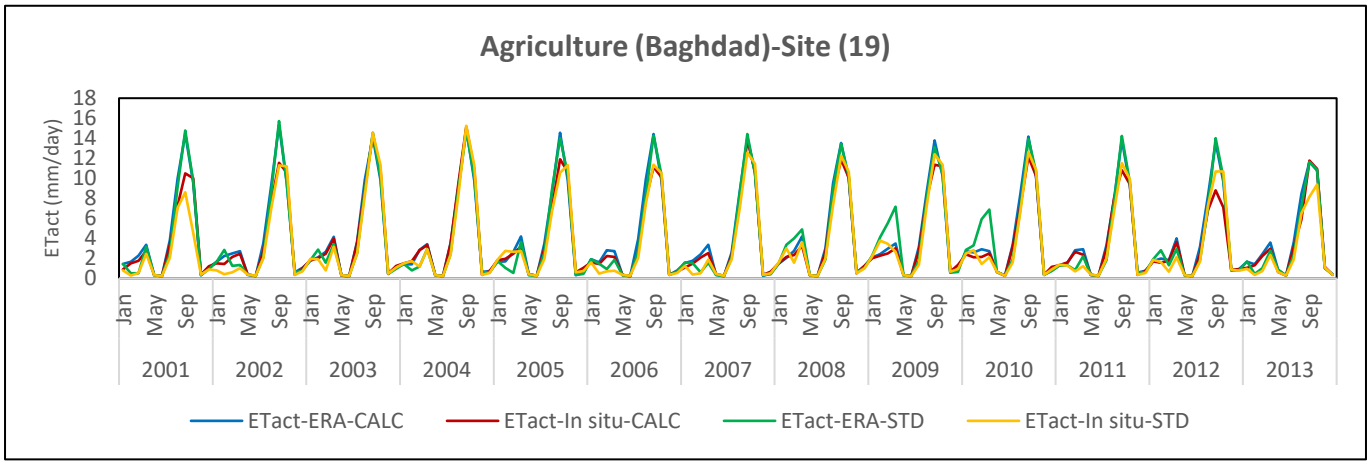
Agriculture (Baghdad)-Site (19)
ETact (mm/day)
0
2
4
6
8
10
12
14
16
18
Jan May Sep
2001 2002 2003 2004 2005 2006 2007 2008 2009 2010 2011 2012 2013
ETact-ERA-CALC
ETact-In situ-CALC
ETact-ERA-STD
ETact-In situ-STD

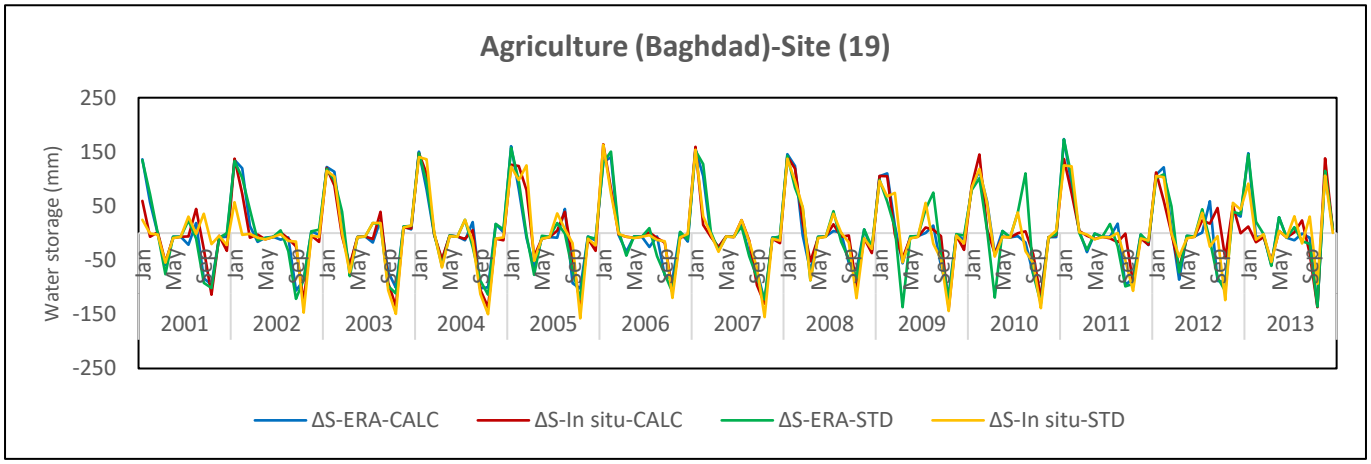
Agriculture (Baghdad)-Site (19)
Water storage (mm)
250
150
50
-50
-150
-250
Jan May Sep
2001 2002 2003 2004 2005 2006 2007 2008 2009 2010 2011 2012 2013
ΔS-ERA-CALC
ΔS-In situ-CALC
ΔS-ERA-STD
ΔS-In situ-STD

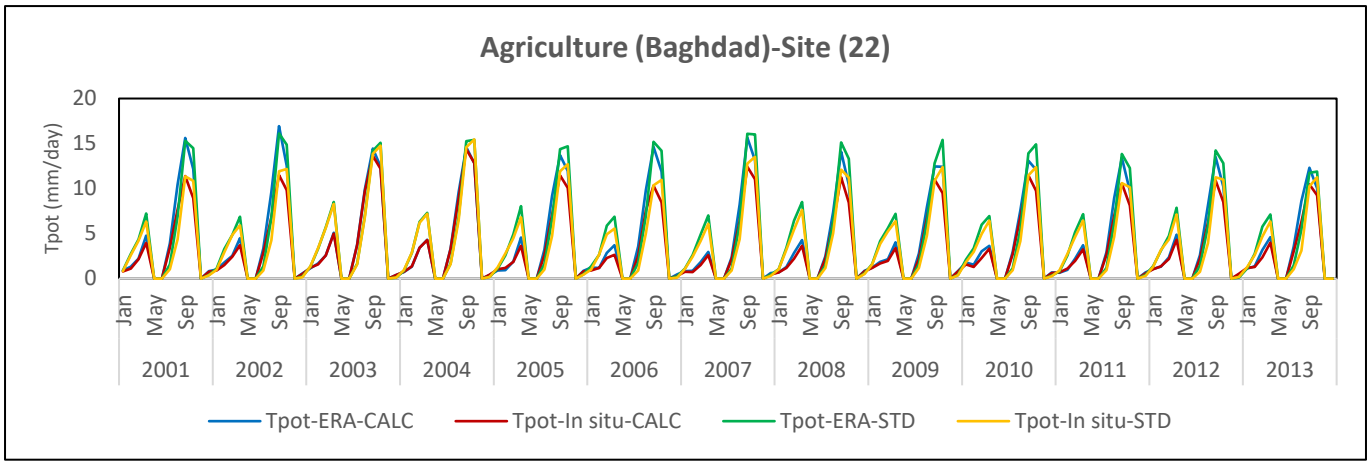
Agriculture (Baghdad)-Site (22)
Tpot (mm/day)
0
5
10
15
20
Jan May Sep
2001 2002 2003 2004 2005 2006 2007 2008 2009 2010 2011 2012 2013
Tpot-ERA-CALC
Tpot-In situ-CALC
Tpot-ERA-STD
Tpot-In situ-STD

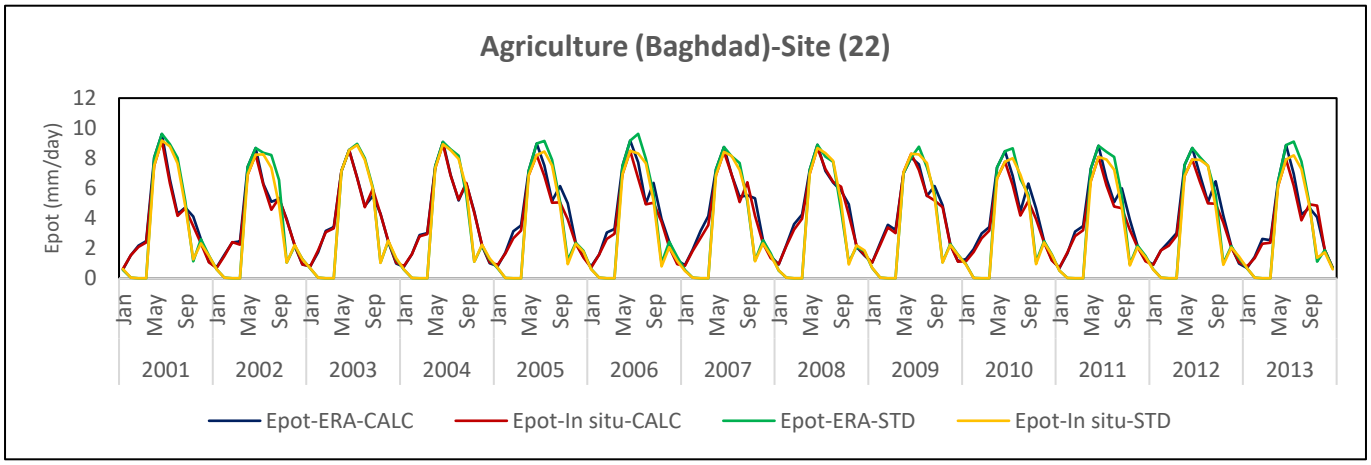
Agriculture (Baghdad)-Site (22)
Epot (mm/day)
0
2
4
6
8
10
12
Jan May Sep
2001 2002 2003 2004 2005 2006 2007 2008 2009 2010 2011 2012 2013
Epot-ERA-CALC
Epot-In situ-CALC
Epot-ERA-STD
Epot-In situ-STD

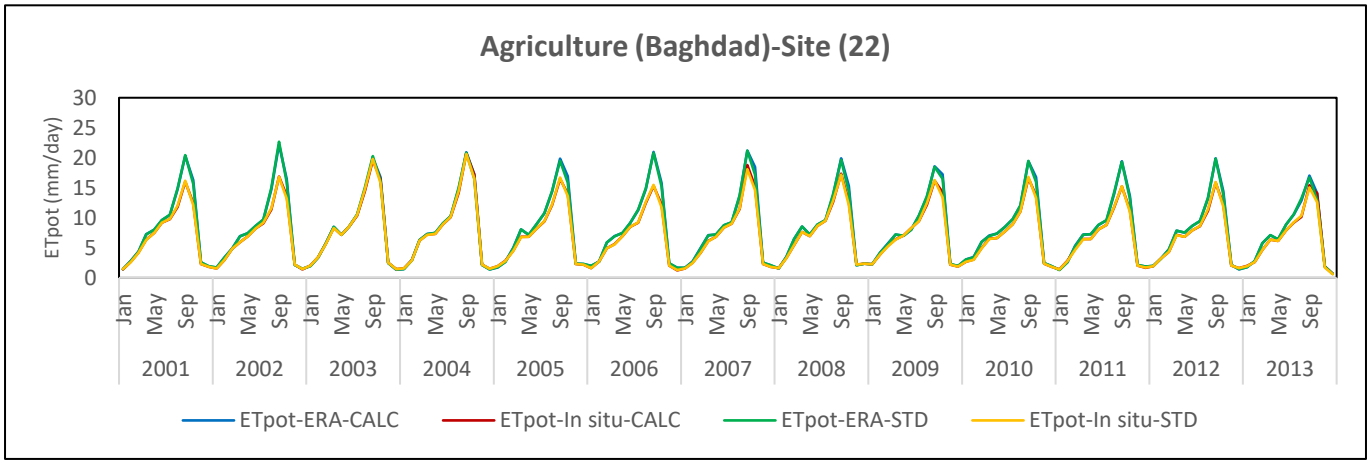
Agriculture (Baghdad)-Site (22)
ETpot (mm/day)
0
5
10
15
20
25
30
Jan May Sep
2001 2002 2003 2004 2005 2006 2007 2008 2009 2010 2011 2012 2013
ETpot-ERA-CALC
ETpot-In situ-CALC
ETpot-ERA-STD
ETpot-In situ-STD

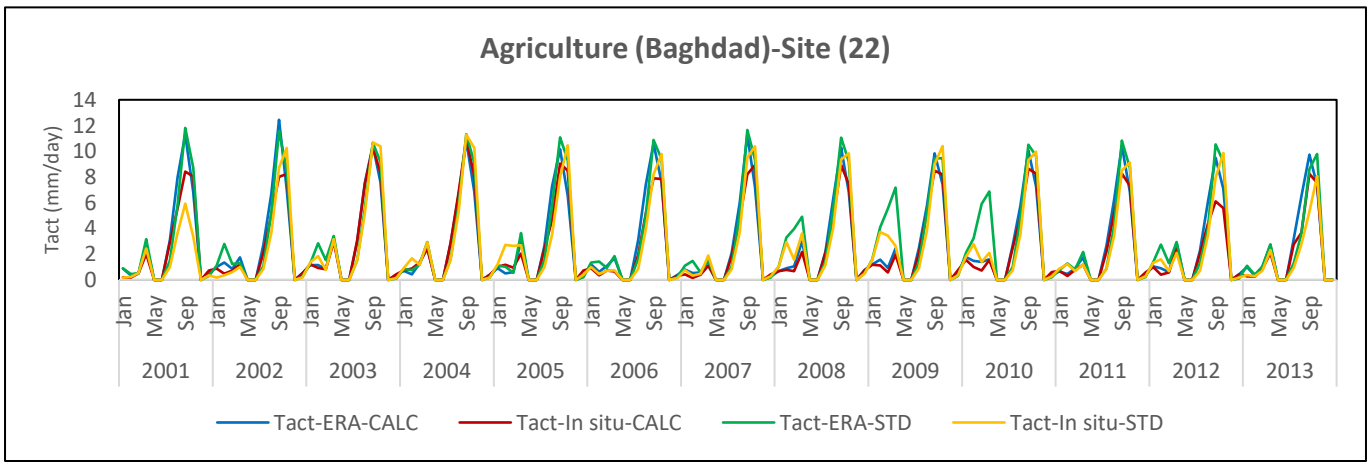
Agriculture (Baghdad)-Site (22)
Tact (mm/day)
0
2
4
6
8
10
12
14
Jan May Sep
2001 2002 2003 2004 2005 2006 2007 2008 2009 2010 2011 2012 2013
Tact-ERA-CALC
Tact-In situ-CALC
Tact-ERA-STD
Tact-In situ-STD

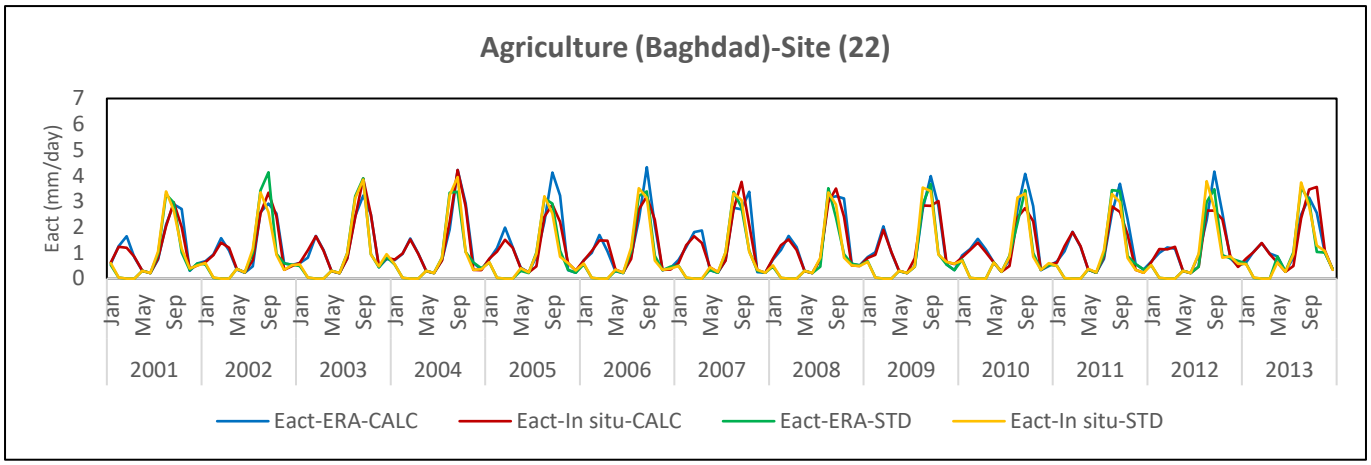
Agriculture (Baghdad)-Site (22)
Eact (mm/day)
0
1
2
3
4
5
6
7
Jan May Sep
2001 2002 2003 2004 2005 2006 2007 2008 2009 2010 2011 2012 2013
Eact-ERA-CALC
Eact-In situ-CALC
Eact-ERA-STD
Eact-In situ-STD

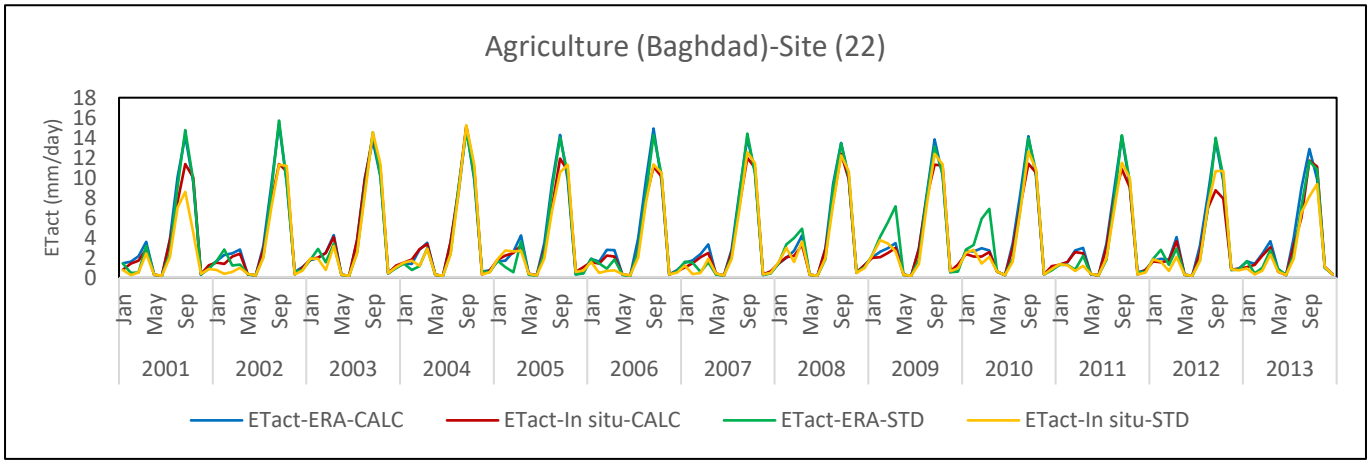
Agriculture (Baghdad)-Site (22)
ETact (mm/day)
0
2
4
6
8
10
12
14
16
18
Jan May Sep
2001 2002 2003 2004 2005 2006 2007 2008 2009 2010 2011 2012 2013
ETact-ERA-CALC
ETact-In situ-CALC
ETact-ERA-STD
ETact-In situ-STD

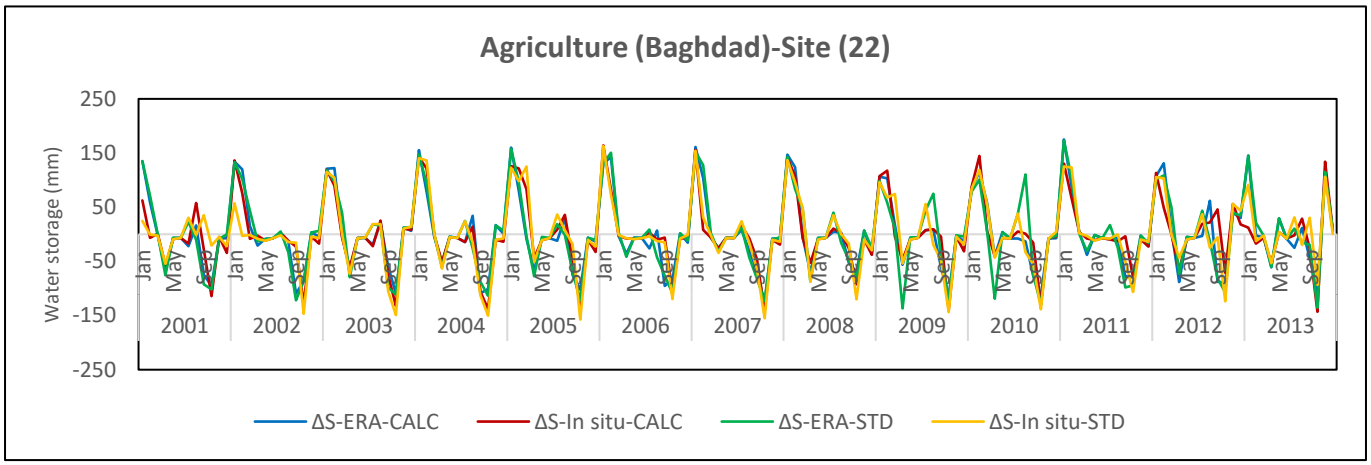
Agriculture (Baghdad)-Site (22)
Water storage (mm)
-250
-150
50
150
250
Jan May Sep
2001 2002 2003 2004 2005 2006 2007 2008 2009 2010 2011 2012 2013
ΔS-ERA-CALC
ΔS-In situ-CALC
ΔS-ERA-STD
ΔS-In situ-STD